Zhikang Xu,
Xiaojun Huang
Lingshu Wan

Surface Engineering of Polymer Membranes

ADVANCED TOPICS
IN SCIENCE AND TECHNOLOGY IN CHINA

ADVANCED TOPICS
IN SCIENCE AND TECHNOLOGY IN CHINA

Zhejiang University is one of the leading universities in China. In Advanced Topics in Science and Technology in China, Zhejiang University Press and Springer jointly publish monographs by Chinese scholars and professors, as well as invited authors and editors from abroad who are outstanding experts and scholars in their fields. This series will be of interest to researchers, lecturers, and graduate students alike.

Advanced Topics in Science and Technology in China aims to present the latest and most cutting-edge theories, techniques, and methodologies in various research areas in China. It covers all disciplines in the fields of natural science and technology, including but not limited to, computer science, materials science, life sciences, engineering, environmental sciences, mathematics, and physics.

Zhikang Xu
Xiaojun Huang
Lingshu Wan

Surface Engineering of Polymer Membranes

With 184 figures

ZHEJIANG UNIVERSITY PRESS
浙江大学出版社

Springer

AUTHORS:

Prof. Zhikang Xu
Institute of Polymer Science,
Zhejiang University,
Hangzhou 310027, China
Email: xuzk@zju.edu.cn

Dr. Xiaojun Huang
Institute of Polymer Science,
Zhejiang University,
Hangzhou 310027, China
Email:hxjzxh@zju.edu.cn

Dr. Lingshu Wan
Institute of Polymer Science,
Zhejiang University,
Hangzhou 310027, China
Email: lswan@zju.edu.cn

Cover design: Frido Steinen-Broo, EStudio Calamar, Spain
Printed on acid-free paper

Preface

Surface Engineering of Polymer Membranes embraces those processes which modify membrane surfaces to improve their in-service performance. It means 'modifying the surface' of a membrane to confer surface properties which are different from its bulk properties. The purpose may be to minimize fouling, modulate hydrophilicity/hydrophobicity, enhance biocompatibility, act as a diffusion barrier, provide bio- or chemical functionalities, mimic a biomembrane, fabricate nanostructures or simply improve the aesthetic appearance of the membrane surface. The book begins with the basics of the surface engineering of polymer membranes, including surface modification, biomimicking, enzyme immobilization, molecular imprinting and the various methods of the spectroscopic and structural study of membrane surfaces. These are followed by descriptive treatments of topics such as surface modification by graft polymerization and macromolecule immobilization, the construction of biomimetic surfaces and their functionalities, enzyme immobilization and bioactivity, molecular recognition and nanostructured surfaces. This book provides a unique synthesis of our knowledge of the role of surface chemistry and physics in membrane science and technology. I sincerely hope and anticipate that this book, which contains plentiful information on the many and varied aspects of membrane surfaces, will be useful to anyone interested or involved in this fascinating and technologically important research area.

It is indeed a great pleasure to extend my "thank you" to all my colleagues and students for their dedication to our research projects. Especially, Chapter 3 profits from the work of Bei-Bei Ke, Chapter 4 is part of the thesis by Meng-Xin Hu, Chapters 5 and 7 are based on the parts of theses by Qian Yang and Zheng-Wei Dai respectively, Chapter 8 profits from the work by Ai-Fu Che and Yun-Feng Yang, and Chapters 9 and 10 are benefit from the thesis by Zhen-Gang Wang. Their efforts are deeply appreciated and acknowledged. Finally, I would like to thank the editorial staff of Springer Verlag and Zhejiang University Press for their assistance.

Zhi-Kang Xu
Hangzhou
December 2007

Contents

1

Surface Engineering of Polymer Membranes: An Introduction

Polymeric separation membranes develop rapidly and have been applied in many fields. Filtration with polymer membranes covers the separation of industrial chemicals, purification of laboratory products and treatment of drinking water. For all these processes, the performance limits are clearly determined by the membrane itself. Flux and rejection of a membrane process such as microfiltration or ultrafiltration are mainly influenced by size exclusion. Nevertheless, surface properties of the membrane also play a crucial role. It is because membrane fouling, induced by adsorption of matter onto the membrane surface or deposition into the pores, is mainly controlled by the surface properties. For example, a hydrophobic membrane surface is apt to cause adsorption of protein or other solutes due to hydrophobic interactions. As is well known, membrane fouling will decline the flux and deteriorate the selectivity. Meanwhile, the products must meet the ever stricter environmental or safety standards. A membrane separation system should consist of a membrane with stable and reliable performance. Therefore, the first objective of polymer membrane surface engineering is to enhance the surface properties of the membrane by modulating its surface chemistry and physics, and hence improve the performance of the membrane.

Another important objective is to achieve surface functionalization for polymer membranes. It is well known that the membrane process has been used in many applications. Some of them are relatively mature, while others are still in the course of development. The developing technologies, including those for biocatalysis and sensing, generally require a functional membrane surface. What is more, their performances mainly depend on the functionality of the membrane surface. For instance, a functional surface immobilized with enzyme can be applied in an enzyme-membrane bioreactor as well as in biosensors, in which the activity retention and stability of the immobilized enzyme are essential. It is accepted that characteristics of the membrane surface can remarkably affect the enzyme activity and stability. Therefore, based on the strategies for surface modification, a functional membrane surface can

also be constructed. This objective is exciting because it means that the areas of application for polymer membranes can be greatly extended.

To achieve the two above-mentioned objectives, it is easy and effective to use surface modification in the surface engineering of polymer membranes. "Grafting from" and "grafting to" are two commonly used strategies. The "grafting from" method utilizes active species existing on a membrane surface to initiate the polymerization of monomers from the surface. Usually this strategy is accomplished by treating a substrate with plasma and glow-discharge to generate immobilized initiators, followed by polymerization. On the other hand, for the "grafting to" method, polymer chains carrying reactive anchor groups at the end or on the side chains are covalently coupled to the membrane surface, which is also referred to as macromolecules immobilization in this book. Chapters 4 and 5 mainly focus on these two methods, respectively. In these two chapters, surface modifications of polymer membranes are comprehensively summarized, which include chemical graft polymerization, plasma or glow-discharge induced graft polymerization, UV-induced graft polymerization, high energy radiation-initiated graft polymerization, and immobilization of synthetic polymers and biomacromolecules. Applications of these surface modified membranes are also discussed from various aspects.

As inspired by the cell membrane, biomimetic modification is also introduced to realize membrane surfaces with the desired surface properties or functions. According to the fluid mosaic model proposed by Singer and Nicholson, the cell membrane is composed of a semipermeable lipid bilayer, which consists of three classes of amphipathic lipids, i.e. phospholipids, glycolipids and steroids. The relative composition of each depends upon the type of cell, but in the majority of cases phospholipids are the most abundant. Thus, the construction of membrane surfaces with phospholipid moieties is discussed in Chapter 6. In this chapter many kinds of membrane surfaces with phospholipid moieties are present. It is not hard to see that the modified membranes are highly biofouling resistant because they possess considerably biocompatible surfaces. This type of membrane can also suppress non-specific adsorption of proteins or cells, which is also beneficial to its biomedical applications.

Differing from phospholipid, carbohydrates have often been found on the surface of nearly every cell membrane in the form of polysaccharides, glycoproteins, glycolipids or/and other glycoconjugates. The carbohydrates on the external cell membrane, known as the glycocalyx, play essential roles in many biological functions which can be classified in two opposing ways. One serves as sites for the docking of other cells, biomolecules and pathogens in a more or less specific recognition process. The other contributes to steric repulsion that prevents the undesirable non-specific adhesion of other proteins and cells. Both these two functions rely on the carbohydrate-protein interactions. Advances in membrane surface glycosylation constitute Chap-

ter 7 in which modification with natural polysaccharides, such as heparin and chitosan, as well as synthetic glycopolymers is described. The surface glycosylation provides the membrane with a surface of high hydrophilicity and biocompatibility. Furthermore, the specific recognition between the carbohydrates and proteins endows the membranes with some interesting functions, which may be useful in protein isolation/purification.

A molecular imprinting technique is also a way of creating a membrane surface with a specific recognition function, which forms Chapter 8. Compared with a glycosylated surface, a molecular imprinted surface is even more flexible. As we know, molecular recognition involves selection and recognition according to the shape, size and the interaction characterized with selectivity between a ligand and a given receptor. A molecular imprinting technique just originates from molecular recognition, which can also achieve recognition at the molecular level. A molecular imprinted membrane can be used to separate template molecules from others of similar molecular size, or to concentrate template molecules. This extends the size exclusion mechanism for a separation membrane by introducing specific recognition. For example, such membranes can separate amino acid from its enantiomers though the molecular size is the same. Moreover, a molecular imprinted membrane can act as a recognition element for sensor design. In Chapter 8, the basic theory of the molecular imprinting technique, methods for molecular imprinted membrane preparation (including surface imprinting method), the separation mechanism of the molecular imprinted membranes and their applications are summarized.

A membrane with a biocatalytic surface is another important example of surface functionalization, which is the topic of Chapter 9. The enzyme is a kind of catalyst that is not only efficient and safe but also environmentally benign and resource and energy saving. Using a membrane as the support for enzyme immobilization can simultaneously realize the functions of catalysis and separation. However, there are many factors affecting the performance of an immobilized enzyme, such as surface chemistry, membrane structure, immobilization procedure as well as enzyme characteristics, enzyme loading and reaction condition. In this chapter, immobilization of an enzyme on polymer membranes is thoroughly reviewed. Various procedures for the immobilization of different kinds of enzymes on a great variety of membrane materials, including natural and synthetic materials, are present here. In addition, the applications of membranes with a biocatalytic function in bioreactors and biosensors are also summarized.

In the past decade, nanofibrous membranes prepared via an electrospinning technique have received considerable interest because of their large surface area to volume ratio and high porosity. Most importantly, an electrospinning technique is versatile and shows a good prospect for the fabrication of nanofibrous membranes on a large scale. When compared with traditional filter media such as a phase inversion membrane or fibrous membrane at the

micron scale, an electrospun nanofibrous membrane used for filtration may have an extremely high efficiency. It should be attributed to the nano-sized fibers. Thus, this topic is sufficiently important to warrant its own treatment in Chapter 10. In this chapter, we focus on the functionalization of nanofibrous membranes, and those with a biocatalytic function and affinity function are particularly emphasized.

Before the specific description of the modification and functionalization of polymer membrane surfaces, some general methods for surface modification and characterization, which are closely related to polymer membranes, are introduced in the following chapters. Characterizing the modified surface is not only important to understand the relationship between the membrane surface structure and its properties but also important to provide guidance for surface modification. It is well known that membrane surface properties are affected by many factors such as the chemical composition, morphologies and structures, wettability, and biocompatibility. Therefore, in Chapter 2 membrane surface characterization is introduced from the above-mentioned aspects. The following characterization techniques are briefly introduced: attenuated total reflectance Fourier transform infrared (ATR-FTIR) spectroscopy, X-ray photoelectron spectroscopy (XPS), static secondary ion mass spectrometry (SSIMS), energy dispersive X-ray spectroscopy (EDS), optical microscopy, laser confocal scanning microscopy (LCSM), scanning electron microscopy (SEM), environmental scanning electron microscopy (ESEM), atomic force microscopy (AFM), contact angle measurement, and some evaluation methods for the biocompatibility of membrane surfaces. On the other hand, methods for the functionalization of the polymer membrane are summarized in Chapter 3 from the aspects of surface modification, molecular imprinting, and enzyme immobilization. For surface modification in particular, several methods are presented, which include coating, self-assembly, chemical treatment, plasma treatment, and graft polymerization.

Overall, membrane science and technology is still in a period of enormous progress and development. The steady rise to 3.442 in 2006 of the impact factor of the *Journal of Membrane Science*, the top journal in this field, is excellent proof. In our view, surface engineering is one of the most important fields in all of membrane science. In this book, an attempt has been made to cover the most important trends in the area of surface modification and functionalization of polymer membranes. However, due to the wide diversity of the field, selections have to be made which also reflect the particular interests of the authors.

2

Techniques for Membrane Surface Characterization

In recent years, the surface engineering of polymer membranes through surface modification and surface functionalization has received significant attention. Since the properties of a membrane surface are very important for practical applications, it is important to have the means to characterize and measure those structures and properties. In fact, surface characterization is not only important for understanding the relationship between the membrane structure and its properties but also for guiding surface modification. It is well known that various aspects of a membrane surface, which include chemical composition, morphology and topography, wettability, and biocompatibility, can affect the properties and applications remarkably. Many kinds of surface characterization techniques may be applied to study the surface properties of polymer membranes. In this chapter, techniques for the characterization of a polymer membrane surface are reviewed, which include attenuated total reflectance Fourier transform infrared (ATR-FTIR) spectroscopy, X-ray photoelectron spectroscopy (XPS), static secondary ion mass spectrometry (SSIMS), energy dispersive X-ray spectroscopy (EDS), optical microscopy, laser confocal scanning microscopy (LCSM), scanning electron microscopy (SEM), environmental scanning electron microscopy (ESEM), atomic force microscopy (AFM), contact angle measurement, and some evaluation methods for the biocompatibility of membrane surfaces.

2.1 General Principles

2.1.1 Sample Preparation

A number of general ideas can be applied to all polymeric surfaces. Of course, a polymeric membrane surface is not the exception. Sample preparation is of great importance for every characterization method, which determines the reliability of the obtained results. Bad sample preparation gives rise to artifacts.

Needless to say, a sample for characterization should reflect, as closely as possible, the membrane being subjected to the separation process, whether it be the chemical composition or the physical morphologies. Therefore, first of all, contamination on the membrane surface should definitely be avoided. Every step in the analysis procedure must be carefully performed. Contamination is easily introduced from the environment such as from the atmosphere and even from the packaging bag. On the other hand, some residual matter may also act as a contaminant, especially for the membrane after modification. For example, the subjected membrane grafting polymerization process should be thoroughly rinsed or cleaned to remove the residual un-reacted monomers or the embedded un-grafted polymer. Secondly, unlike other smooth polymer film surfaces, a polymer membrane is porous and hence preserving the original look of the porous membrane is a matter of special importance in most cases. For some characterization methods, a vacuum is required and then drying is necessary for sample observation. Consequently, problems can arise if a wet membrane specimen is dried under intense conditions because the membrane porous structure may be damaged or altered by the capillary forces (Mulder, 1996). Various methods can be employed to prevent this. For example, as water has a high surface tension, a sequence of non-solvents for the membrane such as water, ethanol and hexane can be used one by one to reduce the capillary forces during drying. In this sequence, the surface tension of the non-solvent decreases gradually and the last hexane has a very low surface tension and can be easily removed.

2.1.2 Where is the Surface?

It is well known that the surface property is very important. However, what is meant by a membrane surface? Where is the surface? Ideally the surface should be defined as the plane at which the membrane terminates, in other words, the last atom layer before the adjacent phase begins (Bubert and Jenett, 2002). Unfortunately such a definition is impractical because the effect of termination extends into the solid beyond the outermost atom layer, especially for a membrane which is porous and rough. Furthermore, the "surface" is sometimes a changeable concept for different methods of analysis, because different methods provide varying degrees of information at different depth profiles. For example, attenuated total reflectance Fourier transform infrared (ATR-FTIR) spectroscopy is a most widely used surface characterization technique and supplies the characteristic absorption bands of functional groups with a depth of 0.1~10 μm. But another technique, X-ray photoelectron spectroscopy (XPS), is more surface-sensitive, which provides the amount and state of elements presented in the surface layer with a depth of about 10 nm. In addition, it is worth noting that the analysis depth may be different or changeable even for a certain kind of characterization technique, which is very useful in analyzing a chemically gradient surface. As we know, the analysis depth for XPS changes with the take-off angle while that

of ATR-FTIR varies a lot with the wavelength, incident angle, etc. In conclusion, it is extremely important to choose a suitable technique for the surface characterization. The analysis depth profiles of some typical techniques are shown in Fig.2.1.
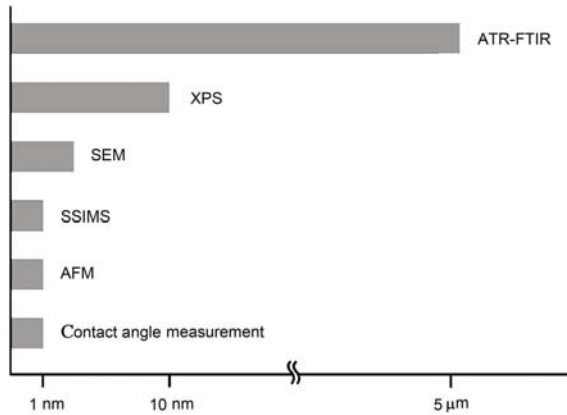
Fig. 2.1. Estimated analysis depth profiles of some characterization techniques

2.1.3 Is it Really the Surface?

If you want to observe a polymer surface (a polymer membrane surface is of course included), it does not seem to be such a very easy matter. Maybe the surface works like magic. That is because solid polymers have non-equilibrium structures with chains rotating and repeating and exhibit a range of relaxations and transitions in response to time, temperature and other environmental changes. Surface reconstruction of polymers has been reported extensively from both theoretical and experimental points of view (Chen and McCarthy, 1999). In general, reconstruction tends to concentrate at the surface of the component that is the most similar to the phase above it. As we know, some membrane processes, such as wastewater treatment, ultrapure water production, hemodialysis and seawater desalinization, are performed in an aqueous environment. Meanwhile, in most cases, additives are used for membrane preparation to modulate the structure or enhance the performance. These additives, including some kinds of water-soluble polymers, are often highly hydrophilic. They will be enriched at the membrane surface in an aqueous environment. However, under vacuum or in the atmosphere they may bury into the membrane bulk and be replaced by other components with a low surface energy. As a result, the possible changes induced by the environments should be considered before the analysis of a membrane surface. The reconstruction of a polymer surface is illustrated in Fig.2.2.
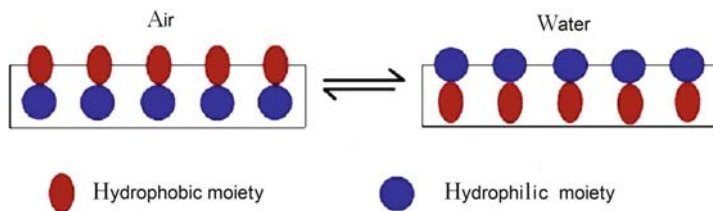
Fig. 2.2. Illustrated reconstruction of polymers under different environments

2.1.4 Invasive or Non-invasive

Although a membrane surface is at the forefront of interacting with its surroundings and the surface influences many crucially important properties of the membrane, up to now observation of the surface in a simple, direct, *in situ* and high-resolution way, presenting a real world of atoms or molecules at the outermost surface layer, is still challenging. Mainly because reconstruction of a membrane surface can take place, techniques that provide *in situ* real-time monitoring of the membrane surface during membrane processes are attractive. Methods requiring a high vacuum, such as scanning electron microscopy (SEM), are generally invasive while most optical techniques are non-invasive (Chen et al., 2004). These non-invasive techniques can be used to monitor the changes of the surface state, such as the adsorption of protein or the formation of membrane fouling. Unfortunately, the optical techniques are mostly of low resolution and other special conditions such as transparent membranes are required. Phase contrast X-ray micro-imaging with synchrotron radiation has been shown to be a powerful tool for non-invasive observation of phenomena occurring in membrane filtration processes (Yeo et al., 2005). This technique is able to observe the deposition of particles inside the lumen of a hollow fiber membrane and also detect deposition and fouling within the membrane structure. This means that the inside surface of a membrane may be observed *in situ*. Besides, the resolution of this technique is of the order of 1 μm, which is superior to other available non-invasive techniques. More and more techniques are becoming available for *in situ* real-time observation. Therefore, the real world and original appearance of the membrane surface will be progressively approached.

2.2 Chemical Composition of Membrane Surfaces

In most cases, analysis of the chemical composition of the membrane surface is necessary. For example, we want to know the chemical changes of the surface before and after surface modification. We also want to know what kind of foulants is adhered to the membrane surface. As a result, the following important questions should at least be answered:

(1) Which elements are present at the membrane surface?

(2) What chemical states of these elements are present?

(3) How much of each chemical state of each element is present?

(4) What is the spatial distribution (especially for different depth profiles) of each element in the membrane?

Many kinds of techniques have been applied to characterize the membrane surface. Various types of probe beams (i.e. photons, electrons, ions), analysis beams, sampling depths, detection limits, special resolution, and chemical information are involved. Here we will focus on the principles and applications of some typical methods applied to membrane chemistry characterization, including ATR-FTIR, XPS, static secondary ion mass spectrometry (SSIMS) and energy dispersive X-ray spectroscopy (EDS).

2.2.1 Attenuated Total Reflectance Fourier Transform Infrared (ATR-FTIR) Spectroscopy

FTIR spectroscopy is based on the interaction of infrared (IR) radiation with a material, in which molecular vibrations are analyzed. Imagine atoms as masses joined by bonds with spring-like properties. Some atoms have a large mass, and others have a small mass; some bonds are stiff, and others are easily deformed. When molecules are exposed to infrared (IR) light, radiation at frequencies matching the fundamental modes of vibration is absorbed, with the additional restriction that absorption occurs only for those vibrations that induce oscillating dipoles perpendicular to the surface. FTIR spectra show peaks corresponding to the frequencies at which radiation is absorbed. Because groups of atoms have unique fundamental modes of vibration, the peaks in a FTIR spectrum represent specific chemical bonds and chemical functional groups; each spectrum is a "fingerprint" for that material (Bellamy, 1974; Dee et al., 2002).

The IR technique has had a long and successful history in surface or near-surface chemical composition characterization, which includes ATR-FTIR spectroscopy, diffuse reflectance spectroscopy (DRS), etc. Among them, ATR-FTIR spectroscopy has been successfully applied in membrane surface analysis, which includes the characterization of chemical composition, physical structure as well as protein adsorption (Chan and Chen, 2004). This technique is performed by using IR spectrophotometers configured with a standard ATR accessory. For analysis a sample is pressed against an internal reflection element (IRE) which is a high refractive index material, maybe a block of zinc selenide (Fig.2.3). Total internal reflection can occur at the interface between media with different refractive indices. If the angle of incidence exceeds a critical value, radiation cannot pass into the medium with the lower refractive index; instead, it is totally reflected. In an internal reflection measurement, IR radiation covering a certain frequency range (corresponding to wavenumbers in the IR spectrum, e.g., between 4000 and 400 cm^{-1}) is focused onto the end of the IRE where the beam undergoes total internal

reflection before exiting and arriving at a detector. At each internal reflection the IR beam penetrates a short distance from the surface of the IRE into the sample, forming an evanescent wave at the interface. ATR-FTIR analysis is thus based on the interaction between the evanescent wave and the contacted membrane. The band positions and shapes are slightly different from those in transmission spectra, but not enough to affect qualitative identification.
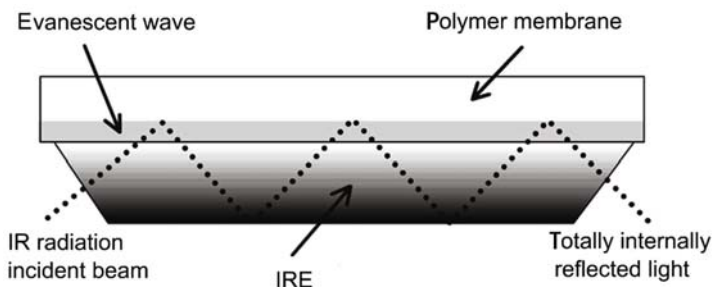
Fig. 2.3. Diagram illustrating ATR-FTIR

The penetration depth, d_p, of the light into the lower refractive index material for ATR-FTIR measurement is defined as the depth at which the field amplitude has fallen to $1/e$ of its value at the surface. For two materials, with refractive indices n_1 and n_2, it is given by:

$$d_p = \lambda_1/[2\pi(\sin^2\theta - n_{21}^2)^{1/2}], \tag{2.1}$$

where θ is the incident angle of light on the surface of the element, λ_1 is the wavelength in the higher refractive index material (i.e. IRE) and is related to the incident wavelength λ by the expression $\lambda_1 = \lambda/n_1$.

The intensity of an ATR-FTIR spectrum depends on the distance that the evanescent wave extends into the sample and on the number of reflections. The higher refractive index of IRE reduces this distance, giving a smaller penetration depth and then a weaker spectrum. The depth of penetration is proportional to the wavelength, so that when ATR-FTIR spectra are compared with transmission the intensities at longer wavelengths appear enhanced. For example, if θ is 45° while refractive indices of the polymer membrane and ZnSe element are 1.50 and 2.4, respectively, at a wavenumber of 2243 cm^{-1} (typically for cyano group) $d_{p,2243}$ is $\sim$0.89 μm and at a wavenumber of 1666 cm^{-1} (e.g. for carbonyl group) $d_{p,1666}$ is $\sim$1.20 μm.

Although ATR-FTIR measurements are very conveniently compared with other techniques, there is the problem of ensuring good optical contact between the sample and the IRE when measuring a solid stiff membrane. The accessories have devices that clamp the sample to the IRE surface and apply pressure. This works well with elastomers and other deformable materials,

and also with most polymer membranes. But some other solids give very weak spectra because the contact is confined to small areas. The poor contact is greatest at shorter wavelengths where the penetration depth is lowest. Therefore, new accessories with very small IRE, typically about 2 mm across, have been developed to overcome the problem of contact (Lindon et al., 2000).

ATR-FTIR spectroscopy can be used to characterize a polymer membrane and to monitor the modification and fouling of the membrane. Belfer et al.(2000) modified polyethersulfone ultrafiltration membranes by radical grafting and characterized the unmodified, modified and protein fouled membrane surfaces. The results indicated that the chemical changes on the modified membrane surfaces could be well characterized by ATR-FTIR spectroscopy. In addition, it was also shown that the ATR-FTIR technique enables the recognition of albumin absorption on the membrane surfaces. To determine the orientation of adsorbed albumin, the incident beam was polarized in the p-direction (perpendicular to the plane of incidence) or the s-parallel direction. Furthermore, spectral techniques such as subtracting and Fourier self-deconvolution could be applied to recognize the conformation of albumin absorbed on the membrane surface, by analysing the overlapping peaks comprising the broad amide I band.

Besides traditional spectral techniques, new equipment and theory are being developed. Recently, high-resolution FTIR spectroscopy has been commercialized in which an actual spectral resolving capability of better than 0.09 cm^{-1} for the natural separation of two identical lines is achieved. Rapid-scan based on continuous-scan mode allows the study of reactions or processes as fast as 13 ms (or 77 spectra/s) at a spectral resolution of 16 cm^{-1} (Jiang, 2003). This rapid-scan is favorable for collecting time-resolved spectra of small molecules diffusion, protein adsorption, etc. Two-dimensional infrared (2D IR) has been proposed in 1989 by Noda (1989; 1990), which is a spectro-mathematical tool that correlates spectra synchronously and asynchronously in a third dimension defined by a physical parameter in a dynamic system under study. This novel method is able to probe the specific order of certain events taking place with the development of a controlling physical variable. Using 2D correlation analysis on ATR-FTIR spectra, absorption behavior of small molecules such as water and the state of water molecules in the membrane can all be studied. As an example, the time-resolved ATR-FTIR spectra for the processes of absorption/desorbing of water molecules into/from the polymeric membrane and their corresponding 2D correlation spectra are shown in Fig.2.4 (Wan et al., 2007).

2.2.2 X-ray Photoelectron Spectroscopy (XPS)

Properly speaking, ATR-FTIR spectroscopy is not a surface-sensitive technique because its penetration depth is at the level of a micron. XPS, or electron spectroscopy for chemical analysis (ESCA), is a more surface-sensitive
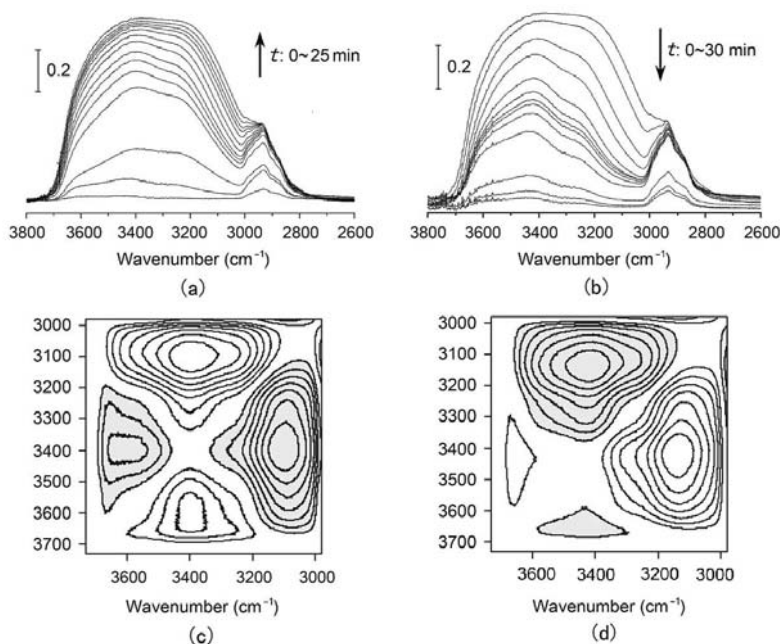
Fig. 2.4. Temporal changes of ATR-FTIR spectra in the range of 3800–2800 cm^{-1} wavenumbers during the water-absorbing (a) and water-desorbing (b) processes of PANCNVP membrane. 2D IR spectra (c) and (d) were obtained from (a) and (b), respectively. Reprinted with permission from (Wan et al., 2007). Copyright (2007) American Chemical Society

analytical method, which is also one of the most popular spectroscopic methods for surface chemical analysis of polymers. It provides qualitative and quantitative information on the atomic composition down to a depth of typically 0.5∼10 nm depending on the take-off angle. The spatial resolution possible with various commercially available XPS spectrometers is about 10 µm (Adamsons, 2000). This kind of technique supplies information not only about the type and amount of elements present but also about their oxidation state and chemical surroundings.

XPS is a technique based on a photo-electronic effect (Fig.2.5). Under X-ray (photon) exposure, photoelectrons are emitted with energy values characteristic of the elements present at the surface. The energy of the emitted photoelectrons is then analysed by the electron spectrometer and the data presented as a graph of intensity versus electron energy. The kinetic energy (E_K) of the electron is the experimental quantity measured by the spectrometer, but this is dependent on the photon energy of the X-rays employed and is therefore not an intrinsic material property. The binding energy of the electron (E_B) is the parameter which identifies the electron specifically, both in terms of its parent element and atomic energy level. The Einstein equation

gives the relationship between photon energy $(h)\nu$, E_K and E_B:

$$E_B = h\nu - E_K - \phi, \tag{2.2}$$

where ϕ is the work function of the analyzer detector. As all three quantities on the right-hand side of the equation are known or measurable, it is a simple matter to calculate the binding energy of the electron. In practice, this task will be performed by the control electronics or data system associated with the spectrometer and the operator merely selects a binding or kinetic energy scale to confirm which is the more appropriate (Watts and Wolstenholme, 2003).
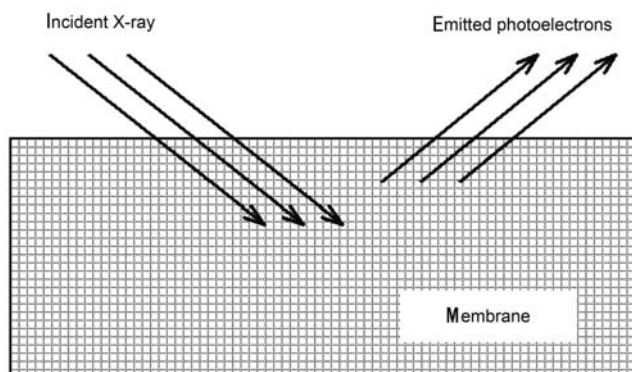
Fig. 2.5. Schematic illustration of the principle of XPS

When an electron is ejected from an atom, the binding energy will be recorded. Thus the photoelectron spectrum will reproduce the electronic structure of an element quite accurately since all electrons with a binding energy less than the photon energy will feature in the spectrum. Those electrons which are excited and escape without energy loss contribute to the characteristic peaks in the spectrum; those which undergo inelastic scattering and suffer energy loss contribute to the background of the spectrum.

A block diagram of a typical XPS experimental arrangement is shown in Fig.2.6. The various modules necessary for analysis by XPS are: a source of the primary beam; sample inlet system; an electron energy analyser and detection system, all contained within a vacuum chamber; a data system which is nowadays an integral part of the system. Energetic X-ray photons, commonly in the range of 1000∼2000 eV, are used as source for core electron ionizations. The source should be monochromatic and of high photo intensity. There are many metals which can be used as anodes to generate irradiation. However, in most cases Mg or Al is used due to their narrow line width; their energy/line width is 1253.6 eV/0.7 eV and 1486.6 eV/0.85 eV, respectively.
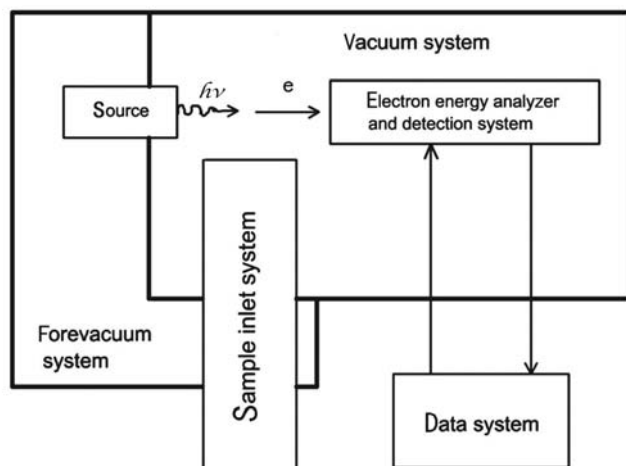
Fig. 2.6. Block diagram of a typical XPS experimental arrangement

The depth of analysis in XPS varies with the kinetic energy of the electrons under consideration. It is determined by a quantity known as the attenuation length (λ) of the electrons, which is related to the inelastic mean free path. The intensity of electrons (I) emitted from all depths greater than d in a direction normal to the surface is given by the Beer-Lambert relationship:

$$I = I_0 \exp(-d/\lambda), \tag{2.3}$$

where I_0 is the intensity from an infinitely thick, uniform substrate. For electrons emitted at an angle θ to the surface normal, this expression becomes:

$$I = I_0 \exp(-d/(\lambda \cos \theta)). \tag{2.4}$$

Eqs.(2.3) and (2.4) show that by considering electrons that emerge at 90° to the sample surface, some 65% of the signal in electron spectroscopy will emanate from a depth of less than λ, 85% from a depth of less than 2λ, and 95% from a depth of less than 3λ (Watts and Wolstenholme, 2003). In general, the depth for collecting 95% of information, 3λ, is defined as the depth of XPS analysis. A typical depth list of XPS analysis under various conditions is shown in Table 2.1 (Briggs, 1998).

As shown in Table 2.1, if electrons are detected at some angle to the normal of the sample surface, the information depth is reduced by an amount equal to the cosine of the angle between the surface normal and the analysis direction (see Eq.(2.4)). This is the basis for a powerful analysis technique, angle-resolved XPS. One of the reasons for the usefulness of the method is that it can be applied to membranes on which an ultrathin coating or grafting layer exists. Another reason for using angle-resolved XPS is that it

Table 2.1. Depth list of XPS analysis under various conditions

Core shell	Binding energy (eV)	Analysis depth (95% information, nm)					
		Mg Kα			Al Kα		
		10°	45°	90°	10°	45°	90°
F 1s	686	0.8	3.4	4.8	1.1	4.5	6.3
O 1s	531	1.0	4.1	5.8	1.3	5.2	7.3
N 1s	402	1.1	4.7	6.6	1.4	5.7	8.0
C 1s	287	1.3	5.2	7.3	1.5	6.2	8.7
Si 2p	102	1.5	5.9	8.4	1.7	6.9	9.7

is a non-destructive technique which can provide chemical state information. The analysis of a surface layer with gradient chemical composition by angle-resolved XPS is illustrated in Fig.2.7.
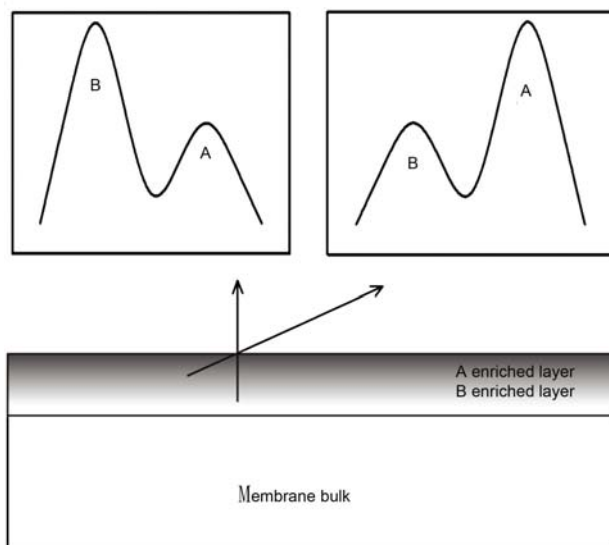
Fig. 2.7. Illustration of angle-resolved XPS measurement. Components A and B are enriched at the outermost surface layer and the near surface layer, respectively

XPS can be used for both qualitative and quantitative analyses as mentioned above. The first step to be taken in characterizing the surface chem-

istry of the membrane under investigation is the identification of the elements present. To achieve this goal it is usual to record a survey, or wide scan, spectrum over a region (generally 0∼1000 eV) that will provide fairly strong peaks for all elements in the periodic table except for hydrogen and helium. The survey spectrum in XPS will generally be followed by the acquisition of spectra around the elemental peaks of interest. As the spectrum contains valuable chemical state information these regions will be recorded at a higher resolution. Thus a high-quality core level spectrum can be obtained. Furthermore, for a specific element in the core level spectrum, small changes in electron energy as a result of the chemical environment of the emitting atom can also be observed. They can be distinguished generally by peak fitting. By converting peak intensities (peak areas) to atomic concentrations, the spectrum from XPS can be quantified. But it should be pointed out that there are many factors which must be considered when attempting to quantify the XPS spectrum.

Although XPS is surely a powerful technique for surface chemistry analysis, the samples must be stable within the ultrahigh vacuum chamber of the spectrometer. Very porous materials such as a membrane with high porosity may pose problems as well as those having a solvent residue. Besides, when peak fitting is performed, one should be careful to prevent arbitrary fitting.

2.2.3 Static Secondary Ion Mass Spectrometry (SSIMS)

Mass spectrometry of polymers and polymeric surfaces represents a very broad field of active research (Hanton, 2001). Several mass spectrometric techniques have been developed to analyze surfaces among which SIMS is by far the dominant method. In SIMS, samples are bombarded by a beam of positive ions (frequently argon ions). The primary ions penetrate the surface and transfer energy through a collision cascade, with the emission of a variety of types of secondary particle, including secondary electrons, Auger electrons, photons, neutrals, excited neutrals, positive secondary ions and negative secondary ions (Fig.2.8). SIMS is concerned with the last two of these, positive and negative secondary ions. These secondary ions are analyzed with a mass spectrometer, which allows identification of all elements as well as their isotopes. The spectra of both positive and negative secondary ions are collected to reflect the composition of the material.

The instrumentation for SSIMS can be divided into parts (Bubert and Jenett, 2002): (a) vacuum system; (b) sample inlet system; (c) the primary ion source in which the primary ions are generated, transported and focused towards the sample; (d) the mass analyzer in which sputtered secondary ions are extracted, mass separated and detected; and (e) data process system.

Several ion sources are particularly suited for SSIMS. The first produces positive noble gas ions (usually argon) either by electron impact or in plasma created by a discharge. The ions are then extracted from the source region, accelerated to the chosen energy, and focused in an electrostatic ion-optical
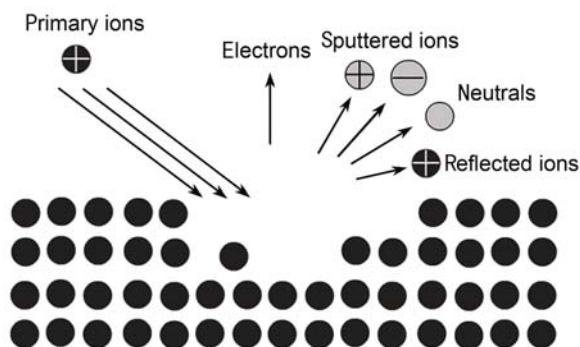
Fig. 2.8. Effects of positive ions on polymer surface

column. According to the difference of the primary ion current density, SIMS can be conducted in two modes. In static SIMS (SSIMS, the ion density is less than 10^{12} ions/cm^2), surface sensitivity is ensured by maintaining the ion beam at low intensity. Ideally, each ion impacting the surface will hit areas previously undisturbed. The outermost one to two atomic layers (0.5∼1 nm) can be characterized with SSIMS. In dynamics SIMS, bombardment with high intensity primary ions causes emission of secondary ions from continuously increasing depth into the material so that in-depth concentration profiles can be measured. Therefore, SSIMS is a more surface-specific technique.

To minimize surface damage, SSIMS should be as efficient as possible to detect the total yield of secondary ions from a surface. So the mass analyzer is very important. In early work, a quadrupole mass spectrometer has been used for many years in which a continuous ions beam is adopted. The combination of a pulsed ion source with a time-of-flight (TOF) mass analyzer results in a powerful analytical tool characterized by high sensitivity, high-mass resolution, and high surface specificity. This technique is commonly referred to as TOF-SIMS. In a TOF mass analyzer, all sputtered ions are accelerated to a given potential voltage (2∼8 keV), so all ions have the same kinetic energy. The ions are then allowed to drift through a field-free drift path of a given length before striking the detector. Light ions travel the fixed distance through the flight tube more rapidly than identically charged heavy ions. Thus, measurement of the time taken of ions with mass-to-charge ratio provides a simple means of mass analysis. Because a very well defined start time is required for flight time measurement, the primary ion gun must be operated in a pulsed mode to enable delivery of discrete primary ion packages (Bubert and Jenett, 2002).

Just like any other mass spectrum, an SSIMS spectrum consists of a series of peaks of different intensity (i.e. ion current) occurring at certain mass numbers. The relationship between the peaks in an SSIMS spectrum and the surface chemistry is not as straightforward as in XPS or other methods. On

the other hand, many of the more prominent secondary ions from metal or semiconductor surfaces are singly charged atomic ions, which makes allocation of mass numbers slightly easier. However, in the case of polymer membrane surface analysis, it is more complicated. Because of the large number of molecular ions that occur in any SSIMS spectrum from a polymer surface, much chemical information is obviously available in SSIMS. But this means that detailed insight into molecular composition can also be provided by SSIMS spectra, except for evidence of the elements present.

In some cases, the clusters observed are definitely characteristic of the material (Bletsos et al., 1986). The SSIMS spectrum from polystyrene measured in a TOFMS contains peaks spaced at regular 104-mass-unit intervals, corresponding to the polymeric repeat unit. Flosch et al. (1992) characterized the modifications at the surface of poly (vinylidene difluoride) membranes by XPS and SIMS. Significant differences in the surface chemistry were observed between the two membranes, i.e. those with hydrophilic and hydrophobic surfaces. Another mass spectroscopy, matrix-assisted laser desorption ionization mass spectrometry (MALDI-MS) is very useful in analysis of a protein-fouled membrane surface, as reviewed by Chan and Chen (2004).

As with XPS, SSIMS is typically run under ultrahigh vacuum, which makes it almost impossible to observe the membrane surface *in situ*. Besides, ions can be detected as arising either from the substrate material itself, from the introduced molecules or other species on the surface, or from contaminations and impurities on the surface. The interpretation of the spectra is also difficult. However, SSIMS has the benefits of full elemental coverage and great surface sensitivity and is a powerful technique for membrane surface characterization. A comparison of XPS and SSIMS is shown in Table 2.2.

Table 2.2. Comparison of XPS and SSIMS

	XPS	SSIMS
Qualitative analysis	Elements except hydrogen	All elements
Quantitative analysis	Yes	No
Sensitivity	0.2% atoms	10^{-6}
Information	Chemical groups	Molecular level
Depth	Variable, 1∼10 nm	Changeless, 0.5∼1 nm
Spatial resolution	∼50 μm	∼50 μm

2.2.4 Energy Dispersive X-ray Spectroscopy (EDS)

Energy dispersive X-ray spectroscopy (EDS) is a chemical microanalysis technique, which is often applied in combination with a scanning electron microscope (SEM). As we know, when a beam of high energy electrons is focused on a specimen, the electrons are absorbed or scattered by the specimen, and secondary electrons, Auger electrons, characteristic X-rays and backscattered electrons are emitted from the sample during bombardment (Fig.2.9). For an

SEM, images are constructed from the emitted secondary electrons; while the EDS technique utilizes the characteristic X-rays.
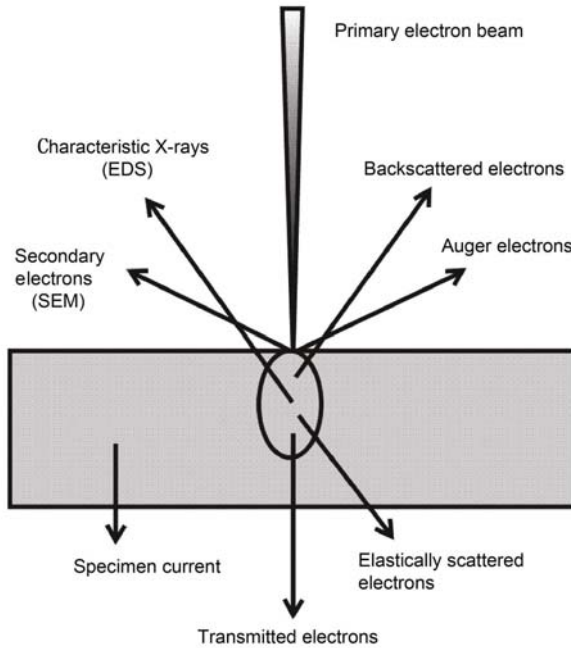
Fig. 2.9. The interactions of beam electrons and sample atoms generating a variety of signals

At rest, an atom within the sample contains ground state (unexcited) electrons situated in concentric shells around the nucleus. The incident electron beam, however, excites an electron in an inner shell, prompting its ejection and results in the formation of an electron hole within the atom's electronic structure. An electron from an outer, higher-energy shell then fills the hole, and the excess energy of that electron is released in the form of an X-ray. The release of X-rays creates spectral lines that are highly specific to individual elements; thus, the X-ray emission data can be analyzed to characterize the sample in question.

In EDS spectra the X-ray intensity is usually plotted against energy. They consist of several approximately Gaussian-shaped peaks being characteristic of the elements present. Most of the chemical elements can be identified by EDS. The only limit is whether the particular type of detector window registers soft X-ray of the light elements (Bubert and Jenett, 2002). The following analytical information can be provided by EDS:

(1) Qualitative analysis: Elements with atomic numbers from that of beryllium to uranium can be detected. The minimum detection limits vary from about 0.1 weight percent to a few percent depending on the element and matrix. Fig.2.10 gives an example of an EDS spectrum, which was collected from a polypropylene microporous membrane surface. Surface initiated atom transfer radical polymerization (ATRP) was performed on the membrane surface by introducing surface-immobilized bromide. As shown in Fig.2.10, peaks of bromine including BrK and BrL can be clearly observed.
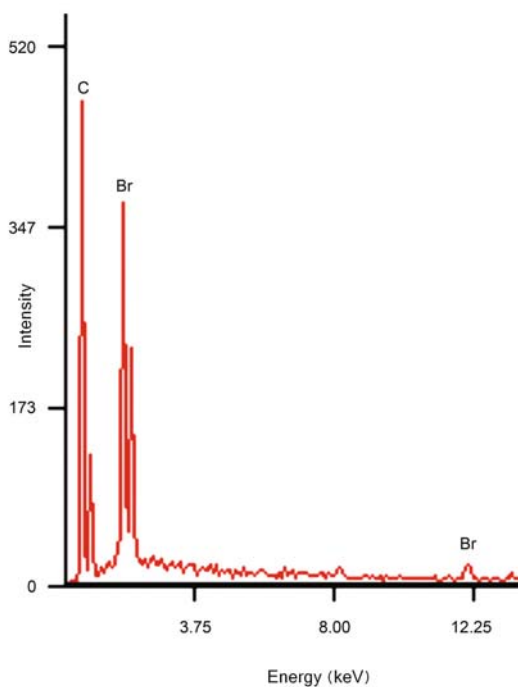
Fig. 2.10. Energy dispersive X-ray spectrum of a polypropylene membrane grafted with bromide

(2) Quantitative analysis: Quantitative results are readily obtained without standards. The accuracy of standardless quantitative analysis is highly sample dependent. Greater accuracy is obtained using known standards with similar structure and composition as those of the unknown sample.

(3) Line profile analysis: The electron beam is scanned along a preselected line aided by an SEM image across the sample while X-rays are detected for discrete positions along the line. Analysis of the X-ray energy spectrum at each position provides plots of the relative elemental concentration for

each element versus position along the line. This technique is very useful in analyzing the distribution of elements on the surface or at the cross-section of a membrane (de los Rios et al., 2007).

(4) Elemental mapping: Characteristic X-ray intensity is measured relative to lateral position on the sample surface. Variations in X-ray intensity then indicate the relative elemental concentrations across the surface. Maps are recorded using image brightness intensity as a direct function of the local concentration of the elements present. Lateral resolution of about 1 μm is possible.

2.3 Morphologies and Microstructures of Membrane Surfaces

2.3.1 Surface Morphology of Membrane

For polymeric materials the term morphology can be defined as the form and organization of a size scale above the atomic arrangement but smaller than the size and shape of the specimen. Microstructure is a concept slightly different from morphology, with more emphasis on local atomic and molecular details. But in most cases they are interchangeable. Here these two terms are used together to represent the surface state of the membranes. Content of morphology and microstructures of polymeric materials include the surface topography, the crystallization, the microphase separation for multiphase polymers, the size, shape and distribution of fillers for composite polymers, etc. (Sawyer and Grubb, 1987). For membranes the first important aspect of morphology and microstructure is the size, shape, quantity of pores (if they are visible), which play important roles in the performance of the membrane.

To study the surface morphology and microstructure of a polymer membrane, various characterization techniques are available, such as X-ray diffraction, neutron scattering and microscopy technology. Of all these technologies, microscopy offers the most convenient and powerful methods. The history of microscopes can be traced back to as early as 400 years ago. Modern microscopy technology has supplied us with a huge family of microscopes with different resolving power from which a suitable one can be chosen according to practical requirements.

2.3.2 Introduction to Microscopy

Microscopy is a technique to visualize fine structures of the object with a microscope. Janssen and his son, Zacharias, are often considered to be the first to have invented the compound optical microscope in 1595. From then on, scientists have done their best to build new types of microscopes with better resolving power employing the most advanced technology of the age. In 1933, Ruska invented the first electronic microscope. In 1981 Binnig and

Rohrer built the first scanning tunneling microscope. Together with the help of the electronic microscope and scanning tunneling microscope, scientists are now able to make observations of the atomic world. Modern microscopes can be divided into three categories: optical microscopes, electronic microscopes, and scanning probing microscopes (SPM). Optical microscopes can reach a resolution of several hundreds of nanometers. Typical electron microscopes can resolve to several nanometers. And certain types of SPM such as STM and AFM can have an atomic scale resolution. The investigative environment should usually be a high vacuum for the electron microscope, but SPM and optical microscopes do not have such a restriction. Generally speaking, to choose a suitable type of microscope, factors needing consideration include the resolution requirement, the sample components, the method of preparation, the information to investigate, etc. In most cases many types are employed together to study one specimen from different perspectives.

2.3.3 Basic Conceptions in Microscopy

Resolution and contrast. Resolution is defined as the minimum distance between two object features when they can still be distinguished from each other, while contrast is the fractional change in image brightness caused by the object feature. Resolution and contrast are two basic parameters of the microscope system which add up to determine the investigation power of the microscope. To discern two features on the object, there are two preconditions to be fulfilled. Firstly the contrast must be high enough (the typical value is 0.05) to make the two features visible from the environment background signals. Secondly, the distance between the two features must be within the resolving limitation so that they can be discerned one from the other.

Depth of field and field of view. Depth of field is the thickness of the specimen that appears simultaneously in the microscopy image. And field of view is the area of the specimen included in the imaging domain. These two parameters determine the convenience for the user and the amount of information contained in the image. Images with a larger depth of field will be able to reveal the three-dimensional information of the specimen.

Bright field and dark field. Bright field and dark field are two different modes of imaging. Bright field images have a bright background while features of the specimen are shown as dark areas. Bright field is the common mode when imaging with a microscope. But if the contrast of the feature is low, or the size is tiny, it will be hard to discern it from the background because of the interference of the strong background signal. Dark field technology can solve this problem. A dark field image is almost the negative type of the bright field image. Features show up as bright areas while the background is full of darkness.

Resolving ability limitation by diffraction. Under certain circumstances, a lens has the ability to form an image of a spot light source on the other side of the lens. However, since light is a form of electromagnetic wave, the

wave-like behavior of the light will make the image into a small round plate composed of a bright spot at the center and less intensive light and dark holes around it. This spot is named "Airy disk", as illustrated by Fig.2.11(a). The radius of the Airy disk (r_A) is defined as the radius of the first minimum of the intensity distribution from the center, as Fig.2.11(b). The value is $1.22F\lambda/d$, where F is the focal length, λ is the wavelength of the light, and d is the diameter of the lens. According to calculation, in the center peak of the intensity distribution, about 84% of light energy is contained.
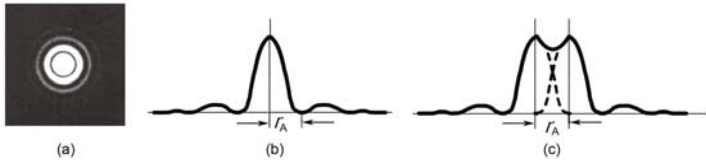
Fig. 2.11. Airy disk and Rayleigh criterion. (a) Image of Airy disk; (b) Intensity distribution of Airy disk; (c) Rayleigh criterion

To discern two different spot light sources, their images have to be far enough. According to Lord Rayleigh, the limitation will be reached when the intensity maximum of the first Airy disk falls into the intensity minimum of the second one. That is to say, the two points are discernable only when the distance between their images is no less than $1.22F\lambda/d$. This criterion is named after Rayleigh as "Rayleigh criterion", as shown in Fig.2.11(c).

At the limitation state, the minimum light intensity between the two Airy disks is about 20 % lower than that at the center of the Airy disk. And 20 % of light intensity difference is commonly assumed to be the minimum difference for human eyes to recognize. Thus the Rayleigh criterion is reasonable.

In 1873, the German optician Abbe published a theory in which he stated that the minimum resolvable distance of a certain microscope system can be expressed as $d_0 = 0.61\lambda/(n\sin\alpha)$, where λ is the wave length of the illuminant, α is the half angle of incident rays to the top lens of the objective and n is the refractive index in the space between the object and the objective lens. The expression $n\sin\alpha$ is defined as "Numerical Aperture (NA)", and is an important parameter of the object lens. For a system taking air as the environment of the object and the objective lens, the value of d_0 is 0.6λ. Even for an oil immersion system, the minimum resolvable distance is no less than 0.5λ. Therefore we can see that the wavelength of the light plays an important role in deciding the final limitation of the resolving distance of a microscope system. If we use white light as a light source, the limitation is about 0.3 μm, and for ultraviolet and quartz lens this value turns out to be about 0.15 μm. Obviously this is not enough for characterization of a membrane surface. To see more, we have to use a shorter wavelength. Electron beams will meet the requirement.

2.3.4 Optical Microscopy

2.3.4.1 Imaging Principles

As can be seen from Fig.2.12(a), optical refraction will happen when a light beam goes with a certain incidence angle through the interface of two materials with different refractive indices as follows:

$$\frac{n_1}{n_2} = \frac{\sin \gamma}{\sin \alpha}. \tag{2.5}$$

According to the refraction principle, special shaped lenses with the ability to form virtual or real images of the object are designed and become the basic unit used in an optical microscope system.
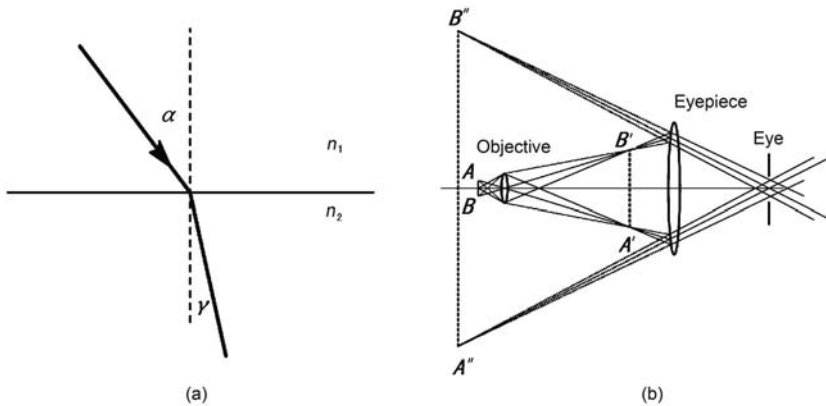
Fig. 2.12. (a) Refraction; (b) Imaging principle of optical microscopes

Optical microscopes can be divided into two types. One is a simple microscope with only one imaging lens. Because such a type of microscope cannot operate at high magnification, it is seldom used in modern research. The second type is a compound microscope with more than one lens for imaging. It can work with high magnification and resolution, revealing more details of the specimen. Typical compound optical microscopes have an objective lens group and an eyepiece with a very complicated structure (Fig.2.12(b)). Light goes through and is refracted by these series of lenses following the rules of geometrical optics, with the image of the object becoming magnified and finally projected into the eyes of the user. The objective lens forms the inverted real image of the object, and the eyepiece is posed at a chosen position so it forms a greatly enlarged virtual image of the object from its real image. This virtual image can be seen by the user's eyes.

A typical configuration of a modern optical microscope includes a magnification unit composed of the objective lens and the eyepiece, a stage to

fix the specimen and an illumination source to supply the light beam. Also a mechanical structure is designed to hold all the above configurations. The magnification ability of the eyepiece and objective lens decides the magnification ability of the microscope. A common optical microscope system can show fine details of the specimen at a range of $2\times \sim 2000\times$ magnifications, according to different situations. The simplest type of illumination source is just a mirror to reflect the daylight. But an advanced optical microscope system often uses a man-made controllable light source. The type of light beam ranges from infrared to ultraviolet. The shorter the light's wavelength, the higher the resolution limitation will be, although for a light source other than visible light, special detectors are needed. To manage the quality and intensity of the light, diaphragms and filters are required too. Usually the light is transmitted through the specimen to form the image, but a reflecting mode is also available by alternation of the system.

2.3.4.2 Applications and Advantages

Compared with the electron microscope and scanning probing microscope, the optical microscope is really an old type. But due to the simple operation, the comprehensively understood principle, the easy sample preparation and the low cost, this technology is still useful for the characterization of the membrane. Optical microscope characterization is often taken as the first step in microscopy observations to supply a low-resolution overview. It is also a convenient strategy using an optical microscope to characterize the surface layer of a membrane by indirectly observing its cross-section. Furthermore, because of the features of an optical microscope, it is possible to connect it to a digital camera to do online investigation of the membrane preparation process, the fouling process and the filtration mechanism. The recent development of such technology includes DOTM (direct observation through membrane) and DVO (direct visual observation) systems to monitor surface deposition during filtration (Chen et al., 2004).

In recent years many advanced types of optical microscopes have been developed to fulfill special requirements, which have greatly enlarged the application area of optical microscopes. They include the following types. (1) Stereo optical microscopes, which supply images of views from slightly different directions through the two eyepieces. This enables the user to form a 3D image with his eyes. (2) Phase contrast microscopes, which transfer the alternation of phase into intensity of the light so that the human eye can feel. (3) Interference microscopes and differential interference microscopes, which use the interference of the light to form images. (4) Polarizing microscopes, which employ the polarized light as a detector to investigate a specimen with anisotropy, such as crystallized polymers or liquid crystals. (5) Fluorescent microscopes, which are used to investigate the fluorescent samples. (6) Laser confocal scanning microscopes. This is a new type of optical microscope which

is especially useful for investigation of the membrane surface, and in the following segments we will introduce it in detail.

2.3.5 Laser Confocal Scanning Microscopy (LCSM)

2.3.5.1 Principles of Fluorescence

A laser confocal scanning microscope (LCSM) can work in fluorescence mode or reflecting mode. Certain kinds of materials emit fluorescence when exposed to external light. The wavelength of fluorescence is usually longer than that of the exciting light. The difference between the wavelength of the emitted light and the exciting light is named as Stokes shift and this is summarized as Stokes law. The time delay between the exciting and the emitting behaviors is one millionth of a second or smaller. Light emitted beyond this time delay belongs to phosphorescence.

Principles of fluorescence can be expressed by the Jablonski diagram as in Fig.2.13 which was first conceived by Jablonski in the 1930's. S_0 represents the basic unexcited energy level of the atom, also referred to as the ground state. There are two types of excited energy state: one is called the excited singlet state denoted as S_n, and the other type is called the triplet state, represented by T_n. Excitation from the ground state S_0 to a excited singlet state of S_n does not change the spin state of the electron, while excitation of a triplet state T_n will involve a change of spin state, which is called forbidden transition in quantum theory, meaning that there is a low possibility of such a transition. So the molecule is mainly excited to singlet states by the external photons.
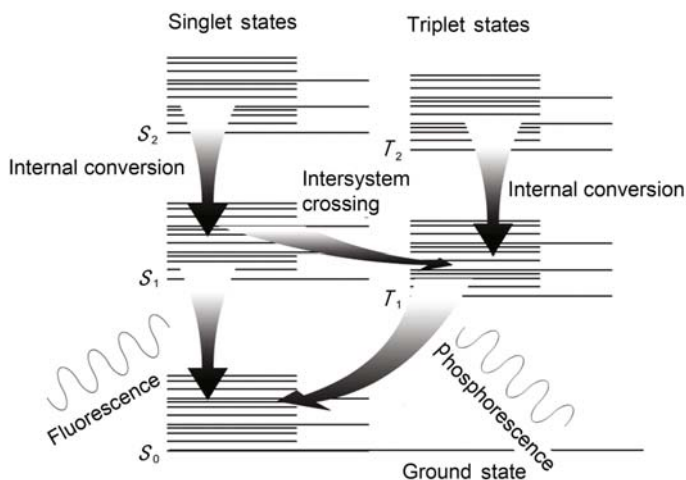
Fig. 2.13. Principles of fluorescence

The excited state is not a stable state of a molecule, and the excited molecule tends to return to the ground state by losing the excess energy. These energy loss transitions can be divided into two categories, radiationless transitions such as internal conversion, intersystem crossing or vibration conversion, or radiative transitions, including fluorescence or phosphorescence. Internal conversion is the isoenergetic transition from a state with low vibration energy but high electron orbits to a new state with a higher vibration energetic level and low electron orbits. Intersystem crossing is the transition between the excited singlet state and the excited triplet state. Normally such a transition is a "forbidden transition" as referred to previously.

The molecular falls back into the lowest energy level of S_1 and T_1 shortly after the excitation and the following transition from S_1 to S_0 causes the emission of fluorescence, while the transition from T_1 to S_0 generates phosphorescence. Since the energy level of T_1 is lower than S_1, the wavelength of phosphorescence is longer than that of fluorescence. Also, because the transition from T_1 to S_0 is a forbidden transition, the emission of phosphorescence comes later than that of fluorescence.

2.3.5.2 Emission Spectrum and Excitation Spectrum

Emission spectrum. As shown in Fig.2.14, the emission spectrum is the intensity distribution on different wavelengths of the fluorescence when excited by certain excitation light. Theoretically, protons with energy lower than the energy gap between S_0 and S_1 are not able to cause the emission of fluorescence. Once the exciting protons have a wavelength shorter than that limitation, the fluorescence will be observed. In this case, the distribution of the wavelength of the emitted light, i.e. the emission spectrum, is independent of the exciting protons. Also, the direction of the emitted light has no relationship with the exciting light, which makes it possible to observe the fluorescence in the direction the exciting light is coming from.

Excitation spectrum. The excitation spectrum (Fig.2.14) is obtained by recording the fluorescence intensity at the maximum emission of the emission spectra when changing the wavelength of exciting light continually. The excitation spectrum is similar to the UV-vis spectrum but with a higher sensitivity.

2.3.5.3 Confocal Scanning

The resolution of a common optical microscope is restricted by the limitation of the diffraction. By using technology of confocal scanning represented by Minsky in 1955, it is possible to overcome this limitation with an optical microscope system. The objective lens and the collector lens share the same focus just at the specimen. Normally the spacial resolution of the image is confined by the size of the Airy disk. But Minsky introduced a small pinhole
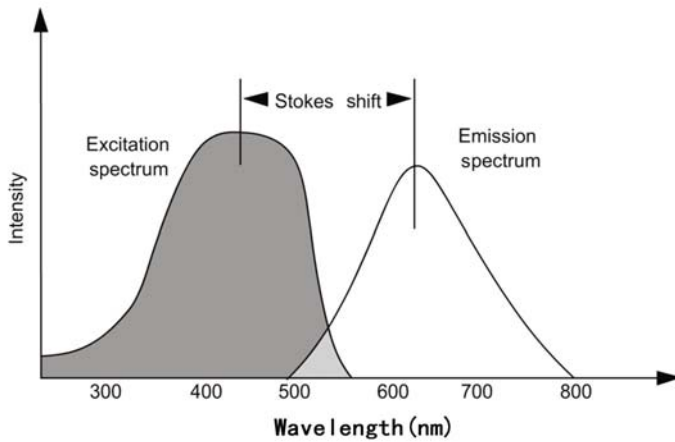
Fig. 2.14. Emission spectrum and excitation spectrum

in front of the detector which allows only the central part of the Airy disk to reach the detector so that higher spacial resolution than that decided by the Airy disk was achieved (Fig.2.15). Because of the special working manner of the confocal optical microscope, in which only one point of the specimen is detected at one time, a scanning system is needed, by which the detecting point rasters through the specimen in both x and y directions, to form finally the full image of the specimen.
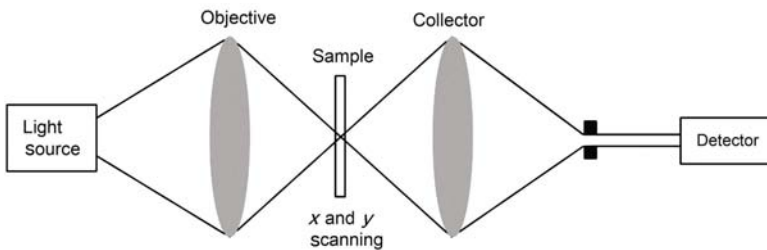
Fig. 2.15. Principle of confocal scanning

2.3.5.4 Basic Configuration of LCSM

As schematically illustrated in Fig.2.16, modern practical LCSM works with reflecting light. The light source is designed to produce a beam of scanning laser from the focus point of the objective lens. The scanning laser is focused by the objective lens onto the specimen which is posed at the focus plane of the objective lens. According to the principle of optics, light reflected (in

reflecting mode) or emitted (in fluorescent mode) from the focus point at the specimen is focused by the objective lens back onto the first focus point again. A diachroic mirror is introduced to move the focusing point of the collected light to another place from the pinhole of the light source. The collected light forms an Airy disk at the new focusing point, where a pinhole is set to allow only the center part of the Airy disk to reach to detector to form the signal of the scanning point on the specimen.
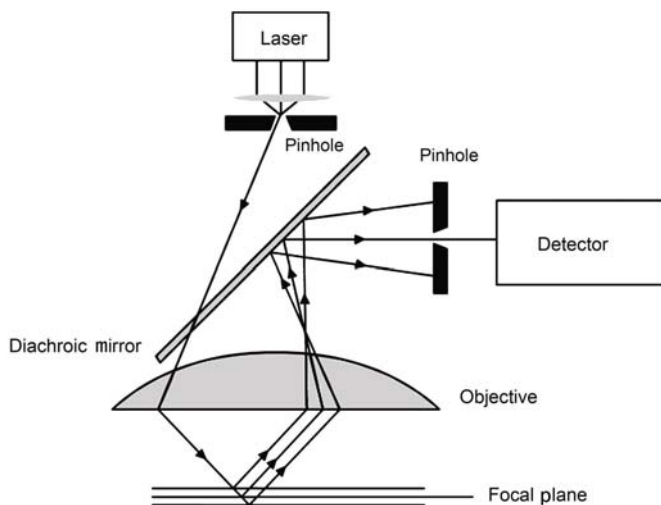
Fig. 2.16. Principle of LCSM

A detecting beam of a modern LCSM laser has several advantages: (1) Accurate point focus can be formed by the objective lens because of low divergence and monochromaticity with a laser beam; (2) One of the problems for the original confocal system is that the intensity of the detecting beam and the imaging signal is low. The application of a laser can solve this problem because the laser beam owns a high energy intensity; (3) The wavelength can be selected precisely with a narrow spectrum width.

Although it can be applied in a reflective mode, applications of LCSM often involve the technology of fluorescent labeling. Special configuration to LCSM for the fluorescent imaging mode is mostly like that of the common fluorescence optical microscope. And to gain an image with good resolution an oil immersion objective lens is needed. Some membrane materials have an inherent fluorescence capacity but in most cases fluorescence has to be induced by physical or chemical treatments. Such treatments include: (1) Treating the sample with specific stains; (2) Chemical binding of the fluorescent groups onto the molecular chain; (3) Binding fluorescent-labeled molecules onto the interested components by specific affinity (Ferrando et al., 2005).

A prominent feature of LCSM is its ability of optical sectioning. Since LCSM images mainly contain the information of the focal plane, a three dimensional structure can be reconstructed from a series of images at different heights. This feature facilitates the study of three dimensional surface topography, the pore structure and structure fouling on the membrane surface.

Recently LCSM is being used more and more for the surface characterization of membranes. These applications include the characterization of membrane surface morphology (Charcosset and Bernengo, 2000; Charcosset et al., 2000), investigation of filtration principles (Hayama et al., 2003), research of protein-membrane interactions (Reichert et al., 2002), etc. Most of these applications employed the ability of three dimensional image reconstruction to investigate the distribution of structure features and external adsorptions in a certain depth.

The limitation of LCSM for characterization of the membrane lies in the resolution confinement. In the best case, LCSM offers a resolution of 180 nm in the focal plane and only 500~800 nm along the optic axis. This is obviously not enough for the characterization of the fine structure of membranes.

2.3.6 Scanning Electron Microscope

2.3.6.1 Introduction to Electron Microscope

Wavelength of Electron Beam. Electrons are particles of a certain mass. Usually the mass of an electron is denoted as m_e, and has a value of 9.109534×10^{-31} kg. Electron beams are a group of electrons moving along in the same direction. According to de Broglie, moving electrons have a dual personality called by wave-particle duality. This means that they also behave as a radiation wave. The relationship of the associated wavelength of the moving electron and its mass and velocity can be expressed as

$$\lambda = h/(mv), \tag{2.6}$$

where m and v are the mass and velocity of the electron respectively and h is Planck's constant whose value is 6.62×10^{-34} J·s. The kinetic energy of a moving electron is

$$V_e = 1/(2mv^2). \tag{2.7}$$

After substituting V_e for v and putting in numerical values for h, m, Eq.(2.7) can be changed to Eq.(2.8)

$$\lambda = \frac{1.23}{\sqrt{V_e}} \tag{2.8}$$

From Eq.(2.8) we can deduce that a 50 keV electron has an associated wavelength of 0.0055 nm. This is rather a small value comparing to that of a visible light.

The wavelength of a moving electron achieved from Eq.(2.8) still works in Ernst Abbe's theory. If we could build a microscope system using an electron beam as the working illumination, and supposing that NA of the newly built system is 1.4, we shall see that a 50 keV electron beam will be able to resolve details as small as 0.0024 nm. This is a size much smaller than that of an atom. This means that we can discern something as small as an atom within the diffraction limitation.

Family of Electron Microscope. Taking the electron beam as the basic element of the system, electron microscopes can be divided into the following types: (1) Transmission Electron Microscope (TEM). TEM is the first type of electron microscope invented. The specimen prepared for TEM testing is always thin enough for the electron beam to get through and form a signal carrying the information of the specimen. Detectors are posed at the back of the specimen to collect the transmitted radiations and particles. HRTEM (high-resolution TEM) is the high-resolution version of a TEM. The magnification ability of an HRTEM system can reach 50 million times, which enables the system to discern carbon atoms in a diamond separated by only 0.89 Å (89 picometers) and atoms in silicon at 0.78 Å (78 picometers). This makes TEM a powerful tool for research work in nano science; (2) Scanning Electron Microscope (SEM). The SEM system employs the signals emitted from the specimen by the interaction of a rastering electron beam with specimen. Generally speaking, the SEM system has a lower resolution than the TEM system. However, it has a much greater depth of view, and the resulting image will reflect the three dimensional structure of the specimen surface; (3) Scanning Transmission Electron Microscope (STEM). An STEM is a combination of TEM and SEM. It is like SEM because the sample is scanned in a raster fashion. But the detector collects the transmitted electrons rather than the secondary electrons, which is the way a TEM system works. STEM can supply more information than the traditional TEM system while it offers higher resolution than the SEM system. Also, an annular dark field image (ADF) mode is available to gain higher resolution than TEM. Another important advantage of STEM is that any analytical signal, such as X-ray fluorescence spectroscopy and electron energy loss spectroscopy (EELS), can also be obtained at a high resolution (0.1 nm in the very best, aberration-corrected STEM system); (4) Reflection Electron Microscope (REM). Like TEM, REM also uses incident electron beams. But instead of using the transmitted (TEM) or secondary (SEM) electrons, it detects the reflected electrons. This technique is typically coupled with Reflection High Energy Electron Diffraction and Reflection High-energy Loss Spectrum (RHELS); (5) Environmental Scanning Electron Microscope (ESEM). ESEM is unique because of its ability to work in a relatively low vacuum. This is meaningful for the characterization of membranes.

2.3.6.2 Interactions between the Electron Beam and the Specimen

SEM is the most widely used electron microscope in the characterization of the membrane surface. It is based on the interactions of the electron beam and the specimen to obtain the image. These interactions include:

Backscattered Electrons. Collision of the moving electrons with the atoms causes scattering of the electrons. Some of the scattered electrons are subjected to minor or no energy loss and their moving directions are usually changed greatly, while others are subjected to great energy loss (to excite the atom to a higher energy state) but small directional change. The former electrons are called elastic scattered electrons and the latter are called inelastic electrons.

Backscattered electrons (BEs) are electrons reflected back by collision with the specimen atoms. BEs can be divided into elastic BEs and inelastic BEs, according to the energy loss of the BEs. Elastic BEs experience only once or a few times the large angle elastic scattering process and are reflected from the specimen surface with approximately no energy loss. But inelastic BEs are defined as those reflected by the inelastic scattering process dozens or even hundreds of times. Energy of BEs is higher than 50 eV, and the direction of each is different. The number of BEs is related to the incidence angle and the average atomic number of the specimen. A higher average atomic number means a bigger ratio. BEs come out of a depth of 10∼1000 nm. The resolution of a BEs image is 50∼200 nm. And this mode is mainly used to research the atomic number distribution.

Secondary Electrons. Some of the incident electrons lose their energy to excite atoms of the specimen to higher energy state. In some cases, if the extra-nuclear electrons obtain enough energy to escape the binding of the atoms they will run out to form secondary electrons (SEs). The energy of SEs is between 0∼50 eV. And most are within the energy range of 2∼3 eV, so that SEs formed deep inside the specimen surface cannot be emitted from the surface. The emitting depth of SEs is between 2∼10 nm. Emitting of the SEs is greatly influenced by the topology and the chemical physical statement of the surface, so that the SEs image can reveal rich information of the surface microstructure. Resolution of the SEs image can reach 5∼10 nm. And it is especially suitable for surface topography research.

Adsorbed Electrons. Inelastic scattering will cause energy loss to the incident electrons. If such a process happens many times for one incident electron, the electron will finally be captured by the specimen bulk. This will cause a current signal in the circle between the specimen and the ground which is the signal of adsorbed electrons (AEs). After proper amplification, the AEs signal can also be employed to form an AEs image. It is almost the negative pattern of the BEs image, but with a soft contrast. The AEs image does not have a good resolution. Its typical value is several microns.

Transmitted Electrons. When the specimen is as thin as 1 nm or under special operation mode, the incident electrons will transmit the specimen

to form transmitted electrons (TEs). Images formed by TEs can reveal the chemical composition, the thickness and crystallization state of different spots on the specimen. The resolution of TEs images is almost equal to the diameter of the electron beam, i.e. 5~10 nm.

Characteristic X-rays. Incident electrons can excite the extra-nuclear electrons of K-, L- and M-shell onto a higher energy state or out of the atomic bondage, leaving the energy levels unoccupied so that electrons originally at higher energy states will fall down into these unoccupied shells, with the extra energy released in the form of X-rays. Since each kind of atoms has a unique group of energy levels, the X-rays emitted by different atoms are different from each other, i.e., each X-ray is characteristic to the atom number. So measurement of the wavelengths of the X-rays emitted will enable us to decide what kinds of chemical compounds the specimen contains, and investigation of the intensity of the X-rays will help us to evaluate the ratio of different chemical compounds contained in the specimen. The depth of a characteristic X-rays image is about 1~7 μm, and the resolution is merely about several microns.

2.3.6.3 Imaging Principles and Instruments of SEM

Each SEM system contains an electron gun to supply the electron beam, a series of condenser lenses to manipulate the electron beam path, some scanning coils for scanning control, a sample chamber to hold the sample, and a set of detectors to collect the signal (see Fig.2.17). The electron beam is generated and accelerated by the electron gun as a divergent beam, reconverged and focused by the condenser lenses, and finally made into a beam scanning across the sample. Each kind of particle and electromagnetic wave can be a potential signal available to form the image.

For an electron microscope the electron gun is the most important part. Currently three types of electron guns are available: (1) thermionic emission W-filament; (2) heated LaB_6; (3) cold field emission filaments. For the three types of electron guns, the electron source brightness (the beam current density) of the cold field emission is the best, and heated LaB_6 is the next best, with a thermionic emission W-filament the worst. But the vacuum requirements and the costs are of an opposite order. The two former types emit electrons through thermionic emission, by heating the materials to supply the electrons with energy sufficient to overcome the work function. The field emission guns used a high electric field to narrow the energy barrier of the emission so that electrons can be emitted at low temperature. Field emission guns can produce an electron beam with the crossover size as small as 10 nm, while for LaB_6 this value is 10 μm and for a tungsten hairpin 50 μm. The beam brightness of field emission guns can reach up to $10^7 \sim 10^8$ A/(cm^2·sr). This is rather a high value compared with the LaB_6 cathode ($10^5 \sim 10^6$) and W hairpin ($10^4 \sim 10^5$). For field emission guns, foreign atoms on the surface of the cathode will impede the work function severely. So a high vacuum is
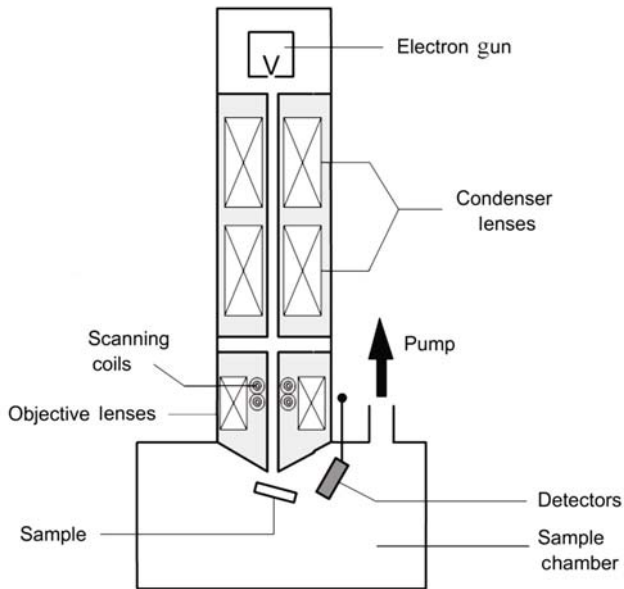
Fig. 2.17. Basic configuration of SEM

needed. To keep the cathode warm (at 2300 K) is also helpful since the landed atoms evaporate at once.

2.3.6.4 Performance of SEM

Generally speaking, an SEM has a higher resolving ability than optical microscopes. Its resolution is mainly limited by several factors: (1) Spot Size: Spot size of the electron beam is the basic limitation for the resolution. The smallest spot size can be obtained by low beam current, high accelerating voltage, and short working distance; (2) Volume of Interaction: Volume of interaction is defined as the area on the specimen where the emitted signals escape from the surface and are collected for imaging. In most cases the volume of interaction is much larger than the spot size, so actually it becomes the critical factor; (3) Accelerating Voltage: The effect of acceleration voltage is complicated. Firstly it will raise the volume of interaction by generating signals with higher emitting energy. Secondly it can reduce lens aberrations in the electron column to produce an electron beam with smaller spot size; (4) Sample Composition: The sample composition affects the resolution by changing both the signal depth and the interaction volume.

The SEM is a widely used characterizing technology because of its good performance: (1) Relatively simple sample preparation: A specimen from an SEM can be directly taken from the samples without further procedures. For

some nonconducting materials a metal coating procedure is needed, but the surface morphology of the original specimen is not changed because the metal membrane has a limited thickness; (2) Magnification can be modulated in a wide range continuously. The range is from several dozen to a value as high as several hundreds of thousands. Even at a high magnification, images with good resolution and enough brightness can still be obtained; (3) Long field depth and large field of view: At a magnification of $100\times$, an optical microscope has a field depth of 1 µm while the SEM can reach a field depth as long as 1 mm, 1000 times that of optical microscopes. Even when the magnification reaches up to ten thousand times, the SEM still has a field depth of 1 µm, which means that the SEM image contains more information about the direction perpendicular to the surface, and from the image the microstructure of the surface topography can be directly observed; (4) High resolving ability: According to the previous description, the wavelength limitation of the optical microscope is about 200 nm, but it is not difficult for the SEM to reach a resolution as good as below 10 nm; (5) Capability to take a comprehensive analysis of the specimen: Equipped by various kinds of probes, the SEM can analyze the local chemical structure and map the composition of each point into an image. This breaks the restriction that chemical analysis can only be used for the specimen as a whole.

The SEM is now a nearly a standard tool for investigating surface properties of membranes, including the surface topography, the change of surface by modification, the adsorption of biomacromolecules, fouling, etc. The SEM is also applied in the observation of the cross section of the membranes. Cross-section investigation is extremely useful for characterization of the asymmetric membranes and complicated membranes. By the surface and cross-section investigation of an SEM, basic parameters such as thickness and pore diameters can be decided. Because the imaging area of the SEM is rather tiny, it is necessary to obtain the average of different areas as the final value.

SEM sample preparation is always a process needing careful consideration. Metal coating is needed since most of the polymeric membranes are nonconductive. Drying of wet membranes requires a freeze-drying treatment. Another choice is to replace the water in the membrane by liquid with low surface tension to avoid the destruction by the capillary force. For the preparation of a cross-section sample a freeze-fracturing operation is required to prevent the deformation of the porous structure.

2.3.7 Environmental Scanning Electron Microscopy

2.3.7.1 Introduction

Although finding wide applications in research works, the SEM still has limitations, making it an imperfect tool. One of these limitations is that it requires a high operation vacuum. Vacuum requirements of the SEM originate from three aspects: (1) Modern SEM usually employs a field emission electronic

gun to obtain an electron beam with high brightness. But a filed emission gun needs vacuum as high as 10 nPa or better to eliminate air atoms landing on the filament. Even in warm mode, the requirement is still at the level of 100 nPa; (2) The path of the electron beam should be as free of any air atoms as possible to avoid scattering; (3) SEM images are mainly obtained with the secondary electrons, most of which have an energy level as low as 2∼3 eV. A high vacuum requirement means not only that a pressure resistant specimen chamber and a high quality pump system are needed so that air can be withdrawn from the chamber to a very low pressure, but also that the specimen should be clean enough. Any volatile component can be a polluting source, let alone the water. This is a serious problem for the research of the membrane separation mechanism and fouling because in these cases the *in situ* investigation of the membrane is usually required with the membrane full of volatile components such as water, in particular.

A second limitation of the SEM is that the specimen must have a conductive surface so that the captured incident electrons will not stay and accumulate on the surface to deform the image by electrostatic effect. For a nonconductor specimen, which is always the case with a polymeric membrane, a metal coating is usually the solution. But it is possible that a fine structure will not survive this process. Also, the metal layer is not always exactly the copy of the membrane's surface topology.

ESEM is the technology to solve these problems. An ESEM system is basically an SEM system but with special alternations to allow the varying of the specimen environment through a range of vacuum, temperature and gas compositions. Even at a pressure as high as 50 Torr, or at a temperature as high as 1500 °C, ESEM still offers high resolution secondary electron images.

2.3.7.2 Principles of Imaging

In an ESEM system, the sample chamber is separated by a Multiple Pressure Limiting Apertures (MPLA) device from the other parts so that the vacuum of the sample chamber can be kept at 50 Torr, while that of the electron gun chamber and the condenser columns can still be reserved at 10^{-5} Torr or better.

Fig.2.18 shows the basic structure of a two degree MPLA system. In ESEM, a selected type of gas is let in from the sample chamber, and flows through the limiting apertures into the condenser column and electron gun chamber, and is finally pumped out. The effect of the MPLA system is to limit the gas flow to the minimum available degree so that a high pressure gradient can be generated between the gun chamber and the sample chamber. Besides confining the flow stream of the gas, the size of the limiting aperture also affects the electron beam. Because of this conflict, the ideal pressure gradient cannot be achieved with only one pressure limiting aperture, so the MPLA system is needed (Optics, 1998).
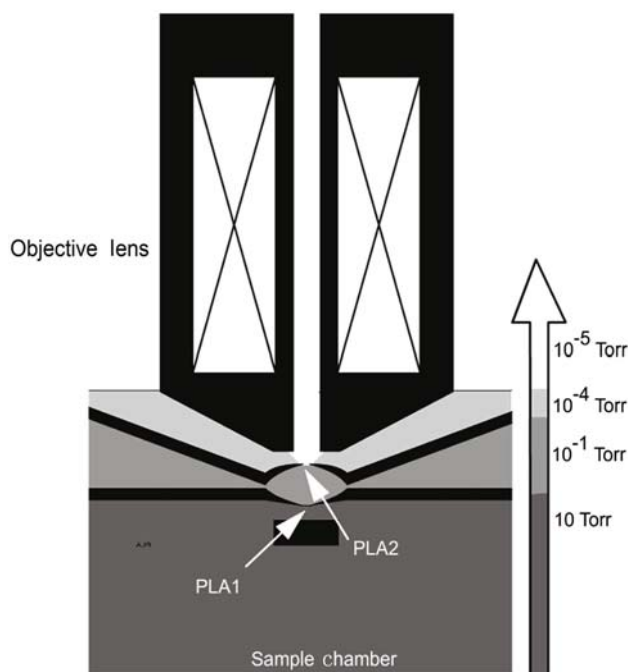
Fig. 2.18. Configuration of MPLA system

The ESEM system also employs special secondary electron detectors, named as environmental secondary detector (ESD) and gaseous environmental secondary detector (GSED) (schematically shown in Fig.2.19) to collect the secondary electron signal for imaging. The ESD collects the secondary electrons as well as the environmental secondary electrons which are generated by the collision of the accelerated electrons with the gas atoms. This supplies the imaging signal with an amplification. GSED is developed from ESD, and it can eliminate the interference from the BEs and the type III secondary electrons which are formed from the collision of the BEs with the wall of the sample chamber. Because of these features, the ESEM system can obtain images with fine details where the SEM cannot.

Except for the environmental electrons, the collision of the accelerated electrons with the gas atom also creates positive ions. These positive ions are attracted onto the specimen surface by the electrons accumulated there, and finally the charging artifacts are eliminated, while with SEM this is always a problem for nonconductor samples. The absence of artifacts supplies the ESEM technology with the convenience that the sample does not need a special preparation technology, such as coating.
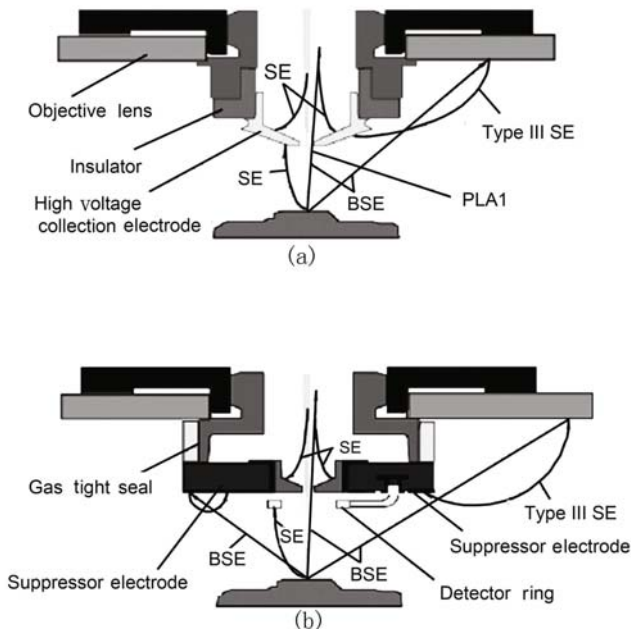
Fig. 2.19. (a) ESD and (b) GSED

2.3.7.3 Features and Applications

Merits of ESEM compared to SEM include: (1) ESEM is of low sensitivity to contaminates: So a specimen with water, gaseous emission, and volatile matter can be investigated by the ESEM system; (2) ESEM is able to provide a saturated water vapor environment for a hydrated specimen; (3) Elimination of charging artifacts supplies several advantages. Firstly it is not necessary that the sample is a conductor so that investigations for insulators such as a polymeric membrane is also possible. Secondly the sample need not be specially prepared, for example with a metal coating. This means that the delicate structure of the sample can be preserved. Also, the sample can be observed just in its natural state. Thirdly the absence of the coating layer interference facilitates the X-ray analysis with less complex, higher energy K-lines. The enhancing of the accelerating voltage is unconfined by the charging balance; (4) The ESEM system supplies a controllable environment for the specimen. An increase in the temperature level to as high as 1500 °C is possible. The environmental pressure can also be adjusted within a certain range. A different gaseous atmosphere can be chosen for special applications; (5) The state of the sample need not to be fixed, which means that a dynamic process such as tension and deformation can also be recorded as a sustain-

ing course. Considering all these merits, ESEM is a very promising tool for the investigation of polymeric membrane materials, especially for membrane fouling (Choi et al., 2005; Yu and Lencki, 2004). But since the resolution is still limited, in many cases it will be hard to obtain an image with an ideally fine structure (Le-Clech et al., 2007).

2.3.8 Atomic Force Microscopy

2.3.8.1 Introduction

An AFM (Atomic Force Microscope) is a kind of SPM (Scanning Probing Microscope). Imaging principles of the SPM are quite different from those of optical microscopes and electron microscopes. It obtains the image by scanning certain probes across the specimen surface. Because of the special imaging method an SPM supplies a resolution which is not confined by the diffraction. Development of SPM technology is rapid and many new types have been invented. AFM belongs to the type called scanning force microscope (SFM), which forms the image by a force signal generated from the tip-specimen interaction. Different kinds of SFM identify themselves by the nature of tip-specimen interaction employed to generate the force signal. SFM mainly includes: AFM, LFM (Lateral Force Microscope), MFM (Magnetic Force Microscope), EFM (Electric Force Microscope), CFM (Chemical Force Microscope), etc. Among all these types AFM is the most preeminent one and is most widely used.

Compared with STM (Scanning Tunneling Microscope), which is the first type of SPM to have the atomic scale resolving ability, AFM overcomes the limitation that the specimen must be conducting, while still reserving good resolution. Banach, Quate and Gerber invented the first AFM at Stanford in 1986. A year later Quate published the high resolution AFM images of atoms of HOPG (Highly Ordered Pyrolytic Graphite) and HOPBN (Highly Ordered Pyrolytic Graphite BN). And HOPBN is the first insulator of which the images with atomic scale resolution are taken by AFM. Resolution of AFM is at the level of subnanometer and is more than one thousand times better than the optical diffraction limitation.

Apart from the ability to capture an atomic scale image, AFM is also famous for its amazing power to manage macromolecules and to do nano-scale processing. This makes AFM an indispensable tool in nanotechnology.

2.3.8.2 Principles of Imaging

Fig.2.20 shows the basic structure of an AFM system. The central component of an AFM system is the cantilever with one end fixed to the basement and the other end fabricated with a sharp tip. In the process of the investigation, the tip is brought slightly into contact with the specimen. Interactions between the specimen atom and the tip will exert a tiny force on the tip, of which

the value is only $10^{-8} \sim 10^{-6}$ N. Such force will cause the cantilever some deformation. The deformation is so small that a special technology is needed to detect it. The relationship of the force F and the deformation z obeys Hooke's rules, as in Eq.(2.9):

$$F = k\Delta z, \tag{2.9}$$

where k is the force constant of the cantilever. So the value of the tip-specimen force of a certain site on the specimen can be obtained by detecting the deformation of the cantilever. The AFM relies on the signal from the force mentioned above or the height of the tip to form the image. Mapping of these signals collected by scanning the tip on the specimen in both x and y directions will form the ATM image. Generally there are two types of imaging modes, the constant height mode and the constant force mode.
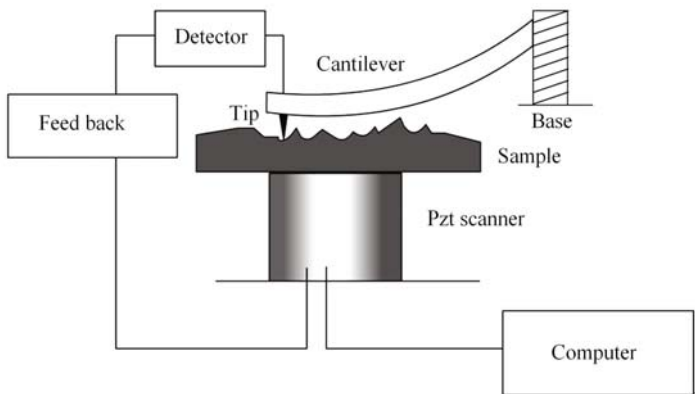
Fig. 2.20. Configuration of AFM

If the specimen is flat enough, the distance between the tip and the specimen can remain constant during the scanning in x and y directions, and the tip-specimen force is taken directly as the imaging signal. Such a mode is called "Constant Height Mode". But for a specimen with a rough surface the constant height mode is not applicable any more, because if the tip still scans at a constant height, there will be a risk of collision with the specimen surface, which will cause damage both for the specimen and for the tip. Hence a feedback mechanism is employed to adjust the tip-to-sample distance to maintain a constant force between the tip and the sample. And this scanning mode is named the "Constant Force Mode", which is most widely used, since most of the specimens do not have a flat surface.

2.3.8.3 Instruments

Cantilever and Tip. To reach a certain resolution, the cantilever must be designed to meet certain requirements. These requirements include: (1) The elastic coefficient of the cantilever should be within the range of $10^{-2} \sim 10^2$ N/m so that force below a nano-Newton can still be detected, and the cantilever can always recover its original state; (2) The natural frequency of the cantilever must be high enough to catch the fluctuation of the surface topography. A typical frequency generated by the fluctuation of the surface topography can be as high as 10 kHz. So the nature frequency of the cantilever must be no less than this value. To fulfill both the first two requirements, the size of the cantilever must be as small as several micrometers; (3) The lateral rigidity should be high so that the effects of lateral movement can be minimized; (4) Existence of the tip should be at one end of the cantilever. Commercially available cantilevers are mostly made up by Si or Si_3N_4, with the shape of character "V" to increase the lateral rigidity. A sharp tip, whose radius of curvature is below 10 nm, is fixed onto the apex of the "V" shape.

Tip Position Detecting System. To detect the height change of the tip, several technologies have been developed: (1) Optical Reflection Technology: The laser beam is reflected by the reflecting plate at the back of the cantilever and collected by an array of photodiodes. This technology has a good resolution, though not the best, among these detecting methods with a value of 0.03 nm when the wavelength of the laser is 670 nm, and is used most widely in commercial AFM; (2) Tunnel Current Technology: This technology relies on the tunnel current to sense the distance between the cantilever and a fixed electrode just above it. The resolution can reach 0.01 nm, but the signal-noise ratio is relatively low. This system needs a vacuum environment to work well; (3) Optical Interferometry Technology: The position of the tip is calculated out from the phase of the beam formed by the two polarized light beams that detect the fixed end of the cantilever and the tip, respectively. It has the best resolution among all these choices, which is 0.001 nm, with a rather high signal-noise ratio; (4) Capacitive Sensing Technology: A parallel-plate capacitor system is built with the cantilever as one of its electrodes and the other one fixed just above the cantilever. By monitoring the capacity of the parallel-plate capacitor the position of the tip can be determined. In this method the resolution is 0.03 nm, which is relatively low; (5) Piezoresistive Cantilevers: The cantilevers are fabricated with piezoresistive elements acting as a strain gage. Strain in the cantilever can be directly calculated with the help of a Wheatstone bridge. But it is not sensitive enough.

Scanning System. The scanning system works in such a way that the tip keeps its position unchanged while the specimen mounted on the scanning system moves along the x and y directions. Typically the scanning system is made up of a piezoelectric tube which can move the specimen in z direction to maintain a certain force, as well as moving in x and y directions for the scanning function. Also there is a kind of "tripod" configuration of three piezo

crystals, each responsible for movement in one direction. The merit of such a configuration is that it can avoid the distortion effect with the tube scanner. As a result, a map of the area $s=f(x,y)$ represents exactly the topography of the specimen.

2.3.8.4 Operation Modes

As can be seen from Fig.2.21, the imaging mode of AFM mainly includes: (1) the contacting mode; (2) the non-contacting mode; (3) the tapping mode; (4) the lifting mode.

Contacting Mode. The contacting mode is the regular operation mode of ATM, in which the tip keeps in contact with the specimen and slides across the surface of the specimen during the scanning process at a constant height or constant strength. This stable mode can be used to obtain a high-resolution image. But it is not applicable for biomacromolecules or a specimen with a low elastic module or one prone to be moved or deformed.
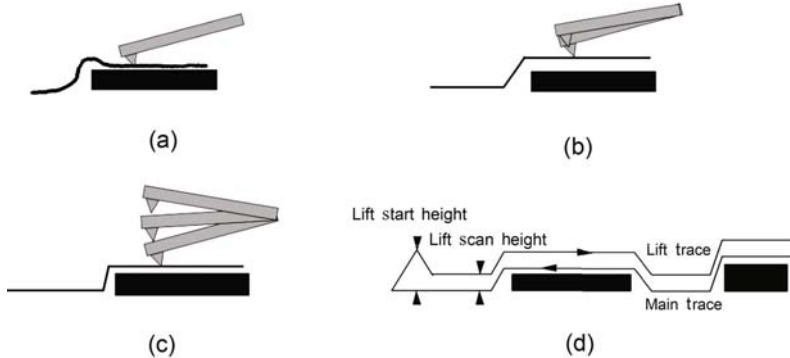
Fig. 2.21. Operation modes. (a) Contacting mode; (b) Non-contacting mode; (c) Tapping mode; (d) Lifting mode

In an atmospheric environment, because of the capillary force, the adsorption effect between the tip and the specimen is strong, and the extra force exerted onto the specimen during the scanning may cause damage to the surface of the specimen. Also, this adsorption effect will enlarge the specimen-tip contact area and decrease the resolving ability of the system. There are two ways to solve this problem. One is to make a surface modification of the tip to lower its surface energy so that the interaction of the contact area can be decreased. The second method is to immerse both the tip and the specimen into a liquid system so that the capillary effect can be overcome.

Non-contacting Mode. In non-contacting mode, the tip vibrates above the surface of the specimen without making contact with the specimen at any

time. Interactions detected by the tip are long-range interactions such as van der Waals' force and the electrostatic forces which do not cause any damage to the specimen. Although this increases the sensitivity, the resolving capacity is decreased in non-contacting mode, and the operation is also more difficult than in other modes.

Tapping Mode. In tapping mode the cantilever is oscillated close to or exactly at its natural frequency. The tip taps the surface slightly from time to time. The oscillation amplitude of the cantilever reaches the maximum value when the tip is free. But when the tip taps the specimen, the oscillation amplitude will drop. The feedback system will make sure that the oscillation amplitude of the cantilevers remains unchanged. So the position of the tip can be moved according to the surface topography of the specimen. And a tapping mode AFM image is obtained by mapping values from the height of the tip to the coordinates.

Resolution of this mode is as good as for the contacting mode. Also, because the contacting time is short, interaction between the specimen and the tip is rather low, with the tip-specimen force in the range of one pico-Newton to one nano-Newton. As a consequence, a decrease in resolving ability, and damage to the specimen surface caused by the shear force during scanning, almost vanish. So the tapping mode is especially good for the investigation of biological systems and soft materials such as polymeric membranes. For specimens which cannot be strongly fixed to the base, the movement caused by the scanning process is rather low.

The tapping mode will also work in a liquid environment. Because of the damping force of the liquid, specimen-tip interaction becomes smaller. So in a liquid environment the damage to the specimen by the shear force is decreased further. Therefore, the tapping mode in liquid is able to investigate living biological systems, or reactions taking place in liquid.

The tapping mode can also be applied to the phase imaging technology, in which the difference between the oscillation of the cantilever and the external driving force can reveal information about the specimen surface property. Phase imaging technology can be used to investigate the surface fraction or the viscoelasticity of the material. Chemical analysis by phase imaging technology is also possible.

The common tapping mode of the AFM uses the method of Amplitude Modulation to do constant strength scanning. Technology of Frequency Modulation can also be used to detect the frequency modification during the scanning process. This modulation method increases the signal-noise ratio greatly and enhances the sensitivity.

Lifting Mode. This mode is mainly applied to imaging by electrostatic force or magnetic force when it is required to eliminate the effect of the topology. The cantilever works as follows: Topology information is acquired by the first scan, then the tip is raised up to a certain height (typically 10∼100

nm), and another scan is done along the obtained topography in the path of the first scan, as Fig.2.21(d) shows.

2.3.8.5 Performance of AFM

A lot of work has been done to enhance the resolving capability of the AFM system. The scanning device has been improved for more precise control. A special design has been created to lower the noise from the external vibration and the acoustic wave. The AFM is equipped with a newly developed detecting system. New modulation methods are employed such as force modulation and frequency modulation. In an existing AFM system the following factors should be considered first if you want to enhance its resolving capability. Firstly, choose a tip with a small radius of curvature to decrease the contact area of the tip and the specimen. Secondly, ensure the cleanliness of the environment. Contamination of the tip by dust will cause fake imaging. Contamination of the specimen by dust will also pollute the tip during the scanning process. Thirdly, the capillary effect is always a factor to consider when imaging in air. To avoid this effect, a vacuum system is needed, or else the image should be taken in N_2 atmosphere, or in a liquid environment.

Although other kinds of SPM also find applications, AFM is most widely used for characterizing a membrane surface. Because of the pore structures of the membrane surface, the tapping mode is always chosen as the operation mode. Since the scanning can be done in a common environment and the sample does not need special treatment using AFM, the membrane surface can be characterized in its natural state. Through such characterization the pore size and porosity can be determined. But for membranes with a coarse surface it is sometimes hard to decide the porosity (Mulder, 1996). AFM colloid probe technology is also a powerful tool for researching the surface interactions of membranes with external molecules, such as proteins and other macromolecules (Asatekin et al., 2006; Brant and Childress, 2004).

2.4 Wettability of Membrane Surfaces

2.4.1 Wettability and Surface Properties of Membrane

The spreading of liquids over solid surfaces is a routine daily occurrence. The study of the wettability of polymer surfaces is of great importance because of the applications of polymers for various industrial uses and, for example, in the choice of coating. The wettability of a membrane surface is also clearly important. On the one hand, various membrane processes require membrane materials with different degrees of wettability. For most membrane processes, including ultrafiltration and microfiltration, they are used for the separation of aqueous media. Thus a hydrophilic membrane is preferable or even definitely necessary. However, for other membrane processes, such as membrane

distillation, a hydrophobic membrane is often required. In this case, two aqueous solutions at different temperatures are separated by a porous hydrophobic membrane and because of a difference in partial pressure (i.e. temperature difference) vapor transport takes place through the pores of the membrane from the hot side to the cold side. Evaporation of the liquid occurs on the high temperature side while the vapor condenses on the low temperature side (Mulder, 1996). The solutions may not wet the membrane. So only a hydrophobic membrane can be used in the concentration and purification of aqueous solutions by a membrane distillation process.

On the other hand, wettability of the membrane surface plays a crucial role in governing biocompatibility and biofouling. When membranes are used in a separation of liquids containing biomacromoleales, the membrane fouling induced by the adsorption of proteins reduces the flux and deteriorates the membrane performance. Membranes can also be applied in the medical field, such as dialysis for the treatment of patients with kidney failure. During this type of membrane process, it is important to avoid the interactions between membrane and blood components including blood proteins, platelets, and other blood cells. Although many factors can influence the biocompatibility of materials, it is generally recognized that a hydrophilic surface reduces the non-specific adsorption of proteins as well as cells and then improves the biocompatibility. Meanwhile, the resistance of protein adsorption can enhance the ability of anti-biofouling for membranes. Therefore, characterization of the wettability of a membrane surface is important.

2.4.2 Principle of Contact Angle

The basic parameter for liquid wetting of a solid surface is the contact angle as defined in Fig.2.22 for a sessile drop. It is formed by a tangent to the liquid at the air/liquid/solid line of contact and a line through the base of the liquid drop where it contacts the solid. Contact angle measurements can be used to assess changes in the wetting characteristics of a surface to indicate changes in surface wettability. Information that one obtains largely depends on the interpretation of the contact angle in terms of Young's equation:

$$\gamma_L \cos\theta = \gamma_S - \gamma_{SL}, \tag{2.10}$$

where γ_L is the liquid-vapor, γ_S the solid-vapor, and γ_{SL} the solid-liquid interfacial tension, respectively, and θ the measured angle with respect to the surface, as illustrated schematically in Fig.2.22.

Several assumptions are involved in defining Young's equation, which include the facts that the capillarity and gravity can be ignored and that the solid surface is level and flat. It is immediately obvious that few real materials meet all these requirements fully and simultaneously. Nonetheless, contact angle measurements can be used to obtain meaningful surface information. Surface energy is the combination of dispersion (non-polar) and polar energy.
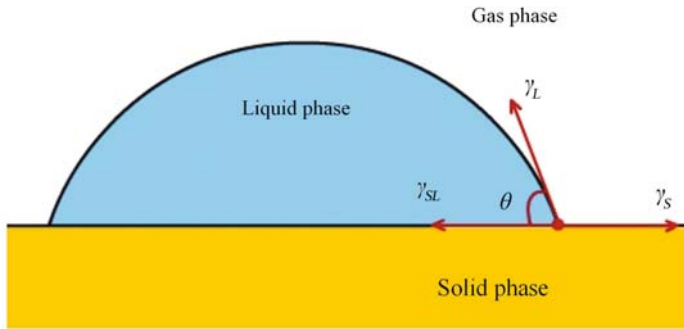
Fig. 2.22. Sessile drop profile showing surface tensions acting at the three phase lines of contact

As shown in Fig.2.23, many kinds of interactions exist between the testing drop and the solid surface, which include acid-base interactions, hydrogen bonding, dipole-dipole interactions, and even interactions induced by surface contaminants. Therefore, various theories based on contact angle measurements have been developed to predict the surface tension and surface energy of organic solids. Typically they include the Fox-Zisman theory, geometric mean theory, harmonic mean theory, and acid-base theory. The following discussion takes acid-base theory as an example (Klee and Hocker, 1999; Vancso et al., 2005).
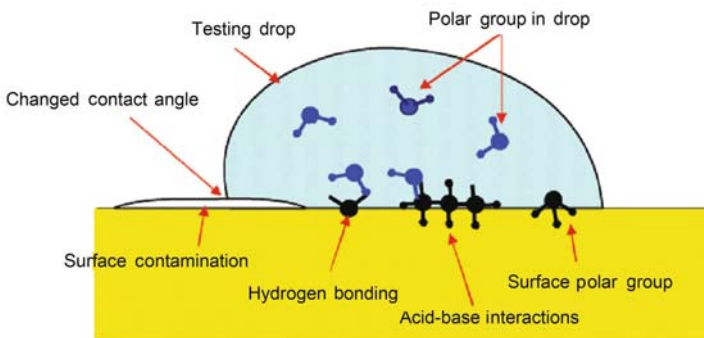
Fig. 2.23. Interactions between dropped liquid and solid surfaces

Fowkes proposed that the work of adhesion (W_a) for a liquid on a solid surface is given by (Yildirim, 2001):

$$W_a = W_a^d + W_a^{nd}, \tag{2.11}$$

where W_a^d represents the contributions from dispersion (non-polar) interactions, and W_a^{nd} represents the same from non dispersion (polar or ionic) interactions. It is generally accepted that all solids would be hydrophobic if $W_a^{nd}=0$, i.e., if the surface is free of polar groups on which water molecules can be bonded.

In the last twenty years significant advances have been made in the thermodynamic treatment of surface free energies, largely due to the pioneering work of Fowkes et al., and Van Oss, Chaudhury and Good. According to these approaches the surface free energy of a phase i is given by:

$$\gamma_i = \gamma_i^{LW} + \gamma_i^{AB}, \tag{2.12}$$

where γ_i^{LW} and γ_i^{AB} refer to the apolar and polar (acid-base) components of surface free energy, respectively. The former can be represented by the Lifshitz-van der Waals (or LW) interactions that include the dispersion, induction and orientation components. The polar interactions are generally considered to be intermolecular interactions between Lewis acids (electron acceptor) and bases (electron donor) on the surface.

According to the Van Oss-Chaudhury-Good (OCG) approach the surface free energy change upon two interacting surfaces (e.g. solid and liquid) is given by:

$$\Delta G_{SL} = -2\sqrt{\gamma_S^{LW}\gamma_L^{LW}} - 2\sqrt{\gamma_S^+\gamma_L^-} - 2\sqrt{\gamma_S^-\gamma_L^+}. \tag{2.13}$$

The changes in free energy associated with the solid-liquid interaction is given by the following relationship:

$$\Delta G_{SL} = \gamma_{SL} - \gamma_S + \gamma_L. \tag{2.14}$$

Substituting Eq.(2.14) into Eq.(2.13), one obtains:

$$\gamma_{SL} = \gamma_S - \gamma_L - 2\left(\sqrt{\gamma_S^{LW}\gamma_L^{LW}} + \sqrt{\gamma_S^+\gamma_L^-} + \sqrt{\gamma_S^-\gamma_L^+}\right), \tag{2.15}$$

which allows one to determine the interfacial surface tension of two interacting surfaces (e.g. water and membrane). As shown, there are four unknowns for the calculation of γ_{SL}, i.e. γ_S, γ_S^{LW}, γ_S^+ and γ_S^-, which are the surface free energy components of solid. The surface free energy components of liquids are generally available in the literature or handbooks. The surface free energy components of solids can be determined by using the Van Oss-Chaudry-Good (OCG) equation that is derived as follows.

Work of adhesion or Gibbs free energy of interaction can be related to the interfacial energies through Young's equation (Eq.(2.10)). Combining Eq.(2.10) and Eq.(2.15),

$$-\Delta G_{SL} = \gamma_L \left(1 + \cos\theta\right) = W_{ad}. \tag{2.16}$$

Substituting Eq.(2.16) into Eq.(2.13), one obtains:

$$(1 + \cos\theta)\,\gamma_L = 2\left(\sqrt{\gamma_S^{\mathrm{LW}}\gamma_L^{\mathrm{LW}}} + \sqrt{\gamma_S^+\gamma_L^-} + \sqrt{\gamma_S^-\gamma_L^+}\right), \tag{2.17}$$

which is very useful information for characterizing a solid surface in terms of its surface free energy components, i.e., γ_S^{LW}, γ_S^+ and γ_S^-. To determine these values, it is necessary to determine contact angles of three different liquids with known properties (in terms of γ_L^{LW}, γ_L^+ and γ_L^-) on the surface of the solid of interest. One can then set up three equations with three unknowns, which can be solved to obtain the values of γ_S^{LW}, γ_S^+ and γ_S^-. Some reference books or databases provided by makers of contact angle equipment give the liquids that can be used for contact angle measurements, along with the values of γ_L, γ_L^{LW}, γ_L^+ and γ_L^-. Apolar liquids suitable for contact angle measurement include hexane, heptane, cyclohexane, benzene, methylene iodide, etc. while polar liquids include water, glycerol, formamide, etc.

If an apolar liquid is placed on the surface of a membrane sample and its contact angle is measured, Eq.(2.17) can be reduced to:

$$(1 + \cos\theta)\,\gamma_L = 2\sqrt{\gamma_S^{\mathrm{LW}}\gamma_L^{\mathrm{LW}}}, \tag{2.18}$$

because γ_L^+ and γ_L^- are zero. Thus, Eq.(2.18) can be used to determine γ_S^{LW} from a single contact angle value, provided that the contact angle measurement is conducted with an apolar liquid of known γ_L and γ_L^{LW} (In fact, $\gamma_L = \gamma_L^{\mathrm{LW}}$; γ_L^+ and γ_L^- are zero). As the value of γ_S^{LW} is already estimated from Eq.(2.18), Eq.(2.17) can now be used to determine the values of γ_S^+ and γ_S^- by solving two simultaneous equations.

Once the three surface tensions, i.e. γ_S^{LW}, γ_S^+, and γ_S^-, are known, the surface tension of the solid, γ_S, can be determined as follows:

$$\gamma_S = \gamma_S^{\mathrm{LW}} + \gamma_S^{AB} = \gamma_S^{\mathrm{LW}} + 2\sqrt{\gamma_S^+\gamma_S^-}. \tag{2.19}$$

The surface free energy, γ_S, is a material specific parameter which, when known for two materials, can be used to estimate the wettability, work of adhesion and the changes in the Gibbs free energy upon interaction.

2.4.3 Methods for Contact Angle Measurement

Several methods are available to measure contact angles (Fig.2.24) (Klee and Hocker, 1999). Accordingly, different kinds of contact angles have been proposed and they can be divided into the static contact angle and the dynamic contact angle. In the case of a static determination the contact angle of a drop with an immobile solid/liquid/gas interface is determined microscopically (sessile drop). In the captive bubble method the contact angle of an air bubble, which is located under the solid surface in contact with the liquid, is measured. In contrast to the sessile drop method, in the captive bubble method the contact angle is measured on a completely wet surface.
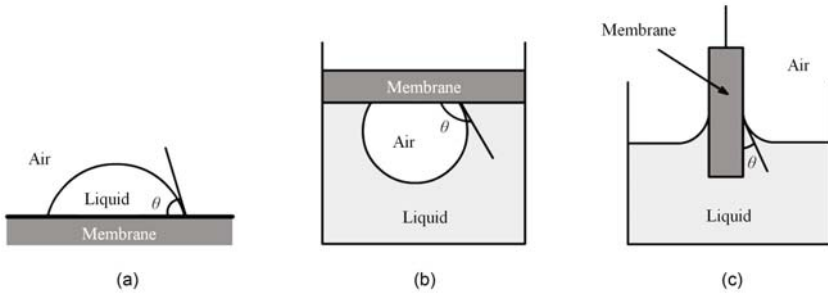
Fig. 2.24. Schematic illustration of dynamic and static contact angle measurements using the (a) sessile drop method, (b) captive bubble method, and (c) Wilhelmy plate method

The Wilhelmy plate method is a dynamic method which permits the contact angle measurement between a sample with perimeter p and a liquid with a surface tension γ_L during immersion and withdrawal of the sample measuring the force F. The contact angles on immersion θ_a (advancing contact angle) and on withdrawal θ_r (receding contact angle) are calculated according to Eq.(2.20):

$$F_{a,r} = \gamma_L p \cos \theta_{a,r}. \tag{2.20}$$

Advancing and receding contact angles can also be measured by other two methods. It is generally recognized that the former relates to surface energy and wettability while the latter relates to surface roughness and repellency. As shown in Fig.2.25, by adding/withdrawing liquid to/from the sessile drop, advancing and receding contact angles can be obtained. They correspond to the critical angles at which the edge of liquid contact line expands/retracts, respectively.
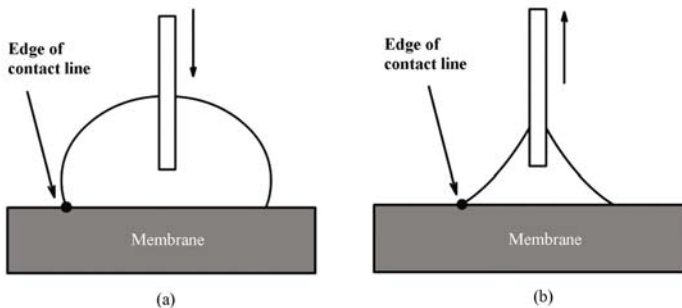
Fig. 2.25. Schematic illustration of measurements of (a) advancing and (b) receding contact angles by adding and withdrawing of liquid, respectively

There is another method which can also be used to measure advancing and receding contact angles. With the aid of a tilting stage, contact angles on either side of the drop on the tilted sample surface are measured, as illustrated in Fig.2.26.
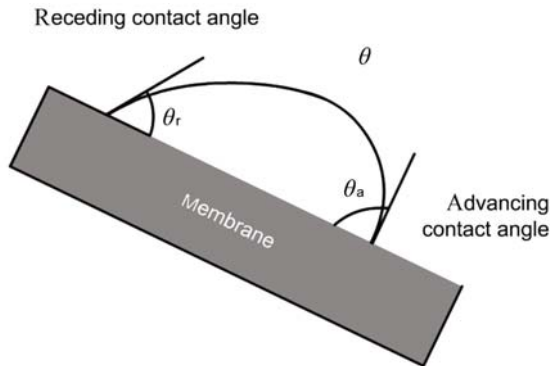
Fig. 2.26. Schematic illustration of measurements of advancing and receding contact angles by tilting sample surface

2.4.4 Contact Angle Hysteresis

The difference between the maximum (advancing) and minimum (receding) contact angle values is called the contact angle hysteresis. A great deal of research has been carried out to analyze the significance of hysteresis. It has been used to help characterize surface heterogeneity, roughness and mobility. Briefly, for surfaces which are not homogeneous there will exist domains on the surface which present barriers to the motion of the contact line. In the case of chemical heterogeneity these domains represent areas with different contact angles to the surrounding surface. For example, when wetting with water, hydrophobic domains will pin the motion of the contact line as the liquid advances, thus increasing the contact angles. When the water recedes the hydrophilic domains will hold back the draining motion of the contact line, thus decreasing the contact angle. From this analysis it can be seen that, when testing with water, advancing angles will be sensitive to the hydrophobic domains and receding angles will characterize the hydrophilic domains on the surface. For situations in which surface roughness generates hysteresis the actual microscopic variations of slope on the surface create the barriers which pin the motion of the contact line and alter the macroscopic contact angles.

2.4.5 Factors Influencing the Contact Angle on Membrane Surfaces

Many factors can influence the contact angle on a membrane surface, which include surface heterogeneity, surface roughness, the volume of dropped liquid, measurement time, measurement temperature, surface contamination and others. These factors should receive attention in respect of contact angle measurements on a membrane surface because most polymer membranes have a porous and rough surface.

Chemical Heterogeneity. For membranes fabricated from blendings or copolymers, the surface is often chemically heterogeneous. For example, in the process of membrane formation, an additive is usually added to modulate the structure and performance. Thus chemical heterogeneity should be considered for contact angle measurement on a membrane surface. On a chemically heterogeneous surface hydrophobic and hydrophilic domains can be formed. Generally speaking, an advancing contact angle is sensitive to the lower surface free energy component (hydrophobic domain) while a receding contact angle is sensitive to the higher surface free energy component (hydrophilic domain).

The effect of heterogeneity on the equilibrium contact angle has been known for some time. The apparent contact angle on a heterogeneous solid surface equals the equilibrium contact angle if the line tension is negligible. Cassie and Baxter (1944)demonstrated the additive nature of wetting over a chemically heterogeneous surface :

$$\cos \theta_e = f_1 \cos \theta_e^1 + f_2 \cos \theta_e^2, \qquad (2.21)$$

where f_1 is the fractional area of the surface with an equilibrium contact angle of θ_e^1. For a surface with two kinds of phases, $f_1 + f_2 = 1$. Generally the deviation is such that the measured value of $\cos\theta$ is lower than the Cassie prediction. The contact line on heterogeneous surfaces has been shown to be meta-stable, resulting in a range of possible values of $\cos\theta$, ranging between advancing or receding values.

Furthermore, chemical heterogeneity can also be induced and deepened by surface reconstruction.

Surface Roughness. Ideally, the contact angle should be measured on a flat and smooth solid surface. However, almost all membrane surfaces are rough. It is generally recognized that surface roughness amplifies hydrophobicity. The construction of superhydrophobic surfaces is a good example, which is often a highly rough surface with nano- and micro-structures.

Young's equation, Eq.(2.10), is valid only for the wetting of a flat surface. Wenzel showed that roughness makes a significant contribution to the wetting behavior of a solid surface and defined the surface roughness, r, to obtain an apparent contact angle for a liquid that completely covers the rough surface. He defined r as the ratio of the true, wetted area of the surface divided by the

projected surface area below the droplet. He then showed that the apparent liquid contact angle on a rough surface, θ_r, is related to Young's equilibrium contact angle by:

$$\cos \theta_r = r \cos \theta_e. \qquad (2.22)$$

Cassie and Baxter extended the Wenzel model to include porous surfaces. In their model a liquid sits on a composite surface made of a solid and air. Therefore the liquid does not fill the grooves of a rough solid. If f_1 is the fractional area of the liquid in contact with the solid while f_2 is the fractional area of the air, $\cos \theta_e^2 = \cos 180° = -1$. Thus Eq.(2.21) can be transformed as:

$$\cos \theta_e = f_1 \cos \theta_e^1 - f_2. \qquad (2.23)$$

Belfort et al. also studied the effect of surface roughness on the contact angles including captive bubble sessile contact angles and advancing/receding contact angles. They took ultrafiltration membranes with a different molecular weight cutoff as a model surface and corrected the contact angle values by taking into consideration surface roughness, which is determined by atomic force microscopy (Taniguchi et al., 2001).

Volume of Dropped Liquid. The drop size dependence of contact angles is also a kind of contact angle multiple-value phenomenon, just like contact angle hysteresis. On ideal solid surfaces, the drop size dependence of contact angles is due to the line tension effect only. For simple, ideal solid-liquid systems, the line tension should be positive as required by the condition of stable thermodynamic equilibrium. However, on real solid surfaces, the observed drop size dependence of contact angles depends not only on the line tension but also on the surface roughness and surface heterogeneity. These non-line-tension factors can cause different patterns in the drop size dependence of contact angles (Li, 1996).

Measurement Time. Generally, the contact angle decreases with time and then reaches a platform, i.e. the equilibrium contact angle. For a series of samples the contact angle is usually calculated from the drop with the same time, for example 20 s. Measurement of the time dependence of the contact angle is often performed to characterize the reconstruction of the polymer surface. But both the evaporation of dropped liquid and penetration into the pores of membranes should be taken into consideration to avoid misleading results.

Rate of Drop Motion. The rate of motion of drop (i.e. the motion of a three-phase line) can also affect the contact angle measurement. For example, contact angles of different liquids on smooth and homogeneous films of Teflon were studied as a function of the rate of motion of the three-phase line by Tavana and Neumann (2006). For liquids with a dynamic viscosity of well below 10 cP, neither advancing nor receding angles are influenced significantly by the rate of motion up to ~12 mm/min. On the other hand, for more viscous liquids increasing the rate of motion causes the advancing angles to increase

and the receding angles to decrease. Such dynamic contact angles may not be used in conjunction with Young's equation.

Some other factors can also affect the contact angle measurements, which include measurement temperature, surface contamination, etc. In conclusion, the contact angle is a convenient, sensitive, versatile technique for surface property characterization. But it is also a vulnerable technique.

2.5 Characterization of Biocompatibility of Membrane Surfaces

2.5.1 Non-specific Adsorption of Proteins

The polymer membrane is not only useful in the filtration of biological fluids or solutions containing proteins but also widely applied in biomedical devices such as hemodialysis (artificial kidney). Among them, the adsorption of proteins is very important. It is commonly accepted that the first readily observable event at the interface between a material and a biological fluid is protein adsorption. Clearly other interactions precede protein adsorption: water adsorption and possibly absorption, ion bonding and electrical double layer formation, and the adsorption and absorption of low molecular weight solutes such as amino acids. The protein adsorption event must result in major perturbation of the interfacial boundary layer which initially consists of water, ions, and other solutes (Andrade and Hlady, 1986).

The treatment and understanding of protein adsorption requires familiarity with modern concepts of protein structure and function. Proteins are biological macromolecules constructed for specific and unique functions. They are high molecular weight polyamides produced by the specific co-polymerization of up to 20 different amino acids. The properties of proteins influence their adsorption behaviors, which include the size and shape, charge, structure stability, unfolding rate, amino acid sequence, etc.

Proteins of larger size are likely to interact with surfaces because they are able to contact the surface at more sites (Dee et al., 2002). For example, an albumin molecule (67 kDa) forms about 77 contacts with a silica substrate while fibrinogen (340 kDa) forms about 703 contacts per molecule. However, size is not the sole determinant, because hemoglobin (65 kDa) exhibits greater surface activity than the much larger fibrinogen.

Charged amino acids are generally located on the outside of proteins and are readily available to interact with surfaces. Consequently, the charge as well as the distribution of charge on the protein surface, can greatly influence protein adsorption. Interestingly, proteins often show greater surface activity near their isoelectric point (the pH at which the protein molecule exhibits zero charge, denoted pI). One explanation is that at the isoelectric point, reduced electrostatic repulsion between uncharged adsorbing molecules can allow more protein to bind. A second explanation relates to alterations in

protein structure because of changes in the charge of amino acids. If the conformation is altered, different amino acids could be exposed on the surface of the protein, which could consequently change the way the molecule binds to the substrate.

Many other properties of proteins can also influence their adsorption. The case is more complex for system with more than two kinds of proteins. In fact, body fluids or some industrial fluids (e.g. in the food industry) contain numerous types of proteins. When a surface is exposed to different proteins or a multicomponent solution, the adsorption behavior of different types of proteins varies a lot. For example, Palacio et al. studied the fouling with protein mixtures in microfiltration. It was found that for pepsin-bovine serum albumin (BSA) mixtures, the initial fouling appears to be dominated by the BSA. However, the fouling in the case of BSA and lysozyme mixtures is dominated by the lysozyme. Generally, certain proteins will be preferentially deposited from the multicomponent solution. Furthermore, time-dependent changes in the composition of the adsorbed layer can occur, until a pseudo-steady state is reached. In other words, at the initial stage of adsorption, a small protein with larger diffusion coefficient will arrive at the surface quickly and occupy the binding sites. Then proteins with higher affinity while with a lower diffusion rate will reach the surface of the material or the adsorbed protein layer. Substitution between these two kinds of proteins may take place but it is not very easy because substitution means desorption of the previously adsorbed proteins.

It is worth noting that although the adsorption of proteins is also a dynamic process, it does not mean desorption can take place easily. Desorption is the reverse of adsorption: molecules previously bound to a surface detach and return to the bulk phase. For desorption to occur, all contacts between protein and surface must be simultaneously broken. Unlike small molecules such as gases, desorption of proteins is slow or nonexistent. Unless dramatic changes are made in the interfacial environment, such as increased ionic strength, lowered pH, and use of chaotropic agents or detergents, protein adsorption is largely irreversible because of the requirement of simultaneous dissociation of all interactions between protein and surface. The difficulty or improbability of simultaneous disruption of all contacts is increased further by large proteins, which can form a greater number of bonds with the surface.

Understanding of the above-mentioned protein adsorption behavior is very important for the design of a protein-resistant membrane surface. In this chapter we are much more concerned about characterizing the non-specific adsorption of proteins. Fortunately Chan and Chen (2004) have reviewed the characterization of protein fouling on membranes. They reviewed the development of techniques used for membrane protein-fouling characterization, as summarized in Table 2.3.

Table 2.3. Summary table of the techniques used for membrane protein-fouling characterization. Reprinted from (Chan and Chen, 2004), Copyright (2005), with permission from Elsevier

Technique	Sample preparation	Capabilities	Sensitivity
SEM	May involve one or more of fixing in cacodylate buffer/glutaraldehyde; washing in sodium cacodylate buffer; postfixing with buffered osmium tetroxide; dehydration using ethanol-water mixtures and absolute alcohol, critical-point drying; drying, freezing, fracturing and/or metal coating	Spatial imaging of fouled surfaces	4 nm spatial resolution; 0.6∼3 nm for SEM with field emission; 0.5 nm analysis depth
Spectrophotometric determination (not including SDS protein stripping)	Requires solubilized protein samples. For protein-fouled membrane samples, can be achieved by water-washing followed by treatment using 5 wt.% SDS solution	Assays for the quantitative measurement of total protein concentration	0.1∼25µg
Radiolabelling	Requires radioactive labels chemically attached to protein molecules	Quantitative measurement of adsorbed (labelled) proteins	0.01 mg BSA/m^2
XPS	No known sample preparation procedures required	Detection of proteins via atomic composition	0.1 at.%; 1∼25 nm analysis depth
TEM	Staining of proteins required; dehydration and embedding samples in resin; thin sections (∼70 nm) of sample need to be cut using an ultramicrotome	Spatially resolved images of location of adsorbed proteins	0.2 nm spatial resolution; 20 nm analysis depth-dependent on sample thickness
Microspectrophotometry	Staining of membrane samples containing adsorbed proteins using dye such as coomassie blue (0.25 wt.%); sonication; washing in absolute alcohol; air drying	Spatial total protein coverage; potential for quantitative measurement	
EPRS	Chemical attachment of spin labels to protein molecules	Quantification of protein fouling; detection of protein denaturation	2.3 ng of labeled BSA

Technique	Sample preparation	Capabilities	Sensitivity
ATR-FTIR	For fouled membranes, washing and drying overnight at room temperature; for flow-cell operation, a thin polymer (dip-cast) coating needs to be applied to the IRE	Quantification of protein fouling; depth profiling; in situ measurement using polymer film under flow-cell conditions	1 mol%; analysis depth 1∼5 μm
Ellipsometry	Spin-coating of polymer on a reflecting surface of high refractive index	Quantification of protein fouling; thickness measurement; in situ measurement using polymer film; direct analysis of membrane also possible	<0.1μm for thickness measurement
SANS	Membranes need to be transparent to neutrons; no known other preparation procedures required	Quantification and location of protein fouling; thickness measurement; structural characterization; in situ measurement using filtration apparatus	
Confocal microscopy	Fluorescent labeling of proteins and membranes	Protein differentiation using fluorescent labels; depth measurement; potential for quantitative measurement	Analysis depth 50 μm
MALDI-MS	For conventional MALDI-MS, requires dissolved analyte and matrix solutions to be deposited/mixed on metallic target/substrate and dried; for redissolution MALDI-MS, requires application of matrix solution followed by drying 100:1∼50,000:1 molar ratio of matrix to analyte is optimal for ion production	Protein differentiation based on molecular weight; quantitative measurement; potential for depth measurement by varying laser power	Mass resolution $(m/\Delta m)$ of 300∼500; 1 pmo∼1 fmol
AFM	No known sample preparation procedures required; analysis can be performed in solution	Topography measurement; protein-protein and protein-membrane force measurement; modes: contact, non-contact, tapping	0.1 nm lateral resolution, 0.01 nm vertical resolution; typically 10^{-8} to 10^{-7} N; 10^{-12} N in air for non-contact mode

(To be continued)

Technique	Sample preparation	Capabilities	Sensitivity
SFA	Spin-coating of polymer film to mica analyzing surfaces; proteins physisorbed or chemisorbed to mica surfaces	Protein–protein and protein–membrane force measurement; measurement in liquid, including aqueous electrolyte solutions	10^{-9} N
Streaming potential	No known sample preparation procedures required	Measurement/ estimation of charge (zeta potential) on clean or fouled membrane in-situ measurement	MV
SPR	Thin polymer coating applied to metal (gold or silver) film	Quantification of protein fouling—thickness in-situ measurement using polymer film under flow-cell conditions	
NMR	No known sample preparation procedures required, although membrane must fit into magnetic coils	Non-invasive, in situ imaging of concentration polarization under flow conditions	10 µm
SIMS	Drying of samples under vacuum; freeze-drying of samples preferred in order to avoid artifacts, especially for biological samples	Differentiation of adsorbed proteins using PCA or neural network analysis; examination of orientation and conformation of adsorbed proteins	1 nm∼1 µm analysis depth
ESEM	No known sample preparation procedures required	Imaging in hydrated/natural state	Resolution generally lower than conventional SEM
ISE	As for ellipsometry	High-resolution imaging of topography over wider areas than conventional ellipsometry	<100 nm for thickness measurement

2.5.2 Interactions between Blood and Membrane

The medical use of membranes has been evolving since the 1940s. Today microfiltration membranes and ultrafiltration membranes are widely used as blood-contact devices in blood apheresis and purification for blood collection or disease therapies, e.g. hemodialysis (artificial kidney), plasmapheresis, plasma fractionation, leukofiltration and artificial liver (Sun et al., 2003). In

these processes, hemolysis, blood coagulation or other damage to blood cells should be definitely avoided.

Blood is a mixture of plasma (a solution of water, salts and proteins), various kinds of cells, and platelets (biologically active cellular fragments) (Dee et al., 2002). Because of the complexity of blood, its interaction with materials is also considerably complex while important. Generally, when blood makes contact with a membrane surface, the proteins adsorb first, followed by the adhesion of platelets as well as their activation. The hemostatic mechanism is designed to arrest bleeding from injured blood vessels. The same process may produce adverse consequences when artificial surfaces are placed in contact with blood, and involve a complex set of interdependent reactions between the membrane, platelets, coagulation proteins, resulting in the formation of a clot or thrombus which may subsequently undergo removal by and fibrinolysis. So platelets play a key role in blood-membrane interactions.

Platelets are non-nucleated, disk-shaped cells having a diameter of 3∼4 μm, and an average volume of 10^{-10} mm^3 (Ratner et al., 1996). Platelets are produced in the bone marrow, circulate at an average concentration of about 250,000 cells per microliter, and occupy approximately 0.3% of the total blood volume. One of the platelets' main roles in the vasculature is essentially to "plug holes" in blood vessels by adhering to and covering sites of injury, preventing blood loss from the vessel. Platelets can also cause catalyzing coagulation reactions, leading to the formation of fibrin, because platelets contain a variety of chemicals. The formation of a blood clot (coagulation) is not a simple event but a result of cascading chemical reactions of plasma proteins (clotting factors). The coagulation cascade can be divided into an extrinsic pathway and an intrinsic pathway. They are briefly illustrated in Fig.2.27.

It is worth noting that the coagulation cascades can be viewed as a complex engineering system, with potential feedback and feed-forward loops, which allows us to identify the following control points within the cascades that are vital to controlling the process (Dee et al., 2002).

Calcium. Calcium ions are required for all reactions in the coagulation cascades except for the activation of factor XII and factor XI. In the absence of calcium ions, blood will not clot. Precipitating or chelating calcium (with, for example, ethylenediamine-tetraacetic acid (EDTA)) is one way to allow storage of blood outside the body without inducing coagulation.

Thrombin. Note that thrombin is a key element in the common pathway and in feedback loops. It is then logical that controlling the availability and reactivity of thrombin would allow a good deal of control over the end stages of coagulation.

Platelet Contributions. Platelets adhere quickly to foreign (nonendothelial) surfaces, initiating an outbreak of platelet aggregation. Understanding how platelets adhere to surfaces may allow the design of biomaterial surfaces that could be largely "ignored" by platelets. Moreover, platelet phospholipids
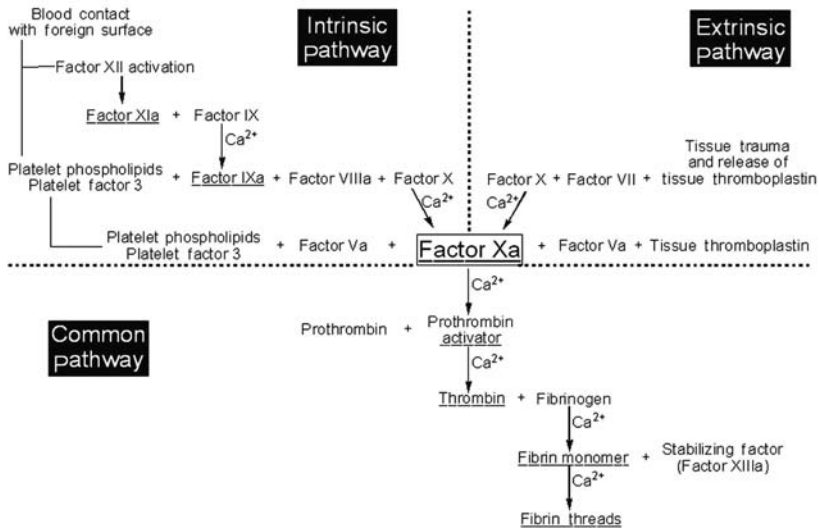
Fig. 2.27. The coagulation cascades of intrinsic and extrinsic pathway

(either released from the membranes of disrupted platelets or displayed on the surface of adherent and aggregating platelets) play roles in both the extrinsic and intrinsic pathways. In many ways, the platelet membrane can be viewed as a surface catalyst for coagulation.

Clotting Factors. Factor X is the link between the extrinsic and intrinsic pathways, making this factor a key control point. Deficiency of factor VIII is the cause of hemophilia A, a disease caused by a recessive defect of the X chromosome. Patients with hemophilia A experience excessive bleeding from mild trauma, sometimes only subsiding on an injection of factor VIII.

Based on the interactions between blood and membranes, hemocompatibility testing of membranes can be performed according to a standardized procedure (such as ISO 10993-4) (Seyfert et al., 2002). The in vitro testing includes contact activation, complement activation, thrombin generation, fibrinogen-fibrin conversion, fibrinolysis, hemolysis, proteolysis, platelet activation, etc. Among them, platelet adhesion is often performed in a laboratory in which the amount and morphology of the adhered platelets can be evaluated. Ko et al.(1993) classified the shape change of activated platelets into five stages in the following sequence: discoid, dendritic (early pseudopodial), spread-dendritic (intermediate pseudopodial), spreading (late pseudopodial and hyaloplasm spreading), and fully spreading (hyaloplasm well spreading and no distinct pseudopodia), as shown in Table 2.4.

Table 2.4. Five stages of platelet morphological changes upon adhesion to foreign surfaces

Stage	Morphology description
Round	Round or discoid, no pesudopodia present
Dendritic	Early pesudopodial, no flattening evident
Spread dendritic	Intermediate pesudopodial, one or more pesudopodia flattened, hyaloplasm not spread between pseudopodia
Spreading	Late pesudopodial, hyaloplasm spreading
Fully spread	Hyaloplasm well spread, no distinct pseudopodia

2.5.3 Interactions Between Cells and Membrane

Since synthetic membranes were introduced in the extra-corporal treatment of kidney failure, significant efforts were made to develop membranes with better hemocompatibility. In general, polymer membranes must possess specific functional characteristics to be used in extra-corporal devices for hemodialysis, like selective permeability, biostability and low interactions with proteins and cells. Hence, most of the membranes developed for conventional blood-contacting biomedical applications are optimized to be inert and non-interacting with the blood proteins, as well as with cells. Membranes for some other applications such as water treatment also require suppression of cell adhesion to reduce membrane fouling.

On the other hand, tissue engineering usually requires a scaffold of porosity. Many methods for preparing separation membranes especially microporous membranes, such as thermally induced phase separation, are suitable techniques to fabricate scaffolds for cell culture. Therefore, membranes have been applied for cell culture. Membranes considered for the immobilization of tissue cells, like hepatocytes, ought to support cell attachment and promote the proliferation and function of these cells. Biohybrid liver support systems are based on the immobilization of hepatocytes on membranes, which should function over distinct periods of time to replace the liver function in cases of fulminant hepatic failure (Krasteva et al., 2002).

The interactions between cells and membrane are just like those for other materials, which are quite complicated. Numerous factors may influence cell behavior on the membrane surface. They include the surface properties of the membrane, such as the porosity, roughness, surface wettability, surface charge, surface chemistry, etc. Beside this, different types of cells exhibit dissimilar behavior even on the same substratum. Therefore, the characterization of interactions between cells and membranes depends on the type of cell. Generally, cell attachment, morphology, proliferation and functions should be investigated in detail. For example, Krasteva et al.(2002) studied the interactions between human hepatoblastoma C3A cells and four kinds of membranes, which are possibly applicable in biohybrid liver support systems. In their work, the ability of the membranes to support cell attachment, morphology, proliferation and function of the cells was studied.

References

Adamsons K (2000) Chemical surface characterization and depth profiling of automotive coating systems. Prog Polym Sci 25:1363-1409

Andrade JD, Hlady V (1986) Protein adsorption and materials biocompatibility: A tutorial review and suggested hypotheses. Biopolymers/Non-Exclusion HPLC, Heidelberg

Asatekin A, Menniti A, Kang S, Elimelech M, Morgenroth E, Mayes AM (2006) Antifouling nanofiltration membranes for membrane bioreactors from self-assembling graft copolymers. J Membrane Sci 285:81-89

Belfer S, Fainchtain R, Purinson Y, Kedem O (2000) Surface characterization by FTIR-ATR spectroscopy of polyethersulfone membranes-unmodified, modified and protein fouled. J Membrane Sci 172:113-124

Bellamy LJ (1974) The Infrared Spectra of Complex Molecules. Chapman and Hall, New York

Bletsos IV, Hercules DM, Benninghoven A, Greifendorf D (1986) SIMSV. Springer-Verlag, Berlin

Brant JA, Childress AE (2004) Colloidal adhesion to hydrophilic membrane surfaces. J Membrane Sci 241:235-248

Briggs D (1998) Surface analysis of polymers by XPS and static SIMS. Cambridge University Press, UK

Bubert H, Jenett H (2002) Surface and thin film analysis: Principles, instrumentation, applications. Wiley-VCH Verlag GmbH, Weinheim

Cassie ABD, Baxter S (1944) Wettability of porous surfaces. Transac Farad Soc 40:546-551

Chan R, Chen V (2004) Characterization of protein fouling on membranes: opportunities and challenges. J Membrane Sci 242:169-188

Charcosset C, Bernengo JC (2000) Comparison of microporous membrane morphologies using confocal scanning laser microscopy. J Membrane Sci 168:53-62

Charcosset C, Cherfi A, Bernengo JC (2000) Characterization of microporous membrane morphology using confocal scanning laser microscopy. Chem Eng Sci 55:5351-5358

Chen V, Li H, Fane AG (2004) Non-invasive observation of synthetic membrane processes–a review of methods. J Membrane Sci 241:23-44

Chen W, McCarthy TJ (1999) Adsorption/migration of a perfluorohexylated fullerene from the bulk to the polymer/air interface. Macromolecules 32:2342-2347

Choi H, Zhang K, Dionysiou DD, Oerther DB, Sorial GA (2005) Effect of permeate flux and tangential flow on membrane fouling for wastewater treatment. Sep Purif Technol 45:68-78

de los Rios AP, Hernandez-Fernandez FJ, Tomas-Alonso F, Palacios JM, Gomez D, Rubio M, Villora G (2007) A SEM-EDX study of highly stable supported liquid membranes based on ionic liquids. J Membrane Sci 300:88-94

Dee KC, Puleo DA, Bizios R (2002) An introduction to tissue-biomaterial interactions. John Wiley & Sons, New York

Ferrando M, Rozek A, Zator M, Lopez F, Guell C (2005) An approach to membrane fouling characterization by confocal scanning laser microscopy. J Membrane Sci 250:283-293

Flosch D, Lehmann HD, Reichl R, Inacker O, Gopel W (1992) Surface analysis of poly(vinylidene difluoride) membranes. J Membrane Sci 70:53-63

Hanton SD (2001) Mass spectrometry of polymers and polymer surfaces. Chem Rev 101:527-569

Hayama M, Miyasaka T, Mochizuki S, Asahara H, Yamamoto KI, Kohori F, Tsujioka K, Sakai K (2003) Optimum dialysis membrane for endotoxin blocking. J Membrane Sci 219:15-25

Jiang EY (2003) Advanced FT-IR spectroscopy. Thermo Electron Corporation, Madison

Klee D, Hocker H (1999) Polymers for biomedical applications: Improvement of the interface compatibility. Adv Polym Sci. 149:1-57

Ko TM, Lin JC, Cooper SL (1993) Surface characterization and platelet adhesion studies of plasma-sulphonated polyethylene. Biomaterials 14:657-664

Krasteva N, Harms U, Albrecht W, Seifert B, Hopp M, Altankov G, Groth T (2002) Membranes for biohybrid liver support systems – investigations on hepatocyte attachment, morphology and growth. Biomaterials 23:2467-2478

Le-Clech P, Marselina Y, Ye Y, Stuetz RM, Chen V (2007) Visualisation of polysaccharide fouling on microporous membrane using different characterisation techniques. J Membrane Sci 290:36-45

Li D (1996) Drop size dependence of contact angles and line tensions of solid-liquid systems. Colloid Surf A: Physicochem Eng Asp 116:1-23

Lindon J, Tranter G, Holmes J (2000) Encyclopedia of spectroscopy and spectrometry. Academic Press, San Diego

Mulder M (1996) Basic principles of membrane technology. Kluwer Academic Publishers, Dordrecht

Noda I (1989) Two-dimensional infrared spectroscopy. J Am Chem Soc 111:8116-8118

Noda I (1990) Two dimensional infrared (2D IR) spectroscopy: Theory and applications. Appl Spectrosc 44:550-561

Optics PE (1998) Environmental scanning electron microscopy: An introduction to ESEM. Robert Johnson Associates, Dorado Hills

Palacio L, Ho CC, Prádanos P, Hernández A, Zydney AL (2003) Fouling with protein mixtures in microfiltration: BSA-lysozyme and BSA-pepsin. J Membrane Sci 222:41-51

Ratner BD, Hoffman AS, Schoen FJ, Lemons JE (1996) Biomaterials science: An introduction to materials in medicine. Academic Press, San Diego

Reichert U, Linden T, Belfort G, Kula MR, Thommes J (2002) Visualising protein adsorption to ion-exchange membranes by confocal microscopy. J Membrane Sci 199:161-166

Sawyer LC, Grubb DT (1987) Polymer microscopy. Chapman & Hall, New York

Seyfert UT, Biehl V, Schenk J (2002) In vitro hemocompatibility testing of biomaterials according to the ISO 10993-4. Biomol Eng 19:91-96

Sun SD, Yue YL, Huang XH, Meng DY (2003) Protein adsorption on blood-contact membranes. J Membrane Sci 222:3-18

Taniguchi M, Pieracci JP, Belfort G (2001) Effect of undulations on surface energy: A quantitative assessment. Langmuir 17:4312-4315

Tavana H, Neumann AW (2006) On the question of rate-dependence of contact angles. Colloid Surface A 282-283:256-262

Vancso GJ, Hillborg H, Schonherr H (2005) Chemical composition of polymer surfaces imaged by atomic force microscopy and complementary approaches. Adv Polym Sci. 182:55-129

Wan LS, Huang XJ, Xu ZK (2007) Diffusion and structure of water in polymers containing N-vinyl-2-pyrrolidone. J Phys Chem B 111:922-928

Watts JF, Wolstenholme J (2003) An introduction to surface analysis by XPS and AES. John Wiley & Sons, Chichester

Yeo A, Yang P, Fane AG, White T, Moser HO (2005) Non-invasive observation of external and internal deposition during membrane filtration by X-ray microimaging (XMI). J Membrane Sci 250:189-193

Yildirim I (2001) Surface free energy characterization of powders. Virginia Polytechnic Institute, Blacksburg

Yu J, Lencki RW (2004) Effect of enzyme treatments on the fouling behavior of apple juice during microfiltration. J Food Eng 63:413-423

3

Functionalization Methods for Membrane Surfaces

Surface functionalization of materials is one of the efficient techniques that can endow these materials with novel properties and transform them into valuable finished products. It has been widely applied to polymeric membranes in many fields and has progressed rapidly in recent years. In this chapter, therefore, important approaches to the surface functionalization of polymeric membranes are briefly described.

3.1 Introduction

Membrane filtration has been considered a technically important separation process over 40 years. Up to now, membrane processes have been developed for a wide range of applications such as microfiltration (MF), ultrafiltration (UF), nanofiltration (NF), reverse osmosis (RO), electrodialysis (ED), membrane electrolysis (ME), diffusion dialysis (DD), gas separation (GS), vapour permeation (VP), pervaporation (PV), membrane distillation (MD), and membrane contactor (MC). The number of such applications is still growing. To further enlarge the applications of the existing polymeric membranes in the advent fields, the surface functionalization of preformed (established) membranes has already become a key point in membrane science and technology. It can improve the performance of the existing polymeric membranes either by minimizing undesired interactions (adsorption or adhesion) that reduce the performance (membrane fouling) or by introducing additional interactions (affinity, responsiveness or catalytic properties) for entirely novel functionalities. In this chapter different functional methods — surface modification, enzyme immobilization and molecular imprinting, all based on an even surface coverage of the entire surface of polymeric membranes — are covered briefly.

3.2 Functionalization of Polymeric Membranes by Surface Modification

Generally, some polymeric materials that have excellent physical bulk and chemical properties often do not possess the suitable surface properties required for specific applications. For this reason, surface modification of polymeric membranes has been of prime importance in various applications from the advent of membrane-involving industries. It offers a versatile means for improving the surface properties (such as hydrophilicity, hydrophobicity, biocompatibility, anti-fouling, surface roughness, antistatic and antibacterial properties, and even conductivity) while preserving the bulk structure of the base membrane. Herein, various methods of surface modification for polymeric membranes have been proposed, e.g. coating, self-assembly, chemical treatment, plasma treatment, and surface graft polymerization.

3.2.1 Coating

Coating is a physical modification method (Mackerle, 2005). The principle and operation of coating is very simple. Hydrophilic or biocompatible materials are physically deposited on the membrane surface via one (or more) of the following mechanisms: (1) adsorption/adhesion — the functional layer is only physically fabricated on the base polymer; the binding strength can be increased via multiple interactions between functional groups in the macromolecular layer and on the solid surface; (2) interpenetration by mixing between the added functional material and the base polymer in an interphase; (3) mechanical interpenetration (macroscopic entanglement) of an added material layer and the pore structure of the membrane. By coating these functional materials on the membrane, the surface property of the membrane could change from hydrophobic or non-biocompatible to hydrophilic and biocompatible. However, this method cannot gain a stable surface, for the materials absorbed on the membrane surface run away easily (Dickson et al., 1998).

3.2.2 Self-assembly

Self-assembly is a very common phenomenon in nature. Many super-molecular structures and complex systems are formed by self-assembly. Self-assembly involves self-assembled monolayers (SAMs) and layer-by-layer (LBL) assembly, which is a new technique for membrane surface engineering. SAMs are ordered molecular assemblies formed by the adsorption of an active surfactant on a solid surface (Ruckenstein and Li, 2005; Ulman, 1996). The order in these two-dimensional systems is produced by a spontaneous chemical synthesis at the interface, as the system approaches equilibrium. Since surface properties are generally considered to be controlled by the outmost 5~10 Å

on a polymeric film, SAMs are especially suited for the control of surface functional group concentration. These surfaces can be produced with different surface energies or surface tensions, which are models for studying the principle of surface interaction.

In 1991, Decher and co-workers introduced a related method for film assembly by means of alternate adsorption of linear polycations and polyanions, or bipolar amphiphiles (Lvov et al., 1993). The process is schematically depicted in Fig.3.1. In this method the crucial feature is excessive adsorption at every stage of the polycation/polyanion assembly that leads to recharging of the outermost surface at every step of film formation. The build-up is easy, and the procedure can be adopted to almost any surface as long as surface charges are present. This technique is very suitable for membrane surface functionalization due to its simplicity and versatility. The process has many important advantages over other techniques for preparing functional materials, for example, the assembly is based on spontaneous adsorptions and no stoichiometric control is necessary to maintain surface functionality, the assembled molecular layers exhibit a much larger thermal and mechanical stability. Most of all, the method is not restricted to substratum and can be used for designing a surface on nanoscale.
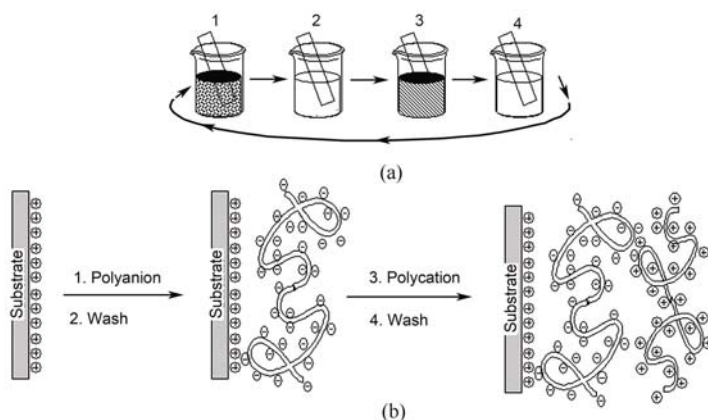
Fig. 3.1. (a) Schematic representation of the film deposition process using slides and beakers. Steps 1 and 3 represent the adsorption of a polyanion and polycation, respectively, and steps 2 and 4 are washing steps; (b) Simplified molecular picture of the first two adsorption steps depicting film deposition starting with a positively charged substrate. From (Decher, 1997). Reprinted with permission from AAAS

3.2.3 Chemical Treatment

Chemical treatment is one of the familiar methods for endowing a membrane surface with types of functional groups and the modified surface is relatively stable. This modification retains the mechanical properties of the membrane while the interfacial properties are changed. Chemical treatments include oxidation, addition, substitution and hydrolysis. Oxidative treatment is the dominant means for chemically modified reactions, which generally involve dry or wet oxidation (Barton et al., 1997; Lu et al., 2005; Pradhan and Sandle, 1999). In the case of dry oxidation, a gaseous oxidation agent, like oxygen, ozone or carbon dioxide is often used. Oxygen-containing groups such as hydroxyl and carboxyl are introduced onto the membrane surface by flame treatment or corona discharge in these gases. These groups can also be introduced onto a membrane by wet oxidation. Wet chemical oxidation involves the use of nitric acid, sulfuric acid, phosphoric acid, alone or in combination with hydrogen peroxide, sodium hypochlorite, permanganate, chromate or dichromate of potassium, transition metal nitrates, etc. The other reactions are also very useful for introducing functional groups to the accessible materials. For example, the nitrile group of polyacrylonitrile (PAN) can be easily hydrolyzed by NaOH or amine, and converted into carboxyl, acrylamide or amide groups. Hydrophilicity of PAN-based membranes can be remarkably increased by this process. These chemical treatments gain a relatively stable modified surface, which can be applied to modify the physical and chemical properties of the polymeric membranes surface.

3.2.4 Plasma Treatment

Plasma, which can be regarded as the fourth state of matter, is composed of highly excited atomic, molecular, ionic, and radical species. Plasma is a highly unusual and reactive chemical environment in which many plasma-surface reactions occur. Surface modification with plasma is an effective and economical surface treatment technique for a membrane (Chu et al., 2002; Denes and Manolache, 2004; Forch et al., 2005; Kang et al., 2001). The unique advantage of plasma modification is that the surface properties and biocompatibility can be enhanced selectively while the bulk attributes of the membrane remain unchanged. As shown in Fig.3.2, plasma treatment for the surface modification of membranes includes plasma sputtering, etching, implantation, and spraying.

3.2.4.1 Plasma Sputtering

Plasma sputtering is a simple and physical plasma treatment process. During the process, inert gases such as neon and argon are activated to form plasma and accelerated towards the substrate. Their energy is transferred to the surface atoms via elastic and inelastic collisions with the materials. Some
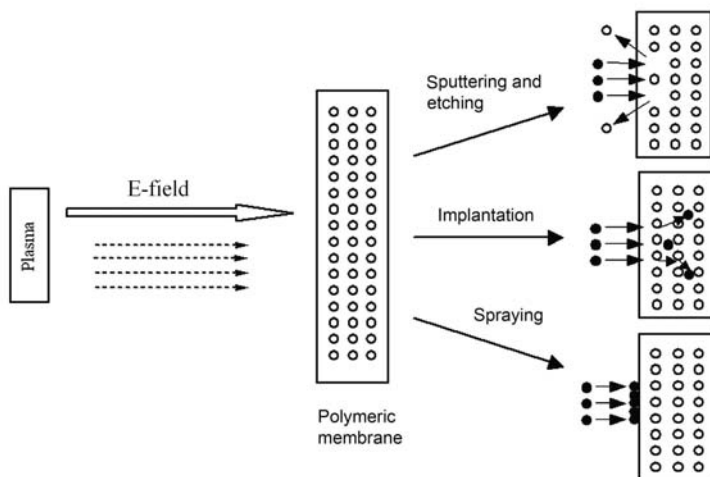
Fig. 3.2. Schematic illustration of plasma treatment technique

surface atoms will acquire enough energy and escape from the substrate to the vacuum chamber. With sufficient sputtering time, surface contamination will be cleaned off, so this process is also called plasma cleaning.

3.2.4.2 Plasma Implantation

Implantation can introduce elements onto the membrane surface without thermodynamic constraints. When polymeric membranes are exposed to plasma and if the plasma density and treatment time are correct, many functionalities will be created near the surface and crosslinked polymer chains can be formed. In a typical plasma implantation process, hydrogen is first abstracted from the polymer chains to create radicals at the midpoint of the polymer chains, and the polymer radicals then recombine with simple radicals created by the plasma gas to form oxygen or nitrogen functionalities. Generally, formation of oxygen functionalities by ion implantation can convert the membrane surface from hydrophobic to hydrophilic, which improves the adhesion strength, biocompatibility, and other pertinent properties. Besides oxygen functionalities, chlorine functionalities that can contribute to an increase in the hydrophilicity are formed using $CHCl_3$ and CCl_4 plasmas. On the other hand, if one wants to improve the hydrophobic properties of the polymer, higher-degree fluorinated compounds such as SF_6, CF_4, and C_2F_6 are used as plasma gases.

3.2.4.3 Plasma Spraying

In atmospheric pressure plasma spraying, the powders of the sprayed materials are introduced into the plasma area of the plasma torch. Because of

the high-temperature and flux velocity of the plasma, the melted or partially melted powders are accelerated towards the substrate at high speed, forming a coating with a lamellae structure. This technique can conveniently treat specimens with a complex geometry and can handle a wide spectrum of materials. It has spurred applications in the area of corrosion resistant, high-temperature, and ablation resistant coatings.

3.2.5 Graft Polymerization

Surface grafting is a chemical modification method. In surface graft polymerization, the modification is achieved by tethering suitable macromolecular chains on the membrane surface through covalent bonding. The key advantage of this technique is that the membrane surface can be modified or tailored to acquire distinctive properties through the choice of different grafting monomers, while maintaining the substrate properties. It also ensures an easy and controllable introduction of tethered chains with a high density and exact localization onto the membrane surface (Bhattacharya and Misra, 2004; Kato et al., 2003). Compared with the physical modification methods such as coating, the covalent attachment of polymer chains onto the membrane surface avoids desorption and maintains the long-term chemical stability of the modified surface.
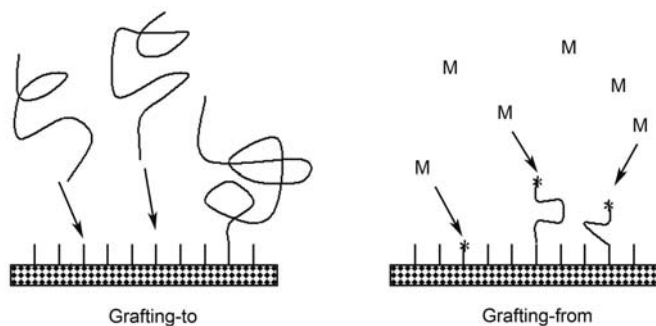
Fig. 3.3. Functionalized polymer membranes by 'grafting-to' and 'grafting-from'. Reprinted from (Zhao and Brittain, 2000), Copyright (2000), with permission from Elsevier

As shown in Fig.3.3, the grafting methods can be generally divided into two classes, i.e., 'grafting-to' and 'grafting-from' processes. In the case of the 'grafting-to' method, preformed polymer chains carrying reactive groups at the end or side chains are covalently coupled onto the membrane surface. The 'grafting-from' method utilizes active species existing on the membrane surfaces to initiate the polymerization of monomers from the surface toward the

outside bulk phase. These techniques can also be classified as chemical, radiation, photochemical, and plasma-induced, according to the different methods used for the generation of reactive groups.

3.2.5.1 Grafting Initiated by Chemical Means

Chemical grafting can proceed by activating functional groups on the membrane surface and reacting with monomers or macromolecules. The path of the grafting process, including free radical and ionic, is determined by the species of initiator. In these two paths, active sites are produced from the initiators and transferred to the substrate to react with the monomer and then to form grafted co-polymers. Typical free radical grafting is generated by a redox reaction, viz. M^{n+}/H_2O_2, persulphates. On the other hand, alkali metal suspensions in a Lewis base liquid, organometallic compounds, and sodium naphthalenide are useful initiators in an ionic mode. In recent years, methods of 'Living Polymerization' have been developed to provide great potential for grafting reactions. In these cases, they provide living polymers with regulated molecular weights and low polydispersities, which mean that a controlled and uniform polymer layer can be generated on the membrane surface.

3.2.5.2 Grafting Initiated by Radiation Technique

Interaction of a membrane with irradiation can cause homolytic fission of polymer chains and thus form free radicals on the surface for further grafting polymerization. Radiation grafting proceeds in two major ways: (1) pre-irradiation and (2) mutual irradiation techniques. In the pre-irradiation technique, the membrane surface is first irradiated and then the radical-possessing substrate is grafted with a monomer. On the other hand, with the mutual irradiation technique, membrane and monomer are irradiated simultaneously, to form free radicals and subsequent graft polymerization. Since the monomers are not exposed to radiation in the pre-irradiation technique, an obvious advantage is that this method is relatively free from homopolymer formation, which occurs in the process of mutual irradiation. However, due to direct irradiation on the membrane surface, a decided disadvantage of the pre-irradiation technique is the scission of the polymer chains, which can result in decrease of mechanical strength.

Many factors affect the results of radiation grafting, for example, the properties of membrane and monomer, concentration of the monomer, the duration of radiation, reaction temperature, the medium, etc. In addition, high-energy radiation goes through the uppermost layer of the membrane, and may change the physical or chemical properties of the substrate.

3.2.5.3 Photochemical Grafting

When groups on the membrane surface absorb light, they go to excited states, which may generate reactive radicals and then initiate the grafting process (Dyer, 2006). The outstanding feature of this technique is that takes place at the outmost surface of the membrane and does not change the properties of the original polymer. The grafting process by a photochemical technique can proceed in two ways: with or without a sensitizer, which can promote the generation of reactive radicals. The mechanism 'without sensitizer' involves the generation of free radicals on the backbone, which react with the monomer free radical to form a grafted co-polymer. On the other hand, in the mechanism 'with sensitizer', the sensitizer forms free radicals, which can abstract hydrogen atoms from the base polymer, producing the radical sites required for grafting.

3.2.5.4 Plasma-grafting Polymerization

When a polymeric membrane is exposed to plasma, radicals are created on the surface. These radicals can and do initiate polymerization reactions when put in contact with monomers in the liquid or gas phase. As a result, grafted copolymers are formed on the surface. Since the plasma and membrane surface produces radicals only close to the surface of the membrane, plasma-grafting polymerization is restricted to the near surface. It is usually conducted by first exposing a membrane to a plasma such as argon, helium, or nitrogen for a short time (a few seconds), introducing many radicals onto the membrane surface. Afterwards, the membrane is brought into contact with the vapor of a monomer at an elevated temperature for a period of time. Oxygen in the monomer vapor or dissolved in the monomer solution inhibits the reactions and should be avoided. Plasma-grafting polymerization is often employed to alter the surface hydrophilicity of a membrane.

3.3 Functionalization of Polymeric Membrane by Molecular Imprinting

Molecularly imprinted membranes combine the characteristics of membrane separation technology (such as continuous operation, low energy consumption and high efficiency of transport) with the highly selective recognition of the molecular imprinting technique. It is regarded as a novel functional polymer membrane in possession of potential perspectives for application (Piletsky et al., 1999; Ulbricht, 2004). Up to now, several methods have been commonly mentioned to prepare a molecularly imprinted membrane, e.g. bulk polymerization, physical mixing and surface imprinting. Generally speaking, the permeability of the former two kinds of membrane is relatively low, which will limit their applications in affinity separation. In addition, some of the

imprinted sites are embedded in the membranes resulting in low availability of efficient imprinting sites. However, in the surface imprinting method, due to the high porosity and good mechanical properties of the support membrane, the resultant composite membrane, with a large surface area to volume ratio, has excellent permeability, binding capability and good stability. Furthermore, the available imprinted sites are mostly located on the membrane surface, facilitating fast recognition, especially for natural macromolecules. Therefore, molecular imprinting on the membrane surface has attracted much attention in recent years. Several methods have been developed to form imprinting sites on the surface.

3.3.1 Formation of Imprinting Sites by Surface Photografting

This is also regarded as a "grafting-from" approach, as can be seen in Fig.3.4. The starter radicals are commonly yielded on the membrane substrate under UV excitation, and the imprinted layers are covalently anchored and cover the entire surface of the support membrane. It can be an intrinsic initiation of photosensitive groups introduced onto the membrane surface by graft or block polymerization instead of added photo-initiators (Wang et al., 1997). Despite the higher surface selectivity of initiation, it is limited to a few polymers and the efficiency is rather low. As a result, this approach is not used widely, and only for special materials. The other approach can be a coated initiation via a hydrogen-abstracting photoinitiator yielding polymer starter radicals on the substrate (Ulbricht et al., 2002). It is adapted to any kind of membrane with the presence of C-H bonds, e.g. a porous polypropylene membrane. Compared with the intrinsic initiation, this approach is widely adopted due to its simplicity in preparation and to its relatively extensive applicability.
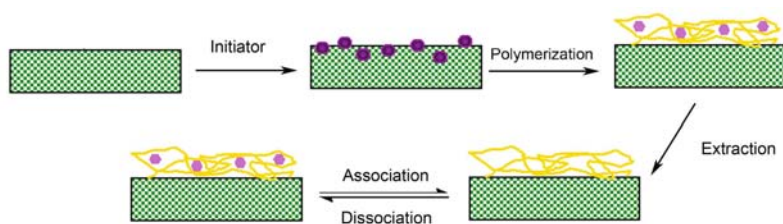
Fig. 3.4. Illustration of surface photo-grafting for the formation of molecularly imprinting sites. Reprinted with permission from (Ulbricht and Yang, 2005). Copyright (2005), American Chemical Society

3.3.2 Formation of Imprinting Sites by Surface Deposition

Surface deposition is an approach used in preparing a thin-layer MIP composite membrane using a very efficient coated α-scission photoinitiator, e.g.

benzoin ethyl ether (BEE) (Kochkodan et al., 2002), yielding starter radicals close to the membrane surface under UV excitation. Because the support membrane is relatively inert to the photoinitiator, no chemical bonding is formed between the imprinted layer and the base membrane. In consequence, this approach is generally considered as a deposition process. In comparison with surface photo-grafting, it is agreed that surface deposition is a more general approach due to its applicability for any kind of membrane surface. Up to now much work on surface imprinting has been focused on this approach. It is worth noting that an important problem is how to control the thickness of the deposited layer for a higher capacity. As we know, controlled/living radical copolymerization is a feasible route to achieve a superior relationship between imprinted efficiency and binding capacity (Ruckert et al., 2002; Titirici and Sellergren, 2006).

3.3.3 Formation of Imprinting Sites by Emulsion Polymerization on the Surface

Emulsion polymerization on the surface has been developed for imprinting recently (Han et al., 2003). Briefly, the process is that a porous membrane is dipped into water-in-oil emulsion containing functional polymers and template and followed by a photo-induced polymerization. Consequently, a thin MIP layer is formed on the support membrane, as shown in Fig.3.5. The advantage of this approach is that imprinted sites are all near or at the surface, reducing mass transfer limitations. More importantly, the imprinting process can be carried out in an aqueous medium rather than in an organic solvent, which may offer a possible approach for imprinting large molecules of biological interest, e.g. protein.
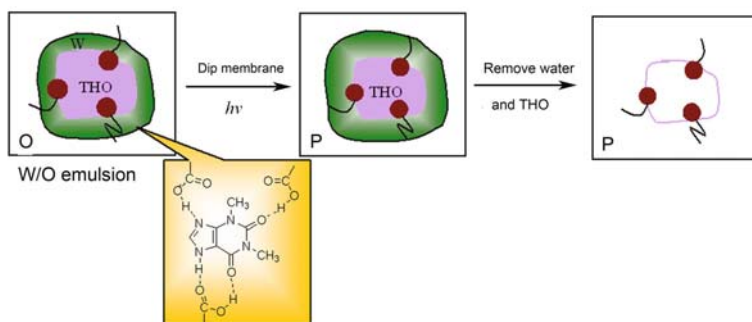
Fig. 3.5. Schematic representation of a novel water-in-oil method for surface imprinting recognition sites onto a microporous substrate. Reprinted with permission from (Han et al., 2003). Copyright (2005), American Chemical Society

3.4 Functionalization of Polymeric Membrane by Enzyme Immobilization

Traditional membrane technology has provided considerable insight into separation and reaction. However, new advances in membrane technology will require synergy between the strength and processing properties of traditional polymeric membranes and the selectivity, through molecular recognition, of biological membranes, so-called biofunctional membranes (Ahuja et al., 2007; Turkova, 1999; Zhao and Brittain, 2000). Biofunctional membranes are entities in which biomacromolecules and/or a collection of cells are immobilized on polymeric matrices cast in the form of membranes.

An enzyme is a kind of biocatalyst. Compared to conventional chemical catalysts, enzymes exhibit a number of features that make their use advantageous. Foremost among them is a high level of catalytic efficiency, often far superior to chemical catalysts, and a high degree of specificity that allows them to discriminate not only between reactions but also between substrates, similar parts of molecules and even optical isomers. In addition, enzymatic catalysis generally operates under mild conditions of temperature, pressure and pH value. By introducing an enzyme to membranes, these biofunctional membranes can combine the functions of separation and catalysis together (Alkorta et al., 1998; Girelli and Mattei, 2005; Girono and Drioli, 2000; Krajewska, 2004). Hereafter we briefly introduce the methods of enzyme immobilization, including physical absorption, chemical binding and entrapment.

3.4.1 Enzyme Immobilization by Physical Absorption

Physical absorption is the most simple and direct method for enzyme immobilization. In this process, the enzyme gets adsorbed on the membrane surface due to the interactions of H-binding, static interaction, electron or ion affinity and hydrophobic force (Arica et al., 2001). This method operates under mild conditions and the residual activity of the immobilized enzyme is relatively high compared to chemical immobilization. However, this process has some known disadvantages. For example, the binding forces are weak and easily change with pH or temperature, and absorption is limited to one monolayer on the membrane surface, hence the amount of enzyme incorporated is very small.

3.4.2 Enzyme Immobilization by Chemical Binding

In order to achieve increased lifetime stability for the immobilized enzyme, it is necessary to have strong and efficient bonding between the enzyme and the substrate. Hence, chemical binding of enzyme biomacromolecules on the membrane is an efficient immobilization method (El-Masry et al., 2000). Usually, the functional groups on the enzyme and the substrate are covalently

bound together, and the enzyme is immobilized onto the substrate. Chemical binding is available for most systems, and it is the most useful method for enzyme immobilization. The groups of enzyme for covalent bonding are the amino group, carboxyl group, phenol group, imidazole group, and indole group. The reactive groups of substrate include the hydroxyl group, carboxyl group, hydroxymethyl group, amino group, etc. Functional groups can be also introduced to the substrate without reactive groups, by grafting. Glutaraldehyde and carbodiimides are two common coupling agents for chemical enzyme immobilization.

Immobilization by chemical binding also involves crosslinking. In this method, the enzyme or bio-macromolecules are joined together by a coupling agent. As a result, enzymes are fixed to or within polymeric supports by crosslinking. An enzyme immobilized by chemical binding has a higher stability, but lower residual activity compared to an enzyme immobilized by physical absorption as a result of denaturalization of enzyme protein during the chemical reaction (Jancsik et al., 1982).

3.4.3 Enzyme Immobilization by Entrapment

As schematically shown in Fig.3.6, entrapment involves two different types, network-like and microcapsule-like (Gekas, 1986). The former is the method where the enzyme is entrapped in a polymer gel network, whereas the enzyme is embedded in a semipermeable microcapsule in the latter method. For enzyme immobilization by entrapment, the secondary structure of the enzyme protein does not change, which normally means the enzyme will have high residual activity. Because big molecules cannot diffuse into the polymer gel or network, this immobilization method can only be applied to the enzyme that prefers small substrate and product. This method also has the disadvantage of low stability like the physical absorption method. To improve the stability of the immobilized enzyme, crosslinking is always used. Absorption/crosslinking and entrapment/crosslinking are two common coupling methods.

(a)   (b)
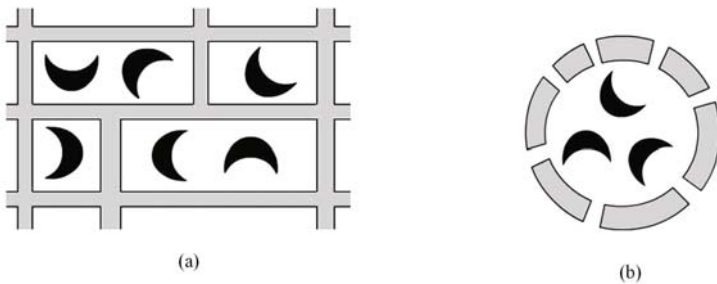
Fig. 3.6. Schematic illustration of two entrapment immobilization methods. (a) Network-like entrapment; (b) Microcapsule-like entrapment

3.4.4 Other Methods for Enzyme Immobilization

The procedures mentioned above for enzyme immobilization have been applied extensively. Nevertheless, they suffer from low reproducibility and poor spatially controlled deposition. In recent years many novel methods have been developed, such as electrochemical immobilization and site-specific immobilization.

Electrochemical entrapment is one of the electrochemical methods. An electrode coated with porous polymer is put into an enzyme solution. When a suitable voltage is applied, the enzyme with a negative charge moves to the anode and is entrapped in the membrane, forming the enzyme immobilized electrode. This method has good operational stability and high catalytic activity (Shan et al., 2006).

In traditional methods, enzymes are always randomly immobilized on the membrane surface. One major disadvantage is that the activity of the immobilized enzyme is often significantly decreased because the active site may be blocked from substrate accessibility, multiple point-binding may occur, or the enzyme protein may be denatured. Site-specific immobilization can overcome these difficulties (Butterfield et al., 2001). Using the power of molecular recognition, enzymes are attached to the membrane surface in a highly ordered array. The active sites of enzymes are away from the attached point, which benefits the diffusion of the substrate (Fig.3.7). These enzymes have superior catalytic properties compared to enzymes that have been immobilized randomly.
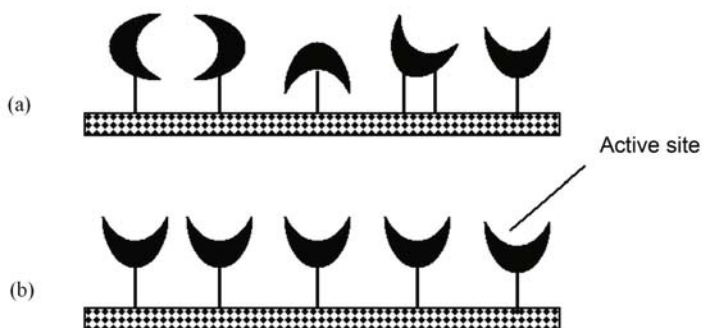
Fig. 3.7. (a) Random immobilization of enzymes; (b) Site-specific immobilization of enzymes to form an array of similarly oriented proteins. Reprinted from (Butterfield et al., 2001), Copyright (2001), with permission from Elsevier

3.5 Conclusion

Various methods for the surface functionalization of polymeric membranes are summarized in this chapter. Surface modification methods, such as coating, self-assembly, chemical treatment, plasma treatment and graft polymerization, can be used to endow surface functionalities while preserve the bulk properties of polymeric membranes. The high selectivity of molecular imprinting technique inspires novel strategies for the functionalization of polymeric membrane. Among them the surface imprinting method is the most efficient to facilitate fast recognition. Immobilization of enzymes on membrane surfaces, by synergying the selective separation functions of polymeric membranes with the catalytic properties of enzymes, provides hints for the preparation of biofunctional membranes.

References

Ahuja T, Mir IA, Kumar D, Rajesh (2007) Biomolecular immobilization on conducting polymers for biosensing applications. Biomaterials 28:791-805

Alkorta I, Garbisu C, Llama MJ, Serra JL (1998) Industrial applications of pectic enzymes: A review. Process Biochem 33:21-28

Arica MY, Kacar Y, Ergene A, Denizli A (2001) Reversible immobilization of lipase on phenylalanine containing hydrogel membranes. Process Biochem 36:847-854

Barton SS, Evans MJB, Halliop E, MacDonald JAF (1997) Acidic and basic sites on the surface of porous carbon. Carbon 35:1361-1366

Bhattacharya A, Misra BN (2004) Grafting: A versatile means to modify polymers – Techniques, factors and applications. Prog Polym Sci 29:767-814

Butterfield DA, Bhattacharyya D, Daunert S, Bachas L (2001) Catalytic biofunctional membranes containing site-specifically immobilized enzyme arrays: A review. J Membr Sci 181:29-37

Chu PK, Chen JY, Wang LP, Huang N (2002) Plasma-surface modification of biomaterials. Mat S Eng R 36:143-206

Decher G (1997) Fuzzy nanoassemblies: Toward layered polymeric multicomposites. Science 277:1232

Denes FS, Manolache S (2004) Macromolecular plasma-chemistry: An emerging field of polymer science. Prog Polym Sci 29:815-885

Dickson JM, Childs RF, McCarry BE, Gagnon DR (1998) Development of a coating technique for the internal structure of polypropylene microfiltration membranes. J Membr Sci 16:25-36

Dyer DJ (2006) Photoinitiated synthesis of grafted polymers. Adv Polym Sci 197:47-65

El-Masry MM, De Maio A, Di Martino S, Diano N, Bencivenga U, Rossi S, Grano V, Canciglia P, Portaccio M, Gaeta FS, et al. (2000) Modulation of immobilized enzyme activity by altering the hydrophobicity of nylon-grafted membranes – Part 1. Isothermal conditions. J Mol Catal B-Enzym 9:219-230

Forch R, Zhang ZH, Knoll W (2005) Soft plasma treated surfaces: Tailoring of structure and properties for biomaterial applications. Plasma Process Polym 2:351-372

Gekas VC (1986) Artificial membranes as carriers for the immobilization of biocatalysts. Enzyme Microb Technol 8:450-460

Girelli AM, Mattei E (2005) Application of immobilized enzyme reactor in on-line high performance liquid chromatography: A review. J Chromatogr B 819:3-16

Girono L, Drioli E (2000) Biocatalytic membrane reactors: Applications and perspectives. Trends Biotechnol 18:339-349

Han MN, Kane R, Goto M, Belfort G (2003) Discriminate surface molecular recognition sites on a microporous substrate: A new approach. Macromolecules 36:4472-4477

Jancsik V, Beleznai Z, Keleti T (1982) Enzyme immobilization by poly(vinyl alcohol) gel entrapment. J Mol Catal B-Enzym 14:297-306

Kang MS, Chun B, Kim SS (2001) Surface modification of polypropylene membrane by low-temperature plasma treatment. J Appl Polym Sci 81:1555-1566

Kato K, Uchida E, Kang ET, Uyama Y, Ikada Y (2003) Polymer surface with graft chains. Prog Polym Sci 28:209-259

Kochkodan V, Weigel W, Ulbricht M (2002) Molecularly imprinted composite membranes for selective binding of desmetryn from aqueous solutions. Desalination 149:323-328

Krajewska B (2004) Application of chitin- and chitosan-based materials for enzyme immobilizations: A review. Enzyme Microb Technol 35:126-139

Lu AH, Li WC, Muratova N, Spliethoff B, Schuth F (2005) Evidence for C-C bond cleavage by H_2O_2 in a mesoporous CMK-5 type carbon at room temperature. Chem Commun 5184-5186

Lvov Y, Decher G, Möhwald H (1993) Assembly, structural characterization, and thermal behavior of layer-by-layer deposited ultrathin films of poly(vinylsulfate) and poly(allylamine). Langmuir 9:481-486

Mackerle J (2005) Coatings and surface modification technologies: A finite element bibliography (1995-2005). Model Simul Mater SC 13:935-979

Piletsky SA, Panasyuk TL, Piletskaya EV, Nicholls IA, Ulbricht M (1999) Receptor and transport properties of imprinted polymer membranes – a review. J Membr Sci 157:263-278

Pradhan BK, Sandle NK (1999) Effect of different oxidizing agent treatments on the surface properties of activated carbons. Carbon 37:1323-1332

Ruckenstein E, Li ZF (2005) Surface modification and functionalization through the self-assembled monolayer and graft polymerization. Adv Colloid Interf Sci 113:43-63

Ruckert B, Hall AJ, Sellergren B (2002) Molecularly imprinted composite materials via iniferter-modified supports. J Mater Chem 12:2275-2280

Shan D, He YY, Wang SX, Xue HG, Zheng H (2006) A porous poly(acrylonitrile-co-acrylic acid) film-based glucose biosensor constructed by electrochemical entrapment. Anal Biochem 356:215-221

Titirici MM, Sellergren B (2006) Thin molecularly imprinted polymer films via reversible addition-fragmentation chain transfer polymerization. Chem Mater 18:1773-1779

Turkova J (1999) Oriented immobilization of biologically active proteins as a tool for revealing protein interactions and function. J Chromatogr B 722:11-31

Ulbricht M (2004) Membrane separations using molecularly imprinted polymers. J Chromatogr B 804:113-125

Ulbricht M, Belter M, Langenhangen U, Schneider F, Weigel W (2002) Novel molecularly imprinted polymer (MIP) composite membranes via controlled surface and pore functionalizations. Desalination 149:293-295

Ulbricht M, Yang H (2005) Porous polypropylene membranes with different carboxyl polymer brush layers for reversible protein binding via surface-initiated graft copolymerization. Chem Mater 17:2622-2631

Ulman A (1996) Formation and structure of self-assembled monolayers. Chem Rev 96:1533-1554.

Wang HY, Kobayashi T, Fujii N (1997) Surface molecular imprinting on photosensitive dithiocarbamoyl polyacrylonitrile membranes using photograft polymerization. J Chem Technol Biotechnol 70:355-362

Zhao B, Brittain WJ (2000) Polymer brushes: Surface-immobilized macromolecules. Prog Polym Sci 25:677-710

4

Surface Modification by Graft Polymerization

Membrane technologies have now been widely exploited and utilized on a large scale due to the unique separation principles of membranes. For further progress, however, membranes with favorable properties and functionabilities must be designed and prepared. Based on existing membrane materials, modification of them is necessary. Among different technologies, graft polymerization is a universal modification method for preparing a "tailored" membrane surface with desired functions. The grafted polymer chains on the membrane surface play an important role in membrane applications. In this chapter methods of graft polymerization on the membrane surfaces and the relative applications are introduced.

4.1 Introduction

Surface modification is a way to minimize undesired properties or introduce additional functions for a polymer separation membrane (Ulbricht, 2006). "Grafting-from" and "grafting-to" are two commonly used strategies. The "grafting-from" method utilizes active species existing on a membrane surface to initiate the polymerization of monomers from the surface, which is also termed graft polymerization in this chapter. On the other hand, for the "grafting-to" method, polymer chains carrying reactive anchor groups at the end or on the side chains are covalently coupled to the membrane surface. Compared with "grafting-to", the "grafting-from" method using functional monomers has proven to be much more flexible and versatile (Kato et al., 2003; Zhao and Brittain, 2000). Firstly, with graft polymerization a "tailor-made" membrane with specific properties can be obtained by introducing specific chains. Secondly, a great variety of grafting densities and chain lengths can be achieved in a convenient way. Thirdly, through graft polymerization the base membrane can be endowed with permanent, advanced and novel functions. Therefore, the modified membranes have been widely used

in various ways, such as in separation processes for liquid and gaseous mixtures (gas separation, reverse osmosis, pervaporation, nanofiltration, ultrafiltration, microfiltration), biomaterials, catalysis (including fuel cell systems), and "smart" membranes.

4.2 Graft Polymerization on Membranes

For graft polymerization, initiators that begin the grafting of a monomer on the membrane surface can be divided into three classes. One is a pre-prepared redox initiator. Another is a photoinitiator. The third includes those generated on the membrane by plasma or glow-discharge treatment, UV irradiation, electron-beam (EB) irradiation, γ-ray irradiation, ozone treatment, laser irradiation, etc. By choosing desired monomers and suitable experimental procedures, as shown in Fig.4.1, a membrane surface grafted with different polymer chains can be realized.
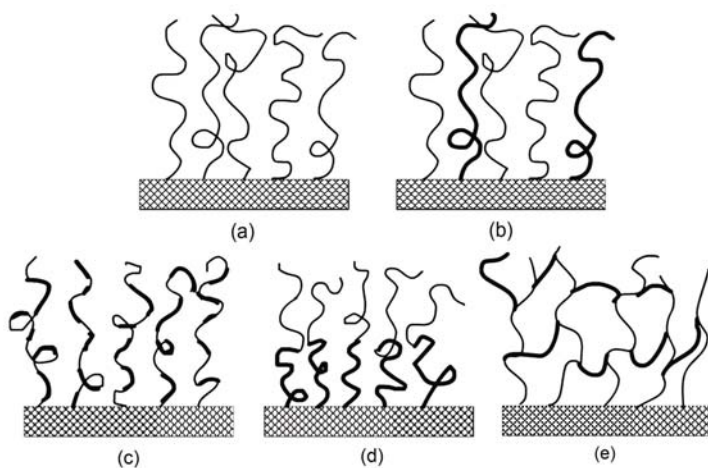
Fig. 4.1. Polymer chains grafted on membrane surface. (a)Flexible homopolymer chains; (b)Mixed homopolymer chains; (c)Random copolymer chains; (d)Block copolymer chains; (e)Crosslinked copolymer chains. Reprinted from (Zhao and Brittain, 2000), Copyright (2000), with permission from Elsevier

4.2.1 Surface Modification by Chemical Graft Polymerization

In the chemical graft process the role of the initiator is very important as it determines the path of the grafting process (Bhattacharya and Misra, 2004). Usually there are two types of initiators used in the solution phase. They

are the redox initiator and the free radical initiator. Occasionally they are chosen based mainly on the reaction temperature, predominantly for the free radical initiator (Desai and Singh, 2004). Free radicals are produced by the decomposition of initiators and transfer to the membrane on which initiating monomers form graft polymers. Apart from the general free-radical mechanism, living graft polymerization is an alternative interesting technique for surface modification.

4.2.1.1 Free-Radical Graft Polymerization

The redox initiator has been widely used in free-radical graft polymerization on the membrane surface and the free radicals are produced indirectly. A redox initiator, e.g. $K_2S_2O_8/Na_2S_2O_5$ was used to modify commercial polyamide (PA) reverse osmosis (RO) and nanofiltration (NF) membranes with vinyl monomers by many researchers(Belfer et al., 1998; 2004; Freger et al., 2002; Gilron et al., 2001). These monomers contain various functional groups. It was shown that the oxidant results in the abstraction of hydrogen from the PA membrane (Avlonitis et al., 1992; Glater et al., 1983). The modified membranes were characterized by FTIR-ATR and contact angle measurements. It was observed that the polymerization could take place not only on the membrane surface but also inside the pores, particularly when a high grafting degree (GD) was achieved (Freger et al., 2002). This phenomenon is undesirable and should be avoided by optimizing graft conditions so that grafting only takes place on the active surface. They also prepared layered polyacrylonitrile (PAN) membranes grafted with charged vinyl monomers by sequential redox-initiated procedures (Belfer, 2003; Belfer et al., 2005). Results showed that grafting of monomers with sulfo-acidic groups was promoted when conducted on a membrane previously grafted with oppositely charged monomers such as 2-dimethylamino-ethylmethacrylate (DMAEMA). It revealed that electrostatic attraction between the membrane surface and the monomers in the reaction solution had a positive effect on the GD.

Jimbo et al. (1998a; 1998b; 1998c; 1999) prepared amphoteric membranes by a chemical free-radical graft of anionic and cationic monomers onto PAN membranes using redox systems. The monomers they used include acrylic acid (AAc), (methacryloxy) ethyl phosphate (MOEP), DMAEMA, (N,N-dimethylamino propyl) acrylamide (DMAPAA) and methylacrylic acid (MAA). Redox system Fe^{2+}/H_2O_2 was used for anionic monomers, while $NaHSO_3/(NH_4)_2S_2O_8$ was used for cationic monomers. With the redox initiator, graft polymerization was performed at 25 °C. The low temperature ensured that structures of the grafted membranes were not damaged because grafting induced by heat often leads to structural deformation (Jimbo et al., 1998a; 1998b). ξ-Potentials measurement (Jimbo et al., 1998c) and FTIR-ATR measurement (Jimbo et al., 1999) were adopted to get macroscopic and microscopic information of the amphoteric PAN membranes. Results concerning the isoelectric point, dissociation constant, surface charge density,

and acid-to-base ratio were obtained. These parameters are of importance for clarifying and describing phenomenological performances of the charged membranes, such as transport properties of electrolytes and protein adsorption in membrane fouling.

A marked, rapid and reversible pH-response membrane was prepared by grafting MAA on a phenolphthalein poly(ether sulfone) (PES) membrane with a redox system, $K_2S_2O_8/Na_2SO_3$ (Wang et al., 2007). The GD increased remarkably with the monomer concentration as reported by Belfer et al. (2000; 1998) and Jimbo et al. (1998a; 1998b).

Except for redox systems, direct oxidation of the polymer backbone with certain transition metal ions can also generate free radical sites on the polymer backbone through the alcohol groups present on them, to initiate graft polymerization. In general, metal ions with low oxidation potential are preferred for better grafting efficiency. The proposed mechanism for such a process has been ascribed to the formation of an intermediate, i.e. metal ion-polymer chelate complex. Ceric ion is known to form a complex with hydroxyl groups on a polymeric backbone, which can dissociate via one electron transfer to give free radicals (Fig.4.2) (Hsueh et al., 2003; Mino et al., 1958; Zhang et al., 2003). Initiated by ceric ammonium nitrate (Zhang et al., 2003), cellulose membranes were grafted with a zwitterionic vinyl monomer, N-dimethyl-N-methacryloxyethyl-N-(3-sulfopropyl) ammonium (DMMSA), to improve the hemocompatibility. The amount of poly(DMMSA) grafted onto the cellulose membranes increased with the feed monomer concentration.

$$Ce^{4+} + R_{polym}OH \longrightarrow complex \longrightarrow R_{polym}O \bullet + Ce^{3+} + H^+$$

$$R_{polym}O \bullet + M \longrightarrow R_{cell}OM \bullet \longrightarrow R_{polym}OMM \bullet$$
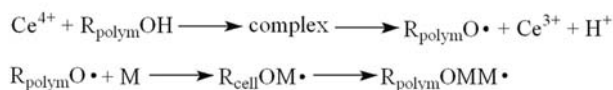
Fig. 4.2. The mechanism of graft polymerization initiated by ceric ion. Reprinted from (Bhattacharya and Misra, 2004), Copyright (2004), with permission from Elsevier

In addition, a free radical initiator can decompose into free radicals upon heating and then initiate graft polymerization. This involves azo compounds, peroxides, hydroperoxides, and peroxide diphosphate. For example, Carroll et al. (2002) introduced a macroinitiator (Fig.4.3) onto polypropylene (PP) hollow-fibre microfiltration membranes by adsorption. It is known that only 50%~60% of the perester groups are effective starting points for the polymerization (Steinert et al., 1999). Due to thermally breaking of the perester linkage the resulting reactive species initiated charged and non-charged hydrophilic monomers to graft on the membranes. The grafted polymers acted as a flexible layer on the surface and resulted in a membrane whose flux depends on the polymer conformation. Childs et al. (2002) chemically bound

a heat-sensitive radical initiator, 4,4'-azo-bis(4-cyanovaleryl chloride), into polyethylenimine-coated hydrophobic PP or polyethylene (PE) membrane and prepared pore-filled microfiltration (MF) membranes by grafting AAc, 4-(vinylpyridine) (4-VP) or styrene (St) at 75 °C. This method can effectively restrain the homopolymerization. The membranes exhibited hydraulic fluxes and pH valve effects consistent with molecular brushes grafted within the pores of the membranes. With azobis(isobutyronitrile) (AIBN) as the initiator, St was first grafted on PE membranes at 70 °C with divinylbenzene (DVB) as the crosslinker, followed by subsequent sulfonation reaction (Son et al. 2006). It was found that the GD increased substantially with the concentration of AIBN and DVB. However, using an excessive amount of DVB and AIBN caused damage to the membrane.
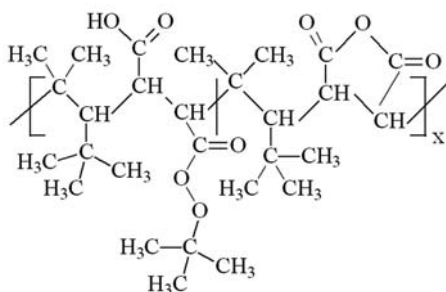
Fig. 4.3. Chemical structure of the macroinitiator based on poly(trimethyl-2-pentene-alt-maleic acid anhydride). Reprinted from (Carroll et al., 2002), Copyright (2002), with permission from Elsevier

4.2.1.2 Living Graft Polymerization

In recent years living polymerization has been developed as a method for grafting reactions. In the case of living polymerization, polymer chains with controlled length and low polydispersity are grafted on membranes. Thus the preparation of membranes with controllable structures and properties becomes possible.

Kang's research group (Ying et al., 2004) grafted AAc on ozone-pretreated poly(vinylidene fluoride) (PVDF) MF membranes by reversible addition-fragmentation chain transfer (RAFT) mediated graft copolymerization. The membranes tethered with poly(AAc) macro chain transfer agents, or the living membrane surfaces, could be further functionalized via surface-initiated block copolymerization with N-isopropylacrylamide (NIPAAm) to obtain PVDF-g-poly(AAc)-b-poly(NIPAAm) MF membranes, which exhibited both pH- and temperature-dependent permeability in aqueous media. In addition they prepared another "surface-active" copolymer membrane via graft

copolymerization of an inimer, 2-(2-bromoisobutyryloxy)ethyl acrylate, on the ozone-pretreated PVDF (Zhai et al., 2004). This "surface-active" membrane allowed the initiation of atom transfer radical polymerization (ATRP) of functional monomers, such as poly(ethylene glycol) methacryate (PEGMA) (Zhai et al., 2004) and DMAEMA (Zhai et al., 2005), to gain antifouling or antibacterial properties, respectively. The pore size distribution and surface morphology of the modified membranes was found to be much more uniform than that of the corresponding membranes prepared by the "conventional" free-radical graft copolymerization process.

Recently, surface-initiated ATRP was employed to tailor the functionality of a nylon membrane. The procedure is shown in Fig.4.4 (Xu et al., 2007). 2-Hydroxyethyl methacrylate (HEMA) and PEGMA were first grafted on the membrane surface through the ATRP method. After that the dormant chain ends of the grafted poly(HEMA) and poly(PEGMA) could be reactivated for the consecutive surface-initiated ATRP. Therefore membranes functionalized by poly(HEMA)-b-poly(PEGMA) and poly(PEGMA)-b-poly(HEMA) diblock copolymer brushes were prepared.
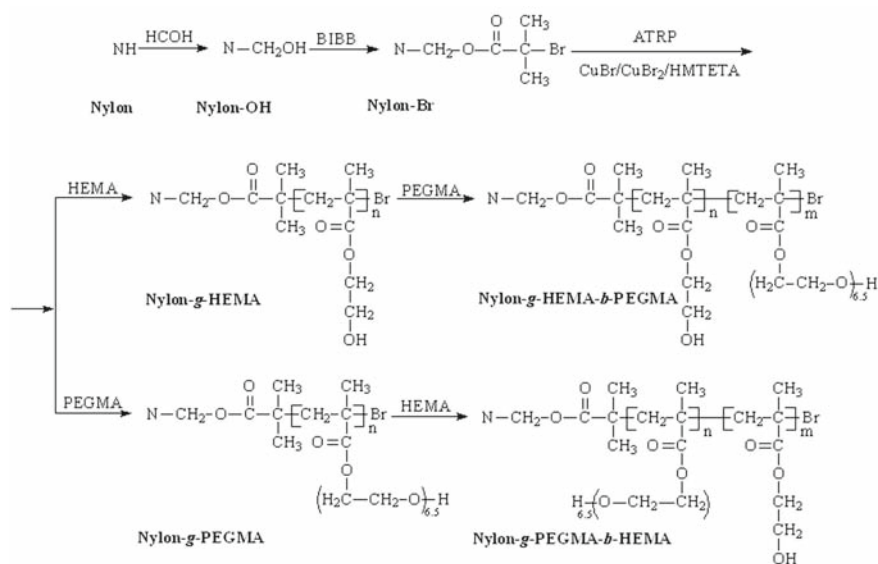
Fig. 4.4. Diagram illustrating the activation and the surface-initiated ATRPs on nylon membrane. Reprinted with permission from (Xu et al., 2007). Copyright (2007) American Chemical Society

In conclusion, these membranes with an "active surface" not only endow membranes with special properties but also offer opportunities for further functionalization of membranes by living graft polymerization techniques.

4.2.2 Surface Modification by Plasma-induced Graft Polymerization

Surface modification by plasma or glow-discharge mainly includes three kinds of methods: plasma treatment, plasma polymerization, and plasma-induced graft polymerization (Zhao et al., 2004). With various gases (such as oxygen, argon, nitrogen, and hydrogen) and active monomers, a wide range of surface properties are utilized for different applications.

4.2.2.1 Plasma Treatment

Plasma or glow-discharge treatment can change the surface properties of a membrane by introducing some polar groups, such as hydroxyl and amino groups. However, there is still one major drawback that is sometimes called 'hydrophobic recovery'. It alters the targeted surface properties with the time of storage. This behavior is believed to be caused by gradual reorientation of the surface chain segments in response to interfacial forces when the membrane surface is exposed to air or to other nonpolar media. This reorientation may lead to the time dependency of surface properties of the plasma treated membrane. In contrast, plasma polymerization and plasma-induced graft polymerization can endow a membrane surface with a permanent effect. And the alternative is to utilize the introduced polar groups to initiate graft polymerization on membranes.

Electrospun polysulfone (PS) fibrous membranes were pretreated by air glow-discharge plasma to produce a large amount of hydroxyl groups. These groups can form a redox-initiating system with Ce(IV) to initiate the graft polymerization of MMA on membranes (Ma and Ramakrishna, 2006). Compared with the initiating system without Ce(IV), high GD of poly(MAA) was gained with the aid of Ce(IV) (Fig.4.5).

In addition, Xu and his co-workers (Liu et al., 2003) made use of the amino groups generated by ammonia plasma to initiate the ring opening polymerization of N-carboxyanhydride (NCA) of γ-stearyl-L-glutamate on microporous PP hollow fiber membranes. Amino group densities on the membrane surfaces increased with the glow-discharge time, as shown in Fig.4.6. The mechanism for the synthesis of polypeptide initiated by primary amines is shown in Fig.4.7. The plasma-treated PP membranes were then dipped in the monomer solution and the graft polymerization lasted 3 d at 35 °C in N_2 atmosphere. Unfortunately, although the polypeptide, poly(γ-stearyl-L-glutamate) (PSLG), was successfully grafted onto the membrane surface, the polymerization degree of the polypeptide was low to some extent. Similar work was also reported by Ito et al. (1997).

4.2.2.2 Plasma Polymerization

Plasma polymerization is a method for which graft polymerization is proceeded by plasma treatment after membranes were previously swelled with
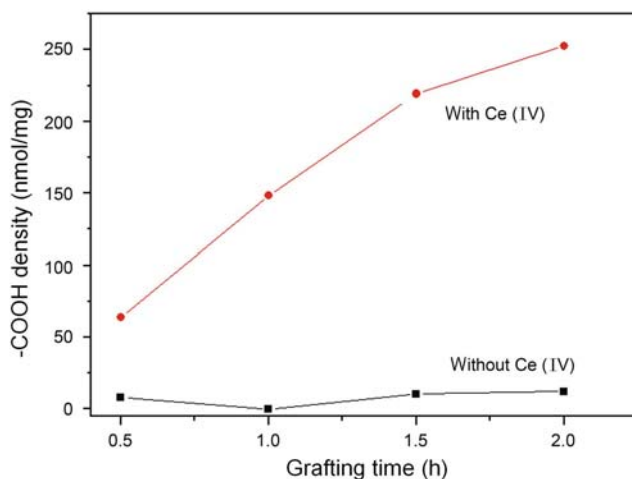
Fig. 4.5. Effects of the addition of Ce(IV) on the grafted carboxy group densities (Ma and Ramakrishna, 2006). Copyright (2006). Reprinted with permission of John Wiley & Sons, Inc.
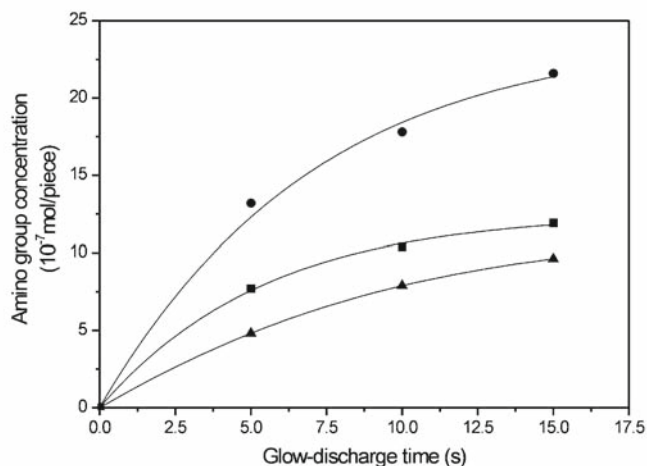
Fig. 4.6. Effects of glow-discharge time on the density of amino groups on the surface of membrane. Electric power was ($\bullet$) 40 W, ($\blacksquare$) 20 W, and ($\blacktriangle$) 10 W. Reprinted from (Liu et al., 2003), Copyright (2003), with permission from Elsevier

monomers. According to this method, plasma-induced grafting of HEMA on chitosan membranes was carried out by Li et al. (2003). The membranes were swelled with HEMA aqueous solution for 48 h, and then treated with nitrogen plasma. But there are some disadvantages for plasma polymerization.
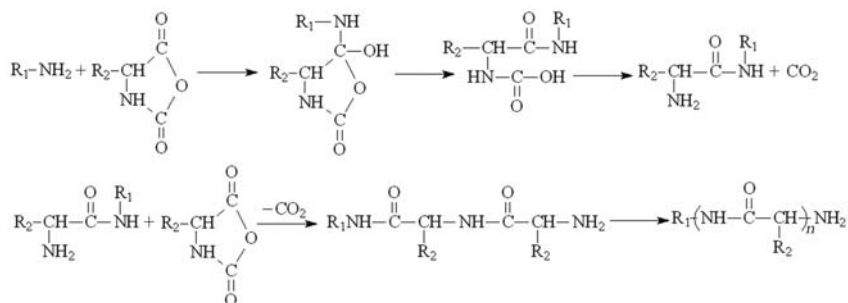
Fig. 4.7. Mechanism of synthesis of polypeptide from NCAs. Reprinted from (Liu et al., 2003). Copyright (2003), with permission from Elsevier

For example, grafts are often accompanied by a lot of homopolymers, and the GD is relatively low.

4.2.2.3 Plasma-Induced Graft Polymerization

Generally speaking, plasma-induced graft polymerization consists of two steps: the first step is a plasma treatment to generate radicals on the base membrane, and the second is graft polymerization of monomers initiated by the radicals. Thus, homopolymerization of monomers in solution can be avoided and the GD can be modulated by changing the reaction time or other experimental conditions.

By both plasma-induced graft polymerization (both in solution and vapor phase) and plasma polymerization, AAc was grafted on PS membranes (Gancarz et al., 1999). Grafting in solution resulted in hydrophobic membranes with significantly reduced pore size. In contrast, grafting in the vapor phase generated brush-like structures and the corresponding membrane possessed a hydrophilic surface as well as unique filtration properties in basic aqueous solutions. It was assumed that grafting in solution gave long chains of poly(AAc) while grafting in the vapor phase formed short polymer brushes. On the other hand, plasma polymerization of AAc on the PS membrane surface only achieved a low GD.

Most of the research involves the treating of a porous membrane with plasma, which only affects its outer surface, leaving the bulk properties unchanged (Lee and Shim, 1997). For example, Lee and co-workers (Lee et al., 1995; Lee and Shim, 1997) reported the grafting of AAc and NIPAAm for the construction of pH and temperature sensitive PA membranes by argon plasma graft polymerization. Goto et al. (1994) prepared an acrylamide (AAm) grafted hollow-fiber polytetrafluoroethylene (PTFE) membrane in which the grafted layer was only formed on the outer surface of the membrane instead of in the pores.

However, for porous PE membranes Yamaguchi et al. (1991; 1993; 1996; 1999; 2001) reported that after plasma treatment radicals were not only generated on the membrane surface but also at the pore walls. They called this kind of graft polymerization plasma-initiated filling polymerization. The so-called filling-polymerized membrane was composed of a porous substrate, which prevented membrane swelling (Yamaguchi et al., 1997) and polymer grafted in the pores, which exhibited permselectivity on the basis of the different solubilities of feed components. Yamaguchi et al. (1996) found that the location of grafted polymer depended on the balance between the diffusivity and reactivity of monomers. Varying the monomer solvent composition could affect the graft polymerization rate (Wang et al., 2002) by changing the monomer diffusivity relative to the reactivity (Yamaguchi et al., 1996). Thus the grafted membrane morphology could be controlled by varying the monomer solvent. A much higher polymerization rate was achieved in water than in organic solvents. Correspondingly, when using water as solvent, grafting mainly occurred at the surface of the porous substructure and was non-uniform; however, a more uniform grafting was obtained when using a water and methanol mixture as solvent. Choi et al. (2007) investigated the effects of reaction conditions on the graft distribution by examining plasma-induced graft polymerization in detail. According to Fick's second law of diffusion, the mass balance for a monomer including a thickness of infinitesimal size within the membrane (x) is given by:

$$R_{\mathrm{p}} + \frac{\mathrm{d}c}{\mathrm{d}t} = D\frac{\mathrm{d}^2 c}{\mathrm{d}x^2}, \tag{4.1}$$

where c is the monomer concentration, t is the time, D is diffusion coefficient, R_{p} is the rate of monomer disappearance with thickness, $\mathrm{d}c/\mathrm{d}t$ is the change in the monomer concentration with thickness with time, and $D(\mathrm{d}^2 c/\mathrm{d}x^2)$ is the change in the rate of diffusion in and out of the thickness. In ordinary free-radical polymerization, the grafting rate at any membrane thickness is given by:

$$R_{\mathrm{p}} = \left(\frac{k_{\mathrm{p}}}{k_{\mathrm{t}}^{1/2}}\right) R_i^{1/2} c, \tag{4.2}$$

where R_i is the rate of initiation, k_{p} and k_{t} are the rate constants for propagation and bimolecular termination, respectively. As is known from Eqs.(4.1) and (4.2), transport of the monomer through the membrane is determined by the diffusion rate and reaction rate (Odian et al., 1975). So uniform graft distribution could be obtained in the case of a high diffusion rate and low reaction rate, while non-uniform graft distribution was obtained when these conditions were reversed (Fig.4.8). Among the grafting conditions, control of the reaction temperature was found to be the most effective for selectively preparing the membrane with uniform or non-uniform graft distribution. Glycidyl methacrylate (GMA) grafted PP membranes were prepared at 1 °C and

40 °C, and the graft distribution in the membranes was directly observed by a microscopic FT-IR mapping method and FESEM (Fig.4.9). Uniform graft distribution was achieved when the reaction was conducted at 1 °C because of the relatively rapid diffusion and the slow reaction of the monomer, while non-uniform graft distribution occurred at higher reaction temperatures. The effect of solvent was the same as in (Yamaguchi et al., 1996). On the other hand, the higher the concentration of monomer solution used, the more non-uniform the distribution. In addition, the graft distribution in a thicker porous substrate (>30 μm) can also be modulated by plasma discharge power or gas pressure. Higher plasma discharge power and lower gas pressure result in more uniform graft distribution (Choi et al., 2003).
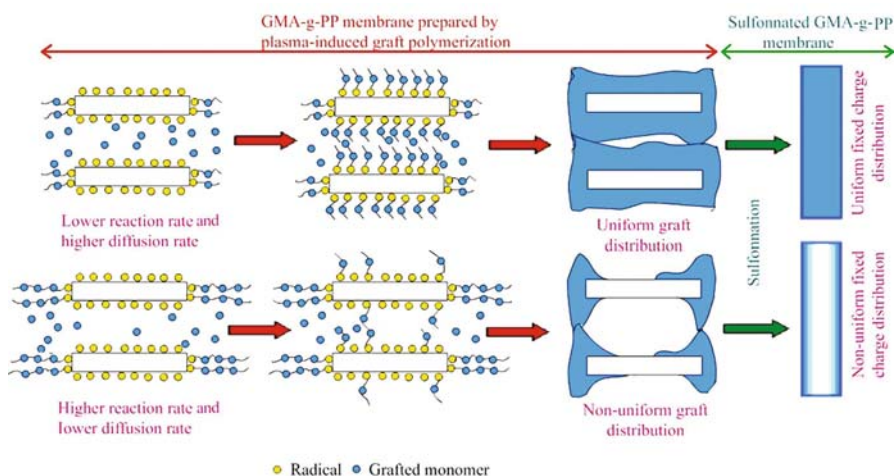
Fig. 4.8. Control of the fixed charge distribution of the ion-exchange membrane. Reprinted with permission from (Choi et al., 2007). Copyright (2007), American Chemical Society
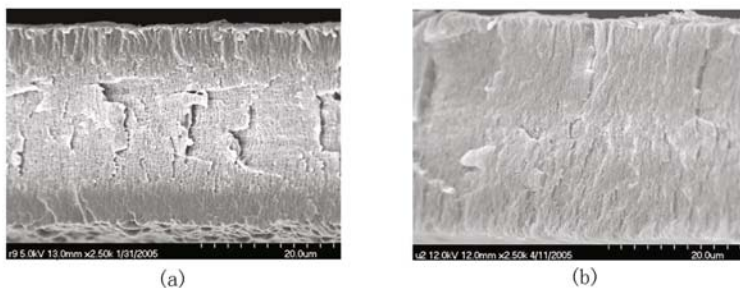
Fig. 4.9. Cross-sectional FESEM images of GMA-*g*-PP membranes with GD 156 wt.% at different reaction temperatures. (a) 40 °C; (b) 1 °C. Reprinted with permission from (Choi et al., 2007). Copyright (2007), American Chemical Society

The grafted polymer formation profile in the membrane was demonstrated by the microscopic FTIR mapping method (Yamaguchi et al., 1999). Spectra were collected at each step of 10 μm or less across, in the direction of the membrane thickness. As shown in Fig.4.10, NIPAAm or benzo[18]crown-6-acrylamide (BCAm) grafted polymer was formed inside the membrane, which is similar to other studies using different monomers (Yamaguchi et al., 1991; 1996). Thereafter the grafted polymer gradually decreased as the distance from the membrane surface increased.
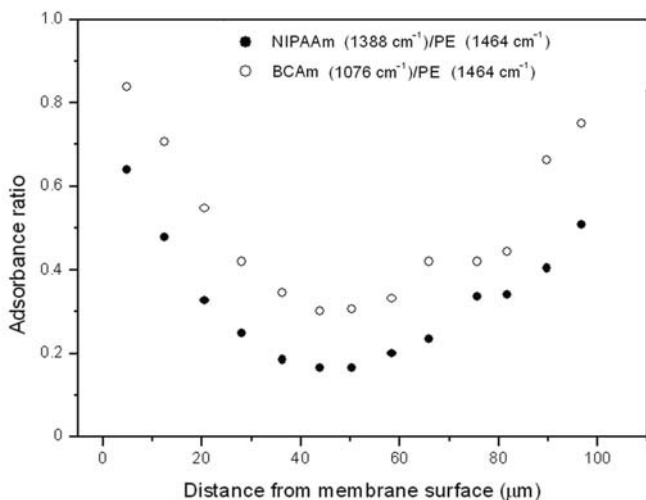
Fig. 4.10. Grafted polymer formation profile in the membrane. Reprinted with permission from (Yamaguchi et al., 1999), Copyright (1999), American Chemical Society

NIPAAm could be grafted uniformly inside the PE membrane pores by the plasma graft-filling polymerization technique, which was also demonstrated by the microscopic FTIR mapping method (Ito et al., 2005). As shown in Fig.4.11, it was found that the ratio of peak areas for peaks occurring at $1550\ cm^{-1}$ (amide II) and $1450\ cm^{-1}$ (CH_2), which represents the ratio of the grafted polymer to the PE substrate, was independent of the position along the cross-section of the membrane (Choi YJ et al., 2000). Xie et al. (2005) gained similar results on polycarbonate track-etched (PCTE) membranes. NIPAAm was grafted on the surface and inside the pores throughout the entire membrane thickness. No dense poly(NIPAAm) layer formed on the membrane surface even at a GD as high as 76.1 wt.%. As shown in Figs.4.12 and 4.13, with the pore-filling ratio increasing, the pore diameters of modified membranes became smaller.
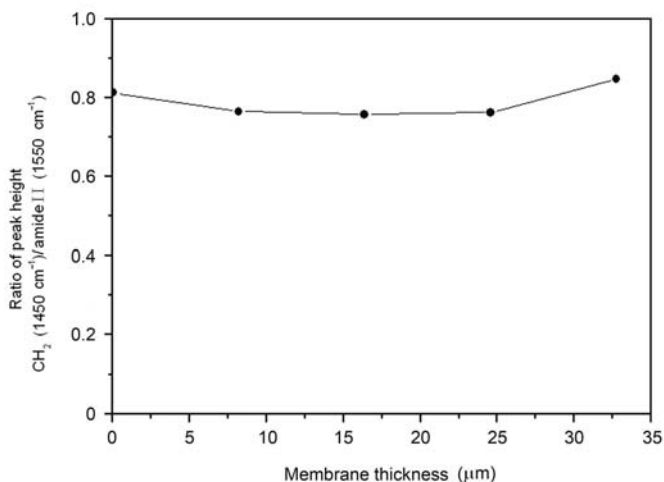
Fig. 4.11. Grafted polymer formation profile in the NIPAAm grafted PE membrane. Reprinted from (Ito et al., 2005). Copyright (2005), with permission from Elsevier
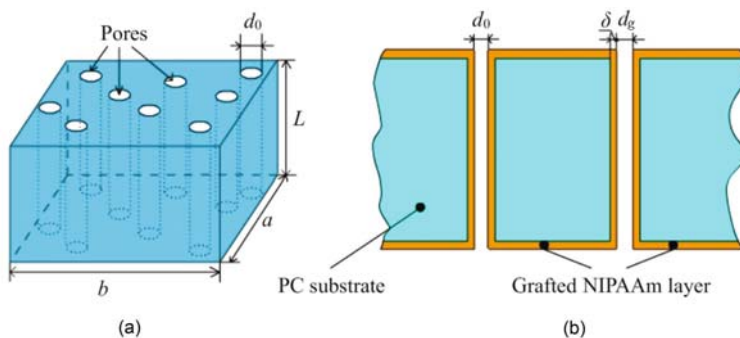
Fig. 4.12. Schematic illustration of PCTE membrane. (a) Three-dimensional structure of ungrafted PCTE membrane; (b) Cross-section of NIPPAAm-g-PCTE membrane. Reprinted from (Xie et al., 2005). Copyright (2005), with permission from Elsevier

As previously mentioned, with suitable grafting conditions different polymer grafted membranes with uniform or non-uniform structures could be gained. Kai et al. (2000) prepared a methyl acrylate (MA) grafted hollow-fiber PE membrane with the graft polymer not only filling the pores of the hollow-fiber substrates but also forming a thick grafted layer of 20 μm on the outer surface. In addition, Kai et al. (2005) prepared crosslinked pore filling PE membranes using MA as grafting monomer and vinyl acrylate (VA)
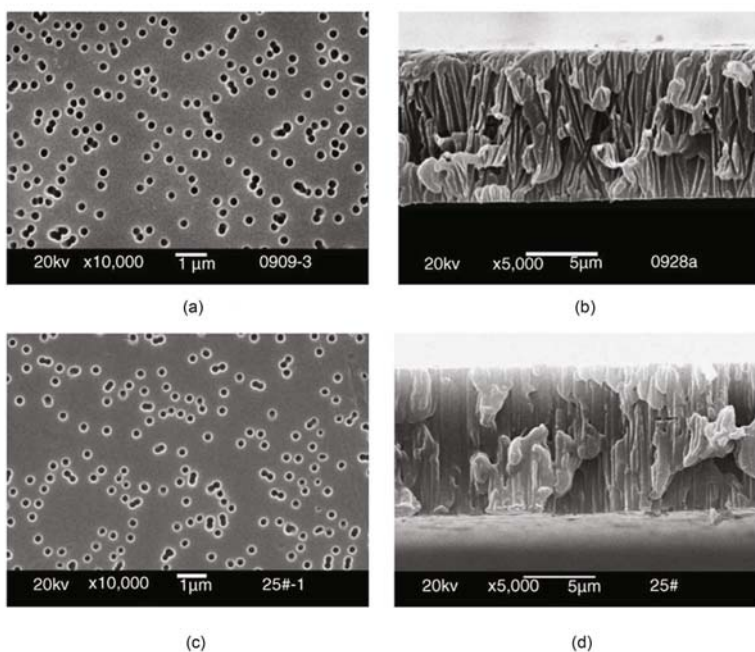
Fig. 4.13. SEM photographs of the surfaces and cross-sections of PCTE membranes grafted with NIPAAm: (a, b) GD=0, and (c, d) GD= 76.1wt.%. Reprinted from (Xie et al., 2005). Copyright (2005), with permission from Elsevier

and N, N'-methylene bis(acrylamide) (MBAAm) as crosslinkers. Results indicated that pressure durability of the membranes was improved remarkably.

In addition, the properties of membrane materials have an influence on grafting polymerization. Taking hydrophilic Nylon-6 (N6) and hydrophobic PVDF porous membranes as substrates, Xie et al. (2007) fabricated thermo-responsive membranes through plasma induced graft polymerization by adding hydrophilic (AAm) or hydrophobic (butyl methacrylate, BMA) monomers to an NIPAAm monomer solution (Fig.4.14). In the experiments poly(NIPAAm-*co*-BMA) (PNB) was mainly grafted on the surface of the membrane rather than into the pores when using PVDF as substrate. This was probably because the hydrophobic monomer BMA first adsorbed onto the hydrophobic PVDF membrane, and the polymerization of adsorbed monomers choked membrane pores and prevented NIPAAm and BMA entering the pores during the subsequent polymerization. To ensure that enough monomers entered the pores of membranes during graft polymerization, PNA was grafted onto the PVDF membrane while PNB was grafted onto the N6 membrane.

As described above, membranes possess various functionalities and reactivity after plasma-induced graft polymerization. So the grafted membranes

(a)

(b)
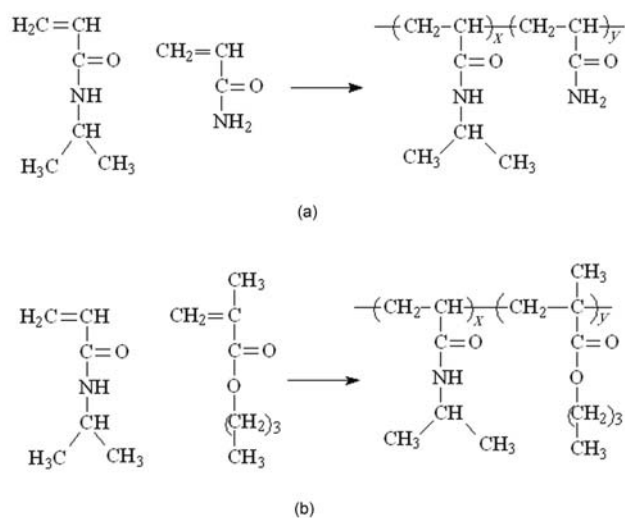
Fig. 4.14. Thermo-responsive copolymers PNA (a) and PNB (b) for grafting polymerization on porous membranes. Reprinted from (Xie et al., 2007). Copyright (2007), with permission from Elsevier

could be further modified with other monomers. Husson et al. (Singh et al., 2005) firstly grafted GMA on PVDF membranes by plasma induced polymerization. Then the epoxide groups of poly(GMA) reacted with vapor-phase bromoacetic acid to introduce a bromoacetate group, which is capable of initiating the graft of 2-vinylpyridine (2-VP) via ATRP. Results indicated that by changing ATRP time it is possible to tune the GD and average pore size. A polymerization time of 24 h reduced the pore-diameter polydispersity from 2.05 to 1.44. Most importantly, the pore-size distribution of a membrane that is initially broad may become narrower after graft polymerization.

4.2.3 Surface Modification by UV-induced Graft Polymerization

UV-induced graft polymerization is also a desirable method for surface modification of polymer membranes for a number of reasons (Hu et al., 2006; Uyama et al., 1998). Firstly, photochemically produced triplet states of carbonyl compounds facilitate hydrogen abstraction, thus graft polymerization can be initiated without prior modification. Secondly, a high concentration of active species is produced locally at the interface between the membrane and the monomer solution. Thirdly, in addition to the simplicity and cleanness of the procedure, the cost of the energy source is lower when compared with other radiation, such as ionizing radiation. Fourthly, UV-induced polymerization is well suited for integration with other technologies, such as microcontact printing and photolithography, to produce a chemically desired

surface in well defined two-dimensional regions. Fifthly, the wavelength of UV irradiation can be adjusted specifically to initiate the reaction and hence undesired side reactions can be avoided or at least reduced to a great extent (Allen and Edge, 1992). Moreover, UV-induced graft polymerization is versatile for various vinyl monomers with desirable functionality.

When a chromophore on a polymer membrane absorbs light it goes to an excited state, which may dissociate into reactive free-radicals, hence the grafting process is initiated directly on polymer chains (Bhattacharya and Misra, 2004). If the absorption of light does not lead to the formation of free-radical sites through bond rupture, this process can be promoted by the addition of photoinitiators or photosensitizers. Therefore UV-induced graft polymerization can proceed in two ways: with or without photoinitiators.

4.2.3.1 UV-Induced Graft Polymerization without Photoinitiators

Without photoinitiators, free radicals can be generated on polymer backbones directly under UV irradiation, which react with monomers to form the grafted polymer. Poly(arylsulfone) (PAS) membranes are light sensitive in the UV range (200∼320 nm) (Kuroda et al., 1990) and hence do not need a photoinitiator for radical production, i.e. they self-initiate and can produce sufficient radicals for vinyl grafting of various functional groups (Crivello et al., 1995). The chemical structures of the PAS membranes, such as PS and poly(ether sulfone) (PES), are shown in Fig.4.15. The mechanism of graft polymerization on PAS membranes was systemically studied by Belfort's group (Yamagishi et al., 1995b; Pieracci et al., 2000; Kilduff et al., 2000; Taniguchi et al., 2003b), shown in Fig.4.16. When these PAS membranes immersed in either water or methanol containing vinyl monomers in the absence of a photosensitizer were irradiated, it was found that extensive polymerization of the monomer took place only on the surface of the membrane (Yamagishi et al., 1995a). HEMA, GMA and MAA were directly bound to the PAS membrane surface according to this method. In these instances no homopolymerization of the vinyl monomer was observed in the solution (Kaeselev et al., 2001).

Two different techniques were adopted to modify the PAS membranes with N-vinyl-2-pyrrolidinone (NVP): a dip modification and an immersion modification (Pieracci et al., 2000). In the dip method the membranes were modified by irradiating them in nitrogen after they had been dipped in the monomer solution for 30 min with stirring. In the immersion method, however, the membranes were modified by irradiating them while they were immersed in the monomer solution. Both the techniques produced membranes with essential wettability. The immersion-modified membrane with the best performance exhibited no adsorptive fouling, similar permeability and higher rejection compared with the regenerated cellulose membrane. The dip-modified membranes exhibited simultaneous loss of bovine serum albumin (BSA) rejection and permeability, which suggested that although radiation
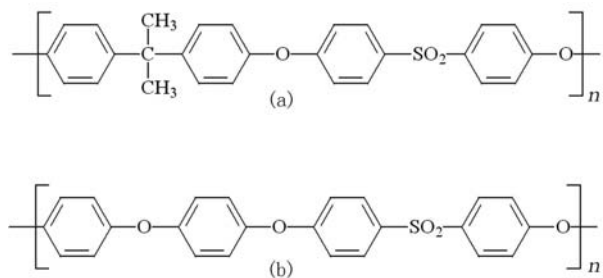
Fig. 4.15. Chemical structures of poly(arylsulfone) membranes. (a) PS ; (b) PES. Reprinted from (Yamagishi et al., 1995a). Copyright (1995), with permission from Elsevier
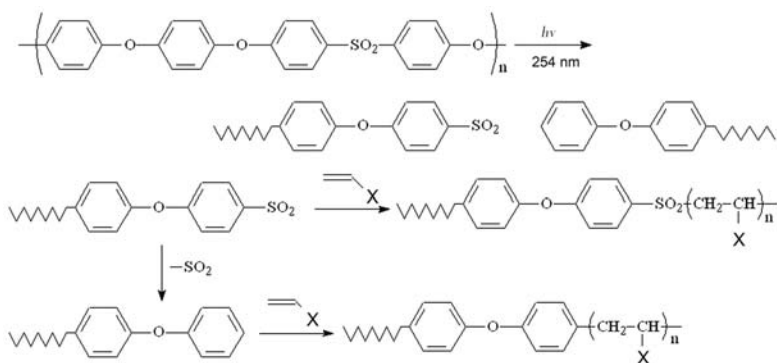
Fig. 4.16. Proposed mechanism for the photochemical modification of PES with vinyl monomers. Reprinted from (Yamagishi et al., 1995a). Copyright (1995), with permission from Elsevier

cleaved PES bonds and enlarged the pores the high GD of polymer chains on the surface blocked the pores and decreased the permeability.

It should be noted that although the two PAS membranes, PS and PES, are both photosensitive, PES is far more sensitive to UV-induced graft polymerization and thus requires far less energy to attain a desired degree of grafting than PS (Kaeselev et al., 2001). In addition, UV wavelengths for irradiating PES membranes influenced the modified PES membrane rejection (Pieracci et al., 2002a; 2002b). UV lamps normally used have an emission wavelength maximum of 300 nm and two specially selected UV light filters, benzene and aromatic polyester films to filter out 254 nm wavelength light which was found to be responsible for severe loss of protein rejection. Membranes modified with such kind of UV lamp had a higher surface wettability than the base membrane, which translated into lower irreversible flux loss.

Resulting from NVP grafted PES UF membranes, there appear to be three critical aspects for optimizing UF performance with protein solutions

(Taniguchi et al., 2003b), which include modification conditions (monomer type and concentration and energy of irradiation with 300-nm lamps), membrane structures (skin thickness), and washing conditions after modification (with ethanol or water). A universal linear plot of the net amount of grafted NVP versus its concentration times irradiation energy (only for $E < 4\,\text{kJ/m}^2$) was obtained. Ethanol was able to effectively remove entrapped homopolymer and other free fragments resulting from chair-scission, while water was less efficient. In addition, UV irradiation with time less than or equal to 60 s minimized any pore enlargement.

The type of monomer chosen also has an important effect. The sensitivity of UV-induced graft polymerization and the filtration performances of PES membranes were studied by Taniguchi and Belfort (2004) using six different monomers, i.e. NVP, HEMA, AAc, 2-acrylamidoglycolic acid (AAG), 3-sulfopropyl methacrylate (SPMA), and 2-acrylamido-2-methyl-1-propanesulfonic acid (AMPS) (Fig.4.17). It was found that several characteristics such as size [(molar volume)$^{1/3}$], sensitivity of grafting/polymerization, and dissolving power had effects on the grafting efficacy and thus on the filtration performance of the modified membranes. The smallest monomer in terms of (molar volume)$^{1/3}$, AAc, was the most sensitive to UV oxidation and polymerization. And thus it was widely used to prepare pH-sensitive membranes (Shim et al., 1999).
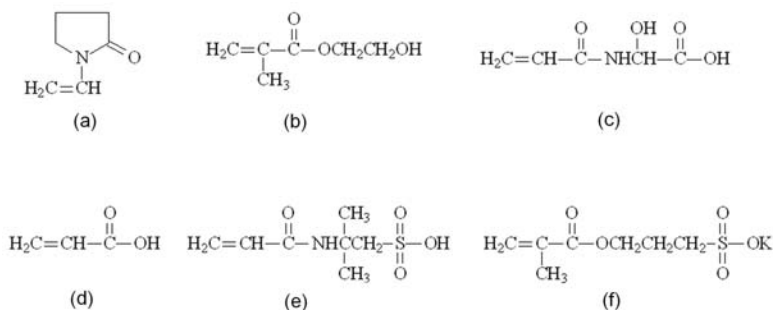
Fig. 4.17. Chemical structures of different monomers used for photo-induced graft polymerization of PES membranes. (a) NVP; (b) HEMA; (c) AAG; (d) AAc; (e) AMPS; (f) SPMA. Reprinted from (Taniguchi and Belfort, 2004). Copyright (2004), with permission from Elsevier

Recently, vinyl spiropyran was photografted onto the 30-kDa PES UF membranes by exposing the membranes previously adsorbed with spiropyran monomer to 300-nm UV radiation, by which an optically reversible switching membrane was prepared (Nayak et al., 2006). ATR/FTIR was used to demonstrate that the vinyl monomers had been grafted onto the PES membranes. When the dry modified membrane was exposed to visible light for 5

min, the peak at about 1663 cm^{-1} increased whereas the peak at 1720∼1725 cm^{-1} decreased. In contrast, under 254 nm UV radiation for 1 h, the peak at about 1663 cm^{-1} decreased whereas that at 1720∼1725 cm^{-1} increased. Because spiropyran contains a light-switchable photochromic group, it represents a colored polar "open" merocyanine form and a white nonpolar "closed" form when exposed to UV and visible light, respectively. Therefore, the vinyl spiropyran grafted PES membrane showed different colors after exposure to UV or visible light (Fig.4.18).
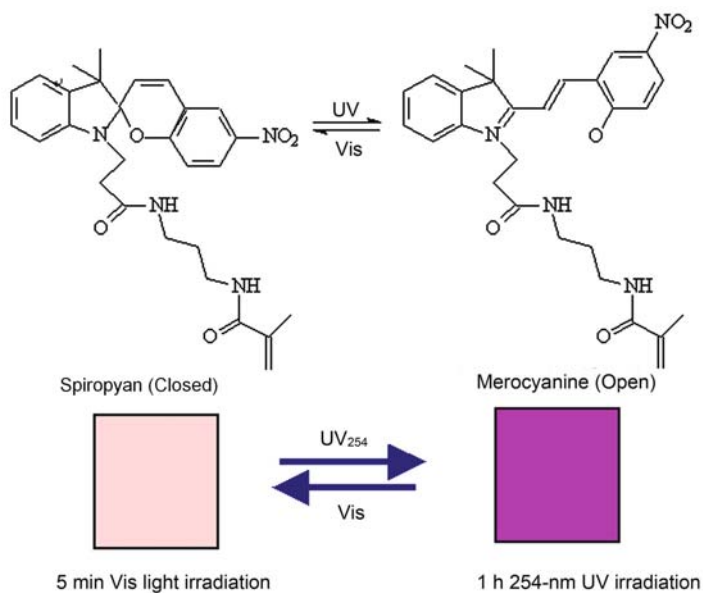
Fig. 4.18. Color change of spiropyran-grafted PES membrane after exposure to UV irradiation at 254 nm for 1 h and visible light for 5 min in air (Nayak et al., 2006). Copyright (2006). Reprinted with permission of John Wiley & Sons, Inc.

It should be pointed out that for intrinsically photosensitive polymers, as mentioned above, an additional photoinitiator is not required when a direct UV excitation of the base polymer is used for the initiation of the graft polymerization; however, it may suffer from a severe degradation of the base membrane's pore structure resulting from polymer chain scission under UV irradiation.

4.2.3.2 UV-Induced Graft Polymerization with Photoinitiators

Surface graft polymerization on a PES membrane was also possible using a photoinitiator (benzophenone, BP, or benzoylbenzoic acid, BPC), which

induced radicals by H-abstraction from the methyl groups of PES instead of the backbone. Except for intrinsically photosensitive polymers, introduction of a photoinitiator is essential for other polymers to achieve UV-induced graft polymerization. Until now, by means of UV-induced graft polymerization with photoinitiators, a number of vinyl monomers were successfully used to modify and functionalize polymer membranes, such as PP, PE, PAN, PS, PU, PET, PVDF, nylon and SBS membranes (as shown in Table 4.1) (Geismann and Ulbricht, 2005; Hickea et al., 1999; Hilal et al., 2004; Hu et al., 2006; Kim et al., 2001; Ma et al., 2000; Mika et al., 1995; 1997; Nouzaki et al., 2002; Peng and Cheng, 1998; 2001; Ulbricht, 1996; Ulbricht et al., 1995; 1996a; 1996b; 1998; Ulbricht and Schwarz, 1997; Ulbricht and Yang, 2005; Wenzel et al., 2000; Yang and Yang, 2003; Yang et al., 1997a; 1997b; 1997c; 1999; Zhou and Liu, 2003). The most used photoinitiators are BP and its derivatives. Generally the graft polymerization of monomers not only takes place on the membrane surface but also at the pore wall.

As reported, HEMA could be grafted on PP MF membrane by ozone treatment (Gatenholm et al., 1997; Kang et al., 2001; Wang et al., 2000) and γ-ray irradiation (Fang et al., 1998a; Shim et al., 2001). However, it has not been reported that poly(HEMA) can be tethered on this kind of membrane surface in the presence of conventional and widely used photoinitiators such as BP. Hu et al. (2006) described a novel process to modify a PP MF membrane with HEMA by UV-induced graft polymerization using BP and $FeCl_3$ as photoinitiator. It was found that HEMA could be successfully grafted onto a PP membrane only when $FeCl_3$ was introduced into the reaction system, although a relative low GD was obtained. Evans and Uri (1949) found that Fe^{3+} in aqueous media was subject to photodecomposition into Fe^{2+} and hydroxyl radicals. The hydroxyl radicals could react rapidly with water soluble vinyl monomers. Therefore ferric ions were the photosensitizer for the polymerization of these monomers (Oster and Yang, 1968). As shown in Fig.4.19, with the addition of a small quantity of $FeCl_3$ into the BP solution, a "synergistic effect" of the two photoinitiators took place, especially in the case of the immersion method. To explore this synergistic effect the influence of BP concentration on the grafting degree was further examined with the immersion method. Typical results are shown in Fig.4.20. It can be seen that with a fixed Fe^{3+} concentration at 0.00165 mol/L, the GD of HEMA increased significantly with the BP concentration at first and then maintained almost a constant of approximately 35 wt.% when the BP concentration exceeded 0.033 mol/L. Therefore 0.033 mol/L of BP was enough for the graft polymerization under this condition. The synergistic effect of BP and Fe^{3+} in the system with UV irradiation might be described as follows: (1) In aqueous solution Fe^{3+} ions produced a number of free radicals which initiated polymerization and then formed monomer radicals and propagating chains of HEMA. PP macroradicals also could be produced via chain transfer from the growing chains or by abstracting hydrogen atoms from the membrane
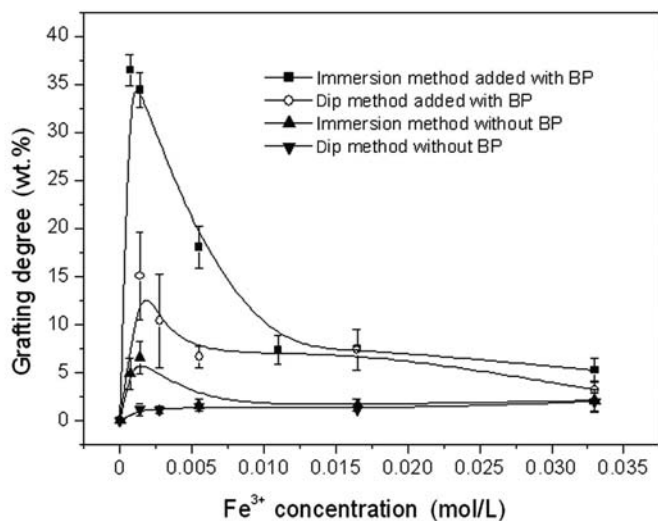
Fig. 4.19. Effect of Fe^{3+} concentration on the grafting degree with two methods. Conditions: BP, 0.033 mol/L; 20%(v/v) HEMA; 25 min UV irradiation for all experiments. Reprinted from (Hu et al., 2006). Copyright (2006), with permission from Elsevier
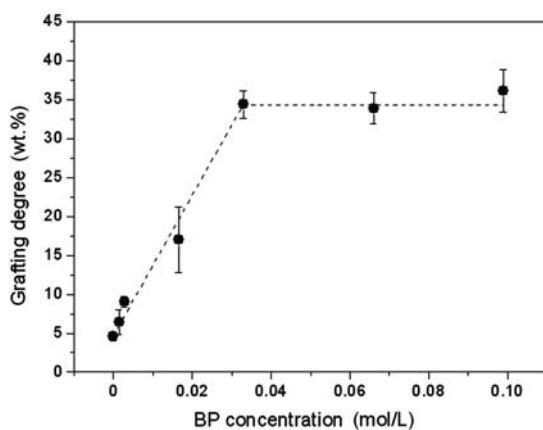
Fig. 4.20. Effect of BP concentration on the grafting degree with the soak method under conditions of 20%(v/v) HEMA in solution and 25 min UV irradiation, 0.033 mol/L Fe^{3+} concentration in solution. Reprinted from (Hu et al., 2006). Copyright (2006), with permission from Elsevier

Table 4.1. Surface modification of polymer membranes by UV-induced graft polymerization with photoinitiators

Membrane	Photoinitiator	Monomer	GD	Ref.
PS, PES UF	BP, BPC	AAc	up to 3.6 mg/cm^2	(Ulbricht et al., 1996b)
SBS	BEE	4-VP, DMAEMA	8.6 mg/cm^2; 4.72 mg/cm^2	(Yang et al., 1997a; 1997b; 1997c; 1999)
PE, PP MF	BEE	4-VP	125.3 wt.%; 126.2 wt.%	(Mika et al., 1995; 1997)
PAN UF	Irgacure 907	MePEGA	55.9 wt.%	(Kim et al., 2001)
PET	BP	AEMA	0.018 mg/cm^2	(Hickea et al., 1999)
PET	BP	NIPAAm 4-VP	2.7 wt.%; 2.54 wt.%	(Yang and Yang, 2003; 2005)
PP	BP	AAc	15.0 μmol/cm^2	(Ma et al., 2000)
PU	BPO	VAc	3.1 wt.%	(Zhou and Liu, 2003)
PP	BP	AAc, AAm, MBAA	up to 4.8 mg/cm^2	(Ulbricht and Yang, 2005)
PAN UF	BP	AAc	7.2 wt.%	(Ulbricht et al., 1995)
PP nylon	BP	AAc	up to 2.3 mg/cm^2	(Bondar et al., 2004; Ulbricht, 1996)
PAN	BP	AAc, HEMA, PEGMA MePEGA	1∼3 mg/cm^2	(Ulbricht et al., 1996a; Ulbricht and Schwarz, 1997)
PAN	BP	Various acrylates or methacrylates	up to 1.0 mg/cm^2	(Ulbricht et al., 1998)
PAN	BP	AAc	0.82 mg/cm^2	(Nouzaki et al., 2002)
PVDF	BP	DMAEMA AMPS	0.71 mg/cm^2	(Hilal et al., 2004)
PET	BP, BPC, BPN	AAc	4 μg/cm^2	(Geismann and Ulbricht, 2005)
PE	Xanthone	NIPAAm, MAA	up to 449 wt.%	(Peng and Cheng, 1998; 2001)
PAN UF	BP	MA	90 wt.%	(Wenzel et al., 2000)
PP MF	BP, FeCl$_3$	HEMA	35.67 wt.%	(Hu et al., 2006)

surface by hydroxyl radicals and monomer radicals. So only with Fe^{3+} could HEMA be grafted on the PP membrane; (2) BP abstracted hydrogen atoms from the membrane to directly create grafting sites on the surface. However, the hydrogen atoms of monomer HEMA were less labile than those of PP, so the monomer radicals were not easy to form. In addition, HEMA had a relatively larger steric hindrance than other vinyl monomers, like AAc or AAm, as far as the chemical structure was concerned. Hence, when BP existed alone, HEMA was hard to polymerize on the PP membrane; (3) Those monomer

radicals and propagating chain radicals might be terminated with Fe^{3+}, or reacted with PP macroradicals on the membrane via coupling termination, which made HEMA grafting on the PP membrane successful.

Ma et al. (2000) described a novel sequential UV-induced living graft polymerization method to modify PP membranes with AAc. This method consists of two steps: first, the photoinitiator, BP, was grafted onto the surface under UV irradiation, yielding a benzpinakol; second, far-UV irradiation was used to cleave this bond again and a "quasi-living" graft polymerization of monomer via recombination and photocleavage of benzpinakol was adopted (Fig.4.21). Results demonstrated that the GD and the chain length of grafted polymer could be controlled by changing the reaction conditions in the first step or in the subsequent step(s) independently. Besides, this procedure is more effective when compared with traditional graft polymerization. The ratio of the amount of grafted polymer to the total amount of polymer by this living method was 4 times greater than that of the simultaneous grafting method.
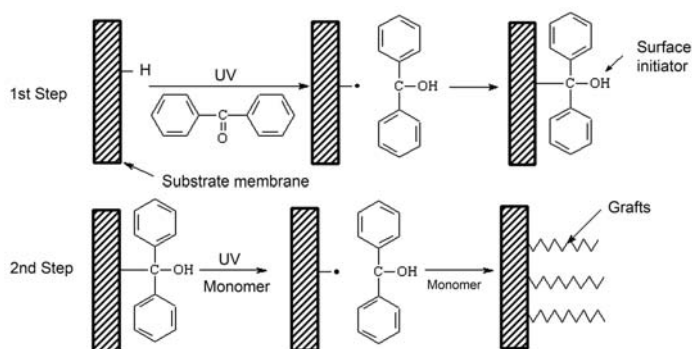
Fig. 4.21. Schematic diagram of the novel photo-induced living graft polymerization method. Reprinted with permission from (Ma et al., 2000). Copyright (2000), American Chemical Society

However, UV irradiation may also cause the photodegradation of polymer membranes (Ulbricht and Yang, 2005). Consequently, an effective and non-degradative surface-initiated graft polymerization will be preferable. An alternative is to physically adsorb the photoinitiator on the membrane surface (Geismann and Ulbricht, 2005; Hilal et al., 2004; Nouzaki et al., 2002; Ulbricht, 1996; Ulbricht et al., 1995; 1996a; 1996b; 1998; Ulbricht and Schwarz, 1997). With the adsorbed photoinitiators, heterogeneous modifications of PAN UF membranes with monomers in water solution by either simultaneous or sequential UV irradiation-initiated graft polymerization were reported (Ulbricht et al., 1996a). Simultaneous grafting from monomer solutions was surface selective when the photoinitiator adsorbed on the membranes was high

enough. However, bulk polymerization in the solution cannot be suppressed completely. By contrast, during sequential grafting process, polymerization chain transfer reactions could be suppressed. Peng and Cheng (1998) reported that NIPAAm was grafted on LDPE membranes with xanthone as photoinitiator, which was adsorbed on the surface and pores of the membranes before the UV irradiation. Furthermore, a multi-stimuli responsive membrane was prepared by co-grafting of NIPAAm and MAA (Peng and Cheng, 2001). The poly(NIPAAm) grafted PE membrane was soaked in methanol for 8 h followed by soaking in an MAA aqueous solution overnight. Then graft polymerization was conducted under UV irradiation without additional photoinitiator. Thus temperature and pH responsive membranes with a wide range of GD and composition were prepared by the sequential UV-induced grafting method. This process showed living radical polymerization characteristics leading to a di-block co-graft structure.

Nevertheless, the physically adsorbed photoinitiator can be desorbed from the membrane surface reversibly. An advanced way is to entrap the initiator in a thin surface layer of the membrane. Ulbricht and Yang (2005) used two different methods to coat BP on PP MF membranes. One was the commonly used adsorption method. The other was a novel entrapping method, which was based on preswelling of the PP membrane in heptane, subsequent solvent exchange, and then entrapping BP in the surface layer of the PP membrane. Because heptane can moderately swell PP, it was used for the entrapping method. Methanol was the solvent for the adsorption method. As shown in Fig.4.22, for the adsorption method a significant fraction of BP was desorbed after immersion in water. In contrast, for the entrapping method less than 10 wt.% BP could be removed by methanol and there was no release into the water. These two findings confirmed a permanent entrapping of the BP under polar solvent conditions. Compared with the adsorption method, the BP entrapping method yielded a less dense grafted layer with longer poly(AAc) chains at the same DG. This was due to somewhat lower immobilized BP amounts, but less side reactions induced by the desorbed BP. To avoid desorption of the physically adsorbed photoinitiator, another method is to graft a monomer from the gas phase. Ulbricht et al. (1995) reported that AAc in the gas phase was grafted on a BP coated PAN UF membrane. The graft and total polymer yield increased with BP loading and UV irradiation time. In addition, in the presence of the transmembrane MA vapor atmosphere, grafting polymerization on the membrane has proved to be effective for filling pores (Wenzel et al., 2000).

4.2.4 Surface Modification by High-energy Radiation-initiated Graft

In the high-energy radiation-induced graft polymerization (RIGP) method, active sites are formed on the polymer backbone and allowed to react with monomer units, which then propagate to form side chain grafts (Nasefa and
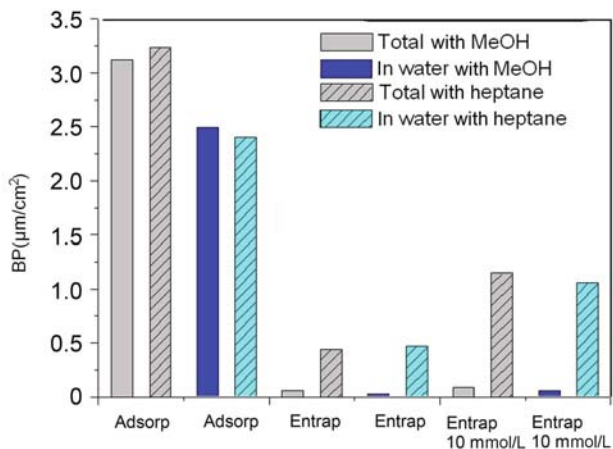
Fig. 4.22. Amounts of BP on/in PP membranes after adsorption or entrapping method (using 1 mmol/L or 10 mmol/L BP concentration) determined by extraction with methanol or heptane. Total: samples after coating via adsorption or entrapping method and subsequent drying; In water: samples after adsorption or entrapping method and subsequent transfer into water for 2 h. Reprinted from (Ulbricht and Yang, 2005). Copyright (2005), American Chemical Society

Hegazy, 2004). At present electron beam (EB) and γ-ray radiation are the mostly used high-energy radiations. A comparison between them is shown in Table 4.2.

Generally the RIGP proceeds in three different ways: pre-irradiation, peroxidation and a mutual irradiation technique (Bhattacharya and Misra, 2004). In the pre-irradiation technique, the polymer backbone is first irradiated in vacuum or in an inert gas atmosphere to form free radicals and then treated with the monomer. In the peroxidation grafting method the membrane is subjected to high-energy radiation in the presence of air or oxygen to form hydroperoxides or diperoxides. These peroxy groups are then treated with the monomer at a higher temperature to decompose to radicals initiating grafting. On the other hand, with the mutual irradiation technique, the membrane and the monomers are irradiated simultaneously to form free radicals and subsequent addition. Often the solution contains an inhibitor to retard homopolymerization in the liquid phase.

4.2.4.1 Electron Beam Irradiation

The surface treatment of polymer membranes by EB irradiation is useful for the preparation of various functional membranes such as ion exchange membranes. However, it is well known that a polymer can be crosslinked by EB irradiation (Hwang and Ohya, 1996; 1997; Ohya et al., 1995).

Table 4.2. Comparison between γ-ray radiation and EB radiation. Reprinted from (Nasefa and Hegazy, 2004). Copyright (2004), with permission from Elsevier

Features	γ−ray radiation	EB radiation
Penetration depth	High	Limited to acceleration energy
Operation	VSimple	Relative complex
Mode of operation	Single	Dual (X-ray and electrons)
On/Off function	No	Yes
Throughput	Low	High
Radiation direction	Scattered	Well-directed
Power, energy and geometry	No control	Well-controlled
Dose rate	Low	High
Processing time	Long	Short
Nuclear waste	Yes	No
Cost	Cheap	Relatively high

Recently a number of vinyl monomers were grafted on membranes such as polyimide, PE, PDMS, and a PVDF membrane by pre-irradiation of EB with or without crosslinkers (Grasselli et al., 2003; Hegazy et al., 2000b; Liu et al., 2007; Mishima et al., 2001; Saito et al., 2002a; Terada et al., 2005; Yanagishita et al., 2004). Washio's group prepared proton exchange membranes (PEMs) by grafting St without or with DVB into crosslinked PTFE (RX-PTFE) (Li et al., 2005a; 2005b; 2006a) and fluoropolymer alloy (Asano et al., 2005) membranes and successively sulfonating. The RX-PTFE membranes were first crosslinked by EB irradiation above their melting temperature, which resulted in remarkable improvements in radiation resistance and mechanical properties (e.g. yield strength and Young's modulus) when compared with those non-crosslinked. The grafting was then achieved by peroxidation of RIGP. The existing of DVB in the grafts, which formed the network structure in the grafts, induced a remarkable improvement in the chemical stability for the modified PEMs. And it was found that there are mainly poly(St) brushes on the surface of the St modified RX-PTFE membranes, while there are mainly PTFE chains on the surface of the RX-PTFE membranes grafted by St together with DVB (Li et al., 2005b). Holmberg et al. (2002) prepared PEMs with the combination of EB pre-irradiation grafting with a living radical polymerization technique, which allows the polymerization to be controlled and facilitates the smart construction of well-defined macromolecular architectures. They introduced ATRP into the preparation of PEMs. Firstly vinylbenzyl chloride (VBC) was grafted on the irradiated PVDF membranes. Then the benzyl chloride groups on the PVDF-g-poly(VBC) membranes functioned as the initiator for the ATRP of St. The poly(St)-grafted membranes, which can still act as an ATRP initiator, were further grafted with tert-butyl acrylate (tBA). Different ATRP systems were investigated and the best one was the homogeneous system with CuBr as the catalyst. Besides, PEMs were also prepared by combining EB preirradiation grafting with nitroxide-mediated polymerization (NMP) (Holmberg et al., 2004). The pre-irradiated PVDF membrane was used to tether 2,2,6,6-

tetramethylpiperidinyl-1-oxy (TEMPO) on them at first. Then St was grafted on the membrane mediated with TEMPO.

Saito's group (Asai et al., 2005; Hagiwara et al., 2005; Kim and Saito, 2000; Kiyohara et al., 1997; Kubota et al., 1997a; 1997b; Miyoshi et al., 2005; Okamura et al., 2002; Ozawa et al., 2000; Saito et al., 1999; 2002b; 2004; Sasagawa et al., 1999; Tsuneda et al., 1998) prepared affinity and ion-exchange membranes (IEMs) by the RIGP method and subsequent chemical modifications. Radiation creates radicals throughout the trunk polymer because of its high energy. Therefore, when PE is used as a trunk polymer, the formation sites of the graft chains on the porous membrane are classified into two types: graft chains embedded in the matrix and those extending from the pore surface (as illustrated in Fig.4.23). The former chains allow the matrix to swell, and the latter chains, referred to as a polymer brush, acquire the mobility of expansion and shrinkage in response to environmental variations, such as pH, ionic strength and temperature.
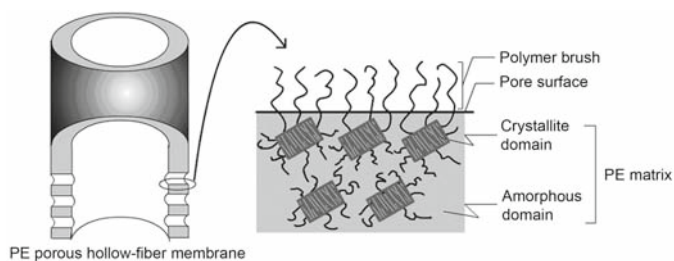
Fig. 4.23. Definitions for polymer brushes grafted onto the pore surface of a porous hollow-fiber membrane. Reprinted from (Okamura et al., 2002). Copyright (2002), with permission from Elsevier

A fluorescence probe technique was used to investigate the characteristics of the polymer chain grafted on a PE MF membrane after labelling with dansyl groups (Tsuneda et al., 1998). The conformational changes of the grafted polymer chain in various solvents were monitored by considering that the steady-state fluorescence emission spectrum of the dansyl group was affected by the polarity of the solvent, the polyethylene, and the graft chain itself. The shift of the emission wavelength of the graft chains demonstrated that the graft chains containing amino groups stretched in water and methanol while shrank in dimethylformamide, acetone, and benzene. These results corresponded to changes in solvent permeability through the membrane pore.

4.2.4.2 γ-Ray Irradiation

The ^{60}Co γ-ray is often used for graft polymerization, which is very simple and penetrating. Therefore it is also an interesting way to modify membranes

with various vinyl monomers for desired functions. Surface modification with γ-ray irradiation can be performed in three ways: pre-irradiation (Choi et al., 2001; Siu et al., 2006; Zhang and Jin, 2006), peroxidation (Kang et al., 2001) and a mutual irradiation technique (Filho and Gomes, 2006; Hegazy et al., 2000a; Hsiue et al., 1988; Nasef et al., 2004; Yang and Hsiue, 1990).

Li et al. (2004; 2005c) and Sato et al. (2003) developed partially fluorinated PEMs for polymer electrolyte fuel cell (PEFC) applications by γ-ray pre-irradiation induced graft polymerization of St into RX-PTFE membranes. It was found that a lower grafting temperature induced higher DG of St on the membrane because of radical annihilation at higher temperature (Sato et al., 2003). The highest GD achievable for RX-PTFE membranes exceeded 130 wt.%. The apparent activation energies were calculated as 39.7 kJ/mol for RX-PTFE membranes and 59.5 kJ/mol for PTFE membranes, which were larger than the reported value 27.9 kJ/mol (Gupta et al., 1994) of fluorinated ethylene propylene copolymer (FEP) resulting from its amorphous and non-crosslinked structure and relatively thin thickness. On the other hand, the dependence index of absorbed doses at pre-irradiation for an RX-PTFE membrane is 0.66, and for a PTFE one it is 1.57 (Li et al., 2004).

After graft polymerization the structure of the membrane may undergo considerable changes at different steps in its preparation, depending on the nature and the amount of the monomer being grafted. These changes may be in the form of thermal stability, crystallinity, glass transition temperature, melting behavior and the compatibility of the grafted component with the backbone polymer. Gupta and Anjum (2001) investigated the properties of PE membranes grafted with AAm by a γ-ray pre-irradiation technique. It was found that the grafting led to a considerable decrease in the heat of fusion and crystallinity of PE membranes because of the cumulative impact of the dilution effect induced by the grafted poly(AAm) chains and the crystal distortion by amorphous poly(AAm) chains. The surface roughness could be strongly affected by the addition of solvents such as acetone and methanol to the grafting medium, which caused the nonhomogeneity on the surface (Gupta and Anjum, 2002).

In addition, because γ-rays are very penetrating, γ-ray irradiation could improve the GD. Liu et al. (2004) found that although NVP can be grafted on PP membranes by UV-induced graft polymerization, the GD was never higher than 2.0 wt.% with the monomer concentration ranging from 10%(v/v) to 70%(v/v). Therefore they adopted another method, γ-ray pre-irradiation, to enhance the GD. It can be seen from Table 4.3 that the GD increased quickly at first. The highest GD was up to 64.7 wt.% when the dose was 15 kGy. However, when the dose was larger than 15 kGy, the GD decreased remarkably. This might be due to the interactions between the irradiation-induced free radicals and the recombination of them, which greatly reduced the amount of active sites for the graft polymerization and resulted in the decline of GD. Therefore, when compared with UV-induced graft polymer-

ization, it was apparent that γ-ray pre-irradiation grafting was more efficient for the tethering of PVP to the PP membrane surface.

Table 4.3. Effect of pre-irradiation dose on the grafting degree PVP on PPMM[a]. Reprinted from (Liu et al., 2004). Copyright (2004), with permission from Elsevier

Pre-irradiation dose (kGy)	GD (wt.%)
5	4.20 ± 0.21
15	64.70 ± 3.11
25	20.91 ± 1.04
35	3.92 ± 0.20

[a]Grafting solution composition: NVP/water = 15/85 (v/v); reaction temperature: 75 °C; reaction time: 10 h

With γ-ray radiation technology there are some other methods for improving the GD or for suppressing the homopolymerization of the monomers. For example, Choi and Nho (1999) found that H_2SO_4 and DVB could enhance the GD of St on PE hollow fiber membranes initiated by γ-ray pre-irradiation. PE, silicone rubber (SR) and poly[1-(trimethylsilyl)-1-propyne] (PTMSP) membranes were grafted with AAc by peroxidation of γ-ray in the presence of Mohr's salt, which could effectively restrain the homopolymerization (Yang and Hsiue, 1998). Taher et al. (1996) reported that AAc and MAA were grafted onto poly(tetrafluoroethylene-perfluoropropylvinyl ether) membranes by mutual γ-ray irradiation technique. The addition of an inhibitor such as Mohr's salt, $FeCl_3$ and $CuCl_2$, was used to inhibit homopolymerization of the monomer. Similarly, grafting of NVP, AAm and their mixtures onto PP membranes was also investigated using this technique (Dessouki et al., 1998).

In addition, Fang et al. (1997) studied the kinetics of RIGP of vinyl acetate on ethylene-*co*-propylene rubber membranes. The membranes were immersed in the monomer solution containing Cu^{2+} and then irradiated with γ-ray. The work established the relationship of the initial grafting rate (dg_0/dt) with various effect factors: $\ln(dg_0/dt) = 20.61 - 5894(1/T) + 1.95\ln[M]_0 + \ln D + 0.5\ln[Cu^{2+}]$. The apparent activation energy and collision frequency factor of the grafting polymerization are 49 kJ/mol and $8.9 \times 10^8 G\% \cdot L^{2.45}/(kGy \cdot h \cdot mol^{2.45})$.

4.2.5 Other Methods

Except for the previously mentioned methods, some techniques, such as ion beam radiation, laser radiation and ozone treatment, may also be chosen to initiate graft polymerization on polymer membranes. Saito et al. (1997) developed a laser-induced surface graft polymerization method in which surface radicals were generated upon laser irradiation. This method enables surface graft polymerization with dimensional precision at the micron scale. Thus they extended this method to prepare a surface-charge-mosaic-modified UF

membrane (Saito and Yamashita, 1998). Firstly the surface of a UF membrane was treated with 4-VP after laser irradiation using a striped photomask. Subsequently the striped photomask was shifted and the surface that was initially shaded from the laser beam by the photomask was exposed to laser irradiation and treated with AAc. Oxygen and carbon distribution maps, determined by scanning XPS analysis and TOF-SIMS maps for $^{16}O^-$ and $^{26}CN^-$ ions showed that the surface of the treated membrane had striped domains composed of poly(4-VP) and poly(AAc).

Under the ozone treatment polymer membranes are oxidized and hydroperoxides are formed (Yamauchi et al., 1991). When exposed to heat the hydroperoxides break into radicals that are able to initiate graft polymerization. Using this technique DEGMA and HEMA were grafted onto PP membranes and the thin grafted hydrogel layers were evenly distributed on the surface (Karlsson and Gatenholm, 1996). An improved wettability was obtained for the DEGMA-grafted surface. In addition, the peroxide generated by the ozone treatment could also be decomposed by redox reaction with $FeCl_2$ and could then initiate HEMA graft polymerization at mild temperatures (Wang et al., 2000). The GD increased from 4 wt.% to 23 wt.% with an increase in the ozone treatment time. The addition of Mohr's salt greatly enhanced the GD of HEMA up to 600 wt.% at 50 °C for 60 min, which behaved as a hydrogel more than as a membrane (Gatenholm et al., 1997).

4.3 Applications of Surface Modified Membranes

The surface modified membranes can be applied in various fields as they can be tailored to satisfy the requirements of functionality. In the following sections the applications of the modified membranes will be discussed from the aspect of environmental stimuli-responsive gating membranes, antifouling membranes, adsorption membranes, pervaporation and reverse osmosis membranes, membranes for energy conversion, gas separation membranes and biomedical membranes.

4.3.1 Environmental Stimuli-responsive Gating Membranes

In the past decade much attention has been drawn to environmental stimuli-responsive gating membranes with porous membrane substrates and stimuli-responsive functional gates, because their surface and permeation properties can be controlled or adjusted by the gates according to an environmental chemical and/or physical stimulus, such as temperature, pH, ionic strength, glucose concentration, electric field, photo-irradiation, or substance species. These environmental stimuli-responsive membranes could find various applications, including in controlled drug delivery, bioseparation, chemical separation, water treatment, chemical sensors, tissue engineering, and so on. The

fabrication of these "intelligent" or "smart" membranes is of both scientific and technological interest.

4.3.1.1 Temperature Responsive Membranes

Grafting NIPAAm on polymer membranes is a common way to prepare temperature responsive membranes. When NIPAAm was grafted on a PE membrane (Wang et al., 2002), the results of SEM, XPS, and the streaming potential study indicated that the grafted poly(NIPAAm) chains exhibited different configurations around the lower critical solution temperature (LCST) (Huang et al., 2002). The amide groups of the grafted poly(NIPAAm) tended to distribute outwards when the chains were in the swelling state, while enveloped by the nonpolar main chains when in their shrinking state. For the poly(NIPAAm)-grafted PE membranes (Peng and Cheng, 1998), two distinct types of temperature responses were observed, depending on the GD. The permeability of the graft membrane increased with temperature at low GD, while it decreased with temperature at high GD. A mechanism explaining the dual valve function of the graft membrane was proposed based on the location of the grafted polymers on the membrane. As illustrated in Fig.4.24, at high GD the poly(NIPAAm) layer shrinks with temperature increase and becomes more compacted and more resistant to diffusion, resulting in decreased permeability. However, it is different for the graft membrane with low GD.
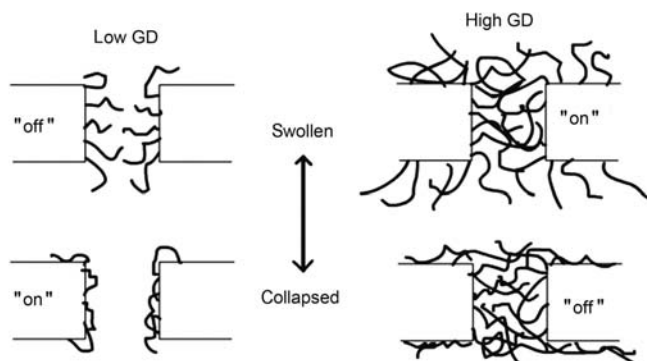
Fig. 4.24. Illustration of the dual-response mechanism (Peng and Cheng, 1998). Copyright (1998). Reprinted with permission of John Wiley & Sons, Inc.

Xie et al. (2005) found that the thermo-responsive gating characteristics of the water flux of poly(NIPAAm) grafted PCTE membranes were mainly dependent on the pore size change induced by the phase transition of poly(NIPAAm) chains rather than the variation of membrane/pore surface hydrophilicity. Xie et al. (2007) also found that when hydrophilic or

hydrophobic monomers were added to NIPAAm monomer solution in the fabrication of thermo-responsive membranes, the response temperatures of grafted gating membranes linearly increased with the molar ratio of the hydrophilic monomer AAm in the NIPAAm co-monomer solution, but linearly decreased with the molar ratio of hydrophobic monomer BMA. These results provided valuable guidance for the design and preparation of thermo-responsive gating membranes with desired response temperatures for different applications. In addition, the effects of the physical and chemical properties of porous substrates on the thermo-responsive gating characteristics were investigated (Yang et al., 2006). Hydrophilic N6(nylon 6) and hydrophobic PVDF porous membranes were used as substrates. As shown in Fig.4.25, the poly(NIPAAm)-grafted N6 membranes exhibited a much larger thermo-responsive gating coefficient (R) than the poly(NIPAAm)-grafted PVDF membranes. This phenomenon should be attributed to the differences in the physical and chemical properties of the porous substrates, such as the hydrophilicity and microstructure. Because of the hydrophilicity of N6, the membrane could allow water to pass easily through the pores. As schemed in Fig.4.26, the PVDF membranes were featured with finger-like pores with a thin functional top layer. After grafting only the grafted poly(NIPAAm) in the functional top layer with controlling pore size could act as a thermo-responsive gate. On the other hand, the N6 membranes were of honeycombed porous structure with comparable pore sizes and hence the grafted poly(NIPAAm) chains in the pores could work effectively throughout the membrane thickness.
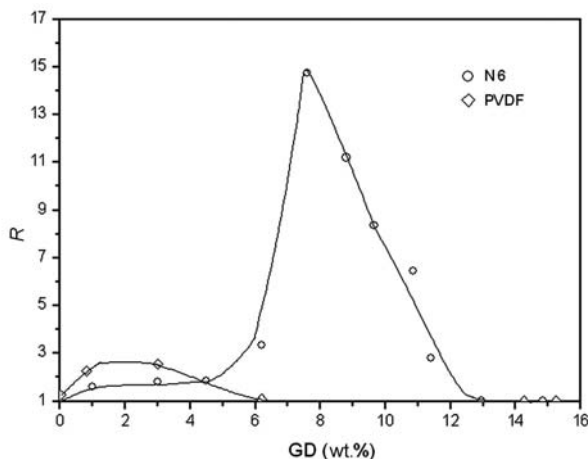
Fig. 4.25. Effects of grafting yield on the thermo-responsive gating characteristics of poly(NIPAAm)-grafted membranes with different substrates (Yang et al., 2006). Copyright (2006). Reprinted with permission of John Wiley & Sons, Inc.
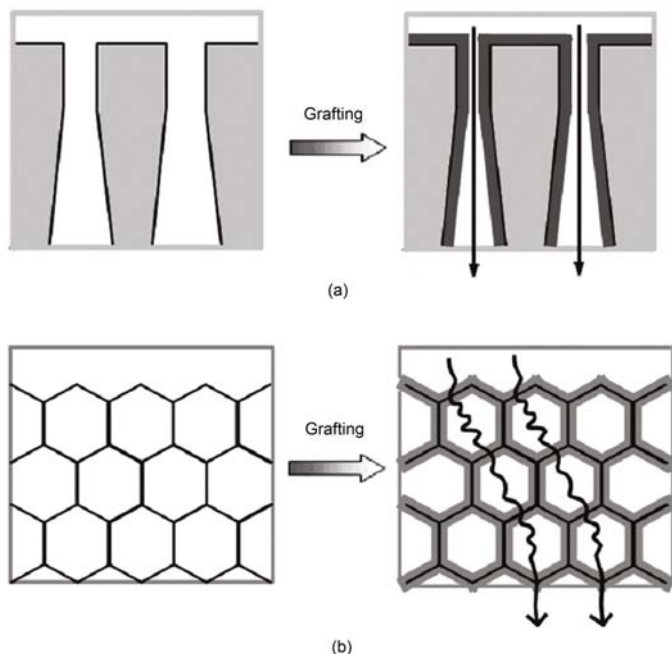
Fig. 4.26. Schematic illustration of the microstructures of cross-sections of poly(NIPAAm) grafted membranes with different porous substrates prepared by plasma-graft pore-filling polymerization (Yang et al., 2006). (a) PVDF substrate and graft membrane; (b) Nylon 6 substrate and graft membrane. Copyright (2006). Reprinted with permission of John Wiley & Sons, Inc.

As mentioned above, almost all the thermo-responsive gating membranes have positive thermo-responsive characteristics, i.e. the membrane permeability increases with environmental temperature. It is because almost all the thermoresponsive functional gates were constructed from poly(NIPAAm). Recently Chu et al. (2005) prepared a negatively thermo-responsive N6 membrane through grafting of AAm/AAc-based IPN polymers in the pores. The membranes with AAm/AAc-based IPN gates showed satisfactorily reversible and reproducible thermo-responsive permeation characteristics. In addition, poly(NIPAAm) grafted PE membranes (Chu et al., 2003) could change from a positive thermo-response to a negative thermo-response by increasing the pore-filling ratio to around 30%. Predicted diffusional coefficients of solutes across the poly(NIPAAm) grafted membranes, which were developed by the phenomenological models, fitted the experimental values well.

For poly (NIPAAm)-grafted PP MF membranes above the LCST of poly (NIPAAm) the fluxes of water and solution containing 500×10^{-6} of dextran (molecular weight: 1.67×10^5 g/mol) were about 6 and 85 times higher than those below the LCST, respectively. Therefore it is clear that the thermo-

response membrane can show multifunctional characteristics, i.e. MF above the LCST and UF below (Liang et al., 1999).

In addition, if the grafted poly(NIPAAm) brushes are not long enough to cover the membrane pores, a crosslink agent is necessary. However, a high crosslink degree may limit the shrinkage of the grafted poly(NIPAAm) and result in the shift of critical temperature to a high temperature (Yang and Yang, 2003).

4.3.1.2 pH Responsive Membranes

Iwata et al. (1998) prepared a pH-responsive membrane grafted with poly(AAc) brushes. It was found that the filtration rate of the membrane with a GD of 0.30 μg/cm^2 was 28 times higher at pH 2.4 than at pH 5.4. As determined by AFM, the thickness of the graft layer was several tens of nanometers at pH 2.6 and increased to 20∼430 nm at pH 7.6, depending on the GD of poly(AAc). Combining the two results it can be concluded that the poly(AAc) graft chains dynamically opened and closed the pores in response to the medium pH, functioning as a molecular valve to regulate the permeation characteristics. Similarly, Shim et al. (1999) prepared a pH-responsive poly(AAc)-grafted PS membrane. A distinctive flux decline of riboflavin solution appeared in the range of pH 4.0∼5.0. Above pH 4.8 the grafted poly(AAc) chains extended and blocked the membrane pores caused by the electrostatic force among the dissociated carboxyl groups. Furthermore, the poly(AAc) grafted PVDF membranes can be used in drug release (Akerman et al., 1998). Permeability of these membranes was controlled by environmental factors such as pH and ionic strength. Besides, the drug properties had an important role in the release. The drug can diffuse through the membrane quite easily at low pH. However, at pH 7 the grafted chains partially blocked the pores and the diffusional flux of bigger drug molecules (M_w 9400) decreased by five orders of magnitude and also the flux of smaller molecules was clearly reduced. Furthermore, this type of membranes facilitated the transport of cationic drugs and repelled anionic ones. All of these trends were reasonably predicted by a mathematical model based on the Donnan equilibrium and measured transport number data.

Mika et al. (1995; 1997; 1999) prepared poly(4-VP)-grafted PP or PE membranes which exhibited a dramatic pH-valve effect. The valves opened at pH>5 where the anchored poly(4-VP) was largely in its unionized form but closed at low pH where the anchored poly(4-VP) was protonated. Most importantly, at low pH, i.e. under closed-valve conditions, these membranes were capable of separating simple inorganic salts from aqueous solutions. The hydraulic properties of the membrane can be analyzed in terms of two morphological models: the brush model or the pore-filled model (Mika et al., 1999). However, using polyelectrolyte theory it is just possible to select the more adequate model for a given situation.

4-VP was also grafted on PET track membranes to design a pH-switching membrane with a novel pore-covering structure (Yang and Yang, 2005). Differing from AAc-grafted pore-covering membranes, these 4-VP-grafted pH valves showed no obvious open and close configurations under AFM. As a consequence of thin surface grafting layer the pore covering was impaired under pressure. In the pressure driving filtration tests the grafted membranes had no retention capacity to BSA. On the contrary, with pressure free, high DG samples could trap it completely whether in an open or closed state. The special pore-covering structure and the performance of reversible fully open/close predicted potential applications in self-adapting micro-reactor and micro-fluidic systems.

It is worth noting that the rate of water permeation through a polypeptide-grafted PTFE membrane was also pH-dependent and found to be slow under high-pH conditions and fast under low-pH conditions (Ito et al., 1997). Under high-pH conditions, randomly coiled graft chains extended to close the pores. The chains formed a helix structure and opened the pores under low-pH conditions. The magnitude of the permeation rate was dependent upon the length and density of the graft chains. Ionic strength also affected the permeation rate.

AAc and NIPAAm grafted polyamide membranes showed multi-stimuli responsive permeability. The phase transition temperature increased from 31 °C to about 50 °C depending on the amount of AAc added to the NIPAAm reaction medium as a comonomer (Lee and Shim, 1997). In addition, poly(AAc)-b-poly(NIPAAm) block polymer chains were grafted on the PVDF membrane resulting in a membrane with pH- and temperature-sensitivity to aqueous media at the same time (Ying et al., 2004). Peng and Cheng (2001) prepared poly(NIPAAm)-b-poly(MAA) diblock brushes grafted PE membranes having pH- and temperature-sensitive permeability. The co-grafted membrane with the poly(MAA) content ranging from 7.6 wt.% to 67.1 wt.% showed the LCST at pH 7.4. By contrast, the co-grafted membrane with the poly(MAA) content above 22 wt.% showed no LCST at pH 4.4 due to complexation between poly(NIPAAm) and poly(MAA) blocks.

4.3.1.3 Photo-Irradiation Responsive Membranes

Chung et al. (1994) first reported a photo-irradiation responsive polymer membrane. The permeability of the membrane could be photocontrolled by grafting with methacrylate containing a spiropyran group, which is able to be a zwitterionic merocyanine form under UV-light irradiation and to isomerize back to the neutral spiropyran under visible-light irradiation. The permeability of the graft membrane varied with UV- or visible-light irradiation. Nayak et al. (2006) also achieved an optically reversible switching membrane. They demonstrated, through two related experiments, that the switchable hydrophilic (on exposure to 254-nm UV light) and hydrophobic

(with visible light) surfaces exhibited low and high protein adsorbabilities, respectively, and then displayed high and low buffer-permeations rates.

4.3.1.4 Ion Responsive Membranes

Ito et al. (2002) and Yamaguchi et al. (1999) developed an 'ion gating' membrane, based on the surface modification of a PE MF membrane with a grafted copolymer of NIPAAm and crown ether-functionalized AAm. As shown in Fig.4.27, when the crown ether host captured specific metal ions, such as Ba^{2+}, the grafted polymer in the pores swelled and closed the pores. When metal ions were removed from the crown ether host, the polymer shrank and opened the pores. The response time was very short and when the feed solution was changed the state of pores changed within 30 s. The response mechanism of this membrane had been clarified based on the understanding of the phase transitions and lower critical solution temperature of the functional copolymer in the presence or absence of ions with high affinity for the crown ether 'receptors'. This membrane may be useful not only as a molecular recognition ion gate, but also as a device for spontaneously controlling the permeation flux and solute size.
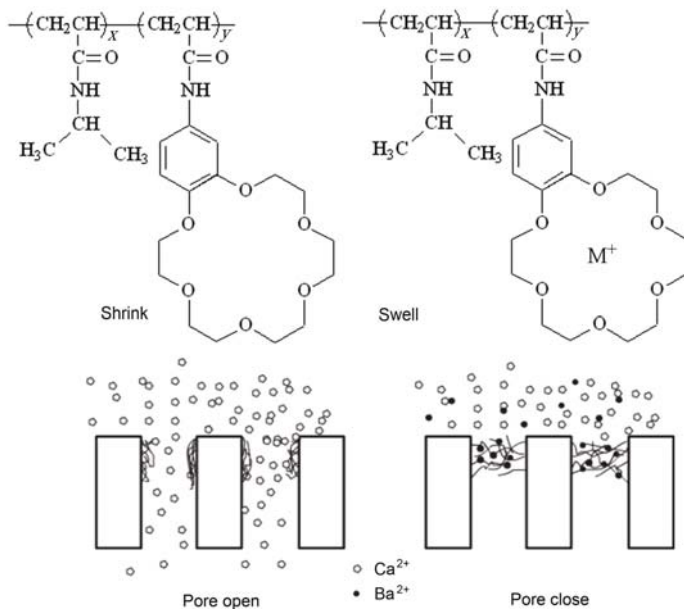
Fig. 4.27. A molecular recognition ion gating membrane based on the surface modification of a PE MF membrane with a grafted copolymer of NIPAAm and crownether-functionalized AAm. Reprinted with permission from (Ito et al., 2002). Copyright (2002), American Chemical Society

Furthermore, the poly(4-VP)-grafted PE and PP MF membranes were ion responsive membranes and showed a higher rejection of polyvalent co-ions and a lower rejection of polyvalent counter-ions compared to monovalent ions in the separation experiment. And the salt rejection strongly depended on the feed concentration (Mika et al., 1995).

4.3.1.5 Substance Species Responsive Membranes

Yanagioka et al. (2003) prepared a molecular recognition membrane by grafting a thermosensitive polymer with a host receptor, β-cyclodextrin (CD), on the PE membrane. The membrane exhibited a high selectivity, in which CD moieties specifically recognized guest molecules and poly(NIPAAm) controlled the molecular recognition ability. In detail, the thermosensitive volume change of the grafted polymer chains had an influence on the degree of steric hindrance to the host-guest interaction. This membrane can be applied as a novel affinity separation system.

The glucose-sensitive membranes were other substance species responsive membranes and were prepared by immobilizing glucose oxidase on the membrane (Cartier et al., 1995; Chu et al., 2004). By measuring the permeability of the membrane, it was found that the prepared membrane responded rapidly to changes in glucose concentration and could be used in drugs (such as insulin) release.

4.3.2 Antifouling Membranes

Protein-induced membrane fouling is caused by protein adhesion on the membrane surface and protein deposition in membrane pores. Membrane fouling during filtration can result in significant loss of performance like selectivity and permeation flux, and thus restricts the membrane application. Usually, hydrophilic membranes can effectively reduce protein fouling. Therefore it is feasible to minimize protein fouling by modifying hydrophobic membranes with hydrophilic monomers.

The permeability experiments of BSA solution revealed that the grafting of poly(NVP) (Pieracci et al., 2000; 2002b; Taniguchi et al., 2003b) and poly(AAc) (Zhu et al., 2007) endowed the modified PES membranes with enhanced fluxes and anti-fouling properties. The antifouling properties of poly(HEMA)-grafted PP membranes were investigated by BSA filtration experiment (Hu et al., 2006; Shim et al., 2001). The modified membrane showed a higher solution flux, lower BSA adsorption and better flux recovery when compared with the unmodified PP membrane. In particular, a 40.6 wt.% grafted membrane showed a two-fold increase in BSA solution flux, a 62% reduction in total fouling and a three-fold increase in flux recovery after chemical cleaning (Shim et al., 2001). The adsorptive BSA on the PP membranes decreased from 2.56 to 0 g/m^2 when the GD increased from 0 to 24.67 wt.%

(Hu et al., 2006). Kang et al. (2001) discussed in detail the effects of BSA adsorption on poly(HEMA)-grafted PP membranes. It was confirmed from the BSA filtration results that the modified membrane had a faster rate of permeation than the unmodified one because the grafted poly(HEMA) layer prevented the initial contact of BSA with the surface of the membrane, resulting in a low specific resistance. In addition, the low adsorption of BSA with the increase of GD was crucially affected by the contribution of higher roughness and hydrophilicity rather than by the contribution of repulsive interaction between two species. Furthermore, Koehler et al. (2000) studied the correlations between intermolecular forces and UF measurements for a hydrophilic modified PS membrane during hen egg-white lysozyme (Lz) filtration. The results demonstrated that the hydrophilic surface exhibited reduced adhesion forces, reduced adsorbed amount, and reduced protein fouling. Their findings provided a fundamental molecular basis to this widely reported and observed phenomenon.

Natural organic matter (NOM) is considered as another contributor to membrane fouling in water treatment applications (Jimbo et al., 1998c; Kabsch-Korbutowicz et al., 1999; Maartens et al., 2000). It is a heterogeneous mixture of complex organic materials consisting primarily of humic substances (humic and fulvic acids) as well as small amounts of hydrophilic acids, proteins, lipids, carboxylic acids, amino acids, and hydrocarbons. The hydrophilic-modified polyamide RO membranes adsorbed less NOM and were more easily cleaned than unmodified membranes with specific fluxes, not changing by more than 0~25% and NaCl rejection was unchanged or increased slightly (Gilron et al., 2001). In particular, a membrane modified with uncharged monomer, HEMA, showed an increase in rejection of chloride on both synthetic and effluent feed streams (Belfer et al., 2004). Kilduff et al. (2000) prepared a poly(NVP)-grafted PES and sulfonated PS NF membrane. It was found that fouling by NOM was reduced significantly. Furthermore, six different hydrophilic monomers were grafted on PES UF membranes to evaluate their ability to reduce fouling by NOM (Taniguchi et al., 2003a). All of them increased NOM rejection excepting NVP. The weak acid AAc modified membranes could reduce irreversible fouling to zero and exhibited excellent filtration performance over multiple runs, in contrast to other strongly hydrophilic monomers such as HEMA and AAG, which increased irreversible fouling relative to the unmodified membrane. Reversible fouling resulting from cake formation was only weakly dependent on membrane surface chemistry; by contrast, irreversible fouling exhibited a marked dependence on surface chemistry. They concluded that hydrophilicity is not an appropriate parameter for estimating reduced fouling potential for NOM feeds, as it is for feeds containing protein. This conclusion was confirmed in their further work, namely that NVP, AMPS and AAc of the six monomers modified PES membranes show superior performance (high protein retention, high protein solution flux, and low irreversible fouling) in the BSA filtration

experiment (Taniguchi and Belfort, 2004). Carroll et al. (2002) reported a polyelectrolyte-grafted MF membrane to control fouling induced by NOM in drinking water. They found that non-ionic and cationic hydrophilic grafts had rates of flux decline by NOM fouling up to 50% lower than an ungrafted PP membrane. Thereafter anionic hydrophilic grafts had initial flux increases up to 140% at high GDs due to multi-valent ions in the natural water, although the pure water flux was substantially lower than for the unmodified membrane.

In addition, Susanto et al. (2007) found that a poly(PEGMA)-grafted PES UF membrane showed excellent antifouling performance, especially for polysaccharides. This membrane can be used to filtrate sugarcane juice. Similarly, a poly(AAc) grafted PAN membrane showed higher rejection with a dextran aqueous solution than with an unmodified one (Nouzaki et al., 2002). Commercial PVDF MF membranes were surface modified with quaternized DMAEM, AMPS and polyehtyleneimine (PEI) (Hilal et al., 2004). And the membrane modified with quaternized DMAEM and PEI had a strong bactericide effect on *E. coli* bacteria. It was attributed to the penetration of polymeric polycationic chains through the wall of the bacteria cell to induce the death of the cell. This membrane could be potentially more resistant to biofouling in water treatment applications.

Yu et al. (2005; 2006a; 2006b; 2007) compared the antifouling characteristics of a series of monomers including AG, PVP, AAc and AAm modified PP hollow fiber microporous membranes in a submerged membrane-bioreactor (SMBR). It was found that the flux recovery increased by 29.0%, 10.0%, 23.0% and 55.0%, and the relative flux ratio increased by 90.0%, 79.0%, 152.0% and 32.0%, respectively. It is clear that the modified PP membranes showed good anti-biofouling properties.

4.3.3 Adsorption Membranes

Separations with membrane adsorbers are a very attractive and rapidly growing application field for functional macroporous membranes (Ulbricht, 2006). The key advantage of the membrane in comparison with conventional porous adsorbers (beads, typically having a diameter of $\geqslant 50$ μm) is the increased diffusion rate which results in a high separation speed.

4.3.3.1 Biomolecules and Cell Adsorption

The efficient recovery of labile biomolecules requires rapid, reliable separation processes using mild conditions. Compared with conventional chromatographic packed beds, adsorptive membranes exhibit low backpressure, short residence time, high volumetric throughputs and a negligible diffusional mass-transfer resistance. Therefore, adsorptive membranes are available in the clarification, concentration, fractionation and purification of biomolecules (Roper

and Lightfoot, 1995). There have been some reviews focusing on special membranes (Kawai et al., 2003; Zeng and Ruckenstein, 1999) or on the various applications (Charcosset, 1998; Ghosh, 2002; Lightfoot and Moscariello, 2004; Zou et al., 2001). The membranes with grafted polymer brushes can adsorb proteins based on ion-exchange, hydrophobic and affinity interactions (Kawai et al., 2003). It has been proposed that proteins were captured in multilayers by the ion-exchange group-containing polymer brushes due to the formation of a three-dimensional space for protein binding via the electrostatic repulsion of the polymer brushes (Kawai et al., 2003). In contrast, proteins are captured in a monolayer at most by the polymer brushes containing hydrophobic or affinity ligands. Besides, it is well known that either a hollow-fiber or a flat-sheet porous membrane as a matrix provides a high protein purification rate (Koguma et al., 2000).

Saito's group (Koguma et al., 2000; Kubota et al., 1996; 1997a; Saito et al., 1999; Tsuneda et al., 1995) functionalized poly(GMA)-grafted PE hollow fiber membranes with anion-exchange groups, namely amino (AM), ethylamino (EA), and diethylamino (DEA) groups, for protein purification. Because mass transfer of the protein was enhanced by the convective flow of the protein solution through the membrane pores, the EA modified membrane exhibited higher recovery rates and recovery capacities of proteins compared to conventional gel-bead-packed beds (Kubota et al., 1996). The multilayer binding of proteins on membranes was determined by internal and external factors. Effects of pH, temperature and NaCl concentration on the multilayer binding of BSA to DEA modified hollow-fiber membranes was also elucidated (Tsuneda et al., 1995). With increasing salt concentration or pH of the protein buffer solution, the graft chain shrank and BSA binding capacity decreased. On the other hand, the BSA binding capacity slightly increased with increasing temperature. Internal factors include the effects of different anion-exchange groups. Multilayer binding was observed for membranes containing EA and DEA groups, with conversions of epoxy groups to EA or DEA groups of higher than 80%, whereas adsorption onto the hollow fiber containing the AM group remained constant irrespective of the conversion. This dependence on the degree of multilayer binding of protein on the ion exchange group density was consistent with that of the flux (Koguma et al., 2000). Irrespective of the flow-rate, the dynamic binding amount of BSA of the membrane module was constant at a high level, and the performance was stable over five adsorption and elution cycles (Kubota et al., 1997a). Besides, the long grafted polymer brush was favorable for protein binding (Okamura et al., 2002) The anion-exchange membrane could be used to purify gelsolin from bovine plasma (Hagiwara et al., 2005). Furthermore, Sasagawa et al. (1999) reported another kind of ion-exchange membrane containing SO_3H-group. It was found that the membrane can adsorb Lz in multilayers. After crosslinking by Mg^{2+} or Ca^{2+}, the membrane can also be used in the purification of egg-white protein that contains Mg and Ca ions.

Ulbricht's group (Ulbricht and Yang, 2005; Yusof and Ulbricht, 2006) prepared ion-exchange membranes by grafting different carboxyl polymer brush layers on PP membranes for reversible protein Lz binding. The binding was performed at low salt concentrations and elution was achieved by increasing the salt concentration. It is worth noting that both poly(AAc-*co*-AAm) and crosslinked poly(AAc-*co*-MBAA) layers showed Lz binding capacities more than 10 times higher than monolayer adsorption onto the unmodified PP membrane surface, and the quantitative recoveries were similar to that of poly(AAc) with the same DG.

Okamura et al. (2005) prepared a poly(NIPAAm)-grafted PP membrane containing an adsorbed monoclonal antibody specific to the target cell. Due to the thermo-responsive phase transition of poly(NIPAAm) that at 32 °C water-insoluble (hydrophobic) and water-soluble (hydrophilic) states interconvert, adsorption of the cell onto the membrane at 37 °C and its desorption at 4 °C took place. With this method, mouse CD80- or mouse CD86-transfected cells were enriched from a 1:1 cell suspension to 72% or 66%, which was simple and of high yield.

Lee et al.(1996) described a grafted-type DEA-containing membrane with a capturing rate constant for *S. aureus* cells that was 1000-fold higher than that of commercial crosslinked-type beads. The ability to capture cells was evaluated for DEA-containing PE membranes with two different coexisting functional groups, epoxy (EO) group or EA group. *S. aureus* and *E. coli* cells were taken as representative for Gram-negative and Gram-positive microbial cells, respectively. The coexistence of the EO group with the DEA group on the membrane was found to be an important factor for the capture of *S. aureus* cells due to the electrostatic and hydrophobic interactions. And better results for *E. coli* cells capture might be obtained by quaternizing the DEA group to append charges onto the graft chains. In addition, the graft polymer chains on the membrane formed favorable three-dimensional binding sites to capture cells (Lee et al., 1997).

4.3.3.2 Metal Adsorption

Selective removal and recovery of metals from wastewater is an important strategy for environmental protection and is of economic concern (Hegazy et al., 2000b). The ability of certain polymers to form polymer-metal complexes has been used for removal, separation and purification of metal ions from contaminated water and solid wastes. With membrane permeation, a high-speed recovery of the metal ion can be achieved because the time required for the diffusion of the metal ion to the chelating group is much shorter than the residence time of the solution across the membrane.

Poly(AAc) grafted PE membranes were found having higher affinity for K^+, Na^+ and Li^+ ions compared to other alkali metals. When the membranes were further converted into –CONH-OH form, they changed to be highly selective towards zirconium and consequentially can be used in the removal of

zirconium from uranium (Hegazy et al., 2000a). Saito et al. (2002a) prepared a cation-exchange porous hollow-fiber PE membrane with crosslinked polymer brushes which can capture Na^+ during the permeation of NaCl solution. The capturing efficiency increased with the degree of crosslinking. The similar membranes functionalized with 2,2'-iminodiethanol, di-2-propanolamine, N-methylglucamine, and 3-amino-1,2-propanediol enabled a high speed recovery of germanium during permeation of a germanium oxide solution. The adsorption capacity did not deteriorate after repeated use of adsorption and elution (Ozawa et al., 2000). When the membrane was functionalized with iminodiacetate groups, it can be used in removal of copper ions from water (Saito et al., 2002b). Furthermore, $-SO_3H$ groups containing membranes can capture Pb ions from solution, which resulted in increase of the flux because crosslinking of the graft chains by Pb ions led to enlarged pores (Kim and Saito, 2000). On the other hand, this kind of membrane could adsorb Co^{2+} from solution and showed a good regeneration property. The adsorbed amount increased with increasing $-SO_3H$ content (Choi and Nho, 1999). The poly(AAc)-grafted membrane can be used as cation-exchange membranes in the recovery of metals from an aqueous solution, and the Hg^{2+} ion content of the membrane was more than that of either the K^+ or Ag^+ ions (El-Sawy and Al Sagheer, 2002).

In addition to the direct chelation of metal ions by ion-exchange membranes, Asai et al. (2005) reported that PE hollow fiber membranes modified with hydrophobic n-octadecylamino groups impregnated bis(2-ethylhexyl)phosphate, which can act as an extractant for liquid-liquid extraction, exhibiting a high selectivity for yttrium ions. The impregnated membrane was rather stable during repeated adsorption-elution cycles. Modification of the PE membrane was also performed in other ways. For example, Saito et al. functionalized the poly(GMA) grafted PE membrane with N-methylglucamine (NMG) and 3-amino-1,2-propanediol (APD) for the recovery of antimony(III). The equilibrium binding capacity to the NMG-ligand-containing membrane, 96 g Sb/kg, was 10 times higher than that of the APD membrane. The equilibrium binding ratios for NMG groups to antimony(III) were all approximately 2 which were in agreement with the results of computational structural analysis (Saito et al., 2004). The poly(AAm)-grafted PE membranes had an excellent binding capacity for mercury ions. Almost 99% mercury separation was achieved from 200×10^{-6} mol/L metal solution and the metal binding capacity was not affected significantly by the pH of solution. The binding capacity achieved 6.2 mmol/g in a membrane with 590 wt.% grafting (Gupta et al., 2002).

Dessouki et al. (1998) studied the effect of grafting modification of PP membrane with NVP, AAm or their mixture on the permeability of lead acetate solutions. The results proved that the modified membrane could remove heavy metals from solution effectively. However, in contrast to the aforemen-

tioned references, the concentration of metal ion in the permeate increased with the GD.

Besides the anionic and cationic polymer brushes grafted membrane, the synergistic effects of these two kinds of polymer brushes on the selective removal, separation and recovery of metals were also studied. Hegazy et al. (1997) investigated the properties of a cationic/anionic (poly(AAc/4-VP)-grafted) PE membrane as well as a cationic (poly(AAc)-grafted) membrane. It is worth noting that the stability constant and complexation bond strength between the metals and functional groups increase due to the incorporation of pyridine rings because a lone pair of electrons on the nitrogen atoms can easily form quaternary pyridinium metal salts or chelate. Furthermore, they prepared a cationic/anionic membrane with a homogeneous distribution of charge. The poly(AAc/2-VP)-grafted membrane showed a higher affinity towards metal chelation than that of the poly(AAc/4-VP)-grafted one, due to the high polarity and chelation effect of N atoms adjacent to 2-VP (Hegazy et al., 2000b). These membranes all showed high selectivity to the Fe^{3+} ion in the presence of other metal ions.

4.3.4 Pervaporation and Reverse Osmosis

Pervaporation (PV) and reverse osmosis (RO) are the two major membrane separation processes used in liquid separation. RO is already used commercially in the separation of aqueous solutions, such as desalination and concentration of fruit juices. However, it is difficult to apply the RO technique to organic liquid separation systems, such as ethanol/water mixtures, due to the high osmotic pressure of these separation systems. In contrast, PV can be used in: (1) dehydration of organic solvents; (2) removal of organic compounds from aqueous solutions; (3) separation of organic mixtures. During the PV process, permselectivity of the membrane is determined by the solubility and diffusivity of liquid in the membrane. Generally, diffusion of small molecules through a dense membrane is favored and the solubility of a component in a polymer is governed by the chemical affinity between the penetrant and the membrane (Teng et al., 2000). Therefore, focus is put on improving the solubility of the membrane by surface modification with graft polymer brushes. However, enhancement of solubility may cause swelling which impairs the separation properties.

### 4.3.4.1 Separation of Aqueous Solution

Separation of water-ethanol mixtures is useful in industrial applications. Generally there are two types of permselective membranes, i.e. water permselective and ethanol permselective membranes. Hydrophilic membranes are usually water permselective and hydrophobic membranes are ethanol permselective. However, it is crucial for water permselective membranes to meet

the requirements of hydrophilicity without dissolution. A useful method is to graft hydrophilic monomers onto the membrane with good stability.

Hirotsu et al. (1987) obtained water permselective membranes through grafting AAc onto a PP membrane. They found that a membrane with an ionized poly(AAc) layer was more effective with an increase in permselectivity. However, with AAc (or AAm) the graft polymerization also occurred in the bulk of the membrane resulting in a decrease in the permselectivity. When choosing MAA that is less reactive as a monomer, the constancy of the permselectivity of the membranes with a GD of more than 1.0 mg/m^2 was maintained, although the separation factor was relatively low (about 30) (Hirotsu, 1987).

Teng et al. (2000) reported on a poly(AAm)-grafted aromatic PA membrane. The separation factor and permeation rate of the modified membranes were higher than those of the unmodified membrane. Optimum PV was obtained by a membrane with a GD of 20.5 wt.% for a 90 wt.% ethanol feed concentration, giving a separation factor of 200 and a permeation rate of 325 g/(m^2·h), while the optimum PV performance was obtained using a poly(AAm)-grafted PTFE membrane with a GD of 21 wt.%, giving a separation factor of ~7500 and a permeation rate of 648 g/(m^2·h) (Tu et al., 2004). As shown in Fig.4.28, the permeation rate and separation factor increased with an increase in the ethanol concentration in the feed mixtures. In addition, membrane swelling prevention with poly(AAm)-grafted PTFE as substrate resulted in high permselectivity.
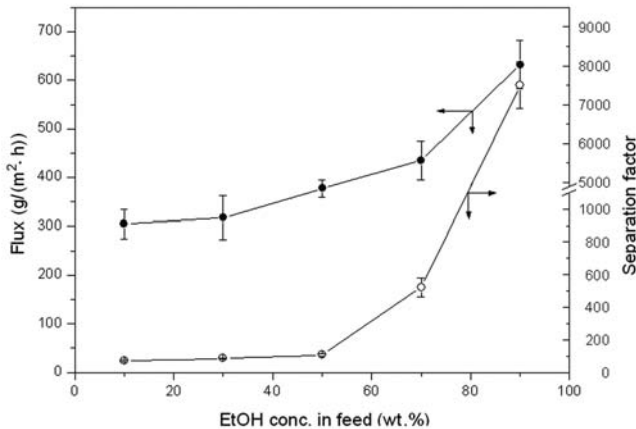
Fig. 4.28. Effect of feed concentration on the performances of poly(AAm)-grafted PTFE membrane with a GD of 21%. Reprinted from (Tu et al., 2004). Copyright (2004), with permission from Elsevier

Nakagawa's group (Mishima et al. 1999; 2001; Mishima and Nakagawa 1999; 2003) reported that grafting of hydrophobic monomers, such as HDFN-MA, fluoroalkyl methacrylates (FALMA) and alkyl methacrylates (AMA) on the PDMS membrane enhanced the selectivity for chlorinated hydrocarbons which contaminate the groundwater and wastewater. The grafted hydrophobic polymer had a much stronger affinity to the chlorinated hydrocarbons like trichloroethylene (TCE) and tetrachloroethylene (PCE) than to water. Besides, the permselectivity was significantly larger for a TCE solution with a higher concentration.

4.3.4.2 Separation of Organic Mixtures

In applying a polymer membrane to separate organic liquid mixtures there is a problem of membrane swelling, which reduces selectivity due to its plasticization effect. Therefore, to obtain good permselectivity, it is important to prevent the swelling of the membrane as well as increasing the solubility difference among the mixed organics. In PV the grafted polymer formed on the membrane surface shows little permeation resistance due to its further swelling, and that formed in the membrane pores exhibits permselectivity according to grafted polymer solubility. Thus the "pore-filling" polymerized membranes were proven to be suitable candidates for organic-liquid pervaporation which suppresses the swelling by the matrix of the support (Yamaguchi et al., 1992). The membrane must be inert to organic liquids, and the filling polymer must be soluble only in a specific component in the feed mixture (Yamaguchi et al., 1991).

Yamaguchi et al. (1991; 1992; 1993) prepared a composite membrane composed of two different polymers: a PE matrix that can suppress membrane swelling and a pore-filling polymer that exhibits selectivity. The permeability of a single component by PV could be controlled through the copolymer composition as well as by solubility control. And PV performance of the membranes showed the same tendency as solubility results. They also prepared crosslinked pore filling-type membranes using a plasma-graft polymerization technique to carry out the PV and RO of organic liquid mixtures. The grafted MA polymer was crosslinked to improve the pressure durability. Then the PE-g-MA/MBAAm membranes exhibited an improved stability and a reasonable separation performance at pressures as high as 12 MPa (Kai et al., 2005).

Ulbricht and Schwarz (1997) prepared pore-filling PAN membranes to remove methanol from less polar hydrocarbons (cyclohexane or methyl t-butyl ether). High selectivities ($\alpha_{\text{methanol/cyclohexane}} \leqslant 2000$) and extraordinarily high permeate fluxes ($J \leqslant 8$ kg/(m^2·h)) were achieved. Another pore-filling PAN membrane was investigated by Frahn et al. (2001; 2004). It was found that modification with $DG \geqslant DG_{\text{crit}}$ was necessary to block all separation layer pores of the UF membrane. In all cases the aromatic compound passed the membrane faster than other compounds. The order in which the feed components passed the membrane was as follows: Bz > Tol $\gg$ Hx $\geqslant$

Chx ($>$ Hep) $>$ Oct. The membranes with poly(ethylene oxide) (PEO) carrying poly(MA) layers showed excellent behavior in an aromatic/aliphatic PV separation. The separation factor α_{Tol} achieved between 4 and 8.5, and permeate fluxes between 0.3 and 5.0 kg/(m^2·h) could be obtained.

Interestingly, metal ions were introduced to prepare the membrane for PV. Yang and Hsiue (1997; 1998) developed swollen composite membranes of PE-g-AAc-Ag$^+$, silicone rubber (SR)-g-AAc-Ag$^+$ and poly[1-(trimethylsilyl)-1-propyne] (PTMSP)-g-AAc-Ag$^+$ with Ag$^+$ distribution for olefin/paraffin separation. The Ag$^+$ was more effective than the Cu$^+$ and Cu^{2+} in facilitated olefin transport. The interaction between olefin and polymer was higher than those between paraffin and polymer in PE-g-AA-Ag$^+$ and SR-g-AA-Ag$^+$ membranes, while the PTMSP-g-AA-Ag$^+$ showed high gas permeability coefficient and high olefin/paraffin (isobutene/isobutane) selectivity.

4.3.5 Membranes for Energy Conversion Applications

The ion exchange membranes can be applied in energy conversion applications such as the polymer electrolyte fuel cell (PEFC), the direct methanol fuel cell (DMFC) and batteries where a significant improvement in current density is required (Anantaraman and Gardner, 1996). In such applications, cation exchange membranes are preferred for use as solid polymer electrolytes over anion exchange membranes, as reviewed by Nasefa and Hegazy (2004). It is worth noting that, for stability reasons, membranes bearing sulfonic acid characters are favored for use in PEFCs whereas carboxylic acid membranes are preferred in batteries (Risen, 1996). A membrane used for a fuel cell is to separate the two compartments of the cell, whilst providing a conducting pathway for cations from the anode to the cathode across the cell (Dell, 2000).

4.3.5.1 Polymer Electrolyte Fuel Cell

In principle, PEFC is a device for converting the free energy of a fuel gas (hydrogen) into electricity in the presence of an oxidant gas (oxygen) (Larminie and Dicks, 2000). The protons produced by dissociation of the hydrogen at the anode pass through the membrane aqueous phase to the cathode and the associated electrons flow in the external circuit to the cathode, leading to production of DC current (Prater, 1994; Watkins, 1993). Nafion membranes are the most popular polymer electrolytes used in PEFC. However, these membranes are very expensive and have difficulty in humidity control which strongly influences the properties (such as the transport properties) of cation exchange membranes (Anantaraman and Gardner, 1996; Bae and Kim, 2003). Therefore the development of cheaper and better fluorinated or non-fluorinated proton conducting membranes is imperative in this situation. Table 4.4 shows a summary of the advances in the preparation of grafted sulfonic acid membranes for PEFC (Nasefa and Hegazy, 2004).

Table 4.4. Summary of the advances in preparation of radiation grafted proton exchange membranes for PEFC

Monomer	Base polymer/ Thickness (µm)	Radiation source/method	GD (wt.%)	IEC (meq/g)	Specific resistivity (Ωcm)	Ref.
St	FEP/50	γ-radiation/ simultaneous	13~52	0.72~2.5	22.0~2.0	(Gupta et al., 1993; Rouilly et al., 1993)
St	FEP/50	γ-radiation/ simultaneous	6.5~40	0.59~1.26	160~3.2	(Gupta and Scherer, 1994)
St/DVB	FEP/125	γ-radiation/pre-irradiation	19.4 and 19.6	1.07~2.15	10.3~36.0	(Bühi et al., 1995b)
St/DVB/TAC	FEP/75	γ-radiation/pre-irradiation	39	1.92	6.2	(Bühi et al., 1995a)
St/DVB	FEP/50	γ-radiation/ simultaneous	11~34; 13~27	0.78~2.08	23.0~3.0	(Gupta et al., 1996; Holmberg et al., 1996)
St	PVDF/125	EB/pre-irradiation	13~275	-	200.0~8.0	(Holmberg et al., 1996)
St	PVDF/80	EB/pre-irradiation	30	1.70	33.0	(Flint and Slade, 1997)
St/DVB/TAC	ETFE/25	γ-radiation/pre-irradiation	25[a]	2.4	17.0[b]	(Brack et al.,1999)
St/DVB St/BVPE	PVDF/80	EB/pre-irradiation	18~73; 19~103	0.48~2.51; 0.19~2.95	10000.0~10.0; 10000.0~7.7	(Holmberg et al., 1998)
St	PVDF/80	EB/pre-irradiation	24~132	1.9~2.3	-	(Holmberg et al., 2002)
St	PVDF/80	EB/pre-irradiation	14~40; 15~60	0.96~1.73; 0.19~2.08	-	(Hietala et al., 1997; Holmberg et al., 2004)

(to be continued)

(Table 4.4.)

Monomer	Base polymer/ Thickness (μm)	Radiation source/method	GD (wt.%)	IEC (meq/g)	Specific resistivity (Ωcm)	Ref.
St	PFA/120	γ-radiation/ simultaneous	6.3~48.7	0.63~2.35	2000.0~21.7	(Nasef et al., 2000a)
St	FEP/120	γ-radiation/ simultaneous	5.0~52.0	0.39~2.27	1190.0~20.0	(Nasef et al., 2000b)
St	PTFE/100	γ-radiation/ simultaneous	5~36	0.36~2.2	10200.0~34.5	(Nasef et al., 2000c)
St	ETFE/50	γ-radiation/pre-irradiation	32~46	2.13~3.27	3.3~5.3	(Chuy et al., 2000)
St/DVB	PFA/120	γ-radiation/ simultaneous	17 and 24	1.62 and 1.59	158.7~62.9	(Nasef and Saidi, 2003)
St	PE/125 ETFE/50 PVDF/50	γ-radiation/pre-irradiation	9; 34; 33	0.72; 2.24; 1.51	-	(Horsfall and Lovell, 2001)
St/DVB	ETFE/100	EB/pre-irradiation	31 and 42	1.49 and 1.88	-	(Arico et al., 2003)
St/DVB	FEP/25	pre-irradiation	19.5	1.44 mmol/g	132 mΩ·cm^2	(Gubler et al., 2004)
St	PTFE RX-PTFE	γ-radiation/peroxidation	1.9~15.6; 135.9	> 3.0	-	(Li et al., 2004)
MSt/St/DVB	RX-PTFE/8-10	EB/peroxidation	17.7~40.7	1.1~2.2	-	(Li et al., 2006b)
St/DVB	RX-PTFE/8-10	EB/pre-irradiation	21~63	1.5~2.8	-	(Li et al., 2005a)
St	PTFE/FEP	EB/peroxidation	77	3.0	-	(Asano et al., 2005)
	Nafion 105/107/112		0; 0	1; 0.89; 1	56; 51	(Kallio et al., 2002)

BVPE: bis(vinyl-phenyl)ethane; TAC: triallyl-cyanorate; [a]mol %; [b]measured *in situ*

Seen from Table 4.4, sulfonated membranes were often used for PEFC applications. Washio's group (Li et al., 2004; 2006b; Sato et al., 2003) grafted St on RX-PTFE and PTFE membranes by γ-irradiation graft polymerization and subsequently sulfonation of the grafted membranes for PEFC applications. It was found that the mechanical properties decreased with increasing GD. Ionic exchange capacity (IEC) of the sulfonated RX-PTFE membrane reached 1.1 meq/g while maintaining the mechanical properties (Sato et al., 2003). The grafted RX-PTFE membranes, which showed good mechanical properties and radiation resistance in comparison with the PTFE membrane, reduced gas permeability and then increased the cell efficiency and lifetime usage. And the highest IEC value gained was over 3 meq/g (Li et al., 2004).

However, for the sulfonated membranes, the crossover of the oxidative gas like O_2 will form very reactive OH· radicals, which attack the α-hydrogen atom on the grafted PSSA chains resulting in the degradation of the PSSA chains, thus shortening the lifetime of the PEFC (Assink et al., 1991). The crosslinking of PSSA side chains by DVB could reduce the gas permeation rate and extend the lifetime of the polymer electrolyte (Li et al., 2005a). And IEC values ranging from 1.5 to 2.8 meq/g were obtained. But DVB only crosslinked the PSSA side chains which cannot restrain the decomposition of the crosslinking structure. Therefore modification of the α-position of St monomer is accepted as an effective way of improving the chemical stability of the membranes. Recently Li et al. (2006b) improved the properties of the PEFC by introducing α-methylstyrene in the graft polymerization. The increase in the concentration of α-methylstyrene improved the chemical stabilities of the resulting PEMs. The same modification was actualized on PTFE/FEP polymer-alloy membranes. The IECs achieved 3.0 meq/g which were three times higher than those of commercial perfluorosulfonic acid (PFSA) membranes (Asano et al., 2005). Büchi et al. (1995b) also prepared FEP(Nafion 117)-g-crosslinked PSSA membranes by the radiation grafting method. The introduction of the crosslinking agent during grafting polymerization improved the fuel cell performance by reducing the gas permeability.

Furthermore, living polymerization techniques were recently adopted to prepare proton-conducting membranes with controllable structures. Holmberg et al. (2002) synthesized proton-conducting membranes by grafting St onto PVDF membranes by ATRP. After sulfonation, the proton conductivities of these membranes were as high as 70 mS/cm, which was high enough for use in a fuel cell. Also Holmberg et al. (2004) grafted St on PVDF membranes by nitroxide stable free radical polymerization (SFRP) to control the graft polymer structure. The membranes were used in a fuel cell for 930 h at 70 °C without any drop in current density. In contrast, their previously prepared PSSA-grafted PVDF membranes with conventional pre-irradiation grafting failed within 150 to 200 h under similar conditions (Hietala et al., 1999).

4.3.5.2 Direct Methanol Fuel Cell

DMFC is another type of fuel cell. It oxidizes methanol fuel directly at the fuel cell anode, which contains a catalyst with a mixture of platinum and a less noble metal such as ruthenium, to produce electricity and hydrogen ions crossing the membranes (Nasefa and Hegazy, 2004). Up to now the perfluorinated ionomer membrane (i.e. Nafion) has been used almost exclusively as the proton conductor in DMFC. Reducing methanol permeation and enhancing proton conductivity of the membranes are two essential steps towards improving the performance of DMFC.

Some research focused on modification of Nafion membranes. For example, Bae et al. (2006) prepared PSSA-grafted Nafion 117 membranes via plasma-induced polymerization to reduce the methanol permeability in DMFCs as well as to increase the crosslinking density, resulting in higher proton conductivity. The methanol permeability was decreased because of reduced ionic cluster size and crosslinked PSSA layer thickness.

Other types of membranes were also developed for DMFC. Yamaguchi et al. (2003) used pore-filled polyelectrolyte as alternative DMFC membranes. Proton conductivity occurred through the filling electrolyte polymer. Swelling of the electrolyte polymer (poly(vinylsulfonic acid/acrylic acid)) was used to control methanol permeation, and the substrate (PTFE membrane) had good mechanical strength at high temperature. Nasef et al (2006) prepared pore-filled PVDF membranes by irradiation. The membranes of bigger pore size with GD of 40 wt.% and 45 wt.% possess an excellent combination of high ionic conductivity and low methanol permeability compared to the Nafion 117 membrane. The values of the ion conductivity and methanol permeability of the three membranes, are 54×10^{-3}, 61×10^{-3} and 53×10^{-3} S/cm and 1.4×10^{-6}, 0.7×10^{-6} and 3.5×10^{-6} cm^2/s, respectively.

In addition, a layer-by-layer deposition method has been applied in the preparation of a proton conducting membrane. Son et al. (2006) prepared multilayer proton conducting membranes through layer-by-layer deposition on a PE membrane by which depression of methanol-crossover was achieved. Four- and six-fold decreases in the permeability of methanol for the multilayer membrane were observed when compared with those of Nafion 117 (1.474×10^{-6} cm^2/s) and 115 (2.375×10^{-6} cm^2/s). The impact of the multilayer structure on the methanol permeability is evident.

4.3.5.3 Membranes for Battery

A battery possesses two electrodes separated by an electrolyte which should be chemically stable and sufficiently durable. The electrolyte provides physical separation between the anode and the cathode. It also provides a source of cations and anions to balance the redox reactions (Nasefa and Hegazy, 2004).

The regenerated cellulose membranes used as separator in alkaline silver oxide batteries lack durability (Safranj et al., 1986). Researchers have found that AAc, MAA, AN and MAA grafted PE and PTFE membranes were potential separators to replace the cellulose membranes in alkaline batteries (Choi et al., 2000a; Ishigaki et al., 1981; Lawler and Charlesby, 1980; Okamoto, 1987). The two cation-exchange PE membranes modified with AAc and MAA were found to have increasing KOH diffusion flux with the increase of GD. However, the electrical resistance decreased rapidly with GD. The IECs for these two membranes were 2.6 and 2.4 mmol/g with GD 140 wt.%, respectively (Choi SH et al., 2000). In addition, grafting of AAc with DEGMA as crosslinker on PP membranes was found to improve the wettability of the separator of the secondary lithium batteries. The cycling results also showed the possibility of working with high Li salt concentrations (Gineste and Pourcelly, 1995).

The α-methylstyrene (tertiary hydrogen is replaced by a methyl group) grafted and sulfonated PTFE membranes were more stable than the St (contains a tertiary hydrogen) modified membranes during exposure to an oxidizing aging solution. The energy efficiencies of α-methylstyrene grafted membranes were 82.6% and 83.0% for 700 test cycles and showed no chemical degradation during this period. Thereby they were found to be potential separators for zinc/ferricyanide batteries, while the energy efficiencies of St-grafted membranes decreased rapidly to less than 60% after 60 or 80 cycles in a cycling test cell (Assink et al., 1991).

An alternative polymer electrolyte membrane for lithium batteries was based on St grafted PVDF membranes, which was prepared by chemical activation with $LiPH_6$ in ethylene carbonate and diethylene carbonate (Nasef et al., 2004). The membrane had high liquid electrolyte uptake capacity and high ionic conductivity at room temperature, both of which increased with the increased GD. Conductivity in the order in 10^{-3} S/cm was achieved at a GD of 50%.

Chen et al. (2006) synthesized a polymer-polymer nanocomposite membrane with polyelectrolyte nanodomains oriented normal to the plane of the membrane. Commercial PCTE membranes were used as a host matrix and modified by oxygen plasma-induced surface graft polymerization. This type of membrane can be used in fuel cells because of its ability to enhance transport in the desired direction. Oxygen plasma treatment of the PCTE host matrix improved pore-filling of an aqueous reaction solution and ensured uniform grafting of poly(AMPS) on the pore walls. The membrane combined the mechanical stability of the hydrophobic matrix and the functionality of the polyelectrolyte domains while enhancing transport in the desired direction for a variety of membrane processes.

4.3.6 Nanofiltration Membrane Preparation

NF membranes have been applied in many areas, especially in rejecting ions and charged organic pollutants. Compared with RO membranes they have excellent properties such as low operating pressure, high flux, high retention to multivalent salts, low investment and operating costs. However, up to now it is difficult to find new materials for preparing NF membranes except aromatic PA although the aromatic PA membranes are easily fouled on account of the hydrophobicity. Therefore the application of NF membranes in some new fields such as biotechnology and pharmacy may be restricted. A potential way to develop new NF membranes is to modify UF membranes by surface grafting polymerization with various monomers, by which the NF membranes can be endowed with desirable functions like hydrophilicity.

Qiu et al. (2005; 2006; 2007) prepared a hydrophilic NF membrane by the photo-grafting of AAc and sodium ally sulfonate (SAS) on a PEK-C UF membrane. The retention of sodium chloride and sodium sulfate on the membrane with grafted poly(AAc) were 57% and 95.7%, respectively; while the water flux of the membrane was ca. 25 L/(m·h), at 0.8 MPa. The changes in membrane permeability and salt retention with different grafting parameters suggested that enough poly(AAc) chains were grafted on the pores wall to convert the UF membrane to the NF-type membrane (sodium sulfate retention close to 100%) within a few minutes (Qiu et al., 2005). The pore size of the skin layer of the original PEK-C UF membrane was reduced with the graft polymerization. The prepared hydrophilic NF membranes yielded an unexpectedly large permeation flux without loss of salt retention (Qiu et al., 2007).

NF membranes were also prepared by grafting AAc (Zhao et al., 2004) and NVP (Zhao et al., 2005b) onto PAN UF membranes. Results from DSC measurement demonstrated that the pores in the membranes modified by grafting AAc became smaller and the distribution of pores narrowed. For surface hydrophilization with an improved permeability change, short graft reaction time ($\sim$10 min) of AAc was recommended. Saccharose retention of this NF membrane was 76%. The NF membrane grafted with NVP had a retention of 83.5% to salts (0.03 mol/L $MgSO_4$ + 0.02 mol/L NaCl), while only 16.9% for the original membrane, at 2 MPa and 30 °C filtration conditions.

On the other hand, Li's group (Chen et al., 2007; Zhao et al., 2005a) prepared hydrophobic NF membranes from PAN UF membranes by plasma graft polymerization of St from the vapor phase. The grafted membrane exhibited a decrease in pore size and an increase in surface hydrophobicity which is potentially used to recover the dewaxing solvent from the dewaxed lube oil. For the feed composition of 83.94% dewaxed solvent, the solvent in permeate solution was 98.42%, and the rejection of lube oil was up to 90.2%.

4.3.7 Gas Separation

Facilitated transport membranes for gas separation have attracted attention as they have a very high selectivity compared with conventional polymeric membranes (Way and Noble, 1992). The high selectivity is attributed to carriers incorporated into the membranes which can react reversibly with the permeant species. Generally there are two types of facilitated transport membranes. One is a supported liquid membrane (SLM), the other is a carrier fixed membrane where the stability is higher than that of SLM.

Matsuyama et al. (1994) prepared a type of cation-exchange membrane by grafting AAc on a PE membrane followed by further modification. The grafted membrane containing ethylenediamine showed remarkably high CO_2 permeability and selectivity of CO_2 over N_2. These excellent results are probably attributed to the high IEC and the high water content. The 2-(N,N-dimethyl)aminoethyl methacrylate (DAMA) grafted PE membrane also had high selectivity of CO_2 over N_2, with a separation factor up to 130 in a water swollen condition. In a dry state the facilitated transport of CO_2 was probably based on the acid-base interaction between CO_2 and amine moiety in the membrane. On the other hand, the CO_2 hydration reaction might occur in the water containing membrane (Matsuyama et al., 1996). Similarly, because the PEO segment can dissolve a large amount of acidic gases, the gas permeation flux through the PEO segment may also be high. Thus MePEGA was grafted on a PAN membrane for CO_2 separation. It was found that the membrane displayed good performance for CO_2/N_2 separation: the highest selectivity of CO_2 over N_2 reached 34.0 at 30 °C (Kim et al., 2001).

4.3.8 Biomedical and Biological Applications

Surface modified membranes by graft polymerization have been widely used in biomedical and biological applications. When the membranes were grafted with some hydrophilic monomers, such as NVP, HEMA, AAc, MAc, the hydrophilicity and biocompatibility of the membranes were improved. Odian et al. (1968) prepared hemodialysis membranes by grafting vinyl alcohol and NVP on PE membranes. The modified membrane showed a ten-fold increase in the solute permeability compared with commercial dialysis membranes. Poly(HEMA)-grafted chloroprene rubber, γ-methyl-l-glutamate and PP membranes showed higher permeability toward urea and uric acid when compared with the un-grafted membranes (Fang et al., 1998a; 1998b; Yuee and Tianyi, 1988). Besides, grafting poly(HEMA) on a PP membrane was an efficient and achievable way to improve its hemocompatibility (Hu et al., 2006).

The surface modified membranes that resist protein adsorption can be used for biomedical purposes. In contrast the modified membranes can also be applied as carriers for protein and cell adsorption or enzyme immobilization. In addition some biomimic monomers, like phospholipid, saccharide, amino

acid analogous monomer, have been chosen to functionalize the membranes to construct a bioactive surface, which is useful in protein isolation and enzyme immobilization. These topics will be discussed in the following chapters.

4.4 Conclusion

Surface modification of membranes by graft polymerization is a versatile and promising method for realizing surface functionalization for polymer separation membranes. The modified membranes have more functions than just being selective barriers with high performance (flux, stability, etc.). In this chapter we reviewed various surface graft methods for membrane modification as well as applications. Apart from conventional grafting processes, the controlled living radical polymerization, which develops rapidly and provides polymers with regulated molecular weight and low polydispersity, has attracted much attention recently. With this novel method graft polymer chains with a well-defined structure can be primarily created. Accordingly these membranes have the potential to achieve controlled functions in applications. Therefore surface modification of membranes with controlled living graft polymerization will be more and more important in the future.

References

Akerman S, Viinikka P, Svarfvar B, Jarvinen K, Kontturi K, Nasman J, Urtti A, Paronen P (1998) Transport of drugs across porous ion exchange membranes. J Control Release 50:153-166

Allen NS, Edge M (1992) Fundamentals of polymer degradation and stabilization. Kluwer Academic Publishers, Dordrecht.

Anantaraman A, Gardner C (1996) Studies on ion-exchange membranes. I. Effect of humidity on the conductivity of Nafion. J Electroanal Chem 414:115-120

Arico A, Baglio V, Creti P, Di Blasi A, Antonucci V, Brunea J, Chapotot A, Bozzi A, Schoemans J (2003) Investigation of grafted ETFE-based polymer membranes as alternative electrolyte for direct methanol fuel cells. J Power Sources 123:107-115

Asai S, Watanabe K, Sugo T, Saito K (2005) Preparation of an extractant-impregnated porous membrane for the high-speed separation of a metal ion. J Chromatogr A 1094:158-164

Asano S, Mutou F, Ichizuri S, Li JY, Miura T, Oshima A, Katsumura Y, Washio M (2005) Fabrication of PEFC membrane based on PTFE/FEP polymer-alloy using radiation-grafting. Nucl Instrum Meth B 236:437-442

Assink R, Arnold JC, Hollandsworth R (1991) Preparation of oxidatively stable cation-exchange membranes by the elimination of tertiary hydrogens. J Membrane Sci 56:143-151

Avlonitis S, Hambury WT, Hodgkiss T (1992) Chlorine degradation of aromatic polyamides. Desalination 85:321-334

Bae B, Ha HY, Kim D (2006) Nafion (R)-graft-polystyrene sulfonic acid membranes for direct methanol fuel cells. J Membrane Sci 276:51-58

Bae B, Kim D (2003) Sulfonated polystyrene grafted polypropylene composite electrolyte membranes for direct methanol fuel cells. J Membrane Sci 220:75-87

Belfer S (2003) Modification of ultrafiltration polyacrylonitrile membranes by sequential grafting of oppositely charged monomers: pH-dependent behavior of the modified membranes. React Funct Polym 54:155-165

Belfer S, Bottino A, Capannelli G (2005) Preparation and characterization of layered membranes constructed by sequential redox-initiated grafting onto polyacrylonitrile ultrafiltration membranes. J Appl Polym Sci 98:509-520

Belfer S, Fainshtain R, Purinson Y, Gilron J, Nystrom M, Manttari M (2004) Modification of NF membrane properties by in situ redox initiated graft polymerization with hydrophilic monomers. J Membrane Sci 239:55-64

Belfer S, Fainshtain R, Purinson Y, Kedem O (2000) Surface characterization by FTIR-ATR spectroscopy of polyethersulfone membranes-unmodified, modified and protein fouled. J Membrane Sci 172:113-124

Belfer S, Purinson Y, Kedem O (1998) Surface modification of commercial polyamide reverse osmosis membranes by radical grafting: An ATR-FTIR study. Acta Polym 49:574-582

Bhattacharya A, Misra BN (2004) Grafting: a versatile means to modify polymers —Techniques, factors and applications. Prog Polym Sci 29:767-814

Bondar Y, Kim HJ, Yoon SH, Lim YJ (2004) Synthesis of cation-exchange adsorbent for anchoring metal ions by modification of poly(glycidyl methacrylate) chains grafted onto polypropylene fabric. React Funct Polym 58:43-51

Brack H, Büchi FN, Rota M, Scherer G (1999) Development of radiation-grafted membranes for fuel cell applications based on poly(ethylene-alt-tetrafluoroethylene). In: Pinnan I, Freeman BD(Eds.), Membrane formation and modification, ACS Symposium Series No. 744. ACS, Washington, DC, p174

Büchi FN, Gupta B, Haas O, Scherer GG (1995a) Performance of differently crosslinked, partially fluorinated proton exchange membranes in polymer electrolyte fuel cells. J Electrochem Soc 142:3044-3048

Büchi FN, Gupta B, Haas O, Scherer GG (1995b) Study of radiation-grafted FEP-*g*-polystyrene membranes as polymer electrolytes in fuel cells. Electrochim Acta 40:345-353

Carroll T, Booker NA, Meier-Haack J (2002) Polyelectrolyte-grafted microfiltration membranes to control fouling by natural organic matter in drinking water. J Membrane Sci 203:3-13

Cartier S, Horbett TA, Ratner BD (1995) Glucose-sensitive membrane coated porous filters for control of hydraulic permeability and insulin delivery from a pressurized reservoir. J Membrane Sci 106:17-24

Charcosset C (1998) Review: Purification of proteins by membrane chromatography. J Chem Technol Biot 71:95-110

Chen H, Palmese GR, Elabd YA (2006) Membranes with oriented polyelectrolyte nanodomains. Chem Mater 18:4875-4881

Chen J, Li JD, Zhao ZP, Wang D, Chen CX (2007) Nanofiltration membrane prepared from polyacrylonitrile ultrafiltration membrane by low-temperature plasma: 5. Grafting of styrene in vapor phase and its application. Surf Coat Tech 201:6789-6792

Childs RF, Weng JF, Kim M, Dickson JM (2002) Formation of pore-filled microfiltration membranes using a combination of modified interfacial polymerization and grafting. J Polym Sci Pol Chem 40:242-250

Choi EY, Bae B, Moon SH (2007) Control of the fixed charge distribution in an ion-exchange membrane via diffusion and the reaction rate of the monomer. J Phys Chem B 111:6383-6390

Choi SH, Jeong YH, Ryoo JJ, Lee KP (2001) Desalination by electrodialysis with the ion-exchange membrane prepared by radiation-induced graft polymerization. Radiat Phys Chem 60:503-511

Choi SH, Nho YC (1999) Adsorption of Co^{2+} by stylene-g-polyethylene membrane bearing sulfonic acid groups modified by radiation-induced graft copolymerization. J Appl Polym Sci 71:2227-2235

Choi SH, Park S, Nho YC (2000) Electrochemical properties of polyethylene membrane modified with carboxylic acid group. Radiat Phys Chem 57:179-186

Choi YJ, Moon SH, Yamaguchi T, Nakao SI (2003) New morphological control for thick, porous membranes with a plasma graft-filling polymerization. J Polym Sci Pol Chem 41:1216-1224

Choi YJ, Yamaguchi T, Nakao S (2000) A novel separation system using porous thermosensitive membranes. Ind Eng Chem Res 39:2491-2495

Chu LY, Li Y, Zhu JH, Chen WM (2005) Negatively thermoresponsive membranes with functional gates driven by zipper-type hydrogen-bonding interactions. Angew Chem Int Edit 44:2124-2127

Chu LY, Liang YJ, Chen WM, Ju XJ, Wang HD (2004) Preparation of glucosesensitive microcapsules with a porous membrane and functional gates. Colloid Surface B 37:9-14

Chu LY, Niitsuma T, Yamaguchi T, Nakao S (2003) Thermoresponsive transport through porous membranes with grafted PNIPAM gates. Aiche J 49:896-909

Chung DJ, Ito Y, Imanishi Y (1994) Preparation of porous membranes grafted with poly(spiropyran-containing methacrylate) and photocontrol of permeability. J Appl Polym Sci 51:2027-2033

Chuy C, Basura V, Simon E, Holdcroft S, Horsfall J, Lovell K (2000) Electrochemical characterization of ethylenetetrafluoroethylene-g-polystyrenesulfonic acid solid polymer electrolytes. J Electrochem Soc 147:4453-4459

Crivello JV, Belfort G, Yamagishi H (1995) Low fouling ultrafiltration and microfiltratia aryl polysulfone. US Patent 5468390

Dell R (2000) Batteries: fifty years of materials development. Solid State Ionics 134:139-158

Desai SM, Singh RP (2004) Surface modification of polyethylene. Adv Polym Sci 169:231-293

Dessouki AM, Taher NH, El-Arnaouty MB (1998) Gamma ray induced graft copolymerization of N-vinylpyrrolidone, acrylamide and their mixtures onto polypropylene films. Polym Int 45:67-76

El-Sawy NM, Al Sagheer FA (2002) Physicochemical investigation of radiationgrafted poly(acrylic acid)-graft-poly(tetrafluoroethylene-ethylene) copolymer membranes and their use in metal recovery from aqueous solution. J Appl Polym Sci 85:2692-2698

Evans MG, Uri N (1949) Photochemical polymerization in aqueous solution. Nature 164:404-405.

Fang YE, Lu XB, Cheng Q (1998a) Influence of degree of grafting and grafting temperature on the permeabilities of grafted polypropylene membranes. J Appl Polym Sci 68:83-89

Fang YE, Lu XB, Wang SZ, Zhao X, Fang F (1997) Kinetics of radiation-induced graft copolymerization of vinyl acetate onto ethylene-*co*-propylene rubber membranes. Radiat Phys Chem 49:275-278

Fang YE, Ma CX, Chen Q, Lu XB (1998b) Radiation-induced graft copolymerization of 2-hydroxyethyl methacrylate onto chloroprene rubber membrane. II. Characterization of grafting copolymer. J Appl Polym Sci 68:1745-1750

Filho AAMF, Gomes AS (2006) Copolymerization of styrene onto polyethersulfone films induced by gamma ray irradiation. Polym Bull 57:415-421

Flint SD, Slade CT (1997) Investigation of radiation-grafted PVDF-*g*-polystyrene-sulfonic-acid ion exchange membranes for use in hydrogen oxygen fuel cells. Solid State Ionics 97:299-307

Frahn J, Malsch G, Matuschewski H, Schedler U, Schwarz HH (2004) Separation of aromatic/aliphatic hydrocarbons by photo-modified poly(acrylonitrile) membranes. J Membrane Sci 234:55-65

Frahn J, Malsch G, Schwarz FH (2001) Generation of a selective layer on polyacrylonitrile membrane supports for separation of aromatic/non-aromatic hydrocarbon mixtures by pervaporation. Macromol Symp 164:269-276

Freger V, Gilron J, Belfer S (2002) TFC polyamide membranes modified by grafting of hydrophilic polymers: an FT-IR/AFM/TEM study. J Membrane Sci 209:283-292

Gancarz I, Poniak G, Bryjak M, Frankiewicz A (1999) Modification of polysulfone membranes. 2. Plasma grafting and plasma polymerization of acrylic acid. Acta Polym 50:317-326

Gatenholm P, Ashida T, Hoffman AS (1997) Hybrid biomaterials prepared by ozone-induced polymerization. 1. Ozonation of microporous polypropylene. J Polym Sci Pol Chem 35:1461-1467

Geismann C, Ulbricht M (2005) Photoreactive functionalization of poly(ethylene terephthalate) track-etched pore surfaces with "smart" polymer systems. Macromol Chem Phys 206:268-281

Ghosh R (2002) Protein separation using membrane chromatography: opportunities and challenges. J Chromatogr A 952:13-27

Gilron J, Belfer S, Väisänen P, Nyström M (2001) Effects of surface modification on antifouling and performance properties of reverse osmosis membranes. Desalination 140:167-179

Gineste J, Pourcelly G (1995) Polypropylene separator grafted with hydrophilic monomers for lithium batteries. J Membrane Sci 107:155-164

Glater J, Zachariah MR, MaCray SB, McCutchen JW (1983) RO membrane sensitivity to ozone and halogen disinfectants. Desalination 48:1-16

Goto M, Miyata T, Uezu K, Kajiyama T, Nakashioa F, Haraguchi T, Yamada K, Ide S, Hatanaka C (1994) Separation of rare earth metals in a hollow-fiber membrane extractor modified by plasma-graft polymerization. J Membrane Sci 96:299-307

Grasselli M, Carbajal ML, Yoshii F, Sugo T (2003) Radiation-induced GMA /DMAA graft copolymerization onto porous PE hollow-fiber membrane. J Appl Polym Sci 87:1646-1653

Gubler L, Kuhn H, Schmidt TJ, Scherer GG, Brack H-P, Simbeck K (2004) Performance and durability of membrane electrode assemblies based on radiation-grafted FEP-*g*-polystyrene membranes. Fuel Cells 4:196-207

Gupta B, Anjum N (2001) Development of membranes by radiation grafting of acrylamide into polyethylene films: Characterization and thermal investigations. J Appl Polym Sci 82:2629-2635

Gupta B, Anjum N (2002) Surface structure of radiation-grafted polyethylene-g-polyacrylamide films. J Appl Polym Sci 86:1118-1122

Gupta B, Anjum N, Sen K (2002) Development of membranes by radiation grafting of acrylamide into polyethylene films: Properties and metal ion separation. J Appl Polym Sci 85:282-291

Gupta B, Büchi FN, Scherer GG (1994) Cation exchange membranes by pre-irradiation grafting of styrene into FEP films. I. Influence of synthesis conditions. J Polym Sci Pol Chem 32:1931-1938

Gupta B, Büchi FN, Scherer GG, Chapiro A (1993) Materials research aspects of organic solid proton conductors. Solid State Ionics 61:213-218

Gupta B, Büchi F, Staub M, Grman D, Scherer GG (1996) Cation exchange membranes by pre-irradiation grafting of styrene into FEP films. II. Properties of copolymer membranes. J Polym Sci Pol Chem 34:1837-1880

Gupta B, Scherer G (1994) Proton exchange membranes by radiation-induced graft copolymerization of monomers into Teflon-FEP films. Chimia 48:127-137

Hagiwara K, Yonedu S, Saito K, Shiraishi T, Sugo T, Tojyo T, Katayama E (2005) High-performance purification of gelsolin from plasma using anion-exchange porous hollow-fiber membrane. J Chromatogr B 821:153-158

Hegazy ESA, El-Rehim HAA, Ali AMI, Nowier HG, Aly HF (2000a) Characterization and application of radiation grafted membranes in waste treatment. Czech J Phys 50:297-308

Hegazy ESA, El-Rehim HAA, Khalifa NA, Atwa SM, Shawky HA (1997) Anionic/cationic membranes obtained by a radiation grafting method for use in waste water treatment. Polym Int 43:321-332

Hegazy ESA, El-Rehim HAA, Shawky HA (2000b) Investigations and characterization of radiation grafted copolymers for possible practical use in wastewater treatment. Radiat Phys Chem 57:85-95

Hickea HG, Ulbricht M, Becker M, Radosta S, Heyer AG (1999) Novel enzyme-membrane reactor for polysaccharide synthesis. J Membrane Sci 161:239-245

Hietala S, Holmberg S, Näsman J, Ostrovskii D, Paronen M, Serimaa R, Sundholm F, Torell L, Torkkeli M (1997) The state of water in styrene-grafted and sulfonated poly(vinylidene fluoride) membranes. Angew Makromol Chem 253:151-167

Hietala S, Paronen M, Holmberg S, Näsman J, Juhanoja J, Karjalainen M, Serimaa R, Toivola M, Lehtinen T, Parovuori K, et al. (1999) Phase separation and crystallinity in proton conducting membranes of styrene grafted and sulfonated poly(vinylidene fluoride). J Polym Sci Pol Chem 37:1741-1753

Hilal N, Kochkodan V, Al-Khatib L, Levadna T (2004) Surface modified polymeric membranes to reduce (bio)fouling: a microbiological study using *E. coli*. Desalination 167:293-300

Hirotsu T (1987) Graft polymerized membranes of methacrylic acid by plasma for water-ethanol permseparation. Ind Eng Chem Res 26:1287-1290

Holmberg S, Holmlund P, Nicolas R, Wilen CE, Kallio T, Sundholm G, Sundholm F (2004) Versatile synthetic route to tailor-made proton exchange membranes for fuel cell applications by combination of radiation chemistry of polymers with nitroxide-mediated living free radical graft polymerization. Macromolecules 37:9909-9915

Holmberg S, Holmlund P, Wilen CE, Kallio T, Sundholm G, Sundholm F (2002) Synthesis of proton-conducting membranes by the utilization of preirradiation grafting and atom transfer radical polymerization techniques. J Polym Sci Pol Chem 40:591-600

Holmberg S, Lehtinen T, Naesman J, Ostrovskii D, Paronen M, Serimaa R, Sundholm F, Sundholm G, Torell L, Torkkeli M (1996) Structure and properties of sulfonated poly[(vinylidene fluoride)-g-styrene] porous membranes. J Mater Chem 6:1309-1317

Holmberg S, Naesman JH, Sundholm F (1998) Synthesis and properties of sulfonated and crosslinked poly[(vinylidene fluoride)-graft-styrene] membranes. Polym Advan Technol 9:121-127

Horsfall J, Lovell K (2001) Fuel cell performance of radiation grafted sulfonic acid membranes. Fuel Cells 1:186-191

Hsiue GH, Yang JM, Wu RL (1988) Preparation and properties of a biomaterial: HEMA grafted SBS by gamma-ray irradiation. J Biomed Mater Res 22:405-415

Hsueh CL, Peng YJ, Wang CC, Chen CY (2003) Bipolar membrane prepared by grafting and plasma polymerization. J Membrane Sci 219:1-13

Hu MX, Yang Q, Xu ZK (2006) Enhancing the hydrophilicity of polypropylene microporous membranes by the grafting of 2-hydroxyethyl methacrylate via a synergistic effect of photoinitiators. J Membrane Sci 285:196-205

Huang J, Wang XL, Qi WS, Yu XH (2002) Temperature sensitivity and electrokinetic behavior of a N-isopropylacrylamide grafted microporous polyethylene membrane. Desalination 146:345-351

Hwang GJ, Ohya H (1996) Preparation of cation exchange membrane as a separator for the all-vanadium redox flow battery. J Membrane Sci 120:55-67

Hwang GJ, Ohya H (1997) Crosslinking of anion exchange membrane by accelerated electron radiation as a separator for the all-vanadium redox flow battery. J Membrane Sci 132:55-61

Ishigaki I, Sugo T, Senoo K, Takayama T, Machi S, Okamoto J, Okada T (1981) Synthesis of ion exchange membrane by radiation grafting of acrylic acid onto polyethylene. Radiat Phys Chem 18:899-905

Ito T, Hioki T, Yamaguchi T, Shinbo T, Nakao S, Kimura S (2002) Development of a molecular recognition ion gating membrane and estimation of its pore size control. J Am Chem Soc 124:7840-7846

Ito Y, Ochiai Y, Park YS, Imanishi Y (1997) pH-sensitive gating by conformational change of a polypeptide brush grafted onto a porous polymer membrane. J Am Chem Soc 119:1619-1623

Ito Y, Ito T, Takaba H, Nakao S (2005) Development of gating membranes that are sensitive to the concentration of ethanol. J Membrane Sci 261:145-151

Iwata H, Hirata I, Ikada Y (1998) Atomic force microscopic analysis of a porous membrane with pH-sensitive molecular valves. Macromolecules 31:3671-3678

Jimbo T, Higa M, Minoura N, Tanioka A (1998a) Surface characterization of poly(acrylonitrile) membranes graft-polymerized with ionic monomers as revealed by zeta potential measurement. Macromolecules 31:1277-1284

Jimbo T, Tanioka A, Minoura N (1998b) Characterization of an amphoteric-charged layer grafted to the pore surface of a porous membrane. Langmuir 14:7112-7118

Jimbo T, Tanioka A, Minoura N (1998c) Comparison of surface and net charge densities of poly(acrylonitrile) membranes grafted with ionic monomers: Hydrophilic and hydrophobic effects of graft chain. J Colloid Interf Sci 204:336-341

Jimbo T, Tanioka A, Minoura N (1999) Fourier transform infrared spectroscopic study of flat surfaces of amphoteric-charged poly(acrylonitrile) membranes: Attenuated total reflection mode. Langmuir 15:1829-1832

Kabsch-Korbutowicz M, Majewska-Nowak K, Winnicki T (1999) Analysis of membrane fouling in the treatment of water solutions containing humic acids and mineral salts. Desalination 126:179-185

Kaeselev B, Pieracci J, Belfort G (2001) Photoinduced grafting of ultrafiltration membranes: comparison of poly(ether sulfone) and poly(sulfone). J Membrane Sci 194:245-261

Kai T, Goto H, Shimizu Y, Yamaguchi T, Nakao SI, Kimura S (2005) Development of crosslinked plasma-graft filling polymer membranes for the reverse osmosis of organic liquid mixtures. J Membrane Sci 265:101-107

Kai T, Tsuru T, Nakao S, Kimura S (2000) Preparation of hollow-fiber membranes by plasma-graft filling polymerization for organic-liquid separation. J Membrane Sci 170:61-70

Kallio T, Lundström M, Sundholm G, Walsby N, Sundholm F (2002) Electrochemical characterization of radiation-grafted ion-exchange membranes based on different matrix polymers. J Appl Electrochem 32:11-18

Kang JS, Shim JK, Huh H, Loo YM (2001) Colloidal adsorption of bovine serum albumin on porous polypropylene-g-poly(2-hydroxyethyl methacrylate) membrane. Langmuir 17:4352-4359

Karlsson JO, Gatenholm P (1996) Solid-supported wettable hydrogels prepared by ozone induced grafting. Polymer 37:4251-4256

Kato K, Uchida E, Kang ET, Uyama Y, Ikada Y (2003) Polymer surface with graft chains. Prog Polym Sci 28:209-259

Kawai T, Saito K, Lee W (2003) Protein binding to polymer brush, based on ion-exchange, hydrophobic, and affinity interactions. J Chromatogr B 790:131-142

Kilduff JE, Mattaraj S, Pieracci JP, Belfort G (2000) Photochemical modification of poly(ether sulfone) and sulfonated poly(sulfone) nanofiltration membranes for control of fouling by natural organic matter. Desalination 132:133-142

Kim JH, Ha SY, Nam SY, Rhim JW, Baek KH, Lee YM (2001) Selective permeation of CO_2 through pore-filled polyacrylonitrile membrane with poly(ethylene glycol). J Membrane Sci 186:97-107

Kim M, Saito K (2000) Radiation-induced graft polymerization and sulfonation of glycidyl methacrylate on to porous hollow-fiber membranes with different pore sizes. Radiat Phys Chem 57:167-172

Kiyohara S, Kim M, Toida Y, Saito K, Sugita K, Sugo T (1997) Selection of a precursor monomer for the introduction of affinity ligands onto a porous

membrane by radiation-induced graft polymerization. J Chromatogr A 758:209-215

Koehler JA, Ulbricht M, Belfort G (2000) Intermolecular forces between a protein and a hydrophilic modified polysulfone film with relevance to filtration. Langmuir 16:10419-10427

Koguma I, Sugita K, Saito K, Sugo T (2000) Multilayer binding of proteins to polymer chains grafted onto porous hollow-fiber membranes containing different anion-exchange groups. Biotechnol Progr 16:456-461

Kubota N, Konno Y, Saito K, Sugita K, Watanabe K, Sugo T (1997a) Module performance of anion-exchange porous hollow-fiber membranes for high-speed protein recovery. J Chromatogr A 782:159-165

Kubota N, Kounosu M, Saito K, Sugita K, Watanabe K, Sugo T (1997b) Repeated use of a hydrophobic ligand-containing porous membrane for protein recovery. J Membrane Sci 134:67-73

Kuroda S, Mita I, Obata K, Tanaka S (1990) Degradation of aromatic polymers: part IV. Effect of temperature and light intensity on the photodegradation of polyethersulfone Polym Degr Stab 27:257

Kubota N, Miura S, Saito K, Sugita K, Watanabe K, Sugo T (1996) Comparison of protein adsorption by anion-exchange interaction onto porous hollow-fiber membrane and gel bead-packed bed. J Membrane Sci 117:135-142

Larminie J, Dicks A (2000) Fuel cell systems explained. John Wiley & Sons, New York

Lawler J, Charlesby A (1980) Grafting of acrylic acid onto polyethylene using radiation as initiator. Radiat Phys Chem 15:595-602

Lee W, Saito K, Furusaki S, Sugo T (1997) Capture of microbial cells on brush-type polymeric materials bearing different functional groups. Biotechnol Bioeng 53:523-528

Lee W, Saito K, Furusaki S, Sugo T, Makuuchi K (1996) Adsorption kinetics of microbial cells onto a novel brush-type polymeric material prepared by RIGP. Biotechnol Progr 12:178-183

Lee YM, Ihm SY, Shim JK, Kim JH (1995) Preparation of surface-modified stimuli-responsive polymeric membranes by plasma and ultraviolet grafting methods and their riboflavin permeation. Polymer 36:81-85

Lee YM, Shim JK (1997) Preparation of pH/temperature responsive polymer membrane by plasma polymerization and its riboflavin permeation. Polymer 38:1227-1232

Li JY, Ichizuri S, Asano S, Mutou F, Ikeda S, Iida M, Miura T, Oshima A, Tabata Y, Washio M (2005a) Proton exchange membranes prepared by grafting of styrene/divinylbenzene into crosslinked PTFE membranes. Nucl Instrum Meth B 236:333-337

Li JY, Ichizuri S, Asano S, Mutou F, Ikeda S, Iida M, Miura T, Oshima A, Tabata Y, Washio M (2005b) Surface analysis of the proton exchange membranes prepared by pre-irradiation induced grafting of styrene/divinylbenzene into crosslinked thin PTFE membranes. Appl Surf Sci 245:260-272

Li JY, Ichizuri S, Asano S, Mutou F, Ikeda S, Iida M, Miura T, Oshima A, Tabata Y, Washio M (2006a) Preparation of ion exchange membranes by preirradiation induced grafting of styrene/divinylbenzene into crosslinked PTFE films and successive sulfonation. J Appl Polym Sci 101:3587-3599

Li JY, Muto F, Miura T, Oshima A, Washio M, Ikeda S, Iida M, Tabata Y, Matsuura C, Katsumura Y (2006b) Improving the properties of the proton exchange membranes by introducing alpha-methylstyrene in the pre-irradiation induced graft polymerization. Eur Polym J 42:1222-1228

Li JY, Sato K, Ichiduri S, Asano S, Ikeda S, Iida M, Oshima A, Tabata Y, Washio M (2004) Pre-irradiation induced grafting of styrene into crosslinked and non-crosslinked polytetrafluoroethylene films for polymer electrolyte fuel cell applications. I: Influence of styrene grafting conditions. Eur Polym J 40:775-783

Li JY, Sato K, Ichizuri S, Asano S, Ikeda S, Iida M, Oshima A, Tabata Y, Washio M (2005c) Pre-irradiation induced grafting of styrene into crosslinked and non-crosslinked polytetrafluoroethylene films for polymer electrolyte fuel cell applications. II: Characterization of the styrene grafted films. Eur Polym J 41:547-555

Li YP, Liu L, Fang YE (2003) Plasma-induced grafting of hydroxyethyl methacrylate (HEMA) onto chitosan membranes by a swelling method. Polym Int 52:285-290

Liang L, Feng XD, Peurrung L, Viswanthan V (1999) Temperature-sensitive membranes prepared by UV photopolymerization of N-isopropylacrylamide on a surface of porous hydrophilic polypropylene membranes. J Membrane Sci 162:235-246

Lightfoot EN, Moscariello JS (2004) Bioseparations. Biotechnol Bioeng 87:259-273

Liu F, Du CH, Zhu BK, Xu YY (2007) Surface immobilization of polymer brushes onto porous poly(vinylidene fluoride) membrane by electron beam to improve the hydrophilicity and fouling resistance. Polymer 48:2910-2918

Liu ZM, Xu ZK, Wang JQ, Wu J, Fu JJ (2004) Surface modification of polypropylene microfiltration membranes by graft polymerization of N-vinyl-2-pyrrolidone. Eur Polym J 40:2077-2087

Liu ZM, Xu ZK, Wang JQ, Yang Q, Wu J, Seta P (2003) Surface modification of microporous polypropylene membranes by the grafting of poly(gamma-stearyl-L-glutamate). Eur Polym J 39:2291-2299

Ma H, Davis RH, Bowman CN (2000) A novel sequential photoinduced living graft polymerization. Macromolecules 33:331-335

Ma ZW, Ramakrishna S (2006) Ce(IV)-induced graft copolymerization of methacrylic acid on electrospun polysulphone nonwoven fiber membrane. J Appl Polym Sci 101:3835-3841.

Maartens A, Swart P, Jacobs EP (2000) Membrane pretreatment: a method for reducing fouling by natural organic matter. J Colloid Interf Sci 221:137-142

Matsuyama H, Teramoto M, Iwai K (1994) Development of a new functional cation-exchange membrane and its application to facilitated transport of CO_2. J Membrane Sci 93:237-244

Matsuyama H, Teramoto M, Sakakura H (1996) Selective permeation of CO_2 through poly(2-(N,N-dimethyl) aminoethyl methacrylate) membrane prepared by plasma-graft polymerization technique. J Membrane Sci 114:193-200

Mika AM, Childs RF, Dickson JM (1999) Chemical valves based on poly(4-vinylpyridine)-filled microporous membranes. J Membrane Sci 153:45-56

Mika AM, Childs RF, Dickson JM, McCarry BE, Gagnon DR (1995) A new class of polyelectrolyte-filled microfiltration membranes with environmentally controlled porosity. J Membrane Sci 108:37-56

Mika AM, Childs RF, West M, Lott JNA (1997) Poly(4-vinylpyridine)-filled microfiltration membranes: physicochemical properties and morphology. J Membrane Sci 136:221-232

Mino G, Kaizerman S, Rasmussen E (1958) Oxidation of pinacol by ceric sulfate. J Polym Sci 31:242-247

Mishima S, Kaneoka H, Nakagawa T (1999) Characterization and pervaporation of chlorinated hydrocarbon-water mixtures with fluoroalkyl methacrylate-grafted PDMS membrane. J Appl Polym Sci 71:273-287

Mishima S, Kaneoka H, Nakagawa T (2001) Characterization for graft polymerization of alkyl methacrylate onto polydimethylsiloxane membranes by electron beam and their permselectivity for volatile organic compounds. J Appl Polym Sci 79:203-213

Mishima S, Nakagawa T (1999) Plasma-grafting of fluoroalkyl methacrylate onto PDMS membranes and their VOC separation properties for pervaporation. J Appl Polym Sci 73:1835-1844

Mishima S, Nakagawa T (2003) Characterization of graft polymerization of fluoroalkyl methacrylate onto PDMS hollow-fiber membranes and their permselectivity for volatile organic compounds. J Appl Polym Sci 88:1573-1580

Miyoshi K, Saito K, Shiraishi T, Sugo T (2005) Introduction of taurine into polymer brush grafted onto porous hollow-fiber membrane. J Membrane Sci 264:97-103

Nasef MM, Hegazy ESA (2004) Preparation and applications of ion exchange membranes by radiation-induced graft copolymerization of polar monomers onto non-polar films. Prog Polym Sci 29:499-561

Nasef MM, Saidi H (2003) Preparation of crosslinked cation exchange membrane by radiation grafting of styrene/divinylbenzene mixtures onto PFA films. J Membrane Sci 216:27-38

Nasef MM, Saidi H, Nor HM, Ooi MF (2000a) Cation exchange membranes by radiation-induced graft copolymerization of styrene onto PFA copolymer films. II. Characterization of sulfonated graft copolymer membranes. J Appl Polym Sci 76:1-11

Nasef MM, Saidi H, Nor HM, Ooi MF (2000b) Proton exchange membranes prepared by simultaneous radiation grafting of styrene onto poly(tetrafluoroethylene-co-hexafluoropropylene) films. II. Properties of the sulfonated membranes. J Appl Polym Sci 78:2443-2453

Nasef MM, Saidi H, Nor HM, Ooi MF (2000c) Radiation-induced grafting of styrene onto poly(tetrafluoroethylene) (PTFE) films. Part II. Properties of the grafted and sulfonated membranes. Polym Int 49:1572-1579

Nasef MM, Suppiah RR, Dahlan KZM (2004) Preparation of polymer electrolyte membranes for lithium batteries by radiation-induced graft copolymerization. Solid State Ionics 171:243-249.

Nasef MM, Zubir NA, Ismail AF, Khayet M, Dahlan KZM, Saidi H, Rohani R, Ngah TIS, Sulaiman NA (2006) PSSA pore-filled PVDF membranes by simultaneous electron beam irradiation: Preparation and transport characteristics of protons and methanol. J Membrane Sci 268:96-108

Nayak A, Liu HW, Belfort G (2006) An optically reversible switching membrane surface. Angew Chem Int Edit 45:4094-4098

Nouzaki K, Nagata M, Arai J, Idemoto Y, Koura N, Yanagishita H, Negishi H, Kitamoto D, Ikegami T, Haraya K (2002) Preparation of polyacrylonitrile ultrafiltration membranes for wastewater treatment. Desalination 144:53-59

Odian G, Henry R, Koeing R, Mangaraj D, Trung D, Chao B, Derman A (1975) Effect of diffusion on rates and molecular weights in graft polymerization. J Polym Sci Polym Chem Edit 13:623-643

Odian G, Keusch P, Raffo J, Tufano J (1968) A study of the synthesis of hemodialysis membranes. RAI Research Corporation, Progress Report, Pb 182990

Ohya H, Minamihira K, Hwang GJ, Kuwahara T, Kang AS, Aihara M, Negishi Y (1995) Studies on membrane for redox flow battery. IX. Crosslinking of tile membrane by the electron radiation and durability of the membrane. Denkikagaku 63:1033-1039

Okamoto J (1987) Radiation synthesis of functional polymer. Radiat Phys Chem 29:469-475

Okamura A, Itayagoshi M, Hagiwara T, Yamaguchi M, Kanamori T, Shinbo T, Wang PC (2005) Poly(N-isopropylacrylamide)-graft-polypropylene membranes containing adsorbed antibody for cell separation. Biomaterials 26:1287-1292

Okamura D, Saito K, Sugita K, Tamada M, Sugo T (2002) Solvent effect on protein binding by polymer brush grafted onto porous membranes. J Chromatogr A 953:101-109

Oster G, Yang NL (1968) Photopolymerization of vinyl monomers. Chem Rev 68:125-151

Ozawa I, Saito K, Sugita K, Sato K, Akiba M, Sugo T (2000) High-speed recovery of germanium in a convection-aided mode using functional porous hollow-fiber membranes. J Chromatogr A 888:43-49

Peng T, Cheng YL (1998) Temperature-responsive permeability of porous PNIP-AAm-g-PE membranes. J Appl Polym Sci 70:2133-2142

Peng T, Cheng YL (2001) PNIPAAm and PMAA co-grafted porous PE membranes: living radical co-grafting mechanism and multi-stimuli responsive permeability. Polymer 42:2091-2100

Pieracci J, Wood DW, Crivello JV, Belfort G (2000) UV-assisted graft polymerization of N-vinyl-2-pyrrolidinone onto poly(ether sulfone) ultrafiltration membranes: Comparison of dip versus immersion modification techniques. Chem Mater 12:2123-2133

Pieracci J, Crivello JV, Belfort G (2002a) Increasing membrane permeability of UV-modified poly(ether sulfone) ultrafiltration membranes. J Membrane Sci 202:1-16

Pieracci J, Crivello JV, Belfort G (2002b) UV-assisted graft polymerization of N-vinyl-2-pyrrolidinone onto poly(ether sulfone) ultrafiltration membranes using selective UV wavelengths. Chem Mater 14:256-265

Prater K (1994) Polymer electrolyte fuel cells: a review of recent developments. Power Sources 51:129-144

Qiu CQ, Nguyen QT, Ping ZH (2007) Surface modification of cardo polyetherketone ultrafiltration membrane by photo-grafted copolymers to obtain nanofiltration membranes. J Membrane Sci 295:88-94

Qiu CQ, Xu F, Nguyen QT, Ping ZH (2005) Nanofiltration membrane prepared from cardo polyetherketone ultrafiltration membrane by UV-induced grafting method. J Membrane Sci 255:107-115

Qiu CQ, Zhang QTNL, Ping ZH (2006) Nanofiltration membrane preparation by photomodification of cardo polyetherketone ultrafiltration membrane. Sep Purif Technol 51:325-331

Risen JW (1996) Applications of ionomers. In: Schuck S(Ed.), Ionomers: characterization, theory and applications. CRC Press, New Jersey, p281

Roper DK, Lightfoot EN (1995) Separation of biomolecules using adsorptive membranes. J Chromatogr A 702:3-26

Rouilly M, Koetz E, Haas O, Scherer G, Chapiro A (1993) Proton exchange membranes prepared by simultaneous radiation grafting of styrene onto Teflon-FEP films. Synthesis and characterization. J Membrane Sci 81:89-95

Safranj A, Omichi H, Okamoto J (1986) Radiation-induced grafting of methyl-α,β,β-trifluoroacrylate onto tetrafluoroethylene-propylene copolymer. Radiat Phys Chem 27:447-453

Sato K, Ikeda S, Iida M, Oshima A, Tabata Y, Washio M (2003) Study on polyelectrolyte membrane of crosslinked PTFE by radiation-grafting. Nucl Instrum Meth B 208:424-428

Saito K, Saito K, Sugita K, Tamada M, Sugo T (2002a) Cation-exchange porous hollow-fiber membranes prepared by radiation-induced cografting of GMA and EDMA which improved pure water permeability and sodium ion adsorptivity. Ind Eng Chem Res 41:5686-5691

Saito K, Saito K, Sugita K, Tamada M, Sugo T (2002b) Convection-aided collection of metal ions using chelating porous flat-sheet membranes. J Chromatogr A 954:277-283

Saito K, Tsuneda S, Kim M, Kubota N, Sugita K, Sugo T (1999) Radiation-induced graft polymerization is the key to develop high-performance functional materials for protein purification. Radiat Phys Chem 54:517-525

Saito N, Yamashita S (1998) Characterization of surface-charge-mosaic-modified ultrafiltration membranes prepared by laser-induced surface graft polymerization. J Appl Polym Sci 67:1141-1149

Saito N, Yamashita S, Matsuda T (1997) Laser-irradiation-induced surface graft polymerization method. J Polym Sci Pol Chem 35:747-750

Saito T, Kawakita H, Uezu K, Tsuneda S, Hirata A, Saito K, Tamada M, Sugo T (2004) Structure of polyol-ligand-containing polymer brush on the porous membrane for antimony(III) binding. J Membrane Sci 236:65-71

Sasagawa N, Saito K, Sugita K, Kunori S, Sugo T (1999) Ionic crosslinking of SO$_3$H-group-containing graft chains helps to capture lysozyme in a permeation mode. J Chromatogr A 848:161-168

Shim JK, Lee YB, Lee YM (1999) pH-dependent permeation through polysulfone ultrafiltration membranes prepared by ultraviolet polymerization technique. J Appl Polym Sci 74:75-82

Shim JK, Na HS, Lee YM, Huh H, Nho YC (2001) Surface modification of polypropylene membranes by gamma-ray induced graft copolymerization and their solute permeation characteristics. J Membrane Sci 190:215-226

Singh N, Husson SM, Zdyrko B, Luzinov I (2005) Surface modification of microporous PVDF membranes by ATRP. J Membrane Sci 262:81-90

Siu A, Pivovar B, Horsfall J, Lovell KV, Holdcroft S (2006) Dependence of methanol permeability on the nature of water and the morphology of graft copolymer proton exchange membranes. J Polym Sci Pol Phys 44:2240-2252

Son HD, Cho MS, Nam JD, Cho SM, Chung CH, Choi HG, Lee Y (2006) Depression of methanol-crossover using multilayer proton conducting membranes prepared by layer-by-layer deposition onto a porous polyethylene film. J Power Sources 163:66-70

Steinert V, Reinhardt S, Werner K (1999) Poly(propene-*co*-maleic acid) with lateral perester groups as initiator in the emulsion polymerization of styrene. J Polym Sci Pol Chem 37:2045-2054

Susanto H, Balakrishnan M, Ulbricht M (2007) Via surface functionalization by photograft copolymerization to low-fouling polyethersulfone-based ultrafiltration membranes. J Membrane Sci 288:157-167

Taher NH, Dessouki AM, Khalil FH, ElArnaouty MB (1996) Preparation and properties of cationic membranes obtained by radiation grafting of vinyl monomers onto poly(tetrafluoroethylene-perfluoropropylvinyl ether(PFA) films. Polym Int 41:383-389

Taniguchi M, Belfort G (2004) Low protein fouling synthetic membranes by UV-assisted surface grafting modification: varying monomer type. J Membrane Sci 231:147-157

Taniguchi M, Kilduff JE, Belfort G (2003a) Low fouling synthetic membranes by UV-assisted graft polymerization: monomer selection to mitigate fouling by natural organic matter. J Membrane Sci 222:59-70

Taniguchi M, Pieracci J, Samsonoff WA, Belfort G (2003b) UV-assisted graft polymerization of synthetic membranes: Mechanistic studies. Chem Mater 15:3805-3812

Teng MY, Lee KR, Liaw DJ, Lin YS, Lai JY (2000) Plasma deposition of acrylamide onto novel aromatic polyamide membrane for pervaporation. Eur Polym J 36:663-672

Terada A, Yuasa A, Tsuneda S, Hirata A, Katakai A, Tamada M (2005) Elucidation of dominant effect on initial bacterial adhesion onto polymer surfaces prepared by radiation-induced graft polymerization. Colloid Surface B 43:99-107

Tsuneda S, Endo T, Saito K, Sugita K, Horie K, Yamashita T, Sugo T (1998) Fluorescence study on the conformational change of an amino group-containing polymer chain grafted onto a polyethylene microfiltration membrane. Macromolecules 31:366-370

Tsuneda S, Saito K, Sugo T, Makuuchi K (1995) Protein adsorption characteristics of porous and tentacle anion-exchange membrane prepared by radiation-induced graft polymerization. Radiat Phys Chem 46:239-245

Tu CY, Chen CP, Wang YC, Li CL, Tsai HA, Lee KR, Lai JY (2004) Acrylamide plasma-induced polymerization onto expanded poly(tetrafluoroethylene) membrane for aqueous alcohol mixture vapor permeation separation. Eur Polym J 40:1541-1549

Ulbricht M (1996) Photograft-polymer-modified microporous membranes with environment-sensitive permeabilities. React Funct Polym 31:165-177

Ulbricht M (2006) Advanced functional polymer membranes. Polymer 47:2217-2262

Ulbricht M, Schwarz HH (1997) Novel high performance photo-graft composite membranes for separation of organic liquids by pervaporation. J Membrane Sci 136:25-33

Ulbricht M, Matuschewski H, Oechel A, Hicke HG (1996a) Photo-induced graft polymerization surface modifications for the preparation of hydrophilic and low-protein-adsorbing ultrafiltration membranes. J Membrane Sci 115:31-47

Ulbricht M, Oechel A, Lehmann C, Tomaschewski G, Hicke HG (1995) Gas-phase photoinduced graft polymerization of acrylic acid onto polyacrylonitrile ultrafiltration membranes. J Appl Polym Sci 55:1707-1723

Ulbricht M, Riedel M, Marx U (1996b) Novel photochemical surface functionalization of polysulfone ultrafiltration membranes for covalent immobilization of biomolecules. J Membr Sci 120:239-259

Ulbricht M, Richau K, Kamusewitz H (1998) Photomodification of ultrafiltration membranes—Part II—Chemically and morphologically defined ultrafiltration membrane surfaces prepared by heterogeneous photo-initiated graft polymerization. Colloid Surface A 138:353-366

Ulbricht M, Yang H (2005) Porous polypropylene membranes with different carboxyl polymer brush layers for reversible protein binding via surface-initiated graft copolymerization. Chem Mater 17:2622-2631

Uyama Y, Kato K, Ikada Y (1998) Surface modification of polymers by grafting. Adv Polym Sci 137:1-39

Wang M, An QF, Wu LG, Mo JX, Gao CJ (2007) Preparation of pH-responsive phenolphthalein poly(ether sulfone) membrane by redox-graft pore-filling polymerization technique. J Membrane Sci 287:257-263

Wang XL, Huang J, Chen XZ, Yu XH (2002) Graft polymerization of N-isopropylacrylamide into a microporous polyethylene membrane by the plasma method: technique and morphology. Desalination 146:337-343

Wang Y, Kim JH, Choo KH, Lee YS, Lee CH (2000) Hydrophilic modification of polypropylene microfiltration membranes by ozone-induced graft polymerization. J Membrane Sci 169:269-276

Watkins D (1993) Research, development, and demonstration of solid polymer electrolyte fuel cell system. In: Blomen LMM (Eds.), Solid polymer fuel cell system. Plenum Press, New York, p351

Way JD, Noble RD (1992) Facilitated transport. In: Ho WS, Sirkar KK(Eds.), Membrane Handbook. Van Nostrand Reinhold, New York, 833-866

Wenzel A, Yanagishita H, Kitamoto D, Endo A, Haraya K, Nakane T, Hanai N, Matsuda H, Koura N, Kamusewitz H, et al. (2000) Effects of preparation condition of photoinduced graft filling-polymerized membranes on pervaporation performance. J Membrane Sci 179:69-77

Xie R, Chu LY, Chen WM, Xiao W, Wang HD, Qu JB (2005) Characterization of microstructure of poly (N-isopropylacrylamide)-grafted polycarbonate track-etched membranes prepared by plasma-graft pore-filling polymerization. J Membrane Sci 258:157-166

Xie R, Li Y, Chu LY (2007) Preparation of thermo-responsive gating membranes with controllable response temperature. J Membrane Sci 289:76-85

Xu FJ, Zhao JP, Kang ET, Neoh KG, Li J (2007) Functionalization of nylon membranes via surface-initiated atom-transfer radical polymerization. Langmuir 23:8585-8592

Yamagishi H, Crivello JV, Belfort G (1995a) Development of a novel photo-
    chemical technique for modifying poly(arylsulfone) ultrafiltration membranes.
    J Membrane Sci 105:237-247
Yamagishi H, Crivello JV, Belfort G (1995b) Evaluation of photochemically mod-
    ified poly(arylsulfone) ultrafiltration membranes. J Membrane Sci 105:249-259
Yamaguchi T, Ito T, Sato T, Shinbo T, Nakao S (1999) Development of a fast
    response molecular recognition ion gating membrane. J Am Chem Soc 121:4078-
    4079
Yamaguchi T, Miyata F, Nakaoa S (2003) Pore-filling type polymer electrolyte
    membranes for a direct methanol fuel cell. J Membrane Sci 214:283-292
Yamaguchi T, Nakao SI, Kimura S (1991) Plasma-graft filling polymerization:
    preparation of a new type of pervaporation membrane for organic liquid mix-
    tures. Macromolecules 24:5522-5527
Yamaguchi T, Nakao SI, Kimura S (1992) Solubility and pervaporation properties
    of the filling-polymerized membrane prepared by plasma-graft polymerization
    for pervaporation of organic-liquid mixtures. Ind Eng Chem Res 31:1914-1919
Yamaguchi T, Nakao SI, Kimura S (1993) Design of pervaporation membrane
    for organic-liquid separation based on solubility control by plasma-graft filling
    polymerization technique. Ind Eng Chem Res 32:848-853
Yamaguchi T, Nakao SI, Kimura S (1996) Evidence and mechanisms of filling
    polymerization by plasma-induced graft polymerization. J Polym Sci Pol Chem
    34:1203-1208
Yamaguchi T, Nakao SI, Kimura S (1997) Swelling behavior of the filling-type
    membrane. J Polym Sci Pol Phys 35:469-477
Yamaguchi T, Suzuki T, Kai T, Nakao S (2001) Hollow-fiber-type pore-filling
    membranes made by plasma-graft polymerization for the removal of chlorinated
    organics from water. J Membrane Sci 194:217-228
Yamauchi J, Yamaoka A, Ikemoto K, Matsui T (1991) Graft copolymerization of
    methyl methacrylate onto polypropylene oxidized with ozone. J Appl Polym
    Sci 43:1197-1203
Yanagioka M, Kurita H, Yamaguchi T, Nakao S (2003) Development of a molec-
    ular recognition separation membrane using cyclodextrin complexation con-
    trolled by thermosensitive polymer chains. Ind Eng Chem Res 42:380-385
Yanagishita H, Arai J, Sandoh T, Negishi H, Kitamoto D, Ikegami T, Haraya K,
    Idemoto Y, Koura N (2004) Preparation of polyimide composite membranes
    grafted by electron beam irradiation. J Membrane Sci 232:93-98
Yang B, Yang WT (2003) Thermo-sensitive switching membranes regulated by
    pore-covering polymer brushes. J Membrane Sci 218:247-255
Yang B, Yang WT (2005) Novel pore-covering membrane as a full open/close
    valve. J Membrane Sci 258:133-139
Yang JM, Chian CPC, Hsu KY (1999) Oxygen permeation in SBS-*g*-DMAEMA
    copolymer membrane prepared by UV photografting without degassing. J
    Membrane Sci 153:175-182
Yang JM, Hsiue GH (1990) Oxygen permeation in SBS-*g*-VP membrane and effect
    of facilitated oxygen carrier. J Appl Polym Sci 41:1141-1150
Yang JM, Jong YJ, Hsu KY (1997a) Preparation and properties of SBS-*g*-
    DMAEMA copolymer membrane by ultraviolet radiation. J Biomed Mater Res
    35:175-180

Yang JM, Wang MC, Hsu YG, Chang CH (1997b) Preparation of SBS-*g*-VP copolymer membrane by UV radiation without degassing. J Appl Polym Sci 65:109-116

Yang JM, Wang MC, Hsu YG, Chang CH (1997c) The properties of SBS-*g*-VP copolymer membrane prepared by UV photografting without degassing. J Membrane Sci 128:133-140

Yang JS, Hsiue GH (1997) Kinetics of Ag^+ contained polymeric complex membranes for facilitated olefin transport. J Polym Sci Pol Phys 35:909-917

Yang JS, Hsiue GH (1998) Swollen polymeric complex membranes for olefin/paraffin separation. J Membrane Sci 138:203-211

Yang M, Chu LY, Li Y, Zhao XJ, Song H, Chen WM (2006) Thermo-responsive gating characteristics of poly(*N*-isopropylacrylamide)-grafted membranes. Chem Eng Technol 29:631-636

Ying L, Yu WH, Kang ET, Neoh KG (2004) Functional and surface-active membranes from poly(vinylidene fluoride)-graft-poly(acrylic acid) prepared via RAFT-mediated graft copolymerization. Langmuir 20:6032-6040

Yu HY, Hu MX, Xu ZK (2005) Improvement of surface properties of poly(propylene) hollow fiber microporous membranes by plasma-induced tethering of sugar moieties. Plasma Process Polym 2:627-632

Yu HY, Xu ZK, Lei H, Hu MX, Yang Q (2007) Photoinduced graft polymerization of acrylamide on polypropylene microporous membranes for the improvement of antifouling characteristics in a submerged membrane-bioreactor. Sep Purif Technol 53:119-125

Yu HY, Xu ZK, Xie YJ, Liu ZM, Wang SY (2006a) Flux enhancement for polypropylene microporous membrane in a SMBR by the immobilization of poly(*N*-vinyl-2-pyrrolidone) on the membrane surface. J Membrane Sci 279:148-155

Yu HY, Xu ZK, Yang Q, Hu MX, Wang SY (2006b) Improvement of the antifouling characteristics for polypropylene microporous membranes by the sequential photoinduced graft polymerization of acrylic acid. J Membrane Sci 281:658-665

Yuee F, Tianyi S (1988) Polypropylene dialysis membrane prepared by cobalt-60 gamma-radiation-induced graft copolymerization. J Membrane Sci 39:1-9

Yusof AHM, Ulbricht M (2006) Effects of photo-initiation and monomer composition onto performance of graft-copolymer based membrane adsorbers. Desalination 200:462-463

Zeng XF, Ruckenstein E (1999) Membrane chromatography: Preparation and applications to protein separation. Biotechnol Progr 15:1003-1019

Zhai GQ, Kang ET, Neoh KG (2004) Inimer graft-copolymerized poly(vinylidene fluoride) for the preparation of arborescent copolymers and "surface-active" copolymer membranes. Macromolecules 37:7240-7249

Zhai GQ, Shi ZL, Kang ET, Neoh KG (2005) Surface-initiated atom transfer radical polymerization on poly(vinylidene fluoride) membrane for antibacterial ability. Macromol Biosci 5:974-982

Zhang J, Yuan J, Yuan YL, Shen J, Lin SC (2003) Chemical modification of cellulose membranes with sulfo ammonium zwitterionic vinyl monomer to improve hemocompatibility. Colloid Surface B 30:249-257

Zhang L, Jin G (2006) Novel method for bilirubin removal from human plasma within modified polytetrafluoroethylene capillary. React Funct Polym 66:1106-1117

Zhao B, Brittain WJ (2000) Polymer brushes: surface-immobilized macromolecules. Prog Polym Sci 25:677-710

Zhao ZP, Li JD, Chen J, Chen CX (2005a) Nanofiltration membrane prepared from polyacrylonitrile ultrafiltration membrane by low-temperature plasma: 2. Grafting of styrene in vapor phase. J Membrane Sci 251:239-245

Zhao ZP, Li JD, Wang D, Chen CX (2005b) Nanofiltration membrane prepared from polyacrylonitrile ultrafiltration membrane by low-temperature plasma: 4. Grafting of N-vinylpyrrolidone in aqueous solution. Desalination 184:37-44

Zhao ZP, Li JD, Zhang DX, Chen CX (2004) Nanofiltration membrane prepared from polyacrylonitrile ultrafiltration membrane by low-temperature plasma: 1. Graft of acrylic acid in gas. J Membrane Sci 232:1-8

Zhou XD, Liu PS (2003) Study on antistatic modification of polyurethane elastomer surfaces by grafting with vinyl acetate and antistatic agent. J Appl Polym Sci 90:3617-3624

Zhu LP, Zhu BK, Xu L, Feng YX, Liu F, Xu YY (2007) Corona-induced graft polymerization for surface modification of porous polyethersulfone membranes. Appl Surf Sci 253:6052-6059

Zou H, Luo QZ, Zhou DM (2001) Affinity membrane chromatography for the analysis and purification of proteins. J Biochem Bioph Meth 49:199-240

5

Surface Modification by Macromolecule Immobilization

Membrane based processes have attracted great attention in recent years. However, the innate disadvantages of common membrane materials, such as the hydrophobic surface and poor biocompatibility, cause many side effects in practice and hinder further applications. Grafting a new layer onto a membrane surface by macromolecule immobilization is a promising solution for these problems. In addition, macromolecule immobilization can endow the existing membranes with new functions. In this chapter some research is introduced in which surface modification was achieved by macromolecule immobilization on the membrane surface.

5.1 Introduction

Macromolecule immobilization, which is called "grafting to" strategy, is an important method for introducing a functional layer onto the membrane surface (Zhao and Brittain, 2000). To perform the macromolecule immobilization, reactions between the macromolecules and the membrane surfaces are necessary. Ulbricht (2006) classified these reactions in three categories:

• Direct reactions between the functional groups of the macromolecules and membrane materials (Fig.5.1(a)).

• Functionalizing the membrane surface with groups such as hydroxyl, amino, carboxyl, etc. and then coupling these groups with the macromolecules (Fig.5.1(b)). This method is suitable for those membrane materials such as polyethylene and polypropylene which are chemically inert and lacking in functional groups.

• Coupling reaction promoted by outside stimulations such as plasma and UV irradiation (Fig.5.1(c)). This method is relatively versatile.

Compared with "grafting from", the "grafting to" strategy has some advantages. For example, it is easy to control the length and structure of the grafted chains. One can primarily synthesize polymers with a desirable molecular weight, chain structure and even molecular weight distribution before the

immobilization. In addition, this strategy is much more feasible for the immobilization of those natural macromolecules which are difficult to synthesize artificially.
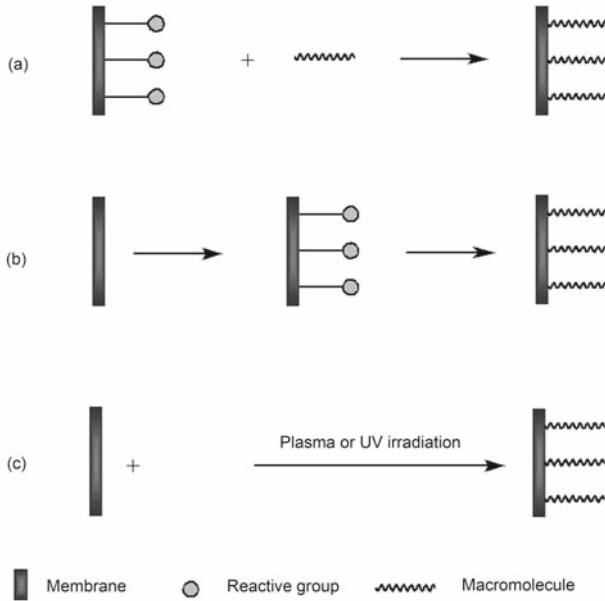
Fig. 5.1. Methods for macromolecule immobilization

5.2 Immobilization with Synthetic Polymers

5.2.1 Polyethylene Glycol (PEG)

PEG has a high solubility in both water and organic solvents (Elbert and Hubbell, 1996; Lee et al., 1995). The molecular structure of PEG is shown in Fig.5.2. Due to its hydrophilicity and large excluded volume, the unique coordination with surrounding water molecules in an aqueous medium (Jo and Park, 2000), PEG is widely used to improve the hydrophilicity and biocompatibility of membranes. PEG has a large excluded volume in water with a Flory Huggins interaction parameter ranging between 0.4~0.5 which indicates that the polymer chain is expanded (Steels et al., 2000) in water. The water molecules associated with PEG create a "hydration shell" where the water molecules are oriented in a structured manner surrounding the PEG chain (Kjellander and Florin, 1981). The grafting of PEG to the surface of

the membrane has been clearly shown to render reduction or prevention of protein adsorption (Ulbricht et al., 1996).

$$H \text{---} (OCH_2CH_2)_n \text{---} OH$$
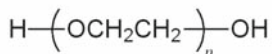
Fig. 5.2. Molecular structure of PEG

Nie et al. (2003) fabricated asymmetric membranes from poly(acrylonitrile-*co*-maleic acid)s (PANCMAs, Fig.5.3(a)). The maleic acid groups were used as functional sites for PEG (molecular weight (MW) = 200) immobilization to improve the biocompatibility of the membrane (Fig.5.3(b)). Compared with PAN and PANCMA membranes, the PEG200 immobilized PANCMA (PANCMA-*g*-PEG) membrane showed lower interactions with platelets as shown in Fig.5.4. It was also found that the immobilization of PEG dramatically decreased the non-specific protein fouling on the membrane surface. As can be seen in Table 5.1, the 1 g/L BSA solution flux of the PANCMA-*g*-PEG membrane was much higher than those of the PAN membrane and the PANCMA membrane. The amount of adsorbed BSA remaining on the membrane after chemical cleaning decreased significantly with an increase of the hydrophilicity in the sequence of PAN, PANCMA and PANCMA-*g*-PEG.

Table 5.1. Filtration Performances of the PAN-Based Membranes[a].Reprinted with permission from (Nie et al., 2003). Copyright (2003), American Chemical Society

Sample	J_{w0} (L/(m^2·h))	J_p (L/(m^2·h))	J_{w1} (L/(m^2·h))	J_{w2} (L/(m^2·h))	BSA adsorption[b] (μg/mg)
PAN	372	104	138	190	14.26
PANCMA	450	233	289	342	7.97
PANCMA-*g*-PEG	871	644	707	782	4.61

[a]The filtration test was conducted at a constant transmembrane pressure of 0.1 MPa and a system temperature of 22 ± 0.2°C. Error range: ±5%
[b]The amount of BSA absorbed onto the membrane after chemical cleaning

Xu et al. (2005) also investigated the influence of PEG MW on the antifouling property of the PANCMA-*g*-PEG membrane. PEGs with MWs of 200, 400, 600 and 1000 were tethered to the membrane surface and permeation experiments were carried out. As the results showed in Table 5.2, with the exception of PANCMA3-*g*-PEG1000, all membranes immobilized with PEG had higher flux values than PAN and PANCMA membranes. Moreover, among all PEG-tethered membranes, the PANCMA-*g*-PEG400 had the high-
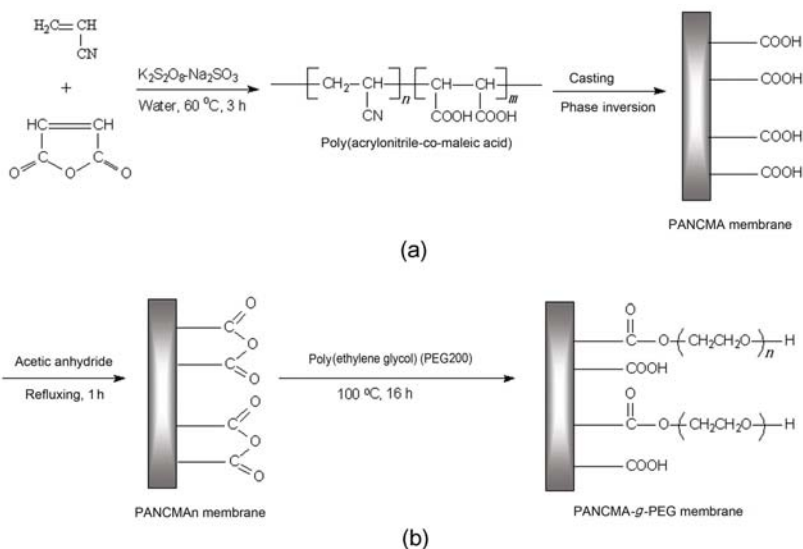
Fig. 5.3. Synthesis of PAN-based copolymers (a) and immobilization of PEG (b). Reprinted with permission from (Nie et al., 2003). Copyright (2003), American Chemical Society
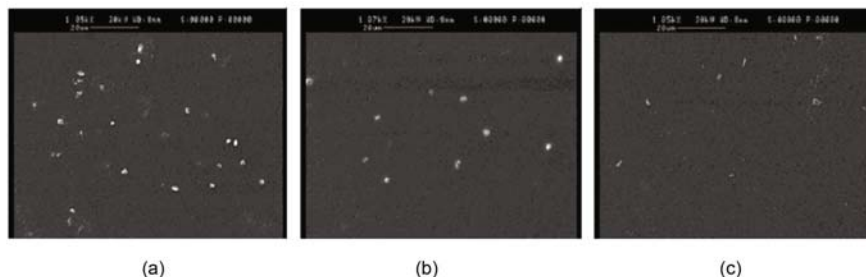
Fig. 5.4. Adhesion of platelets on the PAN (a), PANCMA (b) and PANCMA-*g*-PEG (c) membrane surfaces. Reprinted with permission from (Nie et al., 2003). Copyright (2003), American Chemical Society

est pure water and protein solution fluxes which can be ascribed to the balance between the PEG immobilization density and the content of hydrophilic chain segments.

Zhang et al. (2002) immobilized PEG (MW = 600) onto the PTFE membrane and evaluated the hydrophilicity and biocompatibility of the modified membrane. PTFE membranes were first immersed in PEG solutions with different concentrations (1%, 3%, 5 % (w/v)) and then treated by atmospheric pressure glow discharge plasma. PEG immobilization showed significant re-

Table 5.2. Filtration performances of the PAN, PANCMA and PANCMA-*g*-PEG membranes[a]

Membrane	J_{w0} ((L/m^2·h))	J_p (L/(m^2·h))[b]
PAN	158.5 ± 6.5	17.5 ± 1.5
PANCMA3	323.4 ± 16.8	120.2 ± 5.6
PANCMA3-*g*-PEG200	372.6 ± 22.3	197.6 ± 5.7
PANCMA3-*g*-PEG400	499.4 ± 21.8	312.8 ± 18.3
PANCMA3-*g*-PEG600	450.6 ± 13.5	253.2 ± 12.7
PANCMA3-*g*-PEG1000	311.9 ± 15.6	150.6 ± 6.0

[a]The filtration test was conducted at a constant transmembrane pressure of 0.1 MPa and a system temperature of (22 ± 0.5) °C
[b]The amount of adsorbed BSA on the membrane after chemical cleaning

straint regarding the adsorption of fibrinogen, but increased the amount of albumin adsorbed on the surface (Fig.5.5). This is possibly on account of the chemical and physical properties of the crosslinking network structure of PEG, caused by the plasma treatment. Such a structure endowed the membrane with the ability to selectively adsorb small plasma proteins such as albumin.
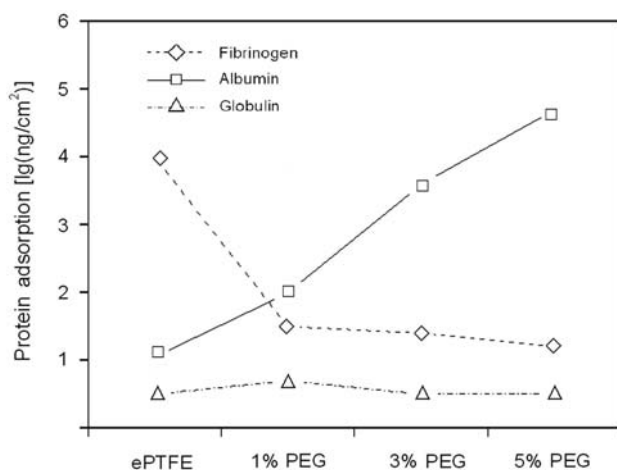
Fig. 5.5. Protein adsorption on PEG immobilized PTFE membrane (Zhang et al., 2002). Copyright (2002). Reprinted with permission of John Wiley & Sons, Inc.

The plasma process may cause damage to the material surface leading to the debasement of surface properties. Thom et al. (1998) proposed a novel PEG immobilization method without affecting the bulk materials. They linked the photoreactive aryl-azide head group onto the PEG chain (α-4-azidobenzoyl ω-methoxy-PEG (ABMPEG), PEG MW = 5000) and employed UV irradiation to tether this macromolecule to the polysulfone (PSf) membrane surface (Fig.5.6). The immobilization degree could be controlled

by the applied ABMPEG concentration during adsorption. The anti-fouling property of the membranes was evaluated by a static BSA adsorption experiment. As shown in Fig.5.7, the amounts of adsorbed protein decreased significantly with the increase of the ABMPEG concentration. When the ABMPEG solution concentration increased to 10 g/L, the protein adsorption amount yielded a reduction of up to 70%.
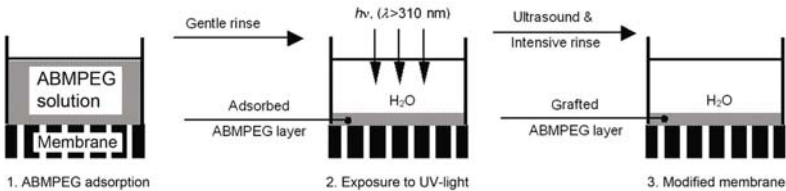
Fig. 5.6. Consecutive steps applied for membrane modification (Thom et al., 1998). Copyright (1998). Reprinted with permission of John Wiley & Sons, Inc.
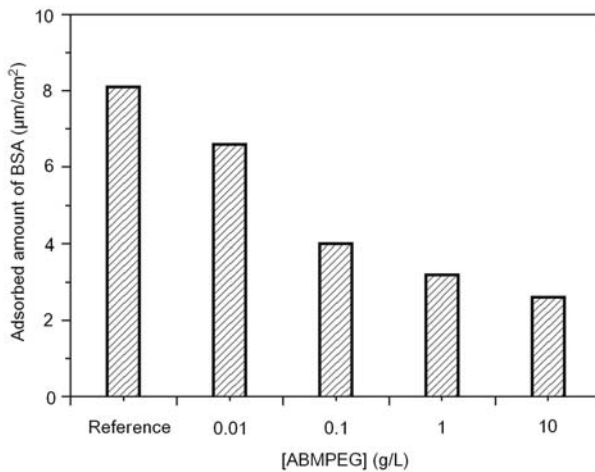
Fig. 5.7. Adsorbed amount of BSA on PSf membranes in dependence on the variation of photo-grafting conditions using aryl azide PEG conjugate ABMPEG, (Thom et al., 1998). Copyright (1998). Reprinted with permission of John Wiley & Sons, Inc.

5.2.2 Poly(N-vinyl-2-pyrrolidone) (PNVP)

PNVP is also a polymer soluble in both water and organic solvents. It has gained a wide range of applications in the fields of additives, cosmetics, coat-

ings and biomedicines because of its excellent biocompatibility and extremely low cytotoxicity. The molecular structure of PNVP is shown in Fig.5.8. Compared with PEG, PNVP has a relatively high Flory Huggins interaction parameter ranging between 0.5~0.6 and subsequently a more collapsed structure in water (Allen et al., 2002). PNVP has also been used to modify the surface properties of polymeric membranes to improve the biocompatibility and to suppress the protein adsorption.
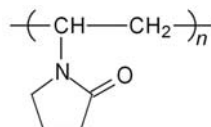
Fig. 5.8. Molecular structure of PNVP
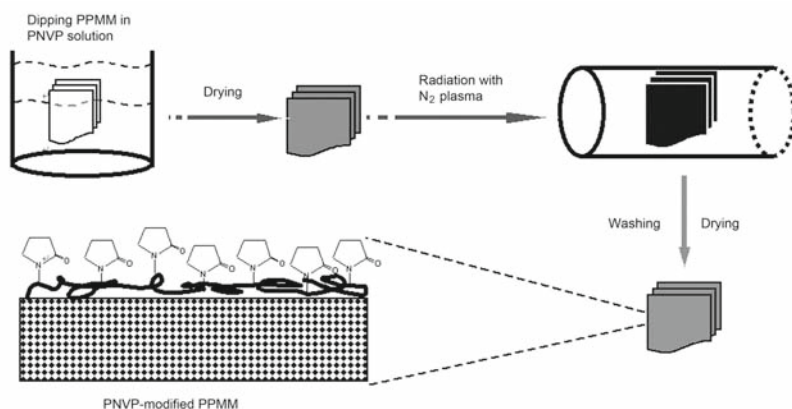
Fig. 5.9. Schematic representation of the immobilization of PNVP on the membrane surface induced by N$_2$ plasma treatment. Reprinted from (Liu et al., 2005b). Copyright (2005), with permission from Elsevier

Liu et al. (2005b) immobilized PNVP on a polypropylene microporous membrane (PPMM) surface by plasma treatment. The process was presented in Fig.5.9. Immobilization of PNVP improved the biocompatibility of the PPMMs significantly. As can be seen in Fig.5.10(a) and Table 5.3, a large number of platelets adhered to the surface of the unmodified PPMM with serious aggregation. Moreover, these adsorbed platelets were deformed and pseudopodia can also be observed. However, after immobilization of PNVP (Figs.5.10(b) and 5.10(c)), the aggregation of platelets and the formation of pseudopodium were suppressed. Also, Table 5.3 shows that the amount
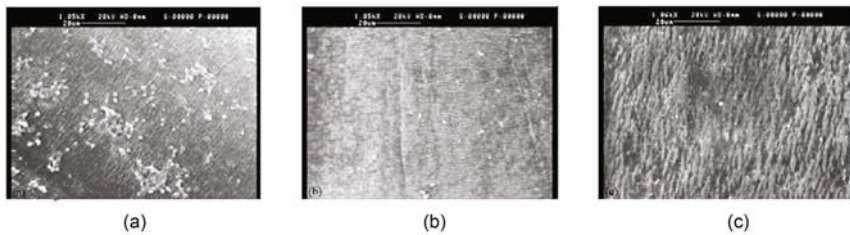
Fig. 5.10. Platelet adhesion on PNVP immobilized PPMMs with different immobilization degrees. (a) 0 wt.%; (b) 6.41 wt.%; (c) 8.13 wt.%. Reprinted from (Liu et al., 2005b). Copyright (2005), with permission from Elsevier

Table 5.3. Average amounts of adsorbed platelets on the surface of PNVP immobilized PPMMs with different immobilization degree. Reprinted from (Liu et al., 2005b). Copyright (2005), with permission from Elsevier

Immobilization degree of PNVP[a] (wt. %)	Amount of adsorbed platelets ($\times 10^{-8}$ m^2 membrane)
0	> 200
1.07	150 ± 8.5
3.03	80 ± 7.6
6.41	46 ± 4.5
7.44	17 ± 2.5
8.13	13 ± 1.2
10.12	8 ± 1.1
12.38	2 ± 0.3

[a]The PNVP-modified PPMMs were prepared with the same plasma treatment time (30 s) with different PNVP adsorption degree

of adhered platelets per unit membrane surface area decreased sharply with the increase in the degree of PNVP immobilization and, when the PNVP immobilization was high enough, only scarce platelets were found on the membrane surface. These results indicated that the hemocompatibility of PPMM was obviously improved by the immobilization of PNVP, which may be ascribed to the hydrophilicity and the biocompatibility of PNVP.

Yu et al. (2006) also employed the same method to treat polypropylene hollow fiber microporous membrane (PPHFMM) and used this membrane in a submerged membrane-bioreactor (SMBR) for wastewater treatment. Filtration results (Table 5.4) obviously demonstrated that the PNVP-immobilized PPHFMMs showed much better anti-fouling behavior in the SMBR than in the nascent one. After continuous operation for about 50 h, the flux recovery, reduction of flux, and relative flux ratio were respectively 53% higher, 17.9% lower and 79% higher than those of the nascent membrane.

Kang et al. (2003) immobilized PNVP to the chlorinated polyvinyl chloride (CPVC) membrane by crosslinking. The PNVP was added to the CPVC solution as the pore-forming and wetting agent. After the membrane fabrication, the PNVP was immobilized by the reaction shown in Fig.5.11. PNVP immobilized CPVC membranes exhibited increased thermal stability and re-

Table 5.4. Flux recovery, reduction of flux and the relative flux ratio for the studied PPHFMMs. Reprinted from (Yu et al., 2006). Copyright (2006), with permission from Elsevier

Immobilization degree (wt. %)	Flux recovery (%)	Reduction of flux (%)	Relative flux ratio
0	36.8	77.1	1.00
4.0	42.5	60.4	1.39
4.8	47.1	62.7	1.63
5.5	62.3	63.7	1.58
6.8	89.8	59.2	1.79

tained a higher hydrophilicity than the untreated ones. However, after PNVP immobilization, a slight decline of pure water flux due to pore narrowing, was also observed.
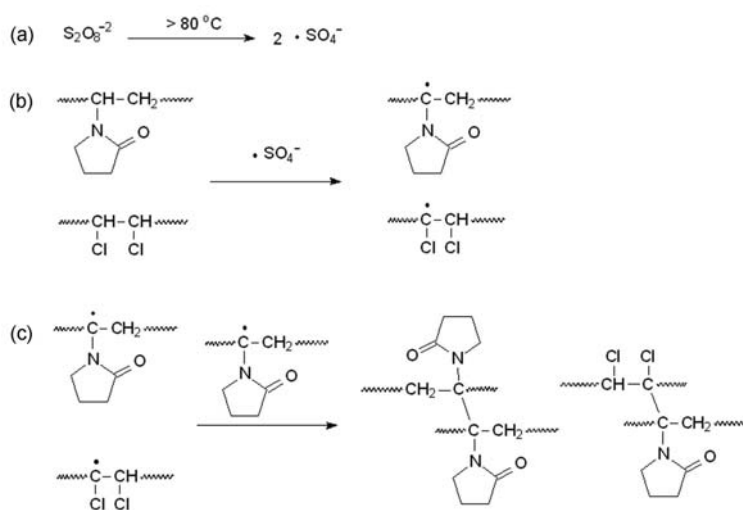
Fig. 5.11. The scheme of the proposed crosslinking mechanism of PNVP. (a) The decomposition of persulphate and the formation of free radicals; (b) the abstraction of hydrogen on PNVP and CPVC by the free radicals; (c) crosslinking. Reprinted from (Kang et al., 2003). Copyright (2003), with permission from Elsevier

5.2.3 Other Synthetic Polymers

Some other polymers were also used to modify membranes by macromolecule immobilization. These polymers were often tethered to the membrane surface to introduce certain unique properties. Generally, stimulation responsive

properties, especially the thermal response property, were most widely investigated. Lue et al. (2007) synthesized crosslinked poly(*N*-isopropylacrylamide) (PNIPAAm) hydrogel by the redox method and grafted this hydrogel onto the track-etched polycarbonate (PC) membrane surface (Fig.5.12). With the PNIPAAm polymer network on the surface, the track-etched PC membrane exhibited rapid and reversible responses to temperature changes (Fig.5.13).
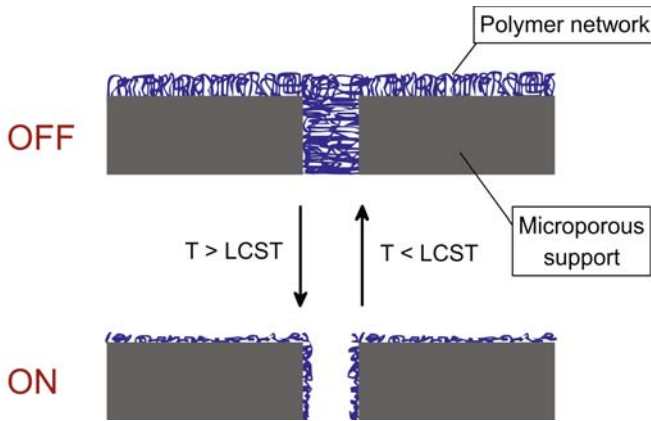

Fig. 5.12. Schematic illustration of the valve mechanism of PNIPAAm grafted onto PC membranes. Reprinted from (Lue et al., 2007). Copyright (2007), with permission from Elsevier
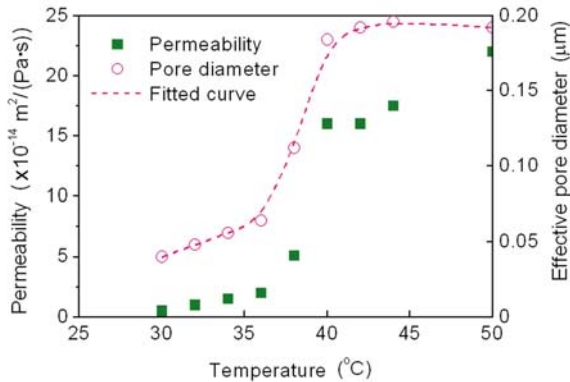
Fig. 5.13. Water permeability and effective pore size of PNIPAAm immobilized PC membrane. Reprinted from (Lue et al., 2007). Copyright (2007), with permission from Elsevier

With the increase in temperature, the water permeability increased significantly. However, at the temperatures above the LCST of PNIPAAm (33.2 °C), the increase in permeability was more significant. This was achieved by the transition between the polymer expansion below the PNIPAAm's LCST and the deswelling above the LCST. Water permeated more significantly at high temperatures because of larger pore diameters during the shrinkage of the grafted polymer chains. While at a low temperature, the grafted polymers swelled and expanded, so that the pores were blocked and in consequence, and the water flux decreased.

Lequieu and co-workers (Lequieu et al., 2005) immobilized thermo-responsive poly(N-vinylcaprolactam) (PVCL) onto the poly(ethylene terephthalate) (PET) track etched membrane surface. First, they incorporated photoreactive azidophenyl groups into the thermo-responsive PVCL chains. Then, the polymers were cast on the PET membrane and suffered irradiation with UV light. Similar to the PNIPAAm grafted membrane, the resulting PVCL immobilized PET membranes also exhibited temperature-responsive permeability behavior. The water permeability increased drastically when the temperature reached the cloud point of the grafted polymer chains as a result of an increased pore diameter (Fig.5.14).
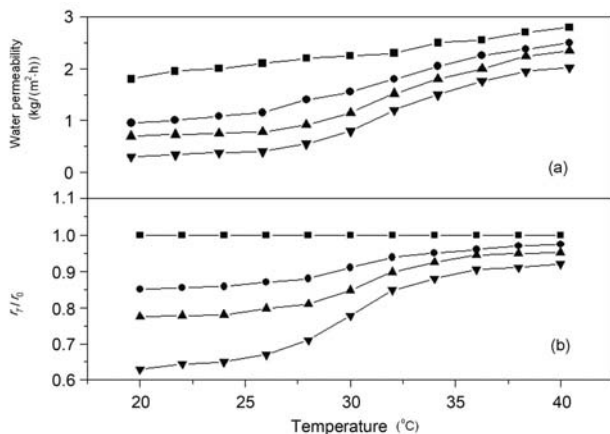
Fig. 5.14. Water permeability (a) and relative pore radius (r_T/r_0) for original PET membrane with initial pore size 0.2 μm (■), and modified membranes with grafting degree of (●) 2.1 wt.%; (▲) 4.4 wt.% and (▼) 7.0 wt.%. $\dfrac{r_T}{r_0} = \dfrac{J_T \eta_T}{J_0 \eta_0}$, where J_T and J_0 are the filtration rates at T (°C) and 20 °C, and η_T and η_0 are the viscosities of the flowing liquid at T (°C) and 20 °C. Reprinted from (Lequieu et al., 2005). Copyright (2005), with permission from Elsevier

5.3 Biomacromolecules

It is envisaged that using the derivatives of native macromolecules existing in biological systems (such as protein and DNA, etc.) to modify membranes can easily offer high biocompatibility. On the other hand, with the biological functions of the biomacromolecules, the modified membrane can be useful in many expanded applications such as bioaffinity separation, immuneassay, immunesensor and chiral separation.

5.3.1 Non-immune Proteins

Liu et al. (2005a) immobilized two plasma proteins, Type I collagen (COL) and human serum albumin (HSA), on a PAN membrane surface to improve its hemocompatibility. The CN groups on the PAN membrane were converted to carboxyl group (PAN-AA) and 1-ethyl-3-(3-dimethyl-aminopropyl) carbodiimide (EDC) was then used as the coupling agent for the following immobilization of COL and HAS (Fig.5.15). Compared with nascent PAN and PAN-AA membranes, the immobilization of platelet-adhesion-inhibiting HSA reduced the platelet adhesion and fibrinogen adsorption. It also prolonged the blood coagulation time (Table 5.5). Though the effect of HAS immobilization on the improvement in hemocompatibility was less than that of heparin immobilization (PAN-HEP), this method could avoid heparin-induced thrombocytopenia. On the other hand, the platelet-adhesion-promoting collagen immobilized PAN membrane exhibited the opposite effect when in contact with blood. Therefore this study demonstrated that the immobilization of HSA on the surface of the PAN membrane might be useful and practicable in improving hemocompatibility and in diminishing the anaphylatoxin formation during hemodialysis treatment.
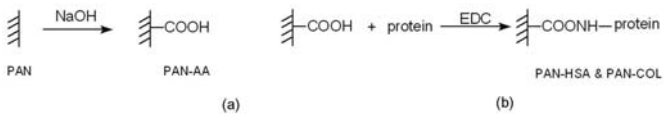
Fig. 5.15. Chemical scheme of protein immobilized PAN membrane. (a) Activation of PAN membrane and inducing the carboxyl groups; (b) Direct immobilization of protein including COL and HSA conjugate onto PAN-AA. Reprinted from (Liu et al., 2005a). Copyright (2005), with permission from Elsevier

Avramescu et al. (2003) immobilized BSA on the cellular-type poly(ethylene vinyl alcohol) (EVAL) microfiltration membrane surface and used this membrane for protein separation. The EVAL membrane was firstly activated both by chemical and plasma treatments and BSA was then immobilized on it.

Table 5.5. Blood coagulation characterization of protein immobilized PAN membranes. Reprinted from (Liu et al., 2005a). Copyright (2003), with permission from Elsevier

Membrane type	Degree of thrombosis[a] (%)	WBCT[b] (s)
PAN	17.4 ± 2.8	320 ± 21
PAN-AA	16.4 ± 2.7	345 ± 13
PAN-HEP	6.7 ± 0.9	851 ± 25
PAN-HAS	9.2 ± 1.2	692 ± 31
PAN-COL	21.8 ± 1.3	253 ± 13

[a]Degree of thrombosis (DT) is defined as follows: $DT=(W_t-W_{\mathrm{dry}})/W_{\mathrm{dry}}\times100\%$, where W_{dry} and W_t are the weight of the dry membrane and the membrane after contact with blood for 120 min
[b]WBCT: whole blood coagulation time

This membrane was used for the affinity separation of bilirubin from aqueous solutions. The BSA-immobilized membranes showed in the static mode a bilirubin retention, which was by a factor of 2.5∼12.5 higher than the 2 mg/g obtained from the bare EVAL membranes.

Dai et al. (2005) immobilized gelatin on the PANCMA membrane and significantly enhanced its biocompatibility and hemocompatibility. They also used EDC as a coupling agent to link the carboxyl groups of the membrane surface and the amine groups of the gelatin molecules (Fig.5.16). It can be seen from Fig.5.17 that with the content of maleic acid in the PANCMA copolymer increased, platelets adhering to both the nascent and the gelatin immobilized membranes obviously decreased and the gelatin immobilized membranes showed an obvious suppression on platelets adhesion. These results revealed that the hemocompatibility of the PANCMA membranes was improved by immobilizing the biomacromolecules on the membrane surface. The anti-fouling property of the PANCMA membrane was also ameliorated by gelatin immobilization as the results showed in Table 5.6. With the increase of maleic acid content in the PANCMA, the fluxes of pure water and BSA solution increased both for the original and the gelatin immobilized membranes. At the same time, all the gelatin-immobilized membranes had a higher flux (both for pure water and BSA solution) than the corresponding PANCMA membranes. All these results demonstrated that gelatin immobilization was an effective way of improving the performances and expanding the application fields of membranes.

5.3.2 Antibodies (IgGs)

Castilho et al. (2000) coated nylon microfiltration membranes with dextran and polyvinylalcohol (PVA). Then protein A was immobilized on the coated membranes. The immobilized protein A served as binding sites for human IgG. These membranes may be useful for immunesensors.

Ahmed et al. (2006) immobilized anti-bovine serum albumin IgG (anti-BSA) and anti-green fluorescent protein IgG (anti-GFP) onto track-etched polycarbonate (PC) membranes and used these membranes to specifically capture BSA and GFP. Firstly, they coated an amine-functional polymer
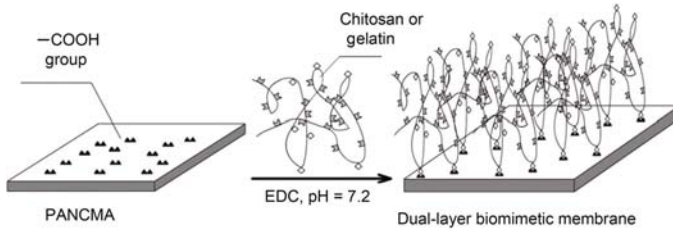
Fig. 5.16. Schematic diagram showing the immobilization of gelatin on the PAN-CAM membrane. Reprinted from (Dai et al., 2005). Copyright (2005), with permission from Elsevier
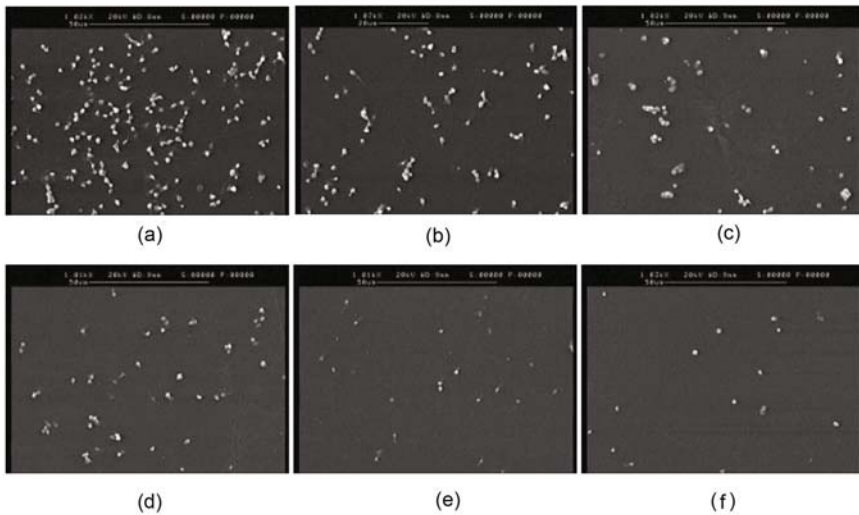

Fig. 5.17. SEM images for the adhesion of blood platelets on the original PANCMA and the gelatin immobilized PANCMA membranes. (a) PANCMA04; (b) PANCMA07; (c) PANCMA11; (d) PANCMA04-gelatin; (e) PANCMA07-gelatin; (f) PANCMA11-gelatin. Reprinted from (Dai et al., 2005). Copyright (2005), with permission from Elsevier

Table 5.6. Filtration performances original PANCMA and the gelatin immobilized PANCMA membranes. Reprinted from (Dai et al., 2005). Copyright (2005), with permission from Elsevier

Membrane	J_{w0} (L/(m^2·h))	J_p (L/(m^2·h))
PANCMA04	385.5 ± 16.5	217.5 ± 11.5
PANCMA07	423.4 ± 26.8	320.2 ± 15.6
PANCMA11	472.6 ± 32.3	397.6 ± 15.7
PANCMA04-gelatin	419.9 ± 21.8	312.8 ± 18.3
PANCMA07-gelatin	450.6 ± 13.5	423.2 ± 22.7
PANCMA11-gelatin	491.9 ± 15.6	450.6 ± 26.0

layer (polyallylamine) on the PC membrane surface and immobilized protein A by the tyrosinase-catalyzed reaction to the amine groups. Then, binding of the antibody to the protein A was carried out. Compared with the conventional method (immobilized through amine-glutaraldehyde chemistry), the tyrosinase-catalyzed immobilization of protein A showed a highly oriented arrangement (Fig.5.18) and the subsequently immobilized antibodies exhibited a much higher specificity for capturing BSA and GFP.
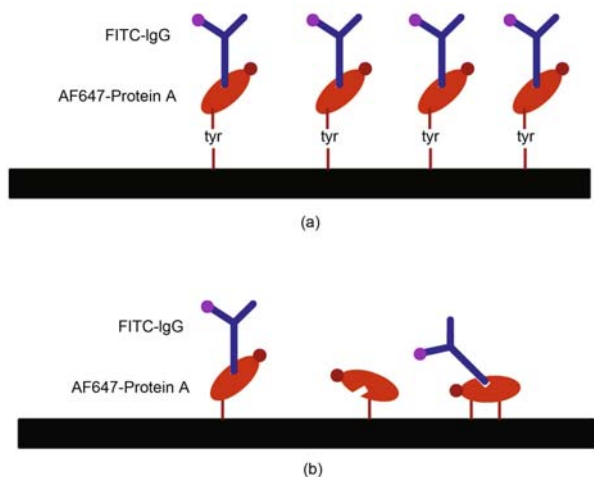

Fig. 5.18. Schematic depiction of antibody attached to an affinity membrane based on (a) favorably oriented protein A immobilized via tyrosinase-catalyzed reaction and (b) randomly oriented protein A immobilized via glutaraldehyde reaction. Reprinted from (Ahmed et al., 2006). Copyright (2006), with permission from Elsevier.

5.3.3 DNAs

DNA also has a biomembrane-like structure, and might be useful for improving the blood compatibility when used as the modification material.

Zhao and Brittain (2000) developed a method of immobilizing the single-strand DNA on the PSf membrane surface. They immersed the PSf membrane in DNA solutions and then dried the membranes at room temperature. Afterwards, UV-irradiation was carried out and the DNA was immobilized. The immobilized DNA was stable in water and in normal saline solution which indicated that this method was an effective way of constructing a DNA tethered PSf membrane surface. With the increase in the concentration of the DNA solution, the amount of immobilized DNA increased. Though the hydrophilicity increased when DNA was immobilized on the membrane (Fig.5.19), the

amount of adsorbed protein was not obviously decreased. However, protein adsorbed on a DNA-immobilized PSf membrane surface showed less conformational change than that on a nascent membrane surface (Fig.5.20), which indicated that the DNA-immobilized membrane might have a better blood compatibility.
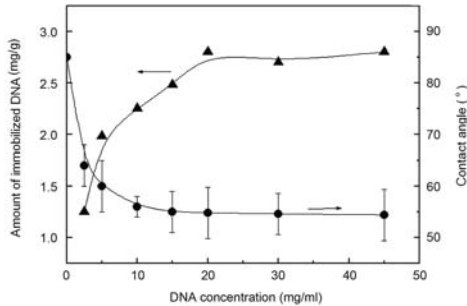

Fig. 5.19. Effect of DNA concentration. (•) contact angle. (▲) amount of immobilized DNA. Reprinted from (Zhao and Brittain, 2000). Copyright (2000), with permission from Elsevier
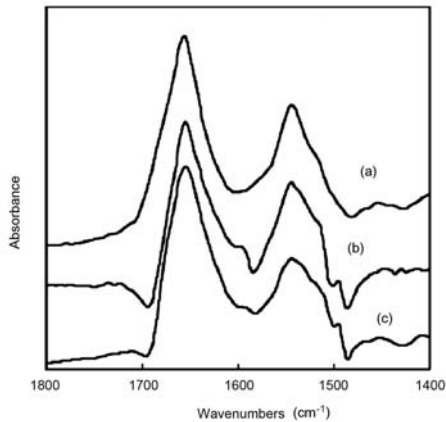
Fig. 5.20. Infrared spectra of the amide I and amide II regions of bovine serum albumin (BSA). (a) Spectra of BSA on ZnSe plate; (b) Spectra of BSA adsorbed on DNA immobilized PSf membrane; (c) Spectra of BSA adsorbed on PSf membrane. Reprinted from (Zhao and Brittain, 2000). Copyright (2000), with permission from Elsevier

The DNA immobilized membrane was also used for the chiral separation. Higuchi's group (Higuchi et al., 2003; Matsuoka et al., 2006) grafted DNA onto the chitosan and cellulose membrane surfaces and performed chiral separation of phenylalanine. These two DNA immobilized membranes showed similar results (Figs.5.21 and 5.22). This indicated that L-phenylalanine was preferentially adsorbed onto the DNA immobilized membrane while D-phenylalanine was left in the solution to permeate through the membrane.
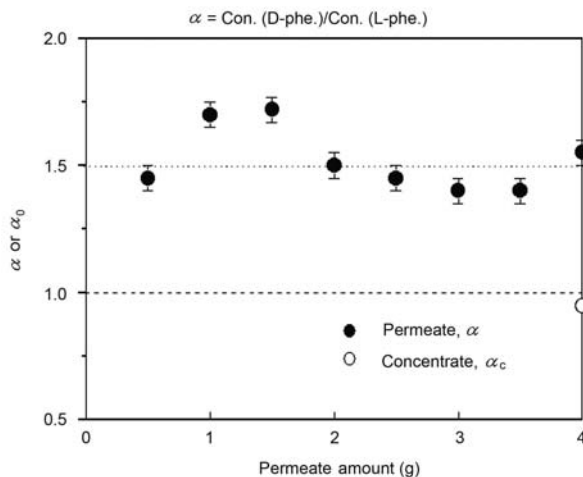
Fig. 5.21. Dependence of the separation factor in the permeate solution through DNA-immobilized chitosan membranes at C_{feed} =6 μM, p = 0.3 MPa, pH 7.0 and 25 °C. The permeate flux was constant during the chiral separation experiment and was (0.005 ± 0.001) m^3/(m^2·d). Data expressed as means$\pm SD$ of four independent measurements. Reprinted from (Matsuoka et al., 2006). Copyright (2006), with permission from Elsevier

5.4 Conclusion

The performance of membranes in many applications relies greatly upon the surface properties. Macromolecules immobilization is an effective way of enhancing the surface properties of membranes. Both synthetic polymers and naturally existing macromolecules can be used as surface modifiers, directly tethered to the membrane surface. Such modifications can be achieved by the reactions between the membrane surface and the macromolecule modifiers. Also, macromolecules can be immobilized with the assistance of outside stimulations such as plasma and UV irradiation. With the surface tethered macromolecules, the biocompatibility and hydrophilicity can be obviously
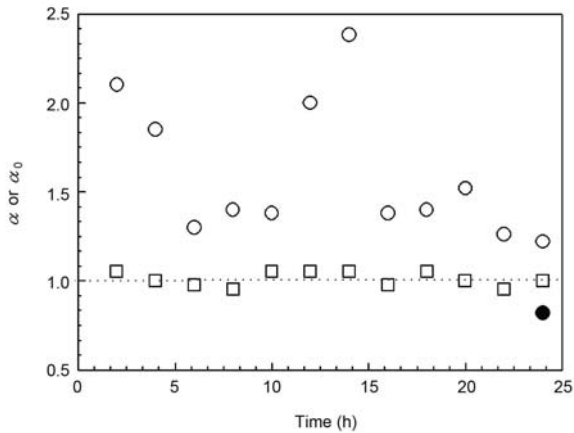
Fig. 5.22. Dependence of separation factors in the permeate (○ and □) and the concentrate (●) solutions during the ultrafiltration of 0.006 mmol/L racemic phenylalanine solution using the DNA immobilized membranes (○ and ●) and the cellulose membranes (□) at pH 7.0 and 25 °C. Reprinted from (Higuchi et al., 2003). Copyright (2003), with permission from Elsevier

improved and the non-specific protein adsorption can be remarkably suppressed. Moreover, affinity membranes can be obtained by immobilization of some bio-functional macromolecules on the surface. Thus, macromolecule immobilization is very useful in the construction of an anti-fouling membrane surface and is a promising method for fabricating membranes in the fields of immunesensors, affinitive capture and chiral separation.

References

Ahmed SR, Lutes AT, Barbari TA (2006) Specific capture of target proteins by oriented antibodies bound to tyrosinase-immobilized protein A on a polyallylamine affinity membrane surface. J Membrane Sci 282:311-321

Allen C, Dos Santos N, Gallagher R, Chiu GNC, Shu Y, Li WM, Johnstone SA, Janoff AS, Mayer LD, Webb MS, et al. (2002) Controlling the physical behavior and biological performance of liposome formulations through use of surface grafted poly(ethylene glycol). Biosci Rep 22:225-250

Avramescu ME, Sager WFC, Wessling M (2003) Functionalised ethylene vinyl alcohol co-polymer (EVAL) membranes for affinity protein separation. J Membrane Sci 216:177-193

Castilho LR, Deckwer WD, Anspach FB (2000) Influence of matrix activation and polymer coating on the purification of human IgG with protein A affinity membranes. J Membrane Sci 172:269-277

Dai ZW, Nie FQ, Xu ZK (2005) Acrylonitrile-based co-polymer membranes containing reactive groups: Fabrication dual-layer biomimetic membranes by the immobilization of biomacromolecules. J Membrane Sci 264:20-26

Elbert DL, Hubbell JA (1996) Surface treatments of polymers for biocompatibility. Annu Rev Mater Sci 26:365-294

Higuchi A, Higuchi Y, Furuta K, Yoon BO, Hara M, Maniwa S, Saitoh M, Sanui K (2003) Chiral separation of phenylalanine by ultrafiltration through immobilized DNA membranes. J Membrane Sci 221:207-218

Jo S, Park K (2000) Surface modification using silanated poly(ethylene glycols). Biomaterials 21:605-616

Kang JS, Kim KY, Lee YM (2003) Preparation of PVP immobilized microporous chlorinated polyvinyl chloride membranes on fabric and their hydraulic permeation behavior. J Membrane Sci 214:311-321

Kjellander R, Florin EJ (1981) Water structure and changes in thermal stability of the system polyethylene oxide-water. J Chem Soc Farad Transac 77:2053-2077

Lee JH, Lee HB, Andrade JD (1995) Blood compatibility of polyethylene oxide surfaces. Prog Polym Sci 20:1043-1079

Lequieu W, Shtanko NI, Du Prez FE (2005) Track etched membranes with thermo-adjustable porosity and separation properties by surface immobilization of poly(N-vinylcaprolactam). J Membrane Sci 256:64-71

Liu TY, Lin WC, Huang LY, Chen SY, Yang MC (2005a) Hemocompatibility and anaphylatoxin formation of protein-immobilizing polyacrylonitrile hemodialysis membrane. Biomaterials 26:1437-1444

Liu ZM, Xu ZK, Wan LS, Wu J, Ulbricht M (2005b) Surface modification of polypropylene microfiltration membranes by the immobilization of poly(N-vinyl-2-pyrrolidone): a facile plasma approach. J Membrane Sci 249:21-31

Lue SJ, Hsu JJ, Chen CH, Chen BC (2007) Thermally on-off switching membranes of poly(N-isopropylacrylamide) immobilized in track-etched polycarbonate films. J Membrane Sci 301:142-150

Matsuoka Y, Kanda N, Lee YM, Higuchi A (2006) Chiral separation of phenylalanine in ultrafiltration through DNA-immobilized chitosan membranes. J Membrane Sci 280:116-123

Nie FQ, Xu ZK, Huang XJ, Ye P, Wu J (2003) Acrylonitrile-based copolymer membranes containing reactive groups: Surface modification by the immobilization of poly(ethylene glycol) for improving antifouling property and biocompatibility. Langmuir 19:9889-9895

Steels BM, Koska J, Haynes CA (2000) Analysis of brush-particle interactions using self-consistent-field theory. J Chromatorg B 743:41-56

Thom V, Jankova K, Ulbricht M, Kops J, Jonsson G (1998) Synthesis of photoreactive alpha-4-azidobenzoyl-omega-methoxypoly(ethylene glycol)s and their end-on photo-grafting onto polysulfone ultrafiltration membranes. Macromol Chem Phys 199:2723-2729

Ulbricht M (2006) Advanced functional polymer membranes. Polymer 47:2217-2262

Ulbricht M, Matuschewski H, Oechel A, Hicke HG (1996) Photo-induced graft polymerization surface modifications for the preparation of hydrophilic and low-protein-adsorbing ultrafiltration membranes. J Membrane Sci 115:31-47

Xu ZK, Nie FQ, Qu C, Wan LS, Wu J, Yao K (2005) Tethering poly(ethylene glycol)s to improve the surface biocompatibility of polyacrylonitrile-co-malele acid asymmetric membranes. Biomaterials 26:589-598

Yu HY, Xu ZK, Xie YJ, Liu ZM, Wang SY (2006) Flux enhancement for polypropylene microporous membrane in a SMBR by the immobilization of poly(N-vinyl-2-pyrrolidone) on the membrane surface. J Membrane Sci 279:148-155

Zhang Q, Wang CR, Babukutty Y, Ohyama T, Kogoma M, Kodama M (2002) Biocompatibility evaluation of PTFE membrane modified with PEG in atmospheric pressure glow discharge. J Biomed Mater Res 60:502-509

Zhao B, Brittain WJ (2000) Polymer brushes: surface-immobilized macromolecules. Prog Polym Sci 25:677-710

6

Membranes with Phospholipid Analogous Surfaces

Since phospholipids, a major component of the outside surface of a biomembrane, were demonstrated to be non-thrombogenic, much attention has been devoted to the use of phospholipid analogous polymers for surface modification in order to improve the biocompatibility of biomaterials with biological systems. In this chapter a variety of approaches for the synthesis of different phospholipid analogous polymers and the surface modification of a polymeric membrane with these phospholipid-containing polymers are briefly described.

6.1 Introduction

Polymeric membranes have been widely used in water treatment, chemical engineering, biochemical product separations, biomedical applications and energy resources. However, most polymeric membranes used nowadays are fabricated from conventional materials such as polypropylene, polyethylene, polysulfone, polyether sulfone, polyacrylonitrile, cellulose acetate, polyvinylchloride, polyvinylidene difluoride. When these polymeric membranes come into contact with proteins or living tissues, the buildup of biofouling on the membrane surface and within the pores will result in performance decline and product loss. Especially when polymeric membranes are used in biomedical and bioengineering applications, such as hemodialysis, the non-biospecific interaction between protein and membrane surface will ultimately result in such events as thrombus formation, inflammation and fibrous encapsulation or bacterial adhesion and infection. There have, therefore, been a number of different methods for modifying polymeric membranes that are necessarily required to come into contact with proteins or tissues, in order to lessen the non-biospecific response (Black, 1992). In recent years, polymers containing phospholipid moieties have received considerable interest in chemical, biological, and medical applications. The fundamental concept is inspired by the mimicry of a cell membrane. It is well known that a cell membrane is mainly composed of various phospholipids and phosphorylcholines. Proteins do not

adsorb irreversibly onto the surface of cells, suggesting that their outer surface is truly biocompatible. Therefore the development of polymeric membranes containing phospholipids, combined with the good mechanical property of a synthetic polymer and the excellent biocompatibility of phospholipids, is one of the most promising methods for fabricating membranes with a biomimetic surface for potential applications in bio-separations and artificial organs.

6.2 Structure and Function of Biomembranes

A biomembrane is a semi-permeable lipid bilayer common to all living cells. It surrounds the cytoplasm of a cell and physically separates the intracellular components from the extracellular environment, thereby serving a function similar to that of skin. A biomembrane plays an important role in all essential biological phenomena, such as maintaining the cell potential, organizing living matter in the cell, creating a fluid two-dimensional matrix, allowing for the controlled transport of solutes, participating in enzyme activity, important in such things as metabolism and immunity, and transporting chemical messages that pass between cells and systems. Most biomembranes in plant and animal cells contain approximately equivalent amounts of lipids and integral membrane proteins which locate in the inside of the biomembrane, the outside, or through-and-through. The famous biomembrane model of Singer and Nicolson (1980) pictures a double layer formed by a lipid matrix and proteins, as depicted in Fig.6.1.

According to the fluid mosaic model of Singer and Nicholson (1980), a biomembrane can be considered as a two-dimensional liquid where all lipid and protein molecules diffuse more or less freely. The bilayer of amphiphilic lipids are spontaneously arranged so that the hydrophobic "tail" regions are shielded from the surrounding polar fluid, causing the more hydrophilic "head" regions to associate with the cytosolic and extracellular faces of the resulting bilayer. The arrangement of hydrophilic and hydrophobic heads of the lipid bilayer prevents hydrophilic solutes from passively diffusing across the band of hydrophobic tail groups, allowing the cell to control the movement of these substances via transmembrane protein complexes such as pores and gates. A biomembrane consists of three classes of amphiphilic lipids: phospholipids, glycolipids and steroids. The relative composition of each depends upon the type of cell, but in the majority of cases phospholipids are the most abundant. It is the lipid bilayer that endows a biomembrane with excellent natural biocompatiblity.

6.3 Biocompatibility of the Phospholipid

With the progress in studies of the biomembrane and the mechanism of thrombus, it was found that a biomembrane is an ideal antithrombotic inter-
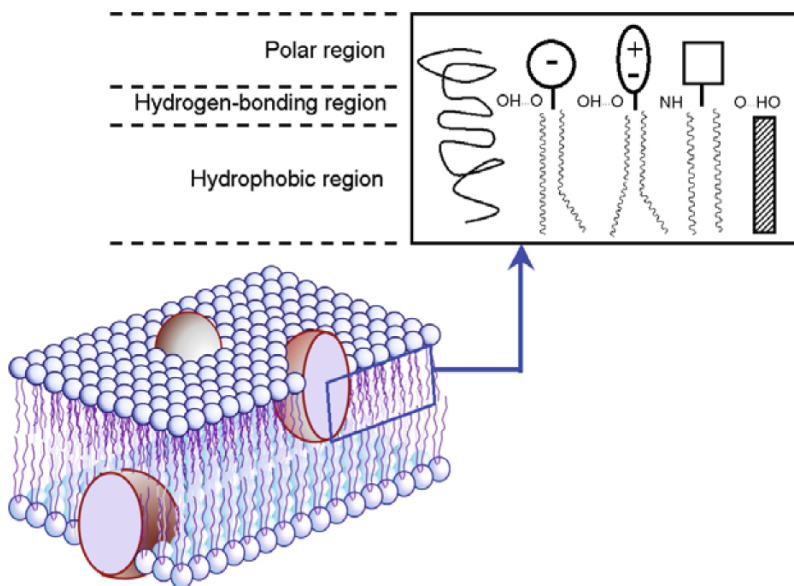
Fig. 6.1. Fluid mosaic model of biomembranes. From (Singer and Nicolson, 1980). Reprinted with permission from AAAS

face. Since the late 1970s lipid-like materials had been widely used to modify surfaces to improve their biocompatibility with biological systems. Yasuzawa et al. (1985b) and Zwaal et al. (1977) found that the phospholipids making up the inside surface of an erythrocye cell membrane were in fact thrombogenic, i.e. would induce coagulation when exposed to blood, while the phospholipids constituting the outside surface were, however, non-thrombogenic. Alone with in-depth studies on biomembranes, it is now known that the lipid bilayer membrane of many cell types has an asymmetric lipid composition in which the inner cytoplasmic surface consists of a larger proportion of negatively charged phospholipids such as phosphatidylserine, while on the outer surface the major component is amphiphilic lipid phosphatidylcholine. The amphiphilic phospholipids possess an equal number of both positively and negatively charged groups within the molecule, thus maintaining overall electrical neutrality. Bird et al. (1988) found that a surface coating of negatively charged phospholipids could induce the intrinsic coagulation pathway leading to clot formation, while that containing amphiphilic phosphatidylcholine was non-thrombogenic.

Based on this knowledge it was thought that the materials and surface containing phosphatidylcholine or structural analogues had potential applications in biomedicine and bioengineering. However, phospholipid membranes are mechanically weak and unstable. It is very difficult to prepare phospholipid bilayers due to their instability. To obtain a stable biomembrane model

and to fabricate biomaterials with biomimetic functions for a variety of practical applications, synthetic phospholipid analogous polymers in particular, and their properties, have been studied extensively during the past three decades.

6.4 Synthesis of Phospholipid Analogous Polymers

In the past three decades, more and more lipid analogous polymers such as polymeric vinyl phosphatidylcholine and phosphatidylethanolamine analogues, polymers with cholesterol moieties and polymeric glycolipid analogues, were synthesized. They could be divided into three types of phospholipid analogous polymers, according to their chemical structure: (1) the side chain type of phospholipid analogous polymers; (2) the main chain type of phospholipid analogous polymers; (3) other phospholipid analogous polymers.

6.4.1 Side Chain Type of Phospholipid Analogous Polymers

6.4.1.1 Phosphate Analogous Polymers

Since 1971 various vinyl phosphate analogous monomers were successfully synthesized by initial approaches (Inaishi et al., 1975; Kimura et al., 1975; 1976). Typical vinyl monomers and polymers bearing phosphate analogues in the side chains are shown in Fig.6.2. These vinyl phosphate analogous monomers can be polymerized in the presence of radical initiator such as AIBN. Some of them can be co-polymerized with other monomers such as acrylonitrile and styrene to obtain the corresponding co-polymers. However, the synthesis and purification of these vinyl phosphate analogous monomers are relatively troublesome, inefficient, non-time-saving, and require uncommon or expensive reagents, or produce the desired products in a low yield. In addition, the corresponding phosphate analogous polymers do not contain the zwitterionic phospholipid head groups and do not possess outstanding biocompatibility. But all of these polymers are valuable precursors in the synthesis of zwitterionic phospholipid analogous polymers.

### 6.4.1.2 Phosphatidylethanolamine Analogous Polymers

Since 1974, a series of valuable zwitterionic phospholipid analogous monomers were successfully synthesized. Among them, phosphatidylethanolamine is the representative one. In 1977, based on the procedure of Billimoria and Lewis (1968), Nakai et al. (1977) further extended and improved this method, and successfully synthesized 2-(methacryloyloxy)ethyl-2-aminoethyl hydrogen phosphate with a high yield of 81% (Fig.6.3(a)). This monomer was
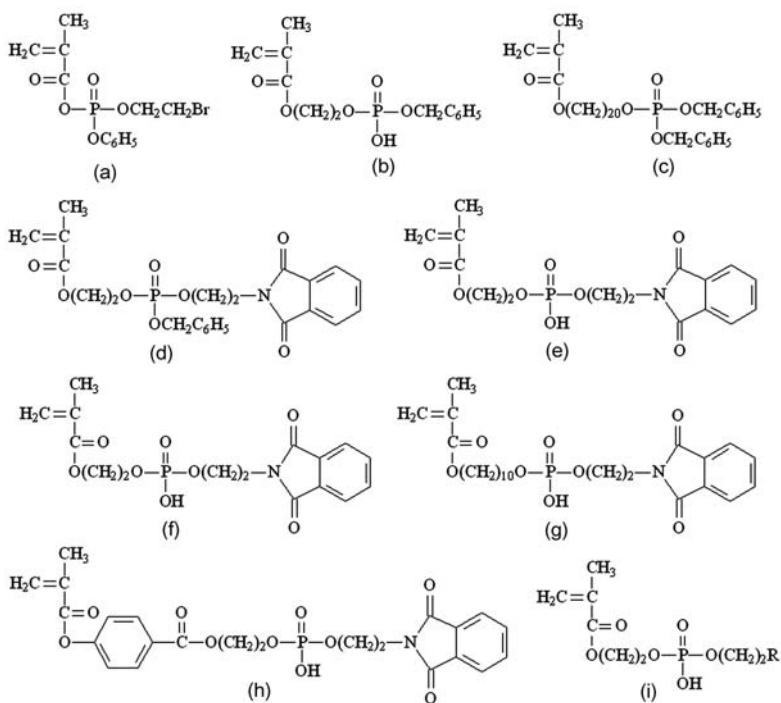
Fig. 6.2. Monomers of phosphate polymer by initial approach. (a) 2-Bromoe-thoxyphenoxyphosphoryl methacrylate; (b) Benzyl 2-(methacryloyloxy)ethyl hy-drogen phosphate; (c) 10-[Bis(benzyloxy)phosphoryloxy]decyl methacrylate (d) Benzyl 2-(methacryloyloxy)ethyl 2′-(phthalimido)ethyl phosphate; (e) 2-(Metha-cryloyloxy)ethyl 2′-(phthalimido)ethyl hydrogen phosphate; (f) Benzyl 2-(p-metha-cryloyloxybenzyloxy)ethyl 2′-(phthalimido)ethyl phosphate; (g) 2-(p-Methacryloy-loxybenzyloxy)ethyl 2′-(phthalimido)ethyl hydrogen phosphate; (h) 2-(Phtha-limido)ethyl 10′-(methacryloyloxy)decyl hydrogen phosphate (i) 2-Chloroethyl 2-(methacryloyloxy)ethyl hydrogen phosphate or 2-bromoethyl 2-(methacry-loyloxy)ethyl hydrogen phosphate

soluble in methanol and polymerized with AIBN as an initiator to give a white polymer. The corresponding polymer is soluble in water, but almost insoluble in methanol, chloroform, and DMF. Subsequently they synthesized another vinyl monomer, 2-aminoethyl 2-(p-methacryloyloxybenzoyloxy)ethyl hydrogen phosphate (Fig.6.3(b)) with the same procedure in 1978 (Nakai et al., 1978). A benzoate group in the corresponding polymer chain in-creased the hydrophobic character to some extent. These two vinyl monomers and their corresponding polymers are early examples of polymeric phos-phatidylethanolamine analogues. The phosphatidylethanolamine analogue

polymer which contains zwitterionic phospholipid head groups could form a zwitterionic species layer under a certain condition.
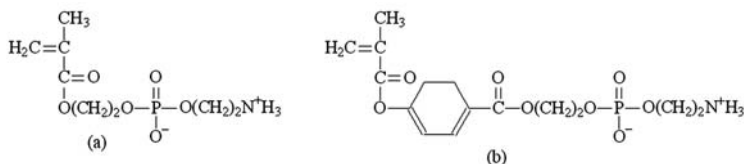
Fig. 6.3. Phosphatidylethanolamine monomers for the synthesis of phospholipid polymers. (a) 2-(Methacryloyloxy)ethyl 2-aminoethyl hydrogen phosphate; (b) 2-Aminoethyl 2-(*p*-methacryloyloxybenzoyloxy)ethyl hydrogen phosphate

6.4.1.3 Phosphatidylcholine Analogous Polymers

A very convenient and useful method for the synthesis of phosphatidylcholine was proposed by Thanh et al. (1974). This method was further extended and improved by Umeda et al. (1982). They successfully obtained the first phosphatidylcholine analogous vinyl monomer, 2-(methacryloyloxy)ethyl-2-(trimethylammonium) ethyl phosphate in 1982. The reaction route to synthesize the phosphatidylcholine analogous vinyl monomer is schematically shown in Fig.6.4.
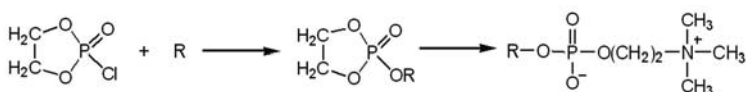
Fig. 6.4. Reaction scheme for the synthesis of phosphatidylcholine analogous vinyl monomer

A common characteristic of phosphatidylcholine analogous vinyl monomers is that they contain a zwitterionic phosphatidylcholine analogous group. Compared with phosphatidylethanolamine, methods for the syntheses of phosphatidylcholine analogous vinyl monomers are convenient and cost-effective. Therefore, various phosphatidylcholine analogous vinyl monomers were completely replaced with phosphatidylethanolamine for preparing phosphlipid analogous polymers in the short term. It was accepted that the successful synthesis of phosphatidylcholine analogous vinyl monomers was a landmark in the development of phospholipid analogous polymers. In fact, using 2-chloro-2-oxo-1,3,2-dioxphospholane (COP) as a starting reagent, three types of phospholipid analogous polymers have been developed to date. They include vinyl monomers and polymers bearing phospholipid analogues in the

side chains, polymers bearing phospholipid analogues in the backbone chains, and others. The reactions route is represented in Fig.6.5 and could be used as a general reaction route to synthesize various phospholipid polymers.
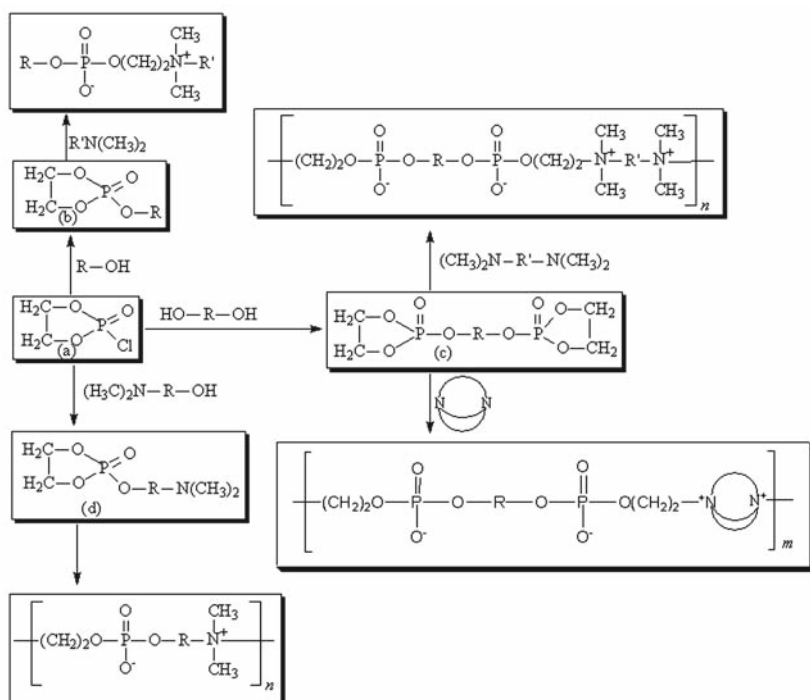
Fig. 6.5. General reaction route to synthesize phospholipid polymers. (a) 2-Chloro-2-oxo-1,3,2-dioxaphospholane; (b) Aliphatic-2-oxo-1,3,2-dioxaphospholane or Aromatic-2-oxo-1,3,2-dioxaphospholane; (c) Bi-aliphatic-2-oxo-1,3,2-dioxaphospholane or Bi-aromatic-2-oxo-1,3,2-dioxaphospholane; (d) Dimethylamino-2-oxo-1,3,2-dioxaphospholane

The general reaction route (Fig.6.5) can be simply summarized as the reaction between COP with aliphatic or aromatic alcohols following the ring-opening reaction with various tertiary amine. For the side chain phosphatidylcholine analogous vinyl monomers, the hydrophobic aliphatic or aromatic chain can be introduced to the molecule in the first reaction stage, while the zwitterionic phosphatidylcholine analogous group was formed in the following reaction stage. By changing the starting alcohols which contain vinyl groups (R contains C=C) or changing ring-opening re-agents which contain vinyl groups (R$'$ contains C=C), various vinyl monomers containing phosphatidylcholine analogues can be obtained and the vinyl group is located in a different structural position.

Using different ring-opening reagents such as trimethylamine (Furukawa et al., 1986; Nakaya et al., 1986; 1994; Seo et al., 1995; Yamada et al., 1995b), 2-dimethylaminoethyl methacrylate or 6-dimethylaminohexyl methacrylate (Yasuzawa et al., 1985a; Zwaal et al., 1977), two types of phospholipid analogous polymers in which the vinyl group is located in a different structural position can be obtained. The two types of phospholipid analogous monomers are shown in Figs.6.6 and 6.7.
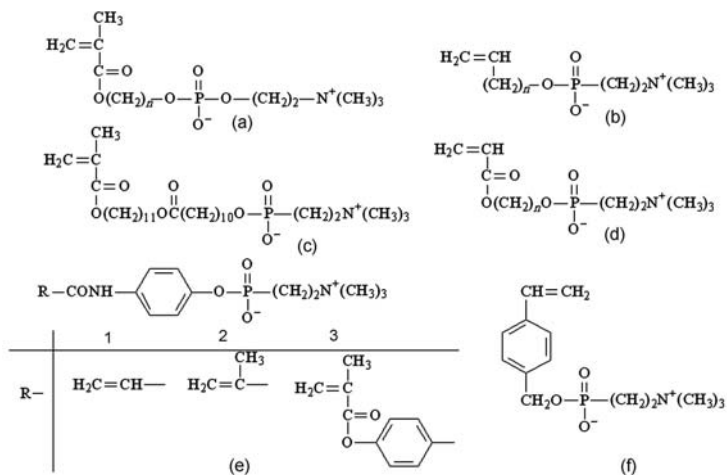
Fig. 6.6. Phosphatidylcholine monomers: trimethylamine as ring-opening reagents. (a) (Methacryloyloxy)ethyl-2-(trimethylammonium)ethyl phosphate; (b) Tricosenyl 2-(trimethylammonium)ethyl phosphate; (c) 10-(11-Methacryloyloxyundecyloxy-carbonyl)decyl 2-(trimethylammonio)ethyl phosphate; (d) (Acryloyloxy)ethyl-2-(trimethylammonium)ethyl phosphate; (e1) p-Acryloylaminophenyl-2-(trim-ethylammonium)ethyl phosphate; (e2) p-Methacryloylaminophenyl-2-(trimethyl-ammonium)ethyl phosphate; (e3) p-Methacryloyloxybenzoylaminophenyl-2-(trim-ethylammonium)ethyl phosphate; (f) p-Vinylbenzyl-2-(trimethylammonium)ethyl phosphate

Using trimethylamine as a ring-opening reagent, a series of phosphatidylcholine analogous vinyl monomers and polymers were synthesized from the reactions of various vinyl aliphatic or aromatic alcohols with COP. Another type of ring-opening reagent, dimethylamine containing a vinyl group such as 2-dimethylaminoethyl methacrylate and 6-dimethylaminohexyl methacrylate, was widely used. Compared with trimethylamine, this kind of ring-opening reagent may produce a different type of vinyl phospholipid monomer whose phosphatidylcholine analogous polar headgroup locates in the middle of the molecule, as well as hydrophobic portions and vinyl groups at both ends. These vinyl monomers were homopolymerized or copolymerized with various polymerizable monomers by radical initiators. The obtained polymers
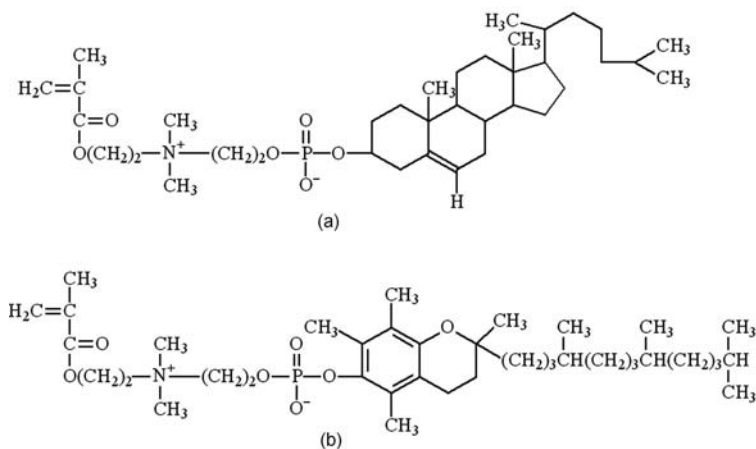
Fig. 6.7. Phosphatidylcholine monomers: 2-dimethylaminoethyl methacrylate or 6-dimethylamino-hexyl methacrylate as ring-opening reagents. (a) 2-[2-(Methacryloyloxy)ethyldimethylammonium]ethyl 5β-cholesten-3-yl phosphate; (b) 2-[2-(Methacryloyloxy)ethyldimethylammonium]ethyl 2R,4′R,8′R-2,5,7,8-tetramethyl-2-(4′,8′,12′-trimethyltridecyl)chroman-6-yl phosphate

showed good mechanical properties, thermal stability and mechanical stability. Some polymers were found to exhibit liquid crystalline behavior and some showed polyelectrolyte behavior.

6.4.1.4 Dipalmitoyl-D,L-α-phosphatidylethanolamine Unit-containing Vinyl Polymers

To develop an improved biomimetic model of natural phospholipid, Nakaya et al. (1990) successfully synthesized a vinyl monomer containing a phosphatidyl ethanolamine unit, dipalmitoyl-D,L-α-phosphatidylethanolmethacylamide in 1990. This monomer could be polymerized by UV and γ-radiation, but not be homopolymerized by radical initiators, and the molecular weight of the obtained polymer was very low. In order to improve the molecular weight of vinyl polymer bearing cephalin units in the side chains, the synthesis and polymerization of 2-(methacryloyloxy)ethyl dipalmitoyl-D,L-α-phosphatidylethanolamide were reported by Nakaya et al. (1989). This monomer could be homopolymerized by radical initiators and the resulting polymer showed liquid crystalline behavior from 35 °C up to 158 °C. The structures of the two vinyl monomers containing dipalmitoyl-D,L-α-phosphatidylethanolamine unit are shown in Fig.6.8.
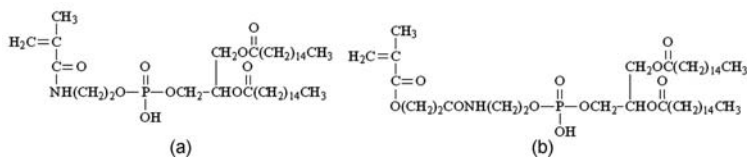
Fig. 6.8. Dipalmitoyl-D,L-α-phosphatidylethanolamine monomers of phospholipid polymers. (a) Dipalmitoyl-D,L-α-phosphatidylethanolmethacylamide; (b) 2-(Methacryloyloxy)ethyl dipalmitoyl-D,L-α-phosphatidylethanolamide

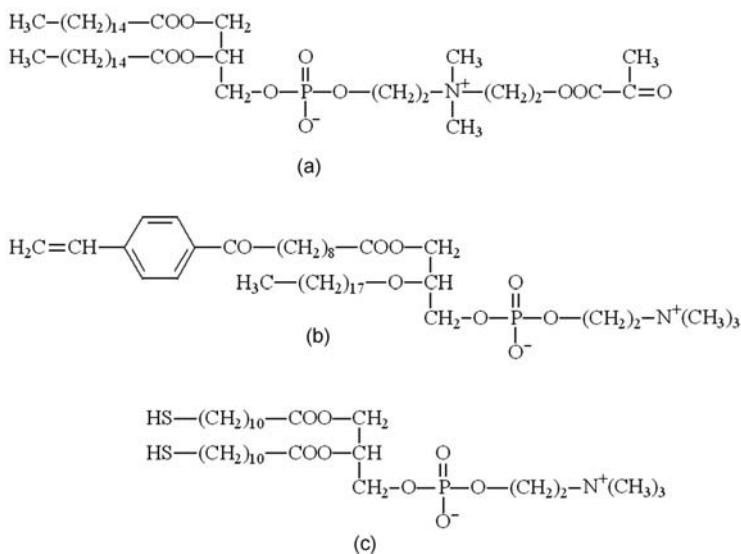## 6.4.1.5 Other Side Chain Types of Phospholipid Analogous Polymers

Besides the four types of side chain phospholipid analogous polymers described above, there are some other analogous systems containing a large number of aliphatic groups which can increase the hydrophobic characteristics (Hasegawa et al., 1984; Kusumi et al., 1983; Regen et al., 1982). These polymerized liposomes are amphiphilic and they contain the highly polar zwitterionic phosphatidylcholine group and hydrophobic alkyl chains, which is in analogy to the natural membrane lipid dipalmitoylphosphatidylcholine (DPPC). The long alkyl chain in the polymerized liposomes can enhance hydrophobic interaction with non-polar polymeric material such as polyethylene to form a more stable film, while having little influence on the biocompatibility of the resulting surface. Fig.6.9 shows other side chain types of phospholipid polymers.

6.4.2 Backbone Chain Types of Phospholipid Analogous Polymers
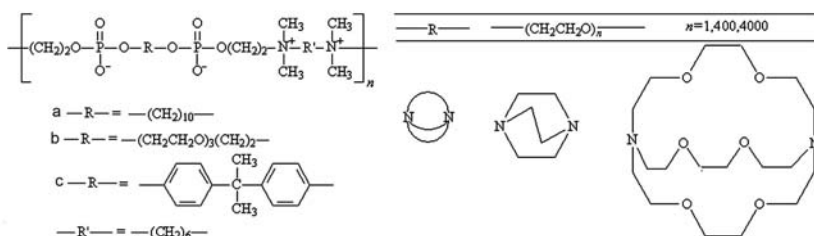
There is considerable interest in the polymers bearing phospholipids in the backbone chains as the structures of these polymers are similar to biological tissues. Several polymers containing a phospholipid in the polymer backbone were synthesized and characterized.

It can be seen from Fig.6.5 that two types of backbone chain phospholipid analogous polymers can be obtained according to the different reaction routes. When COP and diols containing materials were chosen as the starting reagents, intermediates with end-ring groups could be obtained and then reacted with diamine (such as N,N,N',N'-tetramethylhexamethylenediamine and bis(2-dimethylaminoethyl) stearyl-amine) or aza-crown (such as 1,4-diazabicyclo[2.2.2]octane and 4,7,13,16,21,24-hexaoxa-l,10-diazabicyclo[8.8.8] hexacosan) to obtain polymers containing phospholipid analogues in the polymer backbone (Fig.6.10) (Sugiyama et al., 1986; Umeda et al., 1985; Yamada et al., 1995a). These polymers are hygroscopic and soluble in water.

When aliphatic or aromatic hydroxyldimethylamine (such as 2-(dimethylamino) ethanol, 11-(dimethylamino)decanol, and p-[(dimethylamino)ethan-

H₃C–(CH₂)₁₄—COO—CH₂

H₃C–(CH₂)₁₄—COO—CH

CH₂-O-P-O—(CH₂)₂-N⁺-(CH₂)₂-OOC-C=O

(a)

H₂C=CH— —CO—(CH₂)₈—COO—CH₂

H₃C—(CH₂)₁₇—O—CH

CH₂-O-P-O—(CH₂)₂-N⁺(CH₃)₃

(b)

HS—(CH₂)₁₀—COO—CH₂

HS—(CH₂)₁₀—COO—CH

CH₂-O-P-O—(CH₂)₂-N⁺(CH₃)₃

(c)

Fig. 6.9. Other phospholipid monomers. (a) 1,2-Dipalmitoyl[N-2-(methacruloyloxy)ethyl]-D,L-α-phosphatidylcholine; (b) 1-[9-(p-Vinylbenzoyl)nonanoyl]-2-O-octadecyl-rac-glycero-3-phosphocholine; (c) 1,2-Bis(11-mercaptoundecanoyl)-sn-glycero-3-phosphocholine

—(CH₂)₂O-P-O-R-O-P-O(CH₂)₂-N⁺-R'-N⁺—

—R— —(CH₂CH₂O)ₙ— n=1,400,4000

a —R— = —(CH₂)₁₀—
b —R— = —(CH₂CH₂O)₃(CH₂)₂—
c —R— =
—R'— = —(CH₂)₆—

Fig. 6.10. Polymers bearing phospholipid analogues in backbone chains

amido] phenol) were used to react with COP, their subsequent polymerization was carried out by heating in DMF to give the corresponding poly(phosphatidylcholine) analogues (Nakaya et al., 1989). These polymers are hygroscopic and soluble in water and methanol but almost insoluble in acetone, diethyl ether, and benzene. Fig.6.11 shows that some polymers bear phospholipid analogues in the backbone chains. Compared with side chain types of phospholipid analogous polymers, polymers bearing phospholipid analogues in backbone chains were synthesized by thermal ring-opening polymerization without adding any initiator, which is of benefit for the application of these types of polymers in biomedicine.
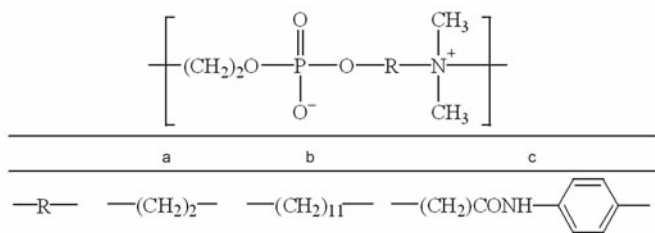
Fig. 6.11. Polymers bearing phospholipid analogues in backbone chains, without adding ring-opening reagent (thermal polymerization)

6.4.3 Other Phospholipid Analogous Polymers

It is well known that the cell membrane is mainly composed of various lipids and proteins which are composed of polypeptide chains. A polypeptide containing phospholipid analogues in the side chains, copoly(g-20-[2-(trimethylammonium)ethyl phosphatidyl]eicosyl L-glutamate, g-methyl L-glutamate) (Fig.6.12(a)) was successfully synthesized in 1988 (Nakaya et al., 1988). Organopolysiloxanes bearing phospholipid side chains were reported in 1995 (Araki et al., 1984). The structure of this polymer is shown in Fig.6.12.
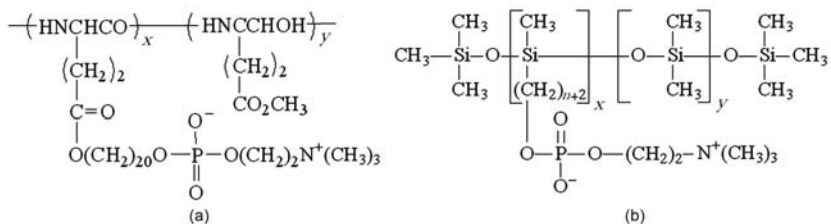
Fig. 6.12. Other phospholipid analogues polymers. (a) Polypeptide bearing phospholipid side chains; (b) Organopolysiloxanes bearing phospholipid side chains

Up to now, there are abundant phospholipid analogous polymers with very useful properties that together have appeared. The properties of these polymers are intimately related to their structure and components.

6.5 Surface Modification of Polymeric Membrane with Phospholipid

Since the zwitterionic phospholipid was demonstrated to be biocompatible and nonthrombogenic, many approaches have been developed for membrane surface modification with a phospholipid, which includes surface adsorption

and coating (Araki et al., 1984; Luo et al., 2001; Michel et al., 2004; Naumann et al., 2002), blending (Ishihara et al., 1999a; 1999b), graft polymerization (Akhtar et al., 1995; Ishihara et al., 2000; Iwasaki et al., 1998; Sugiyama et al., 1998), *in situ* polymerization (Regen et al., 1983) and chemical reaction (Dai et al., 2004; Huang et al., 2005; Nakaya et al., 1988).

6.5.1 Surface Adsorption and Coating

Generally, methods for surface modification can be divided into two classes: physical and chemical. Surface adsorption and coating is a physical modification method. The surface modification is achieved by adsorption or by coating suitable materials on the polymeric membrane surface directly. The key advantage of this technique is that the surface of the polymeric membrane can be simply modified or tailored to acquire very distinctive properties through the choice of different coating materials, while maintaining the substrate properties.

Araki et al. (1984) prepared egg-yolk phosphatidylcholine (EPC) filled or dipalmitoyl phosphatidylcholine (DPPC) filled membrane by immersing a porous cellulose nitrate membrane in the solution of EPC or DPPC in chloroform. It was found that the permeabilities of oxygen, nitrogen, and carbon dioxide through the liposomes-filled membrane were improved, which was ascribed to the higher mobility of the alkyl chain.

Elliott et al. (2003) successfully constructed a phospholipid monolayer on a hydrophobic polystyrene (PS) film by spontaneous vesicle rearrangement, which takes advantage of the self-assembling nature of lipid membranes (Fig.6.13). The long alkyl chain in the phospholipid can enhance the hydrophobic interaction with the hydrophobic polymeric membrane to form a stable film.
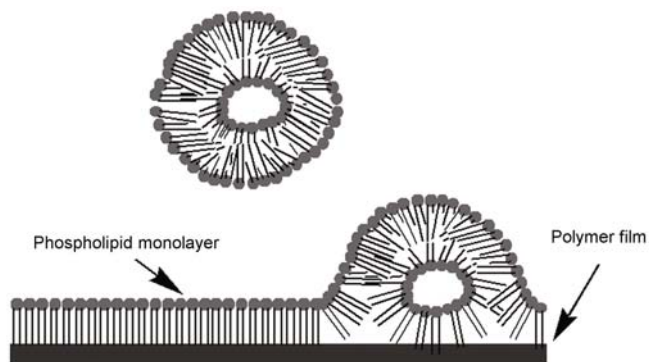
Fig. 6.13. Supporting a phospholipid monolayer on PS films. Reprinted with permission from (Elliott et al., 2003). Copyright (2003), American Chemical Society

Ito et al. (2003) synthesized cationic and anionic 2-methacryloyloxyethyl phosphorylcholine (MPC) copolymers by copolymerization of MPC and *n*-butyl methacrylate (BMA) with 3-(methacryloyloxypropyl)-trimethyl ammonium iodide (MAPTMAI) as the cationic unit or potassium 3-methacryloyloxypropyl sulfonate (PMPS) as the anionic unit, respectively. The polymeric membrane surface with a polyion complex containing phosphorylcholine could be prepared by immersing a poly(ethylene terephthalate) membrane in the anionic and cationic polymer solutions alternately (Fig.6.14). The simplest layer-by-layer deposition for mimicking a biomembrane on a hydrophobic polymeric membrane surface was with a solid-supported, single phospholipid bilayer. The stable polyion complex multi-layer containing phosphorylcholine enabled the polymeric membrane surface to show thermodynamic properties.
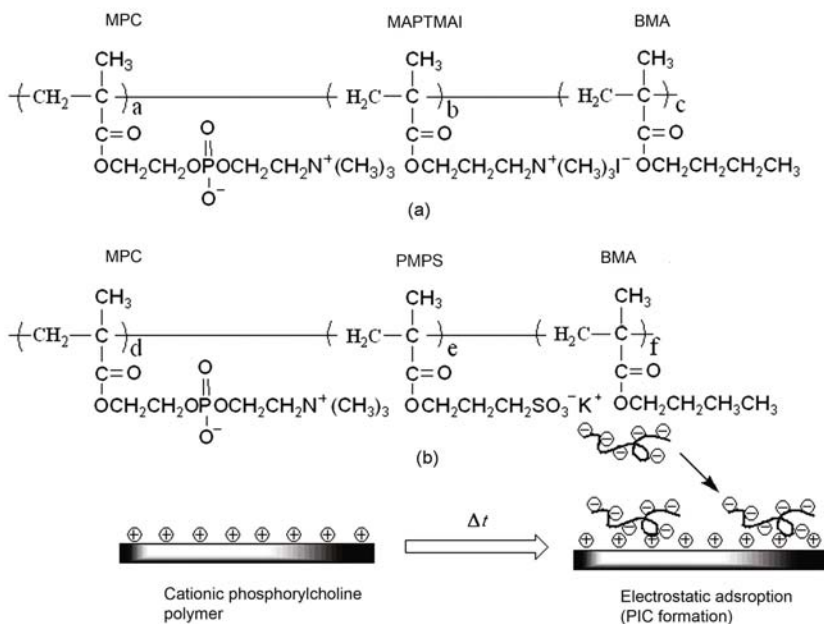
Fig. 6.14. Schematic representation of an electrically controlled polymer surface. (a) PMMB; (b) PMPB. Reprinted from (Ito et al., 2003). Copyright (2003), with permission from Elsevier

Yajima et al. (2002) used the biocompatible copolymers of poly(methacryloyloxy-ethyl phosphorylcholine-*co-n*-butyl methacrylate) and poly(methacryloyloxy-ethyl phosphoryl-choline-*co*-2-ethylhexyl methacrylate) for coating poly(vinyl chloride) (PVC) membranes. The PVC membranes were immersed in different concentration ethanol solutions of MPC copolymer and then air-

dried. The phospholipid analogues polymer layer thus formed could improve the biocompatibility of the PVC membrane and last more than one month. To prepare a blood compatible gas-permeable membrane, Iwasaki et al. (2002) used the copolymers of MPC and dodecyl methacrylate (DMA) as coating materials for a polyethylene (PE) porous membrane. The preparation procedure for a phospholipid polymer skin film adhered to a PE porous membrane is shown in Fig.6.15.
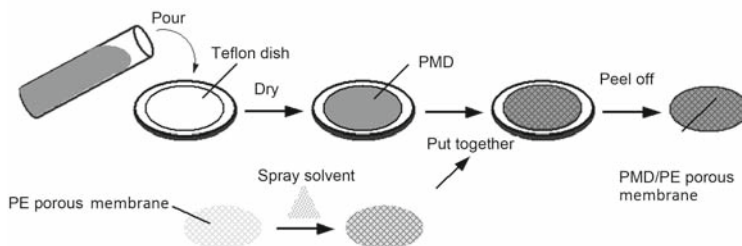
Fig. 6.15. Schematic procedure for the preparation of the PMD/PE porous membrane. Reprinted from (Iwasaki et al., 2002). Copyright (2002), with permission from Elsevier

The poly(MPC-*co*-DMA) (PMD) skin film was quite stable on the PE porous membrane and did not detach from the PE porous membrane even after being soaked in water for more than 6 months. This was attributed to physical anchoring and the affinity of the long alkyl chain of the DMA unit to the hydrophobic PE surface. The PE membrane with the adhered PMD showed an excellent gas-permeability and blood compatibility.

6.5.2 Physical Blending

Blending of blood-compatible polymers such as phospholipid analogous polymers with conventional polymers was an effective method for fabricating a composite polymeric membrane with excellent biocompatibility. Cellulose acetate (CA), which possesses excellent membrane forming properties and good thermal and mechanical stability, had been successfully applied as membrane material in the fields of water treatment, biochemical product purification, and bioseparation systems. But CA could induce serious thrombus formation when the membranes came into contact with blood. To improve the blood compatibility of CA membranes, Ye et al. (2002) blended the copolymers of poly(MPC-*co*-BMA) with cellulose acetate to fabricate an asymmetric and porous structure membrane. CA and poly(MPC-*co*-BMA) were dissolved in solvents such as *N*,*N*-dimethylformamide, acetone, and 2-propanol, respectively. Then the two prepared solutions were mixed together in a given blended composition. The blended solution was spread on a glass plate and

subsequently immersed in a coagulation bath to obtain a blend membrane containing phospholipid analogous polymer. The morphological structure, mechanical properties, and solute permeability of the blend membrane could be conveniently controlled by changing the preparation conditions such as the composition of the solvents and the solvent evaporation time. The blend membranes thus obtained showed solute permeability and excellent protein adsorption resistance compared to the original one because the CA membranes were improved in pore size, porosity, and hydrophilicity on the entire membrane by the addition of the poly(MPC-*co*-BMA) hydrophilic polymer.

Ishihara et al. (2004) used poly(2-methacryloyloxyethyl phosphorylcholine) (PMPC) as the blending material to improve the surface properties of hydrophobic PE membrane. As shown in Fig.6.16, the PE/PMPC blend membrane could be obtained by a combination of solution mixing and solvent evaporation methods using xylene and *n*-butanol mixture as a solvent. In the PE/PMPC blend membrane, the PMPC domains were located not only inside the membrane but also at the surface. The phospholipid polar groups covering the surface could endow the PE/PMPC blend membrane with excellent platelet adhesion resistance.
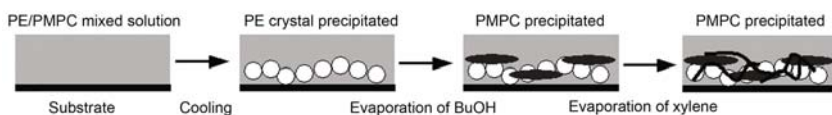
Fig. 6.16. Schematic procedure for preparation of the PE/PMPC membrane. Reprinted from (Ishihara et al., 2004). Copyright (2004), with permission from Elsevier

Other blend polymeric membranes composed of conventional polymers and biocompatible phospholipid analogous polymers were prepared by a similar method, and they were summarized in Table 6.1. It was found that all of the blend polymeric membranes had sufficient hemocompatibility and cytocompatibility.

6.5.3 Surface Grafting Polymerization

Surface graft polymerization is a chemical modification method to modify or tailor a polymeric membrane surface with distinctive properties, while maintaining the substrate properties. Compared with the physically coated and blended ones, the covalent attachment of grafted phospholipid analogous chains onto a polymeric membrane surface can avoid their desorption and maintain a long-term chemical stability. Several surface grafting methods were reported for incorporating phospholipid analogous chains onto the polymeric membrane surface, which include photo-induced grafting, initiator

Table 6.1. Preparation of blend polymers containing phospholipid polymers

| Polymeric materials	Phospholipid monomers	Phospholipid polymers	References
Poly(etherurethane) (PU)	PMPC	(2-methacryloyloxyethyl phosphorylcholine) (MPC)	(Yoneyama et al., 1998; Sawada et al., 2006)
Polysulfone (PSF)	Poly(MPC-*co*-BMA), Poly(MPC-*co*-DMA), Poly(MPC-*co*-MEBU)	*n*-butyl methacrylate (BMA), dodecyl methacrylate (DMA), (2-methacryloyloxyethyl butylurethane (MEBU)	(Ishihara et al., 1999c; 1999d; Ueda et al., 2006)
Poly(*L*-lactide-*co*-glycolide) (PLGA)	Poly(MPC-*co*-MEH)	ethylhexylmethacrylate (EHMA)	(Khang et al., 2001)
Poly(vinyl alcohol) (PVA)	PMPC	(2-methacryloyloxyethyl phosphorylcholine) (MPC)	(Shindo et al., 2003; 2004)
Cellulose acetate (CA)	Poly(MPC-*co*-BMA)	*n*-butyl methacrylate (BMA)	(Ye et al., 2003; 2004)
Polyethylene (PE)	PMPC	(2-methacryloyloxyethyl phosphorylcholine) (MPC)	(Ishihara et al., 2004)
Polyethersulfone (PES)	–	Soybean phosphatidylcholine (SPC)	(Wang et al., 2005)

grafting, corona irradiation grafting and atom transfer radical polymerization (ATRP).

6.5.3.1 Photo-induced Grafting Polymerization

Photo-induced graft polymerization is expected to be a convenient method. It ensures that the grafting chains restrictively locate onto the membrane surface without affecting any bulk properties because of the lower energy source. Ishihara et al. (2000) applied this technique to prepare a PE membrane grafted with PMPC (PMPC-*g*-PE membrane). In order to create reactive sites on the PE membrane surface that can generate further grafting processes, the membrane was immersed in an acetone solution containing benzophenone and then dried under dark conditions. The PE membrane coated with benzophenone was placed in a glass tube containing an MPC solution and the photo-induced polymerization on the PE surface was carried out using an ultra-high pressure mercury lamp. The surface density of the PMPC chain and the grafting layer on the PE membrane could be controlled by changing the preparation conditions such as the concentration of benzophenone and MPC solution, and also photo irradiation time. It was found that the water contact angle and the number of platelets adhered to and activated

on the PE membrane grafted with PMPC decreased with an increase in the amount of PMPC grafted on the membrane surface.

van der Heiden et al. synthesized two compounds containing phospholipid, 1-O-(2-(trimethylammonium) ethylphosphoryl)-triethylene glycol 4-azidobenzoate and 1-O-(2-(trimethylammonium)ethylphosphoryl)-hexanediol 4-azidobenzo- ate, which consist of a photoactivatable 4-azidobenzoyl group, a short spacer chain, and a phosphorylcholine end group (van der Heiden and Koole, 1996; van der Heiden et al., 1997; 1998). Upon UV irradiation, the photoactive 4-azidobenzoyl group could be turned into reactive intermediates that can form covalent bonds with a polymer surface (Fig.6.17). In this way, compounds with phosphorylcholine as end group could be covalently immobilized onto the poly(ether urethane) (PEU) membrane surface under UV irradiation. The modified PEU membrane surfaces showed a decreased underwater contact angle and they suppressed protein adsorption effectively.
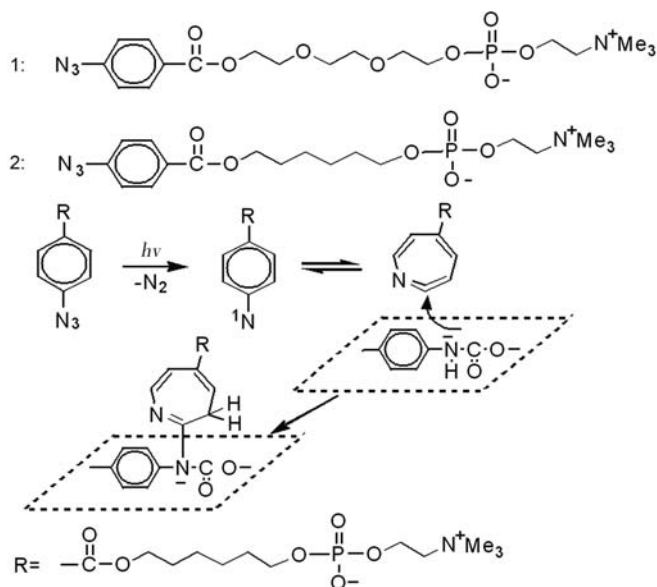
Fig. 6.17. Phosphorylcholine groups are covalently immobilized on the polymer surface by UV irradiation. 1: 1-O-(2-(trimethylammonium)ethyl-phosphoryl)triethylene glycol 4-azidobenzoate; 2: 1-O-(2-(trimethylammonium)-ethylphosphoryl)-hexanediol 4-azidobenzoate. Reprinted with permission from (van der Heiden and Koole, 1996). Copyright (1996), American Chemical Society

6.5.3.2 Initiator Grafting Polymerization

The substrate surface could also be activated by treatment with a chemical reagent and this then generated further grafting polymerization. Korematsu et al. (2002) grafted MPC monomer onto segmented polyurethane (PU) cast film surface. The soft segment of PU was hydroxylated poly(isoprene) diol (HPIP) and the hard segments were 4,4'-methylenediphenyl diisocyanate (MDI) and 1,4-butanediol (BD) as a chain extender. The PU was hydroxylated by potassium peroxodisulfate and MPC was grafted on the surface of hydroxylated using di-ammonium cerium (IV) nitrate (ceric ammonium nitrate, CAN) as a radical initiator (Fig.6.18). The PU membrane modified with PMPC effectively reduced protein adsorption, platelet adhesion, and complemented activation.
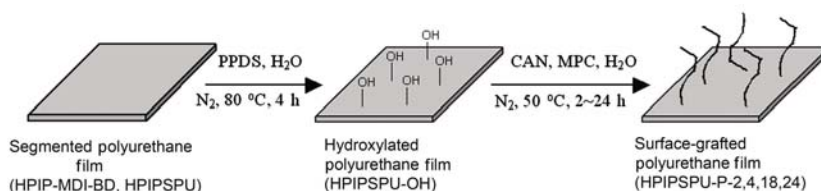
Fig. 6.18. Synthesis scheme for hydroxylated and MPC-grafted PU. Reprinted from (Korematsu et al., 2002). Copyright (2002), with permission from Elsevier

6.5.3.3 Corona Irradiation Grafting Polymerization

As it was mentioned above, graft polymerization can be performed by several methods such as by uv irradiation, by chemical reagent, by plasma treatment, and by corona irradiation, etc. Among them, the corona-discharge treatment is very convenient because this treatment can be performed in the presence of air without a specific chemical reagent. It can produce peroxides on the polymeric membrane surface with corona irradiation and subsequently induce a further grafting process. Iwasaki et al. (1998; 1999) prepared a phospholipid gradient on the PE membrane surface using corona irradiation. To create reactive sites on the PE membrane surface, an additive-free low-density PE sheet membrane was treated with a radio frequency corona-discharge apparatus. A schematic diagram showing the corona-discharge apparatus for the preparation of the PE membrane with phospholipid gradient is shown in Fig.6.19.

The peroxide was produced by corona-discharge treatment, and this peroxide worked as an initiator for graft polymerization. The corona-irradiated PE membrane was subsequently immersed in the ω-methacryloyloxyalkyl phosphorylcholine (MAPC, Fig.6.20) ethanol solutions. MAPC was then

Fig. 6.19. Schematic representation of the corona irradiation apparatus. Reprinted from (Iwasaki et al., 1999). Copyright (1999), with permission from Elsevier

grafted onto the PE sheet membrane. The surface density of poly(MAPC) could be controlled by the energy of the corona and was increased with an increase in the amount of peroxide produced by the corona irradiation. The PE membrane modified with poly(MAPC) effectively reduced protein adsorption, platelet adhesion, and complement activation.

Fig. 6.20. Chemical structure of MAPC

6.5.3.4 ATRP grafting polymerization

ATRP is particularly useful due to its versatility of monomer types, tolerance of impurities, and mild reaction conditions. Recently, Feng et al. (2004) combined an initiator self-assembling monolayer and ATRP techniques to graft MPC from a substrate surface at room temperature. Oligomeric methoxy polyethylene glycol 2-bromoisobutyrate (OEGBr) was used as the initiator and Cu(I)Br/2,2′-bipyridine (bpy) as the catalyst. The procedure of surface-initiated ATRP grafting polymerization is shown in Fig.6.21. The thickness

of the PMPC layer on the substrate surface could be controlled by adding a free initiator or adding an excess deactivator to the polymerization system. Furthermore, a block polymeric brush could be grown on the substrate surface due to the living characteristics of the system, allowing an extension of the grafted PMPC chains with a second block of another monomer.
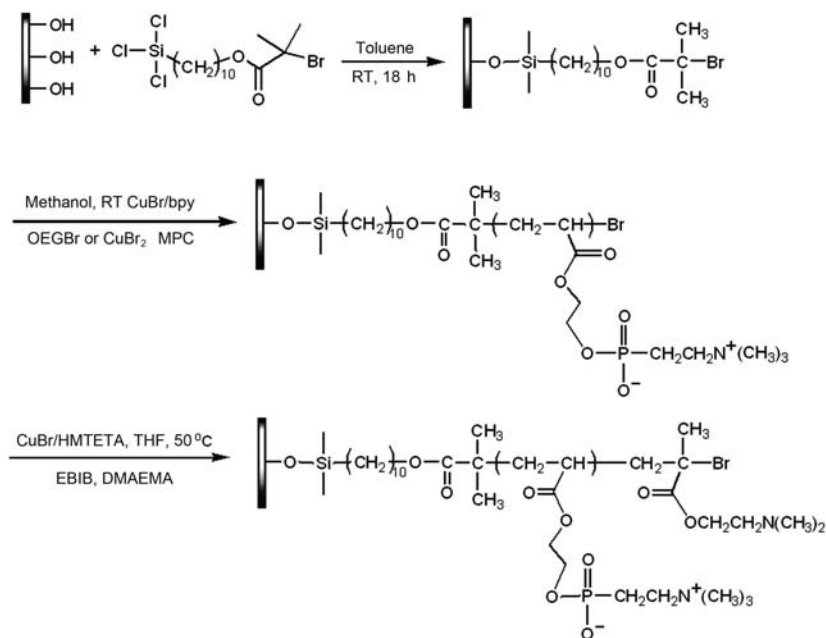

Fig. 6.21. Surface-initiated ATRP grafting polymerization

6.5.4 *In-situ* Polymerization

It is well known that a phospholipid analogous monomer is composed of a hydrophilic head group, a hydrophobic segment, and one or more polymerizable groups. When it was dispersed in an aqueous and insoluble polymer membrane two-phase mixture, a phospholipid layer was adsorbed at aqueous-insoluble polymer membrane phase boundaries. Subsequent polymerization secured the phospholipid layer to the polymer membrane surface through extended hydrophobic interactions, or through covalent linking to alkyl radicals generated on the original surface, and/or by virtue of the insolubility of the newly formed crosslinked network.

To fabricate a stable substrate-supported phospholipid biomimetic layer with the flexible assembly of structurally diverse film constituents, Regen et

al. (1983) synthesized two phospholipid monomers with two or more poly-merizable groups and immersed the PE membrane in the vesicle disper-sion of these phospholipid monomers. The phospholipid monolayer could be adsorbed on the hydrophobic PE surface and the number of phospholipid molecules depended on the concentration used in the aqueous dispersion. The phospholipid layer was polymerized by a heat-initiated free-radical process and formed an insoluble crosslinked network on the PE membrane surface, as shown in Fig.6.22. Phosphatidylcholine modified PE was hydrophilic and the water contact angle was decreased from 100° on the unmodified PE to 35° on the modified one.
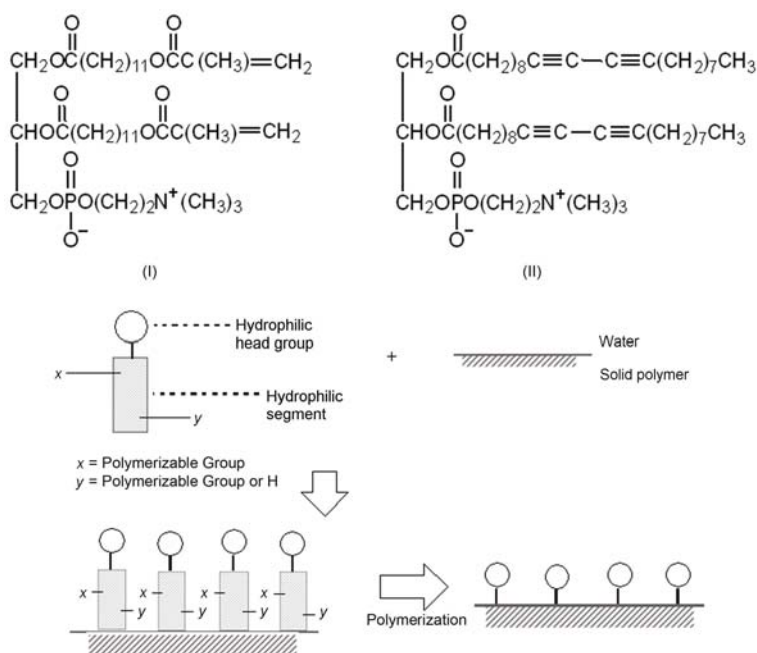
Fig. 6.22. *In situ* polymerization. (I) Bis[l2-(methacryloyloxy)dodecanoyl]-*L*-α-phosphatidylcholine; (II) Diacetylenic phosphatidylcholine. Reprinted with permis-sion from (Regen et al., 1983). Copyright (1983), American Chemical Society

By a similar method, Marra et al. (1997) and Orban et al. (2000) also successfully fabricated a stable substrate-supported phospholipid layer by an *in situ* photo-polymerization instead of by a thermally initiated *in situ* polymerization. As shown in Fig.6.23, a self-assembly of acrylate function-alized phospholipids was prepared on an alkylated support by vesicle fusion and subsequently polymerized by irradiation with visible light, using eosin Y/triethanolamine as a photo-initiating species. It was found that the stabil-

ity of the photo-polymerized flexible films was superior to that observed for polymeric monolayers produced by a thermally initiated free-radical process.
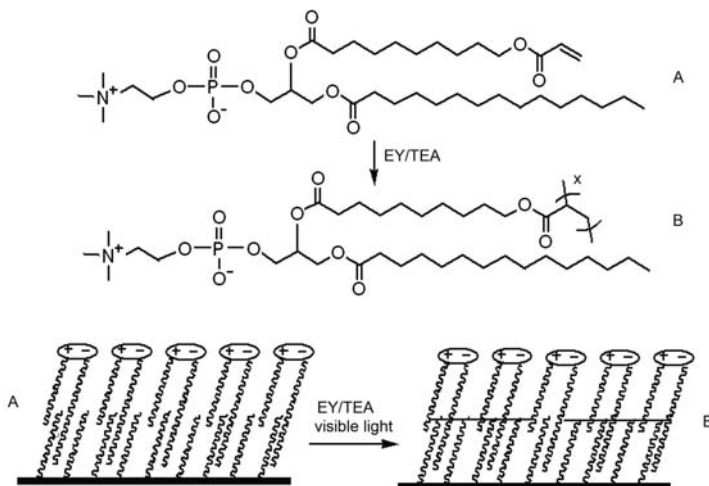

Fig. 6.23. Photo-polymerized phospholipid surface. A: 1-Palmitoyl-2-[12-(acryloyloxy)dodeca-noyl]-*sn*-glycero-3-phosphocholine; B: Polymerized PC monolayer. Reprinted with permission from (Marra et al., 1997; Orban et al., 2000). Copyright (2000), American Chemical Society

To improve the blood compatibility of elastic segmented polyurethanes (SPU), Morimoto et al. (2002) used MPC to modified SPU film by forming a semi-interpenetrating polymer network (semi-IPN). 2-Ethylhexyl methacrylate (EHMA) and triethyleneglycol dimethacrylate (TEGDMA) were used as comonomer and crosslinked reagent. The SPU film was immersed in a solution containing MPC, EHMA and TEGDMA and then polymerized by visible light irradiation. Iwasaki et al. (2003) also prepared semi-IPNs based on a crosslinked MPC-containing copolymer and SPU membrane to improve the mechanical properties of the MPC copolymer gel while maintaining the diffusive release and non-biofouling properties.

### 6.5.5 Surface Chemical Treatment

Chemical treatment is one of the familiar methods for covalently binding phosphorylcholine to the surface and the modified surface is relatively stable because the phospholipid moieties are connected to the substrate by covalent bonding. Lu et al. (2001) proposed the attachment of phosphorylcholine molecular layers onto a silicon oxide surface by chemically anchoring an organic monolayer bearing terminal groups. They described the syntheses of phosphorylcholine compound through coupling of 3-aminopropyl

trimethoxysilane with acryloyloxyethylphosphoryl-choline. As shown in Fig. 6.24, the presence of the labile hydrogen on the secondary amine group of the monomer allowed a subsequent coupling of two monomers with a bridging spacer such as a diisocyanate to form a dimer. The chemically anchored phosphorylcholine monolayer surfaces were as effective as phosphorylcholine polymers or the self-assembly of phospholipid bilayers in inhibiting protein deposition in vitro.
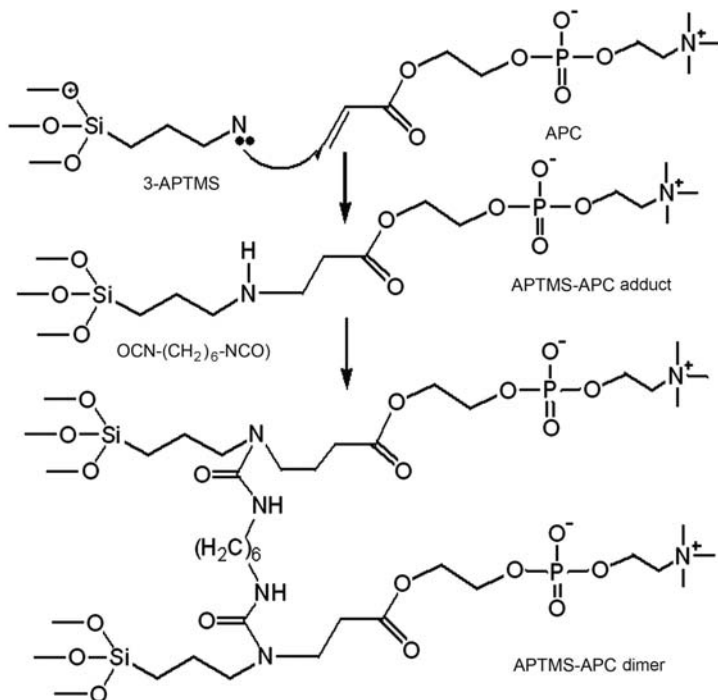
Fig. 6.24. Assembly of chemical fragments leading to phospholipid layers

Yamada et al. (1995b) developed a chemical reaction method to incorporate the phospholipid in organosiloxanes. In order to obtain the desired organopolysiloxanes bearing phospholipid side chains, chloroplatinic acid was used as hydrosilylation catalyst to carry out the hydrosilylation reaction between the alkylhydrogenpolysiloxane and unsaturated vinyl monomers containing phosphatidylcholine analogues. The presence of phospholipid side chains also showed high hydrophilicity and biocompatibility. Organopolysiloxanes having a phospholipid side chain are presented in Fig.6.25.
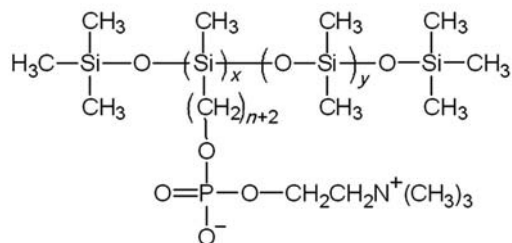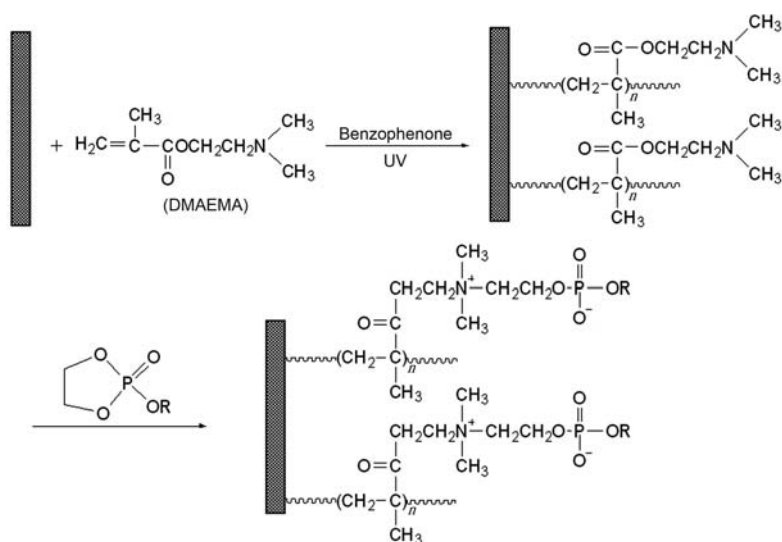
Fig. 6.25. Phospholipid modified organopolysiloxanes

To fabricate a platelet-compatible PE membrane, Liu et al. (1999) synthesized a series of surface-modified PE membranes by introducing phosphorylcholine head groups using UV irradiation and chemical modification techniques. Acrylic acid was firstly graft-copolymerized on the PE membrane surface and then reacted with a series of reactive reagents to anchored phosphorylcholine head groups with various spacer lengths on the PE membrane surface. The reaction procedures are shown in Fig.6.26. Ethylene glycol, butanediol, poly(propyleneglycol), and poly(tetramethylglycol) could be used as spacers. The length of the lipophilic spacer between phosphorylcholine groups and the PE surface affected the biocompatibility and the stability of the phosphorylcholine layer on the membrane surface. A sufficient lipophilic length existing between the phosphorylcholine groups and the PE membrane could stabilize the phosphorylcholine layer, leading to an increase in platelet compatibility of the membrane surface.

Nakaya et al. (1988) described a novel synthetic process to introduce the phosphorylcholine group to the polypeptide chains. The reactant copoly[γ-20-(hydroxy)eicosyl L-glutamate, γ-methyl L-glutamate] was prepared by ester exchange of poly(γ-methyl L-glutamate) with 1,20-eicosanediol, and then the resulting product reacted with COP in the presence of triethylamine in dichloromethane and successfully ring-opened by trimethylamine. The synthetic polypeptide containing phospholipid analogues (Fig.6.27) was more similar to that of biological membranes formed by lipids and proteins, which are composed of polypeptide chains.

Dai et al. (2004) and Xu et al. (2004) conceived an economic and efficient method of attaching phospholipid analogous polymers onto a polypropylene membrane. The synthetic process is schematically described in Fig.6.28. They used N,N-dimethylaminoethyl methacrylate (DMAEMA) as the ring-opening reagent to be photoinduced by graft polymerization onto the polypropylene membrane surface and followed by the ring-opening reaction of grafted poly(DMAEMA) with 2-alkyloxy-2-oxo-1,3,2-dioxaphospholanes. There were five 2-alkyloxy-2-oxo-1,3,2-dioxaphos-pholanes, containing octyloxy, dodecyloxy, tetradecyloxy, hexadecyloxy, and octadecyloxy groups in the molecular structure, which were used to fabricate the modified polypropylene

$$(CH_3)_3N^+CH_2CH_2OH + CH_3COOH \longrightarrow (CH_3)_3N^+CH_2CH_2OH + H_2O$$
$$OH^- \qquad\qquad\qquad\qquad\qquad\qquad CH_3COO^-$$

$$PE \xrightarrow{\text{Acrylic acid}} PE{\sim}COOH \xrightarrow{\text{SOCl}_2} PE{\sim}COCl$$

$$\xrightarrow{\text{Diol}} PE{\sim}COO(CH_2)_nOH$$

$$\xrightarrow{\text{POCl}_3} PE{\sim}COO(CH_2)_n\overset{\overset{\displaystyle O}{\|}}{O}PCl$$
$$\underset{Cl}{}$$

$$\xrightarrow{\text{H}_2\text{O}} PE{\sim}COO(CH_2)_n\overset{\overset{\displaystyle O}{\|}}{O}POH$$
$$\underset{OH}{}$$

$$\xrightarrow[\underset{\text{TPS}}{\overset{\text{CH}_3\text{COO}^-}{(CH_3)_3N^+CH_2CH_2OH}}]{} PE{\sim}COO(CH_2)_n\overset{\overset{\displaystyle O}{\|}}{O}POCH_2CH_2N^+(CH_3)_3$$
$$\underset{O^-}{}$$

Fig. 6.26. Reaction procedures of introducing phospholipid onto PE membrane surface

$$*{-}(NHCHCHOH)_x{-}(NHCHCO)_y{-}*$$
$$\qquad CH_2 \qquad\qquad CH_2CH_2COOCH_3$$
$$\qquad C{=}O$$
$$\qquad O{-}CH_2{-}O\overset{\overset{\displaystyle O}{\|}}{-}P{-}O{-}CH_2CH_2N^+(CH_3)_3$$
$$\qquad\qquad\qquad\underset{O^-}{}$$

Fig. 6.27. Polypeptide with phospholipid analogues

membranes. The length of the alkyloxy chain in the phospholipid analogous polymers had great effects on the hydrophilicity of the modified membranes. The water contact angle was decreased with a reduction in the number of carbon atoms in the long alkyloxy group, while protein adsorption and platelet adhesion were effectively suppressed on all of the modified membranes.

Huang et al. (2005; 2006a; 2006b) synthesized the copolymers of acrylonitrile (AN) with 2-hydroxyethyl methacrylate (HEMA) by a water phase precipitation copolymerization process and fabricated asymmetric porous membranes. To further improve the antifouling property and biocompatibility for these polyacrylonitrile-based asymmetric membranes, the obtained membranes reacted with COP followed by the ring-opening reaction of COP with trimethylamine. As schematically described in Fig.6.29, phospholipid moieties could be directly anchored on the poly(AN-*co*-HEMA) membrane

Fig. 6.28. Schematic representation for the fabrication of modified membranes

surface by chemical syntheses, which could avoid the purification step for the synthesis of vinyl-containing phospholipids. The modified membranes maintained a morphological structure and as good a mechanical property as that of the original membranes, and showed higher water permeability and better blood compatibility than the original ones.
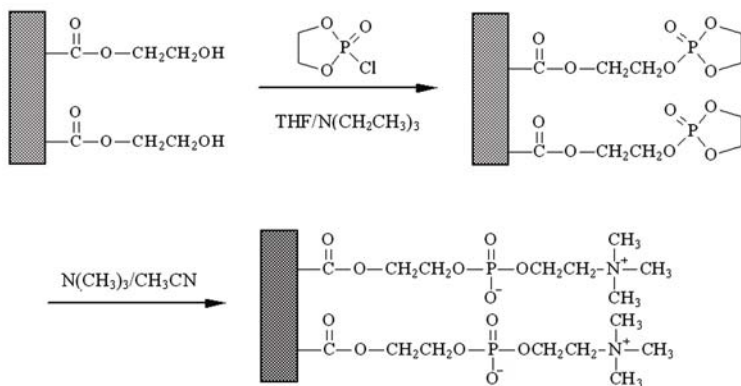
Fig. 6.29. Schematic representation for introducing phospholipid moieties onto the PANCHEMA membrane surface

6.6 Conclusion

Many studies of phospholipid analogous polymers have been reported and have claimed that phospholipid-containing polymers could effectively reduce the adsorption of various proteins and suppress the clot formation following platelet adhesion and activation. The chemical and electronic configuration of the zwitterionic head group in phospholipid allows reversible interaction with biological macromolecules that approach the surface. The initial understanding of the behavior of these phospholipid analogous polymers has been of great benefit in designing new biomaterials. To fabricate phospholipid into polymeric membranes and mimic biomembranes, various approaches have been developed to modify polymeric membranes with phospholipid, as well as to investigate the properties of the modified membranes and to make these membranes with more desirable properties, thereby expanding the range of their applications. All of these biomimetic polymeric membranes containing phospholipid will surely lead to varied applications. It has been suggested that polymer membranes containing phospholipid can be used as artificial biomembranes such as oxygenator membranes, hemodialyzer membranes, and catheter membranes, etc. Phospholipid-containing polymeric membranes can also possibly be used in the fields of ion permeable membranes, bioactive transport membranes, ion-exchange membranes and biosensors.

References

Akhtar S, Hawes C, Dudley I, Reed I, Stratford P (1995) Coatings reduce the fouling of microfiltration membranes. J Membrane Sci 107:209-218

Araki K, Konno R, Seno M (1984) Gas-permeability of phosphatidylcholine impregnated in a porous cellulose nitrate membrane. J Membrane Sci 17: 89-95

Billimoria JD, Lewis KO (1968) The synthesis of phospholipids. Part I. Phosphatidyl and lysophosphatidyl ethanolamines. J Chem Soc C 1404-1412

Bird R, Hall B, Chapman D, Hobbs KEF (1988) Material thrombelastography: An assessment of phosphorylcholine compounds as models for biomaterials. Thromb Res 51:471-4483

Black J (1992) Biological performance of materials. Marcel Dekker, Inc., New York 206-208

Dai QW, Xu ZK, Wu J (2004) A novel approach for the surface modification of polymeric membrane with phospholipid polymer. Chinese Chem Lett 15:993-996

Elliott JT, Burden DL, Woodward JT, Sehgal A, Douglas JF (2003) Phospholipid monolayers supported on spun cast polystyrene films. Langmuir 19:2275-2283

Feng W, Brash J, Zhu SP (2004) Atom-transfer radical grafting polymerization of 2-methacryloyloxyethyl phosphorylcholine from silicon wafer surfaces. J Polym Sci Part A: Polym Chem 42:2931-2942

Furukawa A, Nakaya T, Imoto M (1986) Polymeric phospholipid analogs. 19. synthesis and polymerization of 10-(11-methacryloyloxyundecyloxycarbonyl)decyl 2-(trimethylammonio) ethyl phosphate. Makromol Chem 187:311-316

Hasegawa E, Matsushita Y, Eshima K, Nishide N, Tsuchida E (1984) Synthesis of novel styrene groups containing glycerophosphocholines and their polymerization as liposomes. Makromol Chem Rapid Commun 5:779-784

Huang XJ, Huang XD, Che AF, Xu ZK, Yao K (2006a) Suppression of cell adhesion on polyacrylonitrile-based membranes by the anchoring of phospholipid moieties. Chinese J Polym Sci 24:103-106

Huang XJ, Xu ZK, Huang XD, Wang ZG, Yao K (2006b) Biomimetic surface modification on polyacrylonitrile-based asymmetric membranes via direct formation of phospholipid moieties. Polymer 47:3141-3149

Huang XJ, Xu ZK, Wan LS, Wang ZG, Wang JL (2005) Surface modification of polyacrylonitrile-based membranes by chemical reactions to generate phospholipid moieties. Langmuir 21:2941-2947

Inaishi K, Nakaya T, Imoto M (1975) Synthesis and polymerization of 10-[bis(benzyloxy) phosphoryloxy]decyl methacrylate. Makromol Chem 176:2473-2478

Ishihara K, Fukumoto K, Iwasaki Y, Nakabayashi N (1999a) Modification of polysulfone with phospholipid polymer for improvement of the blood compatibility. Part 1. Surface characterization. Biomaterials 20:1545-1551

Ishihara K, Fukumoto K, Iwasaki Y, Nakabayashi N (1999b) Modification of polysulfone with phospholipid polymer for improvement of the blood compatibility. Part 2. Protein adsorption and platelet adhesion. Biomaterials 20:1553-1559

Ishihara K, Iwasaki Y, Ebihara S, Shindo Y, Nakabayashi N (2000) Photoinduced graft polymerization of 2-methacryloyloxyethyl phosphorylcholine on polyethylene membrane surface for obtaining blood cell adhesion resistance. Colloid Surface B 18:325-335

Ishihara K, Nishiuchi D, Watanabe J, Iwasaki Y (2004) Polyethylene/phospholipid polymer alloy as an alternative to poly(vinylchloride)-based materials. Biomaterials 25:1115-1122

Ito T, Iwasaki Y, Narita T, Akiyoshi K, Ishihara, K (2003) Controlled adhesion of human lymphocytes on electrically charged polymer surface having phosphorylcholine moiety. Sci Technol Adv Mat 4:99-104

Iwasaki Y, Ishihara K, Nakabayashi N, Khang G, Jeon JH, Lee JW, Lee HB (1998) Platelet adhesion on the gradient surfaces grafted with phospholipid polymer. J Biomat Sci-Polym E 9:801-816

Iwasaki Y, Sawada S, Nakabayashi N, Khang G, Lee HB, Ishihara K (1999) The effect of the chemical structure of the phospholipid polymer on fibronectin adsorption and fibroblast adhesion on the gradient phospholipid surface. Biomaterials 20:2185-2191

Iwasaki Y, Shimakata K, Morimoto N, Kurita K (2003) Hydrogel-like elastic membrane consisting of semi-interpenetrating polymer networks based on a phosphorylcholine polymer and a segmented polyurethane. J Polym Sci Part A: Polym Chem 41:68-75

Iwasaki Y, Uchiyama S, Kurita K, Morimoto N, Nakabayashi N (2002) A non-thrombogenic gas-permeable membrane composed of a phospholipid polymer skin film adhered to a polyethylene porous membrane. Biomaterials 23:3421-3427

Khang G, Choi MK, Rhee JM, Lee SJ, Lee HB, Iwasaki Y, Nakabayashi N, Ishihara K (2001) Biocompatibility of poly(MPC-*co*-EHMA)/poly(L-lactide-*co*-glycolide) blends. Korea Polym J 9:107-115

Kimura T, Nakaya T, Imoto M (1975) Synthesis and polymerization of benzyl 2-(methacryloyloxy) ethyl hydrogen phosphate. Makromol Chem 176:1945-1951

Kimura T, Nakaya T, Imoto M (1976) Synthesis of polymers containing phosphoric ester. Makromol Chem 177:1235-1241

Korematsu A, Takemoto Y, Nakaya T, Inoue H (2002) Synthesis, characterization and platelet adhesion of segmented polyurethanes grafted phospholipid analogous vinyl monomer on surface. Biomaterials 23:263-271

Kusumi A, Singh M, Tirrell DA, Oehme G, Singh A, Samuel NKP, Hyde JS, Regen SL (1983) Dynamic and structural properties of polymerized phosphatidylcholine vesicle membranes. J Am Chem Soc 105:2975-2980

Liu JH, Jen HL, Chung YC (1999) Surface modification of polyethylene membranes using phosphorylcholine derivatives and their platelet compatibility. J Appl Polym Sci 74:2947-2954

Lu JR, Murphy EF, Su TJ, Lewis AL, Stratford PW, Satija SK (2001) Reduced protein adsorption on the surface of a chemically grafted phospholipid monolayer. Langmuir 17:3382-3389

Luo GB, Liu TT, Zhao XS, Huang YY, Huang CH, Cao WX (2001) Investigation of polymer-cushioned phospholipid bilayers in the solid phase by atomic force microscopy. Langmuir 17:4074-4080

Michel M, Vautier D, Voegel JC, Schaaf P, Ball V (2004) Layer by layer self-assembled polyelectrolyte multilayers with embedded phospholipid vesicles. Langmuir 20:4835-4839.

Marra KG, Kidani DDA, Chaikof EL (1997) Cytomimetic biomaterials. 2. *In situ* polymerization of phospholipids on a polymer surface. Langmuir 13:5697-5701

Morimoto N, Iwasaki Y, Nakabayashi N, Ishihara K (2002) Physical properties and blood compatibility of surface-modified segmented polyurethane by semi-interpenetrating polymer networks with a phospholipid polymer. Biomaterials 23:4881-4887

Nakai S, Nakaya T, Imoto M (1977) Polymeric phospholipid analog. 10. synthesis and polymerization of 2-(methacryloyloxy)ethyl 2-aminoethyl hydrogen phosphate. Makromol Chem 178:2963-2967

Nakai S, Nakaya T, Imoto M (1978) Polymeric phospholipid analogs. 11. synthesis and polymerization of 2-aminoethyl 2-(*p*-methacryloyloxybenzoyloxy)ethyl hydrogen phosphate. Makromol Chem 179:2349-2353

Nakaya T, Kurio H, Imoto M, Sugiyama K (1989) Polymeric phospholipid analogs. 29. synthesis and polymerization of 2-(methacryloyloxy)ethyl dipalmitoyl-DL-alpha-phosphatidylethanol-amide. Polym J 21:929-935

Nakaya T, Shoji H, Imoto M (1988) Polymeric phospholipid analogs. 22. a synthetic polypeptide with phospholipid analogs. J Macromol Sci A 25:115-119

Nakaya T, Toyoda H, Imoto M (1986) Polymeric phospholipid analogs. 13. synthesis and properties of vinyl-polymers containing phosphatidyl choline groups. Polym J 18:881-886

Nakaya T, Yamada M, Shibata K, Imoto M, Tsuchiya H, Okuno M, Nakaya S, Ohno S, Matsuyama T, Yamaoka H (1990) Polymerized phospholipid langmuir-blodgett multilayer films. Langmuir 6:291-293

Nakaya T, Yasuzawa M, Imoto M (1989) Poly(phosphatidylcholine) analogs. Macromolecules 22:3180-3181

Nakaya T, Yasuzawa M, Imoto M (1994) Synthesis and polymerization of 2-((2-methacryloyloxy)-ethyldimethylammonio)ethyl p-substituted phenyl phosphates. J Macromol Sci A 31:207-215

Naumann CA, Prucker O, Lehmann T, Ruhe J, Knoll W, Frank CW (2002) The polymer-supported phospholipid bilayer: Tethering as a new approach to substrate-membrane stabilization. Biomacromolecules 3:27-35

Orban JM, Faucher KM, Dluhy RA, Chaikof EL (2000) Cytomimetic biomaterials. 4. *In situ* photopolymerization of phospholipids on an alkylated surface. Macromolecules 33:4205-4212

Regen SL, Kirszensztejn P, Singh A (1983) Polymer-supported membranes—a new approach for modifying polymer surfaces. Macromolecules 16:335-338

Regen SL, Singh A, Oehme G, Singh M (1982) Polymerized phosphatidylcholine vesicles. Synthesis and characterization. J Am Chem Soc 104:791-795

Sawada SI, Iwasaki Y, Nakabayashi N, Ishihara K (2006) Stress response of adherent cells on a polymer blend surface composed of a segmented polyurethane and MPC copolymers. J Biomed Mater Res A 79A:476-484

Seo YH, Li YJ, Nakaya T (1995) Preparation and polymerization of 2-(acryloyloxy) ethyl-2-(trimethylammonium) ethyl phosphate and 4-(acryloyloxy) butyl-2-(trimethyl-ammonium) ethyl phosphate. J Macromol Sci A 32:999-1006

Shindo Y, Kozaki M, Fukumoto K, Ishihara K (2004) Properties of blend polymers composed of phospholipid polymer and photocrosslinkable PVA. J Photopolym Sci Technol 17:75-76

Shindo Y, Setoguchi T, Fukumoto K, Ishihara K, Adachi D, Inoue K (2003) Properties of blend films composed of phospholipid polymer and photocrosslinkable PVA. J Photopolym Sci Technol 16:217-218

Singer SJ, Nicolson GL (1980) The fluid mosaic model of the structure of cell membranes. Science 175:720-731

Sugiyama K, Kato K, Kido M, Shiraishi K, Ohga K, Okada K (1998) Grafting of vinyl monomers on the surface of a poly(ethylene terephthalate) film using Ar plasma-post polymerization technique to increase biocompatibility. Macromol Chem Phys 199:1201-1208

Sugiyama K, Nakaya T (1986) Synthesis and properties of polyionenes containing aza-crown ethers and phosphatidylcholine analog moieties. Makromol Chem Rapid Commun 7:679-685

Thanh TN, Chabrier P (1974) New method of preparation for phosphorylcholine, phosphorylhomocholine and their derivatives. Bull Soc Chem Fr 3-4: 667-671

Ueda H, Watanabe J, Konno T, Takai M, Saito A, Ishihara K (2006) Asymmetrically functional surface properties on biocompatible phospholipid polymer membrane for bioartificial kidney. J Biomed Mater Res A 77A:19-27

Umeda T, Nakaya T, Imoto M (1982) Polymeric phospholipid analogs. 14. the convenient preparation of a vinyl monomer containing a phospholipid analog. Makromol Chem Rapid Commun 3:457-459

Umeda T, Nakaya T, Imoto M (1985) Polymeric phospholipid analogs. 16. synthesis and properties of polymers containing phosphatidylcholine analogs in the polymer backbones. Makromol Chem Rapid Commun 6:285-290

van der Heiden AP, Goebbels D, Pijpers AP, Koole LH (1997) A photochemical method for the surface modification of poly(etherurethanes) with phosphoryl-choline-containing compounds to improve hemocompatibility. J Biomed Mater Res A 37:282-290

van der Heiden AP, Koole LH (1996) Photochemical coupling of aryl azides to poly(ether urethane) surface: Studies with a fluorescent model compoud. Macromolecules 29:7012-7015

van der Heiden AP, Willems GM, Lindhout T, Pijpers AP, Koole LH (1998) Adsorption of proteins onto poly(ether urethane) with a phosphorylcholine moiety and influence of preadsorbed phospholipid. J Biomed Mater Res A 40:195-203

Wang T, Wang YQ, Su YL, Jiang ZY (2005) Improved protein-adsorption-resistant property of PES/SPC blend membrane by adjustment of coagulation bath composition. Colloid Surface B 46:233-239

Xu ZK, Dai QW, Wu J, Huang XJ, Yang Q (2004) Covalent attachment of phospholipid analogous polymers to modify a polymeric membrane surface: A novel approach. Langmuir 20:1481-1488

Yajima S, Sonoyama Y, Suzuki K, Kimura K (2002) Ion-sensor property and blood compatibility of neutral-carrier-type poly(vinyl chloride) membranes coated by phosphorylcholine polymers. Anal Chim Acta 463:31-37.

Yamada M, Li YJ, Nakaya T (1995a) Synthesis and properties of polymers containing phosphatidylcholine analogs in the main chains and long alkyl-groups in the side-chains. J Macromol Sci A 32:1723-1733

Yamada M, Li YJ, Nakaya T (1995b) Synthesis of novel organopolysiloxanes having a phospholipid-like structure. Macromolecules 28:2590-2591

Yasuzawa M, Nakaya T, Imoto M (1985a) Polymeric phospholipid analogs. 17. synthesis and properties of vinyl-polymers containing cholesterol and phosphatidylcholine analogous moieties. Makromol Chem Rapid Commun 6:721-726

Yasuzawa M, Nakaya T, Imoto M (1985b) Polymeric phospholipid analogs. 18. synthesis and properties of a vinyl polymer containing both vitamin E and phosphatidylcholine analogous moieties. Makromol Chem Rapid Commun 6:727-731

Ye SH, Watanabe J, Ishihara K (2004) Cellulose acetate hollow fiber membranes blended with phospholipid polymer and their performance for hemopurification. J Biomat Sci-Polym Ed 15:981-1001

Ye SH, Watanabe J, Iwasaki Y, Ishihara K (2002) Novel cellulose acetate membrane blended with phospholipid polymer for hemocompatible filtration system. J Membrane Sci 210:411-421

Ye SH, Watanabe J, Iwasaki Y, Ishihara K (2003) Antifouling blood purification membrane composed of cellulose acetate and phospholipid polymer. Biomaterials 24:4143-4152

Yoneyama T, Ishihara K, Nakabayashi N, Ito M, Mishima Y (1998) Short-term in vivo evaluation of small-diameter vascular prosthesis composed of segmented poly(etherurethane) 2-methacryloyloxyethyl phosphorylcholine polymer blend. J Biomed Mater Res A 43:15-20

Zwaal RFA, Comfurius P, van Deenen LLM (1977) Membrane asymmetry and blood coagulation. Nature 268 358-360

7

Membranes with Glycosylated Surface

Sugar-containing polymers, including natural polysaccharides and synthetic glycopolymers, are highly hydrophilic and biocompatible materials. Sugars also play important roles in many biological processes. Using them as modifiers to modify the membrane surface, which is also called membrane surface glycosylation, can offer properties of both anti-non-specific adsorption and specific recognition. In this chapter we introduce some research in which membrane surface glycosylation was carried out to reduce non-specific adsorption, improve anti-coagulation properties, endow the recognition ability to lectins and even serve as an additional layer to alter the separation performance.

7.1 Introduction

Carbohydrates, ubiquitous in living creatures, have been found on the surface of nearly every cell in the form of polysaccharides, glycoproteins, glycolipids or/and other glycoconjugates. Fig.7.1 shows the molecular structures of some carbohydrates. The carbohydrates on the external cell membrane, known as the glycocalyx, play essential roles in many biological functions which can be classified in two apparently opposing ways. One role is to serve as sites for the docking of other cells, biomolecules and pathogens in a more or less specific recognition process (Dwek, 1996). The other role is to contribute to steric repulsion that prevents the undesirable non-specific adhesion of other proteins and cells (Holland et al., 1998). Both these two aspects rely on the carbohydrate-protein interactions, of which the mechanisms remain controversial even today.

In the past decade there has been a great interest in carbohydrate-protein interactions and many efforts have been made to reveal their underlying essence. Although the mechanism is still not well known, it is clear that in nature carbohydrates binding species typically aggregate into higher-ordered
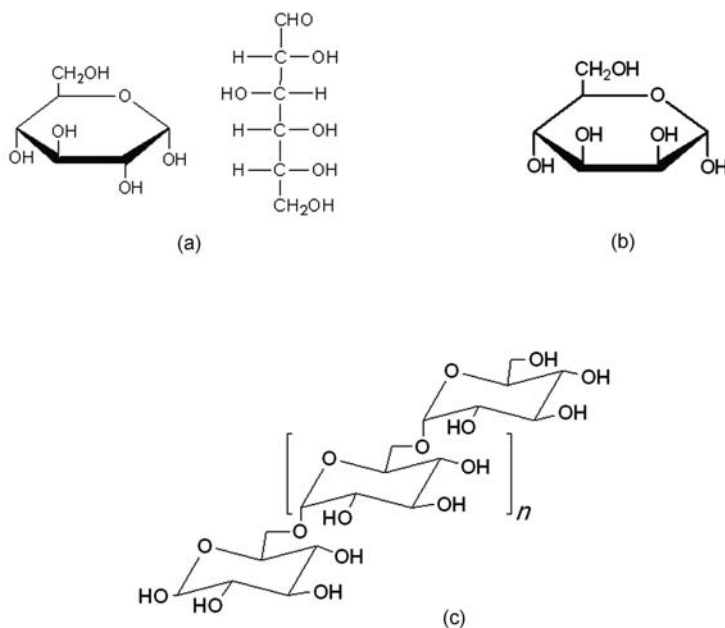
Fig. 7.1. Molecular structures of (a) glucose, (b) mannose and (c) dextran

oligomeric structures, both for prevention of undesirable non-specific adhesion (Holland et al., 1998) and for specific recognition (Lee and Lee, 1995). Actually, highly aggregated surface-tethered carbohydrate ligans, just like the glycocalyx on the cell surface, result in not only the enhancement of binding strength in specific recognition against proteins but also in the minimization of non-specific protein adsorption. Mimicry of the cell surface glycocalyx has led to many promising applications and a large number of different synthetic multivalent glycoligands (such as glycoclusters, glycodendrimers and glycopolymers, etc.) have been designed to interfere effectively with the carbohydrate-protein interactions. The teams of Whitesides (Ostuni et al., 2001) and of Mrksich (Luk et al., 2000) investigated the ability of self-assembled monolayers (SAMs) with different saccharides as end function groups to resist the nonspecific adsorption of proteins. Kissieling's group (Cairo et al., 2002; Gestwicki et al., 2002) studied the structural effects on the interaction between the multivalent ligand with mannose residues and Concanavalin A (Con A).

Recently membrane systems have been receiving increased consideration for biomedical applications such as dialysis, plasmaphorosis and oxygenation of blood during cardiac surgery. However, it is well known that the major obstacle to the extensive use of membrane processes in therapeutic treat-

ment is protein fouling of polymeric membrane materials. Protein deposition on the membrane surface can cause instabilities in transport characteristics and cellular interactions with artificial surfaces are also assumed to be mediated through adsorbed proteins (Deppisch et al., 1998). On the other hand, conventional membrane processes are based purely on a sieving mechanism which often restricts the application of membrane technology, especially in the biomedical field (Klein, 2000). Considering the anti-non-specific adsorption and specific recognition properties of sugars, glycosylating a membrane surface with polysaccharides is a promising solution to these problems. Some research has been done concerning membrane surface modifications with both natural polysaccharides and synthetic glycopolymers.

7.2 Surface Modification with Natural Polysaccharides

7.2.1 Heparin

Heparin is a kind of negatively charged, unbranched carbohydrate polymer and represents the most complex members of the glycosaminoglycan (GAG) superfamily, which further includes dermatan sulfate, chondroitin sulphate, keratan sulfate and hyaluronic acid. It is often applied to modify a membrane surface for the improvement of hemocompatibility.

As is known, membranes fabricated from synthetic polymers such as polyacrylonitrile copolymer, poly(methyl methacrylate) and polysulfon are widely used in dialysis because of their relatively low cost, optimal water permeability and readiness for processing. On the other hand, the main disadvantage is the relatively poor hemocompatibility, which is demonstrated by a rather strong activation of the coagulation and complement system and a drop in the leukocyte count (Cheung et al., 1986; Docci et al., 1988; Steen, 1986). Heparin is often used to avoid complications associated with blood-material interactions. However, administration of heparin usually causes undesired side effects such as internal hemorrhages and, eventually, osteoporoses. Thus immobilization of heparin onto a membrane surface may be a feasible way to improve the hemocompatibility of blood contacting materials and consequently to avoid their side effects. Heparin can be immobilized by physical, ionic or covalent linkages. The covalent linkage is the most widely applied strategy because of its stability and durability.

Hinrichs et al. (1997) heparinized cuprophan hemodialysis membranes using N,N'-carbonyldiimidazole (CDI) as the coupling agent (Fig.7.2). The properties of heparinized Cuprophan membranes were then evaluated. The immobilized heparin partially retained its biological activity and the anticoagulant activity was found to be (12.4 ± 4.2) mU/cm^2 in the thrombin inactivation assay. Moreover, the complement activation induced by the membranes (nascent and heparinized) was determined by measuring the concentration of

fluid phase terminal complement complex (TCC), and the results revealed that the immobilized heparin also displayed an anti-complement activity.
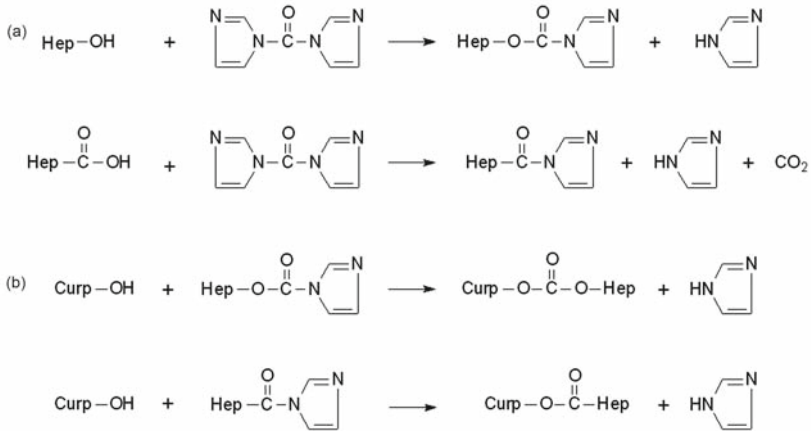
Fig. 7.2. Heparinization of Cuprophan by means of a CDI activation procedure. (a) Activation reactions of heparin with CDI; (b) Immobilization reactions of CDI-activated heparin onto Cuprophan
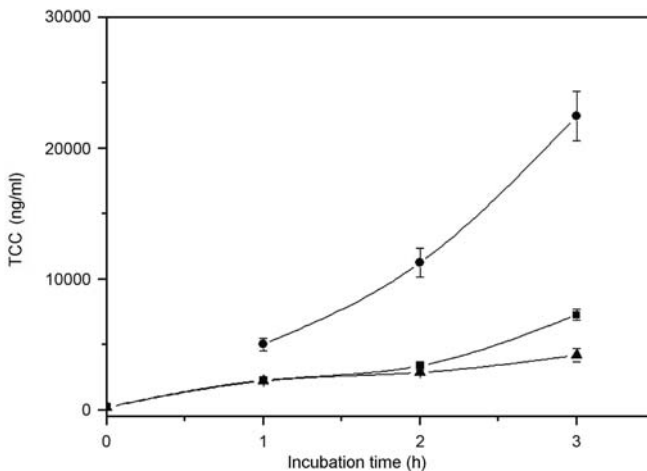
Fig. 7.3. Generation of fluid-phase TCC induced by: nascent Cuprophan membrane: •; heparinized Cuprophan membrane: ■; test tube (polystyrene) alone: ▲. Membranes with a surface area of 3.9 cm^2 were added to 500 ml of serum at 37 °C. The concentration of TCC in serum was measured by means of an ELISA

As shown in Fig.7.3, the nascent Cuprophan membrane induced the generation of substantial amounts of fluid-phase TCC. Moreover, the TCC increased obviously in 3 h of incubation. However, the fluid-phase TCC induced by the heparinized Cuprophan membrane was much lower. The concentration of TCC in the presence of the heparinized Cuprophan membrane also increased with the length of incubation. However, this increase was almost the same as that induced by the test tube (polystyrene) alone, which indicated that the heparinization could significantly reduce the generation of fluid-phase TCC. Reduction of TCC concentration by the heparinized membranes can be ascribed to the restraint of the alternative pathway C3 amplification convertase by the immobilized heparin (Kazatchkine et al., 1979). Also, coverage and modification of the hydroxyl groups on the Cuprophan membrane surface by heprinization were concerned with inhibition of the complement activation (Berlo and Ellens, 1988; Maillet et al., 1990; Yu et al., 1994).
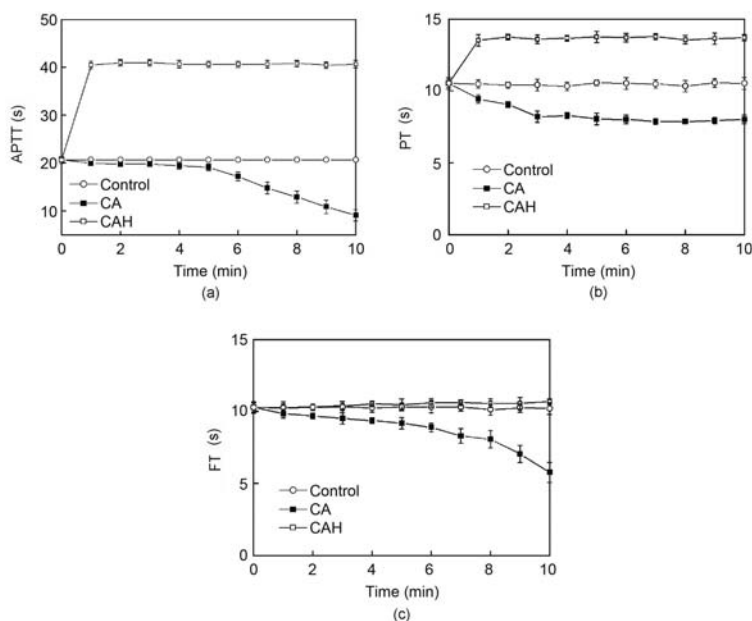
Fig. 7.4. Effects of clotting time on the (a) APTT, (b) PT and (c) FT (Kung et al., 2006). Copyright (2006). Reprinted with permission of John Wiley & Sons, Inc.

Kung et al. (2006) immobilized heparin onto the cellulose acetate (CA) hollow fiber membrane to improve its anticoagulation performance in hemodialysis. The dialysis performance was evaluated by a mini-hemodialysis circle with fresh porcine whole blood. Results from the activated partial thromboplastin time (APTT), prothrombin time (PT), and fibrinogen time (FT) measurements indicated that the dialysis performance and hemocompatibil-

ity of the heparin immobilized CA (CAH) membrane could be improved considerably. Fig.7.4 shows the APTT, PT and FT of the CA membrane, CAH membrane and the control sample. The APTT, PT, and FT of the CA membrane decreased gradually to 25%, 80%, and 60% of that for the control sample after 10 min of clotting time, respectively. On the other hand, the APTT and PT of the CAH membrane increased at the beginning of dialysis and then remained almost constant during the whole process. The FT of the CAH membrane exhibited a relatively stable level during the procedure. Moreover, the APTT, PT and FT of the CAH membrane were 2.0, 1.4, and 1.0 times those of the control sample and 8.0, 1.8, and 1.7 times those of the CA membrane, respectively.

7.2.2 Chitosan

Chitosan is obtained by deacetylation of chitin, which is abundant in nature. It is a linear polyelectrolyte that carries positive charges with a molecular structure of (1,4)-linked 2-amino-2-deoxy-b-D-glucan. It has both amino and hydroxy groups which can be used for further modification. Also, chitosan has been identified as a non-toxic, biodegradable, cell compatible, and biocompatible material (Alsarra et al., 2002; 2004; Lin et al., 2005). Chitosan is often used as a modifier to improve membrane surface biocompatibility and itself is also a good membrane material.

Tan et al. (2002) reported the preparation of a nanofiltration membrane from the PAN membrane through ultraviolet radiation using chitosan as the modifier. This membrane was used to treat $E.$ $globulus$ CTMP (Chemi-Thermao Mechanical Pulp) effluent. The modified membrane showed a remarkable increase in its retention to soda from 2.5% to 40.1%. At the same time the membrane performance such as its rejection of chroma, Chemical Oxygen Demand (COD) and Biochemical Oxygen Demand (BOD) also increased. Musale and Kumar (2000) crosslinked chitosan on the PAN membrane surface with glutaraldehyde as the crosslinker and studied the effect of crosslinking on the sieving characterization of the chitosan/PAN nanofiltration membrane. They found that the surface crosslinked membranes were stable over a 10-h operation for pure water permeation and that the stability increased with increasing glutaraldehyde concentration.

Huang et al. (2006) established a method for the construction of a novel positively charged composite nanofiltration membrane by crosslinking 2-hydroxypropyltrimethyl ammonium chloride chitosan (HACC) on the PAN ultrafiltration membrane surface in the presence of diisocyanate as the crosslinking reagent. The membrane had a molecular-weight cut-off of approximately 560 Da and the pure water flux was 10.59 kg/(h·m^2·MPa). Moreover, they found that the rejection to different salt solutions of this membrane followed the order as: $MgCl_2 > CaCl_2 > NaCl = KCl > MgSO_4 > Na_2SO_4 > K_2SO_4$.

7.3 Surface Modification with Synthetic Glycopolymers

Synthetic sugar-containing polymers are attractive candidates for membrane surface modification because of the definiteness and the controllability of the molecular structure as well as the facility to vary the species of the sugar ligands. Generally there are two methods for preparing synthetic polysaccharides on a membrane surface: graft polymerization of vinyl sugars (glycomonomers) and tethering of sugars onto functionalized synthetic polymers by polymer analogous reactions. For the former strategy difficulties lie in the synthesis of glycomonomers where firstly the hydroxy groups must be protected to avoid unwanted side reactions and secondly the separation and purification process of these glycomonomers is tedious. Moreover in the later method the reaction between sugars and surface functional groups is often sustained because of the space hindrance. For these reasons there are few reports on surface modification of a membrane by synthetic polysaccharides.

Xu's group (Kou et al., 2003; Yang et al., 2005; 2006; 2007) focused on modifying a polypropylene microporous membrane (PPMM) with synthetic polysaccharides in recent years. They established several methods for this purpose, including UV-induced graft polymerization, polymer analogous reactions and surface initiated living polymerizations.

7.3.1 Glycosylation by UV-induced polymerization

Yang at al. (2005a; 2006a; 2007b) and Kou et al. (2003) synthesized two vinyl glycomonomers, 2-gluconamidoethyl methacrylate (GAMA) and α-allyl glucoside (AG), bearing linear and cyclic glucose residues, respectively. Glycosylation of the PPMM surface was carried out by UV-induced graft polymerizations in the presence of benzophenone and plasma treatments (Fig.7.5). The anti-non-specific adsorption properties of PGAMA glycosylated PPMM and the specific recognition properties of PAG glycosylated PPMM were evaluated.

The permeation properties of the PGAMA modified membranes were determined by measuring the pure water and nitrogen gas permeation. The water flux of the nascent and ethanol-wetted membranes was measured and compared with those of the PGAMA modified ones. Fig.7.6 shows the results. The nascent membrane had no detectable water flux. After being wetted by ethanol, the flux of the membrane increased to (340 ± 7) kg/(m^2·h). With the increase of the PGAMA grafting degree from 2.23 wt.% to 6.03 wt.%, the water flux was further increased from (466 ± 26) to (764 ± 28) kg/(m^2·h). In addition it could be observed that the PGAMA modified membranes showed a more stable water permeability than ethanol-wetted ones in which case the water flux obviously declines over a protracted period of time. This indicated that the modification with PGAMA is a durable way of improving the membrane performance.
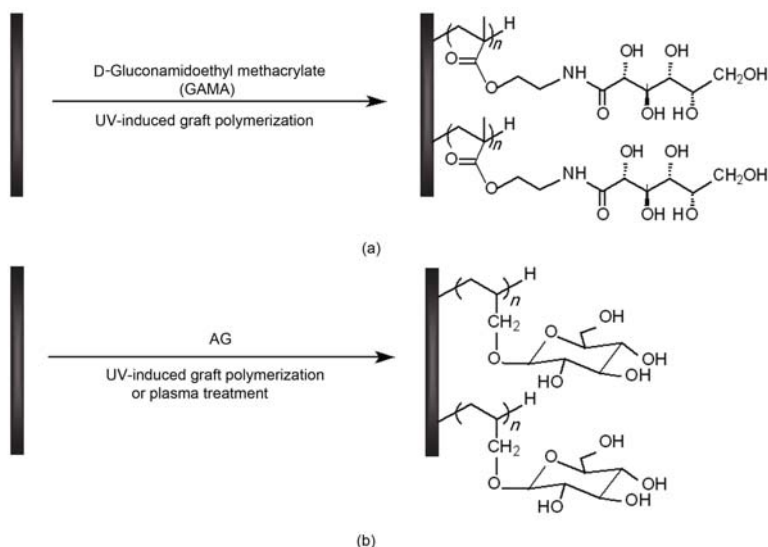
Fig. 7.5. Schematic representation of UV-induced graft polymerizations of GAMA (a) and AG (b) onto PPMM surface
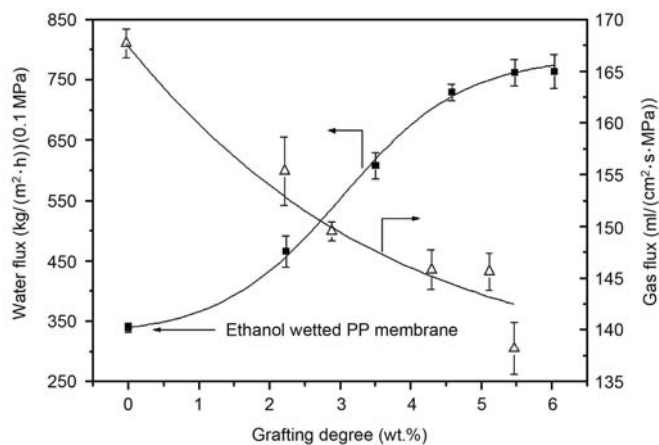
Fig. 7.6. Permeation properties of the nascent and GAMA grafted PPMMs: (■) pure water flux; (△) nitrogen gas flux. Reprinted with permission from (Yang et al., 2005a). Copyright (2005), American Chemical Society

The results also revealed that, with the grafting in progress, the gas flux decreased while the water flux increased. This seemly inconsistant phenomenon can be interpreted as follows. The gas flux was mainly controlled by the pore size and porosity of the membrane, which suffered a serious reduction during the grafting process, while the water flux depends on the surface hydrophilicity to a much higher degree than on the pore properties as long as the grafting degree is low, which was exactly the case in Yang's work (2005a; 2006a; 2007b).

For various (biomedical, especially) applications of polypropylene membranes, protein adsorption is the first problem to conquer and it is expected to be resolved as much as possible (Ho and Zydney, 2001; Kelly and Zydney, 1995; Lim and Bai, 2003). As mentioned above, polysaccharides are promising polymers for the reduction of protein absorption. Thus, in Yang and Kou's work (2003), dynamic protein (BSA as the model protein) solution permeation processes were conducted to evaluate the anti-fouling property of the PGAMA modified membranes. From Fig.7.7 and Table 7.1 it can be found that the flux decreased with the permeation of the BSA solution taking place due to the deposition of proteins on the membrane surface and in the pores. After cleaning in NaOH solution, the flux exhibited some recovery. The ethanol-wetted nascent membrane showed the largest loss of flux from 340 kg/(m^2·h) to 93 kg/(m^2·h) within the measurement time and the RFR is 73%. These results suggested that a large amount of BSA proteins had deposited on the membrane surface and in the pores. However, the flux reduction was restrained by GAMA grafting, which indicated that the GAMA polymer layer was able to prevent the adsorption of BSA effectively. Moreover, the recovery flux increased significantly with the increase in the grafting degree and even at a lower grafting degree a relatively high flux recovery ratio (> 80%) was achieved. This result may be attributed to the fouling mechanism, i.e., how the fouling occurs.

Table 7.1. Permeation and antifouling properties of the studied PPMMs. Reprinted with permission from (Yang et al., 2005a). Copyright (2003), American Chemical Society

Membrane	J_W^a (kg/(m^2·h))	J_P^a (kg/(m^2·h))	J_R^a (kg/(m^2·h))	RFR[b] (%)	FRR[b] (%)
Ethanol-wetted	340 ± 7	93 ± 22	219 ± 22	73	64
2.23 wt.% GAMA grafted	466 ± 26	187 ± 24	390 ± 26	60	84
3.50 wt.% GAMA grafted	608 ± 21	348 ± 37	488 ± 38	57	80
4.58 wt.% GAMA grafted	729 ± 14	452 ± 38	646 ± 30	38	89
5.47 wt.% GAMA grafted	762 ± 22	434 ± 32	658 ± 33	57	86
6.03 wt.% GAMA grafted	764 ± 28	452 ± 25	649 ± 35	59	85

[a] J_P is the pure water flux, J_P is the flux of 1 g/L BSA solution, J_R is the pure water flux of the membrane after cleaning with NaOH solution
[b] RFR (%) = $(1 - J_P/J_W) \times 100$, FRR (%) = $(J_R/J_W) \times 100$

As shown in Fig.7.8(a), for the unmodified membrane or the membranes with a low grafting degree, small protein particles permeated through the membrane pores expediently and protein aggregates deposited in the membrane pores. On the membrane surface a "cake layer" also formed after permeating for a period. Thus the fouling took place on the membrane surface and in the pores. After cleaning in NaOH solution the "cake layer" was removed. However, the protein aggregates deposited in the pores remained. On the other hand, with the grafted PGAMA chains on the membrane surface and in the pores, small protein particles and protein aggregates were kept away from the surface and the pore wall. Thus fouling only took place on the membrane surface in the form of the "cake layer" (Fig.7.8(b)) which could be removed by NaOH cleaning. For this reason the RFR decreased and the FRR increased at a higher PGAMA grafting degree. All these results demonstrated that the anti-fouling properties of the PPMMs could be improved greatly by the grafting of PGAMA.
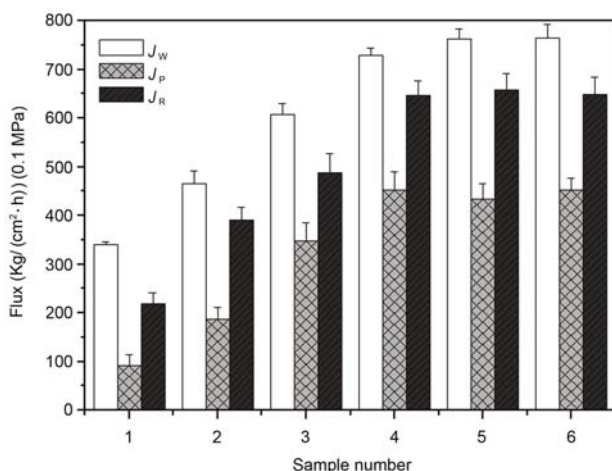
Fig. 7.7. Permeation fluxes of pure water and BSA solution through the nascent and GAMA grafted PPMMs: (1)~(6) 0 wt.%; 2.23 wt.%; 3.50 wt.%; 4.58 wt.%; 5.47 wt.%; 6.03 wt.% GAMA grafted PPMMs, respectively. Reprinted with permission from (Yang et al., 2005a). Copyright (2003), American Chemical Society

Although polymeric biomaterials have been used widely, improving the hemocompatibility of these devices is still a major challenge (Peppas and Langer, 1994). The hemocompatibility of the PGAMA grafted membranes was evaluated by platelet adhesion experiments (Nie et al., 2003; Xu et al., 2004). As shown in Fig.7.9(a), platelets adhered seriously to the nascent PPMM. Such adhesion could be reduced remarkably by the PGAMA grafting (see Figs.7.9(b)~7.9(d)). The restraint of platelet adhesion may be as-
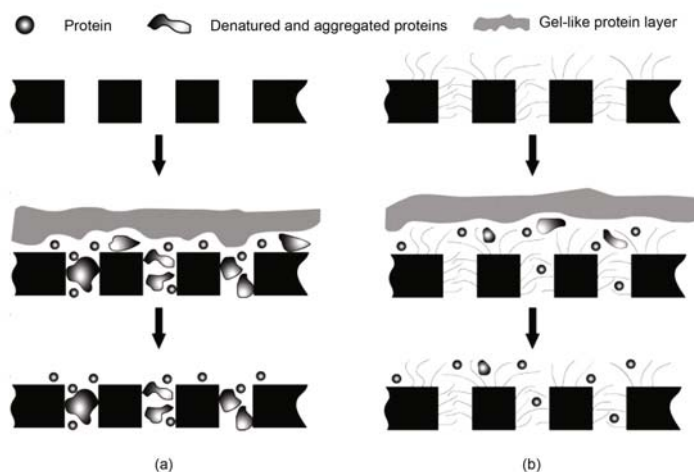
Fig. 7.8. Schematic representation of membrane fouling by proteins before (a) and after (b) glycosylation

cribed to the striking hydrophilicity and the volume restriction of the grafted PGAMA chains. Besides the number of adhered platelets, the morphology of the platelet is also one of the important indices expressing the degree of surface hemocompatibility. As can be seen from Fig.7.9, for the nascent membrane and membranes with a relatively low grafting degree, the adhered platelets show a large size as well as a tendency to aggregation, and hair like filaments can also be found which indicated the activation of the platelets on the surface. In cases of a higher GAMA grafting degree (Figs.7.9(c) and 7.9(d)) the adhered platelets remained in an almost spherical shape, which means that the surface did not activate the platelets. Considering these results, grafting PGAMA onto the membrane surface can sufficiently improve the hemocompatibility of the PPMM.

The grafted PGAMA chains serve as a hydrophilic layer to prevent non-specific adsorption. On the other hand, the PAG chains can act as recognition sites for selective capture because of the specific interaction between cyclic sugar moieties and proteins (lectins). This characteristic makes it a very promising kind of affinity membrane. Lectins are a large group of carbohydrate binding proteins and play key roles in various biological processes (Ambrosi et al., 2005; Kennedy et al., 1995). The biological activities of lectins rely greatly on the carbohydrate binding properties which are achieved by the specific recognition between lectins and carbohydrates. Concanavalin A (Con A), the first to be found and most investigated lectin, which specifically recognizes α-glucopyranoside and α-mannopyranoside residues with free 3-, 4-, and 6-hydroxyl groups, was used as the model protein to evaluate the recognition property of the tethered PAG chains (Goldstein et al., 1965).
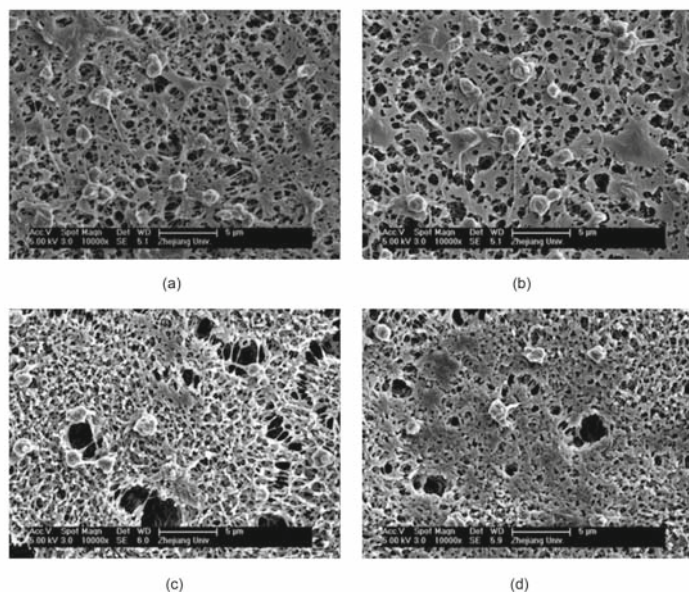
Fig. 7.9. SEM micrographs of adhered platelets on the nascent and modified PP-MMs: (a)∼(d) 0 wt.%; 1.52 wt.%; 4.72 wt.%; 6.28 wt.% GAMA grafted PPMMs, respectively (×10000). Reprinted with permission from (Yang et al., 2005a). Copyright (2003), American Chemical Society

As can be seen from Fig.7.10 and Fig.7.11, the nascent PPMM showed a very little amount of adsorption and weak fluorescence which was caused by physical adsorption of FL-Con A. For the PAG grafted PPMMs with lower GD, weak interactions were also observed and the fluorescence intensity was almost the same as that of the nascent PPMM, which was ascribed to the low affinity ($K_a = 10^3 \sim 10^4$ mol^{-1}) between simple glucoside moieties and Con A. However, when the sugar density on the surface exceeded a critical value (about 90 μg/cm^2 in their case) the interactions obviously increased as a result of the "glycoside cluster effect" (Lee and Lee, 1995; Lundquist and Toone, 2002). Therefore Con A was adsorbed on the membrane surface dramatically. When the sugar density on the membrane surface increased to 220.41 μg/cm^2, the interaction between FL-Con A and glucose residues on the membrane surface obviously increased and bright fluorescence could be observed. Moreover almost no interactions were detected without MnCl$_2$, CaCl$_2$ and NaCl in the buffer solution. Mn^{2+} and Ca^{2+} are two ions essential for the saccharide-binding activity of Con A, while NaCl stabilizes Con A in the solution.

The complex between lectins and glycoligands can be inhibited by the sugar ligands of the same specific lectins (Lis and Sharon, 1998). Fig.7.12
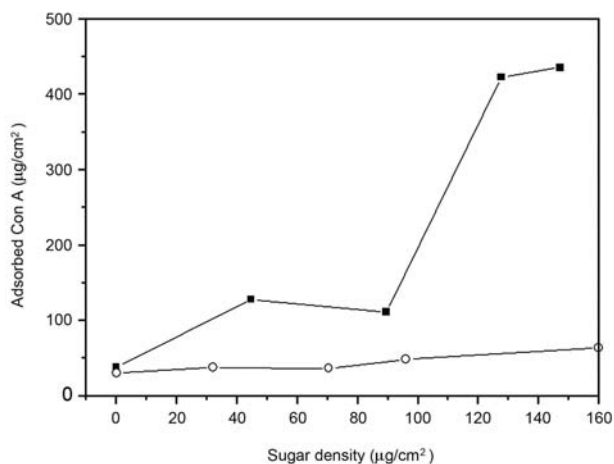
Fig. 7.10. Amount of Con A adsorbed to the PPMM surface with different sugar densities (○: in PBS, ■: in PBS containing 0.1 mmol/L $CaCl_2$, 0.1 mmol/L $MnCl_2$ and 0.1 mol/L NaCl). Reprinted with permission from (Yang et al., 2006a). Copyright (2003), American Chemical Society
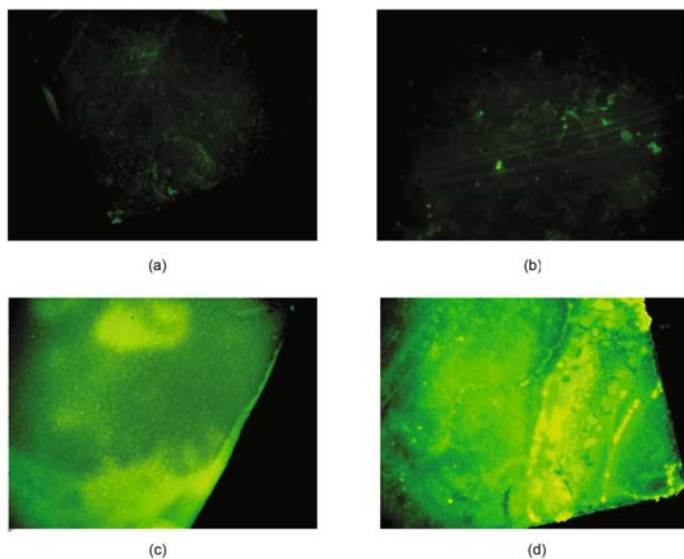
Fig. 7.11. Fluorescence microscope images of PPMMs after FL-Con A adsorption: (a) nascent; (b)∼(d) PPMM-*g*-PAG with grafting densities of 89.80, 187.76 and 220.41 μg/cm^2, respectively. All the images were taken at 40× magnification. Reprinted with permission from (Yang et al., 2008)

shows the fluorescence images of FL-Con A recognized PPMM surfaces after inhibiting with 0.5 g/L glucose solution. As can be seen, FL-Con A banded on the PPMM-*g*-PAG surfaces with higher sugar densities (Figs.7.12(c) and 7.12(d)) was inhibited by glucose solution and the fluorescence intensity clearly decreased. At the same time it was observed that the PPMM-*g*-PAG surface with a sugar density of 220.41 μg/cm^2 showed considerable fluorescence after inhibition with 0.5 g/L glucose solution. This can be ascribed to the strong interactions between the high sugar density surface and FL-Con A. With different sugar concentrations a series of inhibition effects could be achieved. As shown in Figs.7.13(a) and 7.13(b), glucose and mannose exhibit similar inhibition effects. With an increase in the sugar concentration, the fluorescence intensity of the eluent increased first and then reached a platform which indicated the complete inhibition of the recognized Con A. On the other hand, galactose, which is not a Con A binding sugar, has no inhibition effect on the membrane surface recognized by Con A and the eluent solution showed almost no fluorescence (Fig.7.13(c)).
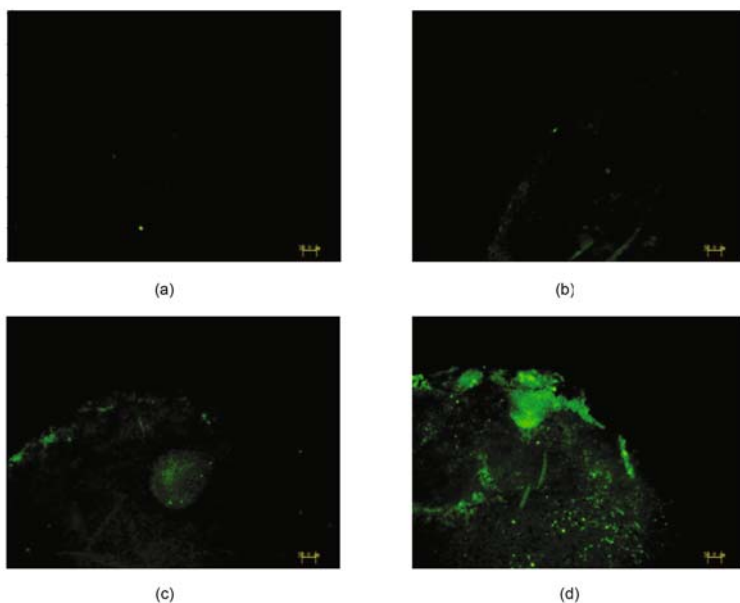
Fig. 7.12. Fluorescence microscope images of FL-Con A adsorbed PPMMs after inhibiting with 0.5 g/L glucose solution: (a) nascent; (b)∼(d) PPMM-*g*-PAG with grafting densities of 89.80, 187.76 and 220.41 μg/cm^2 respectively. All the images were taken at 40× magnification. Reprinted with permission from (Yang et al., 2008).
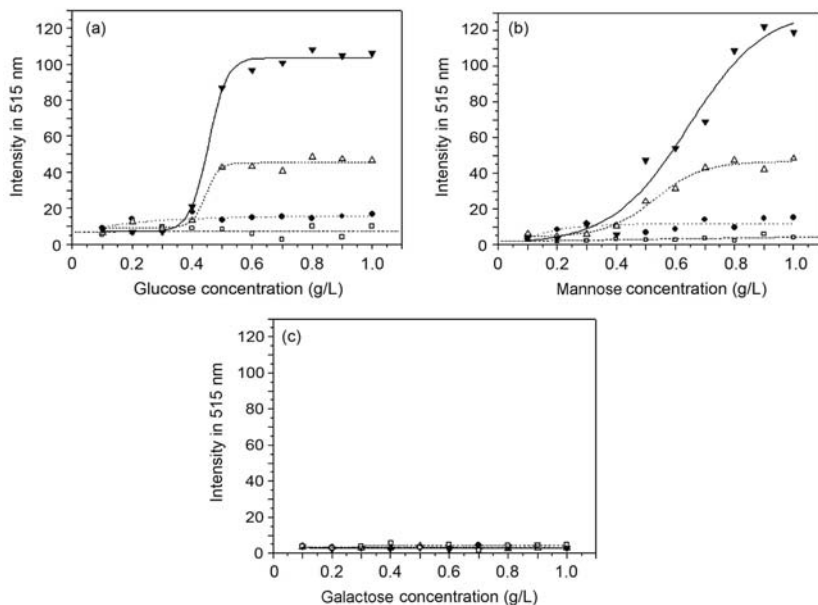
Fig. 7.13. Effect of (a) glucose, (b) mannose and (c) galactose solution concentrations on the fluorescence intensity of the eluent in 515 nm; PAG grafting densities on PPMM: 220.41 (▼), 187.76 (△), 89.80 (●) and 0 (□) μg/cm^2 respectively

7.3.2 Glycosylation by Polymer Analogous Reactions

To avoid complex synthesis procedures, a polymer analogue reaction was also conducted for the construction of the glycosylated membrane surface. Generally two steps were needed. Firstly polymers with functional groups (hydroxyl group, amine group, etc.) were grafted onto the membrane surface. Then sugars were immobilized on the surface by the reactions between the functional groups and sugars. 2-Aminoethyl methacrylate hydrochloride (AEMA) and acrylamide (AAm) were used by Yang et al. (2005b; 2006b) to functionalize the membrane surface and immobilization of linear glucoside moieties was thereafter carried out. They grafted PAEMA chains onto the PPMM surface by UV-induced graft polymerization. Then the hydrochloride protected amine groups were deprotected in the presence of triethylamine and the sugars were immobilized by the reaction between the amine group and D-gluconolactone (Fig.7.14). In another protocol AAm was grafted by UV-induced polymerization and the amide groups were converted to an amine group (Fig.7.15) by Hofmann rearrangement reaction, to immobilize sugars.

After glycosylation, the hydrophilicity of the membrane surface changed and the contact angle measurement over time revealed this variation. The average contact angle of the virgin PPMM was about 142°. After PAEMA grafting all samples exhibited a decrease of hydrophilicity to some extent.
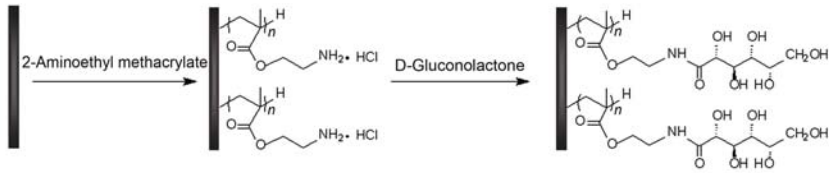
Fig. 7.14. Schematic diagrams illustrating the graft polymerization of AEMA and immobilization of sugars
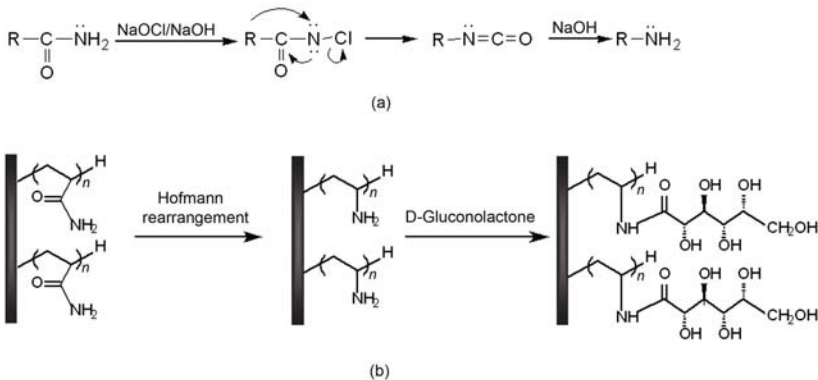
Fig. 7.15. Schematic diagrams illustrating (a) the Hofmann rearrangement reaction and (b) the whole processes for the formation of glycosylated surface

The water drops took about 2000, 2400 and 2800 s to be absorbed into the membrane pores and disappeared completely from the surface of the virgin, 193.20 and 239.46 $\mu g/cm^2$ PAEMA grafted membranes (Figs.7.16(a) and 7.16(b)), respectively. Water generally penetrates into the pores more quickly on the hydrophilic surface than on the hydrophobic one. However, compared with the nascent PPMM, PAEMA grafted membranes had more pores blocked and covered. Thus the latter had a lower water adsorption rate. For the same reason water drops took more time (about 1500 s) to disappear from the glycopolymer tethered membrane surface with a higher sugar density (Fig.7.16(d)), which was more hydrophilic than that with a lower sugar density (about 1250 s, Fig. 7.16(c)).

As mentioned above, the non-specific adsorption of proteins in dynamic filtration can be obviously reduced by surface glycosylation. The anti-fouling property in a static situation was also evaluated. BSA was used as the model protein to evaluate the adsorption of proteins on nascent PAEMA grafted and glycosylated PPMM. Typical results are shown in Fig.7.17. It was found that at low BSA concentrations (1 and 2 g/L) almost the same amount of BSA was adsorbed on these different surfaces. However, the PAEMA grafted membrane still showed some reduction. It could be ascribed to the reason
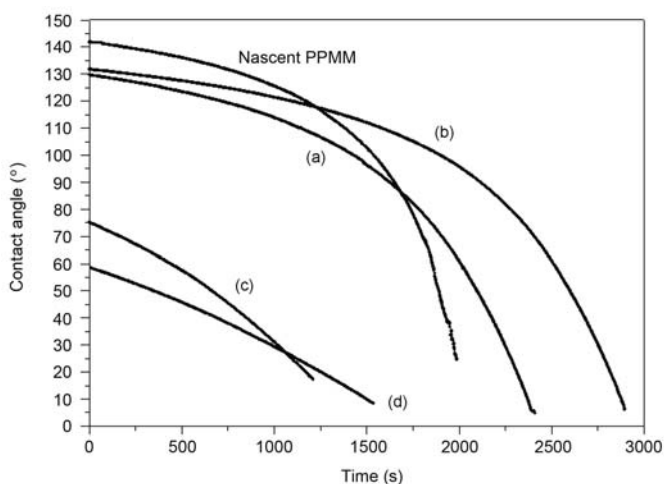
Fig. 7.16. Time dependence of water contact angles: (a) PPMM-*g*-PAEMA (GD = 193.20 μg/cm^2); (b) PPMM-*g*-PAEMA (GD = 239.46 μg/cm^2); (c) PPMM-*g*-GP(BD = 84.36 μg/cm^2); (d) PPMM-*g*-GP (BD = 136.10 μg/cm^2). Reprinted with permission from (Yang et al., 2005b). Copyright (2005), American Chemical Society

that the grafted PAEMA chains were somehow more hydrophilic than in the case of the nascent membrane. For the higher BSA concentration cases (5 and 10 g/L), glycosylated membranes showed the lowest amount of adsorbed BSA.

7.3.3 Glycosylation by Surface Initiated Living Polymerization

Glycopolymers can be introduced onto the polymer membrane surface by UV-induced graft polymerizations and polymer analogue reactions to give high valency ligands tethered surfaces. However, conventional graft techniques suffer a lack of control over molecular structures (molecular weight and polydispersity) and are incapable of further increasing the sugar density (ligand valency). On the other hand, it is also suggested that random clustering of carbohydrates sometimes reduces the strength of affinity with guest proteins owing to the sterically hindered sugar branches (Nagahori and Nishimura, 2001). In other words, the glycopolymer chain length may largely affect the recognition activity (Mann et al., 1998). In consequence, the generation of glycopolymers with a well-defined chain structure and appropriate sugar density is greatly demanded. Yang et al. (2007) established two methods for the construction of a glycosylated membrane surface with controlled molecular weight and structures (linear and comb-like).

For the preparation of the comb-like glycopolymer brushes, poly(2-hydroxylethyl methacrylate) (PHEMA) with hydroxyl groups was grafted to the
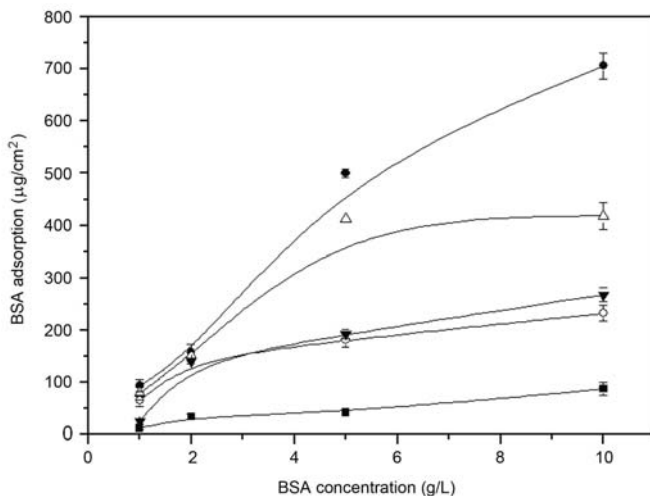
Fig. 7.17. BSA adsorption at (•) nascent PPMM, ($\triangle$) 310.20 μg/cm^2 PAEMA garfted PPMM, (▼) 75.36 μg/cm^2 PGAMA grafted PPMM, (○) 167.00 μg/cm^2 PGAMA grafted PPMM and (■) 225.79 μg/cm^2 PGAMA grafted PPMM surfaces. Reprinted with permission from (Yang et al., 2005b). Copyright (2005), American Chemical Society

PPMM surface by UV-induced graft polymerizations. Then α-Haloester was immobilized to the PHEMA by reaction with the hydroxyl groups and served as the initiator for the further ATRP of the glycomonomer. By varying the ATRP time, comb-like glycopolymer brushes with different chain lengths were introduced to the surface (Fig.7.18(a)). On the other hand, for the linear glycopolymer brushes, bromine was first immobilized to the membrane surface. The membrane was immersed in bromine solution (in CCl$_4$) and then exposed to UV irradiation. Afterwards the surface immobilized bromine initiated ATRP of GAMA and linear glycopolymer was grafted onto the membrane surface (Fig. 7.18(b)).

Different chain structures showed very different images on AFM. As can be seen from Fig.7.19, the nascent PPMM showed a relatively smooth surface and the pores were also visible. After PGAMA grafting the polymer layer could obviously be found and the membrane pores were covered. However, the comb-like PGAMA chains showed a more extended form than that of the linear ones. This can be ascribed to the crowded side chains of the comb-like structure. With the increase in the chain lengths, the comb-like PGAMA chains huddled together and showed an almost conterminous layer. On the other hand, the linear PGAMA chains showed no significant difference with an increase in chain lengths.

Different chain structures also exhibited different performances in preventing non-specific adsorption. As shown in Table 7.2, proteins were adsorbed on
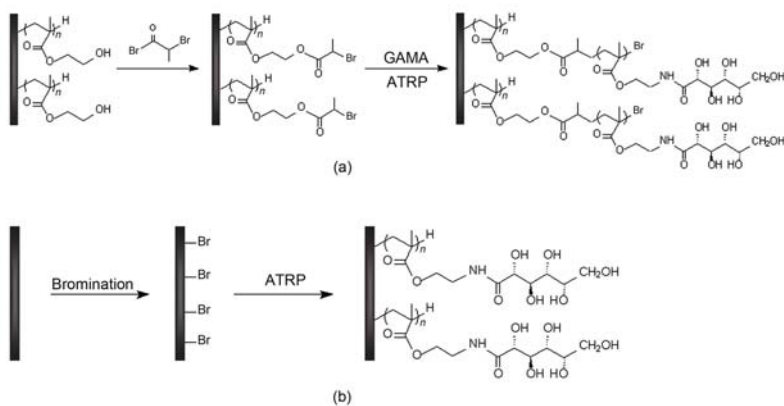
Fig. 7.18. Schematic diagrams illustrating surface initiated living polymerization for construction of comb-like (a) and linear (b) glycopolymer tethered membrane surface
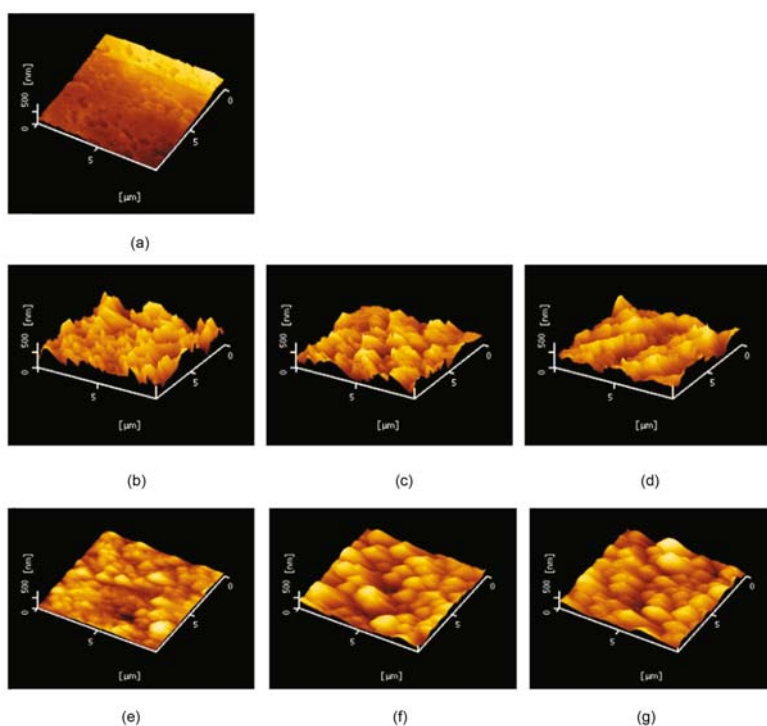
Fig. 7.19. AFM images of (a) nascent PPMM, (b)~(d) PPMM modified by comb-like glycopolymer with chain lengths of 5, 12 and 20 respectively and (e)~(f) PPMM modified by linear glycopolymers with chain lengths of 4, 8 and 12 respectively

brominated PPMM dramatically. PHEMA grafting could reduce the protein adsorption to some extent. After glycosylation the non-specific adsorption of proteins was reduced greatly and the repulsion effect increased with the increase in the chain length. Moreover, the comb-like structure exhibited much stronger repulsion to protein adsorption than the linear one. This may be ascribed to the much denser structure of the comb-like chains (Fig.7.20).

Table 7.2. BSA adsorptions on glycopolymer tethered PPMMs with different chain structures and chain lengths

Chain structure	DP	Adsorbed BSA ($\mu g/cm^2$)
	0^a	282.31 ± 9.64
	4	103.40 ± 10.27
Comb-like	12	0^c
	20	0^c
	0^b	398.64 ± 9.20
	5	115.65 ± 7.17
Linear	10	68.03 ± 8.27
	18	57.14 ± 6.13

[a]PHEMA grafted PPMM after immobilization of BPB; [b]brominated PPMM; [c]changes can not be detected, and the samples showed almost the same absorbance at 595 nm as the original 5 g/L BSA solution
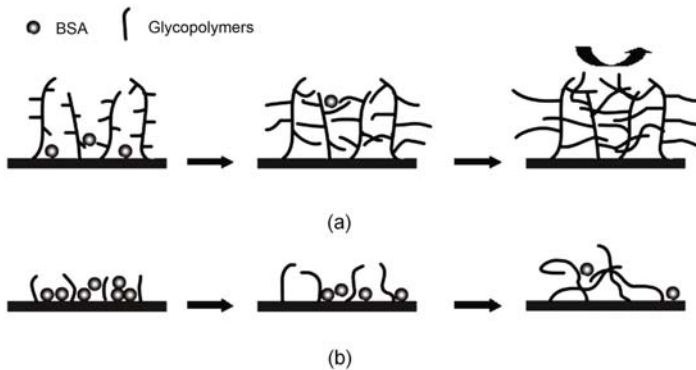
Fig. 7.20. Schematic drawing illustrating protein adsorption on (a) comb-like and (b) linear glycopolymer tethered membrane surfaces

7.4 Conclusion

Membrane surface glycosylation was successfully carried out with both natural polysaccharides, such as heparin and chitosan, and synthetic glycopoly-

mers for different purposes. Naturally existing polysaccharides are abundant and usually have specific characteristics such as anti-coagulation and biocompatibility. In general, natural polysaccharides were immobilized to the membrane surface by the reactions between polysaccharides and the membrane surface. For this purpose the membranes often need activation to generate some active groups (–OH, –NH$_3$, and –OOH, etc.) and sometimes coupling agents are necessary. For glycosylation with synthetic glycopolymers, surface initiated graft polymerizations and polymer analogous reactions were applied. Both conventional techniques, such as UV irradiation and plasma treatment and more advanced living/controlled processes were conducted for graft polymerization. Conventional methods are easy to carry out and are versatile. On the other hand, living/controlled processes gave us a chance to modulate the glycosylation procedure and to control the properties of tethered glycopolymers. By varying the structure of the initiators on the membrane surface, glycosylation with comb-like and linear glycopolymers was achieved. With a different polymerization time, the chain length of the grafted glycopolymer could be controlled. With a glycosylated surface, membrane performances such as water flux, anti-non-specific adsorption and hemocompatibility were obviously improved. In addition, endowing the membranes with a specific recognition property will be a very useful method in fabricating affinity membranes for the selective capture of a virus as well as for drug delivery and protein separation systems.

References

Alsarra IA, Betigeri SS, Zhang H, Evans BA, Neau SH (2002) Molecular weight and degree of deacetylation effects on lipase-loaded chitosan bead characteristics. Biomaterials 23:3637-3644

Alsarra IA, Neau SH, Howard MA (2004) Effects of preparative parameters on the properties of chitosan hydrogel beads containing Candida rugosa lipase. Biomaterials 25:2645-2655

Ambrosi M, Cameron NR, Davis BG (2005) Lectins: tools for the molecular understanding of the glycocode. Org Biomol Chem 3:1593-1608

Berlo AV, Ellens DJ (1988) Biocompatibility of haemodialysis membranes. Adv Exp Med Biol 238:341-358

Cairo CW, Gestwicki JE, Kanai M, Kiessling LL (2002) Control of multivalent interactions by binding epitope density. J Am Chem Soc 124:1615-1619

Cheung AK, Chenoweth DE, Otsuka D, Henderson LW (1986) Compartmental distribution of complement activation products in artifical kidneys. Kindney Int 30:74-80

Deppisch R, Storr M, Buck R, Gohl H (1998) Blood material interactions at the surfaces of membranes in medical applications. Sep Purif Technol 14:241-254

Docci D, Delvecchio C, Turci F, Baldrati L, Gollini C (1988) Effect of different dialyzer membranes on serum angiotensin-converting enzyme during hemodialysis. Int J Artif Org 11:28-32

Dwek RA (1996) Glycobiology: toward understanding the function of sugars. Chem Rev 96:683-720

Gestwicki JE, Cairo CW, Strong LE, Oetjen KA, Kiessling LL (2002) Influencing receptor-ligand binding mechanisms with multivalent ligand architecture. J Am Chem Soc 124:14922-14933

Goldstein IJ, Hollerman CE, Smith EE (1965) Protein-carbohydrate interaction. 11. inhibition studies on the interaction of concanavalin A with polysaccharides. Biochemistry 4:876-883

Hinrichs WLJ, tenHoopen HWM, Engbers GHM, Feijen J (1997) In vitro evaluation of heparinized Cuprophan hemodialysis membranes. J Biomed Mater Res 35:443-450

Ho CC, Zydney AL (2001) Protein fouling of asymmetric and composite microfiltration membranes. Ind Eng Chem Res 40:1412-1421

Holland NB, Qiu YX, Ruegsegger M, Marchant RE (1998) Biomimetic engineering of non-adhesive glycocalyx-like surfaces using oligosaccharide surfactant polymers. Nature 392:799-801

Huang RH, Chen GH, Sun MK, Hu YM, Gao CJ (2006) Studies on nanofiltration membrane formed by diisocyanate crosslinking of quaternized chitosan on poly (acrylonitrile) (PAN) support. J Membrane Sci 286:237-244

Kazatchkine MD, Fearon DT, Silbert JE, Austen FK (1979) Surface-associated heparin inhibits zymosaninduced complement pathway by augmenting the regulatory action of the control proteins on particlebound C3b. J Exp Med 150:1202-1215

Kelly ST, Zydney AL (1995) Mechanisms for BSA fouling during microfiltration. J Membrane Sci 107:115-127

Kennedy JF, Palva PMG, Corella MTS, Cavalcanti MSM, Coelho LCBB (1995) Lectins, versatile proteins of recognition: a review. Carbohyd Polym 26:219-230

Klein E (2000) Affinity membranes: a 10-year review. J Membrane Sci 179:1-27

Kou RQ, Xu ZK, Deng HT, Liu ZM, Seta P, Xu YY (2003) Surface modification of microporous polypropylene membranes by plasma-induced graft polymerization of α-allyl glucoside. Langmuir 19:6869-6875

Kung FC, Chou WL, Yang MC (2006) In vitro evaluation of cellulose acetate hemodialyzer immobilized with heparin. Polym Adv Technol 17:453-462

Lee YC, Lee RT (1995) Carbohydrate-protein interactions: Basis of glycobiology. Acc Chem Res 28:321-327

Lim AL, Bai R (2003) Membrane fouling and cleaning in microfiltration of activated sludge wastewater. J Membrane Sci 216:279-290

Lin WC, Tseng CH, Yang MC (2005) In-vitro hemocompatibility evaluation of a thermoplastic polyurethane membrane with surface-immobilized water-soluble chitosan and heparin. Macromol Biosci 5:1013-1021

Lis H, Sharon N (1998) Lectins: Carbohydrate-specific proteins that mediate cellular recognition. Chem Rev 98:637-674

Luk YY, Kato M, Mrksich M (2000) Self-assembled monolayers of alkanethiolates presenting mannitol groups are inert to protein adsorption and cell attachment. Langmuir 16:9604-9608

Lundquist JJ, Toone EJ (2002) The cluster glycoside effect. Chem Rev 102:555-578

Maillet F, Labarre D, Kazatchkine MD (1990) The role of naturally-occurring antibodies against manmade materials in biocompatibility. Transf Sci 11:33-41

Mann DA, Kanai M, Maly DJ, Kiessling LL (1998) Probing low affinity and multivalent interactions with surface plasmon resonance: Ligands for concanavalin A. J Am Chem Soc 120:10575-10582

Musale DA, Kumar A (2000) Effects of surface crosslinking on sieving characteristics chitosan/poly(acrylonitrile) composite nanofiltration membranes. Sep Purif Technol 21:27-38

Nagahori N, Nishimura SI (2001) Tailored glycopolymers: Controlling the carbohydrate-protein interaction based on template effect. Biomacromolecules 2:22-24

Nie FQ, Xu ZK, Huang XJ, Ye P, Wu J (2003) Acrylonitrile-based copolymer membranes containing reactive groups: Surface modification by the immobilization of poly(ethylene glycol) for improving antifouling property and biocompatibility. Langmuir 19:9889-9895

Ostuni E, Chapman RG, Holmlin RE, Takayama S, Whitesides GM (2001) A survey of structure-property relationships of surfaces that resist the adsorption of protein. Langmuir 17:5605-5620

Peppas N, Langer R (1994) New challenges in biomaterials. Science 263:1715-1720

Steen AVD (1986) Research on dialyzers with improved biocompatibility. Clin Nephrol 26:S39-S42

Tan SZ, Chen ZH, Chen ZH (2002) Preparation of polyacrylonitrile nanofiltration membrane and its separation property in the treatment of papermaking effluent. Transac China Pulp Paper 17:63-66

Xu ZK, Dai QW, Wu J, Huang XJ, Yang Q (2004) Covalent attachment of phospholipid analogous polymers to modify a polymeric membrane surface: A novel approach. Langmuir 20:1481-1488

Yang Q, Hu MX, Dai ZW, Tian J, Xu ZK (2006a) Fabrication of glycosylated surface on polymer membrane by UV-induced graft polymerization for lectin recognition. Langmuir 22:9345-9349

Yang Q, Tian J, Dai ZW, Hu MX, Xu ZK (2006b) Novel photoinduced grafting-chemical reaction sequence for the construction of a glycosylation surface. Langmuir 22:10097-10102

Yang Q, Tian J, Hu MX, Xu ZK (2007) Construction of a comb-like glycosylated membrane surface by a combination of UV-induced graft polymerization and surface-initiated ATRP. Langmuir 23:6684-6690

Yang Q, Wan LS, Xu ZK (2008) Interaction of the glycosylated polypropylene mambrane with lectin. Chinese J Polym Sci 26:363-367

Yang Q, Xu ZK, Dai ZW, Wang JL, Ulbricht M (2005a) Surface modification of polypropylene microporous membranes with a novel glycopolymer. Chem Mater 17:3050-3058

Yang Q, Xu ZK, Hu MX, Li JJ, Wu J (2005b) Novel sequence for generating glycopolymer tethered on a membrane surface. Langmuir 21:10717-10723

Yu J, Lamba NMK, Courtney JM, Whateley TL, Gaylor JDS, Lowe GDO, Ishihara K, Nakabayashi N (1994) Polymeric biomaterials: Influence of phosphorylcholine polar groups on protein adsorption and complement activation. Int J Artif Org 17:499-504

8

Molecularly Imprinted Membranes

Molecular imprinting technology, which originates from the molecular recognition phenomenon in biological systems, has been receiving much attention and already rapid developments have been achieved in recent years. A molecularly imprinted membrane is characterized by selective recognition, high binding capacity and excellent permeability. It is helpful for separation in large-scale applications and especially for the recognition of natural biomacromolecules. In this chapter the basic concept and theory of molecular imprinting are simply described for an understanding of the principles underlying the technique. Then the preparation and application of molecularly imprinted membranes are well presented and summarized.

8.1 Introduction

Molecular recognition is a fundamental biological process characterized by selection and recognition. It is the basis of most biological functions such as enzyme-substrate recognition, antigen-antibody binding, DNA replication, transcription and translation. Thus it is recognized as a universal but special phenomenon in the entire biological world. Over one hundred years ago Fischer in his Noble lecture in chemistry visually described this specific binding using "lock and key" for comparison. Because biomacromolecules such as enzymes, antibodies and receptors easily lose their properties under rigorous conditions, they are hard to be extracted, stored and used. Thus their production and application is greatly limited. For this reason synthetic recognition systems have attracted much attention over the past few decades. In the beginning some scientists attempted to use small ring-like molecules or coronal-like molecules such as crown ether, cyclodextrin and calixarene to simulate biological systems. However, the structures of these small molecules are relatively complicated and multi-step procedures required for the preparation of these hosts are sometimes tedious, causing low yields and the specificity of synthesized materials is not always high. Nowadays how to prepare

a host in a simple operation, at low cost, but with good stability, especially predicted selectivity and binding capability with the enzyme, antibody and receptor turns out to be one of the toughest problems in the world.

Molecular imprinting technology (MIT) originated from the concept of molecular recognition, which can realize special recognition at the molecular level. Based on the interaction of antigen-antibody, molecular imprinting is a new comprehensive subject, studied in combination with the development of biochemistry, structural chemistry and materials chemistry. It is recognized as the necessary outcome of continuous research and exploration of the molecular recognition phenomenon in biology.

8.1.1 Development of Molecular Imprinting Technology

The appearance of MIT benefits from the development of immunology. In 1940s Pauling tried to explain the real reason for the formation of an antibody and proposed the assumption that antigen could be used as the template to synthesize the antibody (Pauling and Campbell, 1942). The basic point of Pauling's theory of antibody formation was that when an antibody was produced, its three-dimensional structure could form multi-point interaction with antigen as much as possible and then antigen would be "memorized" at the binding sites of the antibody. Although Pauling's theory of antibody formation was overthrown by the "Clone technique", it established the theoretical foundation for the development of molecular imprinting.

In 1949 Dickey (1955) proposed the concept of "specific adsorption", which was considered as the threshold of "molecular imprinting". In 1972 Wulff and his co-workers reported their work on the successful preparation of a molecularly imprinted polymer for the first time (Wulff and Sarhan, 1972). Since then MIT has gradually become known. It has achieved vigorous development since Vlatakis et al. (1993) published a paper about a theophylline-imprinted polymer in *Nature* in 1993, and in 1995 MIT was used for the separation and purification of proteins by Kempe and Mosbach (1995). Thus it achieved more rapid development. The annual number of scientific publications increased as a linear rising tendency. In 1992 the number of publications was only 12 and in 1999 it was about 160. By 2001 this number had increased to ca. 270. The detailed statistics of these publications is illustrated in Fig.8.1.

To sum up, MIT has achieved an enormous breakthrough and rapid development in the past 30 years since Wulff's work in 1972. Especially in the past 10 years, molecular imprinting as well as its recognition mechanism has been more clearly known and the corresponding molecularly imprinted materials have been used in extensive applications. Up to now several reviews have been published to report the acquired results in detail (Alexander et al., 2006; Andersson, 2000; Brügemann et al., 2000; Cormack and Mosbach, 1999; Haupt, 2003; Haupt and Mosbach, 2000; Marty and Mauzac, 2005; Mosbach, 2001; Piletsky et al., 1999; 2001; Takeuchi and Haginakab, 1999; Turner et
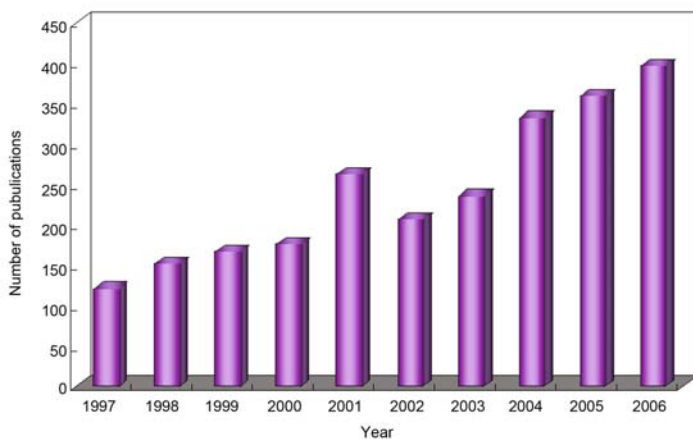
Fig. 8.1. The annual number of scientific publications on the term of "molecular imprinting OR molecularly imprinted", which was provided by Web of Science in 2007

al., 2006; Ulbricht, 2004; Whitcombe and Vulfson, 2001; Wulff, 1995; Ye and Mosbach, 2001).

8.1.2 Basic Theory of Molecular Imprinting Technology

8.1.2.1 Preparation of Molecularly Imprinted Polymer (MIP)

As shown in Fig.8.2, the preparation of a molecularly imprinted polymer is the core part of the molecular imprinting process. It includes three steps: (1) the functional monomers are arranged around the template to form a complex in a proper media; (2) the crosslinkers and initiators are then added into the complex system, thus the interaction between functional monomers and the template is fixed by polymerization under the effect of heat or light; (3) the template is removed from the polymerized complex using a chemical or physical method, then cavities matched exactly with the template by shape, size and the position of functional groups are exposed. Afterwards these cavities of MIP can selectively rebind the template from its substrate solution. The repeated operation can be realized followed by dissociation and association procedures. Thus the MIP can be recycled until the binding sites do not work completely.

8.1.2.2 Binding Types between the Monomer and the Template

Admittedly there are two main types (preorganization and self-assembly) based on various interactions between the monomer and the template during
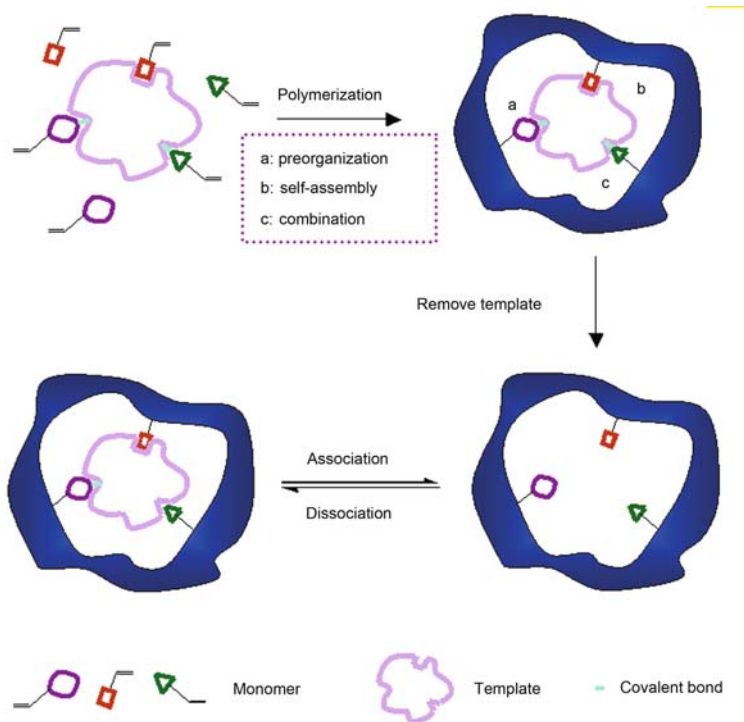
Fig. 8.2. Schematic representation of molecular imprinting process (Alexander et al., 2006). Copyright (2006). Reprinted with permission of John Wiley & Sons, Inc.

a complex formation process. However, it is notable that there is also another type that is deemed as "sacrificial space" utilizing covalent bonding to form the complex and non-covalent bonding to recognize the template.

8.1.2.2.1 Preorganization Method

Preorganization is also called covalent bonding, which was proposed by Wulff and Sarhan (1972) in Germany in the early 1970s. In this method the complex is formed through a reversible covalent bonding between the template and the functional monomer and then polymerization is proceeded by adding crosslinker and initiator. The template is removed by the cleavage of covalent bonding. After that the resultant MIP can rebind the template exactly, through the residual cavities complementary to the removed template covalently. Up to now this method has been commonly applied to some special materials such as boronic esters, shiff base, acetal (ketal), ester, and metal ordination compound.

A typical illustration is the preparation of carbohydrate derivatives imprinted polymers, as shown in Fig.8.3 (Wulff and Schauhoff, 1991). In this work the complex was formed by galactose and 4-vinyl boronic acid via ester-

ification between the two hydroxy groups on the carbohydrate and boronic acid groups and then fixed by free radical polymerization. Under alkaline conditions, the template could be removed from the imprinted polymer. The cavities in the polymer was complementary to the template shape and capable of binding the template selectively.
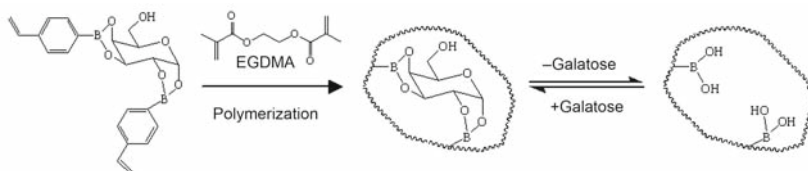
Fig. 8.3. Typical illustration of the preorganization method. Reprinted with permission from (Wulff and Schauhoff, 1991). Copyright (1991), American Chemical Society

The covalent bonding method has many advantages that are comparatively stable template-monomer complex, not rigorous polymerization conditions such as a slightly high temperature, various pH values and highly polar solvent. However, there are still some disadvantages for the imprinting application including : (1) the preparation process of the template-monomer complex is complicated and very costly; (2) the rate of association and dissociation is relatively low due to the formation and cleavage of covalent bonding between the template and the monomer; (3) because of the limited reversible bonding forms, the applied templates and monomers are restricted; (4) what is more important, this interaction differs from natural recognition in biological systems. As a result, the preorganization method progressed slowly.

8.1.2.2.2 Self-assembly Method

The self-assembly method is also called non-covalent bonding, which was proposed by Sellergren et al. (1988) in Sweden in the late 1980s. In this method the template-monomer complex is arranged by one or more kinds of non-covalent interactions and retained in the presence of crosslinker after polymerization. After removal of the template, the resultant imprinted polymer can rebind the template smartly from its substrate solution through the association of non-covalent bonding.

Non-covalent bonding includes hydrogen bonding, electrostatic attraction, metal chelation, charge transfer, hydrophobic interaction and van der Waals force. Among these, hydrogen bonding has been the most widely used up to now. Mathew-Krotz and Shea (1996) selected methylacrylic acid as the functional monomer to interact with 9-ethyl adenine via multiple hydrogen bonding. As a result a highly selective imprinted membrane was obtained, as shown in Fig.8.4.
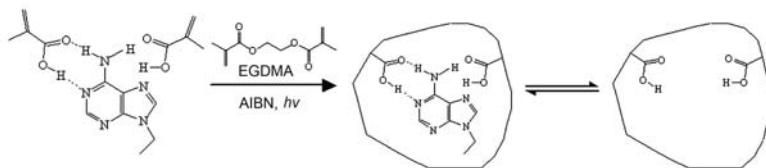
Fig. 8.4. Typical representation of the self-assembling method. Reprinted with permission from (Mathew-Krotz and Shea, 1996). Copyright (1996), American Chemical Society

It is worth mentioning that for one certain template several monomers can be simultaneously used to form the template-monomer complex with the help of different kinds of interactions. In this case uptake of the template by the resultant imprinted polymer is higher relative to that of an imprinted polymer with a single kind of interaction.

In the self-assembly method the polymerization should be realized in a certain condition in order to avoid any possible damage to the non-covalent bonding. Moreover, the presence of nonspecific binding may result in low selectivity. However, compared with the preorganization method, the preparation is relatively easy and the template can easily be removed. In particular, the recognition process is close to the recognition system of natural macromolecules, such as an antigen-antibody and enzyme-substrate. Therefore there are reasons for believing that the self-assembly method has good scope for development.

8.1.2.2.3 Sacrificial Spacer Method

In recent years Whitcombe et al. (1995) has established another new imprinting approach called the "sacrificial spacer" method, which results from the combination of the advantanges of preorganization and self-assembly. In this method the complex was formed with covalent bonding in consistence with the preorganization process, whereas the recognition process was realized by non-covalent bonding. The detailed preparation process is given in Fig.8.5.

The sacrificial spacer method has integrated the high specificity of covalent bonding with the mild operational conditions of non-covalent bonding. Furthermore the applied functional groups are evidently increased, involving amino, mercapto, and hydroxy groups. In addition this approach can also be used for weak hydrogen recognition that can be realized in the self-assembly method.
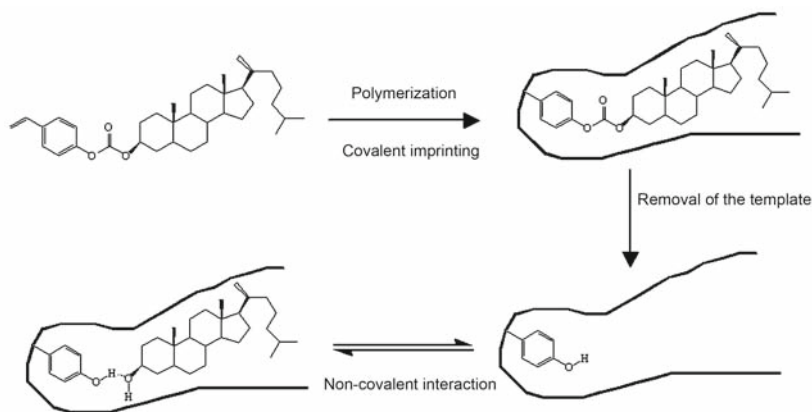
Fig. 8.5. Representative process of the space sacrifice method. Reprinted with permission from (Whitcombe et al., 1995). Copyright (1995), American Chemical Society

8.2 Preparation Methods and Morphologies of Molecularly Imprinted Membranes

Because of its stability, preparation with ease and feasibility in different kinds of conditions, MIPs exhibit extensive perspectives in many fields of application, such as chromatography, solid phase extraction, biosensors and membrane separation. Thus membrane separation, which is characterized by selective transport of a particular target molecule and rejection (or at much lower transport rates) of other molecules, can be operated continuously and easily with high efficiency. Due to less energy consumption compared with other competing separation technologies, membrane separation is always viewed as an example of "green chemistry". Moreover, the process can be used for a large-scale continuous operation, especially in industrial applications. Combining membrane separation with MIT, the molecularly imprinted membrane (MIM) is easily obtained. The specific selectivity of MIM will be greatly improved in comparison with a traditional membrane but without decreasing the separation efficiency. Therefore it is believed that MIM will be one of the materials with the most potential in the new century. So far several reviews have reported achieved results in detail (Piletsky et al., 1999; Ulbricht, 2004; Yoshikawa, 2002).

In order to improve the permeability and selectivity of MIM and simultaneously simplify the preparation process, many methods have been attempted using the continuous efforts of many scientists. Up to now the main preparation methods reported have been summarized, including bulk polymerization, physical mixing and surface imprinting.

8.2.1 Bulk Polymerization

Bulk polymerization is a simple and direct method and thus receives much attention, whereby in situ crosslinking polymerization is firstly introduced to MIT. Later a bulk composite membrane is prepared as a novel material for comparative research.

8.2.1.1 *In situ* Crosslinking Polymerization

MIM was prepared for the first time by Piletsky et al. (1990) using an *in situ* crosslinking polymerization method in 1990. This MIM was successfully used to rebind and separate adenosine monophosphate (AMP).

After which a free-standing imprinted membrane containing 9-ethyl adenine (9-EA) as the template, methyl methacrylic acid as the functional monomer and ethylene glycol dimethacrylate as the crosslinker was prepared on silanized glass slides at 65∼70 °C by Mathew-Krotz and Shea (1996), which was used to study the selective transport of some natural macromolecules. It was found that adenine was transported at a higher rate than cytosine or thymine, but the magnitude was only 10^{-10} mol/(cm²·h) attributable to the closely packed membrane structure observed by scanning electron microscopy (SEM). Furthermore, the selectivity factor defined by the rate ratio of transport for adenosine/guanosine in methanol/chloroform (6/94, v/v) was tested, which could reach 3.4.

To maintain the imprinted cavities, a large amount of crosslinkers are required in this method to fabricate a highly crosslinked network. However, too many crosslinkers may certainly affect the mechanical properties of the imprinted materials, thus leading to the formation of membranes that are fragile and brittle. In the meantime there is another problem, namely that the flux in this method is often low, resulting from the low porosity. Both of these two problems will affect their applications for separation, hence a series of researches about how to solve these problems have been carried out. One idea is to enhance the mechanical properties and flexibility by adding linear polymers into the polymer systems, and the other is to introduce additional pores with the help of porogen.

Atrazine-imprinted membranes, which were prepared by copolymerization of methacrylic acid and tri(ethylene glycol) dimethacrylate in the presence of atrazine in (Sergeyeva et al., 1999), were used as the recognition element of sensitive conductimetric sensors. To improve the flexibility and mechanical stability of these membranes, oligourethane acrylate (OUA) was added to the polymerization system. Simultaneously, chloroform was used as a porogen to increase the porosity. It was shown that when the mass ratio of the crosslinker to OUA was 85/15 and the concentration of porogen reached 30 wt.%, the resulting imprinted membranes had a higher binding capacity and stronger responses to atrazine than its analogous compounds.

Subsequently Sergeyeva et al. (2003) attempted other methods to improve the porosity. Atrazine-imprinted membranes were still prepared as a model by UV-initiated polymerization. To get a high-flux membrane, organic solvents with different polarities such as methyl ethyl ketone, ethyl acetate, chloroform, toluene and dimethylformamide were used as porogens. It was found that the introduction of dimethylformamide as the poor solvent was conductive to the formation of porous membranes. The water flux could reach 3045 L/(m^2·h) due to an earlier onset of phase separation which facilitated the generation of large pores. Linear polymers, like poly(ethylene glycol) (PEG) and polyurethane (Sergeyeva et al., 2007), were further studied in order to increase the through-membrane pores. It was shown that when the polymerization system was added into 15 wt.% PEG (M_w 2000), the water flux of the resultant membranes could be significantly increased to 10791 L/(m^2·h). It was supposed that PEG facilitated phase separation similar to the effect of "poor" solvent, which resulted in a semi-interpenetrating polymer network (semi-IPN) between the crosslinked copolymer and PEG.

An uranyl ion-imprinted membrane was also prepared by Kimaro et al. (2001) using in situ crosslinking polymerization containing styrene as the matrix monomer, divinylbenzene as the crosslinking monomer, and uranyl vinylbenzoate as the ion imprinting complex for the selective transport of metal ions. The polyester was added to create channels directing ion migration to the imprinted sites. As a result, the permeability was greatly optimized and that was favorable for selectively rebinding the uranyl ion.

Recently spin coating has been regarded as a straightforward approach for in situ synthesis of MIP films with good control of the thickness and the porosity. A pre-polymerization mixture was first spread onto a substrate and then a rapid curing of films was realized with UV light. Relative to the non-porous films the use of a low volatility solvent in combination with a linear polymer porogen led to a high porosity and a high binding capacity. Since this technique can easily be adapted to prepare films as thin as tens of nanometers, it could enable its use as recognition elements for a variety of chemical sensing platforms (Das et al., 2003; Schmidt et al., 2005; Schmidt and Haupt, 2005).

8.2.1.2 Membrane Surface Bulk Polymerization

A composite imprinted membrane (thickness of the selectively permeable ultrathin layer is ca. 500 nm) was prepared by Hong et al. (1998) in Martin's group through photopolymerization on the surface of a microporous alumina support membrane. The results indicated that the flux was dramatically improved to 10^{-8} mol/(cm^2·h) and a good selectivity factor ($\alpha = 5.0$) was observed for the template relative to its analogue.

Lehmann et al. (2002) explored a new approach to a bulk composite membrane, as illustrated in Fig.8.6. In this method, L-BFA or D-BFA (a chiral amino acid derivative) imprinted nanoparticles, with a diameter range

of 50 to 100 nm, were firstly synthesized by mini-emulsion polymerization, which served as the recognition parts after the deposition process on a porous polyamide membrane, and then the nanoparticles were covered with another porous polyamide membrane. Hence it seems that the whole structure of the composite membrane is like a hamburger. The imprinted nanoparticles with cost-efficient support membranes could provide a high selective rebinding and have potential application in the purification and sensing process. It is considered a novel and efficient method. However, because of the presence of a dense particle layer, the flow rate is limited and improvement is still required.
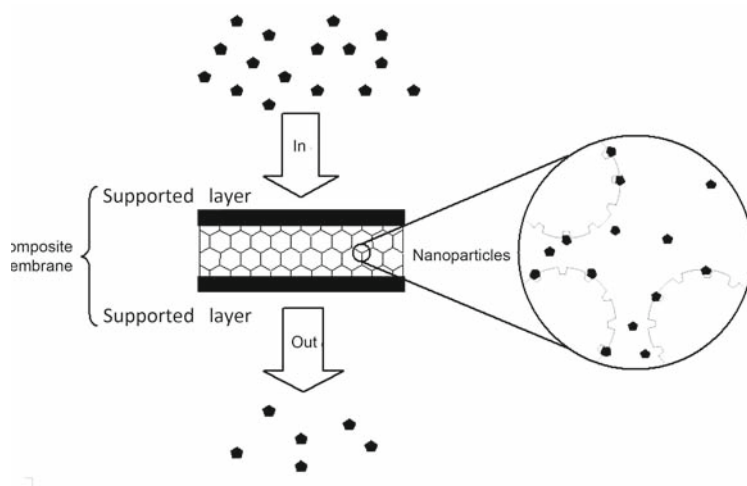
Fig. 8.6. Typical composite membrane proposed by Lehmann. Reprinted from (Lehmam et al., 2002). Copyright (2002), with permission from Elsevier

To obtain mechanically stable and high-flux membranes for separation applications, the imprinted polymers were also in situ synthesized in porous polymer solid supports, such as polypropylene membrane (Donato et al., 2005; Dzgoev and Haupt, 1999), cellulose acetate membrane (Chen et al., 2006), nylon-6 membrane (Hu and Li, 2006) and filtered paper (Kielczynski and Bryjak, 2005). High transport selectivity was normally observed, which confirmed the feasibility of this approach.

8.2.2 Physical Mixing

Although the preparation of MIM by in situ crosslinking polymerization is simple, the flux is relatively low and not applied to selective separation in the absence of the porogen. If a porogen was used in this process, removal of the porogen sometimes would destroy the efficient imprinted cavities and thus

affect the imprinting efficiency. For this reason physical mixing is introduced to fabricate the porous membranes directly, whereby phase inversion is the main method for molecular imprinting research. According to the different preparation conditions, phase inversion can be divided into dry phase inversion and immersed precipitation phase inversion. Moreover, much attention has also been paid to electrospinning in the preparation of MIM recently. The high porosity of an electrospun nanofibrous membrane would facilitate an improvement in permeability.

8.2.2.1 Dry Phase Inversion

Yoshikawa et al. (1995) firstly introduced dry phase inversion into MIT in 1995. In their work a copolymer of acrylonitrile and styrene was used as the membrane matrix and a polystyrene resin bearing a tetrapeptide derivative of H-Asp (OcHex)-Ile-Asp (OcHex)-Glu(OBzl)-CH$_2$-(DIDE-resin) corresponding to Boc-L-amino acids was used as molecular recognition site. N-α-$tert$-butoxycarbonyl-L-tryptophan (Boc-L-Trp) or N-α-$tert$-butoxycarbonyl-D-tryptophan (Boc-D-Trp) was studied as the template. A tetrahydrofuran solution containing polymers and the template was poured onto a flat laboratory dish (8.9 cm diameter). After evaporation of the solvent at room temperature for 24 h, the resultant imprinted membrane with a thickness of 140 to 150 nm was obtained. It was found that the permselectivity towards D- and L-Trp was hardly observed for the Boc-D-Trp-imprinted membrane, whereas D-Trp was preferentially permeated rather than L-Trp through a Boc-L-Trp imprinted membrane and the permeability coefficient ratio was calculated to be 1.4. The effect of solvent composition on chiral recognition ability also led to a better selective binding, and it was found that the optimum composition was a 50% (v/v) ethanol solution (Kondo and Yoshikawa, 2001). The same system was adopted for the adsorption and permeation studies of N-acetyl-D-tryptophan (Ac-D-Trp) and N-acetyl-L-tryptophan (Ac-L-Trp), which demonstrated that this MIT was really a facile technique for introducing chiral recognition sites into polymeric materials (Yoshikawa et al., 1999b).

Subsequently Yoshikawa et al. also prepared a series of similar imprinted polymer membranes using the same method, such as a polystyrene resin bearing a tetrapeptide derivative of H-Asp(OcHex)-Leu-Asp(OcHex)-Glu(OBzl)-CH$_2$-(DLDE-resin) as the functional part for Boc-L,D-Trp (Yoshikawa et al., 1997b), a polystyrene resin bearing a tetrapeptide derivative of H-Glu(OBzl)-Gln-Lys(4-Cl-Z)-Leu-CH$_2$-(EQKL-resin) for Boc-L-Trp and Ac-D,L-Trp (Yoshikawa et al., 1998a), a polystyrene resin bearing a tripeptide derivative of H-Glu(OBzl)-Phe-Phe-CH$_2$-(EFF-resin) for Boc-L-Trp (Yoshikawa et al., 1999a) and a polystyrene resin bearing a tripeptide derivative of H-Glu(OBzl)-Glu(OBzl)-Glu(OBzl)-CH$_2$-(EEE) for Boc-L-Trp (Yoshikawa et al., 2001b).

Similarly, a tetrapeptide derivative of DLDE-resin was employed as a reference system to study the relationship between the chiral recognition ability and the configuration of the target molecule (Yoshikawa and Izumi, 2003). It was found that the Boc-D-Trp imprinted membranes prepared from DLDE derivatives consisting of D-amino acid residues could recognize D-isomer in preference to the corresponding L-isomer and vice versa, as shown in Fig.8.7. It was speculated that this rule was also suitable for other kinds of chiral recognition (Yoshikawa et al., 2005).
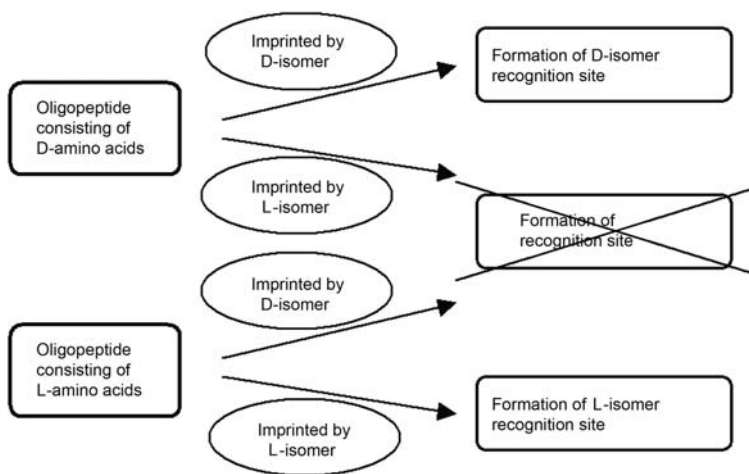
Fig. 8.7. Summary of MIMs bearing oligopeptide for chiral recognition (Yoshikawa and Izumi, 2003). Copyright (2003). Reprinted with permission of John Wiley & Sons, Inc.

Besides, porous MIM could also be obtained using the dry inversion method. For example, modified polysulfone having myrtenal moieties, which acted not only as a functional polymer bearing hydrogen binding sites for amino recognition but also as a membrane matrix, was adopted to prepare porous MIM (Yoshikawa et al., 2006b). It was found that the expression of permselectivity for MIMs was synergistically due to adsorption and diffusion selectivity.

Of course MIMs prepared by this method were not only restricted into the mixture with styrene copolymers and polypeptide derivatives but also could be made of some materials possessing both functionality and membrane-forming properties. Some natural macromolecules, e.g. cellulose acetate (Yoshikawa et al., 1999c; 2001a), and synthesized polymers such as carboxylated polysulfone (Yoshikawa et al., 1998b) were all excellent materials for optical resolution and had already exhibited good selectivity and separation for different amino acids.

8.2.2.2 Wet Phase Inversion

Wet phase inversion is immersed precipitation phase inversion that was employed for the preparation of MIMs by Kobayashi et al. (1995). Poly(acrylonitrile-*co*-acrylic acid) (PANCAA) and theophylline (THO, the template) were fully dissolved in dimethyl sulfoxide (DMSO). The cast solution was coagulated in water (a nonsolvent for PANCAA). As a result imprinted membranes with an asymmetric structure were obtained (Wang et al., 1996). In this case acrylonitrile residues served as membrane formation sites and acrylic acid residues were employed as the functional sites. After removal of the template from the solidified copolymer membranes using 0.1 wt.% acetic acid, the uptake experiments of THO and caffeine (CAF, with a similar structure to THO) were carried out. It was shown that the amount of THO taken into THO-imprinted membranes increased with the increase of THO concentration in the cast solution, due to hydrogen bonding between the THO and COOH groups of copolymers. This result suggested that THO imprinting was occurring during the coagulation of the imprinted membranes. In comparison, CAF uptake into the membranes was much lower than that of the THO template, which indicated that this approach was indeed a feasible method for the preparation of selectively imprinted membranes.

Furthermore, Wang et al. (1997b) studied the effect of the coagulation temperature on THO binding. It was found that the decrease in coagulation temperature caused an increase in THO binding to THO imprinted membranes, because more imprinted sites could be generated at low temperature due to the slow rate of solvent-nonsolvent exchange during the process of membrane formation.

In addition, Kobayashi et al. (1998) discussed the imprinting effect of THO imprinted membranes with different mole fractions of acrylic acid (AA). The results showed that when the AA mole fraction increased from 0 to 15 mol.%, the selectivity of THO increased; and when the AA mole fraction continuously increased, the selectivity decreased instead, due to the increase in nonspecific recognition. Also it was found that the binding amounts of THO strongly depended on the mole ratio of [THO]/[COOH] and the recognition ability was optimal at [THO]/[COOH] = 1 (Kobayashi et al., 2002a).

In addition, poly(acrylonitrile-*co*-methacrylic acid) (PANCMAA) was also used to prepare THO-imprinted membranes and several other structurally analogous substrates (Fig.8.8) were chosen to evaluate the selectivity of THO (Kobayashi et al., 2002a). Due to the presence of methyl groups, PANCMAA exhibited more efficiency in the tailor-made structure of the THO template compared with PANCAA, as illustrated in Fig.8.9. The selectivity was confirmed using CAF and other analogues as references.

Recently MIMs were prepared from the cast solution of PANCMAA with uracil (URA) as the template (Wang et al., 2004). The resultant membranes had typical ultrafiltration structures with porous morphology and showed a permeation flux of 3.5×10^{-5} m^3/(m^2·s) for 32 µmol/L URA aqueous so-
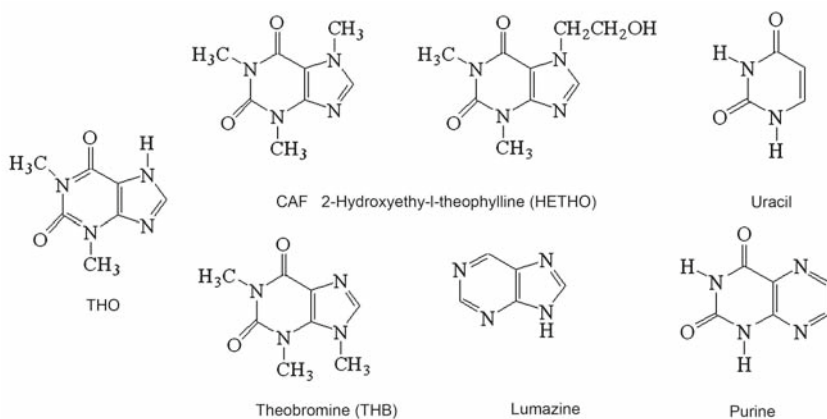
Fig. 8.8. Chemical structures of THO and its analogues
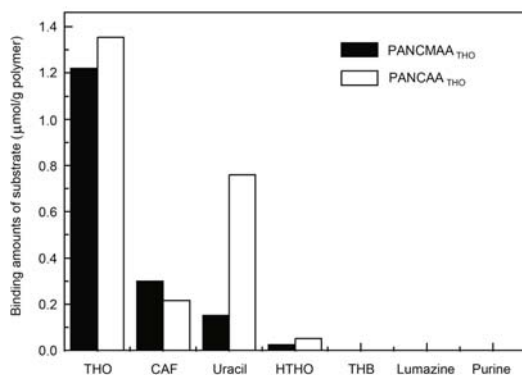
Fig. 8.9. Binding amounts of various substrates to THO-imprinted membranes. Reprinted with permission from (Kobayashi et al., 2002a). Copyright (2002), American Chemical Society

lution. Permselective binding to the template was observed in permeation experiments with a binding capacity of 7.9 μmol/g. When URA concentration in the cast solution reached 2 wt.%, the selectivity factor $\alpha_{U/D}$, defined as the saturated value of URA bound to the imprinted membrane to that of dimethyluracil (DMURA) structurally close to URA, was 13.6.

Furthermore, other polymers such as nylon-6 (Takeda et al., 2005) and polysulfone (Kobayashi et al., 2002b; Son and Jegal, 2007) were also used for the preparation of imprinted membranes. Templates such as uric acid (Cristallini et al., 2004) were also studied, which greatly broadened the application of phase inversion for imprinted membranes.

In an extension of this approach MIMs, which were blended from cellulose acetate (as the matrix polymers) and sulfonated polysulfone (as the functional polymers) with 100/0 (wt./wt.), 95/5 (wt./wt.), 90/10 (wt./wt.) and 85/15 (wt./wt.) compositions using Rhodamine B (Rh B) as the template molecule, were prepared by Ulbricht's group (Malaisamy and Ulbricht, 2004; Ramamoorthy and Ulbricht, 2003; Ulbricht and Malaisamy, 2005). The results indicated that Rh B bound to the MIMs was significantly higher than that bound to the respective blank samples. Wherein the blend membrane with 95/5 (wt./wt.) compositions had the highest binding capacity of 8.5 μmol/g, which revealed that molecular imprinting through phase inversion produced a great number of Rh B binding sites.

Up to now most of the templates used in this approach are small molecules. Trotta et al. (2002) attempted to apply wet phase inversion to macromolecules imprinting. Flavonoid naringin (4,5,7-trihydro- xyflavanone-7-rhamnoglucoside), a component present in the rind of oranges and other citrus fruits that contributes to the bitter taste of orange juice like limonin, was firstly selected as the template to prepare naringin-imprinted membranes using PANCAA as the functional polymers. The resultant membranes were able to bind naringin effectively, but the binding capacity was about 0.13 μmol/g. It was estimated that only 1/3500 of the naringin imprinted sites were able to show effective molecular recognition properties. Subsequently tetracycline hydrochloride (TCH)-imprinted membranes were prepared using the same system to naringin (Trotta et al., 2005). It was surprisingly found that the binding capacity was of the same order of magnitude as the imprinted membranes made for naringin, and only about 1/1500 of TCH imprinted sites were able to exhibit specific binding. Maybe it was the fact that the target molecules were relatively large, and thus most parts of the binding sites were not correctly formed or were not easily available in the bulk of the membranes.

In addition, an MIM for a large-molecular-weight protein (α-amylase) was prepared and studied using the wet phase inversion method (Silvestri et al., 2005). Calorimetric analysis confirmed the strong interaction between α-amylase and the blending component of natural and synthetic polymers.

The strategy mentioned above to prepare imprinted porous membranes using the phase inversion process is a direct approach that introduces recognition sites into membranes during the coagulation process. Although the operation is simple, the binding capacity is relatively low since the porous structure is insufficient to maintain the original shape of the recognition cavities after the removal of the template molecule.

Therefore an innovative approach was recently proposed by Takeda and Kobayashi (2006). Biophenol A (BPA)-imprinted polymer powders made of BPA methacrylate and divinyl benzene (DVB) were hybridized in a porous membrane scaffolding of polystyrene (PS), cellulose acetate (CA), nylon 66 (Ny) and polysulfone (PSf) by an immersed precipitated phase inversion

process for adsorbence and separation. The resulting hybrid imprinted membranes exhibited high capture abilities to BPA. The capacity could reach 148, 142 and 158 µmol/g for hybrid CA, Ny and PSf scaffolds, respectively, and the selectivity factor of BPA to the structural analogue 2-(4-hydroxyphenyl) ethyl alcohol (HPA) was estimated as 11.5, 8.1 and 10.8, correspondingly. However, no evident hybrid effect was caused by the PS hybrid imprinted membrane because the PS scaffold had no binding ability to BPA.

Meanwhile an alternative approach was carried out by Silvestri et al. (2006). As depicted in Fig.8.10, a composite membrane was obtained through the deposition of THO imprinted poly(methyl methacrylic acid-*co*-acylic acid) (PMMACAA) nanoparticles in the bulk or on the surface of PMMACAA porous support membranes fabricated by the phase inversion process. The rebinding tests indicated that the binding capacity of the composite membrane was 5.3 µmol/g, 6 times that of the membrane with non-imprinted nanoparticles and 40 times that with respect to the blank membrane. It also showed that for the membrane with THO-imprinted nanoparticles, the selectivity factor $\alpha_{THO/CAF}$(defined as the binding capacity for the imprinted molecule to the analogue) was detected for 10.
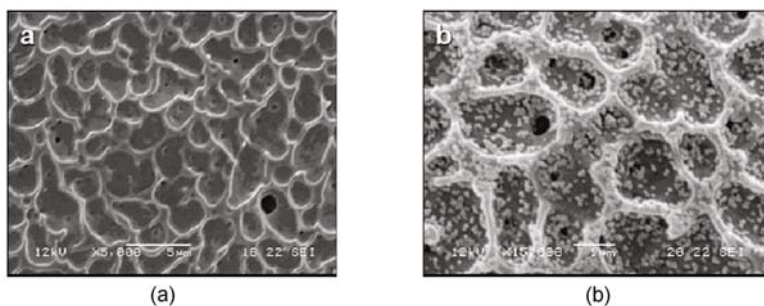
Fig. 8.10. SEM images of the surface of PMMACAA membrane before (a) and after (b) PMMACAA nanoparticle deposition. Reprinted from (Silvestri et al., 2006). Copyright (2006), with permission from Elsevier

In another work cholesterol-imprinted nanoparticles were deposited in porous PMMACAA membranes for application in extracorporeal blood purification. This composite membrane showed a very good rebinding capacity of 115.4 mg cholesterol/g polymer in the buffer solution, and 57 mg cholesterol/g polymer in ethanol (Ciardelli et al., 2006)

8.2.2.3 Electrospinning

Electrospinning is a versatile and efficient approach to produce nano- to micro-scale fibers and the electrospun membrane (mesh) is characterized by

large surface area to volume ratio and high porosity. Therefore it has been paid much attention in recent years.

Most recently the electropinning technique was initially applied to the imprinting field by Chronakis et al. (2006b) in Ye's group. Here electrospun nanofibers were prepared from a mixed solution of poly(ethylene terephthalate) (PET, as a supporting matrix for fiber formation) and polyallylamine (providing functional groups) in the presence of a template molecule, 2,4-dichlorophenoxyacetic acid. When the template was removed, the selective rebinding of the template was obviously compared with a non-imprinted nanofibrous membrane using radioligand binding analysis.

Whereafter THO and 17β-estradiol imprinted nanoparticles, which were prepared by a precipitation polymerization, were encapsulated within PET nanofibers with an average diameter of 150∼300 nm, by electrospinning. This composite nanofibrous membrane had a well-defined morphology and displayed the best selective target recognition, as shown in Fig.8.11 (Chronakis et al., 2006a). Actually this approach provided new application possibilities for molecularly imprinted nanoparticles and electrospun nanofibers.

(a) (b)
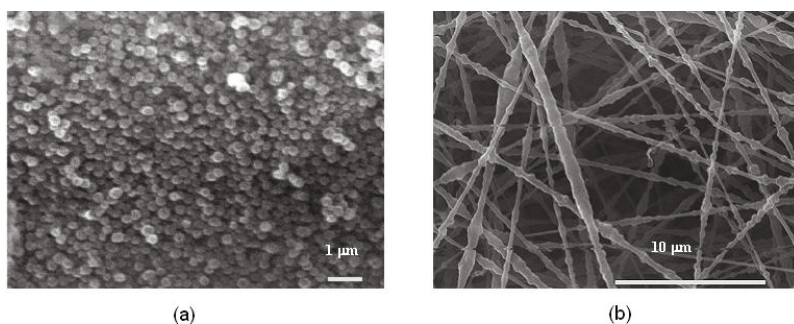
Fig. 8.11. Field emission scanning electron microscope (FESEM) photographs. (a) Molecularly imprinted nanoparticles; (b) The composite nanofibers. Reprinted with permission from (Chronakis et al., 2006a). Copyright (2006), American Chemical Society

In our laboratory a THO-imprinted poly(acrylonitrile-co acrylic acid) nanofibrous membrane was also preliminarily studied by Che et al. (2006). In this case acrylonitrile segments were favorable for the nanofibrous membrane formation and acrylic acid segments provided the functionality for molecular imprinting. These nanofibrous membranes were applied to the crystallization of THO. It was found that the crystallization process could be conducted on the surface of THO-imprinted nanofibrous membranes in saturated THO solution. However, in saturated CAF solution no crystal emerged on the surface of THO-imprinted nanofibrous membranes, which demonstrated the specific selection of imprinted nanofibrous membranes effectively.

Since the electrostatic force supplied by high voltage power may result in the potential destruction of the interaction between the functional groups and the template molecules, the electrospinning technique could only be used for particular imprinting systems. Much work has to be carried out to determine the feasibility of this approach and extend its applications.

8.2.3 Surface Imprinting

As can be seen from above examples, most MIMs, which are prepared by either bulk polymerization or phase inversion, exhibit acceptable affinity and selectivity towards the template molecules in appropriate solvents. However, the permeability of such membranes is relatively low, which limits their application in affinity separation. Furthermore, there is the same problem for the two former methods, namely that imprinted sites and membrane morphology are formed simultaneously. Although it may be easy for the preparation of imprinted membranes, the problem lies in that, in most cases, the conditions required for the optimal formation of imprinted sites are not compatible with those for obtaining optimal pore structure (Ulbricht, 2004). It is well known that pore structure is a crucial factor for membrane separation performance, such as flux. Therefore people started to explore new approaches for combining high-performance binding sites with pore structure allowing efficient membrane separation. In recent years surface imprinting as an excellent imprinting methodology has been widely developed to prepare molecularly imprinted composite membranes. By this method the support membrane possessing optimized pore structure is functionalized by introducing a thin molecularly imprinted layer. Thus the high flux of the support membrane can be retained. In addition, its transport selectivity can be considerably enhanced.

8.2.3.1 Surface Photografting

The preparation of a molecularly imprinted composite membrane by surface imprinting was first reported by Wang et al. (1997a). In that work a polyacrylonitrile membrane containing a photosensitive dithiocarbamate group was employed as the support membrane. In the presence of the template molecule (THO), UV-initiated graft copolymerization of AA and N, N'-methylenebisacylamide (MBAA) led to the formation of a molecularly imprinted layer on the membrane surface, as illustrated in Fig.8.12. The uptake of THO and its analogue CAF by the resulting composite membrane from aqueous solutions were compared. It was found that the polymeric layer of MBAA and AA could take up THO effectively, whereas the binding amount of CAF was much lower. The selectivity factor was up to 5.9. However, the drawbacks were the use of a special support membrane from photosensitive

polymer, the long reaction time of the order of 24 h, and the strong asymmetric pore structure with a mesoporous skin layer resulting in very low permeability.
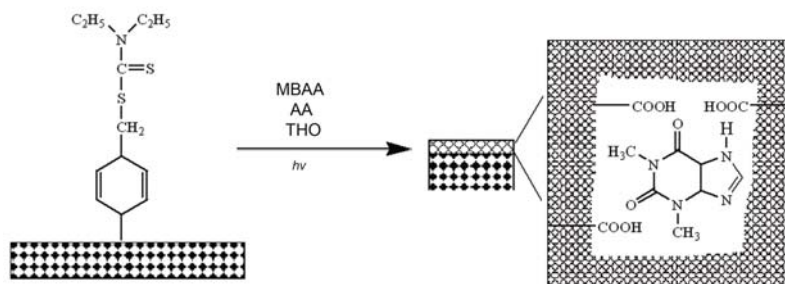

Fig. 8.12. Schematic diagram of membrane surface imprinting by photografting (Wang et al., 1997a). Copyright (1997). Reprinted with permission of John Wiley & Sons, Inc.

Considering the shortcomings resulting from the utilization of such a special membrane, researchers attempted to prepare composite imprinted membranes by modifying commercially available polymeric microfiltration (MF) membranes in possession of high separation performances, and particularly permeability.

In an early study polypropylene MF membranes were photografted, using benzophenone (BP) as the hydrogen-abstracting photoinitiator, with the functional monomer 2-acrylamino-2-methylpropanesulfonic acid and crosslinker MBAA in water (Piletsky et al., 2000). Within a few minutes a thin molecularly imprinted layer was yielded, which was covalently anchored on the outer surface and inner pore walls. Based on BET analysis and the estimation of the grafting degree, it could be calculated that the thickness of the molecularly imprinted layer was below 10 nm. The SEM images further confirmed that the modification was restricted to the surface and thus the high porosity of the support membrane was not blocked. Hence the fluxes of the resultant membrane ($J = 120$ L/(m^2·h)) had been the highest up to then for imprinted membranes (fluxes were usually below 5 L/(m^2·h)). This was very important for the practical application of MIMs that was limited before, particularly on account of their insufficient permeability. Moreover, the accessibility of binding sites and mass transfer were largely improved, which was the advantage of surface imprinting.

Theoretically speaking, BP is capable of abstracting the hydrogen atom of C-H of any polymer (Ulbricht et al., 2002). Thus it can be used as photoinitiator for the surface modification of such polymeric membranes. Nevertheless, for the poly(vinylidene fluoride) (PVDF) membrane, the efficiency of initiation is relatively low. Taking it into account, Sergeyeva et al. (2001)

firstly modified PVDF membranes with polyacrylate, and then fabricated an imprinted layer selective to terbumeton in the same way as above. As expected, the polyacrylate layer improved the photo-grafting efficiency to a considerable degree. Besides, the hydrophilic polyacrylate could minimize non-specific binding occurring during the application of the membrane. The fast filtration experiment was performed to investigate the selectivity of the resulting composite membrane towards terbumeton and other herbicides of similar structure. The results are illustrated in Fig.8.13, indicating that the specificity and selectivity were both high.
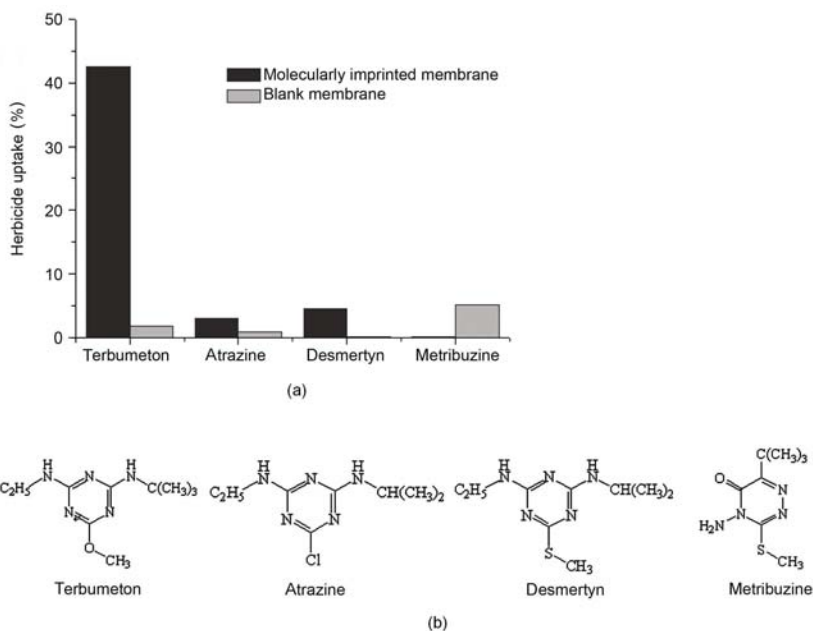
Fig. 8.13. Uptake of (a) the template and (b) its analogues of imprinted and non-imprinted membranes. Reprinted from (Sergeyeva et al., 2001). Copyright (2001), with permission from Elsevier

8.2.3.2 Surface Deposition

A more general approach towards the preparation of a thin-layer molecularly imprinted composite membrane was developed using benzoin ethyl ether (BEE), a very efficient α-scission photoinitiator (Kochkodan et al., 2002). As we all know, radicals generated by BEE are incapable of reacting with the base membrane and initiation takes place exclusively in solution. In this

case the membrane surface can be assumed to be almost inert to the photo-initiation process. Thus it can be reasonably considered that the imprinted polymer is deposited on the membrane surface, rather than anchored via co-valent bonding. Thereby, compared with the photografting method, the main advantage of this novel approach is the potential to synthesize molecularly imprinted composite membranes by controlled deposition of a molecularly imprinted layer onto any kind of polymer support.

In this research field a series of systematic works has been accomplished by Kochkodan and his co-workers (Hilal and Kochkodan, 2003; Hilal et al., 2002; 2003; Kochkodan et al., 2001; 2002; 2003). It was observed, in their early work (Kochkodan et al., 2001), that significant template specificity was only achieved for the MIMs prepared by pre-coating the support with BEE. In contrast, a homogeneous photo-initiated copolymerization in membrane pore volume yielded functional layers with only non-specific binding for the template demetryn. The authors gave as an explanation for this phenomenon that in the pre-coating method the imprinted sites formed were stabilized by the support material, which favors specific recognition, whereas in the latter case the imprinted sites isolated in the pore volume were prone to distortion.

Later, thin molecularly imprinted layers sensitive to 3,5-cyclic monophos-phate (cAMP) were efficiently deposited on PVDF or polyethersulfone (PES) membrane surfaces (Hilal et al., 2003; Kochkodan et al., 2003). Here the func-tional monomers including dimethylaminoethyl mathacrylate (DMAEMA), 2-hydroxyethyl methacrylate (HEMA) and methacrylic acid (MAA) and the crosslinker trimethylopropanethrimethacrylate (TRIM) were used.

In this work the effects of the type and concentration of functional monomers, as well as the concentration of crosslinker and degree of modi-fication (DM) on the binding of cAMP on MIMs during a filtration test were evaluated. It was concluded that the ability of MIMs to bind cAMP was a result of both the specific size and shape of imprinted cavities in addition to the correct position of the functional groups involved in the template bind-ing through ionic and hydrogen binding interactions. It should be noted that, as previously mentioned, the functional layer was only deposited via phys-ical interaction rather than chemical bonding. Therefore a measurement of the adhesion force between the molecularly imprinted layer and the porous polymer support should be carried out to ensure the stability of the compos-ite membrane. In this case atomic force microscopy (AFM), in conjunction with the coated colloid probe technique, has been used to measure interac-tion between a silica sphere coated with imprinted polymer and membrane supports (Hilal and Kochkodan, 2003). The results demonstrated the ac-ceptable adhesion force for application. Other research also confirmed that a uniform crosslinked polyacrylate coating could provide sufficient stability for the composite membrane (Han et al., 2003). Moreover, AFM was used to study surface structure and quantify pore size and surface roughness (Hilal et al., 2002). Fig.8.14 presents the AFM images of composite membranes, which

clearly shows that an increase in the DM led to a systematic decrease in pore size and an increase in surface roughness. Also, as a result of the increase in DM, the total binding capacity of the membrane increased, whereas the permeability and the rate of mass transfer decreased correspondingly. Hence the control of DM, i.e. the thickness of the molecularly imprinted layer, was very important.
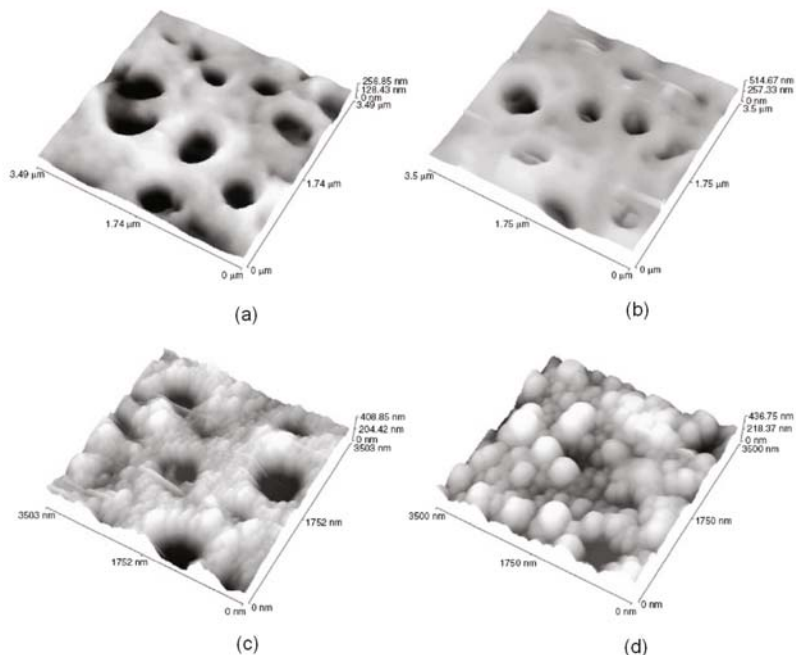
Fig. 8.14. Three-dimensional AFM images of polyethersulphone membranes: (a) conventional; (b) imprinted with DM = 260 µg/cm^2; (c) imprinted with DM = 460 µg/cm^2; (d) imprinted with DM =640 µg/cm^2 (Hilal et al., 2002). Copyright (2002). Reprinted with permission of John Wiley & Sons, Inc.

In order to efficiently adjust the thickness of the molecularly imprinted layer, controlled/living radical copolymerization such as atom transfer radical polymerization (ATRP) and iniferter should be adopted (Ruckert et al., 2002; Sellergren et al., 2002; Titirici and Sellergren, 2006; Wang et al., 2006b; Wei et al., 2005). Using ATRP, Wei et al. (2005) have successfully prepared an ultra-thin (<10 nm) surface-confined molecularly imprinted layer on gold substrates previously modified with a thiol self-assembled monolayer (SAM). It was shown in the experiment that the template could be completely removed (100%) and the binding capacity was relatively high. In particular, the merit of this method is that the thickness of the molecularly imprinted layer

can easily be adjusted according to the demand. More recently the synthesis of the molecularly imprinted nanotube membrane using a porous anodic alumina oxide (AAO) membrane by surface-initiated ATRP was reported by Wang et al. (2006a). The results indicated that the controllable nature of ATRP allowed the growth of molecularly imprinted nanotubes with uniform pores and adjustable thickness in the AAO membrane. Therefore the authors believed that, using the same route, it was possible to tailor the synthesis of molecularly imprinted nanotube membranes with either thicker molecularly imprinted nanotubes for capacity improvement or thinner nanotubes for efficiency improvement.

8.2.3.3 Emulsion Polymerization on Surface

Besides the methods above, water-in-oil emulsion polymerization was also utilized for membrane surface imprinting. Han et al. (2003) introduced molecular recognition sites onto a polypropylene membrane in this way from an aqueous environment. During the competitive binding experiment the surface imprinted sites could discriminate between the template THO and CAF, with a selectivity factor of 4.9±0.8. It was worthy of mention that doing this in an aqueous medium rather than in an organic solvent may offer the possibility of imprinting large molecules of biological interest, e.g. protein. Furthermore, Araki et al. (2005) applied a similar approach to the fabrication of a metal ion-selective composite membrane using pre-hydrophilized PTFE support.

8.3 Separation Mechanism of Molecularly Imprinted Membranes

All along much attention has been focused on the mechanism of selectivity in biological membranes. To date it has generally been accepted that substances transport through cell membranes mainly through carriers and channels, and molecular recognition is central to this selective process. For synthetic polymeric membranes, whether they are non-porous, microporous or macroporous, the transport mechanism is significantly different. The solution-diffusion mechanism governs the transport behavior in a non-porous membrane. However, with regard to the latter two cases, the separation of substances is achieved by aperture sieving. In these cases typical separations of the complex mixture are only fractionations into substance groups. In recent years the affinity membrane, a new functional membrane, has been dramatically developed (Klein, 2000; Ruckenstein and Guo, 2004). The specific binding between the bioactive molecules and ligands immobilized on the membrane offer the possibility of improving the transport selectivity. For MIMs the difference in comparison to the affinity membrane is that template-specific cavities are introduced into the imprinted membrane instead of ligands.

8.3.1 Facilitated and Retarded Permeation

To study the separation mechanism of MIM, besides the imprinted sites the membrane pore barrier has to be considered. It can be reasonably deduced that the imprinted cavities within the volume of a non-porous membrane are not accessible. With porous membranes, apart from seiving, two additional mechanisms for selective transport have been proposed (Piletsky et al., 1999; Ulbricht, 2004):

(1) Facilitated permeation driven by preferential adsorption of the template molecules due to specific recognition (slower transport of non-specific solutes);

(2) Retarded permeation due to affinity binding of the template to molecularly imprinted sites (slower transport of the template).

The facilitated permeation of the template across the MIM was observed in several researches. The first MIMs prepared by Piletsky et al. (1990) possessed selective permeability for the template nucleotide in a diffusion experiment. Subsequently similar results were obtained in the transport study of template adenosine and guanosine through similarly imprinted membranes with MAA as functional monomer and EGDMA as crosslinker (Mathew-Krotz and Shea, 1996; Piletsky et al., 1990). In both single-molecule-transport and two-molecule-transport, i.e. a competitive test, the permeation of adenosine or its derivative was facilitated compared with guanosine. The highest selectivity factor was 3.4. The author thought that selective transport arose from a reversible complex formation between imprinted sites and the template and subsequent shuttling of the template between binding sites in the membrane. Also, such a phenomenon was discovered in *in situ* polymerized molecularly imprinted composite membranes (Chen et al., 2006; Dzgoev and Haupt, 1999; Hong et al., 1998). Thus a typical example came from Hong and co-workers, as mentioned before (Hong et al., 1998). So far it has been the only study that verified facilitated transport by "fixed carrier" i.e. imprinted sites, which was supported by the observation that the transport selectivity increased with a decrease in the solute concentration.

From relevant reports discussed above, it can be concluded that free-standing or composite imprinted membranes by in situ crosslinking polymerization all displayed similar facilitated diffusion behavior (some membranes prepared by dry phase inversion imprinting showed two opposing transport behaviors as a function of the applied driving force. In electrodialysis experiments, facilitated permeation was observed). Although a detailed pore structure analysis has not been carried out for the microporous free-standing or composite imprinted membrane, some conclusions from permeability and other characterization results could be summarized as below (Ulbricht, 2004): (1) There are no large transmembrane pores in MIMs; (2) Template molecules participate in pore formation, which creates specific micropores intersecting macro- and meso-pores. Piletsky et al. (1999) proposed a model for illustrating these conclusions, as represented in Fig.8.15. During the imprinting

process channels could be yielded by the template, which increases the micropore fraction. Meanwhile imprinted sites were produced on larger pore walls. These channels can act as template-specific gates or available diffusion pathways between larger pores, which allows the improvement in selectivity.
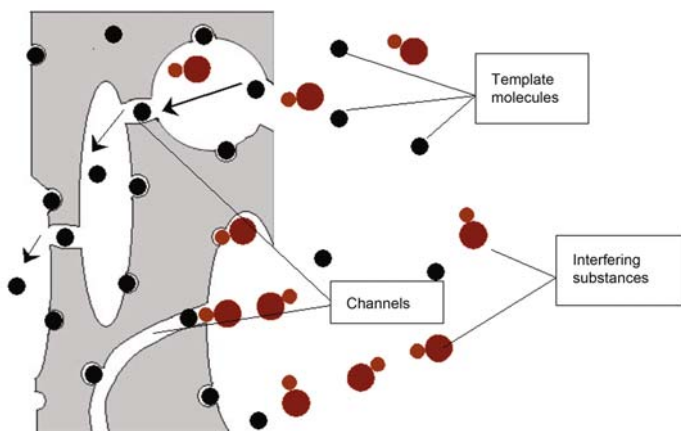
Fig. 8.15. Schematic representation of the possible role of template-specific channels for molecular recognition and transport. Reprinted from (Piletsky et al., 1999). Copyright (1999), with permission from Elsevier

In conclusion, for microporous MIMs the templates can preferentially bind to imprinted sites, followed by hopping and exchange between neighboring molecularly imprinted sites, while the transport of another substance by diffusion is hindered by the micropore barrier of the membrane. Consequently the permeation of the template is facilitated. It should be noted that this process is significantly affected by a few crucial parameters, such as the affinity and density of imprinted sites that need further investigation. The main shortcoming of microporous MIMs lies in their low flux, which can probably be addressed by tailored composite membranes.

Differing from microporous MIMs, macroporous ones usually show retarded permeation for template molecules. According to documents reported up to now, the imprinted membranes prepared by in situ polymerization in the presence of a macromolecular pore-former, wet phase inversion or surface imprinting, can be attributed to macroporous ones. The transport behavior through these membranes is modulated by the combination of diffusion and convection. Thus, selective transport can only be achieved by binding to accessible imprinted sites on trans-membrane pore surfaces. The affinity binding causes retardation for the target molecules, which make these membranes applicable to membrane adsorbers. The macroporous MIM adsorbers possess a high selective binding capacity at a high throughput (Ulbricht, 2004). How-

ever, it should be taken into account that the retarded permeation can only be maintained until the saturation of molecularly imprinted sites with the template molecules.

8.3.2 Gate Effect

The template binding not only leads to facilitated or retarded permeation, as described above, but also can alter the morphology and solute diffusive permeability/conductivity of microporous MIM. The latter phenomenon is termed "gate effect", which was observed by Piletsky et al. for the first time (Piletsky et al., 1995; Sergeyeva et al., 1999). In that work the conductivity of MIM displayed a considerable increase in the presence of the template, which arose from the speedup of ion transfer. Moreover, the diffusion of uncharged species nitrophenole was also accelerated, indicating changes in the micropore structure. In contrast, template binding could also reduce MIM permeability. For a THO-imprinted composite membrane, a great decrease in gas permeability due to sorption of THO was observed while the presence of CAF did not cause obvious changes (Hong et al., 1998).

Two different "gate effects" were observed in covalent and non-covalent imprinted membrane sensors respectively (Piletsky et al., 1998). The electro-conductivity of the two membranes in the presence of templates was compared. It was found that the membranes prepared by non-covalent binding, such as hydrogen bonding or electrostatic interaction, showed a slight increase with an increase in template concentration, whereas the covalent ones exhibited a strong reduction. The latter case could be attributed to significant shrinking of MIM due to the covalent rebinding of the template. The ratio of shrinking could reach 60%~100% (Wulff, 1995). In order to explain such behavior more visually a model of a macroporous crosslinked polymer network proposed by Belokon et al. (1973) and Shea and Stoddard (1991) should be mentioned here. As described in this model (see Fig.8.16), the structure of EGDMA- or DVB-based MIPs could be regarded as a set of highly crosslinked domains (nodules) interconnected by regions of lower crosslinking. The imprinted sites were considered to be located in the highly crosslinked domains. Once the covalent rebinding occurred, the swollen binding cavities due to solvation were occupied by the template sialic acid, which resulted in an even macroscopical shrinking of nodules and a decrease in electroconductivity. However, the case was different for non-covalent binding. A possible explanation may be drawn from the fact that most of the functional groups were homogeneously concentrated inside the selective cavities for the covalent imprinting, but for non-covalent systems a substantial portion of the functional groups were distributed outside cavities all over the polymer. Therefore the rebinding of template molecules could differently impart the structure of these two kinds of MIPs. Piletsky et al. (1998) also suggested that the interactions between templates and binding site domains could alter the surface charge and result in subsequent conformational reorganization of

the polymer network. However, for the non-covalent imprinted membrane, the reasons were not clear and further study was required.
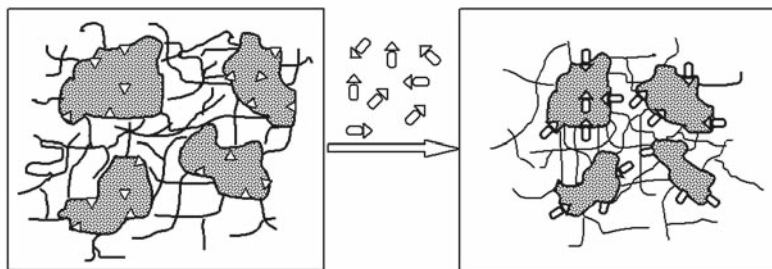
Fig. 8.16. Schematic illustration of possible changes in the MIP network structure resulting from the covalent binding of the template. Reprinted from (Piletsky et al., 1999). Copyright (1999), with permission from Elsevier

In recent years the evidence of the gate effect in an ultrathin layer of THO-imprinted copolymer on a indium-tin oxide electrode or cellulosic dialysis membrane was again reported by Yoshimi and his co-workers (Hattori et al., 2001; 2004b; Yoshimi et al., 2001). Subsequently they pointed out that to optimize morphological changes induced by gate effect, the density, flexibility and the amount of imprinted sites of the molecularly imprinted layer must be tightly controlled during polymerization. In this case living radical polymerization "iniferter" was conducted for controlling the degree of polymerization (Hattori et al., 2004a). It was found that the grafting degree, diffusive permeability and selectivity varied according to the irradiation time. They believed that living radical polymerization might be a promising method, which enables the creation of sophisticated architecture in MIM, allowing for further understanding of the basic nature and mechanism of the gate effect.

8.4 Potential Applications of Molecularly Imprinted Membranes

The combination of molecular imprinting and membrane technology was proposed in 1990, so this is still a recent and developing field. However, as already discussed above, a variety of preparation strategies for MIMs have been developed, which lead to membranes with different morphologies and performances. The existing data in the literature convince us that such membranes will no doubt find applications in many fields, especially in separation technology, sensors and controlled release or delivery.

8.4.1 Separation Technology

Among these applications separation is certainly of major importance. As described in Section 8.3, different separation mechanisms are responsible for the selective transport through MIMs with different barrier structures (macroporous or microporous). Evidently it will result in diverse separation applications. The discussion below will cover two aspects: the respective application of macro- and microporous imprinted membranes.

First of all it should be pointed out that the macroporous MIMs mentioned here refer to the ones prepared by the pre-polymerization method, in situ crosslinking polymerization with the addition of polymeric pore formers, wet phase inversion or surface imprinting. With these membranes, substance separation can only be achieved by the retardation of template molecules. Thus they can function as membrane adsorbers, similar to molecularly imprinted particle solid phase extraction (SPE), which could be used for sample enrichment from a large volume (membrane SPE), recovery and selective decontamination. Because of the macroporous characteristic, convective flow dominates the trans-membrane transport, which can improve separation performance through elimination of diffusion resistance. Therefore the key advantage of an imprinted membrane, compared with other adsorbers such as beads, is its high throughput. Especially in the case of composite membranes with surface imprinting, whose supports are flux-optimized commercial microfiltration membranes, the separation efficiency is very high, which has been characterized in fast filtration experiments (Hilal and Kochkodan, 2003; Hilal et al., 2002; 2003; Kochkodan et al., 2001; 2002; 2003; Piletsky et al., 2000; Sergeyeva et al., 2001). Another advantage of these composite membranes is that a high binding capacity and a high permeability can be adjusted by selecting a support membrane with a suited pore structure (internal specific surface area and average pore size respectively) (Ulbricht, 2004). Moreover the small bed volume of a membrane or membrane stack in comparison with adsorber particles allows faster equilibration of binding cavities and decreases the elution volumes. Hence the macroporous thin-layer molecularly imprinted composite membrane will be an excellent candidate for SPE materials. Molecularly imprinted particle composite membranes were also studied as adsorbers (Lehmam et al., 2002). The results showed that the equilibrium binding capacity was quite high, although the binding experiment needed recirculation and the permeability and accessibility were relatively low. If monodisperse nanoparticles were used instead of traditional micrometer-level molecularly imprinted particles, the separation performance can be further improved. In addition, an interesting work based on incorporation of molecularly imprinted nanoparticles into a wet phase inversion membrane was reported (Silvestri et al., 2006). Generally speaking wet phase inversion should be the most suitable preparation method for the separation membrane. The imprinted membrane obtained in this way demonstrated acceptable binding selectivity. However, the very low permeability of such membranes limits their application as ad-

sorber materials. In examples reported, the uptake measurement can only be conducted at a very low flow rate and the binding plateau value only reached after extensive recirculation. So the phase inversion membranes can be used for decontamination from a large volume stream, but the process requires a relatively long time. More recently Ulbricht and co-workers developed wet phase inversion strategies with a polymer blend instead of a single function polymer (Ramamoorthy and Ulbricht, 2003). In this case the permeability was greatly enhanced, which allowed characterization during fast filtration (SPE). This method open up possibilities for applying MIMs by wet phase inversion to SPE. Additionally, it should be mentioned that the MIMs, which were prepared by in situ crosslinking polymerization in the presence of macromolecular porogens, possess high water flux (Sergeyeva et al., 2003; 2007). They showed attractive potential in separation application, particularly in SPE, even in membrane chromatography.

The microporous MIMs include the ones prepared by in situ monolithic or pore-filling crosslinking polymerization or dry phase inversion. The receptor and transport properties of these membranes are assumed to be based on template-specific recognition sites in trans-membrane microchannels, which serve as "fixed carrier" for facilitated transport. On account of such cognitions, the resolution of enantiomers will be the most promising application. Yoshikawa and co-workers fabricated a series of dry phase inversion membranes, as described before (Kondo and Yoshikawa, 2001; Robertson et al., 2003; Yoshikawa and Izumi, 2003; Yoshikawa et al., 1997a; 1997b; 1998a; 2001b; 2005; 2006a). In their studies the transport of template amino acid enantiomers was facilitated when electrodialysis was adopted as the driving force. Several examples are listed in Table 8.1. As for the membranes derived from in situ polymerization, their relatively low flux may to some extent restrict wide applications (Chen et al., 2006; Dzgoev and Haupt, 1999; Mathew-Krotz and Shea, 1996). Nevertheless, if the preparation techniques become more elegant, these well-defined membranes with "fixed carrier" could serve as systems for the study of cellular trans-membrane transport and mimics of nature receptors.

Table 8.1. Example of MIMs prepared by dry phase inversion

Support materials	Functional polymers	Template molecules	Selectivity factor, α	References
AS	EFF-resin	Ac-L-Trp	$\alpha_{L/D} = 6.8$	(Yoshikawa et al., 1999a)
AS	DIDE-resin	Boc-L-Trp	$\alpha_{L/D} = 6$	(Yoshikawa et al., 1999b)
AS	EEE-resin	Boc-L-Trp	$\alpha_{L/D} = 5$	(Yoshikawa et al., 2001b)
–	CA	Z-D-Glu	$\alpha_{L/D} = 2.3$	(Yoshikawa et al., 1999c)

AS: copolymer of acrylonitrile and styrene DIDE-resin, EFF-resin and EEE-resin refer to the resin containing different oligopeptide residuals

8.4.2 Sensor and Controlled Release

It is well known that a sensor consists of two components: the transducer and the recognition elements. The selectivity, sensitivity and response time of sensors to a large extent depend on the properties of the recognition elements. MIPs as recognition element exhibit very competitive specificity in comparison with biological materials, such as a natural receptor and enzyme (Holthoff and Bright, 2007; Malitesta et al., 1999). However, if traditional molecularly imprinted particles are used, the interface adhesion between the particles and transducer surface may be weak and in particular the response time is extraordinarily long, due to the slow mass transfer. In this situation the thin membrane or film format of MIPs is most suited. A general immobilization approach is that the pre-polymerization mixture is firstly spin-coated on the electrode surface and followed by in situ polymerization, which was demonstrated in several examples (Kobayashi et al., 2001; Schmidt et al., 2004). So far many molecularly imprinted sensors based on different transducer types, such as QCM (Dickert et al., 2004; Ersoz et al., 2005; Fu and Finklea, 2003; Lin et al., 2004; Percival et al., 2002; Tsuru et al., 2006), conductivity (Deore et al., 2000; Suedee et al., 2006), and capacitance (Delaney et al., 2007; Panasyuk-Delaney et al., 2002; Yang et al., 2004; 2005), were developed, showing promising application potential. While such systems only take advantage of the specific binding in the membranes, the transport through the membranes as a selective permeation barrier is also an attractive alternative for transduction (Piletsky et al., 1998).

Controlled release or delivery based on a microporous membrane will be another prospective application field. Targets could be drugs (Bodhibukkana et al., 2006) and environmental pollutants, for instance herbicides (Piletska et al., 2005). More interestingly, the "gate effect" allows biomimetic and smart permeation through imprinted membranes, which is triggered by a stimulus from the environment, such as the binding of a signal molecule at imprinted sites. We can believe that such an intelligent response system will play an important role in biological medicine applications.

8.5 Conclusion and Outlook

The molecular imprinting technique has achieved a breakthrough in recent years due to its outstanding stability, low cost, and the tailor-made recognition ability of MIPs. However, there are still some problems for further discussions, e.g.: (1) the recognition and transport mechanism of the MIM for selective binding are not very clear; (2) the ultimate aim of molecular imprinting is to use a simple synthetic approach to simulate molecular recognition in the biological process, but imprinting in an aqueous solution for natural biomacromolecules is still a challenging subject at present; (3) although the

MIM exhibits a high selectivity, the uptake capacity and transport rates still need to be enhanced.

With the rapid development of biological techniques, synthetic processes and analytical methods, there is considerable reason to believe that MIT will be gradually improved, and thus can be applied to more fields.

References

Alexander C, Andersson HS, Andersson LI, Ansell RJ, Kirsch N, O'Mahony IAN, Whitcombe MJ (2006) Molecular imprinting science and technology: a survey of the literature for the years up to and including 2003. J Mol Recognit 19:106-180

Andersson LI (2000) Molecular imprinting: developments and applications in the analytical chemistry field. J Chromatogr B 745:3-13

Araki K, Maruyama T, Kamiya N, Goto M (2005) Metal ion-selective membrane prepared by surface molecular imprinting. J Chromatogr B 818:141-145

Belokon ZS, Skorobogatova AE, Grybkova NY, Arzhakov SA, Bakeev NF, Kozlov PV, Kabanov VA (1973) Structural-mechanical aspects of crosslinked polymeric glasses deformation. Dokl Acad Sci USSR 214:1069-1071

Bodhibukkana C, Srichana T, Kaewnopparat S, Tangthong N, Bouking P, Martin GP, Suedee R (2006) Composite membrane of bacterially-derived cellulose and molecularly imprinted polymer for use as a transdermal enantioselective controlled-release system of racemic propranolol. J Control Release 113:43-56

Brüggemann O, Haupt K, Ye L, Yilmaz E, Mosbach K (2000) New configurations and applications of molecularly imprinted polymers. J Chromatogr A 889:15-24

Che AF, Yang YF, Wan LS, Wu J, Xu ZK (2006) Molecular imprinting fibrous membranes of poly(acrylonitrile-*co*-acrylic acid) prepared by electrospinning. Chem Res Chinese U 22:390-393

Chen CB, Chen YJ, Zhou J, Wu CH (2006) A 9-vinyladenine-based molecularly imprinted polymeric membrane for the efficient recognition of plant hormone [1]H-indole-3-acetic acid. Anal Chim Acta 569:58-65

Chronakis IS, Jakob A, Hagström B, Ye L (2006a) Encapsulation and selective recognition of molecularly imprinted theophylline and 17β-estradiol nanoparticles within electrospun polymer nanofibers. Langmuir 22:8960-8965

Chronakis IS, Milosevic B, Frenot A, Ye L (2006b) Generation of molecular recognition sites in electrospun polymer nanofibers via molecular imprinting. Macromolecules 39:357-361

Ciardelli G, Borrelli C, Silvestri D, Cristallini C, Barbani N, Giusti P (2006) Supported imprinted nanospheres for the selective recognition of cholesterol. Biosens Bioelectron 21:2329-2338.

Cormack PAG, Mosbach K (1999) Molecular imprinting: recent developments and the road ahead. React Funct Polym 41:115-124

Cristallini C, Ciardelli G, Barbani N, Giusti P (2004) Acrylonitrile-acrylic acid copolymer membrane imprinted with uric acid for clinical uses. Macromol Biosci 4:31-38

Das K, Penelle J, Rotello VM (2003) Selective picomolar detection of hexachlorobenzene in water using a quartz crystal microbalance coated with a molecularly imprinted polymer thin film. Langmuir 19:3921-3925

Delaney TL, Zimin D, Rahm M, Weiss D, Wolfbeis OS, Mirsky VM (2007) Capacitive detection in ultrathin chemosensors prepared by molecularly imprinted grafting photopolymerization. Anal Chem 79:3220-3225

Deore B, Chen ZD, Nagaoka T (2000) Potential-induced enantioselective uptake of amino acid into molecularly imprinted overoxidized polypyrrole. Anal Chem 72:3989-3994

Dickert FL, Hayden O, Bindeus R, Mann KJ, Blaas D, Waigmann E (2004) Bioimprinted QCM sensors for virus detection-screening of plant sap. Anal Bioanal Chem 378:1929-1934

Dickey FH (1955) Specific adsorption. J Phys Chem 59:695-707

Donato L, Figoli A, Drioli E (2005) Novel composite poly (4-vinylpyridine)/polypropylene membranes with recognition properties for (S)-naproxen. J Pharm Biomed Anal 37:1003-1008

Dzgoev A, Haupt K (1999) Enantioselective molecularly imprinted polymer membranes. Chirality 11:465-469

Ersoz A, Denizli A, Ozcan A, Say R (2005) Molecularly imprinted ligand-exchange recognition assay of glucose by quartz crystal microbalance. Biosens Bioelectron 20:2197-2202

Fu Y, Finklea HO (2003) Quartz crystal microbalance sensor for organic vapor detection based on molecularly imprinted polymers. Anal Chem 75:5387-5393

Han MN, Kane R, Goto M, Belfort G (2003) Discriminate surface molecular recognition sites on a microporous substrate: A new approach. Macromolecules 36:4472-4477

Hattori K, Hiwatari M, Iiyama C, Yoshimi Y, Kohori F, Sakai K, Piletsky SA (2004a) Gate effect of theophylline-imprinted polymers grafted to the cellulose by living radical polymerization. J Membrane Sci 233:169-173

Hattori K, Yoshimi Y, Ito T, Hirano K, Kohori F, Sakai K (2004b) Effect of electrostatic interactions on gate effect in molecularly imprinted polymers. Electrochemistry 72:508-510

Hattori K, Yoshimi Y, Sakai K (2001) Gate effect of cellulosic dialysis membrane grafted with molecularly imprinted polymer. J Chem Eng Jpn 34:1466-1469

Haupt K (2003) Molecularly imprinted polymers: The next generation. Anal Chem 75:376A-383A.

Haupt K, Mosbach K (2000) Molecularly imprinted polymers and their use in biomimetic sensors. Chem Rev 100:2495-2504

Hilal N, Kochkodan V, Al-Khatib L, Busca G (2002) Characterization of molecularly imprinted composite membranes using an atomic force microscope. Surf Interface Anal 33:672-675

Hilal N, Kochkodan V, Busca G, Kochkodan O, Atkin BP (2003) Thin layer composite molecularly imprinted membranes for selective separation of cAMP. Sep Purif Technol 31:281-289

Holthoff EL, Bright FV (2007) Molecularly templated materials in chemical sensing. Anal Chim Acta 594:147-161

Hong JM, Anderson PE, Qian J, Martin CR (1998) Selectively-permeable ultrathin film composite membranes based on molecularly-imprinted polymers. Chem Mater 10:1029-1033

Hu XG, Li GK (2006) Application of molecular imprinting technique in sample pretreatment. Chinese J Anal Chem 34:1035-1041

Kempe M, Mosbach K (1995) Separation of amino acids, peptides and proteins on molecularly imprinted stationary phases. J Chromatogr A 691:317-323

Kielczynski R, Bryjak M (2005) Molecularly imprinted membranes for cinchona alkaloids separation. Sep Purif Technol 41:231-235

Kimaro A, Kelly LA, Murray GM (2001) Molecularly imprinted ionically permeable membrane for uranyl ion. Chem Commun 1282-1283.

Klein E (2000) Affinity membranes: a 10-year review. J Membrane Sci 179:1-27

Kobayashi T, Fukaya T, Abe M, Fujii N (2002a) Phase inversion molecular imprinting by using template copolymers for high substrate recognition. Langmuir 18:2866-2872

Kobayashi T, Murawaki Y, Reddy PS, Abe M, Fujii N (2001) Molecular imprinting of caffeine and its recognition assay by quartz-crystal microbalance. Anal Chim Acta 435:141-149

Kobayashi T, Reddy PS, Ohta M, Abe M, Fujii N (2002b) Molecularly imprinted polysulfone membranes having acceptor sites for donor dibenzofuran as novel membrane adsorbents: Charge transfer interaction as recognition origin. Chem Mater 14:2499-2505

Kobayashi T, Wang HY, Fujii N (1995) Molecular imprinting of theophylline in acrylonitrile-acrylic acid copolymer membranes. Chem Lett 927-928

Kobayashi T, Wang HY, Fujii N (1998) Molecular imprint membranes of poly-acrylonitrile copolymers with different acrylic acid segments. Anal Chim Acta 365:81-88

Kochkodan V, Hilal N, Windsor PJ, Lester E (2003) Composite microfiltration membranes imprinted with cAMP. Chem Eng Technol 26:463-468

Kochkodan V, Weigel W, Ulbricht M (2001) Thin layer molecularly imprinted microfiltration membranes by photofunctionalization using a coated alpha-cleavage photoinitiator. Analyst 126:803-809

Kochkodan V, Weigel W, Ulbricht M (2002) Molecularly imprinted composite membranes for selective binding of desmetryn from aqueous solutions. Desalination 149:323-328

Kondo Y, Yoshikawa M (2001a) Effect of solvent composition on chiral recognition ability of molecularly imprinted DIDE derivatives. Analyst 126:781-783

Lehmam M, Brunner H, Tovar GEM (2002) Selective separations and hydrodynamic studies: a new approach using molecularly imprinted nanosphere composite membranes. Desalination 149:315-321

Lin TY, Hu CH, Chou TC (2004) Determination of albumin concentration by MIP-QCM sensor. Biosens Bioelectron 20:75-81

Malaisamy R, Ulbricht M (2004) Evaluation of molecularly imprinted polymer blend filtration membranes under solid phase extraction conditions. Sep Purif Technol 39:211-219

Malitesta C, Losito I, Zambonin PG (1999) Molecularly imprinted electrosynthesized polymers: New materials for biomimetic sensors. Anal Chem 71:1366-1370

Marty JD, Mauzac M (2005) Molecular imprinting: state of the art and perspectives. Adv Polym Sci 172:1-35

Mathew-Krotz J, Shea KJ (1996) Imprinted polymer membranes for the selective transport of targeted neutral molecules. J Am Chem Soc 118:8154-8155

Mosbach K (2001) Toward the next generation of molecular imprinting with emphasis on the formation, by direct molding, of compounds with biological activity (biomimetics). Anal Chim Acta 435:3-8

Panasyuk-Delaney T, Mirsky VM, Wolfbeis OS (2002) Capacitive creatinine sensor based on a photografted molecularly imprinted polymer. Electroanalysis 14:221-224

Pauling L, Campbell D (1942) The manufacture of antibodies in vitro. J Exp Med 76:211-220

Percival CJ, Stanley S, Braithwaite A, Newton MI, McHale G (2002) Molecular imprinted polymer coated QCM for the detection of nandrolone. Analyst 127:1024-1026

Piletska EV, Turner NW, Turner APF, Piletsky SA (2005) Controlled release of the herbicide simazine from computationally designed molecularly imprinted polymers. J Control Release 108:132-139

Piletsky SA, Alcock S, Turner APF (2001) Molecular imprinting: at the edge of the third millennium. Trends Biotechnol 19:9-12

Piletsky SA, Dubey IY, Fedoryak DM, Kukhar VP (1990) Substrate-selective polymeric membranes: selective transfer of nucleie acid components. Biopolym Kletka 6:55-58

Piletsky SA, Matuschewski H, Schedler U, Wilpert A, Piletska EV, Thiele TA, Ulbricht M (2000) Surface functionalization of porous polypropylene membranes with molecularly imprinted polymers by photograft copolymerization in water. Macromolecules 33:3092-3098

Piletsky SA, Panasyuk TL, Piletskaya EV, Nicholls IA, Ulbricht M (1999) Receptor and transport properties of imprinted polymer membranes—a review. J Membrane Sci 157:263-278

Piletsky SA, Piletskaya EV, Elgersma AV, Yano K, Karube I (1995) Atrazine sensing by melecularly imprinted membranes. Biosens Bioelectron 10:959-964

Piletsky SA, Piletskaya EV, Panasyuk TL, El'skaya AV (1998) Imprinted membranes for sensor technology: opposite behavior of covalently and noncovalently imprinted membranes. Macromolecules 31:2137-2140

Ramamoorthy M, Ulbricht M (2003) Molecular imprinting of cellulose acetate-sulfonated polysulfone blend membranes for Rhodamine B by phase inversion technique. J Membrane Sci 217:207-214

Robertson GP, Guiver MD, Bilodeau F, Yoshikawa M (2003) Modified polysulfones. VI. Preparation of polymer membrane materials containing benzimine and benzylamine groups as precursors for molecularly imprinted sensor devices. J Polym Sci Part A: Polym Chem 41:1316-1329

Ruckenstein E, Guo W (2004) Cellulose and glass fiber affinity membranes for the chromatographic separation of biomolecules. Biotechnol Progr 20:13-25

Ruckert B, Hall AJ, Sellergren B (2002) Molecularly imprinted composite materials via iniferter-modified supports. J Mater Chem 12:2275-2280

Schmidt RH, Belmont AS, Haupt K (2005) Porogen formulations for obtaining molecularly imprinted polymers with optimized binding properties. Anal Chim Acta 542:118-124

Schmidt RH, Haupt K (2005) Molecularly imprinted polymer films with binding properties enhanced by the reaction-induced phase separation of a sacrificial polymeric porogen. Chem Mater 17:1007-1016

Schmidt RH, Mosbach K, Haupt K (2004) A simple method for spin-coating molecularly imprinted polymer films of controlled thickness and porosity. Adv Mater 16:719-722

Sellergren B, Lepisto M, Mosbach K (1988) Highly enantioselective and substrate-selective polymers obtained by molecular imprinting utilizing noncovalent interactions. NMR and chromatographic studies on the nature of recognition. J Am Chem Soc 110:5853-5860

Sellergren B, Ruckert B, Hall AJ (2002) Layer-by-layer grafting of molecularly imprinted polymers via iniferter modified supports. Adv Mater 14:1204-1208

Sergeyeva TA, Brovko OO, Piletska EV, Piletsky SA, Goncharova LA, Karabanova LV, Sergeyeva LM, El'skaya AV (2007) Porous molecularly imprinted polymer membranes and polymeric particles. Anal Chim Acta 582:311-319

Sergeyeva TA, Matuschewski H, Piletsky SA, Bendig J, Schedler U, Ulbricht M (2001) Molecularly imprinted polymer membranes for substance-selective solid-phase extraction from water by surface photo-grafting polymerization. J Chromatogr A 907:89-99

Sergeyeva TA, Piletsky SA, Brovko AA, Slinchenko EA, Sergeeva LM, Panasyuk TL, El'skaya AV (1999) Conductimetric sensor for atrazine detection based on molecularly imprinted polymer membranes. Analyst 124:331-334

Sergeyeva TA, Piletsky SA, Piletska EV, Brovko OO, Karabanova LV, Sergeeva LM, El'skaya AV, Turner APF (2003) In situ formation of porous molecularly imprinted polymer membranes. Macromolecules 36:7352-7357

Shea KJ, Stoddard GJ (1991) Chemoselective targeting of fluorescence probes in polymer networks: detection of heterogeneous domains in styrene-divinylbenzene copolymers. Macromolecules 24:1207-1209

Silvestri D, Barbani N, Cristallini C, Giusti P, Ciardelli G (2006) Molecularly imprinted membranes for an improved recognition of biomolecules in aqueous medium. J Membrane Sci 282:284-295

Silvestri D, Cristallini C, Ciardelli G, Giusti P, Barbani N (2005) Molecularly imprinted bioartificial membranes for the selective recognition of biological molecules. Part 2: release of components and thermal analysis. J Biomat Sci-Polym Ed 16:397-410

Son SH, Jegal J (2007) Chiral separation of D,L-serine racemate using a molecularly imprinted polymer composite membrane. J Appl Polym Sci 104:1866-1872

Suedee R, Intakong W, Dickert FL (2006) Molecularly imprinted polymer-modified electrode for on-line conductometric monitoring of haloacetic acids in chlorinated water. Anal Chim Acta 569:66-75

Takeda K, Abe M, Kobayashi T (2005) Molecular-imprinted nylon membranes for the permselective binding of phenylalanine as optical-resolution membrane adsorbents. J Appl Polym Sci 97:620-626

Takeda K, Kobayashi T (2006) Hybrid molecularly imprinted membranes for targeted bisphenol derivatives. J Membrane Sci 275:61-69

Takeuchia T, Haginakab J (1999) Separation and sensing based on molecular recognition using molecularly imprinted polymers. J Chromatogr B 728:1-20

Titirici MM, Sellergren B (2006) Thin molecularly imprinted polymer films via reversible addition-fragmentation chain transfer polymerization. Chem Mater 18:1773-1779

Trotta F, Baggiani C, Luda MP, Drioli E, Massari T (2005) A molecular imprinted membrane for molecular discrimination of tetracycline hydrochloride. J Membrane Sci 254:13-19

Trotta F, Drioli E, Baggiani C, Lacopo D (2002) Molecular imprinted polymeric membrane for naringin recognition. J Membrane Sci 201:77-84

Tsuru N, Kikuchi M, Kawaguchi H, Shiratori S (2006) A quartz crystal microbalance sensor coated with MIP for "bisphenol A" and its properties. Thin Solid Films 499:380-385

Turner NW, Jeans CW, Brain KR, Allender CJ, Hlady V, Britt DW (2006) From 3D to 2D: A review of the molecular imprinting of proteins. Biotechnol Prog 22:1474-1489

Ulbricht M (2004) Membrane separations using molecularly imprinted polymers. J Chromatogr B 804:113-125

Ulbricht M, Belter M, Langenhangen U, Schneider F, Weigel W (2002) Novel molecularly imprinted polymer (MIP) composite membranes via controlled surface and pore functionalizations. Desalination 149:293-295

Ulbricht M, Malaisamy R (2005) Insights into the mechanism of molecular imprinting by immersion precipitation phase inversion of polymer blends via a detailed morphology analysis of porous membranes. J Mater Chem 15:1487-1497

Vlatakis G, Andersson LI, Muller R, Mosbach K (1993) Drug assay using antibody mimics made by molecular imprinting. Nature 361:645-647

Wang HJ, Zhou WH, Yin XF, Zhuang ZX, Yang HH, Wang XR (2006a) Template synthesized molecularly imprinted polymer nanotube membranes for chemical separations. J Am Chem Soc 128:15954-15955

Wang HJ, Zhou WH, Yin XF, Zhuang ZX, Yang HH, Wang XR (2006b) Template synthesized molecularly imprinted polymer nanotube membranes for chemical separations. J Am Chem Soc 128:15954-15955

Wang HY, Kobayashi T, Fujii N (1996) Molecular imprint membranes prepared by the phase inversion precipitation technique. Langmuir 12:4850-4856

Wang HY, Kobayashi T, Fujii N (1997a) Surface molecular imprinting on photosensitive dithiocarbamoyl polyacrylonitrile membranes using photograft polymerization. J Chem Technol Biot 70:355-362

Wang HY, Kobayashi T, Fukaya T, Fujii N (1997b) Molecular imprint membranes prepared by the phase inversion precipitation technique. 2. Influence of coagulation temperature in the phase inversion process on the encoding in polymeric membranes. Langmuir 13:5396-5400

Wang HY, Xia SL, Sun H, Liu YK, Cao SK, Kobayashi T (2004) Molecularly imprinted copolymer membranes functionalized by phase inversion imprinting for uracil recognition and permselective binding. J Chromatogr B 804:127-134

Wei XL, Li X, Husson SM (2005) Surface molecular imprinting by atom transfer radical polymerization. Biomacromolecules 6:1113-1121

Whitcombe MJ, Rodriguez ME, Villar P, Vulfson EN (1995) A new method for the introduction of recognition site functionality into polymers prepared by molecular imprinting-synthesis and characterization of polymeric receptors for cholesterol. J Am Chem Soc 117:7105-7111

Whitcombe MJ, Vulfson EN (2001) Imprinted polymers. Adv Mater 13:467-478

Wulff G (1995) Molecular imprinting in crosslinked materials with the aid of molecular templates—a way towards artificial antibodies. Angew Chem Int Ed 34:1812-1832

Wulff G, Sarhan A (1972) Use of polymers with enzyme-analogous structures for the resolution of racemates. Angew Chem Int Ed 11:341-344

Wulff G, Schauhoff S (1991) Enzyme-analog-built polymers. 27. Racemic resolution of free sugars with macroporous polymers prepared by molecular imprinting. Selectivity dependence on the arrangement of functional groups versus spatial requirements. J Org Chem 56:395-400

Yang L, Wei WZ, Xia JJ, Tao H (2004) Artificial receptor layer for herbicide detection based on electrosynthesized molecular imprinting technique and capacitive transduction. Anal Lett 37:2303-2319

Yang L, Wei WZ, Xia JJ, Tao H, Yang PH (2005) Capacitive biosensor for glutathione detection based on electropolymerized molecularly imprinted polymer and kinetic investigation of the recognition process. Electroanalysis 17:969-977

Ye L, Mosbach K (2001) The technique of molecular imprinting—principle, state of the art, and future aspects. J Incl Phenom Macro 41:107-113

Yoshikawa M (2002) Molecularly imprinted polymeric membranes. Bioseparation 10:277-286

Yoshikawa M, Fujisawa T, Izumi J (1999a) Molecularly imprinted polymeric membranes having EFF derivatives as a chiral recognition site. Macromol Chem Phys 200:1458-1465

Yoshikawa M, Fujisawa T, Izumi J, Kitao T, Sakamoto S (1998a) Molecularly imprinted polymeric membranes involving tetrapeptide EQKL derivatives as chiral-recognition sites toward amino acids. Anal Chim Acta 365:59-67

Yoshikawa M, Izumi J (2003) Chiral recognition sites converted from tetrapeptide derivatives adopting racemates as print molecules. Macromol Biosci 3:487-498

Yoshikawa M, Izumi J, Guiver MD, Robertson GP (2001a) Recognition and selective transport of nucleic acid components through molecularly imprinted polymeric membranes. Macromol Mater Eng 286:52-59

Yoshikawa M, Izumi J, Kitao T (1997a) Enantioselective electrodialysis of amino acids with charged polar side chains through molecularly imprinted polymeric membranes containing DIDE derivatives. Polym J 29:205-210

Yoshikawa M, Izumi J, Kitao T (1999b) Alternative molecular imprinting, a facile way to introduce chiral recognition sites. React Funct Polym 42:93-102

Yoshikawa M, Izumi J, Kitao T, Koya S, Sakamoto S (1995) Molecularly imprinted polymeric membranes for optical resolution. J Membrane Sci 108:171-175

Yoshikawa M, Izumi J, Kitao T, Sakamoto S (1997b) Alternative molecularly imprinted polymeric membranes from a tetrapeptide residue consisting of D- or L-amino acids. Macromol Rapid Comm 18:761-767

Yoshikawa M, Izumi J, Ooi T, Kitao T, Guiver MD, Robertson GP (1998b) Carboxylated polysulfone membranes having a chiral recognition site induced by an alternative molecular imprinting technique. Polym Bull 40:517-524

Yoshikawa M, Kawamura K, Ejima A, Aoki T, Sakurai S, Hayashi K, Watanabe K (2006a) Green polymers from Geobacillus thermodenitrificans DSM465- Candidates for molecularly imprinted materials. Macromol Biosci 6:210-215

Yoshikawa M, Koso K, Yonetani K, Kitamura S, Kimura S (2005) Optical resolution of racemic amino acid derivatives with molecularly imprinted membranes bearing oligopeptide tweezers. J Polym Sci Part A: Polym Chem 43:385-396

Yoshikawa M, Murakoshi K, Kogita T, Hanaoka K, Guiver MD, Robertson GP (2006b) Chiral separation membranes from modified polysulfone having myrtenal-derived terpenoid side groups. Eur Polym J 42:2532-2539

Yoshikawa M, Ooi T, Izumi J (1999c) Alternative molecularly imprinted membranes from a derivative of natural polymer, cellulose acetate. J Appl Polym Sci 72:493-499

Yoshikawa M, Ooi T, Izumi J (2001b) Novel membrane materials having EEE derivatives as a chiral recognition site. Eur Polym J 37:335-342

Yoshimi Y, Ohdaira R, Iiyama C, Sakai K (2001) "Gate effect" of thin layer of molecularly-imprinted poly (methacrylic acid-co-ethyleneglycol dimethacrylate). Sensor Actuat B-Chem 73:49-53

9

Membrane with Biocatalytic Surface

Because of the attractive features associated with enzymes and membranes, their integration has been attracting much attention for many years. This chapter intends to outline the fabrication of a biocatalytic membrane surface through enzyme immobilization. The effects of these kinds of membrane materials and immobilization approaches, as well as methods of surface modification on the properties of enzyme-immobilized membranes are discussed. Furthermore, the preliminary applications of biocatalytic membranes, including membrane bioreactors and biosensors, are also simply reviewed.

9.1 Introduction

Conventional methodologies of chemical processes have been developed in past decades to a high level. They allow the production, separation and analytical determination of an enormous range of sophisticated products. But alternative methodologies, which are not only efficient and safe but also environmentally benign, resource- and energy-saving, are being increasingly sought. Use of enzymes, as green catalysts, is one of the promising strategies for meeting these requirements. Enzymes are featured on account of their unparalleled selectivity and mild reaction conditions (pH, temperature and pressure). A high degree of specificity allows enzymes to discriminate between different substrates (i.e. substrate specificity), similar parts of molecules (i.e. regiospecificity) and optical isomers (i.e. stereospecificity). These specificities prevent the catalysis reaction from being perturbated by side reactions and provide substantially high reaction yields. The mild reaction conditions (such as temperature, pressure, pH, etc.) significantly save energy and reduce manufacturing costs compared with conventional reactions. Therefore the practical use of enzymes is being expanded in fields such as fine-chemical and pharmaceuticals synthesis, food processing and detergent applications, biosensors fabrication, bioremediation and protein digestion in proteomic analysis, as well as in conventional industrial processes and products. Despite the above

unquestionable advantages, a number of problems still exist in the practical use of enzymes. The development of enzymes in large-scale operations has been limited by the instability of enzyme conformation and the high cost of isolation. Many strategies have emerged to improve the functionalities and performances of enzymes for bioprocessing applications, such as genetic and protein engineering, evolution, solvent engineering, chemical modification and immobilization. Among them enzyme immobilization is preferred in almost all large-scale industrial operations, because it allows the easy recovery of enzyme and product, multiple reuses of enzymes, the continuous operation of enzymatic processes, rapid termination of reactions, a significant reduction in the operating cost and a great variety of bioreactors or biosensors. The multipoint attachment between enzyme molecules and host materials reduces the potential deformation of protein conformation, and hence makes them substantially robust and resistant to environmental changes. Traditional membrane technology has provided considerable insight into separation and reaction. As is known, a membrane possesses a porous structure with numerous capillary channels in it, which results in very large surface-to-volume ratio. When a membrane is used as the support for enzyme immobilization, the structure and function characteristics of the membrane endow it with the capability to load high amounts of enzymes as well as the ability to integrate catalytic reaction and separation. Since the cut-off molecular weight of the microporous ultrafiltration membrane is in the order of the molecular weight of typical enzymes, an enzyme can approach the membrane surface either by diffusion or filtration. In general enzymes are immobilized onto/into the membrane by physical adsorption, entrapment and covalent bonding. Each method has its advantages and disadvantages. Compared with physical adsorption, chemical bonding has more potential especially in a membrane-based bioreactor because the leakage of enzymes is prevented during the vigorous flow of the reaction medium. In this immobilization process for a bioreactor, enzyme solution passes through the membrane under transmembrane pressure and bifunctional agents (such as carbodiimide derivatives and glutaraldehyde) are often used to crosslink the enzyme molecules adsorbed on the inner/outer surface.

There are many factors affecting the performance of an immobilized enzyme, such as membrane materials, membrane structures, immobilization methods as well as enzyme characteristics, enzyme loading and reaction conditions. Besides, surface properties of the membrane also have to be considered as playing a significant role. As is known, the behavior of enzymes is usually limited by immobilization, which stabilizes enzymes nevertheless. This is ascribed to a number of factors, two of which are (1) diffusional hindrance to the active sites and (2) non-specific enzyme-surface interactions. The former is the inevitable result of biphasic systems and this problem can be resolved under dynamic conditions to a certain extent. The latter is strongly dependent on the properties of the membrane surface. Most of the enzymes are

separated from natural environments (i.e. living cells). The change of environment may have a significant effect on the enzyme. How to make the membrane surface compatible with the enzyme is critical for improving the performance of the immobilized enzyme, especially when enzyme-immobilized membranes are applied to bioreactors, biosensors, etc. In this respect the development of suitable membranes for enzyme immobilization as well as their applications has been persued for some decades. Therefore, in the following sections, progress in the development of enzyme-membrane systems will be reviewed.

9.2 Enzyme Immobilization

Enzyme-support interactions endow an immobilized enzyme with specific physico-chemical and kinetic properties, which largely decide the practical application of the enzyme. Thus the judicious choice of support can enhance the operational performance of an enzyme-immobilized system. A number of desirable characteristics for the required support were often advanced for enzyme immobilization (Krajewska, 2004), including a high affinity to proteins, the availability of reactive functional groups for direct bonding with enzymes or for chemical modification, moderate hydrophilicity/hydrophobicity, high mechanical stability and rigidity, regenerability, and ease of preparation in different geometrical configurations. Suitable geometrical configurations can provide the system with permeability and a surface area suitable for a chosen biotransformation. These characteristics largely depend on the intrinsic properties of support materials. In other words the kind of support material is an important factor affecting the properties of immobilized enzymes. Support materials can be organic or inorganic, natural or synthetic. They have respective advantages and disadvantages. Concerning the membrane as the support for enzyme immobilization, membranes made from organic polymers will be discussed in detail.

9.2.1 Natural Polymer-based Membranes

Natural polymers, i.e. biopolymers, have been considered as ideal supports for enzyme immobilization, regardless of poor mechanical strength. Biopolymers are compounds that are produced by living organisms and plants, participate in the natural biocycle and are eventually degraded in nature. They generally include cellulose, gelatin, chitin, chitosan, alginate, etc. Among these cellulose, chitin and chitosan are often used as membrane materials for enzyme immobilization, largely due to their ability to form membranes. Their chemical structures are shown in Fig.9.1. Cellulose is a linear polymer of β-(1→4)-D-glucopyranose units in $^4C_1$ conformation. The fully equatorial conformation of β-linked glucopyranose residues stabilizes the chair structure, minimizing its flexibility. Cellulose is abundant in the plant as microfibrils,

which form the structurally strong framework in the cell walls. Chitin and chitosan can be formally considered as analogues of cellulose, where the C-2 hydroxyl groups are replaced by acetamido groups in the case of chitin and by amino groups in the case of chitosan. Chitosan ((1→4)-2-amino-2-deoxy-β-D-glucan) is the principal derivative of chitin ((1→4)-2-acetamido-2-deoxy-β-D-glucan) and these two species are chiefly distinctive in their degree of deacetylation. Chitin serves as a structural component of crustacean shells and fungal cell walls. It is available at very low cost and in large quantities from the wastes of seafood processing. Chitosan is soluble in dilute aqueous solutions of organic acids. Natural polymers have many advantages over most synthetic polymers, such as biodegradability, nontoxicity, physiological inertness, hydrophilicity and remarkable affinity to proteins.
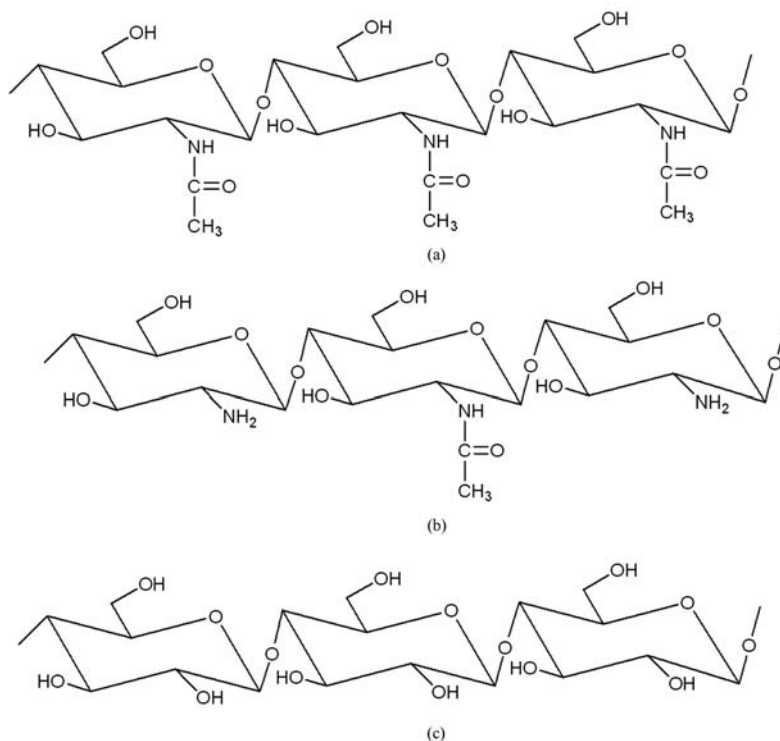
Fig. 9.1. Molecular structure of (a) chitin, (b) chitosan and (c) cellulose

In specific applications such as food, pharmaceutical, medical and agricultural processing, the "green" properties of these natural materials are especially required. Merely from the point of view of enzyme immobilization, the membranes from natural materials are advantageous in possessing

(1) a biofriendly interface and (2) hydroxyl and amino groups which facilitate covalent immobilization of enzymes. Amino groups can be activated by glutaraldehyde and hydroxyl groups by cyanogen bromide, epichlorohydrine, sec-triazines, p-nitrophynyl derivatives, organic sulfonyl chlorides, carbonyldiimidazole and 1-cyano-4-dimethylaminopyridinium tetrafluoroborate (Stollner et al., 2002).

Krajewska et al. (1990) even covalently immobilized urease on glutaraldehydepretreated chitosan membranes (Fig.9.2). The immobilized enzyme retained 94% of its original activity and showed improved pH, temperature, storage and operational stability compared with that of a free one. In the following years this group carried out a series of studies on enzyme-chitosan membrane systems (Krajewska, 1991a; 1991b; Krajewska and Piwowarska, 2005; Krajewska et al., 1997; 2001).
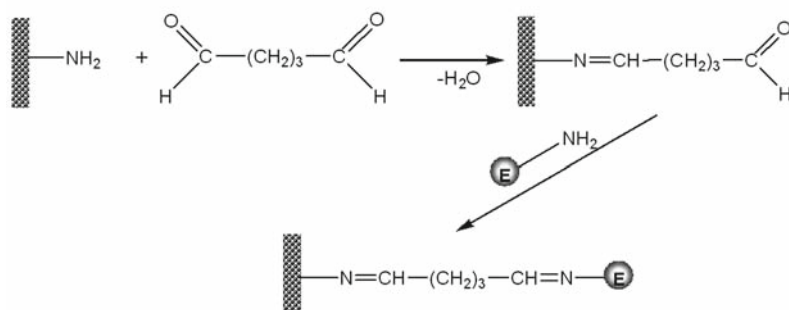
Fig. 9.2. Immobilized urease on glutaraldehyde-activated chitosan membrane

Magalhães and Machado (1998) immobilized urease onto a chitosan membrane to build urea potentiometric biosensors. These urease-immobilized membranes were coupled to all-solid-state nonactin ammonium ion selective electrodes. Enzyme was immobilized through four procedures: (1) adsorption; (2) adsorption followed by reticulation with dilute aqueous glutaraldehyde solution; (3) activation with glutaraldehyde followed by contact with the enzyme solution; (4) activation with glutaraldehyde, contact with the enzyme solution and reduction of the Schiff base with sodium borohydride. The results indicate that procedure (2) could obtain the best response characteristics, such as wide linearity range, fast response and a long lifetime.

Klotzbach et al. (2006) entrapped the glucose oxidase into the chitosan or nafion membrane. Chitosan and nafion were hydrophobically modified with long chain aldehydes and quaternary ammonium bromides, respectively. The hydrophobically modified micellar polymers altered the transport properties of redox species to the electrode surface. The enzyme was effectively immobilized in the membranes and enzymatic activity was maintained. The results indicate that the increase in hydrophobicity enhanced the enzymatic activity,

resulting in a more suitable surface for enzyme immobilization. Furthermore, the biodegradable and biocompatible properties would make the hydrophobically modified chitosan membrane more suitable in applications such as biosensors and biofuel cells.

Murtinho et al. (1998) covalently immobilized catalase, alcohol oxidase and glucose oxidase on cellulose derivatives (cellulose acetate, cellulose propionate or cellulose acetate-butyrate) membranes, which were pre-activated by $NaIO_4$-hexamethylene diamine-glutaraldehyde sequentially. The effects of membrane preparation methods and support properties on the efficiency and stability of coupled enzymes were studied. The results indicate that a cellulose acetate membrane prepared by evaporation produced higher activity of the immobilized enzyme than that prepared by immersion, because the membrane prepared by the latter was more crystalline. The increase in hydrophobicity of cellulose derivatives reduced the activity of the immobilized enzyme but gave better storage stability.

Similarly, lipase was also immobilized (Carneiro-da-Cunha et al., 1999) on cellulose, cellulose derivatives (cellulose acetate and cellulose phthalate) and cellulose composite membranes, which were activated by sodium periodate or carbodiimide. In particular a site-directed immobilization approach was introduced to immobilize subtilisin onto the functionalized cellulose-based membranes and was compared with random immobilization (Liu et al., 2001). Random immobilization was accomplished by bonding aldehyde groups of the membrane with amino groups of the enzyme. Site-directed immobilization was accomplished through the introduction of an octapeptide (FLAG) at the C-terminus of subtilisin by gene fusion of an oligonucleotide sequence coding for the FLAG peptide to the subtilisin gene. The FLAG peptide acted as an affinity tag and was recognized by a monoclonal anti-FLAG antibody, which was also recognized by protein A immobilized on the functionalized cellulose membrane. The catalytic activity of site-directed immobilized subtilisin was found to be three times as high as that of a randomly immobilized one. With respect to the resistance to environmental change, the results show that the immobilized subtilisin possessed good storage stability, thermal and pH stability. Furthermore, the activity of the immobilized subtilisin on cellulose support was more than twice that of a modified polyethersulfone membrane.

When glucose oxidase was immobilized on a functionalized cellulose/cellulose acetate membrane, high activity retention and high stability were also obtained, according to a scanning electrochemical microscope (SECM) (Zhao et al., 2004).

As an alternative to conventional activation methods, a cellulose membrane was activated by a simple photochemical reaction at 365 nm using a photolinker, 1-fluoro-2-nitro-4-azidobenzene (FNAB) (Bora et al., 2005; 2006). The activation of the membrane as well as enzyme immobilization is indicated in Fig.9.3. Nitrene was bound to a C-H bond or N-H bond through insertion reaction; therefore, in route I, the cellulose membrane reacted with

FNAB in the presence of UV light, forming an activated cellulose membrane. Then the amino group of horseradish peroxidase replaced the fluoro group of the activated cellulose, resulting in enzyme immobilization. In route II, when the cellulose membrane was treated with FNAB in basic medium, the hydroxyl group of the cellulose displaced fluorine of FNAB in a nucleophilic reaction to form a photoreactive cellulose membrane, on which the azido group generated a highly reactive intrene in the presence of UV light for the immobilization of glucose oxidase. The results show that the stability of immobilized enzymes was higher than that of free enzymes in an aqueous solution. It suggests that the invoked methods could prevent the drawbacks suffered by the conventional ones: (1) required anhydrous condition; (2) highly toxic reagents; (3) time consuming and cumbersome procedures.
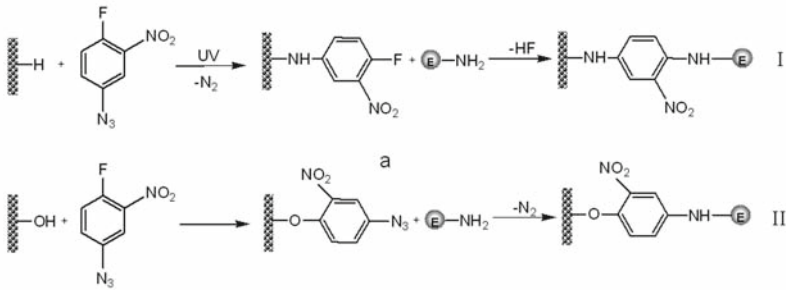
Fig. 9.3. Preparation of a photoreactive cellulose membrane and enzyme immobilization

Cellulose membrane can also be functionalized by plasma-induced grafting polymerization of ethylene diamine (EDA) or n-butylamine (n-BA) to generate amino groups for enzyme immobilization (Biederman et al., 2001). Glucose oxidase labeled by ^{99m}Tc-ertechnetate was then immobilized onto the functionalized membrane. A possible correlation was found between the immobilization capacity and the wettability of the membrane surface.

It was mentioned above that the difference between the effect of natural and synthetic polymer-based membranes on the enzymatic activity and the amount of absorbed enzyme was chiefly attributed to the hydrophilicity/hydrophobicity of the membrane surface, which resulted in the difference in the enzyme-surface interactions. To quantify the enzyme-membrane surface interactions, atomic force microscopy (AFM) was used to probe the force between lipase and the membrane surface (Hilal et al., 2006). The membranes were composed of thin-cellulose or a polyethersulfone active layer and porous non-woven polymer supporting layer. The results are shown in Fig.9.4. In this study, unmodified AFM-tip and lipase-modified AFM-tip were used respectively to measure the interaction between the tip and active layer/supporting

layer. The results show that the hydrophility/hydrophocity largely decided the lipase-surface interactions.
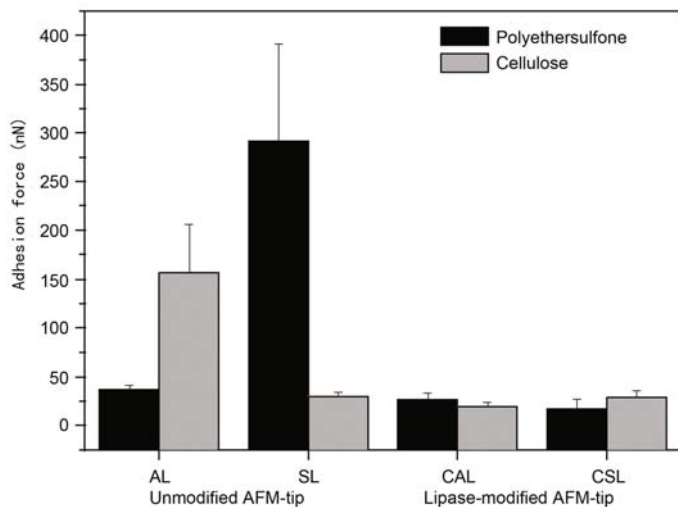
Fig. 9.4. Adhesion interaction measured by AFM technique between an unmodified or covered with lipase AFM-tip and active layer (AL) or supporting layer (SL). Reprinted from (Hilal et al., 2006). Copyright (2006), with permission from Elsevier

Lipase was also immobilized into hydrophilic cellulose or hydrophobic poly(tetra fluorethylene) membranes by embedding crosslinked enzyme aggregates within membrane pores, and the influence of membrane hydrophilicity/hydrophobicity was studied on membrane biocatalytic properties (Hilal et al., 2004). It was found that a hydrophobic membrane showed high affinity to lipase, while a hydrophilic membrane had low sorption ability towards lipase. In detail, spontaneous lipase sorption on the pore surface of hydrophobic membranes formed nuclei of lipase solid phase. Subsequently, lipase aggregates grew from the surface in the depth of pore volume. Because of low lipase sorption on the pore surface of a hydrophilic membrane, nucleation of lipase solid phase started in the pore volume. As a result, lipase aggregates grew from the volume of pores to their surface.

In addition to chitosan and cellulose, silk fibroin membrane was also used to immobilize glucose oxidase (Asakura et al., 1990). Compared with most natural polymers, silk fibroin has the advantage of excellent physical properties, good thermal stability, microbial resistance, etc. In Asakura et al. (1990)'s study different methods were used to insolubilize silk fibrion membranes for glucose oxidase immobilization. Spin-label electron spin resonance (ESR) was used to measure the characteristics of spin-labeled glucose oxidase (the spin label reagent is indicated in Fig.9.5). The results show that

the mobilities of those labeled enzymes were similar, which were correlated to show that thermal and pH stabilities were essentially same among the different enzyme-immobilized membranes. The data of relative enzyme activity suggest that there was no obvious nonspecific enzyme-membrane interaction and inhibition for the enzyme.
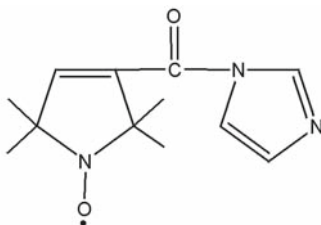
Fig. 9.5. The spin label reagent, N-(2,2,5,5-tetramethyl-3-carbonylpyrroline-1-oxyl)-imidazole (reacting with tyrosine side group of glucose oxidase)

Despite so many advantages of natural polymers, the membranes from natural polymers also suffer from a series of disadvantages, such as poor mechanical strength and chemical instability. For example, the abundance in hydrogen bonding among the polymer chains may result in a decrease in flexibility, the excellent affinity to proteins may make them easily eroded by bacteria and the high hydrophilicity may cause the membranes to swell in a wet atmosphere. These drawbacks limit the direct application of enzyme-immobilized membranes from natural polymers in many fields. However, these drawbacks are absent in membranes from many synthetic polymers. So far it has been thought that the composite membrane from natural and synthetic polymers is more advantageous over that from a single component. The preparation methods include blending, macromolecule modifying and layer building.

In the case of the first method, a blend of cellulose acetate (CA) and poly(methyl methacrylate) was fabricated into a composite membrane and glucose oxidase was immobilized onto the membrane (Rauf et al., 2006). The immobilized glucose oxidase revealed a high resistance to operation, storage and denaturant.

In the case of the second method, a composite membrane from GMA-modified cellulose was prepared, which was used to covalently immobilize trypsin for application in a microbioreactor (Jiang et al., 2000). In the latter case microstructures were specially designed in the composite membranes with a hydrophilic CA layer/hydrophobic poly(tetra fluorethylene)(PTFE) layer for lipase immobilization (Fig.9.6). The microstructure offered a proper microenvironment for enzyme molecules. Firstly, the hydrophilic/hydrophobic layers of a membrane can be wetted by an aqueous and organic phase respectively, so an organic/aqueous interface is formed at

the interface of the hydrophilic/hydrophobic layers. While lipase is entrapped at the interface of hydrophilic/hydrophobic layers, it is also entrapped at the phase interface, which is beneficial for interfacial activation of lipase. Secondly, interfacial entrapment leads to higher enzyme loading in comparison with the enzyme absorption in the pores or on the surface of the hydrophilic layer. Thirdly, lipase in the micropores is not easy to wash away. Typically, a dense CA layer was coated on the porous PTFE layer to prepare a composite membrane and lipase was immobilized by filtration (Xu et al., 2006b). The relatively dense cellulose layer rejected enzymes to control the enzyme loading, which prevented enzymes from being dissolved into the aqueous phase. The porous PTFE layer provided a hydrophobic environment and a large specific surface area for lipase immobilization. It was found that enzymes were absorbed in pores of PTFE layer and deposited on the interface between the two layers after filtration. When used for hydrolysis of olive oil in the biphasic membrane reactor, a high activity was obtained as well as stability to temperature, pH and operation. This specially designed structure of the composite membrane and this immobilization method endowed the membrane reactor with very good performance. A similar lipase-immobilized membrane by filtration was also used for chiral separation of racemic ibuprofen (Wang et al., 2007). In this study the fine imaging of the CA membrane structure was obtained: the CA coating layer facing the PTFE was porous and facing the air was dense. High activity retention, good selectivity and a long half-life were found for the lipase that was entrapped at the interface of the composite membrane.
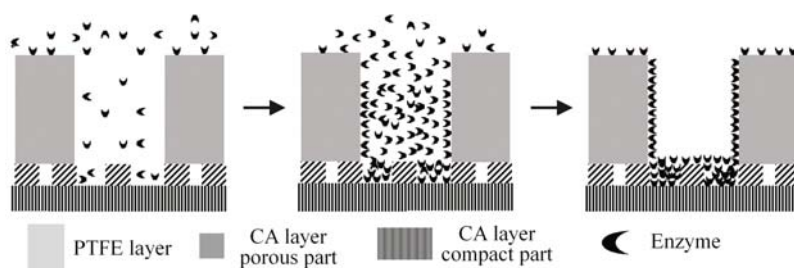
Fig. 9.6. Lipase immobilization on the microstructure of CA/PTFE composite membrane. Reprinted from (Wang et al., 2007). Copyright (2007), with permission from Elsevier

In a recent study a chitosan layer was deposited on the surface as well as on the pore walls of the polyacrylonitrile membrane, which was followed by immobilization of urease (Gabrovska et al., 2007). The results indicate that the enzyme immobilized on a membrane coated with 0.25% chitosan (solution) showed the highest activity.

9.2.2 Synthetic Polymer-based Membranes

Enzyme-immobilized systems based on synthetic polymers membranes have been widely explored in the fields of bioreactors and biosensors. Many synthetic polymers are poor in biocompatibility, biodegradability, hydrophilicity and even cause damage to proteins, while some of their intrinsic properties make them practically much more applicable than natural polymers. These properties chiefly involve the abundance in species, excellent mechanical and processing performance as well as chemical and physical stability, etc. So far there have been thousands of kinds of monomers that can be polymerized into polymers, a large number of which can be fabricated into membranes. These membrane species possess distinctive characteristics, meeting various requests for enzyme catalysis. For example, membranes from polyacrylonitrile, polysulfone and polypropylene are very stable to most chemical reagents and microorganisms to be applied in water and to most organic solvents-involved systems, for a long time. Furthermore, due to the variety of monomers and polymers in properties, the membranes for enzyme immobilization can also be specially designed for this specific purpose.

Enzymes can be either entrapped into the membrane or attached onto the membrane surface. Entrapment ensures that the membrane loads a high amount of enzyme; however, the corresponding membrane materials have to be water-soluble or else the organic solvents will have significant impact on the enzyme conformation. Although surface attachment has few requirements for membrane materials (as long as they can form membranes), the enzyme loading largely depends on factors such as surface properties of the membrane (charge, hydrophobicity/hydrophilicity, porosity, etc.). Concerning the activity, entrapped enzyme tends to be inactivated by the polymerization reaction of surrounding monomers and high-molecular-weight substrate has difficulty in approaching the enzyme. Although the enzyme immobilized through surface attachment is also affected by the coupling process or undesirable surface tension, it is more accessible to the substrate. Furthermore, the microenvironment of the enzyme can be improved by modification of the surface properties of the membrane.

9.2.2.1 Entrapment of Enzymes in Membranes

An enzyme can be entrapped into the membrane by three methods. Firstly, an enzyme can be added into the polymerization system or polymer solution and then the enzyme-involved mixture is fabricated into membranes. Secondly, enzyme solution can be filtrated through the membrane and enzyme molecules are immobilized onto the membrane pore surface. Thirdly, the enzyme can be immobilized between membrane layers.

In the case of the first method, an immobilized β-galactrosidase-membrane system was prepared by UV initiated polymerization of 2-hydroxyle- thyl methacrylate (HEMA) mixing with the enzyme (Arica et al., 1999); such an

enzyme-immobilized membrane was applied to a membrane reactor and used continuously for lactose hydrolysis without any considerable loss of activity. In the Uragami et al. (2006)'s study, two kinds of urease-entrapped polymer membranes were prepared. One was prepared by bulk-copolymerization of a monomer mixture containing vinylized urease (VU) (urease-immobilized poly(VU-AAm-HEMA) membrane). The other one was prepared by ultrafiltration of a mixture of urease and quaternized chitosan into a cellulose acetate membrane, which was mounted onto a porous support (urease-immobilized polyion complex membrane) (Fig.9.7). The results show that the activity of the urease-immobilized poly(VU-AAm-HEMA) membrane was lower than that of the urease-immobilized polyion complex membrane, but stabilities of the former were higher than those of the latter. In another interesting study (Eldin et al., 1998), mutual grafting was used to immobilize β-galactosidase. In detail, γ-radiation-induced polymerization of HEMA and a coating of enzyme were conducted by turns on a poly(tetra fluorethylene) membrane, which was previously grafted with acrylic acid. This double grafting technique greatly improved the catalytic activity of the immobilized enzyme compared with direct grafting of HEMA together with the enzyme.
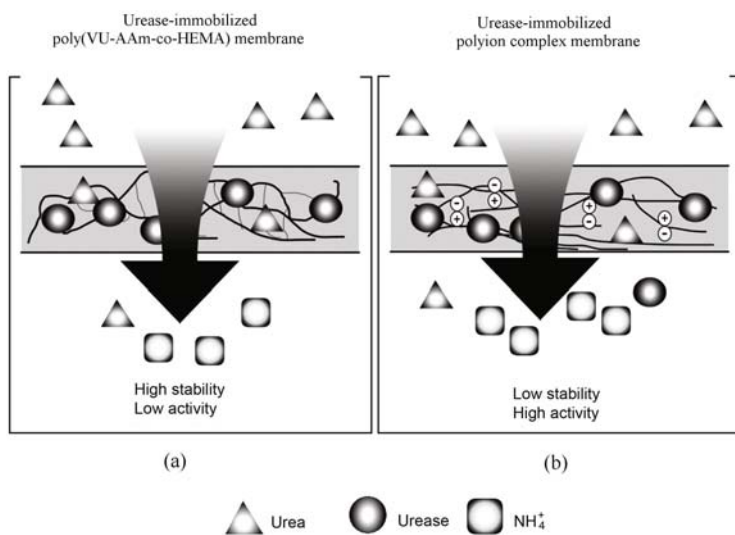
Fig. 9.7. Illustration for performance of the urea-immobilized poly(VU-AAm-HEMA) membranes (a) and urease-immobilized polyion complex membranes (b). Reprinted from (Uragami et al., 2006). Copyright (2006), with permission from Elsevier

In the case of the second method, a series of work was described in (Curcio et al., 2000; Gille and Staude, 1994; Shiomi et al., 1988; Tanioka

et al., 1998). Shiomi et al.(1988) immobilized invertase ionically by circulation of an enzyme solution through a poly(ethylene-*co*-vinyl alcohol) hollow fiber inside surface, which was preliminarily aminoacetalized with AAA ($(CH_3)_2NCH_2CH(OCH_3)_2$). This membrane was applied to separate glucose from the reaction mixture. Gille and Staude (1994) applied polysulfone and substituted a polysulfone membrane for immobilization of invertase and amyloglucosidase through: (1) hydrophobic interactions (unspecific immobilization), (2) covalent bond or (3) coulombic forces. The enzyme immobilized by method (1) showed the lowest activity and that by method (2) showed the highest activity. In the study by Tanioka et al.(1998), the enzyme was entrapped in the pore of a porous membrane. The external surfaces of the porous membrane were covered with polymer thin layers through plasma-induced graft polymerization. The enzymatic activity was retained and this grafted layer from the pores suppressed leakage of enzyme while the substrate was still allowed to pass through. With (Curcio et al., 2000) chymosin was immobilized on the membrane by ultrafiltration of the enzyme solutions, which were continuously fed to the system in a total recycle configuration.

In the case of the third method, the HEMA solution was sprayed on the glucose oxidase-immobilized poly(HEMA) membrane and then polymerized (Arica and Hasirci, 1993). The activity and stability of entrapped glucose oxidase were compared with those of the surface-immobilized one. The entrapment method showed a much higher immobilization efficiency than surface immobilization, while less operational stability and more diffusional difficulty of substrate.

Although entrapment can ensure the immobilization efficiency and activity, and this method has been widely applied for bioreactors, it is the origin of low operational and storage stability, because of the weak interaction between the enzyme and the matrix. Therefore, a molecular recognition process for enzyme immobilization has been developed. This method appears to be an alternative to surface adsorption or covalent bonding. One typical example is that peroxidase or glucose oxidase was immobilized by entrapping biotin-labeled enzyme into an electropolymerized avidin-contained polypyrrole membrane (Amounas et al., 2000). The recognition process was based on the specific interaction between biotin and avidin (Fig.9.8). The results indicate that this method showed higher immobilization efficiency than conventional entrapment and, furthermore, the enzymatic membrane revealed remarkable storage stability.

9.2.2.2 Attachment of Enzyme on Membrane

9.2.2.2.1 On Non-grafted Membrane

Enzyme can be immobilized onto the membrane surface by adsorption or chemical bonding. For the purpose of adsorption, special interaction is usually required between membrane surface and enzyme, such as hydrogen bonding,
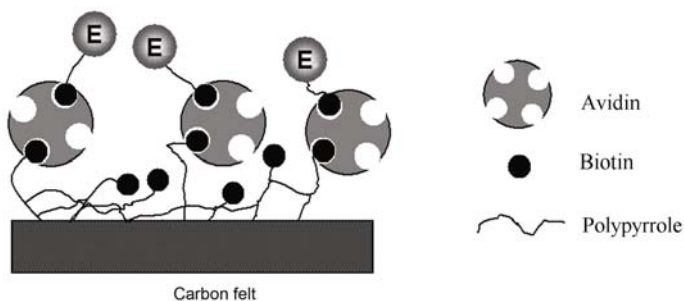
Fig. 9.8. Schematic configuration of the enzymatic membrane structure. Reprinted from (Amounas et al., 2000). Copyright (2000), with permission from Elsevier

electrostatic and hydrophobic interaction, chelation (metal ions (Cu, Ni, Zn) immobilized on the surface are capable of binding with amino acids such as histidine, cysteine and tryptophan). The kind of interaction depends on the chemical composition of the membrane surface, which usually has to be modified according to requirements. For example, Imai et al. (1986) modified a poly(ethylene-*co*-vinyl alcohol) membrane surface using two aminoacetals with different chain lengths. Invertase was then immobilized on the modified membrane through electrostatic interaction. The results show that the Michaelis-Menten constant was smaller for the invertase bound by the longer-chain-length molecule. For the same purpose, *N*-vinylimidazol was introduced into polyacrylonitrile membranes by copolymerization and glucose oxidase was immobilized onto the membrane through electrostatic interaction between a negative-charged carboxyl group and positive-charged imidazol groups (Godjevargova et al., 2000).

On the other hand, to increase the hydrophobicity of the membrane surface, hydrophobic groups can be introduced onto the surface or into the polymer. In a typical case HEMA copolymerized with a hydrophobic group-contained MAPA under UV. Lipase was adsorbed onto the poly(HEMA-*co*-MAPA) membranes by hydrophobic interaction. The adsorption capacity increased as the MAPA ratio in the membrane increased and the adsorbing/desorbing process did not influence this capacity.

In another study L-histidine was introduced onto poly(HEMA) membranes for catalase immobilization. This process was driven by ion-exchange effects and metal recognition (Akgol et al., 2001). The ion-exchange effects were caused by the free carboxyl group and imidazole ring on the grafted L-histidine and the amino acid side-chains of the enzyme molecules. Metal recognition was based on the chelation of trivalent ferric iron of catalase with a histidine molecule on the membrane surface, which was thought of as the interaction between hard Lewis acid (Fe (III)) and hard Lewis base (oxygen of the free carboxyl group and imidazole ring). For urease immobilization through adsorption, Procion Brown MX-5BR was attached onto

the membrane surface and Ni (II) was subsequently incorporated into the dye molecules (Akgol et al., 2002b). The strong binding of the dye-ligands to proteins resulted from the cooperative effect of ion-exchange and/or hydrophobic interactions, as well as metal recognition (between the imidazole group and –SH group of urease and Ni (II) ions on the dye molecule). The dye-Ni (II) attached polyamide hollow fiber membranes were repeatedly used for the adsorption/desorption of enzyme without any obvious loss in adsorption affinity. Similarly, Cibacron Blue F3GA (CB) was also covalently incorporated onto the poly(HEMA) membrane and then complexed with Fe (III) ions for adsorption of catalase (Arica et al., 1997).

For the purpose of covalent bonding, the membranes are usually required to have reactive groups. Some homopolymer-based membranes possess reactive groups, which can be activated for enzyme immobilization (e.g. activation of –OH in poly(HEMA) by epichlorohydrin (Arica, 2000)). In more cases, reactive groups have to be generated additionally. So far the emerging methods mainly include plasma activation, copolymerization and conventional chemical reaction on the surface (e.g. hydrolysis).

Low-temperature plasma was employed for activation of polypropylene, PVDF, or poly(tetra fluorethylene) membrane surfaces under nitrogen or ammonia gas atmosphere (Kawakami et al., 1988). Primary amino groups were attached onto the membranes for subsequent immobilization of glucose oxidase using glutaraldehyde as coupling agent. This enzymatic membrane was applied to sense the glucose concentration in the buffer.

Copolymerization can benefit enzyme immobilization because it can: (1) introduce reactive groups; (2) create the required microenvironment for the immobilized enzyme and (3) improve the mechanical performance of the support to a certain extent. Furthermore, copolymers are more commercially available than homopolymers. For example, to introduce reactive groups onto a polyacrylonitrile membrane, reactive-group-contained comonomers can be used to copolymerize with acrylonitrile. Xu's group (Nie et al., 2004; Ye et al., 2005b; 2005c) synthesized poly(acrylonitrile-co-maleic acid) by means of a water-precipitation copolymerization process, and fabricated this copolymer into the membrane. Lipase was then immobilized onto the carboxyl-contained membrane that was activated by EDC/NHS (as indicated in Fig.9.9). The properties of the free and immobilized lipase were assayed and the results are indicated in Table 9.1. It was found that the immobilization increased the activity of lipase in an organic medium, which was ascribed to several reasons. Firstly, free lipase aggregated because it was insoluble in an organic medium, while immobilized lipase scattering on a large membrane surface area could contact with substrates more easily. Secondly, the formation of covalent bonds between the enzyme and the membrane surface increased the stability of the enzyme conformation against the organic medium. Thirdly, some properties of the membrane surface could benefit the activity of the immobilized lipase, which might include the hydrophobic interaction between

the copolymer backbones on the membrane surface and the hydrophobic domain around the lipases' active site. This hydrophobic interaction was able to stabilize the "open state" conformation of lipase and favored the active site accessibility to substrates. Herein the conformation of lipase has to be specialized. A promising property of lipase is its activation in the presence of a hydrophobic interface. In the absence of interfaces, lipase has some elements of secondary structure (termed the "lid") covering its active site and making it inaccessible to substrates (Fig.9.10(a)). However, in the presence of hydrophobic interfaces, an important conformational rearrangement takes place yielding the "open state" of lipase (Fig.9.10(b)). Its rearrangement results in the exposure of hydrophobic surfaces, the interaction with the hydrophobic interface and the corresponding functionality. Therefore, whether lipase is immobilized through physical adsorption or chemical bonding, the hydrophobic surroundings can obviously affect the activity of lipase.
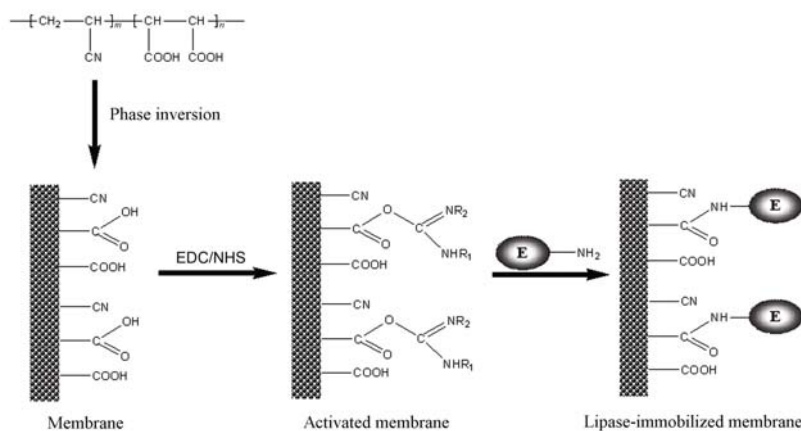
Fig. 9.9. Schematic representatives for the reactions of membrane activation and enzyme binding

Table 9.1. Activity and kinetic parameters for the free and immobilized lipases. Reprinted from (Ye et al., 2005b). Copyright (2005), with permission from Elsevier

Sample	Medium	V_{max} (U/mg)	K_m (mmol/L)	Activity (U/mg)	Activity yield (%)
Free lipase	Aqueous	46.4	0.45	42.1	-
Immobilized lipase	Aqueous	16.1	1.36	14.3	33.9%
Free lipase	Organic	0.269	8.61	0.204	-
Immobilized lipase	Organic	0.277	3.86	0.233	114%

To endow a polyacrylonitrile membrane as support for chemical immobilization of enzyme, epoxy groups containing GMA were also introduced
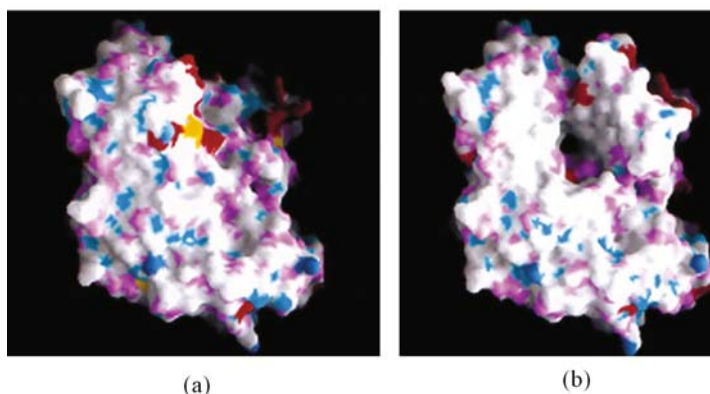
Fig. 9.10. Surface characteristics of CRL. (a) Closed state; (b) Open state in the same orientation. Color scheme: charged oxygens, dark red; polar oxygens, magenta; charged nitrogens, dark blue; polar nitrogens, light blue; sulfurs, yellow. Reprinted from (Cygler and Schrag, 1999). Copyright (1999), with permission from Elsevier

into the membrane by copolymerization (Fig.9.11(a)) and glucose oxidase was immobilized onto the membrane by direct bonding or through a spacer (hexamethylenediamine) and crosslinking agent (i.e. glutaraldehyde) (Godjevargova et al., 1999). It was found that GOD immobilized by direct bonding showed a better performance compared with that by indirect bonding. By copolymerizing HEMA with GMA, an epoxy group was introduced onto the polyHEMA membrane (Fig.9.11(b)) and cholesterol oxidase or invertase was directly immobilized on the poly(HEMA-*co*-GMA) membranes through covalent bonds between amino groups of enzyme and an epoxy group of GMA (Akgol et al., 2002a; Danisman et al., 2004). Similarly, a membrane was prepared for α-amylase immobilization and the enzyme-immobilized membrane was applied to continuous hydrolysis of starch (Bayramoglu et al., 2004). Hydrophobic MAPA was also used to copolymerize HEMA (Fig.9.11(c)) to introduce carboxyl onto the poly(HEMA) membranes and bring a hydrophobic microenvironment for lipase immobilization (Bayramoglu et al., 2002).

Many researchers have devoted themselves to the study of the generation of reactive groups by conventional chemical methods for enzyme immobilization. Among them, the Yang's group (Lin and Yang, 2003a; 2003b; 2003c; Yang and Lin, 2001) and Godjevargova's group (Dayal and Godjevargova, 2005; 2006; Godjevargova et al., 2004; Godjevargova and Gabrovska, 2003; 2005; 2006; Vasileva and Godjevargova, 2004; 2005) donated a lot of relevant research. Their work mainly focused on the direct modification of polyacrylonitrile, acrylonitrile-based copolymers (commercial products that cannot be used to directly immobilize enzyme) and polyamide membranes for subsequent immobilization of different enzymes. In their
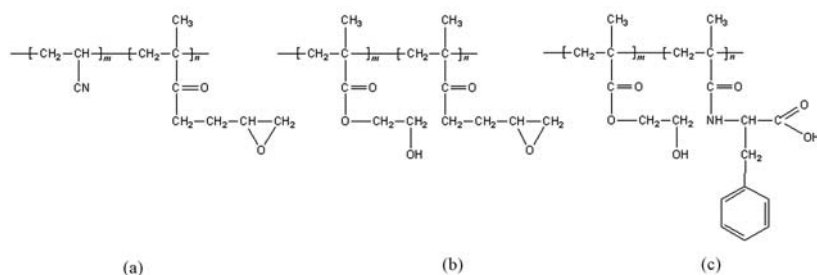
Fig. 9.11. Chemical structure of (a) poly(AN-*co*-GMA); (b) poly(HEMA-*co*-GMA) and (c) poly(HEMA-*co*-MAPA) membrane

work, NaOH/1,6-hexanediamine, hydroxyl amine, hydrazine dihydrochloride, HCl/ethylenediamine and $CH_3OH/NaOH/H_2O_2$ were used respectively as modification agents to modify the membranes, which resulted in the generation of the amino groups or amide for the immobilization of urease, cholesterol oxidase, glucose oxidase or catalase. The results show that different modification reagents had distinct effects on the behavior of immobilized enzymes. Jolivalt et al. (2000) and Sousa et al. (2001) covalently immobilized oxidized laccase and pig liver esterase on the hydrazine-treated PVDF membrane (Fig.9.12(a)) and four-reagent systems-treated nylon membranes (Fig.9.12(b)) respectively. Oxidized laccase-immobilized membranes were applied in the efficient removal of a phenylurea pesticide in wastewater.

In addition, another three membrane surface modifications for enzyme immobilization have to be mentioned because of their particularity. Firstly, Hicke et al. (1996) modified polyacrylonitrile and acrylonitrile-based copolymer membranes with an acyl azide method, which mainly involved the process of hydrazide formation, nitrosation and azido transfer with diphenyl phosphoryl azide to introduce acyl azide groups (Fig.9.13). This method can covalently attach the protein onto solid carriers efficiently and mildly. Three modification methods were used (including modifications a, b and c) and amyloglucosidase (AG) was directly immobilized onto the modified membranes. It was found that among the three modification methods, modification c obtained the best results with respect to AG immobilization while still preserving the separation performance of the initial membrane. Furthermore, under ultrafiltration conditions, AG activity was even improved due to the convective flow of substrate solution through the membrane.

Secondly, a modified poly(tetra fluorethylene) membrane was used as a support for enzyme immobilization. It is well known that poly(tetra fluorethylene) is very chemical-inert; hence, to allow covalent coupling of alliinase to poly(tetra fluorethylene), a poly(tetra fluorethylene) membrane surface was treated using different methods and a variety of coupling agents (the combinations of methods and agents are shown in Table 9.2) (Keusgen et al., 2001). The enzyme was either immobilized by covalent coupling (Fig.9.14(a)) or by
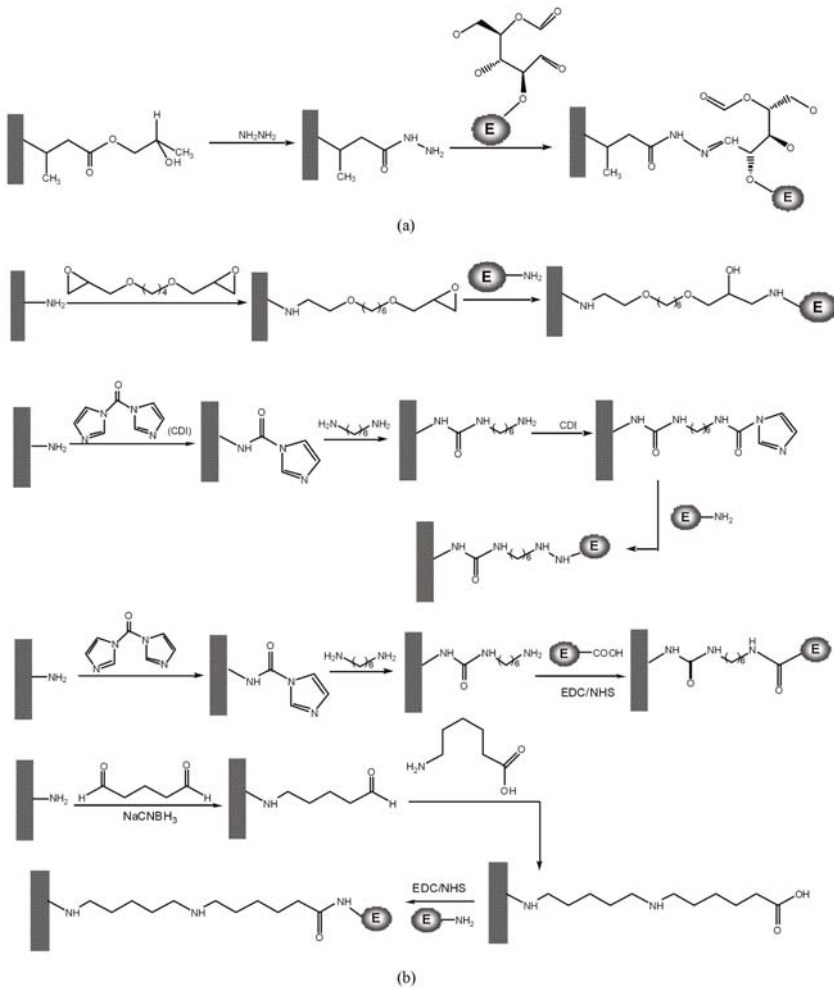
Fig. 9.12. Enzyme immobilization on (a) PVDF membrane and (b) nylon membrane using distinct methods

a sugar-lectin binding (Fig.9.14(b)). Method 29 (coupling of mannan by 1,4-BDDG, followed by a single layer of Con A) obtained the best result for the alliinase immobilization. This method allowed: (1) immobilization of enzymes under physiological conditions; (2) easy achievement of enzyme multilayers for enzymes carrying carbohydrate chains and (3) renewing protein layers.

Recently (as the third method), a bifunctional membrane (with epoxy groups and immobilized copper ions) was constructed for the immobilization and purification of penicillin G acylase (PGA) (Chen et al., 2007). PGA
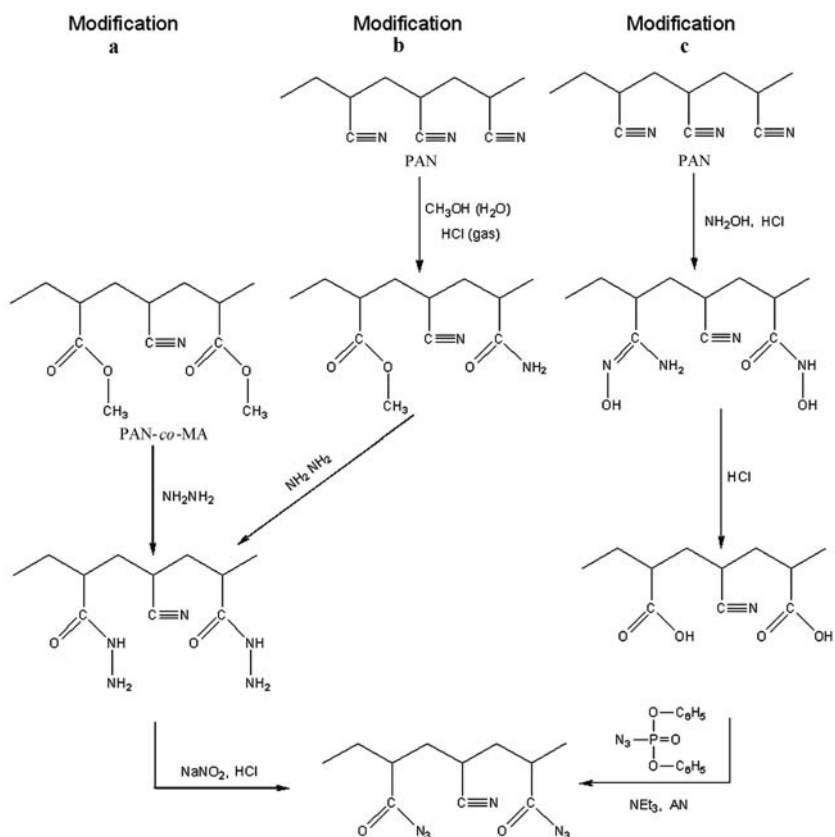
Fig. 9.13. Pathways of polyacrylonitirle modification by acyl azide method (Hicke et al., 1996). Copyright (1996). Reprinted with permission of John Wiley & Sons, Inc.

chelated firstly with the immobilized copper on the membrane and then was covalently bound to the membrane through the epoxy group (Fig.9.15). In the procedures iminodiacetic acid disodium (IDA) played a critical role, especially in the construction of the bifunctional membrane. The results show that the immobilized PGA revealed remarkable stability after 26 times use over more than 2 months. Therefore this immobilization approach has potential for development and application in industrial processes.
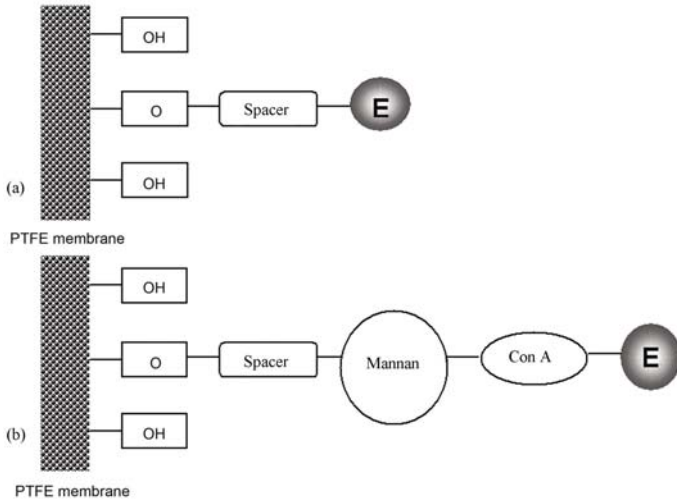
Fig. 9.14. Schematic derivatization procedures applied to poly(tetra fluorethylene) membrane surfaces. The enzyme (alliinase) was either immobilized directly (a) or indirectly (b) by a carbohydrate-lectin complex
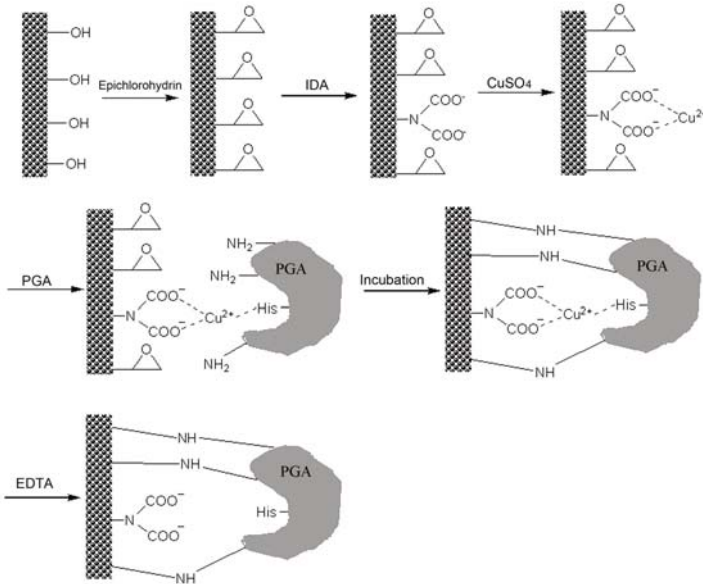
Fig. 9.15. Schematic graph for the bifunctional membrane preparation and PGA immobilization. Reprinted from (Chen et al., 2007) Copyright (2007), with permission from Elsevier

Table 9.2. Derivatization methods used for the immobilization of alliinase on poly(tetra fluorethylene) surfaces (Keusgen et al., 2001). Copyright (2001). Reprinted with permission of Wiley-Liss, Inc., a subsidiary of John Wiley & Sons, Inc.

Reagents	Modification																												
	1	2	3	4	5	6	7	8	9	10	11	12	13	14	15	16	17	18	19	20	21	22	23	24	25	26	27	28	29
Na	x	x											x		x		x		x		x		x		x		x		x
O$_3$			x								x																		
H$_2$O$_2$										x	x																		
Thionylchloride				x	x	x	x	x	x	x		x	x	x	x	x	x	x	x	x	x	x	x	x	x	x	x	x	x
EACA							x	x																					
DCC									x																				
1,4-BDDG												x	x							x	x	x	x						
Benzoquinone														x	x											x	x		
ADT																x	x	x	x					x	x				
Mannan																								x	x	x	x	x	x
Con A						x					x						x	x	x	x	x	x	x	x	x	x	x	x	x
Alliinase	x	x	x	x	x	x	x	x	x	x	x	x	x	x	x	x	x	x	x	x	x	x	x	x	x	x	x	x	x

9.2.2.2.2 On Grafted Membrane

Despite being an alternative method for modifying a membrane surface, the effect of grafting on the enzyme immobilization is obviously different from that of the above-mentioned methods. Firstly, the number of grafting-resulted reactive groups for enzyme immobilization is usually independent of the number of active sites on the original membrane. In other words, the number of reactive groups brought by the direct treatment of the membrane is mainly dependent on the reactive sites on original membrane (such as the nitrile group on the polyacrylonitrile membrane). However, grafting-modified membrane can provide much more reactive groups. Typically, grafting polymerization of acrylic acid brings a great number of carboxyl groups for the membrane.

Secondly, the grafted polymer chain can act as a spacer. As is known, one of the factors that lowers the activity of immobilized enzymes is the multipoint attachment between the enzyme and the support, which restricts conformational freedom of the enzyme and decreases the accessibility of substrate to the active site in the enzyme. The use of spacers can minimize such steric hindrance by distancing the immobilized enzyme from the underlying solid surface. In a word, the introduction of spacer makes the immobilized enzyme more flexible.

Thirdly, grafting usually provides a more suitable microenvironment for enzyme immobilization, such as more hydrophilic/hydrophobic and even highly biomimetic surroundings, because naturally occurring molecules in vivo (saccharide, phospholipids, etc.) can be easily bonded to the polymerized monomers or macromolecular chains.

According to (Ruckenstein and Li, 2005), grafting methods are generally divided into two classes, i.e. "grafting-to" and "grafting-from" processes. The "grafting-from" method uses the active species existing on the material surfaces to initiate polymerization of monomers from the surface toward the outside bulk phase. In the "grafting-to" method, preformed polymer chains carrying reactive groups at the end or side chains are coupled to the surface directly. The former method can control the grafting chains and density as well as the number of reactive groups more easily; however, these kinds of species are fewer because many macromolecules cannot be synthesized by the grafting method, especially some naturally occurring macromolecules (chitosan, etc).

- **Effect of Graft Polymerization (Grafting-from)**

Graft polymerization on the membrane surface can also create a specific affinitive interface or introduce specific reactive groups for enzyme immobilization.

In the case of physical adsorption, some functional chains are usually introduced onto the membrane surface for the specific interaction between enzyme and membrane. Godjevargova (1996) modified acrylonitrile copolymer

and polyamide membrane by radiation grafting of AMPSA (with negatively-charged sulpho groups) and DMAEM (with positively-charged quaternary amino groups) in the presence of Fe^{2+}. Then glucose oxidase was immobilized through electrostatic interaction between AMPSA or DMAEM and the enzyme.

In a similar study (Fujita et al., 2003), poly(GMA) was grafted onto a polyethylene hollow fiber membrane and reacted with ethanolamine to introduce an anion-exchange group. Then collagenase was immobilized onto the membrane through electrostatic interaction and the leakage of enzyme was prevented by glutaraldehyde crosslinking. This immobilized enzyme showed good catalytic efficiency and stability in the production of tripeptide from gelatin.

Deng et al. (2004a; 2004b; 2004c) did a series of studies on the adsorption of lipase on grafted polymer-modified hydrophobic PP membranes. In their studies, hydrophobic polypeptide (poly(γ-ethyl-L-glutamate) (PELG) and poly(γ-stearyl-L-glutamate) (PSLG)) (Fig.9.16(a)), glycopolymer (PAG) (Fig.9.16(b)) and phospholipid analogous polymers (PAPs) (Fig.9.16(c)) were respectively tethered to the membrane surface by graft polymerization of γ-ethyl-L-glutamate, γ-stearyl-L-glutamate, α-allyl glucoside and DMAEMA (followed by reaction with COP). Their studies were based on the construction of biomimetic membranes with retained hydrophobicity for lipase adsorption and activation, because polypeptide, phospholipids as well as glucolipids are the principal components of the natural biomembrane. In addition, the modified membranes have been proved to be biocompatible with a variety of proteins including enzymes. The results (Fig.9.17) show that the adsorption capacity of the membrane decreased after modification, which was ascribed to the decrease in hydrophobicity; however, the activities of lipase on the modified membranes increased to a different extent, because of the biocompatible effect (except for the glycopolymer-modified membrane because of too great an increase in hydrophilicity). Especially in the case of PAPs with octadecyloxy groups (18-PAP), their grafting on the membrane even increased the activity retention from 57.5% to 83.2%. On the other hand, after ring-opening of a poly(GMA)-grafted membrane by positively charged ethanolamine or hydrophobic phenol, α-amylase was immobilized on the membranes through either electrostatic or hydrophobic interaction (Miura et al., 2002).

In the studies of graft polymerization for the covalent immobilization of enzyme, the main purpose of the graft was to provide reactive sites, spacer (Wang and Hsiue, 1993) as well as moderate hydrophilicity/hydrophobicity. Some typical examples are indicated in Table 9.3.
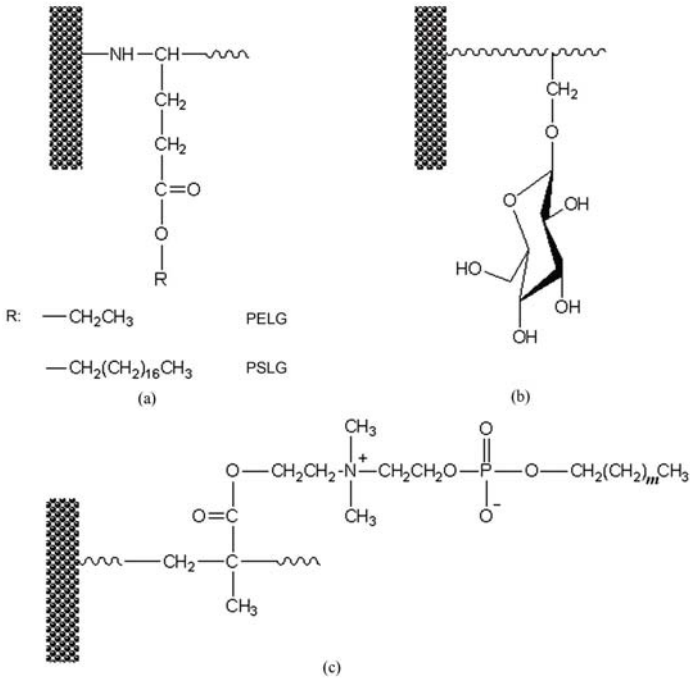
Fig. 9.16. Schematic representation of (a) PELG-/PSLG-; (b) PAG- and (c) PAP-modified membranes
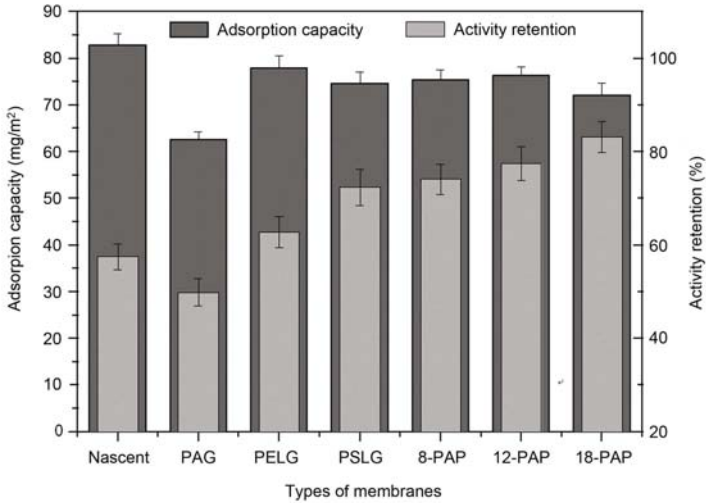
Fig. 9.17. Adsorption amount and activity retention of lipase on different PP membrane

Table 9.3. Covalent bonding of enzyme onto the graft-polymerization modified membranes

Membrane material	Grafted polymer	Coupling agent	Enzyme	Application	Ref.
Polyethylene	Polyacrylic acid	CMC	Glucose oxidase	Glucose biosensor	(Hsiue and Wang, 1990)
Nylon	Poly(BMA)	HMDA+glutaraldehyde	Urease	Non-isothermal bioreactor	(El-Sherif et al., 2001a; 2001b)
Nylon	Poly(DGDA)	Glutaraldehyde	β-Galactosidase	Non-isothermal bioreactor	(Eldin et al., 1999a)
PET	Poly(AEMA)	Glutaraldehyde	Fructosyltransferase	Bioreactor for synthesis of polysaccharides	(Hicke et al., 1999)
Acrylonitrile copolymer	Polyacrylamide	NaOH+GA	Cellulase	Hydrolysis of cellulose	(Yuan et al., 1999)
Poly(tetra fluorethylene)	Poly(HEMA) Poly(MAA)	HMDA+cyanuric chloride,Glutaraldehyde	β-Galactosidase	Glucose determination	(Eldin et al., 1999b)
PVDF	Poly(acrylic acid)	WSC	Glucose oxidase	Glucose determination	(Ying et al., 2002)
Polypropylene	Poly(aniline)	Glutaraldehyde (or adsorption)	Horseradish peroxidase	Biosensor, Affinity seperation	(Piletsky et al., 2003)
Nylon-6	Poly(GMA)	Direct bonding	Urease	Kidney machine	(Teke and Baysal, 2007)

- **Effect of Macromolecules Tethering (Grafting-to)**

Graft polymerization is generally initiated by energy excitation, which is simple and available for most materials and a large number of monomers. Differently, the "grafting-to" method usually needs the generation of reactive groups on the membrane for further reaction; however, this method is able to introduce some macromolecules that are hardly synthesized in common ways (e.g. radical-initiated polymerization). Enzymes can be immobilized on the macromolecules-tethered membrane by physical adsorption or chemical bonding.

In the case of physical adsorption, polyethyleneimine (PEI) was tethered onto poly(HEMA-*co*-GMA) membranes followed by incorporation of Cu (II) ions for immobilization of tyrosinase (Arica and Bayramoglu, 2004). The multi-point interaction was ionic between positively charged PEI and negatively-charged tyrosinase. In addition the enzyme could also bind Cu (II) ions because tyrosinase was a copper-dependent enzyme (the divalent metal ions as soft Lewis acids could interact with soft Lewis bases such as nitrogen and sulfur found in histine and cysteine). The beneficial properties of such an enzyme-membrane system include the mild immobilization conditions and one-step enzyme adsorption at substantially higher levels as well as membrane reusability. They would offer promising potential in several biochemical processes.

Similarly, for immobilization of glucose oxidase, chitosan was tethered onto a poly(HEMA-*co*-GMA) membrane and some of them were chelated with Fe (III) ions (Arica et al., 2007). The incorporated Fe (III) ions were used to immobilize glucose oxidase through adsorption, which was caused by chelation of Fe (III) ions with the phosphate group FAD (flavin adenie dinucleotides). Its molecular structure of glucose oxidase was shown in Fig.9.18. Besides the advantages mentioned in the above case, the tethering of chitosan also offered a biocompatible microenvironment to the guest enzyme.
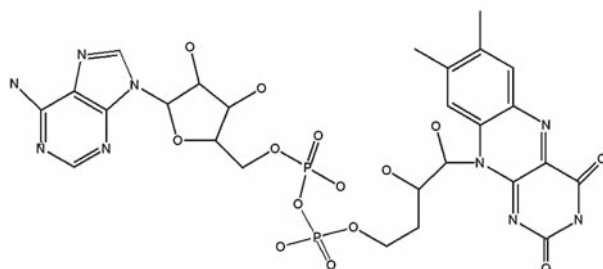
Fig. 9.18. The co-factor FAD in glucose oxidase

Based on the electrostatic interaction between enzyme and tethering-modified membranes, polyelectrolytes were assembled layer-by-layer within

the membrane pore domain for enzyme adsorption (Smuleac et al., 2006). The results show that the incorporated enzyme revealed only minor conformational changes and good reusability and could be easily regenerated.

In fact the macromolecules such as chitosan and gelatin possess a large amount of amino groups that are able to react with both reactive membranes and enzyme. This provides a route for enzyme immobilization by covalent bonding on a macromolecules-tethered membrane surface. As mentioned previously, acrylonitrile was able to copolymerize with other vinyl monomers (i.e. maleic anhydride) to introduce reactive groups (i.e. carboxyl). The copolymerization provided active sites for chitosan or gelatin tethering. In the studies by Ye et al. (2005a; 2006), chitosan or gelatin were tethered onto the EDC-activated poly(AN-*co*-MA) membrane surface and then lipase was immobilized onto the modified membrane (Fig.9.19) using glutaraldehyde as coupling agent. The results show that the construction of a dual-layer membrane increased the activity of immobilized lipase as well as the stability. In addition, the tethering of polycationic chitosan on the copolymer membrane also facilitated the ionic adsorption of lipase due to the electrostatic interaction (Ye et al., 2007).
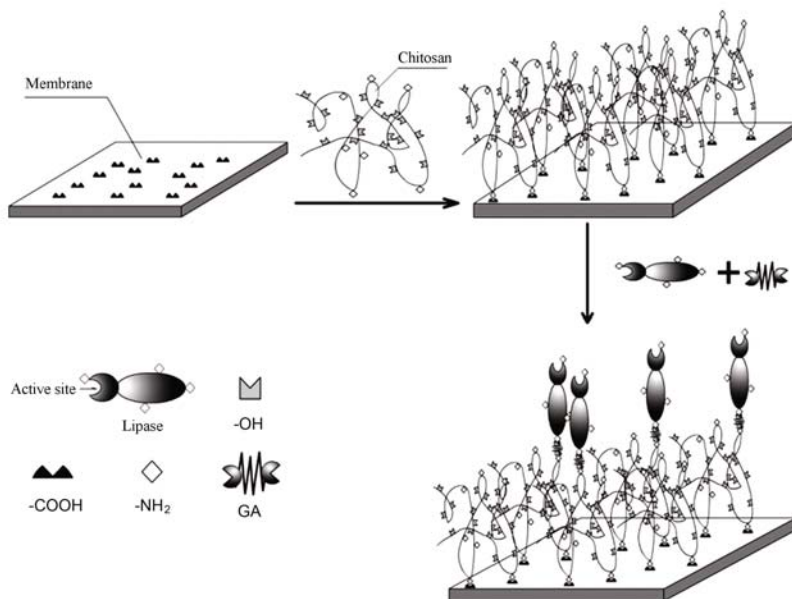
Fig. 9.19. Schematic representative for the preparation of the chitosan-modified membrane and lipase immobilization by glutaraldehyde. Reprinted from (Ye et al., 2006). Copyright (2005), with permission from Elsevier

9.3 Applications

The present applications of enzyme-immobilized membranes chiefly include laboratorial organic synthesis and analytical and medical applications. The former are usually realized by an enzymatic membrane bioreactor, in which enzyme-immobilized membranes are positioned in a unit. In the latter applications, the enzyme-immobilized membranes are mainly used in biosensors to probe the substrate quantitatively.

9.3.1 Membrane Bioreactor

In areas of laboratorial production, the functionality of an enzyme-immobilized membrane is most embodied in the enzymatic membrane bioreactor (EMBR), which realizes simultaneous and continuous product removal. In a membrane bioreactor, the biocatalyst is confined in a well-defined region of space by means of a selective membrane, or immobilized by adsorption on or entrapment within the polymeric matrix. Larger molecular-weight enzymes are kept from diffusing through the membrane by permeation, while low-molecular-weight substrates, products and inhibitors are readily allowed to pass through the membrane.
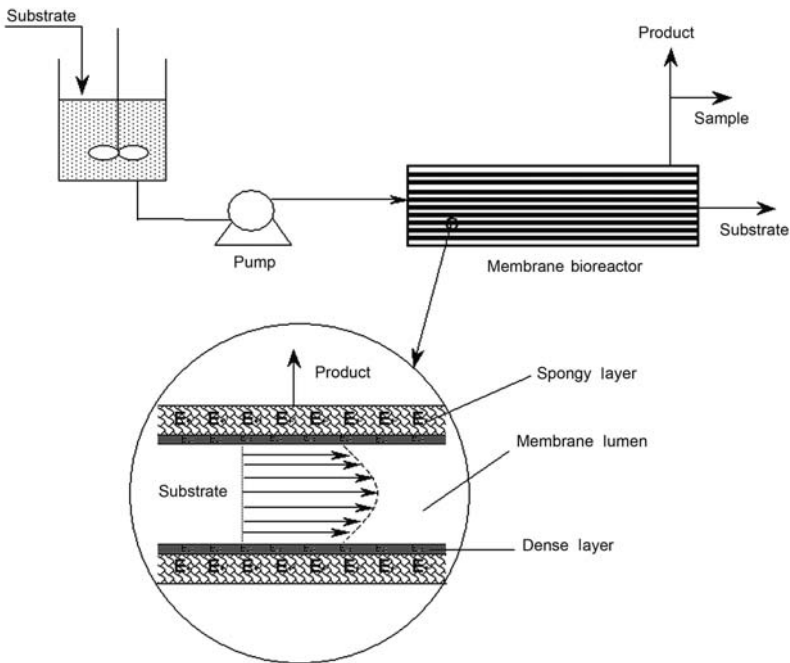
Fig. 9.20. Schematic configuration of enzyme membrane bioreactor

A hollow fiber membrane is considered as an attractive alternative for use in EMBR, due to its large surface area-volume ratio with a variety of module designs and operation modes. With such characteristics, a hollow fiber membrane bioreactor gives high volumetric productivity. The configuration of the general EMBR is shown in Fig.9.20. The membrane reactor generally consists of a bundle of ultrafiltration hollow fibers assembled in a cylindrical cartridge according to a tube and shell configuration. The fibers are asymmetric membranes with integration of a dense surface layer and a spongy support layer. In the bioreactor the substrate continuously flows mainly in the axial direction and partially in the radial direction. Meanwhile substrate is forced by ultra-filtration (under a certain pressure) to permeate through the membrane wall (skin and spongy layer); here it comes into contact with the entrapped enzyme and its bioconversion takes place. Products and unconverted substrate are continuously removed in a radial direction from the permeating stream. So far much research has focused on the development of EMBR (some are listed in Table 9.4) and several researchers put forward models to simulate the bioreactor. Calabrò et al. (2002) analyzed and characterized the behavior of EMBR from a theoretical point of view.

The given model was applied to different reacting systems and agreed well with some experimental data in the literature under some typical operating conditions. Gottifredi et al. (Gonzo and Gottifredi, 2007; Gottifredi and Gonzo, 2005) developed a technique to estimate the effectiveness factor in catalytic pellets so as to greatly simplify the simulation of membrane biocatalyst reactors. The procedure can be applied to any biocatalytic system provided that a single chemical reaction took place.

However, there are two main obstacles restricting the development of EMBR, which are related to the concentration polarization phenomena and the loss of total enzymatic activity. The concentration polarization leads to severe fouling of the membrane and an extremely low production rate, as measured by the mass flux of product. The total activity loss is attributed to several factors, including the thermal inactivation, leakage of enzyme and, furthermore, relatively high shear stress. The effective methods to resolve the problems involve (1) use of a relatively hydrophilic membrane, (2) clearance of the reactor at the time and (3) covalent attachment of enzyme on the membrane, etc. For example (Edwards et al., 1999), a chitosan gel was always coated on the polysulfone capillary membrane for polyphenol oxidase immobilization. The enzyme-composite membrane system was used to construct a bench scale bioreactor for removal of enzyme-generated products during treatment of industrial phenolic effluents. The bioreactor indicated greater efficiency than chitosan flakes and, furthermore, it was demonstrated that the presence of chitosan contributed considerably to the decrease in product inhibition.

Table 9.4. Some typical applications of EMBR

Enzyme	Membrane material/type	Application	Ref.
Fumarase	Polysulfone/Hollow fiber	Conversion of fumaric acid into L-malic acid	(Giorno et al., 2001)
Cellulase	Polysulfone/flat sheet	Hydrolysis of cellulose	(Gan et al., 2002)
Penicilline acylase	-/Hollow fiber	Hydrolysis of Penicilline	(Wenten and Widiasa, 2002)
Glucose oxidase; peroxidase	Polypyrrole/flat sheet	Oxidation of glucose	(Amounas et al., 2000)
Inulinase	Polysulfone/hollow fiber	Coversion of inuline to fructose	(Diaz et al., 2006)
Rhizopus juvanicus lipase	-/Flat sheet or hollow fiber	Hydrolysis of triglycerides (olive oil); peroxidation of fatty acids	(Bouwer et al., 1997)
Candida rugosa lipase; Pseudomonas cepacea lipase	Aromatic polyamide/hollow fiber	Hydrolysis of triglycerides; regioselective transesterification of 5,7-diacetoxyflavone	(Giorno et al., 1997)
Candida rugosa lipase	Poly(vinyl alcohol)-poly(tetra fluorethylene)/flat sheet	Hydrolysis of olive oil	(Xu et al., 2006a)
	Aromatic polyamide/hollow fiber	Chiral resolution of racemic naproxen methyl ester	(Giorno et al., 2007; Sakaki et al., 2001)
	Polyacrylonitrile /hollow fiber	Chiral resolution of racemic ibuprofen ester	(Long et al., 2003; 2005)

Especially because of the characteristics of lipase catalysis, biphasic EMBR is designed. The two-separate phase bioreactor consists of a continuous organic phase (containing the hydrophobic substrate to be converted), an enzyme-immobilized membrane, and a continuous aqueous phase (for extracting product). The membrane keeps the two phases separated and in contact at the same time. The transfer of hydrophobic substrate from the bulk organic phase to the enzyme and the transfer of product from reaction medium to the bulk aqueous solution are realized by diffusion. In the reactor the enzyme-immobilized membrane functions as a reaction interface; therefore the right choice of membrane material and suitable preparation of the membrane can meet the demand of the interface activation for lipase as well as for stability.

It was previously mentioned that Deng et al. (2005) physically immobilized lipase onto the different modified PP membranes. Among them, a glycopolymer-modified membrane was chosen for construction of EMBR, based on the hydrophilization and biocompabilization with the retention of some hydrophobicity. The hydrophobic membrane is physically, chemically and biologically stable especially in severe conditions. However, in the bioreactor the contact zone in hydrophobic membranes between the aqueous and organic phases is very thin because of the poor wettability of membranes, resulting in the low efficient use of an enzyme in the membrane wall. The results show that the lipase-immobilized PP membrane exhibited catalytic efficiency similar to that of some hydrophilic membranes in biphasic EMBR, verifying the feasibility of the employment of hydrophilized PP membranes in such EMR.

In a similar envision, i.e. making a hydrophobic membrane more hydrophilic and biocompatible, the blend of HEMA-terminated polyurethane pre-polymer and GMA was cured, which was coated on the PP membrane under UV (Pujari et al., 2006). Then lipase was immobilized onto the membrane through covalent bonding and the lipase aggregates were further crosslinked by glutaraldehyde. The lipase-immobilized membrane showed high activity and stability in the biphasic membrane bioreactor.

In addition, to improve stability, activity and enantioselectivity of immobilized lipase in the membrane reactor, the technique of emulsion was also introduced. Emulsions provide (1) the organic phase for hydrophobic substrate, (2) the interface with a large area for interfacial reaction and (3) the aqueous phase for extracting the product. Two kinds of procedures were used. In one procedure the lipase-immobilized membrane reactor was fed with an oil-in-water emulsion, in which the dispersed phase consisted of an organic phase containing the racemic ester substrate and the continuous phase was a buffer solution (Giorno et al., 2003). In another procedure the emulsion was first loaded within the membrane together with lipase and then the emulsion/lipase-immobilized membrane was placed between two separate phases, an organic phase containing the substrate and an aqueous phase ex-

tracting the product. The results indicate that immobilized enzymes showed high stability as well as high catalytic activity and enantioselectivity (Giorno et al., 2007).

9.3.2 Biosensor

A biosensor is usually defined as a sensing device consisting of a biological recognition element (e.g. enzymes, nucleic acids, antibodies and cells) in intimate contact with a suitable transducer, which is able to convert the biological recognition reaction or the biocatalytic process into a measurable electronic signal. The obtained electronic signal is proportional to the concentration of the analyte sensed. Different kinds of transducers have been employed in biosensors, viz potentiometric, amperometric, conductometric, thermometric, optical and piezo-electric, most of the current research being placed on the first two. The immobilization of enzyme on/in a support also reveals its advantages in biosensors over free enzyme cluster directly on a transducer's working tip: (1) reusability and (2) stability. A porous membrane as the support can allow the analyte to permeate through the network structure. In principle, because of enzyme specificity and sensitivity, the biosensor can be tailored for nearly any target analyte. Meeting the demand for practical, cost-effective and portable analytical devices, enzyme-based biosensors have enormous potential as useful tools in medicine, environmental in situ and real time monitoring, bioprocess and food control, and biomedical and pharmaceutical analysis.

However, we can deduce here a problem when enzyme is immobilized within the membrane, i.e. mass transfer limitation. Different from the bioreactor, no transmembrane pressure exists in the biosensor system and the analyte has to approach the enzymes by diffusion. If membrane biofouling occurs, the mass transfer of analyte will be further limited and the stability of the biosensor will be even deleteriously affected. Therefore, to resolve the problem, on the one hand the porosity and pore size need to be increased; on the other hand moderate modification of the membrane is required (Wisniewski and Reichert, 2000). Some cases of the enzyme-immobilized membrane explored in laboratorial biosensors are listed in Table 9.5.

Table 9.5. Applications of enzyme-immobilized membranes in biosensors

Enzyme	Membrane	Analyte	Ref.
Glucose oxidase	Plasma treated PP		(Hsiue et al., 1989)
	Polyethylene-g-acrylic acid		(Hsiue and Wang, 1990)
	Poly(tetra fluorethylene)-g-acrylic acid		(Turmanova et al., 1997)
	Poly(vinyl alcohol) cryogel	Glucose	(Doretti et al., 1997; 1998)[a]
	Eggshell		(Choi et al., 2001)
	Poly(8-hydroxyquinaldine)[b]		(Kasem et al., 1998)
	Cellulose acetate		(Alp et al., 2000)
	PEI-adsorbed polyelectrolyte[c]		(Nguyen et al., 2003)
Catalase	Poly(tetra fluorethylene)-g-acrylic acid/PE-g-acrylic acid	H_2O_2	(Silva et al., 1991)
Horseradish perosidase	Poly-o-phenylenediamine	H_2O_2	(Chen et al., 1997)
Uricase	Silk fibrorin	Uric acid	(Zhang et al., 1998)
Sulfite oxidase	Chitosan/poly(HEMA) copolymer	H_2O_2	(Ng et al., 2000)
Tyrosinase	Polyethersulfone	Monophenol; Diphenol	(Climent et al., 2001)
Fructose dehydrogenase	Cellulose acetate (embedding mediator)	D-fructose	(Tkac et al., 2001)
Acetylcholinesterase; Choline oxidase	Poly(HEMA)	Acetylcholine	(Kok et al., 2001)
Multienzyme systems[d]	Polypropylene-g-acrylic acid	Creatinine	(Hsiue et al., 2004)

[a] PEG-modified glucose oxidase; [b] electropolymerized monomers; [c] the polyelectrolyte included polyacrylonitrile and polysulfone-grafted-acrylic acid; [d] sarcosine oxidase/creatinase and sarcosine oxidase/creatinase/creatininase

9.4 Conclusion and Outlook

This chapter reviews how the membrane acted as a support for enzyme immobilization and the applications of enzyme-immobilized membranes in bioreactors and biosensors. The effect of membrane types as well as the modification methods of the membrane on the performance of an enzyme-immobilized membrane are described. Many kinds of membrane materials and enzymes are involved in the study of enzyme immobilization. From these cases we can find that enzyme immobilization on a membrane has been explored extensively and the enzyme-immobilized membranes revealed the good functioning of integrated catalysis and separation, regardless of the application in bioreactors or biosensors. Furthermore, the development of enzyme immobilization on membranes has also provided routes for other bio-catalysts immobilization.

However, the application of enzyme-immobilized membranes is still limited to laboratory scale operation. Several factors are considered that hinder their further development: (1) the absence of commercially available immobilization methods that can retain the activity, the required amount of enzyme and prevention simultaneously of the leakage of enzymes; (2) industrial-scale and continuous production of enzyme-immobilized membranes is still impossible; (3) the mass transfer limitation of substrate/analyte to the enzyme that occurs both in EMBR (concentration polarization) and biosensors (Wisniewski and Reichert, 2000). Therefore, to develop enzyme immobilization on the membrane and further the applications, much work has yet to be carried out. On the other hand, due to the natural instability of enzymes, other active biomolecules should also be considered as alternatives, such as cells. So the techniques of immobilizing other bioactive catalysts need to be pursued. In recent years the emergence and development of electrospinning techniques solved the problems to a certain extent, due to the unique characteristics of an electrospun nanofiberous membrane. This will be detailed in Chapter 10.

References

Akgol S, Bayramoglu G, Kacar Y, Denizli A, Arica MY (2002a) Poly(hydroxyethyl methacrylate-*co*-glycidyl methacrylate) reactive membrane utilized for cholesterol oxidase immobilization. Polym Int 51:1316-1322

Akgol S, Kacar Y, Ozkara S, Yavuz H, Denizli A, Arica MY (2001) Immobilization of catalase via adsorption onto L-histidine grafted functional pHEMA based membrane. J Mol Catal B-Enzym 15:197-206

Akgol S, Yalcinkaya Y, Bayramoglu G, Denizli A, Arica MY (2002b) Reversible immobilization of urease onto Procion Brown MX-5BR-Ni(II) attached polyamide hollow-fibre membranes. Process Biochem 38:675-683

Alp B, Mutlu S, Mutlu M (2000) Glow-discharge-treated cellulose acetate (CA) membrane for a high linearity single-layer glucose electrode in the food industry. Food Res Int 33:107-112

Amounas M, Innocent C, Cosnier S, Seta P (2000) A membrane based reactor with an enzyme immobilized by an avidin-biotin molecular recognition in a polymer matrix. J Membrane Sci 176:169-176

Arica MY (2000) Epoxy-derived pHEMA membrane for use bioactive macromolecules immobilization: Covalently bound urease in a continuous model system. J Appl Polym Sci 77:2000-2008

Arica MY, Baran T, Denizli A (1999) Beta-galactosidase immobilization into poly(hydroxyethyl methacrylate) membrane and performance in a continuous system. J Appl Polym Sci 72:1367-1373

Arica MY, Bayramoglu G (2004) Reversible immobilization of tyrosinase onto polyethyleneimine-grafted and Cu (II) chelated poly(HEMA-co-GMA) reactive membranes. J Mol Catal B-Enzym 27:255-265

Arica MY, Denizli A, Salih B, Piskin E, Hasirci V (1997) Catalase adsorption onto cibacron blue F3GA and Fe (III) derivatized poly(hydroxyethyl methacrylate) membranes and application to a continuous system. J Membrane Sci 129:65-76

Arica MY, Hasirci V (1993) Immobilization of glucose oxidase: A comparison of entrapment and covalent bonding. J Chem Technol Biot 58:287-292

Arica MY, Yilmaz M, Bayramoglu G (2007) Chitosan-grafted poly(hydroxyethyl methacrylate-co-glycidyl methacrylate) membranes for reversible enzyme immobilization. J Appl Polym Sci 103:3084-3093

Asakura T, Yoshimizu H, Kakizaki M (1990) An ESR study of spin-labeled silk fibroin membranes and spin-labeled glucose oxidase immobilized in silk fibroin membranes. Biotechnol Bioeng 35:511-517

Bayramoglu G, Kacar Y, Denizli A, Arica MY (2002) Covalent immobilization of lipase onto hydrophobic group incorporated poly(2-hydroxyethyl methacrylate) based hydrophilic membrane matrix. J Food Eng 52:367-374

Bayramoglu G, Yilmaz M, Arica MY (2004) Immobilization of a thermostable alpha-amylase onto reactive membranes: kinetics characterization and application to continuous starch hydrolysis. Food Chem 84:591-599

Biederman H, Boyaci IH, Bilkova P, Slavinska D, Mutlu S, Zemek J, Trchova M, Klimovic J, Mutlu M (2001) Characterization of glow-discharge-treated cellulose acetate membrane surfaces for single-layer enzyme electrode studies. J Appl Polym Sci 81:1341-1352

Bora U, Kannan K, Nahar P (2005) A simple method for functionalization of cellulose membrane for covalent immobilization of biomolecules. J Membrane Sci 250:215-222

Bora U, Sharma P, Kannan K, Nahar P (2006) Photoreactive cellulose membrane – A novel matrix for covalent immobilization of biomolecules. J Biotechnol 126:220-229

Bouwer ST, Cuperus FP, Derksen JTP (1997) The performance of enzyme-membrane reactors with immobilized lipase. Enzyme Microb Tech 21:291-296

Calabró V, Curcio S, Iorio G (2002) A theoretical analysis of transport phenomena in a hollow fiber membrane bioreactor with immobilized biocatalyst. J Membrane Sci 206:217-241

Carneiro-da-Cunha MG, Rocha JMS, Garcia FAP, Gil MH (1999) Lipase immobilization on to polymeric membranes. Biotechnol Tech 13:403-409

Chen BH, Zhu K, Wu HH, Zhang YZ (1997) Electron transfer of horseradish peroxidase entrapped in poly-*o*-phenylenediamine membrane electrode. Chem J Chinese Univ 18:615-620

Chen CI, Chen CW, Huang CW, Liu YC (2007) Simultaneous purification and immobilization of penicillin G acylase using bifunctional membrane. J Membrane Sci 298:24-29

Choi MMF, Pang WSH, Xiao D, Wu XJ (2001) An optical glucose biosensor with eggshell membrane as an enzyme immobilisation platform. Analyst 126:1558-1563

Climent PV, Serralheiro MLM, Rebelo MJF (2001) Development of a new amperometric biosensor based on polyphenoloxidase and polyethersulphone membrane. Pure Appl Chem 73:1993-1999

Curcio S, Calabro V, Iorio G (2000) An experimental analysis of membrane bioreactor performances with immobilized chymosin. J Membrane Sci 173:247-261

Cygler M, Schrag JD (1999) Structure and conformational flexibility of Candida rugosa lipase. BBA-Mol Cell Biol L 1441:205-214

Danisman T, Tan S, Kacar Y, Ergene A (2004) Covalent immobilization of invertase on microporous PHEMA-GMA membrane. Food Chem 85:461-466

Dayal R, Godjevargova T (2005) Polyacrylonitrile enzyme ultrafiltration and polyamide enzyme microfiltration membranes prepared by diffusion and convection. Macromol Biosci 5:222-228

Dayal R, Godjevargova T (2006) Pore diffusion studies with immobilized glucose oxidase plus catalase membranes. Enzyme Microb Tech 39:1313-1318

Deng HT, Xu ZK, Dai ZW, Wu J, Seta P (2005) Immobilization of Candida rugosa lipase on polypropylene microfiltration membrane modified by glycopolymer: Hydrolysis of olive oil in biphasic bioreactor. Enzyme Microb Tech 36:996-1002

Deng HT, Xu ZK, Huang XJ, Wu J, Seta P (2004a) Adsorption and activity of Candida rugosa lipase on polypropylene hollow fiber membrane modified with phospholipid analogous polymers. Langmuir 20:10168-10173

Deng HT, Xu ZK, Liu ZM, Wu J, Ye P (2004b) Adsorption immobilization of Candida rugosa lipases on polypropylene hollow fiber microfiltration membranes modified by hydrophobic polypeptides. Enzyme Microb Tech 35:437-443

Deng HT, Xu ZK, Wu J, Ye P, Liu ZM, Seta P (2004c) A comparative study on lipase immobilized polypropylene microfiltration membranes modified by sugar-containing polymer and polypeptide. J Mol Catal B-Enzym 28:95-100

Diaz EG, Catana R, Ferreira BS, Luque S, Fernandes P, Cabral JMS (2006) Towards the development of a membrane reactor for enzymatic inulin hydrolysis. J Membrane Sci 273:152-158

Doretti L, Ferrara D, Gattolin P, Lora S (1997) Amperometric biosensor with physically immobilized glucose oxidase on a PVA cryogel membrane. Talanta 44:859-866

Doretti L, Ferrara D, Gattolin P, Lora S, Schiavon F, Veronese FM (1998) PEG-modified glucose oxidase immobilized on a PVA cryogel membrane for amperometric biosensor applications. Talanta 45:891-898

Edwards W, Leukes WD, Rose PD, Burton SG (1999) Immobilization of polyphenol oxidase on chitosan-coated polysulphone capillary membranes for improved phenolic effluent bioremediation. Enzyme Microb Tech 25:769-773

El-Sherif H, De Maio A, Di Martino S, Zito E, Rossi S, Canciglia P, Gaeta FS, Mita DG (2001a) Urease immobilization on chemically grafted nylon membranes Part 2: Non-isothermal characterization. J Mol Catal B-Enzym 14:31-43

El-Sherif H, Martelli PL, Casadio R, Portaccio M, Bencivenga U, Mita DG (2001b) Urease immobilisation on chemically grafted nylon membranes Part 1: Isothermal characterisation. J Mol Catal B-Enzym 14:15-29

Eldin MSM, Bencivenga U, Portaccio M, Stellato S, Rossi S, Santucci M, Canciglia P, Gaeta FS, Mita DG (1998) Beta-galactosidase immobilization on premodified Teflon membranes using gamma-radiation grafting. J Appl Polym Sci 68:625-636

Eldin MSM, De Maio A, Di Martino S, Bencivenga U, Rossi S, D'Uva A, Gaeta FS, Mita DG (1999a) Immobilization of beta-galactosidase on nylon membranes grafted with diethylenglycol dimethacrylate (DGDA) by gamma-radiation: Effect of membrane pore size. Adv Polym Tech 18:109-123

Eldin MSM, Portaccio M, Diano N, Rossi S, Bencivenga U, D'Uva A, Canciglia P, Gaeta FS, Mita DG (1999b) Influence of the microenvironment on the activity of enzymes immobilized on Teflon membranes grafted by gamma-radiation. J Mol Catal B-Enzym 7:251-261

Fujita A, Kawakita H, Saito K, Sugita K, Tamada M, Sugo T (2003) Production of tripeptide from gelatin using collagenase-immobilized porous hollow-fiber membrane. Biotechnol Progr 19:1365-1367

Gabrovska K, Georgieva A, Godjevargova T, Stoilova O, Manolova N (2007) Poly(acrylonitrile)chitosan composite membranes for urease immobilization. J Biotechnol 129:674-680

Gan Q, Allen SJ, Taylor G (2002) Design and operation of an integrated membrane reactor for enzymatic cellulose hydrolysis. Biochem Eng J 12:223-229

Gille M, Staude E (1994) Symmetric enzyme distribution in asymmetric UF polysulfone membranes. Biotechnol Bioeng 44:557-562

Giorno L, D'Amore E, Mazzei R, Piacentini E, Zhang J, Drioli E, Cassano R, Picci N (2007) An innovative approach to improve the performance of a two separate phase enzyme membrane reactor by immobilizing lipase in presence of emulsion. J Membrane Sci 295:95-101

Giorno L, Drioli E, Carvoli G, Cassano A, Donato L (2001) Study of an enzyme membrane reactor with immobilized fumarase for production of L-malic acid. Biotechnol Bioeng 72:77-84

Giorno L, Li N, Drioli E (2003) Use of stable emulsion to improve stability, activity, and enantioselectivity of lipase immobilized in a membrane reactor. Biotechnol Bioeng 84:677-685

Giorno L, Molinari R, Natoli M, Drioli E (1997) Hydrolysis and regioselective transesterification catalyzed by immobilized lipases in membrane bioreactors. J Membrane Sci 125:177-187

Godjevargova T (1996) Radiation grafting of AMPSA and DMAEM onto membranes of acrylonitrile copolymer and polyamide for immobilization of glucose oxidase. J Appl Polym Sci 61:343-349

Godjevargova T, Dayal R, Marinov I (2004) Simultaneous covalent immobilization of glucose oxidase and catalase onto chemically modified acrylonitrile copolymer membranes. J Appl Polym Sci 91:4057-4063

Godjevargova T, Gabrovska K (2003) Immobilization of urease onto chemically modified acrylonitrile copolymer membranes. J Biotechnol 103:107-111

Godjevargova T, Gabrovska K (2005) Kinetic parameters of urease immobilized on modified acrylonitrile copolymer membranes in the presence and absence of Cu (II) ions. Macromol Biosci 5:459-466

Godjevargova T, Gabrovska K (2006) Influence of matrix on external mass transfer resistance in immobilized urease membranes. Enzyme Microb Tech 38:338-342

Godjevargova T, Konsulov V, Dimov A (1999) Preparation of an ultrafiltration membrane from the copolymer of acrylonitrile-glycidylmethacrylate utilized for immobilization of glucose oxidase. J Membrane Sci 152:235-240

Godjevargova T, Konsulov V, Dimov A, Vasileva N (2000) Behavior of glucose oxidase immobilized on ultrafiltration membranes obtained by copolymerizing acrylonitrile and N-vinylimidazol. J Membrane Sci 172:279-285

Gonzo EE, Gottifredi JC (2007) A simple and accurate method for simulation of hollow fiber biocatalyst membrane reactors. Biochem Eng J 37:80-85

Gottifredi JC, Gonzo EE (2005) On the effectiveness factor calculation for a reaction-diffusion process in an immobilized biocatalyst pellet. Biochem Eng J 24:235-242

Hicke HG, Bohme P, Becker M, Schulze H, Ulbricht M (1996) Immobilization of enzymes onto modified polyacrylonitrile membranes: Appplication of the acyl azide method. J Appl Polym Sci 60:1147-1161

Hicke HG, Ulbricht M, Becker M, Radosta S, Heyer AG (1999) Novel enzyme-membrane reactor for polysaccharide synthesis. J Membrane Sci 161:239-245

Hilal N, Kochkodan V, Nigmatullin R, Goncharuk V, Al-Khatib L (2006) Lipase-immobilized biocatalytic membranes for enzymatic esterification: Comparison of various approaches to membrane preparation. J Membrane Sci 268:198-207

Hilal N, Nigmatullin R, Alpatova A (2004) Immobilization of crosslinked lipase aggregates within microporous polymeric membranes. J Membrane Sci 238:131-141

Hsiue GH, Liu CH, Wang CC (1989) Preparation of glucose oxidase membrane for the application of glucose sensor by plasma activation. J Appl Polym Sci 38:1591-1605

Hsiue GH, Lu PL, Chen JC (2004) Multienzyme-immobilized modified polypropylene membrane for an amperometric creatinine biosensor. J Appl Polym Sci 92:3126-3134

Hsiue GH, Wang CC (1990) Glucose oxidase immobilized polyethylene-g-acrylic acid membrane for glucose oxidase sensor. Biotechnol Bioeng 36:811-815

Imai K, Shiomi T, Uchida K, Miya M (1986) Immobilization of enzyme onto poly(ethylene-vinyl alcohol) membrane. Biotechnol Bioeng 28:198-203

Jiang HH, Zou HF, Wang HL, Ni JY, Zhang Q (2000) Covalent immobilization of trypsin on glycidyl methacrylate-modified cellulose membrane as enzyme reactor. Chem J Chinese Univ 21:702-706

Jolivalt C, Brenon S, Caminade E, Mougin C, Pontie M (2000) Immobilization of laccase from Trametes versicolor on a modified PVDF microfiltration membrane: Characterization of the grafted support and application in removing a phenylurea pesticide in wastewater. J Membrane Sci 180:103-113

Kasem KK, Sheets J, Koon N (1998) Modified electrodes with synthetic biocatalytic membranes. Biotechnol Progr 14:791-796

Kawakami M, Koya H, Gondo S (1988) Immobilization of glucose oxidase on polymer membranes treated by low-temperature plasma. Biotechnol Bioeng 32:369-373

Keusgen M, Glodek J, Milka P, Krest I (2001) Immobilization of enzymes on PTFE surfaces. Biotechnol Bioeng 72:530-540

Klotzbach T, Watt M, Ansari Y, Minteer SD (2006) Effects of hydrophobic modification of chitosan and Nafion on transport properties, ion-exchange capacities, and enzyme immobilization. J Membrane Sci 282:276-283

Kok FN, Bozoglu F, Hasirci V (2001) Immobilization of acetylcholinesterase and choline oxidase in/on pHEMA membrane for biosensor construction. J Biomater Sci-Polym Ed 12:1161-1176

Krajewska B (1991a) Chitin and its derivative as supports for immobilization of enzymes. Acta Biotechnol 11:269-277

Krajewska B (1991b) Urease immobilized on chitosan membrane. Inactivation by heavy metal ions. J Chem Technol Biot 52:157-162

Krajewska B (2004) Application of chitin- and chitosan-based materials for enzyme immobilizations: A review. Enzyme Microb Tech 35:126-139

Krajewska B, Piwowarska Z (2005) Free vs chitosan-immobilized urease: Microenvironmental effects on enzyme inhibitions. Biocatal Biotransfor 23:225-232

Krajewska B, Leszko M, Zaborska W (1990) Urease immobilized on chitosan membrane: Preparation and properties. J Chem Technol Biot 48:337-350

Krajewska B, Zaborska W, Leszko M (1997) Inhibition of chitosan-immobilized urease by boric acid as determined by integration methods. J Mol Catal B-Enzym 3:231-238

Krajewska B, Zaborska W, Leszko M (2001) Inhibition of chitosan-immobilized urease by slow-binding inhibitors: Ni^{2+}, F^- and acetohydroxamic acid. J Mol Catal B-Enzym 14:101-109

Lin CC, Yang MC (2003a) Cholesterol oxidation using hollow fiber dialyzer immobilized with cholesterol oxidase: Effect of storage and reuse. Biomaterials 24:549-557

Lin CC, Yang MC (2003b) Cholesterol oxidation using hollow fiber dialyzer immobilized with cholesterol oxidase: Preparation and properties. Biotechnol Progr 19:361-364

Lin CC, Yang MC (2003c) Urea permeation and hydrolysis through hollow fiber dialyzer immobilized with urease: storage and operation properties. Biomaterials 24:1989-1994

Liu JL, Wang JQ, Bachas LG, Bhattacharyya D (2001) Activity studies of immobilized subtilisin on functionalized pure cellulose-based membranes. Biotechnol Progr 17:866-871

Long WS, Bhatia S, Kamaruddin A (2003) Modeling and simulation of enzymatic membrane reactor for kinetic resolution of ibuprofen ester. J Membrane Sci 219:69-88

Long WS, Kamaruddin A, Bhatia S (2005) Chiral resolution of racemic ibuprofen ester in an enzymatic membrane reactor. J Membrane Sci 247:185-200

Magalhães JMCS, Machado AASC (1998) Urea potentiometric biosensor based on urease immobilized on chitosan membranes. Talanta 47:183-191

Miura S, Kubota N, Kawakita H, Saito K, Sugita K, Watanabe K, Sugo T (2002) High-throughput hydrolysis of starch during permeation across alpha-amylase-immobilized porous hollow-fiber membranes. Radiat Phys Chem 63:143-149

Murtinho D, Lagoa AR, Garcia FAP, Gil MH (1998) Cellulose derivatives membranes as supports for immobilisation of enzymes. Cellulose 5:299-308

Ng LT, Guthrie JT, Yuang YJ (2000) UV cured biocompatible membrane for biosensor application. Polym Int 49:1017-1020

Nguyen QT, Ping ZH, Nguyen T, Rigal P (2003) Simple method for immobilization of bio-macromolecules onto membranes of different types. J Membrane Sci 213:85-95

Nie FQ, Xu ZK, Wan LS, Ye P, Wu J (2004) Acrylonitrile-based copolymers containing reactive groups: synthesis and preparation of ultrafiltration membranes. J Membrane Sci 230:1-11

Piletsky S, Piletska E, Bossi A, Turner N, Turner A (2003) Surface functionalization of porous polypropylene membranes with polyaniline for protein immobilization. Biotechnol Bioeng 82:86-92

Pujari NS, Vaidya B, Bagalkote S, Ponrathnam S, Nene S (2006) Poly(urethane methacrylate-co-glycidyl methacrylate)-supported-polypropylene biphasic membrane for lipase immobilization. J Membrane Sci 285:395-403

Rauf S, Ihsan A, Akhtar K, Ghauri MA, Rahman M, Anwar MA, Khalid AM (2006) Glucose oxidase immobilization on a novel cellulose acetate-polymethylmethacrylate membrane. J Biotechnol 121:351-360

Ruckenstein E, Li ZF (2005) Surface modification and functionalization through the self-assembled monolayer and graft polymerization. Adv Colloid Interfac 113:43-63

Sakaki K, Giorno L, Drioli E (2001) Lipase-catalyzed optical resolution of racemic naproxen in biphasic enzyme membrane reactors. J Membrane Sci 184:27-38

Shiomi T, Tohyama M, Satoh M, Miya M, Imai K (1988) Properties of invertase immobilized on the poly(ethylene-co-vinyl alcohol) hollow fiber membrane. Biotechnol Bioeng 32:664-668

Silva MAD, Gil MH, Piedade AP, Redinha JS, Brett MO, Costa JMC (1991) Immobilization of catalase on membranes of poly(ethylene)-g-co-acrylic acid and poly(tetrafluoroethylene)-g-co-acrylic acid and their application in hydrogen peroxide electrochemical sensors. J Polym Sci Polym Chem 29:269-274

Smuleac V, Butterfield DA, Bhattacharyya D (2006) Layer-by-layer-assembled microfiltration membranes for biomolecule immobilization and enzymatic catalysis. Langmuir 22:10118-10124

Sousa HA, Rodrigues C, Klein E, Afonso CAM, Crespo JG (2001) Immobilisation of pig liver esterase in hollow fibre membranes. Enzyme Microb Tech 29:625-634

Stollner D, Scheller FW, Warsinke A (2002) Activation of cellulose membranes with 1,1′-carbonyldiimidazole or 1-cyano-4-dimethylaminopyridinium tetrafluoroborate as a basis for the development of immunosensors. Anal Biochem 304:157-165

Tanioka A, Yokoyama Y, Miyasaka K (1998) Preparation and properties of enzyme-immobilized porous polypropylene films. J Colloid Interf Sci 200:185-187

Teke AB, Baysal SH (2007) Immobilization of urease using glycidyl methacrylate grafted nylon-6-membranes. Process Biochem 42:439-443

Tkac J, Vostiar I, Sturdik E, Gemeiner P, Mastihuba V, Annus J (2001) Fructose biosensor based on D-fructose dehydrogenase immobilised on a ferrocene-embedded cellulose acetate membrane. Anal Chim Acta 439:39-46

Turmanova S, Trifonov A, Kalaijiev O, Kostov G (1997) Radiation grafting of acrylic acid onto polytetrafluoroethylene films for glucose oxidase immobilization and its application in membrane biosensor. J Membrane Sci 127:1-7

Uragami T, Ueguchi K, Watanabe A, Miyata T (2006) Preparation of urease-immobilized polymeric membranes and their function. Catal Today 118:158-165

Vasileva N, Godjevargova T (2004) Study on the behaviour of glucose oxidase immobilized on microfiltration polyamide membrane. J Membrane Sci 239:157-161

Vasileva N, Godjevargova T (2005) Study of the effect of some organic solvents on the activity and stability of glucose oxidase. Mater Sci Eng C-Bio S 25:17-21

Wang CC, Hsiue GH (1993) Glucose oxidase immobilization onto a plasma-induced graft copolymerized polymeric membrane modified by poly(ethylene oxide) as a spacer. J Appl Polym Sci 50:1141-1149

Wang YJ, Hu Y, Xu J, Luo GS, Dai YY (2007) Immobilization of lipase with a special microstructure in composite hydrophilic CA/hydrophobic PTFE membrane for the chiral separation of racemic ibuprofen. J Membrane Sci 293:133-141

Wenten IG, Widiasa IN (2002) Enzymatic hollow fiber membrane bioreactor for penicilin hydrolysis. Desalination 149:279-285

Wisniewski N, Reichert M (2000) Methods for reducing biosensor membrane biofouling. Colloid Surface B 18:197-219

Xu J, Wang YJ, Hu Y, Luo GS, Dai YY (2006a) Candida rugosa lipase immobilized by a specially designed microstructure in the PVA/PTFE composite membrane. J Membrane Sci 281:410-416

Xu J, Wang YJ, Hu Y, Luo GS, Dai YY (2006b) Immobilization of lipase by filtration into a specially designed microstructure in the CA/PTFE composite membrane. J Mol Catal B-Enzym 42:55-63

Yang MC, Lin CC (2001) Urea permeation and hydrolysis through hollow fiber dialyzer immobilized with urease. Biomaterials 22:891-896

Ye P, Jiang J, Xu ZK (2007) Adsorption and activity of lipase from Candida rugosa on the chitosan-modified poly(acrylonitrile-co-maleic acid) membrane surface. Colloid Surface B 60:62-67

Ye P, Xu ZK, Che AF, Wu J, Seta P (2005a) Chitosan-tethered poly(acrylonitrile-co-maleic acid) hollow fiber membrane for lipase immobilization. Biomaterials 26:6394-6403

Ye P, Xu ZK, Wang ZG, Wu J, Deng HT, Seta P (2005b) Comparison of hydrolytic activities in aqueous and organic media for lipases immobilized on poly(acrylonitrile-co-maleic acid) ultrafiltration hollow fiber membrane. J Mol Catal B-Enzym 32:115-121

Ye P, Xu ZK, Wu J, Deng HT, Seta P (2005c) Covalent immobilization of lipase on poly(acrylonitrile-co-maleic acid) ultrafiltration hollow fiber membrane. Chem Res Chinese Univ 21:723-727

Ye P, Xu ZK, Wu J, Innocent C, Seta P (2006) Entrusting poly(acrylonitrile-*co*-maleic acid) ultrafiltration hollow fiber membranes with biomimetic surfaces for lipase immobilization. J Mol Catal B-Enzym 40:30-37

Ying L, Kang ET, Neoh KG (2002) Covalent immobilization of glucose oxidase on microporous membranes prepared from poly(vinylidene fluoride) with grafted poly(acrylic acid) side chains. J Membrane Sci 208:361-374

Yuan XY, Shen NX, Sheng J, Wei X (1999) Immobilization of cellulase using acrylamide grafted acrylonitrile copolymer membranes. J Membrane Sci 155:101-106

Zhang YQ, Shen WD, Gu RA, Zhu J, Xue RY (1998) Amperometric biosensor for uric acid based on uricase-immobilized silk fibroin membrane. Anal Chim Acta 369:123-128

Zhao JS, Yang ZY, Zhang YH, Yang ZY (2004) Immobilization of glucose oxidase on cellulose/cellulose acetate membrane and its detection by scanning electrochemical microscope (SECM). Chinese Chem Lett 15:1361-1364

10

Nanofibrous Membrane with Functionalized Surface

Nanofibers are able to form a highly porous membrane and their attractive features promote their applications in many fields. This chapter covers the studies of the functionalization of the nanofibrous membranes and corresponding applications, including catalysis, micro-detection and target capturing. This review suggests that nanofibrous membranes offer great promise in bioapplications.

10.1 Introduction

10.1.1 Principal and Fundamental Aspects

One principle of nanotechnology is that the reduction in the dimensions of a material leads to new properties, i.e. generally the so called surface effect, small size effect, quantum effect and scale effect, as well as some emerging super-properties (e.g. superconductivity and superparamagnetism) and exceptional properties (e.g. lotus effect). Therefore, because of the unique properties and potential applications, nano-scale materials especially with one dimension have been subject of research. A one-dimensional (1D) nanostructure is mostly generated in the form of fiber, wire, rod, belt, tube, spiral or ring by a large number of methods. Among these methods electrospinning seems the simplest technique for fabricating nanofibers with both solid and hollow interiors that are exceptionally long in length, uniform in diameter and diversified in composition (Li and Xia, 2004). Furthermore, electrospinning is currently the only technique that allows the fabrication of continuous fibers with diameters ranging from several micrometers down to a few nanometers. This method is applicable to synthetic and natural polymers, polymer alloys, polymers loaded with nanoparticles or active agents, as well as to metals and ceramics. Fibers with complex architectures, such as core-shell fibers, can be produced by special electrospinning methods. It is also possible to produce

fibers in ordered arrangements. In short, the technique of electrospinning is highly versatile.

Fig.10.1 shows a schematic illustration of a typical setup for electrospinning. The apparatus consists of three major parts: a high-voltage power supply, a needle-like spinneret, and a grounded conductive collector. The spinneret is connected to a syringe containing polymer solution (or melt). The solution is fed through the syringe to the spinneret at a constant and controllable rate. When a high voltage is applied, the pendent drop of polymer solution at the nozzle of the spinneret is electrically charged and the induced charges are evenly distributed over the drop surface. The electrostatic repulsion between the surface charges and the columbic force exerted by the external electric field will be the major electrostatic forces on the drop. Under these electrostatic interactions the liquid drop will be distorted into a conical object commonly known as the Taylor Cone. At a critical voltage (i.e. once the strength of the electric field has surpassed a threshold value), the electrostatic forces overcome the surface tension of the solution and force a jet to erupt from the tip of the spinneret. The electrified jet is only stable near the tip of spinneret, after which the jet undergoes a stretching and whipping process. As the jet accelerates toward lower-potential regions, the solvent evaporates while the entanglements of the polymer chains prevent the jet from breaking up. In the basic setup a grounded target is used to collect the resultant fibers that are deposited in the form of non-woven mesh. Almost any soluble or fusible polymer with moderate molecular weight can be electrospun. Generally speaking, the ideal electrospinning process should meet such requirements that (Huang et al. 2003): (1) the diameter of the fibers is consistent and controllable; (2) the fiber surface is defect-controllable and (3) continuous single nanofiber is collectable. One of the most important parameters related to electrospinning is the fiber diameter. On the one hand, depending on the jet sizes as well as polymer contents in the jets it has been recognized that during the traveling of a solution jet from spinneret onto the collector the primary jet may or may not be split into multiple jets, resulting in different fiber diameters. On the other hand, regardless of the splitting, the morphology and diameter of fibers are dependent on the intrinsic properties of the solution (such as solubility, glass-transition temperature, melting point, crystallization velocity, molecular weight, molecular-weight distribution, entanglement density, solvent vapor pressure, pH value, electrical conductivity, viscosity or concentration, surface tension of the solvent) and process parameters (such as the strength of electrical field, the distance between spinneret and collector, the feeding rate for the polymer solution as well as the humidity and temperature of the surroundings). In general, if more diluted solution is used the conductivity of the solution is increased by adding some salts or a lower feeding rate for the solution is adopted, and the diameter of the fibers will be significantly decreased.
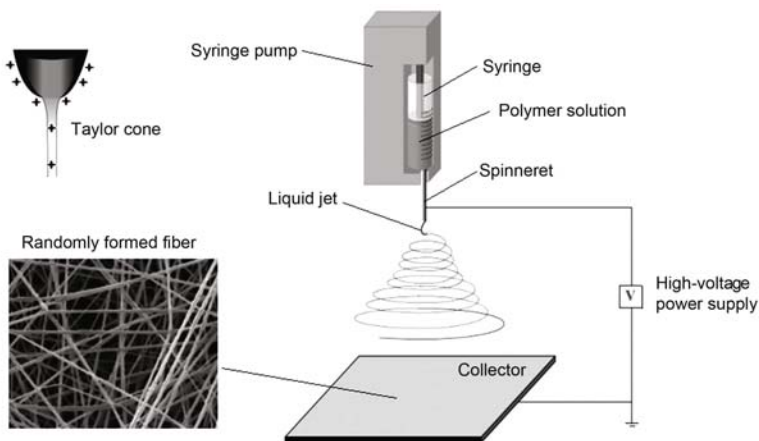
Fig. 10.1. A typical electrospinning setup using a grounded static collector

According to the requirements for the nanofiber assemblies, one can either control the flight of the electrospinning jet through the manipulation of the electric field or design a specific collection device (dynamic or static) or combine both above. These methods have yielded aligned fibers with various degrees of order and fiber directions for two- and three-dimensional assemblies. Many typical apparatuses have been reviewed and discussed in detail to obtain such assemblies (Teo and Ramakrishna, 2006). For example, a high speed rotating drum(Fig.10.2(a)) is commonly used to collect aligned fibers. A pair of parallel conductive electrodes (Fig.10.2(b)) are able to create an electric field so that electrospun fibers are preferentially aligned across the gap between the electrodes. Aligned individual fibers can be positioned on a tapered and grounded disc collector (Fig.10.2(c)) because the tip-like edge substantially concentrates the electric field, which makes a deposited nanofiber repulsive to the next fiber attracted to the tip. To fabricate a tubular scaffold, electrospun fibers are deposited on a rotating tube and the deposited fiber layer is subsequently extracted from the tube. Fiber alignment can be controlled with auxiliary electrodes to create an electric field profile that influences the flight of the electrospinning jet.

10.1.2 Applications of Electrospun Nanofibers

Electrospinning, derived from electrostatic spinning, has its basis in earlier studies. Although the relative phenomenon has been documented in the literature since 1745, the crucial patent appeared in 1934, in which an experimental setup for production of polymer filaments by means of an electrostatic force was described for the first time (Formhals, 1934). Despite these early discoveries the procedure was not used commercially. In 1971 an apparatus was patented for electrospin acrylic fibers with diameters of 0.05 to 1.1
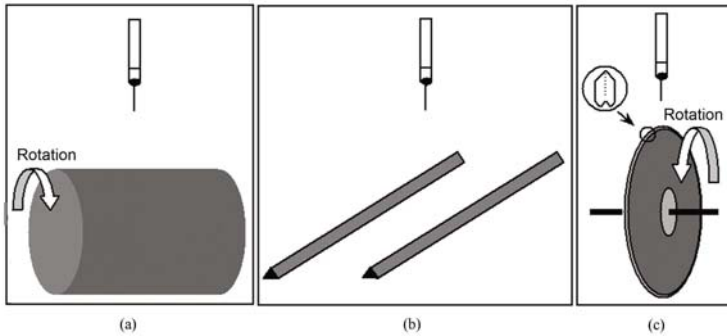
Fig. 10.2. Schematic of electrospinning setups for obtaining various fibrous assemblies. (a) Rotating drum; (b) Parallel electrode; (c) Disc collector. Reprinted from (Teo and Ramakrishna, 2006). Copyright (2006), with permission from IOP Publishing Ltd.

μm (Baumgarten, 1971). However, this work, which was followed by other patents, also remained unnoticed. Electrospinning has gained substantial academic attention since the 1990s partially because of a surging interest in nanotechnology, as this process can fabricate ultrafine fibers or fibrous structures of various polymers with diameters down to submicrons or nanometers. The activities of the Reneker group (Dishi et al., 1995) also played a significant role in furthering the studies on electrospinning.

In addition to the inherent properties of nanostructures, the regained attention of electrospun nanoscale fibers can also be attributed to a number of unique features: (1) extremely long length; (2) large surface area-to-volume ratio and complex pore structure; (3) alignment on the molecular level. These features distinguish electrospun fibers from 1D nanostructures fabricated by other techniques. The electrospinning technique and resultant structures have been drawing considerable attention and have been applied in many fields because of the simplicity of the fabrication scheme, the diversity of materials suitable for electrospinning and the interesting features associated with electrospun nanofibers. In the following sections some applications of the nanofibrous membrane will be simply discussed.

10.1.2.1 Filtration Application

An electrospun nanofibrous membrane, which possesses high porosity, interconnectivity and microscale interstitial space, is an attractive candidate for membrane preparation. Generally speaking, to obtain high filtration efficiency, it is necessary that the sizes of the channels and pores in the filter material be adjusted to the sizes of the particles to be filtered. Nanofibrous membranes had been extensively explored in air filters. Even though an extremely thin layer of electrospun fibrous membrane is used in air filters,

high filtration efficiency could still be obtained. With regard to ultrafiltration/microfiltration, electrospun nanofibrous membranes can also act as the scaffold to make the filter highly permeable and highly separation efficient (Yoon et al., 2006) by means of a layer assemble technique (Fig.10.3).
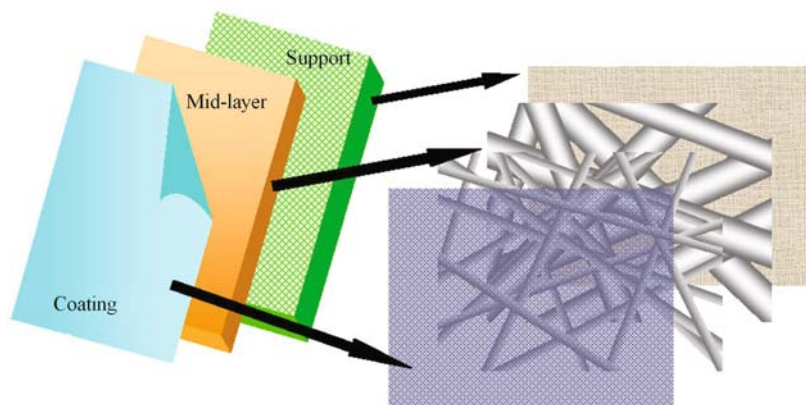
Fig. 10.3. Schematic diagram for the assembly of three-tier composite membrane. Reprinted from (Yoon et al., 2006). Copyright (2006), with permission from Elsevier

10.1.2.2 Reinforcement Application

Fiber-based reinforcement (using glass fiber and carbon fiber, etc.) is one of the most effective strategies for enhancing the strength and other performance of a composite material. The large surface-to-volume ratio associated with nanofibers can significantly increase the interaction between the fibers and the matrix material. The nanoscale fibers can realize "molecular reinforcement" (Greiner and Wendorff, 2007). Because of these two effects, nanofibers can lead to better reinforcement than other kinds of fibers. Much research has demonstrated that the nanofibers reinforced the matrix up to an order of magnitude and several times greater.

10.1.2.3 Biomedical Application

Current biomedical applications of nanostructured polymers are chiefly perused in medicine and pharmacy. One significant consideration is that the nanoscale is particularly relevant for biological systems, because the dimensions of proteins, viruses and bacteria fall in the same size range. Because of the peculiar structure, electrospun nanofibers were preliminarily explored in tissue engineering, drug delivery and wound dressing, etc. For example,

for tissue engineering an ideal scaffold should replicate the structure (three-dimensional fiber network) and function (surrounds cells and supports them) of the natural extracellular matrix as closely as possible, until the cultured cells have formed a new matrix. Therefore an electrospun non-woven mesh seems to be a promising scaffold. In addition, the diversity of materials to be electrospun and the controllable structure of the mesh also drive the studies of cell culture. So far a variety of cells have been seeded onto such carrier matrices for the generation of target tissues.

10.1.2.4 Catalysis Application

Electrospinning provides a series of attractive supports for carrying enzymes and other catalysts, because these supports possess high porosity and large surface-to-volume ratio. Nanofibrous membranes, on the one hand, are able to provide much room for loading catalysts and, on the other hand, have very low restriction on the diffusion of substrates towards catalysts. In addition these nanofibers can be easily recovered from the reaction system, which substantially reduces the production cost. In the case of biocatalysts, in recent years nanofibrous membranes have showed great potential in the immobilization of a variety of enzymes, such as α-chymotrypsin, lipase, cellulase, glucose oxidase, catalase.

In addition, because of the versatility of nanofibers, their applications have branched into areas such as biofuel cells, protective clothing, sacrificial templates, electrode materials and electronic and optical devices, and there is potential in other areas too. It is expected that the applications of nanofibrous membranes will be increasingly extended by further functionalization.

10.2 Nanofibrous Membrane Functionalization

The functionalization of a nanofibrous membrane usually refers to two aspects: the direct application endowed such nanostructured material with special functionality and the modification endows the material with potential for further use. For example, immobilization of catalytic molecules (such as enzyme) can functionalize the nanofibrous membranes with catalytic activity, and can promote the use of the catalysts in more circumstances, such as biofuel cells. Fig.10.4 schematically shows the principle of a typical biofuel cell. The nanofibrous membrane with a high amount of enzyme loading can endow the biofuel cell with high power density. Furthermore, to obtain a higher performance of the immobilized enzyme, the nanofibrous membrane can be functionally modified. In the following sections we will chiefly describe the applications of the nanofibrous membranes in the catalysis of substrates and capture of target molecules.
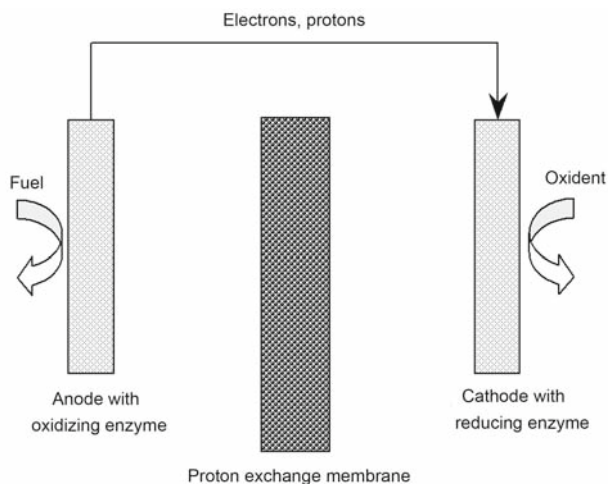
Fig. 10.4. Schematic of enzyme-based fuels

10.2.1 Biocatalytic Electrospun Membrane

Many research groups have devoted a number of studies to this fabrication. In addition to large surface area-to-volume ratio, importance is also attributed to the following: (1) the variety of polymer for electrospinning can meet various requirements for choice of supports; (2) the high porosity and small sizes of units relieve the mass transfer of the substrates; (3) the durability of such inter-connective and continuous structures ensures the repeated use of immobilized enzyme; (4) many nanostructures are well known for stabilizing the proteins; (5) the filtration performance of the nanofibrous membrane can be combined with the biocatalytic properties to realize simultaneously the highly efficient functioning of catalysis and separation.

Enzymes can be immobilized through attachment on the fiber surface or entrapment in the fiber. Surface attachment includes physical adsorption, covalent bonding and a combination of adsorption and crosslinking. Entrapment chiefly refers to the confinement of enzymes in the fibers and can be easily achieved by electrospinning of the mixture of polymer solution and enzymes. Crosslinking of entrapped enzymes is able to further prevent the leakage of enzymes from fibers.

10.2.1.1 Surface Attachment

- **On Pristine Nanofiber Surface**

As previously reported (Jia et al., 2002), α-chymotrypsin was covalently attached to the functionalized polystyrene (PS) nanofibers with a typical diameter of 120 nm (Fig.10.5). The observed enzyme loading was up to 1.4 wt.%,

corresponding to over 27.4% monolayer coverage of the external surface of the PS nanofibers. The specific activity for the immobilized enzyme was over 65% of that for the native enzyme in aqueous solution, which indicates a low diffusional restriction of substrate. When the immobilized α-chymotrypsin was used in organic solvents, such as hexane and isooctane, it exhibited over three orders of magnitude higher activity than that of its natural counterpart.
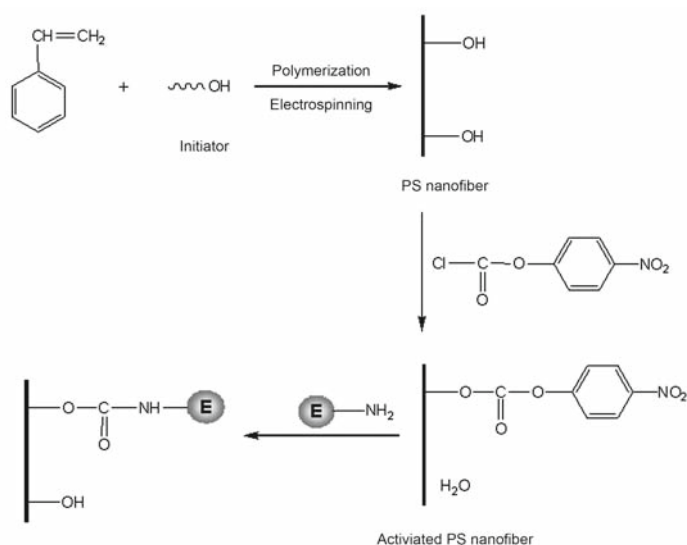
Fig. 10.5. Schematic representation for the fabrication of PS nanofibers and the subsequent enzyme immobilization. E represents the enzyme

Also, using pristine nanofibers as carrier material, electrospun silk fibroin nanofibers were applied as the support for enzyme immobilization (Lee et al. 2005). This silk fibroin (SF) was regenerated from silkworm cocoons. It was found that these SF nanofibers loaded enzymes up to 5.6 wt.%. The specific activity of the immobilized α-chymotrypsin on SF nanofibers was 8 times higher than that on silk fibers and increased as the fiber diameter decreased. The enzyme stability was compared among four SF samples. Sample SF8 (with 205 nm fiber diameter) had excellent stability in aqueous solution at 25 °C and retained more than 90% of the initial activity after 24 h (80% for free enzymes). Sample SF11 (with 320 nm fiber diameter) showed a higher stability in ethanol, retaining more than 45% of the initial activity (5% for free enzyme). This indicates that the enzyme revealed enhanced stability after immobilization on SF nanofibers.

Ye et al. (2006a) used an electrospun nanofibrous membrane from poly(acrylonitrile-*co*-maleic acid) (PAN-MA) as the support for lipase immobilization, considering the excellent performance of a polyacrylonitrile membrane.

In Chapter 8 the hollow fiber membrane from this copolymer was referred to as being used for lipase immobilization. It was found that the activity retention and amount of the immobilized enzyme on a nanofibrous membrane were both higher than those on a hollow fiber membrane. The Michaelis constant (K_m, the reflection of partition and diffusion effects) was also higher for the nanofibrous membrane, suggesting the easier accessibility of the substrate to the active sites of the immobilized enzyme, caused by relieved diffusion limitation.

Kim et al. (2005) developed an approach for the fabrication of enzyme aggregate coatings on the surfaces of electrospun polymer nanofibers (depicted in Fig.10.6). This approach employed the covalent attachment of seed enzyme molecules onto the nanofibers, followed by crosslinking of additional enzyme molecules and aggregates from solution onto the seed enzyme molecule using glutaraldehyde. α-Chymotrypsin (CT) was coated on the nanofibers electrospun from a mixture of PS and poly(styrene-co-maleic anhydride) (PSMA). The results show that the initial apparent activity of the CT-aggregate-coated nanofibers was nine times higher than that of nanofibers with just a monolayer of covalently attached CT molecules. The stability of the CT-aggregate-coated nanofibers had essentially no measurable loss of activity over a month under rigorous shaking conditions. The resultant enzyme-aggregate coating was thought of as bunches of crosslinked enzyme aggregates (CLEAs) that were covalently attached to nanofibers by a linker of each seed enzyme molecule. Furthermore, CLEAs were well known for their high stability. This is the reason why the enzyme-aggregate coating on the nanofibers both led to high overall enzyme activity and stabilized the enzyme activity of the final biocatalytic nanofibers. This approach of enzyme coating on nanofibers, yielding high activity and stability, created a useful biocatalytic system with potential applications in some fields (e.g. biofuel cells, bioconversion, bioremediation, and biosensors).

A blend mixture of biodegradable poly(-caprolactone) and poly(D,L-lactic-co-glycolic acid)-NH$_2$ (PLGA-b-PEG-NH$_2$) was electrospun and used for lysozyme immobilization (Kim and Park, 2006). Close to the previous results, the enzyme loading and catalytic activity of the immobilized lysozyme on the nanofiber was higher than that on casting film. Recently Nair et al. (2007) immobilized lipase onto hydrophobic PS/PSMA (containing maleic anhydride) composite nanofibers. The resultant nanofibers were pretreated in aqueous alcohol solution. Thereafter the tightly aggregated nanofibers could be dispersed in water into a loosely entangled structure for long periods of time. The treated nanofibers increased the enzyme loading up to about 8 times and augmented the steady-state conversion of a continuous flow reactor filled with enzyme-loaded nanofibers.

Using electrospun polyacrylonitrile (PAN) nanofibers as supports, Li et al. (2007) covalently immobilized lipase by an amidination reaction. It was
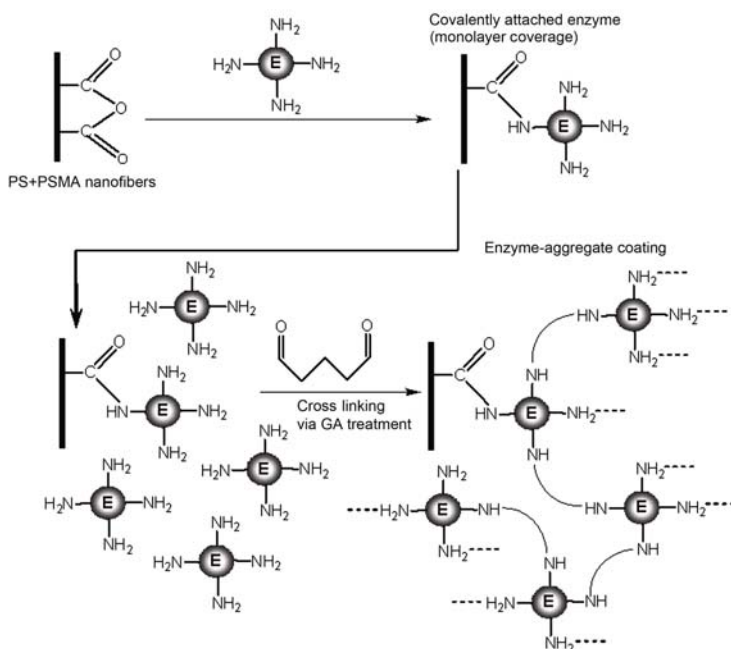
Fig. 10.6. Schematic diagram for the preparation of covalently attached enzymes and enzyme-aggregate coatings on nanofibers using glutaraldehyde as a crosslinker. The nanofibers were electrospun from the mixture of PS and PSMA. E represents the enzyme. Reprinted from (Kim et al., 2005). Copyright (2006), with permission from IOP Publishing Ltd.

found that the immobilization method showed a better performance (activity retention and stabilities) than many other immobilized lipase systems.

Although the nanofiber has low limitation for the diffusion of substrate, the nonspecific interaction between the surface and the enzyme is still an important factor in negatively affecting the activity of the enzyme. By modification of the support surfaces through biocompatiblization or the introduction of spacer, the performance of the immobilized enzyme can be improved. These mechanisms have been introduced in detail in Chapter 8.

- **On Modified Nanofiber Surface**

It has been previously mentioned that lipase could be immobilized onto the nanofibers electrospun from acrylonitrile-based copolymers. Moreover, the carboxyl-contained nanofibers were further modified with chitosan or gelatin, which would favor lipase immobilization with regard to activity and stabilities of loaded enzyme (Ye et al., 2006b). It appeared that the tethered biomacromolecule formed a dual-layer with the support surface. The results indicate that there was an increase in the maximum velocity of en-

zyme catalysis ($V_{\max}$) for the lipase immobilized on the chitosan- or gelatin-modified nanofibers, in comparison with the lipase immobilized on the pristine nanofibers. It has been previously mentioned that the enzymatic activity was increased by the introduction of phospholipid moieties onto polypropylene membranes (also referred to in Chapter 8). Considering this, nanofibers containing phospholipid moieties were fabricated from poly[acrylonitrile-*co*-(2-methacryloyloxyethyl phosphorylcholine)] (PANMPC) and used as the support for lipase immobilization (Huang et al., 2006). Lipase was immobilized on the nanofibers through physical adsorption by means of electrostatic interaction. Once immersed in phosphate buffer, the zwitterionic phospholipid moieties reoriented on the surface of the nanofibers, forming a stable and biocompatible external microenvironment for lipase activation. Fig.10.7 schematically shows preparation of the copolymer nanofiber and the electrostatic interaction between phospholipid moieties and lipase. The results indicate that the activity of adsorbed lipase increased a lot after the phospholipid moities were introduced and high enzyme loading was retained.

Based on the concept of combining hydrophobicity and biocompatibility, electrospun polysulfone (hydrophobic) with poly(*N*-vinyl-2-pyrrolidone) (PVP) or poly(ethylene glycol) (PEG) as additives (biocompatible) were used for immobilizing lipase (Wang et al., 2006a). The results show that the addition of PVP or PEG increased the activity of the immobilized lipase.

An approach was developed to tailor the adsorption behavior and the activity of lipase through modulation of the structure of grafted poly(acrylic acid) (PAA) on the cellulose nanofibers (Chen and Hsieh, 2005). The grafting structure was dependent on the surface initiating mode: a gel-like structure was formed by the ceric-ion initiated reaction and a brush-like structure was formed by methacrylation (with methacrylate chloride) and polymerization. The extensive and entangled polyanions PAA was able to form complex with Ce (III) to form a crosslinked 3D structure, which usually had a stronger ability to seize enzyme molecules. With PAA grafts increased, enzyme molecules adsorbed on the outer layer of the gels might hamper the diffusion and accessibility of additional enzyme molecules to the binding sites underneath, lowering the efficiency of enzyme adsorption. Therefore the diffusion of enzyme molecules became more difficult as the extent of entanglement, crosslinking, and/or the thickness of the 3D network structure increased. The brush-like structures had a lower capacity to entrap enzyme. The results show that the fiber surfaces with fewer but longer PAA grafts had higher adsorption efficiency for lipase, which implies a possible change of enzyme binding from mono-layer to multi-layer. However, the lipase adsorbed on the surfaces with fewer but shorter PAA grafts exhibited higher activities. For the lipase adsorbed in the gel-like structure, the catalytic activity was lower because of the entangled and crosslinked structure of the PAA network, which limited the diffusion of the substrate and the conformational freedom of the adsorbed enzymes. On the ceric ion-initiated grafted surface, the adsorbed lipase pos-
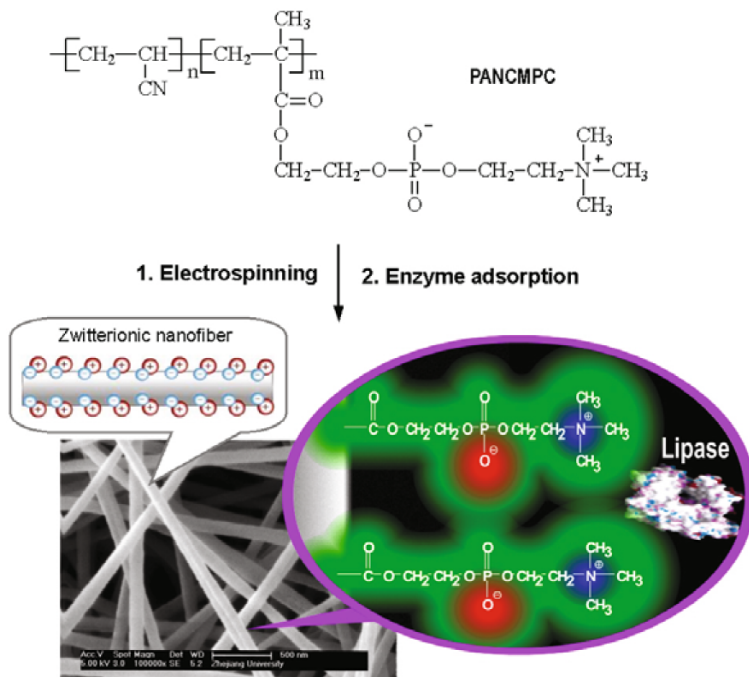
Fig. 10.7. Schematic representation for the fabrication of phospholipid-modified nanofibers and lipase adsorption. The adsorption is driven by the electrostatic interaction between the positively-charged group in the phospholipid moiety and the negatively-charged lipase. The nanofibers are charged by the zwitterionic phospholipid moieties (Huang et al., 2006). Copyright (2006). Reprinted with permission of John Wiley & Sons, Inc.

sessed improved stability to organic solvent over free lipase. In polar solvents, such as alcohol, the greater ability of the PAA grafts to retain water lessened water loss, thus protecting the enzyme, while in non-polar solvents, such as THF and hexane, the multipoint binding sites of PAA prevented the enzymes from exposing more of their hydrophobic domains, stabilizing their conformation. The two structures of PAA grafts are indicated in Fig.10.8.

Introduction of a spacer arm onto the support is another effective method for enhancing the catalytic activity of an immobilized enzyme. The flexible spacers can offer the enzyme greater freedom of movement and minimize steric hindrance caused by solid supports, so that the microenvironment for the immobilized enzyme is 'closed to the free one'.

In a typical case (Wang and Hsieh, 2004) PEG used as an amphiphilic spacer with reactive end groups for lipase immobilization was pre-tethered onto the alkali-hydrolyzed cellulose nanofibers (Fig.10.9). PEG was selected as a spacer because this polyether exhibits attractive biological properties, such as protein resistance. While free lipase retained only 25% of its orig-
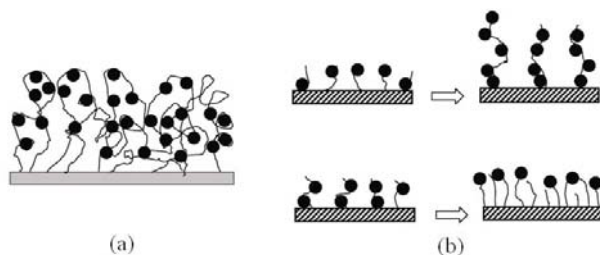
Fig. 10.8. Schematic representation for enzyme immobilization on the poly(acrylic acid) (PAA)-grafted surface of ultra-fine cellulose fiber. The structural model of PAA grafts can be: (a) gel-like structure; (b) brush-like structure with increased grafted-chain length (upside) and increased grafted-chain density (downside). (Chen and Hsieh 2005). Copyright (2005). Reprinted with permission of Wiley-Liss, Inc., a subsidiary of John Wiley & Sons, Inc.

inal activity, the fiber-bound lipase possessed a much higher retention of catalytic activity after exposure to cyclohexane, toluene and hexane. This indicates that the tethered PEG was able to stabilize the conformation of lipase in the non-polar and non-aqueous medium. Furthermore, the fibrous structure was retained throughout the alkaline hydrolysis, activation, coupling, and activity assays. This stabilization effect might be attributed to the hydrophilization of the fibers, because the formed hydrophilic layer on the surface could protect lipase molecules from hydrophobically interacting with the outer surroundings. Such interaction was one of the factors that leads to protein unfolding and subsequent activity loss.
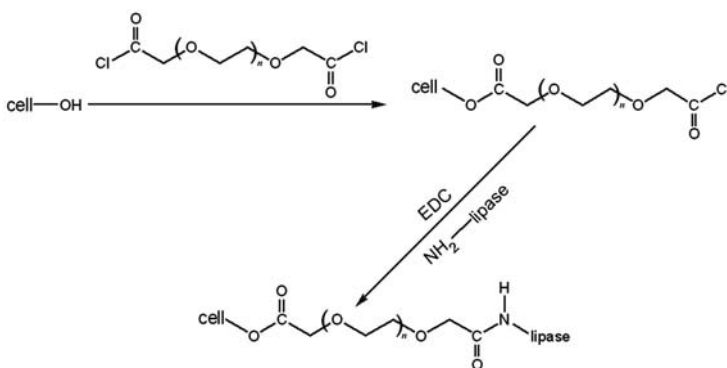
Fig. 10.9. Reactions of PEG diacylchloride with cellulose fibers and immobilization of enzymes to the PEG spacer-grafted nanofibers (Wang and Hsieh, 2004). Copyright (2004). Reprinted with permission of John Wiley & Sons, Inc.

Co-electrospinning of support materials with other components might have a great impact on the performance of the immobilized enzymes, because the properties of the support can be tailored, such as electrical conductivity or biocompatibility. In particular, an increase in electrical conductivity of the support is favorable to redox enzymes because the electron transfer between the enzyme and the substrate can be fastened. This hypothesis has been realized through the fabrication of an electrochemical biosensor. In our studies (Wang et al., 2006b; 2007), a nanofibrous membrane containing carbon nanotubes (CNTs) was used as the support for catalase or horseradish peroxidase immobilization, and it was found that the CNTs had a positive effect on the activity of immobilized enzymes. Preparation of such support was very simple: blending polymer with acid-treated CNTs in the solvent and then electrospinning. Since CNT was discovered by Iijima (1991), it has attracted much interest because of its series of excellent properties, such as superb electrical conductivity, high chemical stability and remarkable mechanical strength. CNTs (Fig.10.10(a)), consisting of cylindrical graphite sheets of nanometer diameter, can be divided into single-walled nanotube (SWNT), double-walled nanotube (DWNT) and multi-walled nanotube (MWNT) according to the number of layers of graphite sheets. As an outstanding conductive material, CNTs have been successfully applied to the biosensor aiming to promote the electron transfer reactions of proteins (including those where the redox center is embedded deeply within the glycoprotein shell). Therefore, in the nanofibers-redox enzyme system, CNTs were also expected to act as the pathway for fastening the electron transfer. It was concluded that in the catalytic reaction, electron transfer between catalase and the substrate H_2O_2 was facilitated by the enhanced-conductive nanofibers (Fig.10.10(b)). Therefore the activity of catalase was increased. According to the Michaelis constant, another property of CNTs might work in the catalytic system, namely the biocompatibility effect of CNTs. The storage stability of the immobilized catalase on modified nanofibers was higher than that on the pristine nanofibers. Compared with chemical modifications, this method is relatively simple and time-saving. Therefore such composite support has the potential to be explored in other fields, such as electrochemistry. As the price of CNT decreases, the membrane even has possible future applications in large-scale operations.

10.2.1.2 Encapsulation

Encapsulation of enzymes in the nanofibers can be achieved by direct electrospinning of enzymes along with other components (organic or inorganic materials). Compared with surface immobilization, this immobilization approach has the advantages of easier processing, high enzyme loading and lower exposure of enzyme to harsh chemicals.

In general it is difficult to electrospin natural proteins into fibers. In the case of casein, over 55% of the amino acids in casein proteins contain polar
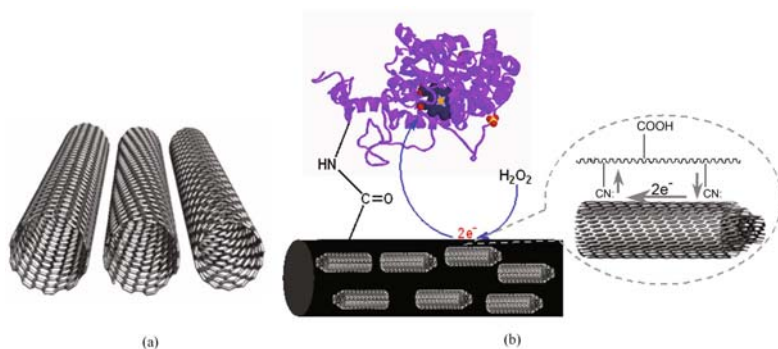
Fig. 10.10. (a) Scheme of carbon nanotubes; (b) Schematic representation for the role of MWCNT in the catalytic system. The arrow points to the direction of electron transfer

groups, i.e., 26% -COOH, 15% -NH$_2$ and 15% -OH. These polar groups enable the formation of intermolecular and intra-molecular hydrogen bonding among the casein molecules, which is the main factor that leads to failure in the electrospinning of this protein. PVA or PEO is often used for blending with natural macromolecules for electrospinning. This is mainly due to the following: (1) they are non-toxic, water-soluble polymers with good chemical and thermal stability; (2) they are easily modified through their hydroxyl groups; (3) they are commercially available in a wide range of molecular weights at a low price; (4) they are biocompatible and (5) they have dissimilar structures to the natural biomacromolecules and a capacity to form secondary bonding with proteins, which would dissociate the hydrogen-bonded molecules (protein, chitosan, etc.) and interrupt the three dimensional structure. An approach was even developed to blend PVA or PEO with the natural protein (Xie and Hsieh, 2003). The PVA/casein or PEO/casein solution was electrospun into nanofibers and subsequently crosslinked with 4,4′-methylenebis(phenyl diisocyanate) (MDI). Both nanofiberous membranes showed great stability in the aqueous medium. A similar method was also used to encapsulate lipase into the nanofiber. The catalytic activity of lipase entrapped in PVA fibers was about 100-fold lower than that of free lipase. The activity of lipase in the nanofibers was over 6 times higher than that in the cast membrane.

PVAs were also electrospun together with cellulose into a nanofibrous membrane followed by crosslinking in the presence of glutaraldehyde vapor (Wu et al., 2005). It was found that the activity of immobilized cellulase in PVA nanofibers was over 65% of that of the free one, and was obviously higher than that in the casting film from the same solution. It was demonstrated that the crosslinking reaction had a great impact on the activity of immobilized enzymes because crosslinking damaged the active site of the enzyme to a large extent. As expected, the catalytic efficiency of the immobilized cellulase

decreased gradually in the process of crosslinking, because cellulase access to the substrate was more difficult and more active sites were damaged. However, -OH in PVA molecules could also participate in the crosslinking, which resulted in a slower decline in the activity of the immobilized cellulase, with a prolonged crosslinking time.

In another study (Ren et al., 2006), PVA/glucose oxidase (GOD) was directly electrospun on the electrode followed by crosslinking using glutaraldehyde. The schematic diagram of the electrospinning setup is shown in Fig.10.11, in which the Pt electrode was used to collect the composite nanofibers. Results of chronoamperometric measurements, namely the linear response range and the lower detection limit indicate that electrospinning was a convenient and efficient method for preparing enzyme electrodes. Also, Sawicka et al. (2005) applied a PVP/urease nanofibers-based biosensor to analyze urea. This biosensor shows advantages over the prior technology, such as a shorter response time, a greater sensitivity to lower concentrations of urea, and a more versatile design.
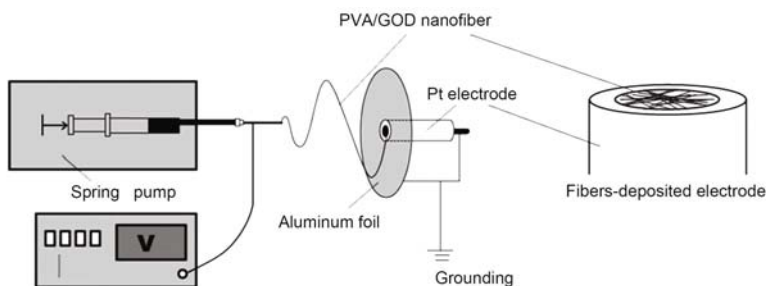
Fig. 10.11. Schematic diagram of the electrospinning setup for the preparation of nanofibers-deposited electrode. Reprinted from (Ren et al., 2006). Copyright (2006), with permission from Elsevier

Generally speaking, encapsulation immobilization possesses a series of advantages over surface attachment. However it still has some insufficiencies:

- The enzyme molecules are not only embedded into the nanofibers, but also reside on the surface, which usually leads to a leakage of enzymes;
- Because most of the enzyme molecules are confined inside the nonporous fibers, the diffusion of the substrate to the enzyme is restricted;
- These nanofiber materials are limited to several kinds of polymers, which are able to form a homogeneous solution with enzyme. As is known, most enzymes are water-soluble. However, only a few polymers can be dissolved in the aqueous medium. Even if the homogeneous solution is electrospun, nanofibers with beads can still be observed in the nanofibrous membrane. Moreover, when the nanofibrous membranes are immersed in solvents,

their water solubility causes them to swell and disintegrate, resulting in enzyme leakage, poor thermal stability and reusability.

- Crosslinking of the enzyme-encapsulated fibers tends to reduce the porosity (as shown in Fig.10.12) and would result in conformational changes of the enzyme molecules, which in turn limits the accessibility of the substrates to the active sites of the enzymes.

(a)   (b)
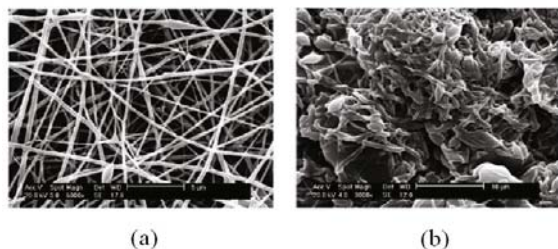
Fig. 10.12. Electrospun PVA/cellulase fibers (a) before and (b) after crosslinking. Reprinted from (Wu et al., 2005). Copyright (2005), with permission from Elsevier

Considering these obstacles, a novel method was proposed to prepare enzyme-encapsulated mesoporous silica nanofibers (Patel et al., 2006). The features of this system included a high surface area to volume ratio facilitating substrate diffusion, no deformation of the fibers with little or no swelling, no enzyme leakage, high thermal stability, increased reusability and the freedom to encapsulate various kinds of enzymes individually. The activity of the encapsulated enzyme in mesoporous silica nanofibers was higher than that in a conventional silica sample and silica powders, thus contributing to biocatalytic applications.

10.2.2 Affinity Electrospun Membrane

Electrospinning can also be used to prepare affinity membranes. Affinity membranes are a broad class of membranes that selectively capture specific target molecules (or ligates) by immobilization of a specific capturing agent (or ligand) onto the membrane surface. In biotechnology, affinity membranes can be applied in protein purification and toxin removal from bioproducts, etc. In environmental industry, affinity membranes can be applied in the removal of organic waste removal and heavy metal in water treatment.

As a biomimetic method, cyclic (α-allyl glucoside, AG) and linear (D-gluconamidoethyl methacrylate, GAMA) sugars were introduced into PAN nanofibers by electrospinning, respectively, and the nanofibrous membranes were used to isolate the protein mixture (Yang et al., 2006). This isolation is based on selective recognition between saccharide residues and proteins,

which is the first step in numerous phenomena based on cell-cell interactions, such as blood coagulation, immune response, viral infection, inflammation, embryogenesis and cellular signal transfer. The saccharide, such as glucose, is well known as having specific recognition to concanavalin A (Con A) that is a kind of lectin, lectins being a large group of carbohydrate binding proteins. It is reported the lectin can specifically recognize α-glucopyranoside and α-mannopyranoside residues through free 3-, 4-, and 6-hydroxyl groups. The results indicate that by recognition through AG moieties, the concentration of Con A in Con A/bovine serum albumin (BSA) mixture solution decreased greatly, revealing that the AG-contained nanofibers had a strong affinity to Con A. On the contrary, the GAMA-contained nanofibers showed very low, or even no affinity to Con A except some non-specific adsorption, because only the pyranose ring form participated in the interaction with Con A. The molecular structures of AG- and GAMA-contained copolymer and the recognition scheme are indicated in Fig.10.13. With glycopolymers bearing different sugar moieties, one can envisage that these materials are very useful in protein isolation, lectin or antibody-binding assay, drug delivery systems, molecularly imprinted polymers.
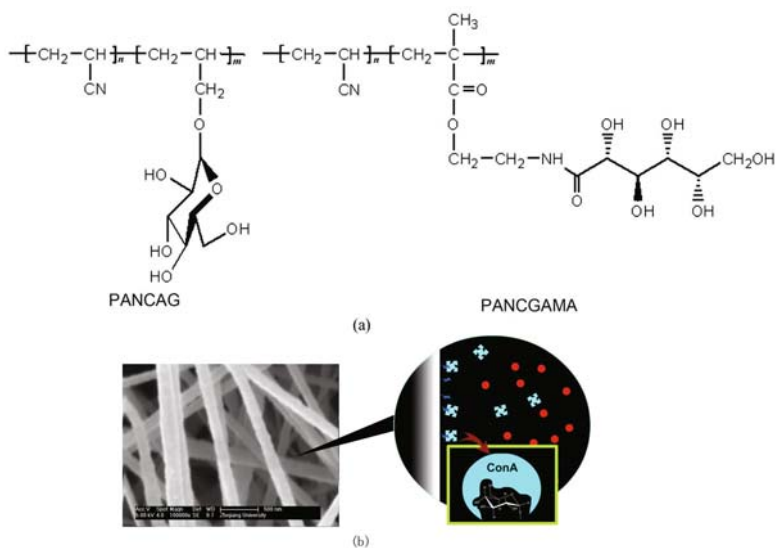
Fig. 10.13. (a) Molecular structures of poly(acrylonitrile-*co*-AG) and poly(acrylonitrile-*co*-GAMA); (b) Recognition of AG to Con A (Yang et al., 2006). Copyright (2006). Reprinted with permission of John Wiley & Sons, Inc.

Ma et al. developed a series of affinity nanofibrous membranes to capture the specific target molecules. For example, Cibacron Blue F3GA (CB) was immobilized onto the cellulose membrane (Fig.10.14(a) (Ma et al., 2005))

and the multi-steps derivatived polysulfone (PSF) membrane (Fig.10.14(b) (Ma et al., 2006b)) respectively to capture BSA molecules. On the other hand, metharylic acid (MAA) was grafted to the nanofiber surface to capture Toluidine Blue O (TBO) molecules ionically and BSA chemically (Ma et al., 2006a). Observation using confocal laser scanning microscope images showed the labeled BSA covered the fiber surface uniformly and distributed evenly into the fibrous membranes (Fig.10.15). These electrospun membranes showed high water permeability, good reusablity and the capacity to capture target molecules (shown in Table 10.1).
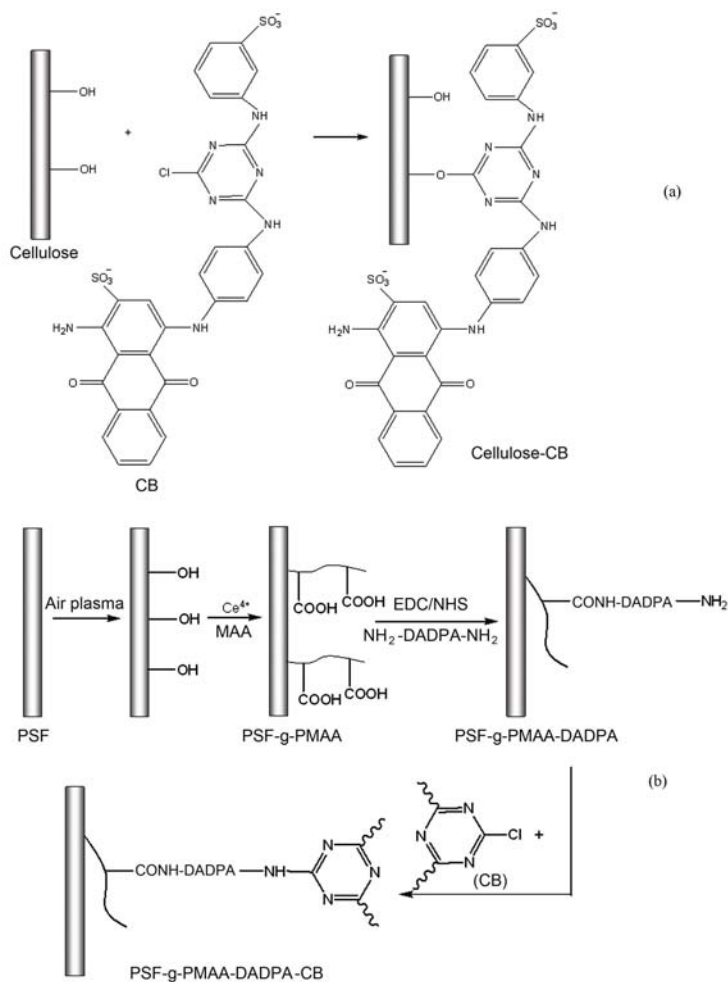
Fig. 10.14. Schematic preparation of affinity (a) cellulose membrane and (b) polysulfone membrane, where NH_2-DADPA-NH_2 represents $NH_2CH_2CH_2CH_2NHCH_2$-$CH_2CH_2NH_2$
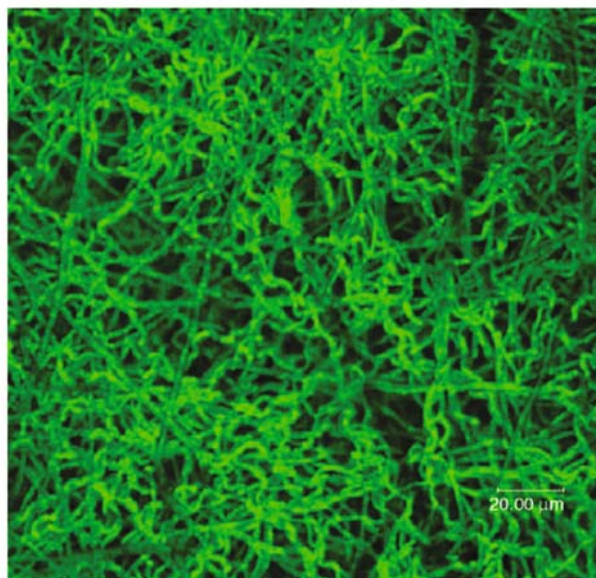
Fig. 10.15. Laser scanning confocal microscope image of polysulfone fiber mesh immobilized with labeled BSA. Reprinted from (Ma et al., 2006a). Copyright (2006), with permission from Elsevier

Table 10.1. The capturing capacity of some affinity membranes

Membrane	Amount of captured BSA (mg/g membrane)
Cellulose-CB	13
PSF-CB	22
PSF-PMAA	17

10.3 Conclusion and Outlook

Electrospinning is a simple and versatile method for fabricating continuous fibers with controllable diameters from several micrometers down to tens of nanometers. The involved materials are rich in variety, including organic polymers, some inorganic polymers and composite materials, and can be processed into nanofibers with hollow structures and aligned arrays or layer-by-layer stacked films through tailoring the electrospinning parameters and the apparatus. The characteristics of the structure (such as the high porosity, interconnectivity, micro-scale interstitial space and large surface-to-volume ratio)

and the electrospinning technique enable this electrospun nanostructure to be practical in many applications, such as filtration, reinforcement, biomedicine, catalysis, etc. In the field of biotechnology dealt with in this chapter, biocatalytic functionalization of the nanofibrous membranes has been explored since the year 2002 and the catalytic membrane was preliminarily applied in biosensors. Preparation of the affinity membranes with a nanofibrous structure was also preliminarily studied in recent years and showed satisfactory results for target capturing and filtration. Nanofibrous membranes have also received extensive and growing interest globally. In other words, functional and highly performing nanofibers have revolutionalised the world of structural materials.

Despite the promising properties of electrospun nanofibrous membranes, some challenges have still to be faced: (1) the subject has only been studied rudimentarily to date and (2) the production of nanofibers is still limited to the laboratory level and needs to be scaled-up for commercial use. However, it can be expected that research into electrospinning will become more interdisciplinary in the near future. With the involvement of a bigger scientific and engineering community, electrospinning will become one of the most powerful tools for fabricating nanostructures and nanomaterials with the broadest range of functionalities and applications.

References

Baumgarten PK (1971) Electrostatic spinning of acrylic microfibers. J Colloid Interf Sci 36:71-79

Chen H, Hsieh YL (2005) Enzyme immobilization on ultrafine cellulose fibers via poly(acrylic acid) electrolyte grafts. Biotechnol Bioeng 90:405-413

Dishi J, Srinivasan G, Reneker DH (1995) A novel electrospinning process. Polym News 20:206-207

Formhals A (1934) Process and apparatus for preparing artificial threads. US patent 1,975,504.

Greiner A, Wendorff JH (2007) Electrospinning: A fascinating method for the preparation of ultrathin fibers. Angew Chem Int Ed 46:5670-5703

Huang XJ, Xu ZK, Wan LS, Innocent C, Seta P (2006) Electrospun nanofibers modified with phospholipid moieties for enzyme immobilization. Macromol Rapid Comm 27:1341-1345

Huang ZM, Zhang YZ, Kotaki M, Ramakrishna S (2003) A review on polymer nanofibers by electrospinning and their applications in nanocomposites. Compos Sci Technol 63:2223-2253

Iijima S (1991) Helical microtubules of graphitic carbon. Nature 354:56-58

Jia HF, Zhu GY, Vugrinovich B, Kataphinan W, Reneker DH, Wang P (2002) Enzyme-carrying polymeric nanofibers prepared via electrospinning for use as unique biocatalysts. Biotechnol Progr 18:1027-1032

Kim BC, Nair S, Kim J, Kwak JH, Grate JW, Kim SH, Gu MB (2005) Preparation of biocatalytic nanofibres with high activity and stability via enzyme aggregate coating on polymer nanofibres. Nanotechnology 16:S382-S388

Kim TG, Park TG (2006) Surface functionalized electrospun biodegradable nanofibersfor immobilization of bioactive molecules. Biotechnol Progr 22:1108-1113

Lee KH, Ki CS, Baek DH, Kang GD, Ihm DW, Park YH (2005) Application of electrospun silk fibroin nanofibers as an immobilization support of enzyme. Fiber Polym 6:181-185

Li D, Xia YN (2004) Electrospinning of nanofibers: Reinventing the wheel? Adv Mater 16:1151-1170

Li SF, Chen JP, Wu WT (2007) Electrospun polyacrylonitrile nanofibrous membranes for lipase immobilization. J Mol Catal B-Enzym 47:117-124

Ma ZW, Kotaki M, Ramakrishna S (2005) Electrospun cellulose nanofiber as affinity membrane. J Membrane Sci 265:115-123

Ma ZW, Kotaki M, Ramakrishna S (2006a) Surface modified nonwoven polysulphone (PSU) fiber mesh by electrospinning: A novel affinity membrane. J Membrane Sci 272:179-187

Ma ZW, Masaya K, Ramakrishna S (2006b) Immobilization of Cibacron blue F3GA on electrospun polysulphone ultra-fine fiber surfaces towards developing an affinity membrane for albumin adsorption. J Membrane Sci 282:237-244

Nair S, Kim J, Crawford B, Kim SH (2007) Improving biocatalytic activity of enzyme-loaded nanofibers by dispersing entangled nanofiber structure. Biomacromolecules 8:1266-1270

Patel AC, Li SX, Yuan JM, Wei Y (2006) In situ encapsulation of horseradish peroxidase in electrospun porous silica fibers for potential biosensor applications. Nano Lett 6:1042-1046

Ren GL, Xu XH, Liu Q, Cheng J, Yuan XY, Wu LL, Wan YZ (2006) Electrospun poly(vinyl alcohol)/glucose oxidase biocomposite membranes for biosensor applications. React Funct Polym 66:1559-1564

Sawicka K, Gouma P, Simon S (2005) Electrospun biocomposite nanofibers for urea biosensing. Sensor Actuat B-Chem 108:585-588

Teo WE, Ramakrishna S (2006) A review on electrospinning design and nanofibre assemblies. Nanotechnology 17:R89-R106

Wang YH, Hsieh YL (2004) Enzyme immobilization to ultra-fine cellulose fibers via Amphiphilic polyethylene glycol spacers. J Polym Sci Part A: Polym Chem 42:4289-4299

Wang ZG, Ke BB, Xu ZK (2007) Covalent immobilization of redox enzyme on electrospun nonwoven poly(acrylonitrile-co-acrylic acid) nanofiber mesh filled with carbon nanotubes: a comprehensive study. Biotechnol Bioeng 97:708-720

Wang ZG, Wang JQ, Xu ZK (2006a) Immobilization of lipase from Candida rugosa on electrospun polysulfone nanofibrous membranes by adsorption. J Mol Catal B-Enzym 42:45-51

Wang ZG, Xu ZK, Wan LS, Wu J, Innocent C, Seta P (2006b) Nanofibrous membranes containing carbon nanotubes: Electrospun for redox enzyme immobilization. Macromol Rapid Comm 27:516-521

Wu LL, Yuan XY, Sheng J (2005) Immobilization of cellulase in nanofibrous PVA membranes by electrospinning. J Membrane Sci 250:167-173

Xie JB, Hsieh YL (2003) Ultra-high surface fibrous membranes from electrospinning of natural proteins: casein and lipase enzyme. J Mater Sci 38:2125-2133

Yang Q, Li JJ, Hu MX, Wu J, Xu ZK (2006) Nanofibrous Sugar Sticks via Electrospinning. Macromol Rapid Comm 42:1942-1948

Ye P, Xu ZK, Wu J, Innocent C, Seta P (2006a) Nanofibrous membranes containing reactive groups: Electrospinning from poly(acrylonitrile-*co*-maleic acid) for lipase immobilization. Macromolecules 39:1041-1045

Ye P, Xu ZK, Wu J, Innocent C, Seta P (2006b) Nanofibrous poly(acrylonitrile-*co*-maleic acid) membranes functionalized with gelatin and chitosan for lipase immobilization. Biomaterials 27:4169-4176

Yoon K, Kim K, Wang XF, Fang DF, Hsiao BS, Chu B (2006) High flux ultrafiltration membranes based on electrospun nanofibrous PAN scaffolds and chitosan coating. Polymer 47:2434-2441

Index